



THE UNIVERSITY
of ADELAIDE

THE LANDSCAPE
EVOLUTION,
GEOCHEMISTRY AND
BIOGEOCHEMISTRY OF
KANGAROO
ISLAND

KATHERINE A. STOATE

Geology & Geophysics
School of Physical Sciences
The University of Adelaide

This thesis is submitted in fulfilment of the
requirements for the degree of Doctor of Philosophy

JUNE 2016

Abstract

This work provides a landscape context and framework for the use of regolith and vegetation in mineral exploration on Kangaroo Island, South Australia. Regolith field observations and the production of a regolith–landform map have improved constraints on the ferricrete plateau formation and also on the landscape history of the Island. The ferricrete and ferruginous materials on Kangaroo Island have been found to be the result of continuous formation but have been largely in place since the Eocene.

Through field observations, microanalysis and a large scale geochemical survey, the nature of the ferruginous materials and the processes that form them have been examined. Ferrolysis and the movement of groundwater have been interpreted to play major roles in the formation of the ferruginous materials. These processes have a significant impact on the use of the weathered materials for mineral exploration as economic and indicator elements are leached early in the weathering process. Ferruginous materials do contain the signature of mineralisation over areas that contain known deposits, however, the apparent lack of dispersion halos makes these materials difficult to use for a large scale geochemical survey for mineral exploration as target zones may be missed by low sampling densities. Despite this, the ferricrete materials can be useful for mineral exploration, as although potentially only providing small target areas, they do highlight areas of mineralisation. Conversely, the underlying weathered bedrock potentially has less use for mineral exploration as the economic metals have been readily mobilised out of the bedrock during the weathering processes on Kangaroo Island.

The biogeochemical surveys were successful in highlighting areas of mineralisation, and displayed a greater dispersion halo than observed in the ferruginous materials. The biogeochemical surveys also helped to provide further information into the processes occurring in the landscape. The eucalypts are interpreted to source groundwater from the weathering zone in the bedrock and effectively pick up elements as they are leached. While displaying a high degree of variability, even over areas of known mineralisation, this dataset was better suited to identifying signals of mineralisation at a larger scale than the ferricrete. A limiting factor on the use

of eucalypt for biogeochemical surveys is the occurrence of systematic inter-species variations. This makes large, regional scale surveys difficult, as there is a high possibility that there will not be a consistent vegetation species, resulting in a dataset in which different species need to be compared and potentially excluded in order to correctly identify meaningful anomalies. The xanthorrhoea, overall, was less successful in taking up elements of interest, most likely due to its shallower root system, which is likely to tap into the already leached saprolite or groundwater that has only been recently recharged by meteoric water (diluting any chemical signature of the underlying bedrock).

This thesis has been able to demonstrate the potential usefulness as well as challenges associated with utilising ferricrete and vegetation for geochemical and biogeochemical sampling for mineral exploration. In doing so it has also furthered understanding of the landscape evolution of Kangaroo Island, building on previous work, and providing a basis for future landscape evolution studies and mineral exploration on the island.

Thesis Declaration

I certify that this work contains no material which has been accepted for the award of any other degree or diploma in my name, in any university or other tertiary institution and, to the best of my knowledge and belief, contains no material previously published or written by another person, except where due reference has been made in the text. In addition, I certify that no part of this work will, in the future, be used in a submission in my name, for any other degree or diploma in any university or other tertiary institution without the prior approval of the University of Adelaide and where applicable, any partner institution responsible for the joint-award of this degree.

I give consent to this copy of my thesis, when deposited in the University Library, being made available for loan and photocopying, subject to the provisions of the Copyright Act 1968.

I also give permission for the digital version of my thesis to be made available on the web, via the University's digital research repository, the Library Search and also through web search engines, unless permission has been granted by the University to restrict access for a period of time.

Katherine Allison Stoate

Table of Contents

Abstract	iii
Statement of Originality	vii
Acknowledgements	xv

Chapter 1: Introduction to Kangaroo Island, Research Themes and Thesis Outline	19
1.1. Introduction	21
1.2. Iron-indurated materials, Ferricrete and Laterites	22
1.2.1. The ‘laterite’ profile	23
1.2.2. Models for evolution and formation of ferricrete/laterite	24
1.3. Kangaroo Island: A case study of ferricrete formation	26
1.3.1. Location and Background	26
1.3.1.1. <i>Climate</i>	27
1.3.1.2. <i>Vegetation</i>	27
1.3.1.3. <i>Landuse</i>	27
1.3.2. Geological Setting	28
1.3.2.1. <i>Mesoproterozoic – Neoproterozoic</i>	28
1.3.2.2. <i>Cambrian</i>	28
1.3.2.3. <i>Permian</i>	28
1.3.2.4. <i>Mesozoic</i>	30
1.3.2.5. <i>Cenozoic</i>	30
1.3.3. Landscape and regolith of Kangaroo Island	31
1.4. Thesis outline	32

Chapter 2: Landscape and Regolith Evolution of Kangaroo Island	35
2.1. Introduction	39
2.3. Geological Background	40
2.3.1. Neoproterozoic & Cambrian	40
2.3.2. Permian	44
2.3.3. Jurassic	44
2.3.4. Cenozoic	45
2.4. Methods	46
2.4.1. Regolith-Landform Mapping	46
2.4.2. Weathering Profiles	48
2.5. Results	51
2.5.1. Stokes Bay Road Weathering Profiles	51
2.5.2. Ferricrete classification and forms	53
2.5.2.1. <i>Ferruginised Basement and Saprolite</i>	54
2.5.2.2. <i>Ferruginised Sediments</i>	54
2.5.2.3. <i>Pisoliths</i>	54
2.5.2.4. <i>Nodular Ferricrete</i>	55
2.5.2.5. <i>Vermiform Ferricrete</i>	55
2.5.3. Permian Sediments	55
2.5.4. Mt Taylor and Mt Stockdale	56
2.6. Discussion	57
2.6.1. Permian to Jurassic palaeo-topography	57
2.6.2. Distribution of marine sediments and implications for Cenozoic tectonics	59
2.6.3. Timing of Ferricrete Formation	62
2.6.4. Formation of ferruginous materials and the ferricrete plateau	63
2.7. Conclusions	67

Chapter 3: Petrographic evidence for complex processes in the formation of the ferruginous component of the regolith of Kangaroo Island.	69
3.1. Introduction	73
3.2. Methods	74
3.3. Results	78
3.3.1. Petrology	78
3.3.1.1. <i>Simple Ferruginous Materials</i> <i>(weathered bedrock and saprolite)</i>	78
3.3.1.2. <i>Complex/Reworked Ferruginous Materials</i> <i>(pisoliths, nodular and vermiform)</i>	83
3.4. Discussion	89
3.4.1. Stage I - The breakdown and weathering of feldspars and the remobilisation of iron to form ‘simple’ ferricretes	91
3.4.2. Stage II - Reworked / Complex Ferricretes	94
3.4.3. Stage III - Mobilisation of indicator/economic elements	97
3.5. Conclusions	97
3.5.1. <i>In situ</i> or transported? The implications for mineral exploration	97
Chapter 4: Geochemical Survey of the ferruginous materials of Kangaroo Island	101
4.1. Introduction	105
4.2. Background	108
4.3. Methods	111
4.3.1. Sampling procedures and geochemical analysis	111
4.3.2. Data treatment	113
4.4. Results	116

4.4.1. Major Element Geochemistry	116
4.4.2. Trace Elements	118
4.5. Discussion	121
4.5.1. The breakdown and weathering primary material; the mobility of the major elements	122
4.5.2. Mobile and Immobile elements	124
4.5.3. Behaviour of the economic elements	126
4.5.4. Geochemical classification of ferricretes	128
4.5.5. Geochemical Mapping	129
4.5.6. Implications for mineral exploration	130
4.6. Conclusions	131
Chapter 5: Biogeochemical Surveys of Kangaroo Island	133
5.1. Introduction	137
5.2. Background	140
5.3. Methods	144
5.3.1. Mineral workings on Kangaroo Island	145
5.3.2. Sampling Procedures	146
5.3.3. Geochemical analysis and data treatment	148
5.4. Results	150
5.4.1. Eucalyptus Results	152
5.4.2. Xanthorrhoea Results	164
5.4.3. Case studies in areas of known mineralisation	166
5.5. Discussion	166
5.5.1. Comparing Xanthorrhoea and Eucalypt Datasets	166
5.5.1.1. <i>Significant spatial variation</i>	168
5.5.2. Mineralised Zones	173
5.6. Conclusions	175

Chapter 6: The Landscape Evolution of Kangaroo Island:

Integrating Datasets	180
6.1. Introduction	182
6.2. Ferricrete on Kangaroo Island: the result of extended periods of formation but largely in place since the Eocene	184
6.3. Identification of <i>in situ</i> and transported ferricrete formation	185
6.4. The mobilisation of major, trace and economic elements: A potentially limiting factor the use of weathered materials in mineral exploration.	187
6.5. The interaction of biogeochemical systems with the regolith and landscape: A suitable sampling material for mineral exploration.	189
6.6. Final Remarks	190
References	193
Appendix A: Geochemical and Biogeochemical Data Tables	
Appendix B: Ferricrete Maps and Plots	
Appendix C: Eucalypt Maps and Plots	
Appendix D: Xanthorrhoea Maps and Plots	

Acknowledgements

Without the help and support of a large number of people, and a selected few who went above and beyond, I would not have been able to complete this thesis.

That this thesis is done is first and foremost due to my mum, Karen, the best, most wonderful person I know. Thanks you for supporting me, for always being there, believing in me, for giving me a shoulder to cry on and the frank advice when I needed it. Without your support I would never have been able to do this. Hopefully I can be you when I grow up.

Alan, thanks for the hugs; for being a solid, reliable (albeit at times infuriating) and unwavering presence in my life. I'm lucky to have such an awesome little brother. Dad, I know you'd be proud. Grandpa, thank you for your love and support, and for the long lunches down at Lake Breeze.

Millie and Morgan, you are both such strong, accomplished women. You've had no problems jumping in and leading me through the chaos that has been the last 3 years, so many, many times. Thank you, thank you, thank you – for without your unwavering support and belief that I could get this thing done (even from different states and continents) I probably wouldn't have. Thank you for talking me through hysterical tears and melt downs, listening to ridiculous rants, talking nonsense with me and letting me crash at your respective houses. I can't begin to say how much I appreciate and admire you both, and how incredibly fortunate I am to have you both in my life. Just call if you ever need anything. I'm there.

Charlotte, you get it better than anyone else. We got there, sanity (mostly) intact. We nailed it. Amy, Bec, Stace, Millie, Bronwyn, Shannon, Cari, Dani - I've got an incredible bunch of friends. Thank you for the support, coffees, dinners, chats, drinks, trips, weddings, flower opportunities and most importantly to me, the laughs and hugs.

Laura, Bonnie, Jade, Kat, Morgan, Charlotte – my beautiful PhD girls. What can I say, you get it. As above, thank you for everything. You're the reason I still have any degree of sanity and I can't tell you how much I love and appreciate you all.

Farid, thank you for the coffees, debriefs, the breath of fresh air and real life when it all got a bit too much, you are a truly wonderful friend. Donnelly, office mate extraordinaire, thank you for chats, gossips and just generally being around, our office was pretty damn awesome and it will be the one thing that I miss about this place. Justin, (my apologies, I did try to keep the Arts student in me suppressed for the thesis, albeit with limited success, however I figured I could go all out for the acknowledgements) thank you for your help, for without the hand holding, the coffees and meetings talking me through sentence by sentence when I was struggling, I would have walked away long ago.

Dave, Steve, Justin and Caroline, thank you for making this thesis better, for your support and guidance over the past 4 years and for all of the opportunities that a post-graduate career has offered. Special thanks to Laura for proof reading this thesis, it was very much appreciated, and contributed to making this a whole lot easier to read. Thanks also go to the incredible scientists and geologists whose work on Kangaroo Island; in biogeochemical and geochemical surveys; and in landscape sciences, I have attempted to build on.

All of the others who have been in and out of my life over the past four years, to those newly entered, those who have come and gone and those who I have neglected terribly over the past 6 months - thank you for being around when you were. Your help and support, through coffees, lunches, dinners, deep and meaningful conversations, weddings, drunken ramblings, hysterical laughter and bouts of tears have been so very much appreciated and is certainly not forgotten. To- Jennie; Karen; Richard; Tori; Ash; Steph; Lachie; Eleanor; Emma; Josh; Elaine; Kel; Jen; Ryan; Sam; Emma & Matt; Blair & Mat; Josh; Tony & Ann; Miranda; Drew; Ben; Josh; Ash; Bel; Lou; Bianca; Funny & Stijn; Alec; Diana; Ros; Chris and anyone else who I have inadvertently missed.

And to the baristas at coffee shops and wait staff at cafes, thank you for the coffee (which was increasingly necessary as this thesis progressed) and the seemingly inconsequential chats. It was a constant and welcome reminder that there was a real world out there.

Now it's time for me to go and join it.

Chapter 1

Introduction to Research Themes,
Kangaroo Island and Thesis Outline

1.1. Introduction

The majority of mineral resources exploited in Australia are sourced from basement terrains of Palaeozoic age or older (Solomon and Groves, 2000). This basement geology is widely covered by younger sedimentary sequences and regolith. Regolith includes the *in situ* products of weathering, transported sediments, concentrations of various minerals due to the movement of ground and surface waters and vegetation (Scott and Paine 2009). Regolith thickness can vary from meters to hundreds of meters and presents challenges for observing and evaluating the nature of buried bedrock geology. This is especially problematic for geochemical mineral exploration, as the chemical signatures of ore deposits are typically modified or obscured by regolith processes and materials. Determining the likely expression of the basement geochemistry through various aspects of the landscape is important for mineral exploration, but is hampered by the dilution and concentration of elements and minerals through weathering and the transport of materials. In Australia, mineral exploration is complicated by these regolith processes and complications amplified by the significant thickness of regolith and the age and extent of reworking of ancient land surfaces.

Laterite and various iron-oxide indurated materials are common regolith components, with widespread global distribution (Figure 1.1). Induration and associated resistance to erosion of these iron-rich materials means that they commonly form plateaux or mesas. This general resistance to erosion also means that once iron indurated materials have formed in the landscape they can be physically reworked and transported, particularly in the form of detrital pisoliths. The processes and mechanisms by which the iron-indurated materials form has been subject to ongoing debate including, but not limited to, the following; (Aleva, 1994; Anand and Paine 2002; Bourman, 1989A; 1989B; 1995; 1993b; Eggleton and Taylor, 1998; Milnes et al., 1987; Ollier and Galloway, 1990; Paton and Williams, 1972; Schellmann, 1994; Stephens, 1971b; Taylor et al., 1992; Twidale, 1983; Twidale and Bourne, 1998).

Iron-indurated materials have been used as a sampling medium for mineral exploration for decades. They are thought to be favourable because of adsorption of trace metals and their widespread distribution. Their utilisation for mineral exploration has added to the need to understand the formation of laterite profiles and ferricretes and the geochemical signatures that they contain. One of the primary aims of this project is to use the widespread

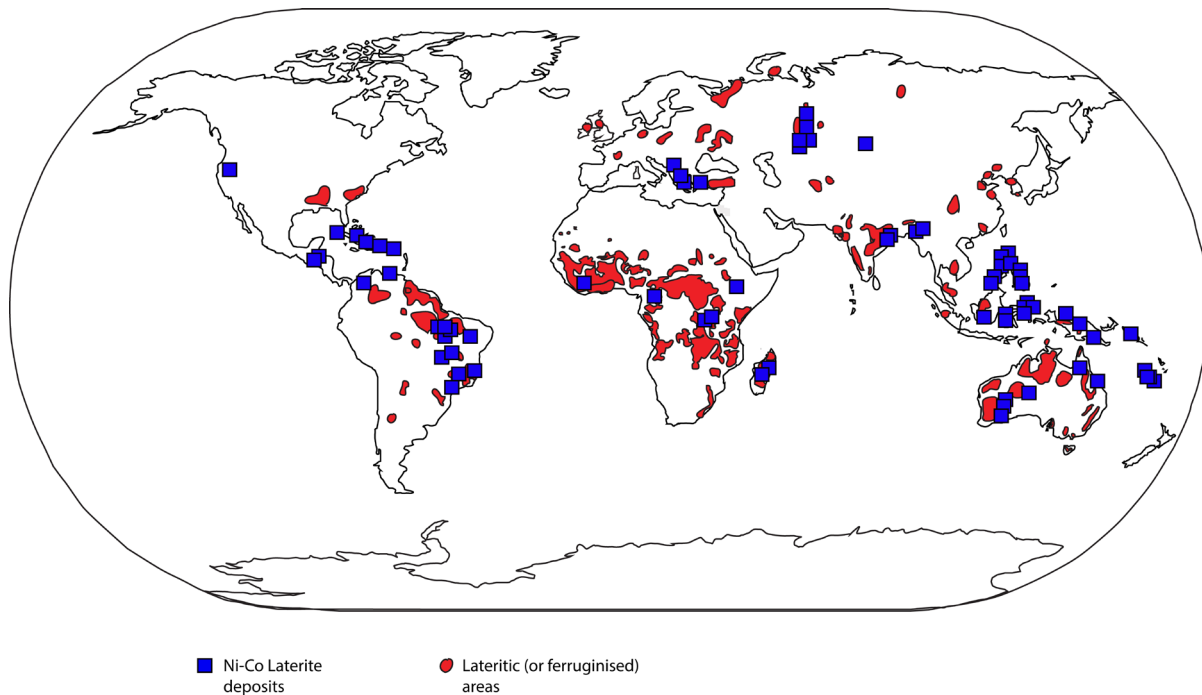


Figure 1.1: Map of the global distribution of laterite, which is marked in red, and Ni - Co laterite deposits are highlighted by the blue squares; modified after Stephens (1971a); Berger (2011) & Lima da Costa (1993).

ferricrete plateau on Kangaroo Island as a case study area to assess the use of iron-indurated materials for mineral exploration. Kangaroo Island contains known mineral systems and a well-defined bedrock geology, allowing for the formation of ferruginous materials to be considered in the wider landscape evolution. This chapter provides an introduction to the nomenclature and current theories on the formation of iron-indurated materials, as well as a summary of the landscape of Kangaroo Island.

1.2. Iron-indurated materials; Ferricrete and Laterite Definitions

The exact definitions of the terms laterite, laterite profile and ferricrete vary depending on the author and their background. Laterite as a term was originally used by Buchanan (1807) in India to describe a particular iron-rich building material that hardened when exposed to air. Since that point laterite has been used to describe many different materials, as well as the profiles from which they originate (Aleva, 1994; Anand, 2002; Bourman, 1989, 1995, 1993b; Bourman and Conacher, 1998; Bourman and Ollier, 2002; Cornelius et al., 2006, 2008; Eggleton and Taylor, 1998; Farmer and Milnes, 1990; Milnes et al., 1987; Ollier and Galloway, 1990; Paton and Williams, 1972; Schellmann, 1994; Stephens, 1971b; Taylor et al., 1992; Twidale, 1983; Twidale and Bourne, 1998). As a result of geochemical research in the 1980s and 1990s there is some agreement on the structure of a 'laterite profile', which

comprises of a weathered bedrock or saprolite zone, pallid zone, mottled zone and iron enriched zone (Figure 1.2; Anand and Butt, 2010; Bourman, 1989, 1993b; Milnes et al., 1985; Ollier and Galloway, 1990). Ferricrete is now preferred as a general term to describe regolith material indurated by iron oxide, as it does not contain the many connotations of laterite. As a consequence, while the term laterite has been used in previous research conducted on Kangaroo Island, ferricrete or ferruginous materials are the terms used in this thesis to describe any iron stained or iron-indurated product on Kangaroo Island.

1.2.1. The 'laterite' profile

The traditional 'laterite' profile includes a zone of weathered bedrock, saprolite, a pallid zone, a mottled zone and an iron enriched zone, which if occurring at the land surface, has generally been hardened due to exposure to air (Figure 1.2). Formation of ferruginous materials in a profile was mostly considered to be the result of chemical weathering in tropical conditions or climates (Bourman, 1993b; Meshram and Randive, 2011; Nash and McLaren, 2011). These conditions are generally thought to be favourable for ferricrete formation due to subdued topography, which limits erosion, the leaching of bases and silica in the upper part of the profile and a fluctuating water table resulting in alternating oxidising and reducing conditions. Upward capillary movement of iron compounds allows for the concentration and hardening at the top of the profile, which forms the typical cap or crust of ferricrete (Bourman, 2007). However, it has been shown that ferricrete formation is not always restricted to tropical conditions (Alley, 1977; Eggleton and Taylor, 1998; Milnes et al., 1985; Paton and Williams, 1972; Sevin et al., 2012; Taylor et al., 1992), and in the case of weathering profiles subjected to continual exposure, regardless of a steady or changing climate (Hunt et al., 1977), there are obvious difficulties in assigning one specific climate regime to the formation of ferricrete.

Many surficial ferricrete deposits do not appear to be monogenetically related to the underlying bedrock (Bourman, 2007) and may contain significant amounts of transported materials. Aleva (1994) suggested that very few ferricrete accumulations are entirely *in situ* or transported, but represent varying mixtures of the two. Bourman (1993b) has suggested that ferricrete deposits are the result of a variable lateral transport of materials, either physically or in solution, with weathering superimposed upon this. The best case for *in situ* processes can be made for mottled or bleached saprolite zones if they contain preserved textures

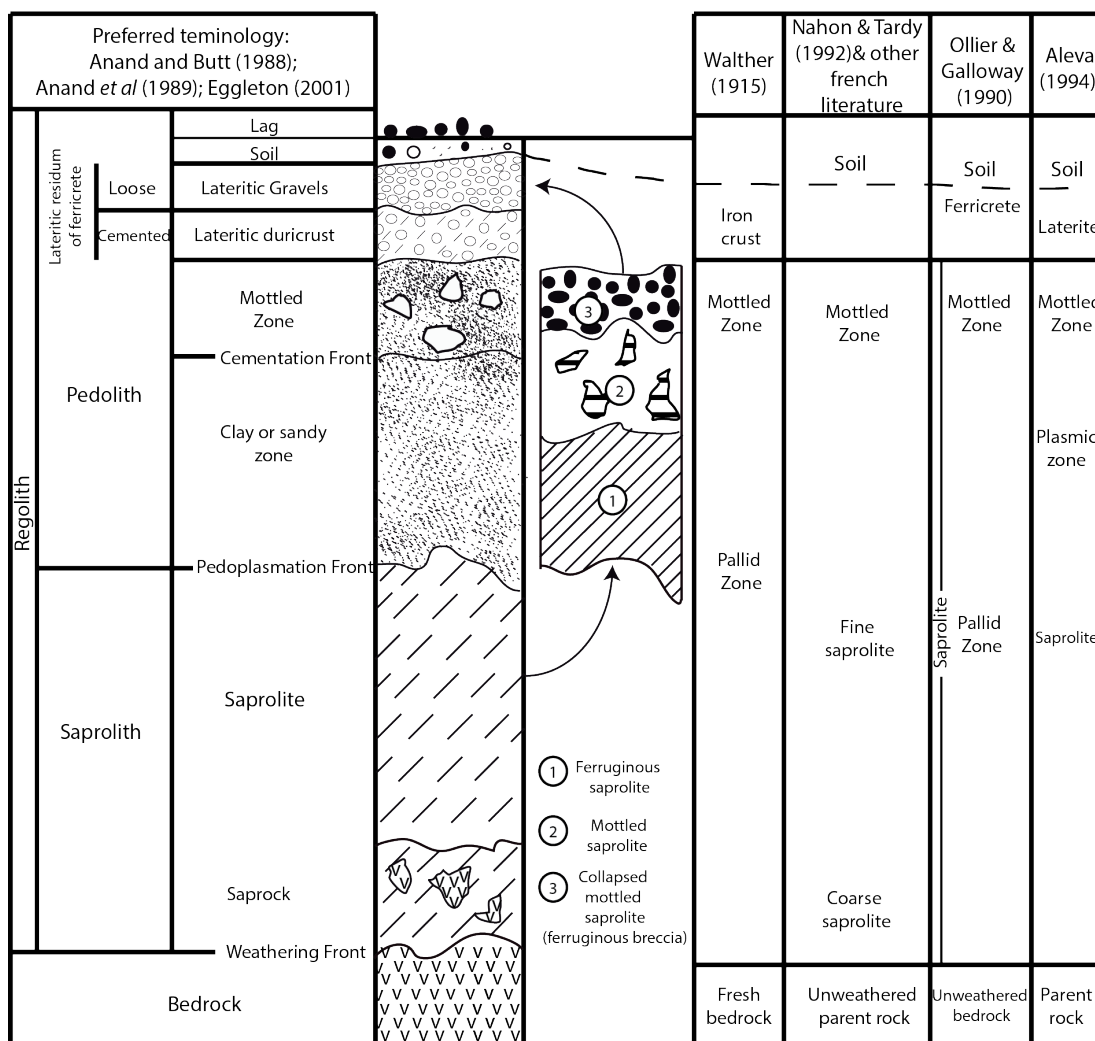


Figure 1.2: Schematic laterite/ferricrete profile and comparison of common nomenclature for the different components. Modified after Anand (2002).

of the original rock but even in these materials there is likely to be local redistribution, weathering and evacuation of minerals associated with these processes (Bourman, 2007).

1.2.2. Models for evolution and formation of ferricrete

There is a great deal of debate regarding the appropriate nomenclature for describing ferruginous materials and the processes of their formation. What follows is by no means an exhaustive, or overly comprehensive, summary of the various models for the evolution and formation of ferruginous materials. Rather, it is a summary of the models and hypotheses that are applicable to the Australian landscape, and the study of Kangaroo Island in particular, relying heavily on the works of Eggleton and Taylor (1998), Anand (2002) and Bourman (1993a, 1995).

Eggleton & Taylor (1998) reviewed a number of theories for the formation of ferruginous material predominately through *in situ* weathering, most which fall within three broad categories, which are detailed below. The schemes of Anand (2002) and Bourman (1993a) relate to specific types of ferricretes forming in different environments and provide greater detail than Eggleton & Taylor (1998).

The first model reviewed by Eggleton and Taylor (1998) is that of ferricrete development beneath a large, flat lying surface with a seasonally wet climate. Examples of locations where ferricrete has formed under these conditions include Northern Cape York, where there is an area of iron enrichment, and an associated aluminium enrichment, forming a bauxite layer. There is an increase in iron and decrease in silica moving up the profile. This model allows for the formation of mesas and caps, if the area were to be incised and the bauxite eroded.

The second model allows for the deep weathering of flat lying rocks, with the development of a localised ferricrete shell through the lateral migration of iron in groundwater and the precipitation of iron, as well as other elements such as aluminium, when it reaches the surface. There are numerous examples of this from the Charters Towers region of north Queensland (Eggleton and Taylor, 1998). Rather than forming an extensive duricrust, the ferricrete forms in localised areas, particularly at zones of groundwater discharge.

The third model is the development of ferricrete as part of a hill slope soil profile. The erosion of bedrock leaves behind the ferricrete as the hardest part of the profile, thereby leading to relief inversion. This is typical of some stream systems, where ferruginised stream sediments overlie slightly weathered bedrock and this alluvium is cemented through the precipitation of Fe^{2+} in the groundwater seepage.

Anand's (2002) scheme includes the formation of specific types of pisolith ferricretes within three different environments. Pisoliths that are formed in soil are homogenous, compound and concentric, formed by replacement or cementation of soil or sediments by iron oxides. Pisoliths formed from saprolite are lithic, may contain preserved rock fabrics and are dominated by goethite, hematite and kaolinite. The third scenario is the formation

of concentric pisoliths in sub-aqueous environments, such as valleys, which have various cores typically surrounded by goethite cutans.

Bourman's (1989, 1993a, 1993b, 1995) work on ferruginous materials centres in southern Australia is perhaps the most relevant to this study, therefore the classification system employed by Bourman is used herein. Ferruginous materials are broadly classified into two categories, 'simple' or *in situ* and 'complex' or reworked. Simple materials include ferruginised bedrock or sediments, where the parent material is identifiable through the preservation of bedrock structures or non-weathered minerals. The formation of these simple ferricretes is suggested to be through local lateral iron enrichment via solution. The other broad classification is the 'complex' or reworked ferricretes, where a single parent material cannot be assigned, and includes pisoliths, nodular and vermiform ferricretes. The formation of these are varied and complex, and will be discussed further in later chapters.

1.3. Kangaroo Island: A case study of ferricrete formation

Kangaroo Island was chosen as a case study in order to examine the processes related to ferricrete and iron-indurated formation, and its use as a geochemical exploration tool. The landscape of Kangaroo Island is dominated by a dissected ferruginous plateau, overlying a relatively homogenous bedrock geology, of the metasedimentary rocks of the Cambrian Kanmantoo Group. This combination of widespread ferruginous regolith, relatively homogenous underlying metasedimentary bedrock and the known mineralised zones makes Kangaroo Island an excellent natural laboratory to address the formation and remobilisation of ferricrete and ferruginous materials and the constraints upon their use for mineral exploration. The use of biogeochemical datasets allows for the geochemical signatures in differing levels of the weathering profile to be assessed, and what effect the landscape has on these sampling media.

1.3.1. Location and background

Kangaroo Island lies 17 km offshore of the Australian mainland in the southern end of the Gulf St Vincent, South Australia (Figure 1.3). It has an area of approximately 4 400 km², is 100 km east-west and about 50 km north-south. Kangaroo Island was first charted by Europeans in 1803 on Matthew Flinders' Investigator voyage (Cooper, 1953) and it was the

original site of European settlement in South Australia in 1836 (Davies, 2002). Evidence of Aboriginal inhabitants dates back at least 12 000 years (Davies, 2002), with spearheads and other tools found at Murray Lagoon. At the time of European discovery, no Indigenous people were recorded as inhabiting the island (Cooper, 1953).

1.3.1.1. Climate

The climate of Kangaroo Island is dominated by the westerly weather systems that affect the majority of southern Australia. The northern coast of the island is protected by the Gulf St Vincent, which results in milder conditions and warmer ocean temperatures than the southern coast, where the next landfall is Antarctica. The northwest area of the island receives significantly more rainfall (up to 900 mm/year) than the area to the southeast (~ 400 mm/year; Davies, 2002). The rainfall difference is due in part to the 200 metre change in elevation between the north and the south of the island, as well as the weather systems being predominately from the west. Mean temperatures in Kingscote (the main town on the island) range from 15 °C (minimum) to 23 °C (maximum) in January, while July temperatures range from 8 °C to 15 °C.

1.3.1.2. Vegetation

The island has two major and distinct vegetation community types which are predominantly controlled by soil type. The limestone and carbonate based soils of the Dudley Peninsula are dominated by the Kangaroo Island narrow leaf mallee (*Eucalyptus cneorifolia*) and other mallee scrub vegetation, as are the low lying coastal regions along the south coast. The ferruginous soils tend to host eucalypt woodland, which can be dense along alluvial channels, dominated by cup gums (*Eucalyptus cosmophylla*), stringybarks (*Eucalyptus baxteri*) and messmate stringybarks (*Eucalyptus obliqua*).

1.3.1.3. Land use

Kangaroo Island is divided into three main land use areas: agricultural for both pastoral and cropping; plantations of both pines and hardwoods (eucalypts); and native vegetation. Approximately one third of the Island is within National Parks, much of which has not been cleared and is dominated by mallee shrubland. Although Kangaroo Island was settled by European inhabitants in the late 1800s, land clearance only began to have a significant

impact on the native vegetation in the 1940s through an increased number of inhabitants and farming as a result of post-World War II ‘soldier-settlement’ schemes. As such, the predominant land use on the island is for pasture and cropping. Within the last decade there has been an increase in the number of tree plantations on the island, with the *Pinus radiata* and eucalypts (e.g. Tasmanian Blue Gums) being the primary plantation crops.

1.3.2. Geological Setting

1.3.2.1. Mesoproterozoic – Neoproterozoic

The oldest exposed rock units on Kangaroo Island are the Neoproterozoic Taracowie Siltstone, Tapley Hill Formation, Sturt Tillite and Sandison Subgroup (Fairclough, 2008). These units are part of a small regional anticline from the Neoproterozoic Adelaide Geosyncline on the Dudley Peninsula (Belperio, 1992; Daily and Milnes, 1972).

1.3.2.2. Cambrian

The main bedrock types of Kangaroo Island are Cambrian metasedimentary rocks of the Kangaroo Island Group to the north and the Kanmantoo Group to the south (Figure 1.3; Belperio, 1995; Flottmann, 1995). The boundary for these units broadly follows the Cygnet–Snelling Fault Zone, suggesting that this structure was also active in the Cambrian (Belperio, 1992; Flottmann, 1995). The Kangaroo Island Group is characterised by platform marine sediments and is up to 2 km thick (Daily et al., 1980; Flottmann, 1995). The Kanmantoo Group includes 7–8 km of alternating sandy and silty sediments interpreted to have been deposited as turbidites in a shelf setting and continues onto the mainland in an arcuate belt (Flottmann, 1995; Haines et al., 2001). The Kanmantoo Group underwent amphibolite to lower granulite facies metamorphism during the Delamerian Orogeny. Localised migmatism occurred around granitoid intrusions during the late Delamerian Orogeny (ca. 500 Ma; Foden et al., 2002; Haines and Flöttmann, 1998). There are various models for the tectonic environment in which the Kanmantoo Group was deposited (Boger and Miller, 2004; Haines et al., 2001). Recent detrital zircon studies suggest that the likely provenance of the sediments is the Ross Orogen in Antarctica (Boger and Miller, 2004; Haines et al., 2001; Ireland et al., 1998), rather than the Gawler Craton as previously suggested (Belperio, 1992). In contrast, clasts of Gawler Range Volcanics in the Kangaroo Island Group indicate that it is likely to have been sourced, at least in part, from the Gawler Craton (Daily et al., 1980; Flottmann, 1995).

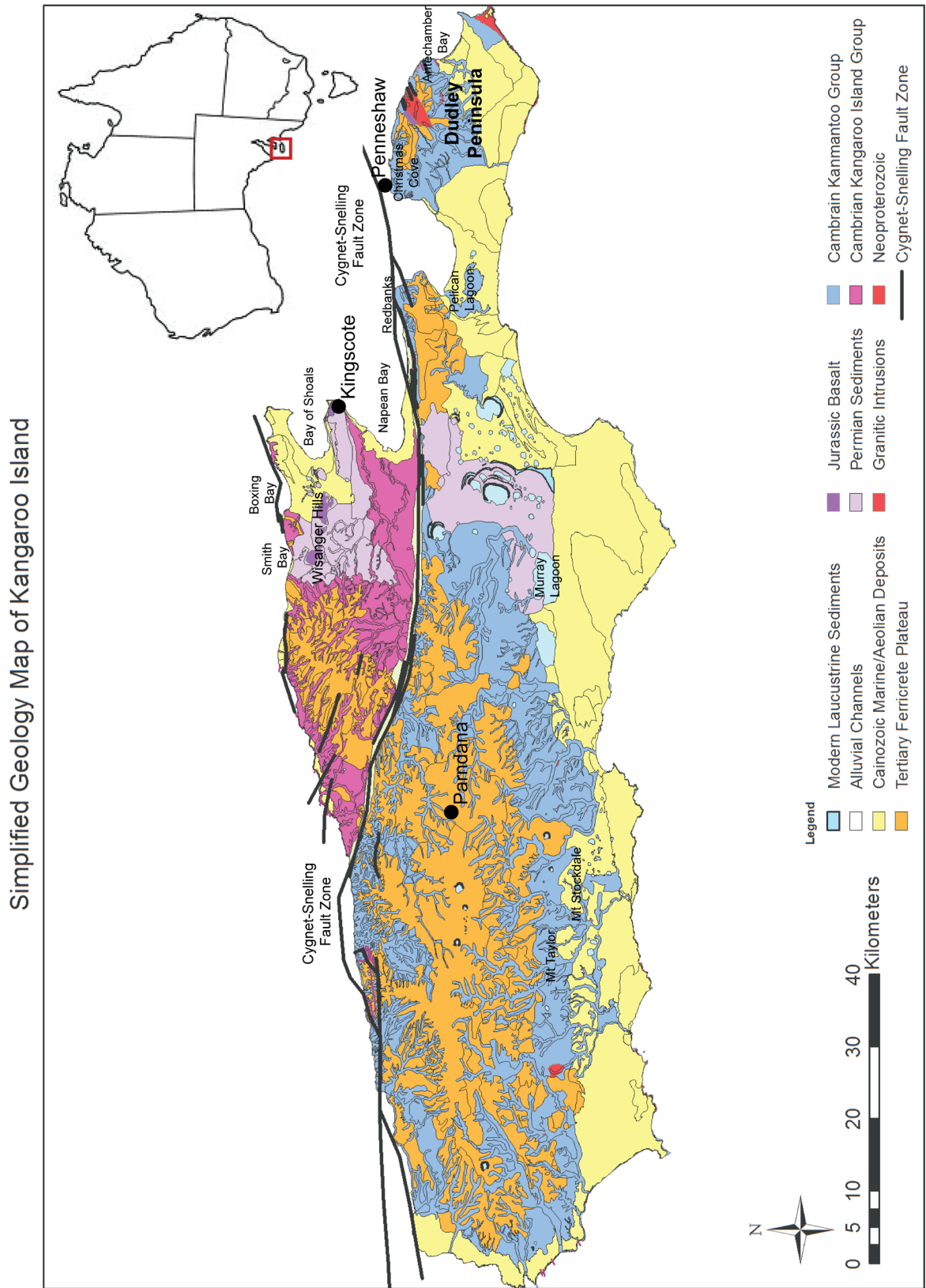


Figure 1.3: Simplified geology map of Kangaroo Island, South Australia, showing the major units and structural controls of the island. Major places names mentioned in the geological background are also included (Belperio 1993; Fairclough 2008).

Inset: Location map of the locality of Kangaroo Island within Australia.

1.3.2.3. *Permian*

The next youngest preserved and exposed rock units are Permian in age, at which time much of the eastern half of the Island was glaciated as part of the Troubridge Basin. Backstairs Passage, which now separates Kangaroo Island from the Fleurieu Peninsula, is thought to be a remnant glacial valley, along with glacial landforms also interpreted at Pelican Lagoon and Christmas Cove (Belperio, 1995; Bourman and Alley, 1999). The Cape Jervis Formation occurs on the Dudley Peninsula at Christmas Cove in Penneshaw, with glacial striae also at Boxing Bay and Smith Bay near Kingscote (Bourman and Alley, 1999). The Cape Jervis Formation also occurs on the main part of the island around Kingscote, preserved as oxidised sediments under the Jurassic-aged Wisanger Basalts. The direction of movement of the glaciation has been determined to be north-northwest from striae measurements (Bourman and Alley, 1999).

1.3.2.4. *Mesozoic*

The Jurassic-aged Wisanger Basalts crop out in the northeastern part of the Island. These tholeiitic basalts are associated with the rifting of Gondwana and the separation of Australia from Antarctica (Milnes et al., 1982). The Wisanger Basalts crop out near Kingscote and overlie Permian sediments, forming the small plateaux of the Wisanger Hills. The basalts are characterised by hexagonal columnar jointing (Drexel, 1995; Milnes et al., 1982) and are remarkably unweathered.

1.3.2.5. *Cenozoic*

During the Tertiary, Kangaroo Island was on the edge of three basins: the St Vincent, Murray and Eucla basins (Drexel, 1995). The Kingscote Limestone was deposited during the Eocene to Oligocene in a shallow marine environment, suggested to be distant from fluvial influence (Milnes et al., 1983). Miocene marine sediments are represented on the southern portion of the Island, most notably the Mount Taylor and Mount Stockdale areas to the southwest (Milnes et al., 1983). These sediments were likely to have been more aerially exposed, suggested by their presence as reworked clasts in younger aeolian calcarenites (Milnes et al., 1983). Marine sediments from the Pliocene are dominated by fossiliferous limestones at lower landscape levels than the Miocene sediments. Pleistocene marine sediments are confined to the lowland area following the current coastline (Milnes et al., 1983) with the Pleistocene Ochre Cove Formation forming the dominant landscape

feature of Redbanks, on the southern side of Nepean Bay (Pillans and Bourman, 2001). The majority of sediments are most likely to have been eroded from areas south of the Cygnet Fault, which was active at the time and would have had similar uplift to that experienced along the Mt Lofty Ranges (Tokarev et al., 1999). Holocene sediments are found in the low lying bay areas, such as Nepean Bay, Antechamber Bay and the Bay of Shoals (Milnes et al., 1983).

1.3.3. Landscape and regolith of Kangaroo Island

The landscape of Kangaroo Island is dominated by the ferricrete plateau (Figure 1.3). The relationship between the regolith materials and the landscape of the Island was first explored by Bauer (1959), who built on the earlier soil division work by Northcote (1946, 1948). This work is included in the later study on the Cenozoic marine sediments by Milnes et al. (1983). Research on the ferricrete has been conducted in three main stages, by Daily and Twidale (1974), Bourman (1989) and followed by Bourman and Pillans (1999) with their palaeomagnetic work on the stratigraphic section at Redbanks.

None of the previous studies on Kangaroo Island have been able to provide a conclusive age of the ferricrete plateau that covers much of the island. Daily et al. (1974) suggested that the age of the ferricrete plateau was older than the Middle Jurassic but younger than the Early Permian, based on stratigraphic, geomorphological and radiometric evidence, with a distinction made between the ferruginised Permian sediments and the ferricrete surface. Climate evidence on a regional scale indicates that Australia experienced tropical to subtropical conditions during the Mesozoic, specifically the Triassic, which would support the formation of the ferricrete during this period (Daily et al., 1974; Twidale, 1983). However, as previously mentioned, a tropical climate is not necessary for the formation of ferricrete (Taylor et al., 1992).

Bourman and Pillans (1997) conducted magnetostratigraphic research on a profile at Redbanks, where they concluded that the age of ferruginisation was 72 ka. However the Redbanks profile is not part of the main ferricrete plateau and is thought to be comprised of much younger sediments that post-date the movement of the Cygnet–Snelling Fault (Pillans and Bourman, 2001). As a consequence these sediments do not provide the opportunity to constrain ferruginisation processes older than this.

Further work has been conducted by Bourman around Kangaroo Island and several other localities within the Fleurieu Peninsula, where deep weathering profiles have been identified (Bourman, 2007). Specifically, an area in the vicinity of Willunga Hill has been used to demonstrate that many of the exposed features are the result of modifications and developments under environmental conditions similar to those of the present. This is an alternative to the view that tropical conditions are needed for the formation of ferricrete (Bourman, 2007). Therefore the age and processes of formation of the ferricrete on Kangaroo Island remain uncertain.

1.4. Thesis outline

This thesis aims to determine whether the use of geochemistry and biogeochemistry can better characterise the landscape system and processes that operate within it. These processes are then examined in relation to the possible use of ferruginous material and vegetation for mineral exploration. The ferruginous materials will be examined at a micro scale, to identify the petrological setting of the geochemical anomalies that might occur.

The indurated iron oxide materials observed in this study will be all referred to as ferruginous materials or ferricrete. This includes all of the iron stained and indurated materials in the regolith, in which iron oxides are visible as an orange to red colouration. These materials can range from slightly oxidised clays of a few percent iron to hardened hematite rich materials containing over 50% iron. In some locations, a near complete 'laterite' profile has been observed from bedrock through saprolite, mottled and pallid zones and a pisolithic cap. The sampling conducted herein focuses on the ferruginous materials that are present at the surface on Kangaroo Island, as the surficial materials present the most effective means of producing a first pass dataset for a geochemical survey. Sampling surficial material also allowed for a greater range of ferruginous materials to be collected and the processes that are involved in ferricrete formation to be more fully examined. These aspects all allow the ferruginous materials to be examined for their usefulness as a medium for mineral exploration.

This thesis comprises of six chapters.

Chapter 1 (this chapter) provides a background on the study area of Kangaroo Island, a brief background to the study of ferricretes and iron-indurated materials and introduces the aims of this thesis.

Chapter 2 is a synthesis of the current knowledge of the geology and the landscape evolution of Kangaroo Island. This is supplemented by new observations and a regolith map for the island. The classifications, morphology and landscape setting for the various ferricretes are also discussed in this context, as well as a model for the formation of ferricretes within the context of Cenozoic tectonics and landscape evolution.

Chapter 3 presents petrography and microanalysis, including electron microprobe imagery of the ferruginous materials sampled. Examining the physical evidence presented at the microscale allows a better understanding of the chemical processes that formed the ferruginous materials. This information can be used to determine the suitability of the ferruginous materials as a sample media for mineral exploration through cover.

Chapter 4 details the regional scale geochemical survey of the ferruginous materials. This chapter uses geochemistry to examine the formation of the ferricretes and ferruginous materials, as well as assessing their suitability as a sampling medium for mineral exploration through cover.

Chapter 5 contains biogeochemical surveys that were conducted on Kangaroo Island, using several eucalypt species and xanthorrhoea, or grass trees. These biogeochemical surveys were conducted to gain a better understanding of expression of the system through the vegetation, as well as to further test the biogeochemical method in relation to its use for mineral exploration.

Chapter 6 is a concluding chapter brings together these large scale datasets and discusses them in context and relation to each other and the wider landscape evolution of Kangaroo Island. The utilisation of different sampling media for mineral exploration is also discussed.

Chapter 2

Landscape and Regolith Evolution of Kangaroo Island

Foreword

As outlined in Chapter 1, there has been a significant amount of work conducted on various aspects of the geology and the landscape of Kangaroo Island (Figure 2.1). However, much of this work has addressed specific aspects of the regolith and geology rather than considering them in part of a wider regolith–landscape evolution context for the region. This chapter aims to address this, first, by compiling and integrating much of the previous work, as well as new observations, into a regolith–landform map (Figure 2.2). The regolith–landform map is then used as the basis for an investigation into the influence of major controls on the evolution of the landscape, such as bedrock lithology, tectonics, eustacy and climate. Understanding the effect and influence of these controls will allow for a better understanding of the processes that form the associated regolith materials in the landscape, as well as the ongoing nature of these processes.

2.1. Introduction

The formation and evolution of a landscape is the result of a number of different factors, including tectonics, climate, eustatic changes and the starting materials that the landscape surface is formed from (Bishop, 2007; Butt and Bristow, 2013; Ollier, 1995; Paton and Williams, 1972; Phillips, 2005; Tucker and Hancock, 2010; Wilford and Thomas, 2013). In cases where landscape systems have experienced long term aridity and tectonic quiescence, the evolution of the landscape has often been thought to be relatively simple. The formation of regolith materials has been considered to be largely controlled by only a select number of factors (Twidale, 1976, 1983, 1998). In recent years, further investigation into the regolith of these tectonically quiescent areas has revealed that the evolution of the landscape is often more complex, reflecting the control of many factors (Butt and Bristow, 2013; Gale, 1992; Ollier, 1995; Wilford and Thomas, 2013). Australian landscapes, in particular, tend to be subject to the view that the formation of the landscape, and the formation of ferricretes in particular, are the result of relatively slow moving processes (Daily et al., 1974; Twidale, 1976, 1983). Kangaroo Island forms an excellent case study for the formation of complex ferricretes and the influence of different factors on landscape evolution.

The ferricretes on Kangaroo Island have long been the topic of debate with uncertainties about their protolith and timing and characteristics of formation (Bourman, 1989, 1993b, 2007; Daily et al., 1974; Milnes et al., 1985; Twidale, 1983). Investigations into the ferricretes can be advanced through the integration of neo-tectonics, landscape processes, field relationships, surface geochemistry and microanalysis of the materials. Understanding the formation of the ferricretes and its interaction with the landscape is important due to its potential as a sampling medium for mineral exploration. This chapter integrates new information with previous studies to expand upon the impact of landscape processes and evolution on the formation of the ferricrete on Kangaroo Island. This provides a framework for subsequent microanalysis, geochemical and biogeochemical surveys.

2.2. Geological Background

The geology on Kangaroo Island ranges from Neoproterozoic through to modern day sediments, including ferricretes and carbonates. These are as follows, and the relationships of the various units to the wider region are highlighted in the time–space plot in Figure 1.

2.2.1. Neoproterozoic & Cambrian

The two main basement rock packages on Kangaroo Island are the Kanmantoo Group and Kangaroo Island Group. These are Cambrian metasedimentary rock packages interpreted as having been deposited in a deep marine setting (Kanmantoo Group) which transitioned into the shallow water sequence, Kangaroo Island Group (Daily et al., 1980; Flottmann et al., 1998; Haines et al., 2001; Jago et al., 2003). A small section of the Neoproterozoic Adelaidean is exposed on the Dudley Peninsula, on the northeast coast of the island. This includes the Taracowie Siltstone, the Tapleys Hill Formation, Sturt Tillite and Sandison Subgroup (Fairclough, 2008).

The Kangaroo Island Group consists of fine grained sandstones deposited intertidally with alluvial layers of coarse grained sandstone and conglomerate (Daily et al., 1980; Flottmann, 1995). The pre-weathering mineralogy of the Kangaroo Island Group changes slightly with differing facies within the unit. The conglomerate of the Boxing Bay Formation is rich in gneissic and granitic clasts whereas the White Point Formation conglomerate contains carbonate-rich clasts (Daily et al., 1980). Sandstones throughout the group generally have abundant feldspar, mica and quartz. The Kangaroo Island Group is interpreted to be sourced from the neighbouring Gawler Craton, due to the degree of clast rounding, the lithologies present in the conglomerates and the palaeocurrent reconstructions within the finer grained facies (Daily et al., 1980).

The Kanmantoo Group comprises 8 units and is characterised by interbedded meta-sandstones, siltstones and mudstones (Daily and Milnes, 1973; Jago et al., 2003). They are

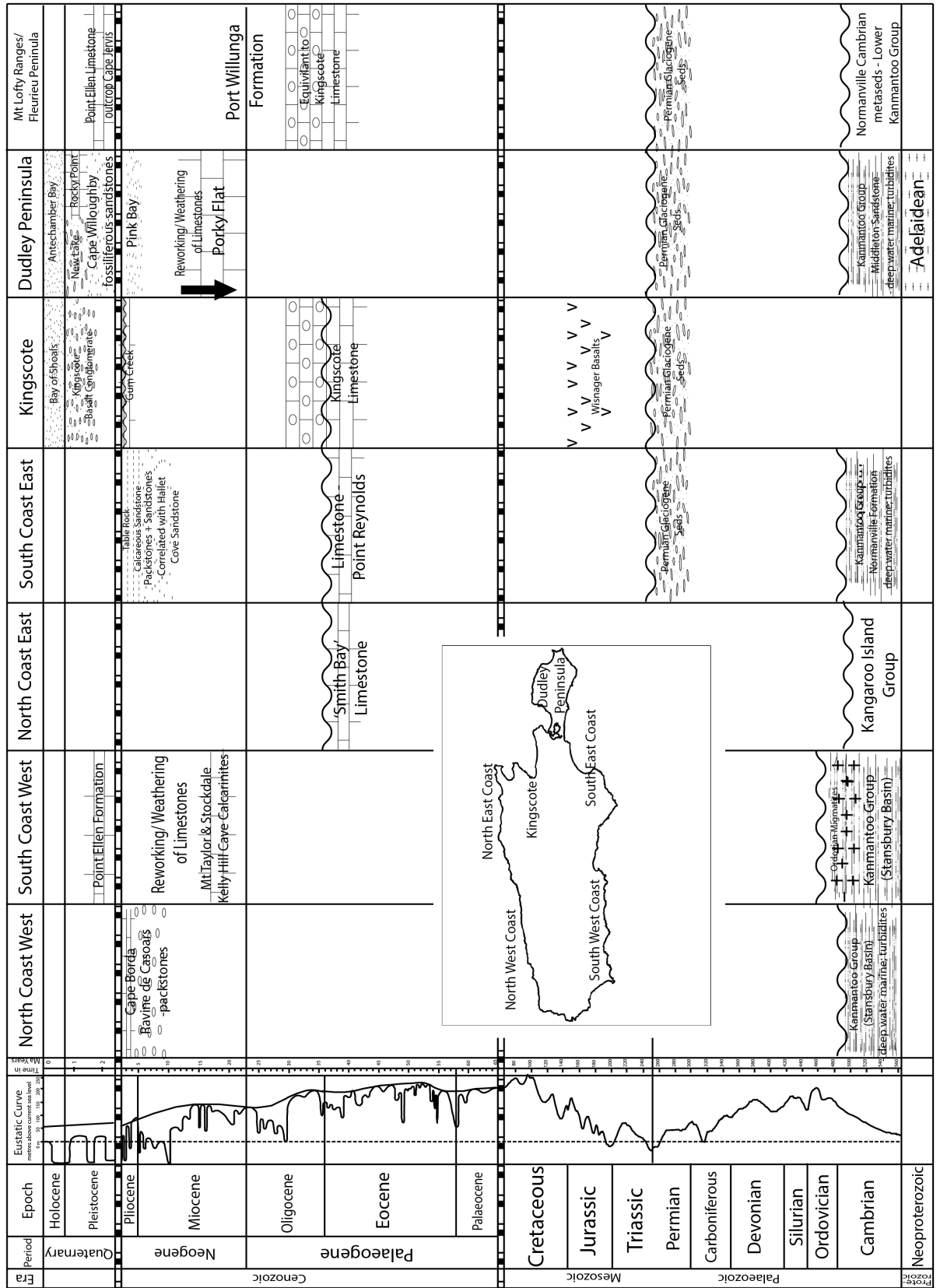


Figure 2.1: Time-space plot for Kangaroo Island and the adjacent regional area, with a global sea level curve adapted from Haq (1988); Haq and Schutter (2008). Geological information from: Belperio (1995a) Bourman and Alley (1999); Bourman et al. (2007, 2010a, 2010b); Flöttmann (1995, 1998); Flöttmann and Cockshell (1996); Haines and Flöttmann (1998) and Milnes et al. (1983).

typically highly micaceous and contain fine grained quartz and feldspar, with proportions varying between the 8 units. Some units are dominated by metasiltstones, such as the Tallisker Formation, while the Balquhiddier Formation includes metasiltstones, metasediments and conglomerate facies (Daily and Milnes, 1973; Jago et al., 2003). The pre-weathering mineralogy of the Kanmantoo Group meta-siltstones and meta-sandstones is quartz + plagioclase + biotite + muscovite \pm calcite \pm chlorite \pm garnet \pm epidote (Daily and Milnes, 1973; Jago et al., 2003). Actinolite, diopside and epidote also occur as secondary minerals in the phyllite and calc-silicate layers in some formations (Daily and Milnes, 1973; Jago et al., 2003).

Exposure of the Kangaroo Island Group away from the coast is limited, but areas that are exposed are weathered in a similar manner to the Kanmantoo Group. This includes formation of kaolinite from feldspars and the formation of ferricretes at the top of profiles. The dominant landscape process acting upon the Kanmantoo Group along the coastline is erosion, with little opportunity for the development or preservation of a weathering profile. Inland, the basement rocks mostly occur in a moderately to highly weathered state (Table 2.1). In alluvial channels where erosion rates are high the basement rocks are only slightly weathered (Table 2.1). The weathered products of both the Kanmantoo and Kangaroo Island Groups can be distinguished from other weathered rock packages on the island by the abundance of micas within the weathering products.

Exposures of granitic intrusions from the Cambrian (Foden et al., 2002) are concentrated around the southern coastal areas, and have been eroded to form castle koppie with tafoni on large radius domes (Twidale, 1981). This is exemplified at the Remarkable Rocks, within the Flinders Chase National Park. The granites are both I- and S-type with slightly different mineralogy. I-type granites are typically biotite- and/or hornblende-bearing and in many cases are titanite-bearing, plagioclase-rich diorite, tonalite, granodiorite and granite (Foden et al., 2002). The S-types are biotite-rich, muscovite-bearing without hornblende, and range

Table 2.1: Weathering index after Eggleton (2001). These terms have been used throughout to describe the type and degree of weathering found in bedrock in the field. These terms are not entirely universal, with terms such as saprock and saprolite also part of the nomenclature for regolith materials.

	Field Criteria	Alteration assemblage/composition
Unweathered	Having no visible signs of weathering	None
Slightly Weathered	Core-stones, if present, are interlocked; few micro fractures; is easily broken with a hammer. Sediments have traces of weathering on the surfaces on sedimentary particles. Some clay or iron oxides may be present, filling voids between coarse particles	Weak iron staining; slight weathering of feldspars. Primary minerals very prominent; some smectite and minor goethite may be present. Ca, Mg, Na appreciably depleted; K, Si show slight depletion.
Moderately Weathered	Marked iron stained common; up to 50% secondary minerals; core stones rectangular and interlocked. Larger particles have a thick weathering skin. Can be broken by a kick (with boots on), but not by hand.	Most feldspars in larger particles are weathers. Most alkalis and alkaline earths have been lost. Primary minerals still dominant, with smectite, kaolin \pm iron oxides and oxyhydroxides present.
Highly Weathered	Strong iron staining, and more than 50% secondary minerals; core-stones are free and rounded, and there are numerous micro fractures. This material can be broken apart by hand with difficulty.	Nearly all feldspars in larger particles are weathered. Appreciable silica has been lost; mineralogy includes kaolin \pm goethite \pm hematite with significant amounts of primary minerals
Very Highly Weathered	Retains structure from the original rock; may be pale coloured and is composed completely of secondary minerals and resistates from the parent material. Core stones, if present, are rare and rounded. It can easily be broken by hand.	All feldspars are weathered; mineralogy is dominated by kaolin \pm goethite \pm hematite with or without residual quartz. Other primary minerals in low abundance or lost.
Intensely Weathered	Only major parent rock features discernible, such as lithological changes or resistate veins; resistate minerals may remain in a matrix of secondary minerals.	Mineralogy is essentially \pm goethite/hematite/maghemite \pm quartz \pm kaolinite \pm gibbsite. High levels >50% of sesquioxides, negligible alkalis and alkaline earths; significant titania.

from granite to granodiorite (Foden et al., 2002). Away from the immediate coastline the granite intrusions tend to form domed hills with a high degree of weathering (Table 2.1).

2.2.2. Permian

A sequence of glacial sediments were deposited on Kangaroo Island during the Permian, which have since been subjected to weathering and iron oxide induration in some areas. Glacial regolith is represented by the Cape Jervis Formation (Belperio, 1995a; Bourman and Alley, 1999), and is one of the main lithologies in the southeastern part of the island. The package is of variable thickness, ranging from only 7 m in outcrop at Christmas Cove to 290 m thick in some bore holes (e.g. the Kingscote Bore) and an estimated 400 m from geophysical surveys in the trough northwest of the Dudley Peninsula (Bourman and Alley, 1999). These sediments include diamictons inter-bedded with fine grained clay and mud, which are poorly consolidated, have poor permeability and can be similar in appearance to the highly weathered Kanmantoo Group (Bourman and Alley, 1999). Drop stones and gravels in the diamicton layers identifies the package as a glacial sediment.

2.2.3. Jurassic

The Wisanger Basalt is the only volcanic rock package on the island and radiometric dating shows it to be from the Jurassic (Drexel, 1995; Milnes et al., 1982). It occurs only in the northeast of the island (Figure 2.2) and forms elevated topographic features. The basalts are fresh to slightly weathered when *in situ*, with only weak iron oxide staining, little to no change in the structure and little to no evidence of weathering or alteration of primary minerals. The occurrence of rounded basaltic clasts within Eocene and Oligocene Kingscote Limestone (Milnes et al., 1982, 1983) suggests that the extent of the Wisanger Basalt was originally more extensive than it is at the present. The relatively fresh state of the basalt is suggested to be the result of either the burial of the material by post-middle Jurassic sediments or from the complete erosion of the weathered material (Milnes et al., 1982).

2.2.4. Cenozoic

Cenozoic regolith materials are dominated by marine sediments and regolith carbonates, aeolian sediments and indurated iron oxides (ferricretes), which make up the majority of the surficial geology on the island. The coastal marine sediments lie parallel to the modern coastlines and extend up to 15 km inland. These are predominantly limestone and in some cases calcareous sandstones, with varying amounts of foraminifera (McGowran, 1989; Milnes et al., 1983). The deposition of Eocene marine sediments, in the low lying areas around Kingscote, are related to a series of global sea level changes (McGowran, 1989; Milnes et al., 1983). Miocene marine sediments were deposited along the south coast, in the Mt Taylor and Mt Stockdale area. The Pliocene sediments, found in low lying areas along the east and west coasts and between the main island and Dudley Peninsula, are also believed to be related to eustatic changes. The Late Pliocene sediments are regarded as evidence of a widespread transgression (Milnes et al., 1983). Regolith carbonates are present along the south coast where the older Tertiary limestones have been reworked, largely by aeolian processes, to form the Quaternary Bridgewater Formation (Drexel, 1995; Milnes et al., 1983).

Aeolian sediments on Kangaroo Island are dominated by aeolian calcarenites and are largely composed of reworked materials from older marine deposits, carbonates and sand. The main geological unit is the Bridgewater Formation. Outcrop of the Bridgewater Formation dominates the south coast, extending up to 15 km inland and also occurs around the coastal cliffs, commonly unconformably overlying Cambrian basement rock. Longitudinal, northwest–southeast to east–west trending dune systems and hardened carbonate deposits capping the cliffs of eroded Cambrian basement are the dominant manifestations of the Bridgewater Formation. The carbonate deposits were originally large scale dunes and back-beach deposits (Drexel, 1995; Milnes et al., 1983) the movement of meteoric water through these deposits has cemented the sediments, through the mobilisation and re-precipitation of calcium carbonate (Twidale, 2002). The Bridgewater Formation is assigned to the

Pleistocene (Belperio, 1992, 1995a, 1995b), although it contains reworked clasts of Miocene and Eocene aged materials (Milnes et al., 1983).

Ferruginous regolith dominates much of the regolith and landscape of the island, particularly inland, with varying morphology and evolution histories. As a consequence, several different classifications have been used in this work depending upon whether the iron oxide induration is *in situ* (simple) or reworked (complex). These classifications are based upon the work of Bourman (Figure 8; 1993a, 1989).

2.3. Methods

Regolith landform mapping, field observations and a detailed analysis of regolith profiles has been undertaken in order to better assess the formation and characteristics of the ferricrete on Kangaroo Island.

2.3.1. Regolith-Landform Mapping

A regolith-landform map of Kangaroo Island (Figure 2.2) was produced from field observations, information from previously published works, the SRTM-derived 1 Second Digital Elevation Models Version 1.0 (DEM) and topographic maps.

The major landscape feature of the Island is the ferricrete plateau, which is generally assumed to be relatively flat lying and homogenous. However, there are variations within the ferricrete and landscape, caused by changes in the basement structure and drainage channels. Within the ferricrete plateau there are several different regolith-landform units mapped. These landform units are not just based upon the physical appearance of the ferricrete, but rather a composite of the elevation, vegetation and ferricrete type. Thus, the regolith-landform units do not correlate exactly with the classifications given to the ferricrete at an outcrop or hand sample scale. The ferricrete plateau is largely composed of the ferruginised basement or saprolite (Table 2.2a), pisolithic (Table 2.2c) and nodular

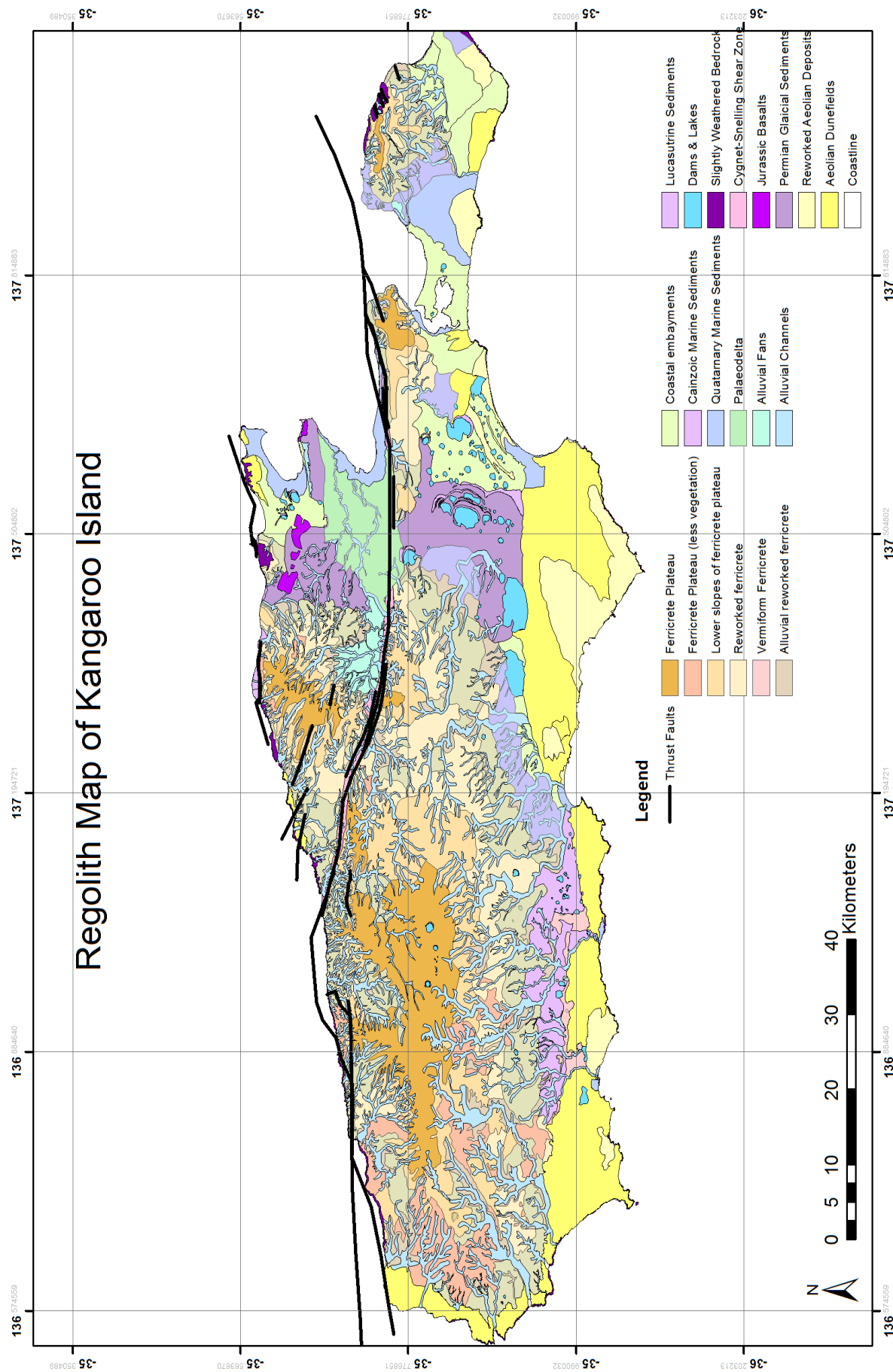


(Table 2.2d) ferricrete. The ferruginised sediments (Table 2.2b) tend to occur closer to coastal areas, although they can be found on the main plateau. Vermiform ferricretes (Table 2.2e) are generally found in lower lying areas off the main plateau (Figure 2.2).

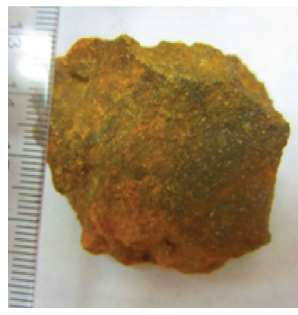




The occurrences of the marine sediments have been mapped from a composite of the previous geological map of the island (Fairclough, 2008), SRTM-derived 1 Second Digital Elevation Models Version 1.0 from Geoscience Australia, topographic maps and field observations. Some areas are remote with little to no access, such as the west coast, and these have been mapped from the aforementioned remote sensing data.

A range of alluvial channels, largely associated with modern drainage systems, are present across the island. The majority of these are ephemeral and flow after winter rainfall. The weathering profile of the Island is best observed in modern alluvial channels, where the channel bed comprises of fresh to moderately weathered basement rock that becomes progressively more weathered up the profile, culminating in highly weathered bedrock (Table 2.1) that is generally capped by pisolithic ferricrete. In a number of alluvial systems there is some reworking of the ferricrete where it has been eroded, transported and redeposited along contemporary valley systems. For example, hematite cemented pisoliths form river terraces along the Cygnet River at the Bonaventura Prospect. These alluvial features tend to follow topographic features within the underlying top of bedrock surface or weathering front, which themselves are expressions of fault movements and scarps. An example is the Cygnet River, which broadly runs parallel to the Cygnet Snelling Fault Scarp and into Nepean Bay.

2.3.2. Weathering Profiles

To better assess the deep weathering of the Island, and the formation of the regolith and landscape, several weathering profiles were examined. These included two road cuttings along Stokes Bay Road. These weathering profiles cut down through the ferricrete

Table 2.2: Classification system of ferricretes on the different morphologies of ferruginous materials on Kangaroo Island.

	Ferricrete Morphology	Simple or Complex ?	Description	Photo
a.	Ferruginised Bedrock and Saprolite	Simple	Weathered bedrock and saprolite which contains some degree of iron staining or induration. Preservation of bedrock features, fabrics and textures.	
b.	Ferruginous Sediments	Simple	Iron oxide impregnated sediments. The lack of a distinct relict fabric makes them unable to be identified as ferruginised bedrock, and they are called sediments instead.	
c.	Pisoliths	Complex	Individual pisoliths, which can display multiple rinds (or cutans), which sometimes are found cemented together.	
d.	Nodular	Complex	Similar to pisoliths, but with a lesser degree of rounding, and slightly bigger main form.	
e.	Vermiform	Complex	Sinuuous, worm like channels between pisoliths. The matrix is often comprised of sands or clays that contrast to the iron rich material.	

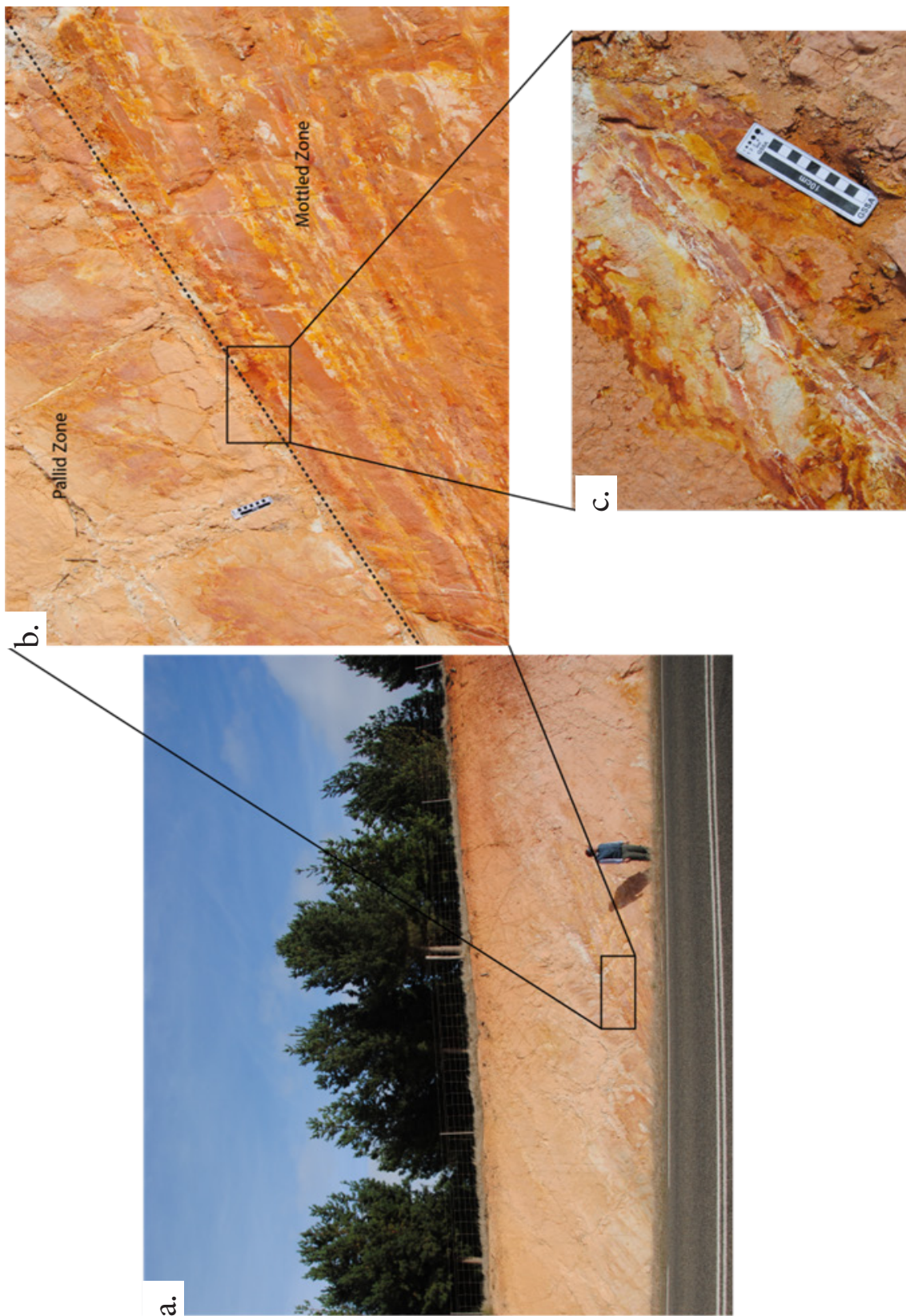


Figure 2.3: Stokes Bay Road weathering profile #1 (a) shows the full extent of the weathering profile. Person for scale is 1.6 m tall. (b) shows the distinct boundary between the pallid and mottled zones; (c) highlights the remnant and overprinted saprolite structures. There was some evidence of de-watering and other structures.

plateau and into the underlying weathered bedrock. The weathering profiles were logged, photographed and assessed for geomorphological and structural features.

2.4. Results

The results provided are a combination of detailed field observations and weathering profile descriptions and include descriptions of key field sites that provide constraints on landscape evolution.

2.4.1. Stokes Bay Road Weathering Profiles

The first of the Stokes Bay Road weathering profiles is a 6 m section where Stokes Bay Road has been cut through a hill (Figure 2.3). The base of the weathering profile is largely made of weathered Kanmantoo Group. Moderately weathered basement rock becomes progressively more weathered to a highly weathered grade (Table 2.1) and there is an increase in iron oxide staining towards the current landsurface. Some original sedimentary structures are retained within the saprolite, which is up to one metre thick; including dewatering and cross-bedding structures (Figure 2.3). The mineralogy of the saprolite changes from angular to sub-angular, interlocked quartz with plagioclase, muscovite and potassium feldspar some which has been replaced by weathering products at the base of the profile, to quartz dominated by smectites and other products of the weathering of the feldspars, stained by iron oxide as highly weathered bedrock at the top of the saprolite layer. The saprolite and bedding structures are truncated by a pallid zone in the upper part of the profile, which in places is over one metre thick. The pallid zone is highly leached with mineralogy dominated by kaolinite. Remnant quartz veins are present in the saprolite and pallid zone although they are disaggregated in parts. The distribution of pallid and mottled layers is partly controlled by the lithology of the original rock and this is particularly evident in sandstone units where the pallid layer has developed to a greater depth. A 50 cm thick mottled zone sits above the pallid zone, where iron oxide staining of 5–10 cm in thickness is present along fractures that continue from the pallid zone. The mottled zone is overlain

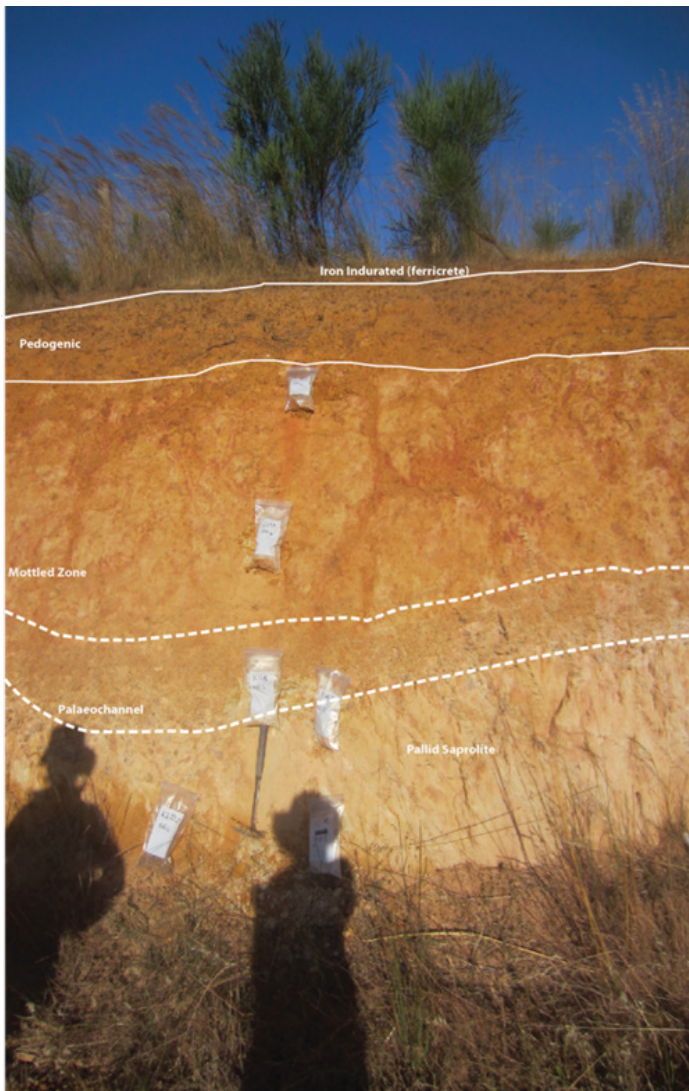


Figure 2.4: Stokes Bay Road Weathering Profile #2. This is the smaller of the two road profiles, in which a palaeochannel can be seen. This profile is topped by pisolithic material, and the different layers within the profile have been annotated on the image.

by a pedogenic/soil profile over one metre in thickness. The mottled zone mineralogy is iron oxide stained kaolinite. The profile is capped by a thin layer (<10 cm) of individual iron oxide pisoliths (2–5 cm in diameter).

The second Stokes Bay Road profile is approximately six metres thick and contains a palaeochannel (Figure 2.4). At the base of the profile is a 60 cm thick pallid zone of highly weathered Kanmantoo Group metasedimentary rocks. The palaeochannel lies on top of the pallid zone, is about 30 cm thick and is comprised of rounded clasts of Kanmantoo Group metasedimentary rocks that are moderately weathered. The palaeochannel has larger clasts (~5 cm in diameter) at the base of the channel, fining upward to small pebble sized clasts (~1 in cm diameter). Above the palaeochannel is a mottled zone, over one metre thick, with

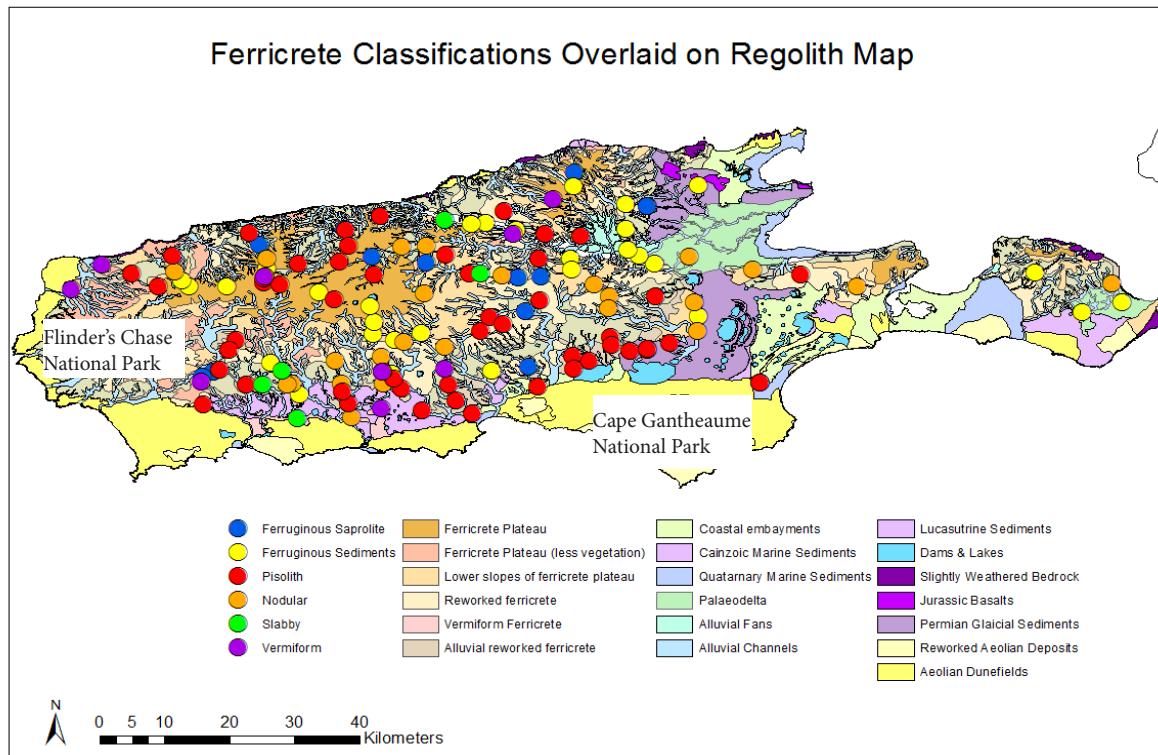


Figure 2.5: Ferricrete classifications overlain on the regolith map of Kangaroo Island. The areas where samples were not collected due to National Park restrictions are highlighted by the two labels for Flinder's Chase National Park and Cape Gantheaume National Park.

2.

areas of iron oxide enrichment, that are especially concentrated in sub-vertical fractures. The mottled zone is topped by a 40 cm pedogenic zone and capped by a thin (<10 cm) layer of pisoliths (2–5 cm in diameter). Iron oxide staining along fractures passes from the weathered Kanmantoo metasedimentary rocks through to the base of the pedogenic zone.

2.4.2. Ferricrete classification and forms

Ferruginous regolith dominates much of the regolith and landscape of the island, particularly inland with varying morphology and evolution histories. As a consequence, several different classifications have been used in this work depending upon whether the iron oxide induration is *in situ* (simple) or reworked (complex). These classifications are based upon the work conducted by Bourman (1993a, 1989), in the Mt Lofty Ranges (Table 2.2). As this field area is geographically and geologically related to Kangaroo Island, this classification was thought to be the most appropriate.

2.4.2.1. Ferruginised Basement/ Saprolite

These are ‘simple’ ferricretes, formed *in situ* from the iron oxide induration of weathered basement or saprolite (Table 2.2a). Most samples preserve basement rock textures and fabrics such as bedding, sedimentary structures, visible muscovite and quartz veining. Mineral fabrics within the ferricrete, where evident, are that of the parent material. Ferruginised bedrock is mainly in exposed road cuttings or alluvial channels, in the higher upland areas of the island, towards the north coast.

2.4.2.2. Ferruginised Sediments

Ferruginous sediments are also classified as *in situ* ferricretes (Table 2.2b). Some of these ferruginised sediments overlap the ferruginised bedrock classification. Where bedrock features could not be identified but the ferruginous material did not fall into one the ‘complex’ categories, it was categorised as a ferruginised sediment. This classification also includes Cenozoic sediments with iron oxide deposition occurring due to movement of Fe-rich groundwater, which generally remain unconsolidated and weakly cemented. These ferruginised Cenozoic sediments are found along the south coast within 20 km of the coastline. Permian sediments found at the Wisanger telephone exchange on Gap Road and at the Kingscote foreshore, underlying the Wisanger Basalt, are also ferruginised. The remaining ferruginised sediments occur across the Island and on the main parts of the plateau.

2.4.2.3. Pisoliths

Pisoliths occur as individual spherical concretions, typically have multiple rinds and are up to 5 cm in diameter (Table 2.2c). They commonly have a goethite outer layer, although the ratio of hematite to goethite can vary. The pisoliths are generally loose on the surface. In some cases pisoliths are cemented in a later matrix of a similar material to the pisoliths, dominated by clays, quartz sand and indurating iron oxides. Pisoliths and pisolithic sediments are spread across the ferricrete plateau, in alluvial channels within the plateau and

in the areas immediately surrounding the plateau. The pisoliths are described and discussed further in Chapter 3.

2.4.2.4. Nodular

Nodular ferricretes are larger (>5 cm diameter) and more angular than the pisoliths (Table 2.2d). They tend to lack the multiple rinds that characterise the pisoliths, and have a slightly higher hematite to goethite ratio than the pisoliths. The nodular ferricretes generally sit lower in the landscape than the pisoliths but still on higher points on the island. They have less rounding than the pisoliths, suggesting a lower level of transportation and reworking. In most cases the angular nature of the nodular ferricrete is interpreted to mean that they were formed *in situ* (Bourman, 1989).

2.4.2.5. Vermiform

The samples classified as vermiform ferricretes, are generally comprised of pisoliths consolidated within a sandy matrix (Table 2.2e). The sand dominated matrix forms sinuous worm-like channels around the iron oxides and pisoliths which can contrast strongly in colour. The pisoliths are weakly consolidated within the sandy matrix and retain concentric banding and iron oxide staining. These are interpreted to be complex, transported ferricretes. Vermiform ferricretes are only found around the south coast of the island in the areas dominated by Cenozoic marine deposits. Vermiform ferricretes are predominately found around the south coast of the island in the areas dominated by Cenozoic marine deposits, however there are other occurrences in the northern areas of the island.

2.4.3. Permian Sediments

Several exposures of Permian sediments were documented in this study that have not previously been identified or mapped (Figure 2.6). These exposures extend the footprint of Permian sediments further west. The Permian sediments are fine grained clay to mud, are poorly consolidated and are distinguished from highly weathered Kanmantoo Group rocks

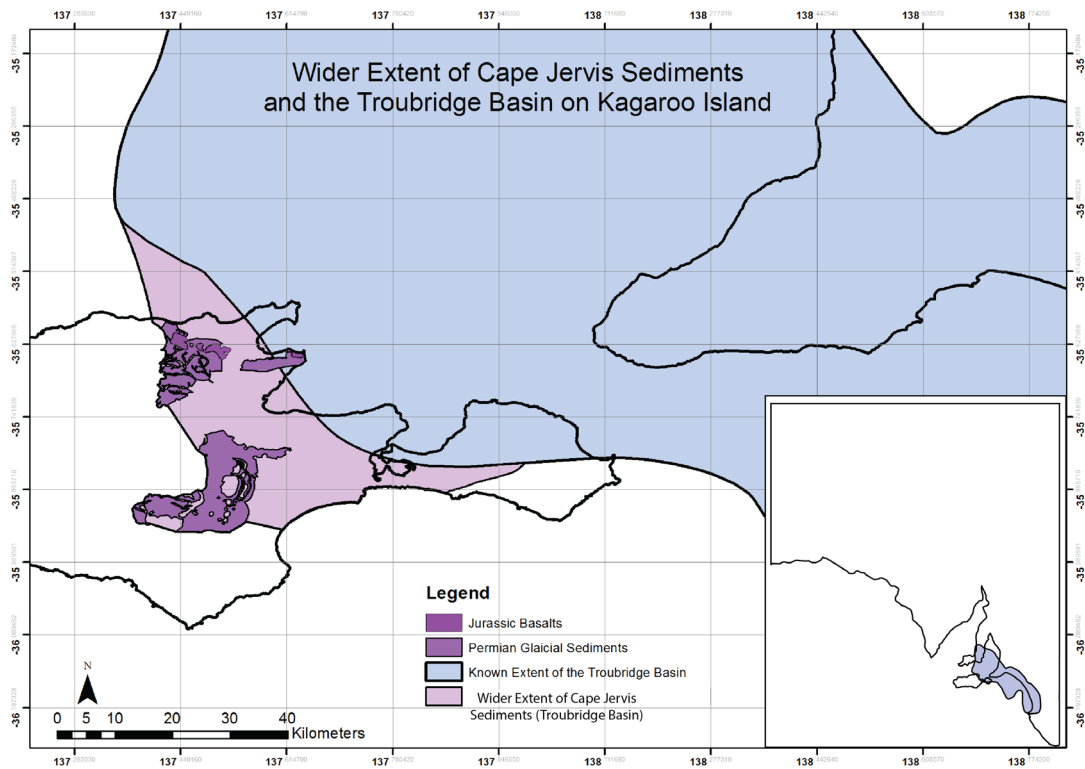


Figure 2.6: A map of the wider extent and landscape context of the Cape Jervis Sediments and the Troubridge Basin on Kangaroo Island and the Fleurieu Peninsula. The light purple areas are the areas suggested that Permian sediments extend to on Kangaroo Island from field observations in this study.

by the lack of muscovite. The presence of drop stones and gravels in some areas of the new occurrences also makes identifies them as glacial sediments. In one exposure in a small road cutting on the South Coast Rd (53H 715737E 6026658N), the sediments are approximately one metre thick. Other occurrences were identified in road scrapings, with striated boulders found. However, the thickness and extent of the package remains unknown.

2.4.4. Mt Taylor and Mt Stockdale

The Mt Taylor and Mt Stockdale region (~15 km by 5 km) is dominated by the ferricrete plateau (Figure 2.2), which dips gently to the southeast. Marine sediments are thought to have been deposited onto an erosional surface that may have then been overlain by the ferricrete plateau (Milnes et al., 1983). These sediments are calcareous, indurated back-beach sediments, which now form prominent high points within the landscape.

2.5. Discussion

This discussion focuses on the long term landscape evolution including ferricrete formation and characteristics of Kangaroo Island. This also includes the wider extent of Permian sediments and the structural and eustatic controls on the landscape. The formation of individual ferricrete types and classifications will be discussed further in Chapter 3.

2.5.1. Permian to Jurassic palaeo-topography

The presence of the Permian Cape Jarvis Group and the Jurassic Wisanger Basalt provides a starting point for establishing a framework for the landscape evolution of Kangaroo Island. These units provide the earliest constraints on post-Delamerian erosional and depositional surfaces.

The Cape Jarvis Group sediments are found throughout the central part of Kangaroo Island, from Penneshaw on the Dudley Peninsula though to Kingscote and Murray Lagoon on the main part of the Island (Figure 2.6). These sediments were deposited as part of the larger Troubridge Basin (Bourman and Alley, 1999). The Troubridge Basin is defined to extend across the southern part of South Australia (inset Figure 2.6) with outcrops identified on the Yorke and Fleurieu peninsulas (Bourman and Alley, 1995; 1999). Glacial sediments have also been intersected in marine exploration drill holes throughout the subsurface of Gulf St Vincent, Investigator Strait, Backstairs Passage, the Coorong and the continental shelf between Kangaroo Island and the Otway Basin (Bourman and Alley, 1995; 1999). The Troubridge Basin is interpreted to be largely formed by the erosional action of Permian glaciers, and glacial erosional surfaces have been recognised at Christmas Cove on the Dudley Peninsula, Hallett Cove and Port Elliot on the Fleurieu Peninsula (Alley et al., 2013; Bourman and Alley, 1990, 1995, 1999; Milnes and Bourman, 1972). Overlying the Permian sediments in the north of Kangaroo Island is the Jurassic-aged Wisanger Basalt. Milnes (1982) has interpreted the Wisanger Basalts to be largely confined to the Troubridge Basin and their genesis is linked to the initiation of rifting between Australia and Antarctica.

The presence of Permian sediments within the low lying areas around the central portion of the Island (Figure 2.6), particularly the areas around Kingscote, American River and Murray Lagoon, supports the hypothesis that the movement of Permian glaciers within the Troubridge Basin created an erosional trough where the retreating glaciers then deposited the Cape Jervis Group sediments. This is also supported by the lack of Permian sediments elsewhere on the Island and the absence of glacial striae on the bedrock in any of the upland areas. The occurrences of Jurassic basalts within the Permian erosional trough potentially suggests that the Troubridge Basin remained a topographic low into the Jurassic due to the lack of basalts found in upland areas and lack of evidence for mass erosion and wastage of the basalts. This also suggests that the area which is now the ferricrete plateau was an upland area during the Permian–Jurassic and has remained so. The current elevation of the basalts is approximately 180 m above current sea levels, slightly lower than the height of the ferricrete plateau, corresponding with the hypothesis that the basalts filled an erosional trough. This basaltic basinal fill may have effectively brought the land surface back to sea level, or at least to a level at which this part of the Troubridge Basin was no longer the sole site of deposition within the Kangaroo Island region.

The Cape Jervis Formation sediments on Kangaroo Island were previously thought to be restricted to the central portion of the Island (Figure 2.6). However, the process of regolith–landform mapping has identified new occurrences further to the southwest. These are mottled and iron oxide stained, however, drop stones and a lack of muscovite (a key indicator of the weathered Kanmantoo Group bedrock) allowed for the identification of these as Cape Jervis Formation sediments. While these are ferruginised, the occurrences of pisoliths are variable, and there are no pisoliths within the ferruginised sediments that occur underlying the Wisanger basalts. This could suggest that the ferruginisation has occurred post-Jurassic, with the ferruginised sediments underlying the basalts being the result of sub-basaltic weathering (Milnes et al., 1982; Schmidt et al., 1976). However, the possibility remains that there are no pisoliths in the profiles under the basalts because the materials

underlying them were not part of the pedogenic zone.

2.5.2. Distribution of marine sediments and implications for Cenozoic tectonics on Kangaroo Island

The marine sedimentary sequences on Kangaroo Island, combined with Phanerozoic sea level curves (Figure 1), provide time and palaeo-elevation constraints on uplift, subsidence and fault movement within the Island. One of the most obvious and dominant controls on neotectonics and land surface evolution is the Cygnet-Snellings Fault Zone. This zone runs eastwest across the island and divides the underlying Cambrian bedrock groups, the Kangaroo Island Group and the Kanmantoo Group.

The movement of Permian glaciers is interpreted to have created an erosional trough in the eastern section of Kangaroo Island (Alley et al., 2013; Bourman and Alley 1999), where retreating glaciers then deposited the Cape Jervis Sediments. There is no evidence of these Permian sediments on the plateau, nor any glacial striae found on bedrock, suggesting it was above sea level during the Permian. The lack of Eocene–Oligocene sediments on the plateau leads to the interpretation that this height difference was maintained or augmented into the Eocene. Global average Eocene sea levels of 200 m (Haq, 1988) indicate the middle section of the island is likely to have been more elevated than its current level and regions of the plateau may have been at least 50 – 100 m higher than the present (Figure 2.7).

Ferruginisation is thought to have occurred during the Oligocene through to the early Miocene. The lack of ferruginous material as detritus in Eocene marine sediments is a strong indicator that it had not been formed previous to that time. It is interpreted that the tilting of the island was prior to the Miocene, due to the Miocene marine sediments only occurring on the south coast (Figures 2.7–8). The deposition of these Miocene marine sediments occurred with a sea level of approximately 150 m above the current sea levels (Haq, 1988). This may be the result of uplift of the northern part of the island as a consequence of the

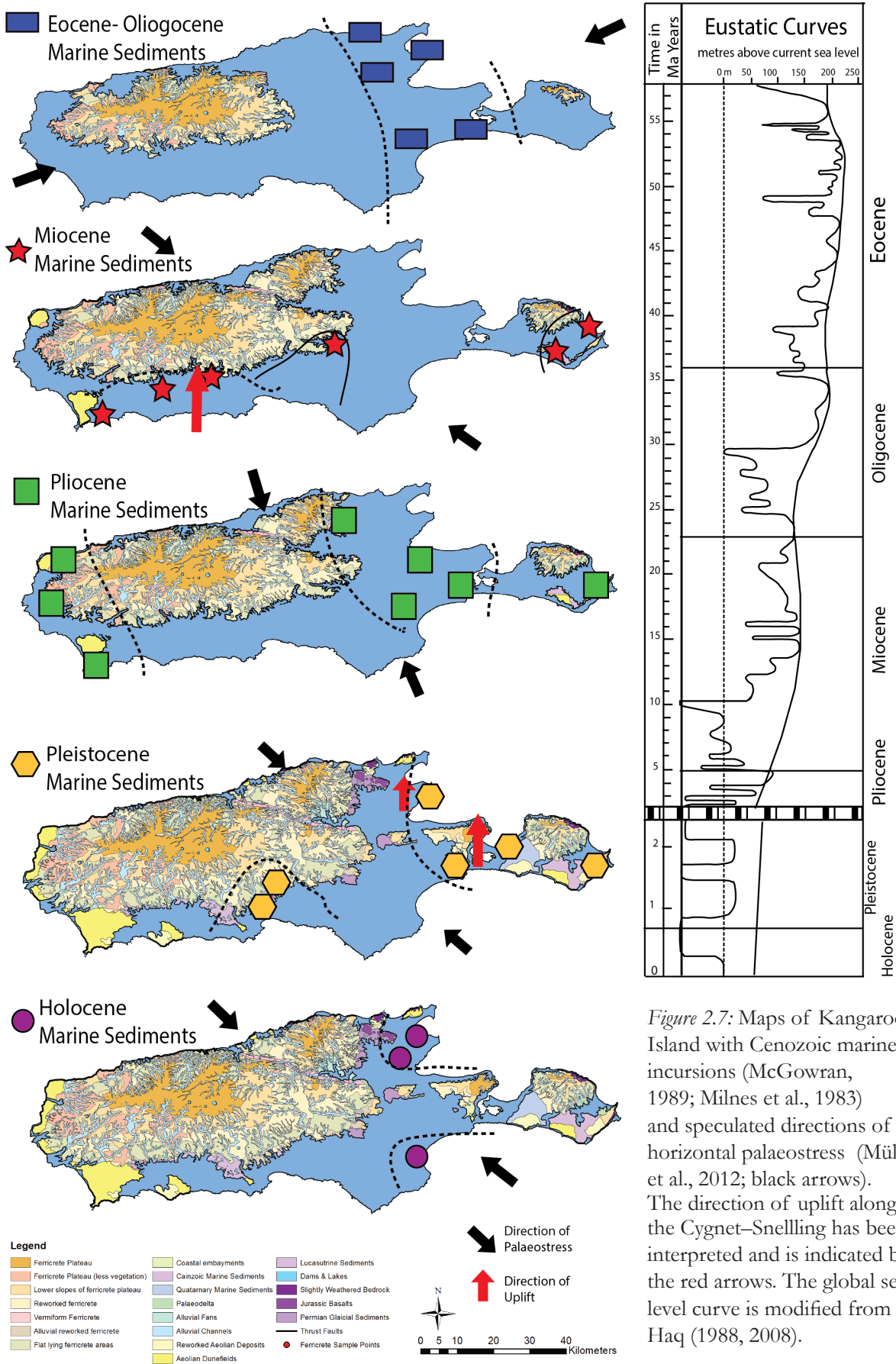


Figure 2.7: Maps of Kangaroo Island with Cenozoic marine incursions (McGowran, 1989; Milnes et al., 1983) and speculated directions of horizontal palaeostress (Müller et al., 2012; black arrows). The direction of uplift along the Cygnet–Snelling has been interpreted and is indicated by the red arrows. The global sea level curve is modified from Haq (1988, 2008).

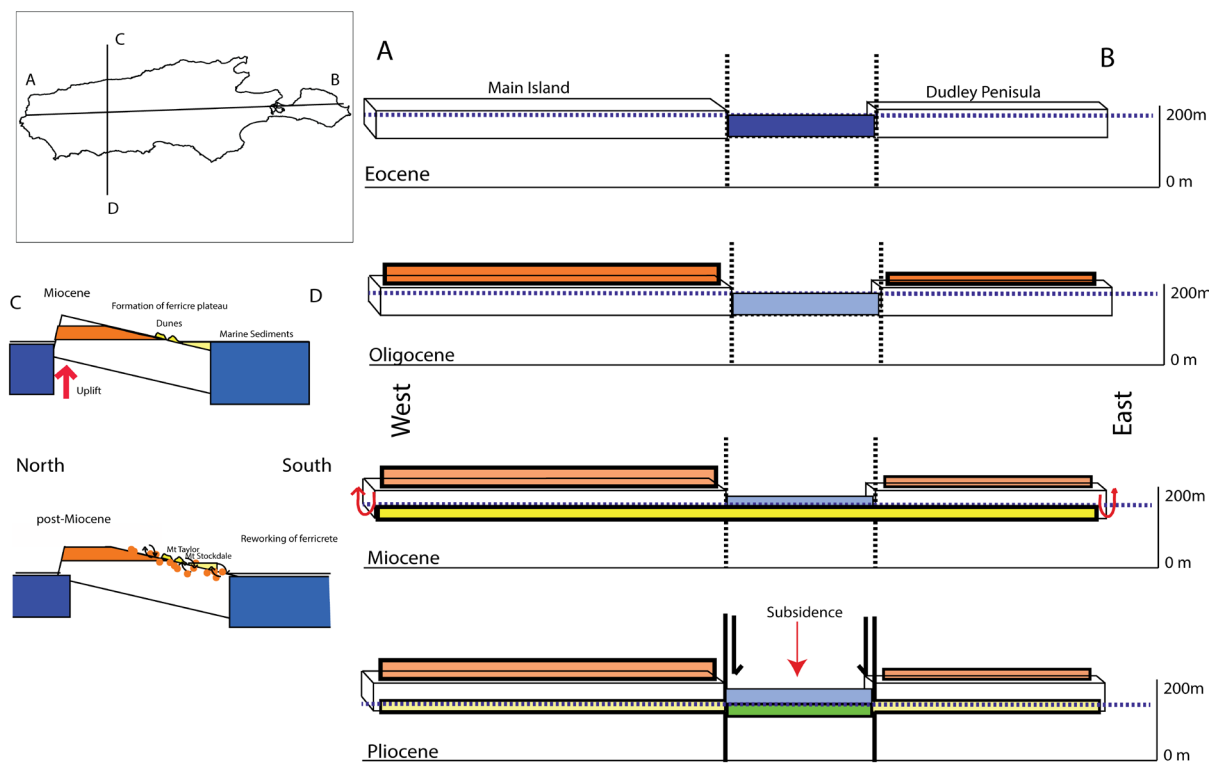


Figure 2.8: Cartoon cross sections of Kangaroo Island, with the East-West sections showing the Cenozoic marine sedimentation and the effect of palaeotectonics. The smaller cross section to the left shows a north-south section of the island, with the uplift of the northern part of the island, the formation of ferruginised material and the deposition of Miocene marine sediments. The red arrows indicate a form of tectonic movement.

reactivation of the Cygnet–Snelling Fault, or because of the subsidence of the south coast relative to the northern edge of the island (Figure 2.8). Only a small amount of movement would be necessary to achieve the current observable landscape, and thus subsidence is perhaps more likely. Regionally, there is also evidence of tectonic movement in the Mt Lofty Ranges and Yorke Peninsula at this time (Tokarev et al., 1999; Wilford and Thomas, 2013). This movement would also mirror what has been proposed to be occurring at a continental scale by Sandiford (2007) and Muller et al. (2013). The lack of preserved Miocene marine sediments overlying the Eocene sediments suggests these areas that had previously been inundated were now above sea level, which is largely accommodated simply by the lower sea level and/or tilting of the island as opposed to major episodes of uplift.

Ongoing movement along faults that are proposed to exist along the margins of the Permian

trough is supported by differential progressive subsidence across the faults (Figure 2.7). This is again evident during the Pliocene, where Pliocene marine sediments occur through the lower lying section of the middle of the island (Figure 2.7). This indicates a palaeostress regime change after the Miocene.

Pleistocene and Holocene marine sediments only occur on the margins of the island and only slightly (<40 m) above current sea levels (Figure 2.7). This indicates recent uplift or subsidence, as evidenced by the 'Redbanks' profile which has been dated to 780 – 1070 ka using magnetostratigraphic methods (Pillans and Bourman, 2001). This profile lies within the Cygnet–Snelling Fault Zone and is now exposed at approximately 15 m above the current sea level indicating that there has been some movement along the fault zone.

2.5.3. Timing of Ferricrete Formation

Understanding the mode of ferricrete formation is integral for the material to be used as an exploration medium. To accurately assess the relevance of geochemical patterns within the ferruginous material, it is necessary to understand its relationship with the landscape as well as the material that it is derived from. The mode of formation of ferricretes is a long debated subject not in the least because of the complexity and the lack of definitive characteristics for the term ferricrete (refer to Chapter 1). Here we refer to all iron oxide materials as ferricretes or ferruginous materials. The age of the ferricrete plateau on Kangaroo Island and the timing of its formation has been a debated topic over a number of years (Bourman, 1989, 1993a, 1993b, 1995; Daily et al., 1974; Milnes et al., 1982, 1985, 1987; Schmidt et al., 1976; Twidale, 1983, 2002). This debate has resulted in two primary theories: firstly, that the ferricrete is a remnant surface that formed and existed prior to the deposition of the Jurassic Basalts (Daily et al., 1974; Twidale, 1983); or secondly, that the ferricrete plateau was formed during the Cenozoic and is the result of a long period of continual reworking (Bourman, 1993a; 1993b; 1995; Bourman and Alley, 1990; Milnes et al., 1985; 1987). Ferricrete is exceptionally difficult to date absolutely as it is subjected

to continual and ongoing weathering processes, however, considering the landscape as a whole can provide relative age constraints.

The ferricrete plateau post-dates the deposition of the Kanmantoo Group and the Delamerian Orogeny, providing an absolute maximum age constraint of ca 500 Ma. There is also a lack of indurated iron oxide clasts within the Permian Cape Jervis Formation sediments, suggesting that the Kanmantoo Group was not ferruginised prior to this time and that the formation of the ferricrete plateau post-dates the deposition of the Permian Cape Jervis sediments. The lack of pisolithic clasts between the Cape Jervis Formation and the overlying Jurassic Wisanger basalts suggests that the formation of the ferricrete plateau also post-dates the deposition of the Jurassic basalts. Thus, the relative maximum age of the formation of the ferricrete plateau is proposed as the end of the Jurassic.

The relative minimum age of the formation of the ferricrete plateau is interpreted to be the Miocene. This is by the occurrence of back-beach, Miocene marine deposits perceived to be onlapping to the pisolith dominated ferricrete plateau at Mt Taylor and Mt Stockdale. While this provides some constraint to the age of primary ferruginisation of the ferricrete plateau the ongoing nature of weathering processes results in these ferruginised materials being continually reworked and new materials forming. Ferruginous materials at Redbanks record a 780 ka polarity shift of the Earth's magnetic field (Pillans and Bourman, 2001). This is the youngest absolute age of ferruginisation recorded on Kangaroo Island. The different morphologies of ferruginous material that have been identified on Kangaroo Island also indicate the ongoing nature of ferruginisation processes. This is indicated by the reworking of pisolithic material shed from the main plateau to form vermiform ferricretes in late Cenozoic to early Quaternary marine sediments.

2.5.4. Formation of ferruginous materials and the ferricrete plateau

Ferruginous materials on and adjacent to the ferricrete plateau take a variety of forms

including pisolithic, nodular and vermiform, ferruginised bedrock and saprolite. The *in situ* ferricretes have been formed by the movement of iron oxides within groundwater and the re-precipitation of these oxides into these slight to moderately weathered rocks. These *in situ* examples can, and do, retain features from the parent rock, including texture, fabric and mineralogy. The pisolithic, nodular and vermiform ferricretes are all classified as complex or reworked ferricretes, as they have no obvious or direct link to a parent material when not viewed within a larger profile. By looking at these complex materials within profiles and the landscape, the relationships indicate that the pisolithic and nodular materials are formed from the bedrock. In the first of the Stokes Bay Road weathering profiles the saprolitic zone preserves bedrock features such as remnant bedding and disaggregated quartz veins (Figure 2.3). The iron leached from the pallid saprolitic zones is interpreted to have formed the pisolithic capping of the profile through capillary action (Bourman, 1995). Bourman (1995) interpreted this to have been the result of repeated wetting and drying cycles, most likely from the movement of the groundwater table. While much of the material in profile two must be transported, as it overlies a palaeochannel, the pisoliths are thought to have formed *in situ*, i.e. where they now lie. A large component of the iron is derived from the underlying Kanmantoo Group evidenced by the fluid channels in the profile that are highlighted by iron staining (Figure 4). The nodular ferricretes are also interpreted to be largely formed *in situ* due to their larger, angular form and their tendency to occur higher within the landscape. Thus, all of the above ferricrete forms could be used for mineral exploration, as they are largely the *in situ* result of weathering processes, both chemical and physical. In this landscape setting, the pisoliths occur at the tops of the profiles, suggesting they have not moved significantly. If this is the case, the pisoliths are likely to record a trace element signature of the groundwater in the area and can offer a useful indicator of the surrounding area. The vermiform ferricretes are the least likely to be useful for mineral exploration, as they were formed as a result of transport off the main plateau and re-cementation in a sandy matrix. This method of formation is consistent with the occurrence of the vermiform ferricretes predominately just off of the plateau and within valleys and

lower parts of the landscape.

The influence of climate on ferricrete formation has received considerable attention within the literature (Anand, 2002; Bourman, 1993b, 1995, 2007; Bourman and Alley, 1990; Bourman and Conacher, 1998; Eggleton and Taylor, 1998; Hachmann and Tietz, 1998; Milnes et al., 1985, 1987; Taylor et al., 1992; Twidale and Bourne, 1998). There is a long held view that ferricrete is formed in tropical conditions with less erosion and distinct wet and dry periods, equating to a rapidly developed deep weathering profile analogous with the modern 'laterite' weathering profiles. However, the view that the formation of ferruginous materials has to be a result of weathering under a tropical climatic conditions is not shared by all researchers (Bourman, 2007; Stephens, 1971; Taylor et al., 1992). Bourman (2007) instead suggests that the upper part of the ferruginous profiles in southern South Australia are experiencing ongoing modification even under present environmental conditions. Milnes (1985) suggests that the present variable regolith materials on terrestrial landscapes are the integrated products of leaching, erosion, complex reworking and ongoing weathering since the Permian. Despite the continual formation of these weathering products, the palaeoclimatic data indicates that climatic conditions experienced in Australia during the proposed period of ferricrete formation go through a 'drying-off' period during the late Miocene, after a period of high rainfall during the Eocene and Oligocene (Macphail, 2007; Martin, 1991; 2006). These climatic conditions produced the wetting and drying cycles 'neede'd for the fomration of ferricretes, albeit on a continental scale.

Other influences on the formation of ferruginous materials include the pH (the acidity or alkalinity of a solution) and Eh (the availability of oxygen) of the groundwater, the necessity of an aqueous solution to be present for weathering to occur, tectonic movement and the long time periods needed for deep weathering to occur in more arid environments. The pH and the Eh are two key factors that will determine the formation of ferricretes, as these are primary controls on the solubility of iron. Iron will be mobilised or precipitated

from solution dependant on the pH and Eh conditions. If the pH and Eh are relatively high then the Fe will be precipitated from solution; if pH and Eh are low then the solubility of Fe may exceed that of silica, and thus move through the system (Norton, 1973). Changes in pH and Eh will result in reversals of mobility, thus changes in enrichment of the solution. Redox reactions will result in the increase of acid produced in the system, thus lowering the pH and increasing the likelihood that the Fe will be mobile in solution. Consequently the mobilisation of Fe creates the conditions needed for Fe to remain mobilised within the system. These reactions are dependent upon the movement of an aqueous solution through the system, therefore the movement of groundwater as well as meteoric waters are important to consider (Nahon, 1991). It has been suggested that minerals are nearly completely altered before their removal, when the supply of water and acidic solution is large relative to the supply of silicate minerals, and the subsequent residence time in weathering environments compared to reaction times is long (West et al., 2005). This appears to be largely the case in regards to the weathering processes that are occurring on Kangaroo Island. Tectonic movement may also have a significant effect on the chemical system, and has even been suggested to have a greater impact than climate (Raymo and Ruddiman, 1992; Riebe et al., 2001; West et al., 2005). Kangaroo Island, like the rest of South Australia, is thought to have remained reasonably tectonically stable for a significant period of time, however the suggestion that the formation of the ferricrete began with a change in weathering conditions induced by tectonic movement along the Adelaide Fold Belt and Cygnet–Snelling Fault during the Miocene, is not unreasonable (Tokarev et al., 1999; Wilford and Thomas, 2013).

Therefore, the ferricrete plateau on Kangaroo Island is likely to be a land surface of considerable age, but subject to ongoing chemical weathering processes. The mobilisation and precipitation of Fe to form ferruginous materials was likely to have occurred under low pH and Eh conditions, possibly precipitated by palaeo-tectonic movement on the island. Despite the age of the landform, it is not necessary that the land surface has remained

static, rather, the processes that form the ferricrete occurred over a long period of time, and these processes are still at work today.

2.6. Conclusions

Using a combination of previously collected data and new field observations, including the production of a regolith - landform map, the following landscape evolution for Kangaroo Island from the Permian is proposed. The area that is currently the ferricrete plateau has been some form of 'uplands' since the Permian, when the mass movement of glaciers created a significant erosional surface through the centre of the island, presumed to follow structural weaknesses in the bedrock. This area remained as an erosional depression through to the Jurassic, when it was flooded with basalt at the beginning stages of the rifting of Australia and Antarctica. There are no recorded deposited materials post the deposition of Jurassic basalts until the deposition of Eocene marine sediments, which corresponded with a rise in global sea levels. It is suggested that the ferricrete formation occurred during the Oligocene to the Miocene, concurrent, and possibly initiated by, tectonic movement on the island. The Pliocene is likely to have also involved the subsidence of the middle portion of the island relative to the main part of the island. The Pleistocene through to the Holocene was characterised by continual reworking of the ferricrete, as well as deposition of marine sediments, the reworking of the marine sediments to form calcareous aeolinite deposits and minor tectonic activity that resulted in the movement of areas such as Redbanks. Understanding the landscape evolution provides new constraints on the age and timing of the ferricrete formation. However, we have been unable to place an exact date on the age of the ferricrete, due to the lack of quantitative and absolute data. Further data on the mineralogy and the geochemistry of the ferruginous materials may place tighter constraints on the time of the ferricrete formation and the processes at work.

Chapter 3

Petrographic evidence for complex processes
in the formation of the ferruginous
component of the regolith of Kangaroo
Island.

Foreword

This chapter investigates the petrography and mineral chemistry of several different types of ferricretes on Kangaroo Island. This was undertaken to facilitate a better understanding of the formation of the ferruginous materials on Kangaroo Island and how these materials may be used for geochemical mineral exploration. The formation and expression of the ferricretes studied reflect different landscape settings, the progression from weathered bedrock and indurated saprolite, through to transported and reworked materials.

3.1. Introduction

Iron (Fe) is one of the most abundant elements on Earth and, due to its mobility within low temperature environments, iron oxide is an abundant product of weathering (McQueen, 2005). This abundance, as well as the ability for iron oxide minerals such as hematite and goethite to host cations of pathfinder and trace elements, means that iron oxides are of particular importance for geochemical exploration (McQueen, 2005). The mechanisms and rates by which ferruginised products are formed during weathering processes have long been contested (Alley, 1977; Bourman, 1989a, 1995, 2007; Bourman et al., 2010; Bourman and Conacher, 1998; Cornelius et al., 2008; Daily et al., 1974; Eggleton and Taylor, 1998; Hunt et al., 1977; McQueen and Munro, 2003; Milnes et al., 1985; 1987; Ollier and Galloway, 1990; Paton and Williams, 1972; Schmidt et al., 1976; Schmidt and Embleton, 1976; Smith and Perdrix, 1983; Stephens, 1971; Twidale, 1983). The formation of ferruginous materials can involve numerous mechanisms within open systems, including the lateral and vertical transport of iron, and associated cations, including pathfinder and trace elements in groundwater (McQueen, 2005; Nahon et al., 1977, 1991). If geochemical sampling of ferricrete is to be used for mineral exploration then it is necessary to understand the mode of its formation, in order to determine where mineral deposit signatures have been derived from.

Research into the genetic processes for ferruginous materials within South Australia have largely been focused on the greater Mt Lofty Ranges, in particular studies conducted by Milnes and Bourman (see Bourman, 1989a, 1989b, 1993a, 2006; Milnes et al., 1985, 1987). These studies have demonstrated that much of the confusion and complexity regarding the formation of the ferruginous material is a result of difficulties in establishing consistent relationships between different materials and their settings. Ferruginised materials can be formed *in situ*, such as ferruginised bedrock, sediments and saprolite, and are termed here 'simple' ferricretes, after Bourman (1989a). Ferruginised materials can also occur as reworked materials, classified here as 'complex' ferricretes after Bourman (1989a), which

include pisoliths, nodular, slabby and vermiform ferricretes. Some studies, which have included petrography and mineralogy, have demonstrated that even within a single location, multiple, discrete, formation events can occur (Bourman, 1993a, 1995). In contrast, other studies have demonstrated that there can be a linear progression towards the formation of ferruginous materials within a profile (Bourman, 2006; Muller and Bocquier, 1986; Nahon et al., 1977). Although larger regional studies have considered the ferruginous materials on Kangaroo Island, detailed work on the ferruginised material has not been conducted recently, and the applications for geochemical mineral exploration have not been considered.

This chapter investigates the petrography and mineral chemistry of several different types of ferricretes on Kangaroo Island. This is done in order to better understand the formation of the ferruginous materials and the processes involved. Understanding these processes will allow for the better assessment of how these materials may then be used for geochemical mineral exploration. The ferricretes studied reflect different landscape settings and the progression from weathered bedrock through to indurated saprolite and moderately weathered *in situ* to transported material.

3.2. Methods

The samples used in this chapter were taken from the ferricrete plateau region, including the Bonaventura mineral prospect, and on the southern margins of the plateau (Figure 3.1). Samples KISB001 and KISB002 are weathered bedrock from the base of the Stokes Bay Road weathering profiles, which are just south of the Cygnet–Snelling Fault Zone. Samples KIFE022, KIFE018 and KIFE019 are ferruginised bedrock and saprolite samples and are all from within the Cygnet–Snelling Fault Zone, with the latter two in close proximity to the Bonaventura mineral prospect. Samples KIFE103 and KIFE105 are also identified as ferruginised bedrock samples, both taken from outside of the main plateau area, KIFE103 north of the Cygnet–Snelling Fault Zone, KIFE105 to the south. Samples KIFE110, KIFE012, KIFE048, KIFE062 and KIFE109 are all complex or reworked ferricretes from

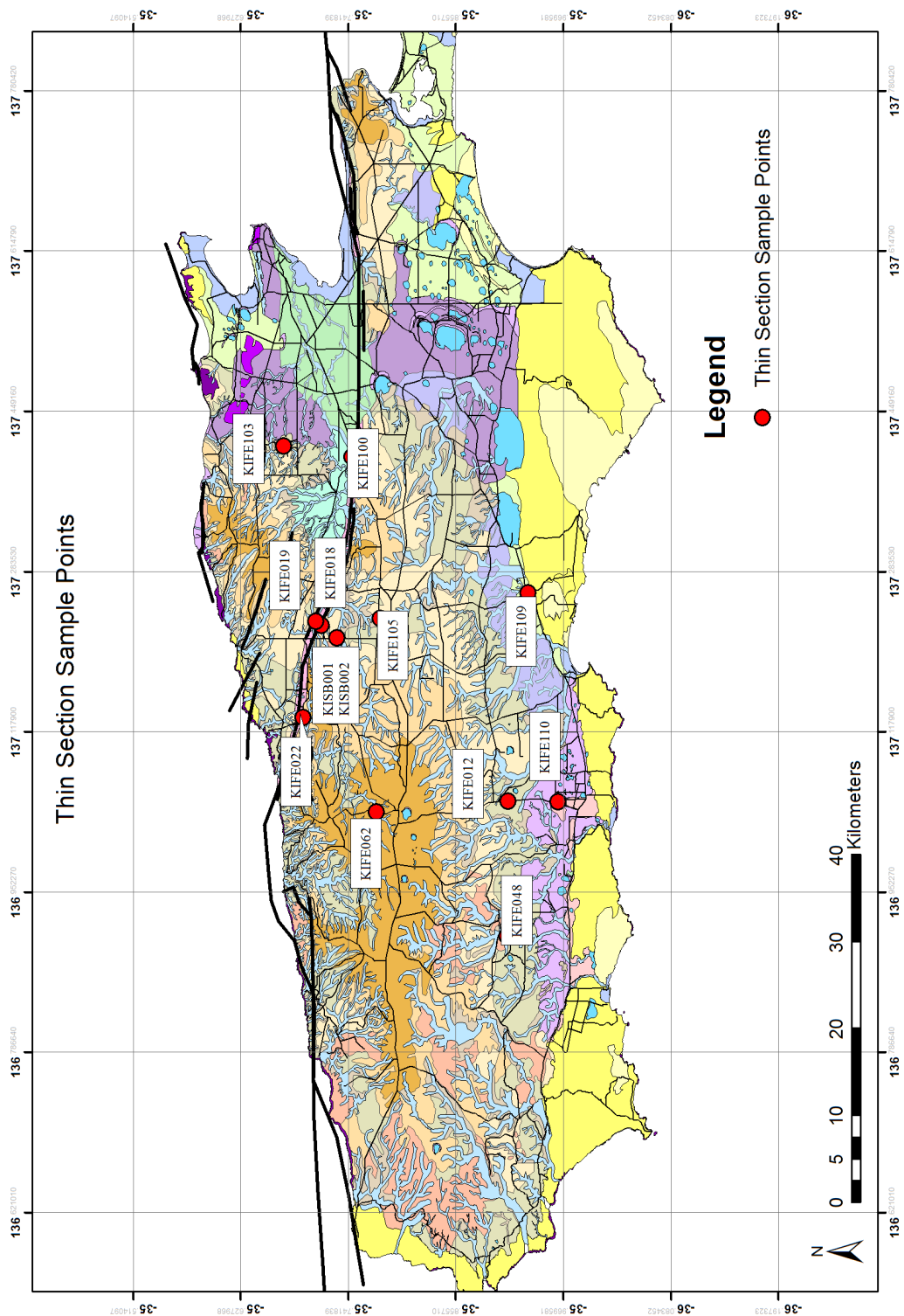


Figure 3.1: Thin sections sample points on the regolith map of Kangaroo Island. The Cygnet–Snelling Fault Zone is mapped in the thick black lines.

various areas of the island, including the main plateau and towards the southern coast (Table 3.1). These samples were chosen to represent a wide range of landscape settings and geographical locations.

Thin sections were made to examine the microscale processes involved in the formation of the end member regolith types that were interpreted from hand samples in Chapter 2. This includes samples of fresh bedrock (from drill core), weathered bedrock and saprolite with relatively little iron oxide induration and iron oxide indurated saprolite (Table 3.1). Individual pisoliths, and pisoliths that have been transported and re-cemented in a matrix, were also examined (Table 3.1). Samples were made into polished thin sections and analysed under plain and cross polarised light.

Thin sections were imaged using backscatter electron imaging using a Phillips XL30 Scanning Electron Microscope (SEM) at Adelaide Microscopy. Images were captured at 20 kV accelerating voltage with a spot size of 3. Mineral phases and compositions were identified using an EDAX energy dispersive spectroscopy detector. SEM imaging was primarily conducted to better identify minerals and examine the best areas to use for subsequent electron microprobe element mapping. Selected samples were mapped and analysed using the Cameca SXFive electron microprobe at University of Adelaide, Adelaide Microscopy, using an accelerating voltage of 15 kV and a pixel size of $\sim 4 \mu\text{m}$. Element maps of Si, Al, Fe, Mg, Mn, Ti and K were collected using wavelength dispersive spectrometers (WDS) and Ca, Cu, Na, P, Pb and Zn were collected simultaneously using EDS. Some issues were encountered with electron beam instability resulting in variations in beam intensity, and subsequently emitted x-ray reductions across the images. This is expressed as gradual colour changes across a number of the images. These elements maps were collected to better determine textural relationships and changes of elemental concentrations within samples. Selected saprolite, pisolith and vermiform samples were analysed to gain a better understanding of key samples and their context within the formation process of

Table 3.1: Summary of samples that were made into thin sections, including ferricrete classification and notes regarding the landscape setting where the samples were taken from.

Sample	Location	Weathering Classification	Brief Description
Kanmantoo #1		Unweathered bedrock	Sample from drillcore
Kanmantoo #2		Unweathered bedrock	Sample from drillcore
KISB001	Stokes Bay Road	Moderately weathered bedrock	Sample from the bottom of the profile, moderately weathered bedrock (still some fabric present)
KISB002	Stokes Bay Road	Highly weathered bedrock/saprolite	Mottled saprolite; fine grained.
KIFE103	Cockatoo Creek Road	Ferruginised bedrock	Mottled bedrock, has schistosity and muscovite present in hand sample
KIFE100	Bark Hut Road	Ferruginised sediments	Pallid zone, part of the weathering profile, near Kohinoor
KIFE018	In the paddock North of Pioneer Bend Road	Vermiform ferricretes	Sample taken from the side of the paddock, just off of Pioneer Bend Road. Higher point within the landscape.
KIFE019	Bonaventura Prospect; on the Cygnet Snelling Fault Zone	Ferruginised bedrock	Sample taken from within 500m of the Grainger Old Mine workings and close to the costean dug for MONAX exploration.
KIFE105	Weatheralls Road	Ferruginised bedrock	Very hematite rich, high point within the landscape.
KIFE109	South Coast Road;	Pisoliths	Ferricrete pit, off the main plateau, transported. Slightly north-west of the sand dunes of Little Sahara.
KIFE110	Mt Taylor Road;	Vermiform ferricrete	Reworked ferricrete, vermiform, within a ferricrete pit, off of the main plateau, transported materials from the plateau.
KIFE012	Mt Taylor Road;	Vermiform ferricrete	As the road moves up to go onto the plateau.
KIFE048	Church Road	Slabby Ferricrete	Unconsolidated, angular hand sample sized blocks.
KIFE022	Range Road	Ferricrete bedrock	Edge of plateau to the North, quite a steep descent off the plateau.
KIFE062	Cooper's Road	Nodular	In plantation, on main part of plateau.

the ferruginous materials. Instrument malfunction resulted in only K and Fe maps being collected for sample KIFE022 (Figure 3.4).

3.3. Results

3.3.1. Petrology

Hand sample identification and classification, (summarised in Chapter 2), has been used to divide the ferricrete samples into two main groups, simple (*in situ*) and complex (reworked) ferruginous materials. Information regarding the landscape setting for each sample can be found in Table 3.1.

3.3.2. Simple Ferruginous Materials (weathered bedrock and saprolite)

Weathered Kanmantoo Group (bedrock) samples KISB001, KISB002 and KIFE103, are predominantly comprised of angular to sub-angular, interlocked quartz grains of 0.2–0.5 mm and exhibit undulose extinction (Figure 3.2). Plagioclase grains of 0.1–0.5 mm typically comprise 5–10% of the sample; muscovite grains of 0.3–<0.1 mm comprise 2–5% of the sample; with potassium feldspar 0.5 mm to 0.3 mm comprise 2–5% of the sample. Chlorite is found throughout and comprises ~2% of the sample. Zircon is present in trace amounts. Potassium feldspar and plagioclase are partially replaced by clay minerals (Figure 3.2e, f). The two Stokes Bay Road samples (KISB001, KISB002) have minimal amounts of iron oxide replacement and enrichment (Figure 3.2e, 3). Sample KIFE103 has a much higher degree of iron oxide replacement (Figure 3.2g). Iron oxide enrichment is variable, largely replacing weathered plagioclase, feldspar and muscovite, ranging from 10–40% of the sample (Figure 3.2e-h). The electron microprobe maps of weathered bedrock sample KISB002, highlight the texture and fabric of the material (Figure 3.3). Quartz grains are angular and typically 0.5–1.0 mm across (Figure 3.3a). Iron oxyhydroxide is present along cracks within quartz grains and coats the outer edge of the grains (Figure 3.3c). The high concentrations of K and Al in the matrix suggest it is dominantly composed of clay minerals produced by the

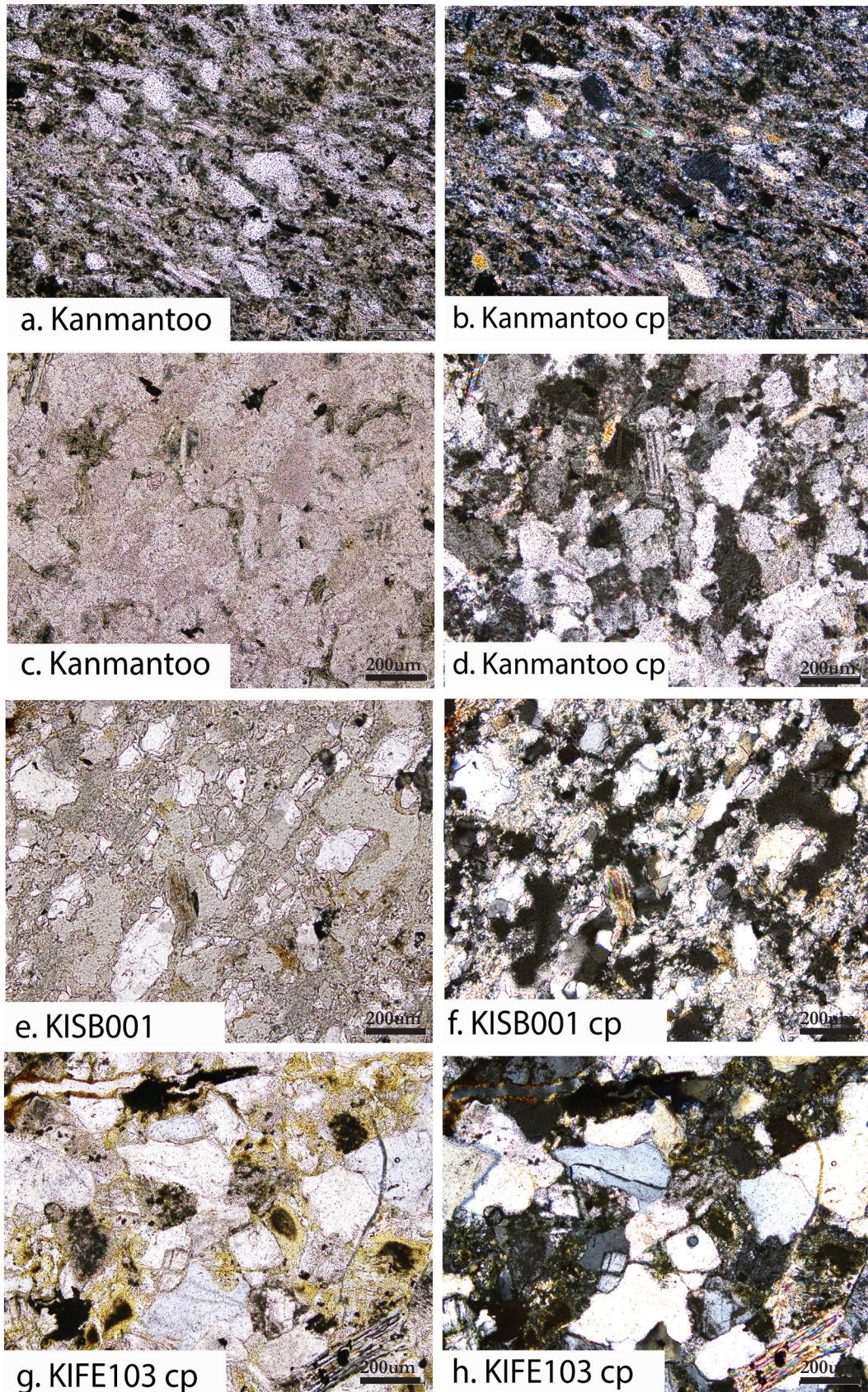


Figure 3.2: a-d) thin section photos (in plane and cross polarised light) of drill core sample from unweathered Kanmantoo Group. Images e, f thin sections photos of saprolite samples from the Stokes Bay Road profiles. Images g, h, are images from a different weathered bedrock sample.

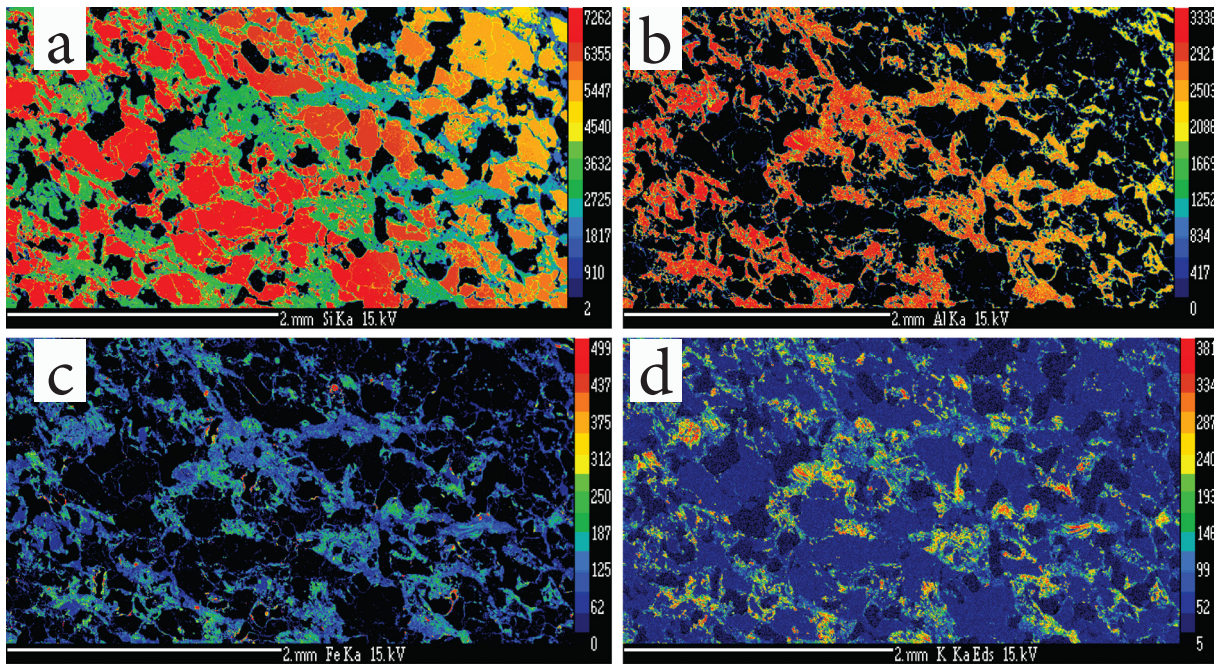


Figure 3.3: Electron microprobe images of KISB002, the sample of weathered bedrock from the Stokes Bay Road Profile. The images show different elements; a) Si; b) Al c) Fe and d) K.

weathering of K feldspar (regions of K and Al, lacking Fe) and biotite (regions containing K, Fe and Al).

From the two electron microprobe maps of sample KIFE022, there is a large degree of Fe (Figure 3.4), with a fabric, as well as the abundance of K within the sample (Figure 3.4b). Potassium distribution again corresponds with biotite, with platy, needle-like structures (Figure 3.4b). What are assumed to be quartz crystals (in the absence of an adequate Si map) and are individual grains and are not aligned into the vein-like structures (Figure 3.4a).

Samples classified as saprolite in hand sample include KIFE018, KIFE019 and KIFE100. Sample KIFE018 is predominantly comprised of sub-angular to rounded quartz grains (0.2–0.5 mm in diameter, Figure 3.5). Approximately 50% of the quartz exhibits undulose extinction. The remainder of the samples are comprised of muscovite flakes typically 2–5% and <0.1–0.3 mm, and small (1%) amounts of plagioclase and potassium feldspar. Trace amounts of detrital zircon are present. Potassium feldspar and plagioclase are almost entirely replaced by clay minerals and iron oxides. Iron oxide enrichment is variable, largely

replacing weathered plagioclase, feldspar and muscovite and ranging from 30–70% by area in different regions of the samples. Sample KIFE018 has remnant textures defined by the presence of muscovite, and a higher Fe-oxide content and lower quartz content than some of the other weathered bedrock samples. Electron microprobe maps of KIFE018 (Figure 3.5), demonstrate a strong relict foliation, evidenced by the ribbon-like nature of quartz grains within the sample. Iron is accumulated around the margins of quartz grains and also surrounding holes in the thin section which appear black in all images (Figure 3.5). These holes presumably represent highly weathered material that is soft and easily lost during thin section preparation. Potassium is hosted by a combination of biotite, muscovite and K feldspar, suggested by the variable morphology of grains (platy vs non-platy) and the presence or absence of Fe within platy grains (Figure 3.5). Sample KIFE019 (Figure 3.6) is predominantly comprised of sub-angular to rounded quartz grains (0.2–0.5 mm). Approximately 50% of the quartz grains exhibit undulose extinction. These samples have no visible or trace amounts of muscovite, plagioclase and potassium feldspar. Iron oxide

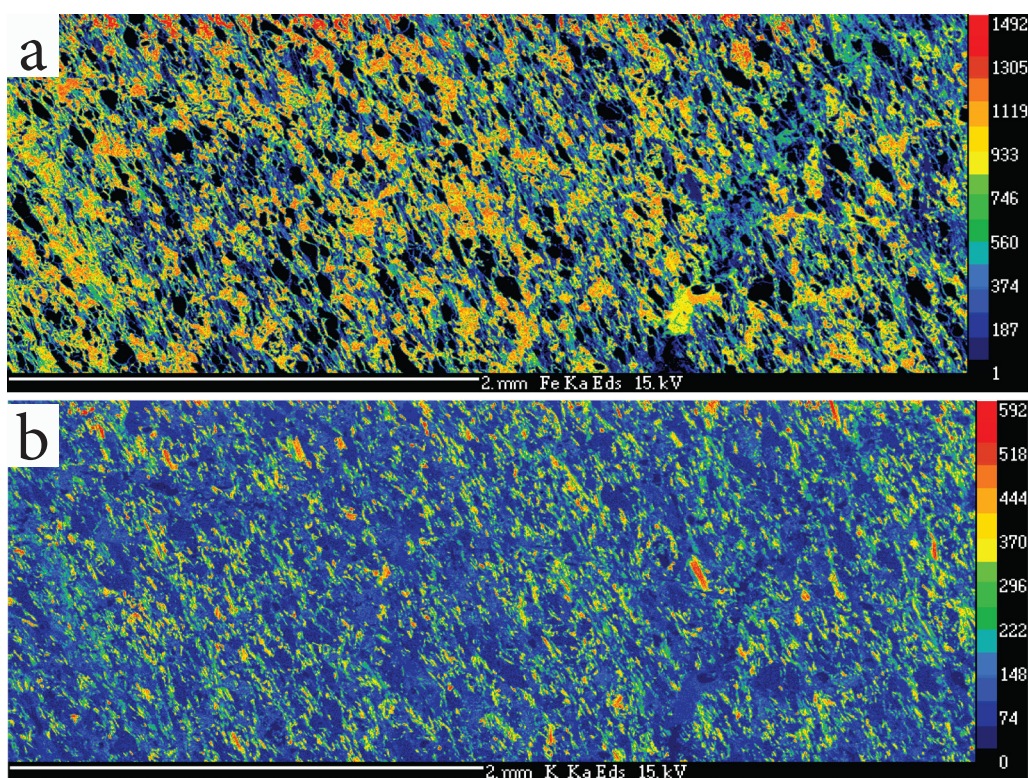


Figure 3.4: Electron microprobe images of KIFE022, a sample of weathered bedrock from the Stokes Bay Road Profile. The images show different elements; a) Fe; b) K.

enrichment is variable, ranging from 40–70% by area in different regions of the samples (Figure 3.6). Native Cu was identified by petrography and SEM imaging (Figure 3.7). Copper crystals occur in a void area within the iron oxide overprinted matrix. This sample also contains the best example of the iron oxides encroaching into the quartz (Figure 3.7). All other textural relationships are adequately captured in the electron microprobe element maps (Figure 3.6). Samples KIFE019 has a higher proportions of iron oxides than samples KIFE018 and KISB002 and an absence of plagioclase, potassium feldspar and trace amounts of muscovite. The electron microprobe maps of Cu for KIFE019 does not show the individual grains of Cu that were observed in the SEM images, possibly due to the larger scale at which the microprobe maps were collected. However, the maps were collected at a resolution that allows many Ti inclusions to be observed. The K in this sample is concentrated in ‘blobs’ rather than in the platy, sheet-like structures previously

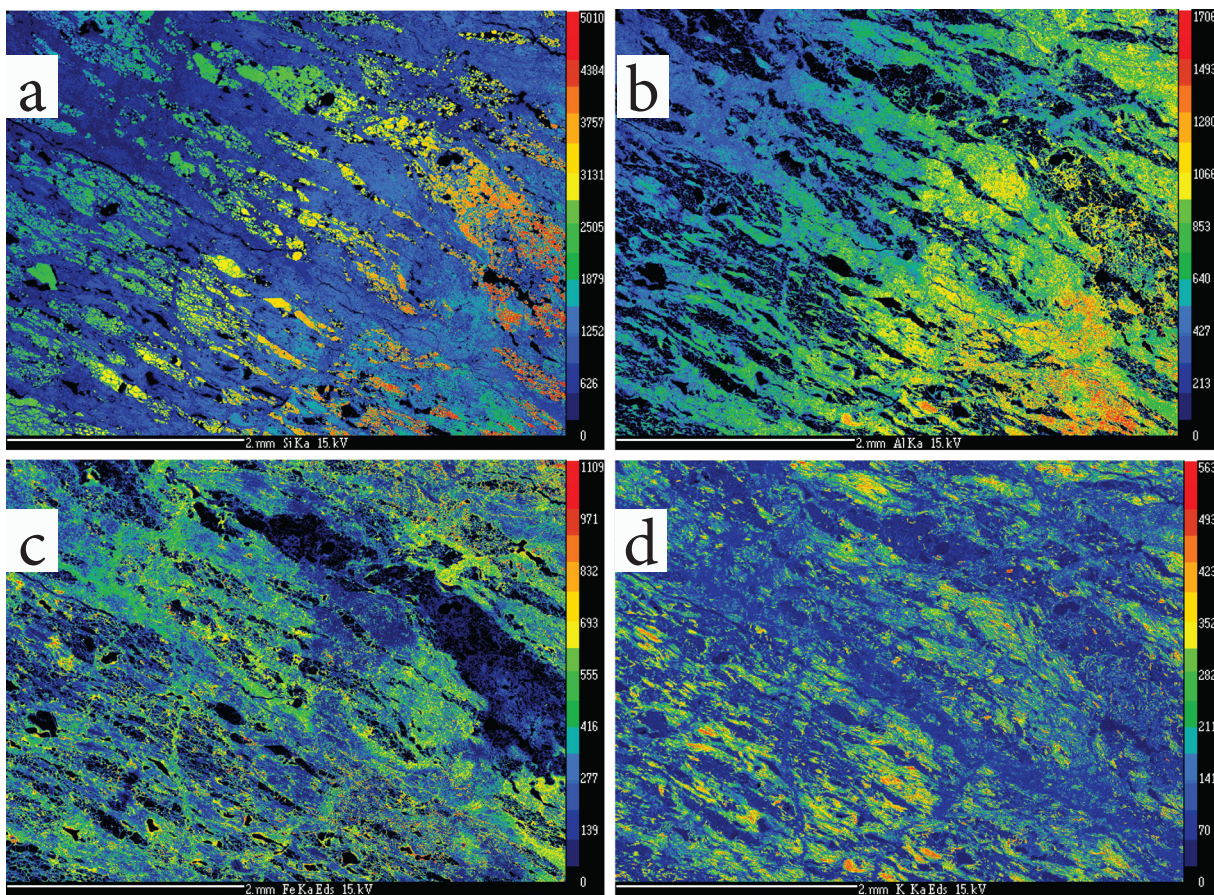


Figure 3.5: Microprobe images of KIFE018, a sample of weathered bedrock from within the paddock at Grainger Old Mine/Bonaventura prospect. The images show different elements; a) Si; b) Al c) Fe and d) K.

described for other samples (Figure 3.6c). Regions of this sample also shows an inverse relationship between Fe and Al, with areas of high Fe abundance (Figure 3.6e). There is an area within the sample, highlighted in Figure 3.6, that may be in the preliminary stages of forming a pisolith, with an increase in Al and Fe and a decrease in Si in a band around the outside, and quartz occurring as broken grains that are clustered towards the centre.

Sample KIFE100 is predominantly comprised of sub-angular to rounded quartz grains (0.2–0.5 mm in diameter). Approximately 50% of the quartz grains exhibit undulose extinction. These samples have no visible or trace amounts of muscovite, plagioclase and potassium feldspar. Iron oxide enrichment is variable, ranging from 40–70% by area in different regions of the samples.

Sample KIFE105 is exceedingly hematite rich, comprising of ~70% hematite and 30% quartz (Figure 3.8). The matrix is a mix of small, sub-angular to sub-rounded quartz grains that are individually surrounded by hematite. The pisoliths are mixed, and include pisoliths that are entirely hematitic, to those that are approximately 20% quartz grains, 80% hematite. There are no other trace minerals that have been identified within the sample. This sample shows the complete Fe-oxide induration of pisoliths within a matrix (Figure 3.8). Potassium is not present and Al is only found in some distinct bands around the pisoliths. The pisoliths appear to be comprised almost entirely of Fe-oxide, with some small inclusions of quartz. The matrix supporting the pisoliths is quartz grains and Fe-oxide.

3.3.3. Complex/Reworked Ferruginous Materials (pisoliths, nodular and vermiform)

Thin sections were made from samples that were classified in hand sample as pisoliths (KIFE109), nodules (KIFE062), vermiform (KIFE110, KIFE012) and slabby (KIFE048) ferricretes.

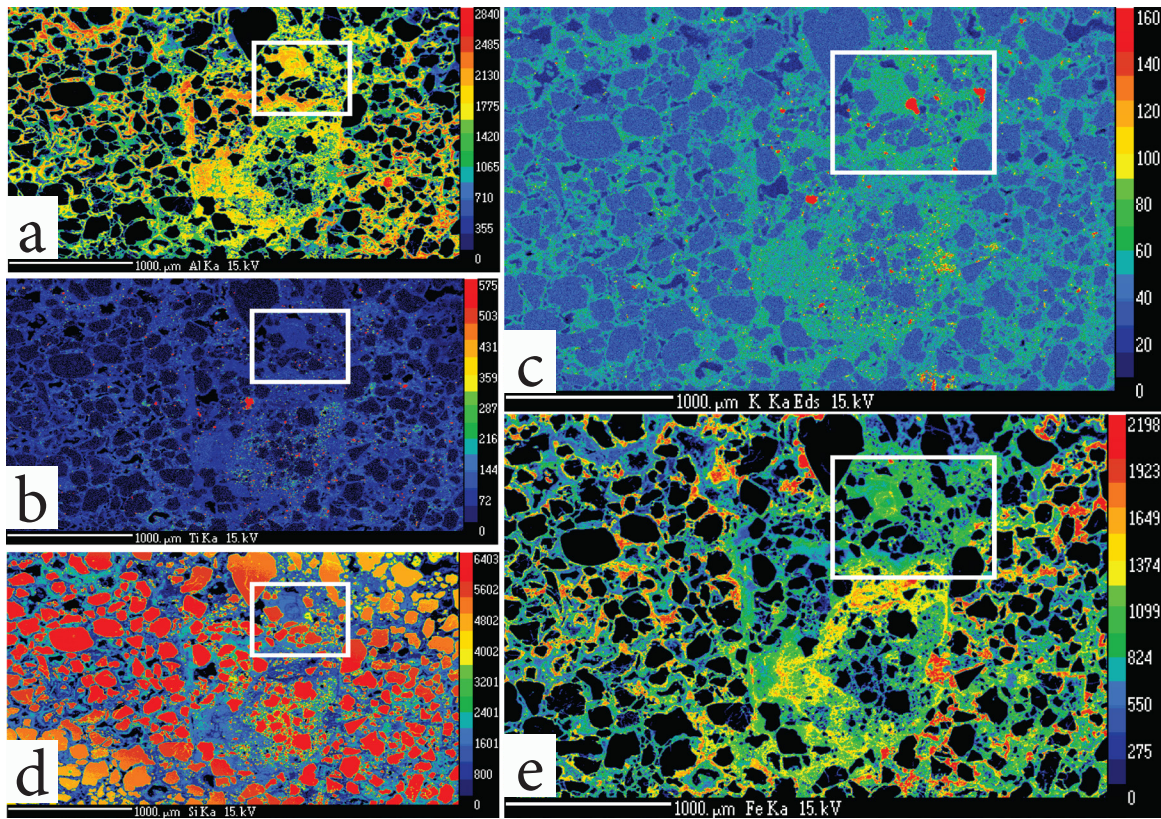


Figure 3.6: Microprobe images of KIFE019, a sample of weathered bedrock proximal to the Bonaventura prospect. The images show different elements; a) Al, b)Ti, c) K, d)Si, e) Fe. The white box highlights the area that is discussed as being as the beginning stages of pisolith formation.

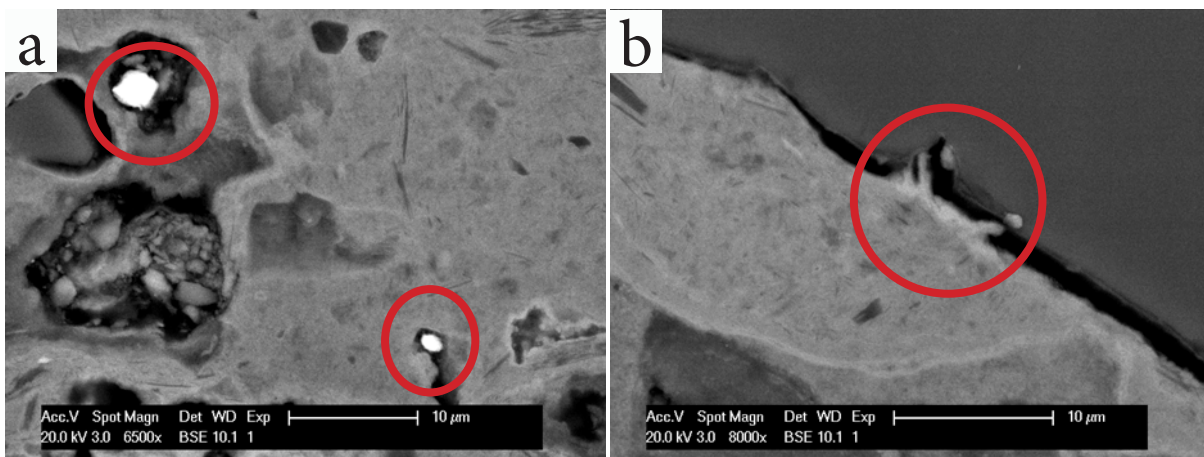


Figure 3.7: SEM images of sample KIFE019, taken from above the Bonaventura Prospect. Highlighted in image a) are grains of native copper; b) images display the encroachment of iron oxide into the quartz crystals.

The sample KIFE048, was classified in hand sample as a slabby ferricrete, but under microanalysis more closely resembles ferruginised bedrock (Figure 3.9). The sample is predominantly comprised of large, sub-angular to rounded quartz grains (0.2–0.5 mm). Approximately 50% of the quartz exhibits undulose extinction. The remainder of the sample is muscovite (typically < 0.1–0.3 mm, 2-5%), and small (1%) amounts of plagioclase and potassium feldspar. Trace amounts of detrital zircon are present. The electronmicroprobe maps show distinct areas that are quartz absent and appear as blue regions (Figure 3.9). These areas are dominated by Fe, and include some Al. Iron oxide enrichment is variable and ranges from 30–70% by area in different regions of the samples (Figure 3.9).

The electron microprobe maps of sample KIFE062 show the edge of an individual nodule (pisolith) (Figure 3.10). The images show the growth of initial pisolith, the edges of which are enriched in Al and depleted in Fe (Figure 3.10). Variations in Fe and K delineate the second and third cutans, both of which are amorphous and relatively smooth, however the third appears to be discontinuous (Figure 3.10). The outer cutan contains high K inclusions and lower amounts of Fe, further suggesting the rinds have developed in two stages (Figure 3.10).

The pisolith sample (KIFE109) is similar to KIFE062 (nodular sample) and is predominantly comprised of sub-angular to rounded quartz grains. Iron oxides appear within the quartz grains and as cutans on the outside of the pisoliths. In both samples, the quartz grains are interlocked in the ‘cores’ of the pisoliths/nodules. In sample KIFE109 there is a noticeable change in size of the quartz grains, from larger, sub-rounded grains in the centres of the pisoliths to angular, smaller grains with iron oxide coatings in the cutans. The iron oxide enrichment is variable between hematite-rich and more goethite-rich areas. The hematite tends to dominate within the pisolith, while goethite is more evident at the edges and within the rims. These rinds do not completely encircle the pisoliths/nodules, rather they tend to be more elliptical in shape. Plagioclase, potassium feldspars and micas were not observed within these samples.

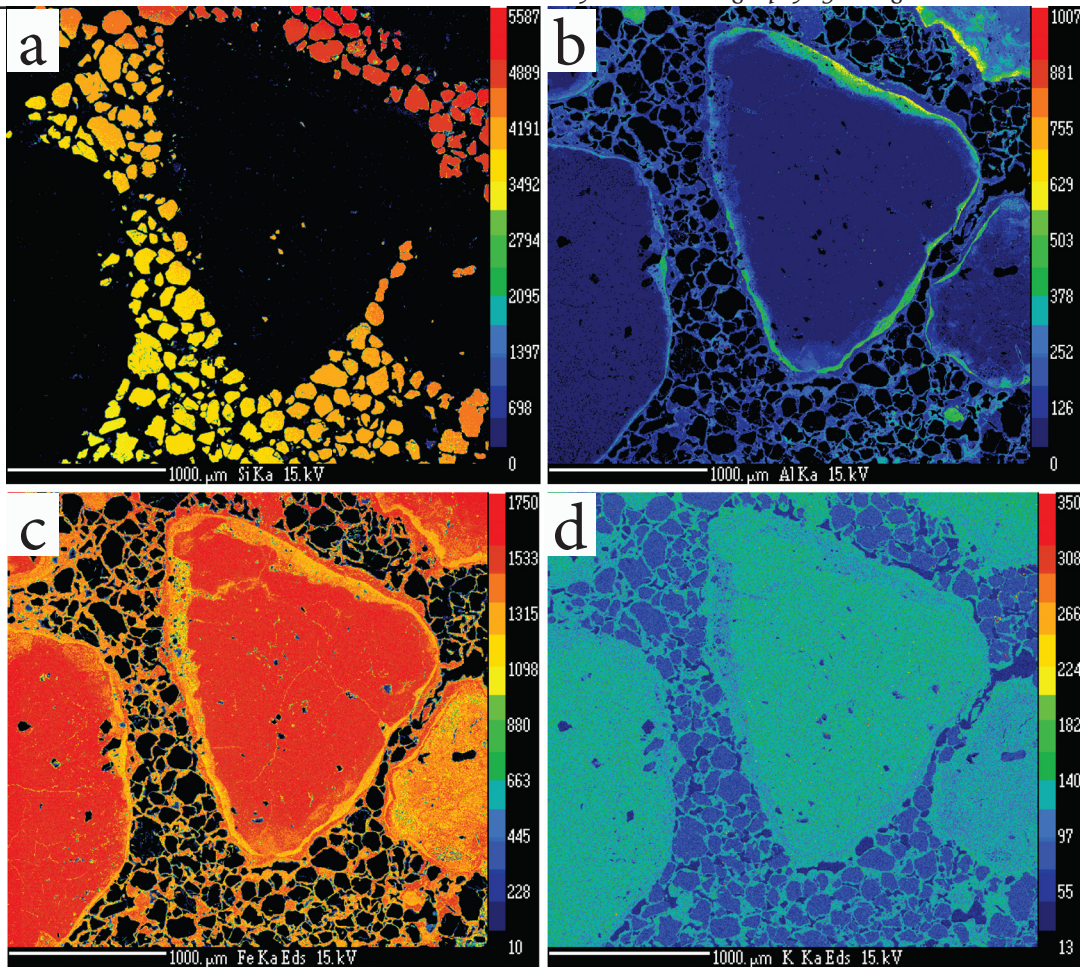


Figure 3.8: Electron microprobe images of KIFE105. The images shows the elements; a) Si; b)Al c) Fe and d) K. The image demonstrates the exceedingly iron-rich nature of this sample.

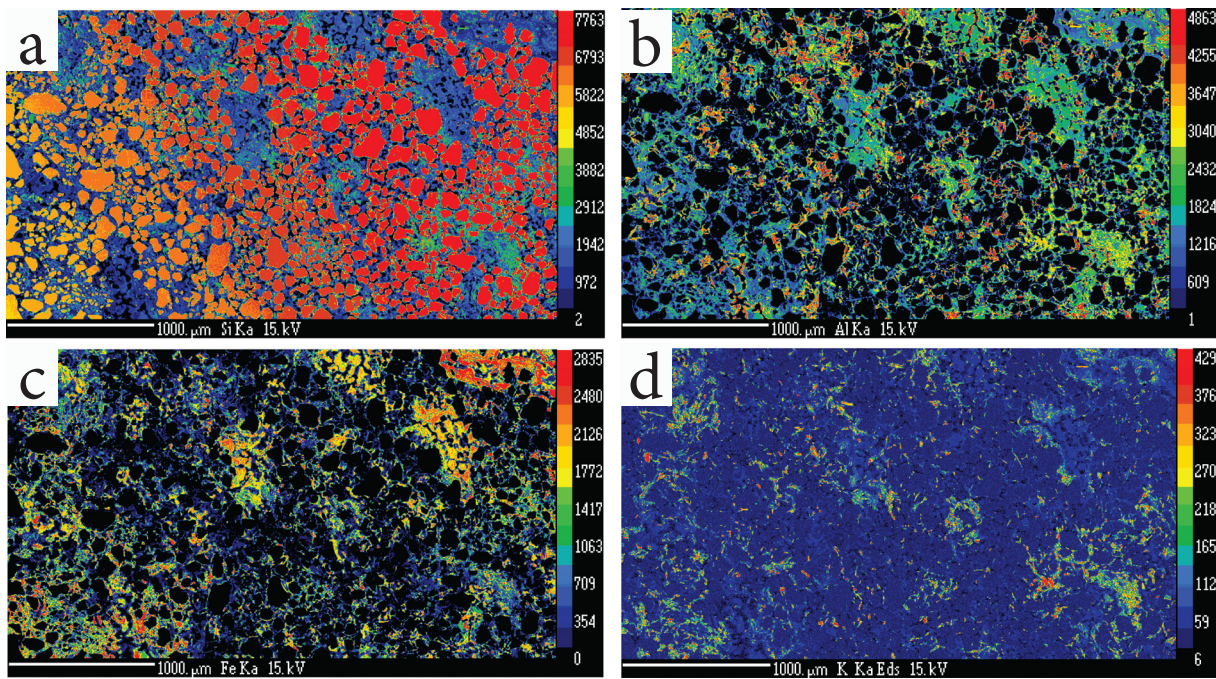


Figure 3.9: Electron microprobe images of KIFE048. The images shows elements; a) Si; b)Al c) Fe and d) K.

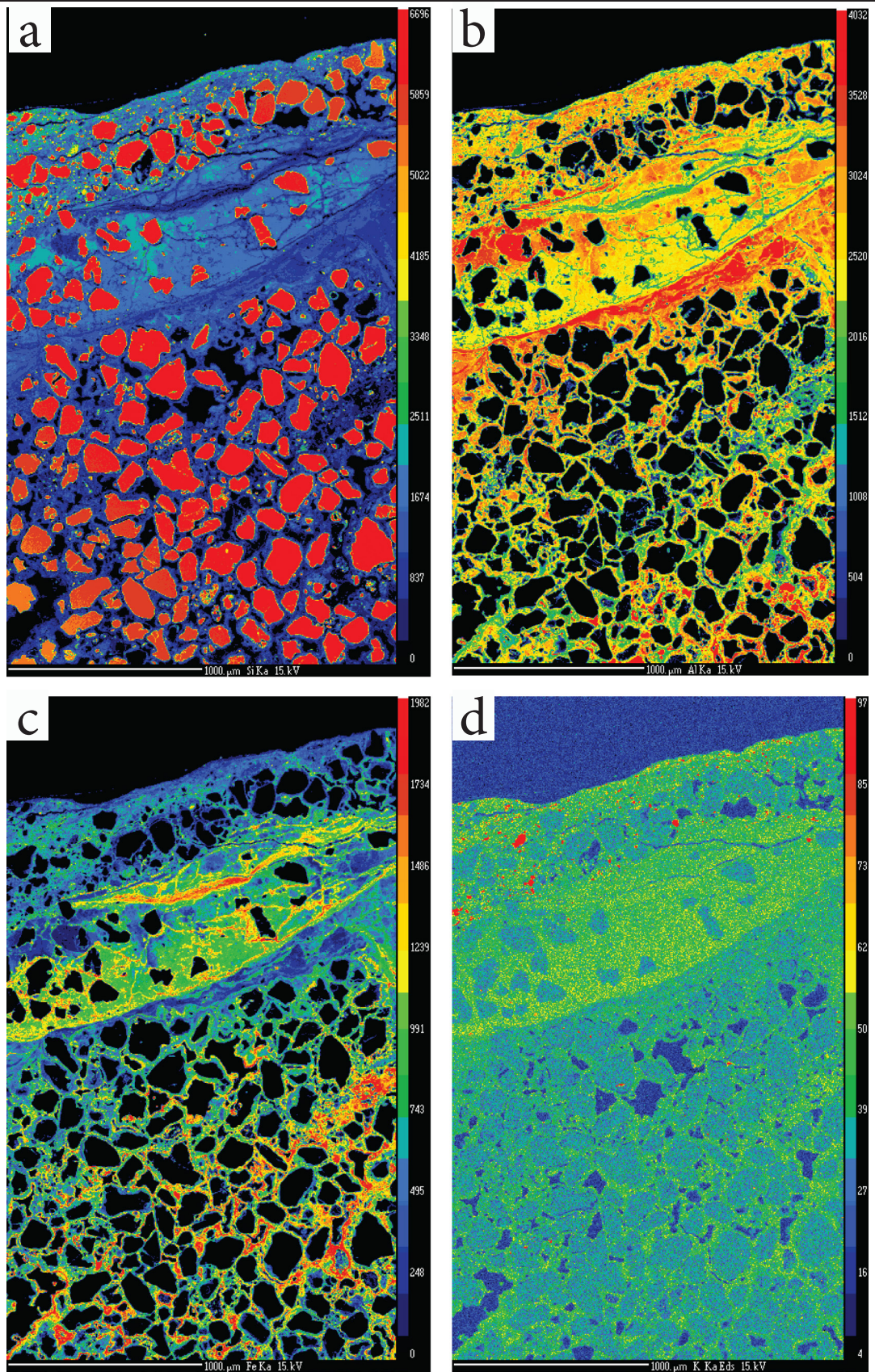


Figure 3.10: Electron microprobe images of KIFE062, a nodular form of ferricrete. The images show elements; a) Si; b) Al; c) Fe and d) K.

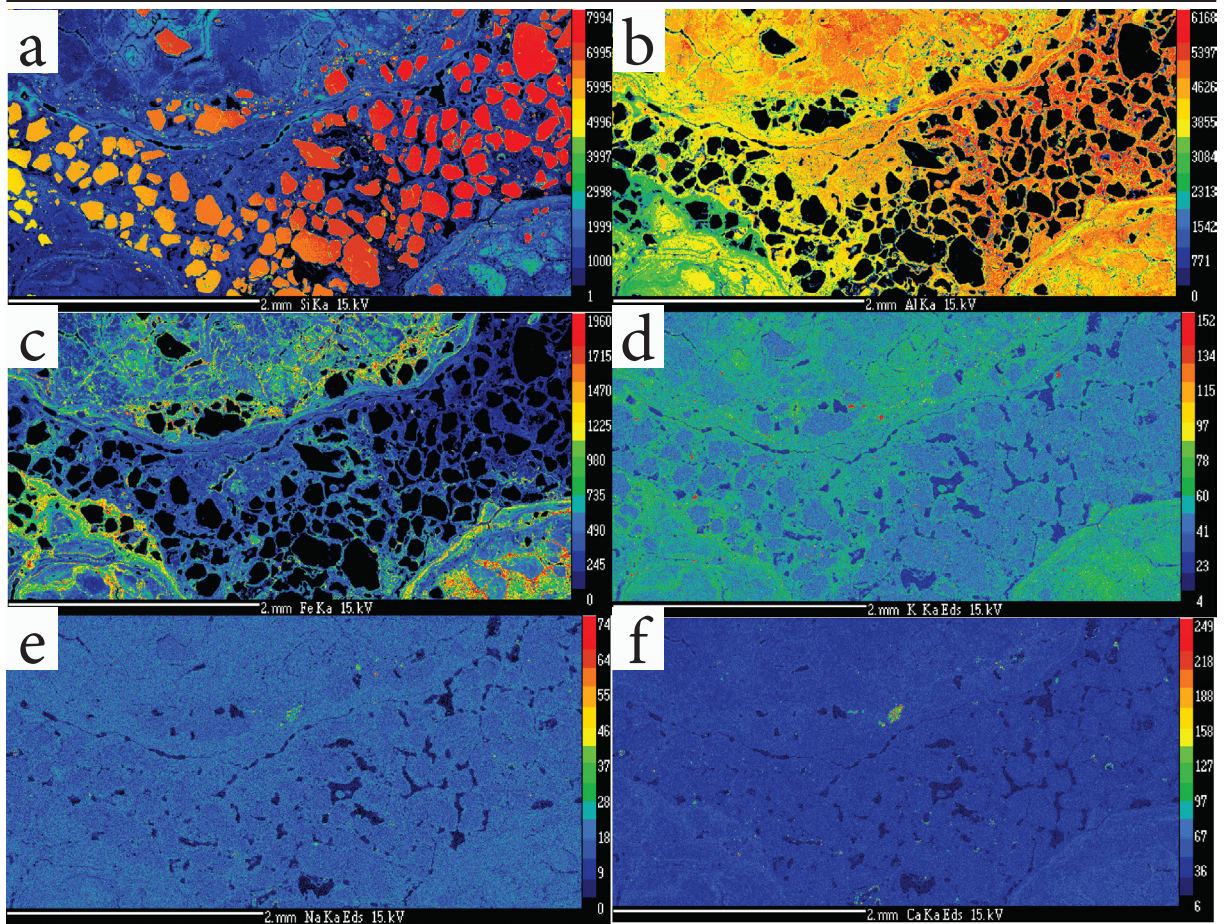


Figure 3.11: Electron microprobe images of KIFE102 (A), a vermiform form of ferricrete. The images show different elements; a) Si; b) Al; c) Fe; d) K; e) Na; d) Ca .

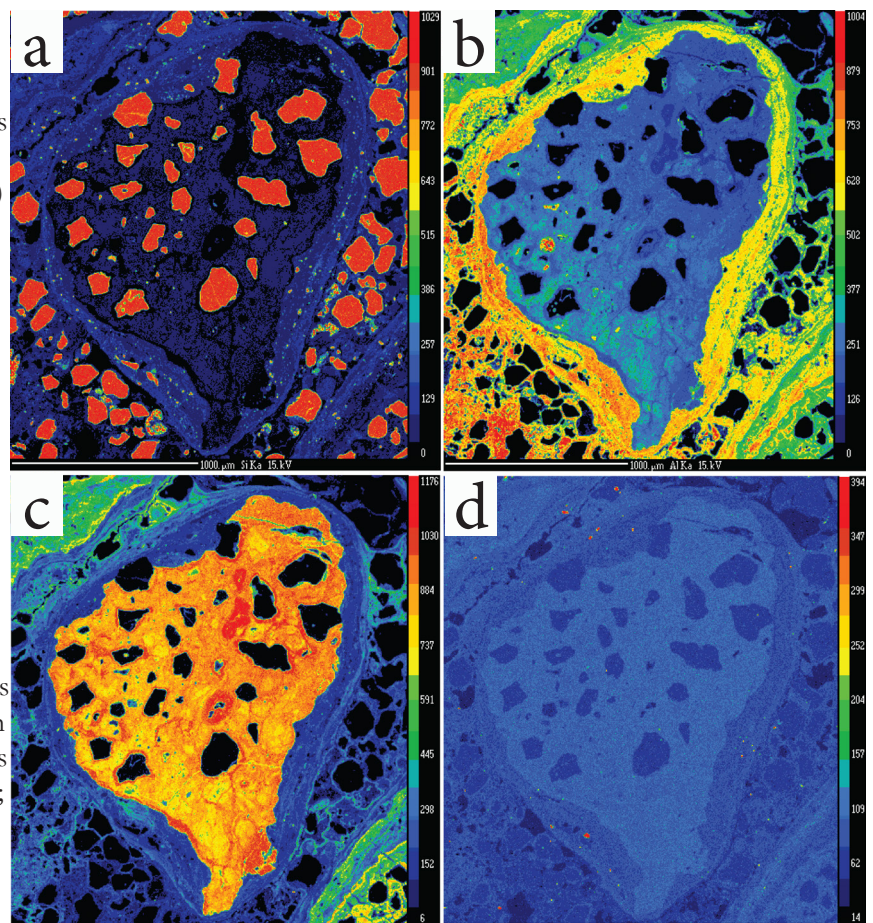


Figure 3.12: Microprobe images of KIFE102 (B), a vermiform form of ferricrete. The images show different elements; a) Si; b) Al; c) Fe; and d) K.

Sample KIFE102 (Figures 3.11–3.13) was classified as a vermiform ferricrete and examined in detail due to its complex nature. This sample contains a variety of pisoliths, supported in a mixed matrix. Figure 3.11, where the edges of several pisoliths are evident, shows the high concentration of Al, within the rind and the matrix. Iron oxide is only visible within the pisoliths. There are also K and Ca rich inclusions with the pisolith rinds. Figure 3.12 demonstrates an individual pisolith in the same sample, at a smaller scale. In this pisolith Al is dominant within the matrix and the rinds, with Fe-oxide only appearing within the pisolith and as thin layers within the rinds (Figure 3.12). In contrast is Figure 3.13 is an example of a pisolith has been completely overprinted by Fe oxides. In this case there is very little Al left within the pisolith, and what is left is concentrated in the outside rinds.

Approximately 30% of the material from vermiform sample KIFE110 was lost during preparation of the thin section, preventing a complete description of the texture of the sample. It is, however, predominantly comprised of angular to sub-angular tightly packed quartz grains (0.2–0.5 mm), with weak iron oxide staining. Some parts of the samples have the form of pisoliths, i.e. rounded shapes with clear boundaries from the outer matrix.

3.4. Discussion

The primary aim of conducting microanalytical work on the ferruginous materials was to provide a link between the wider landscape evolution (Chapter 2) and the geochemistry of the ferricretes (Chapter 4). Microanalysis enables the examination of petrographic evidence of the processes at work within the larger system and allows different ferruginous materials to be studied in greater detail. The microanalysis concentrated on four important aspects:

- a. Relic mineralogy or textures of protoliths, or lack thereof;
- b. Evidence of addition/removal or replacement of material;
- c. Textural relationships consistent with time integrated processes including

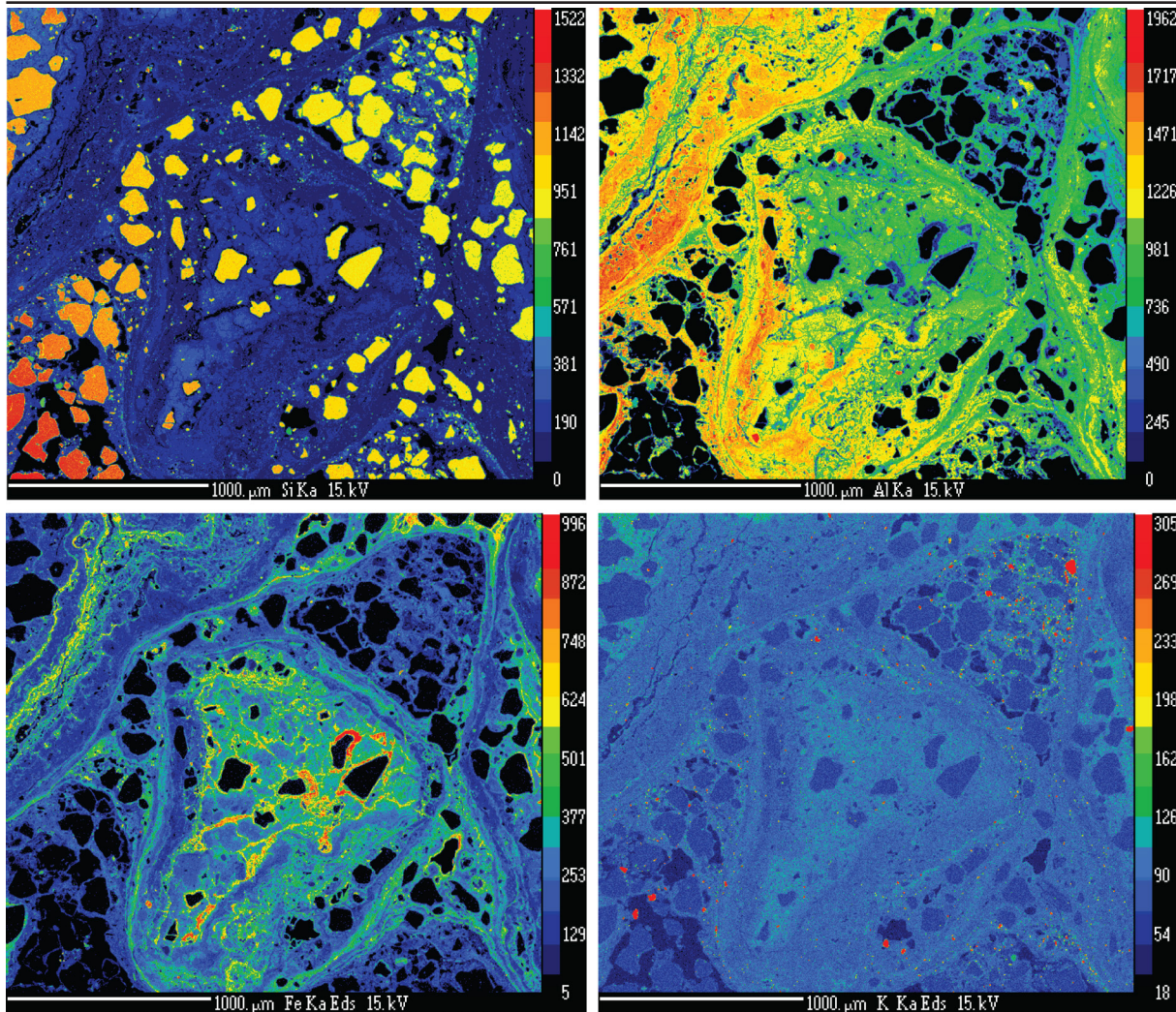


Figure 3.13: Microprobe images of KIFE102 (C), a vermiform form of ferricrete. The images show different elements; a) Si; b) Al; c) Fe; and d) K.

- i. Overprinting textures
- ii. Elemental chemistry changing
- d. Trace element distribution or redistribution.

Examining these key aspects of ferricretes in the context of microanalysis has allowed the identification of three main stages in the formation of the ferricretes on Kangaroo Island:

Stage I - The breakdown and weathering of feldspars and the re-mobilisation of iron and aluminium to form ‘simple’ ferricretes.

Stage II - The formation of the ‘complex’ ferricretes, including wetting and drying cycles to create the cutans of pisoliths.

Stage III - The mobilisation of key indicator/trace/economic elements.

3.4.1. Stage I – The breakdown and weathering of feldspars and the remobilisation of iron to form ‘simple’ ferricretes

Simple ferricretes contain remnants of bedding fabric and products that are in various stages of weathering and are therefore easily identifiable as products of weathering processes acting on the bedrock that they overlie. The means by which simple ferricretes are formed has been debated (Aleva, 1994; Anand, 2002; Bourman, 1989a, 1993b; Eggleton and Taylor, 1998; Ollier and Galloway, 1990; Paton and Williams, 1972; Schellmann, 1994; Stephens, 1971; Twidale, 1983; Twidale and Bourne, 1998). We use the new data to propose a method of formation for the simple ferricretes on Kangaroo Island.

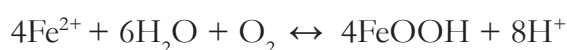
Figure 3.2 shows the comparison of drill core samples of fresh bedrock (Kanmantoo Group metasedimentary rocks) versus the weathered bedrock (KISB002) and the saprolite samples (KIFE048). This shows a breakdown of feldspars and an increase in Fe staining. These samples show progressive weathering towards the present land surface, with an increase in kaolinite, smectite and Fe-oxide and decreasing preservation of protolith fabric or mineral alignment. Thin section imaging shows that these areas are dominated by biotite ($\text{K}(\text{Mg,Fe})_3\text{AlSi}_3\text{O}_{10}(\text{OH})_2$). The breakdown and weathering of biotite increases the Fe content within the most weathered samples, whereas K is removed during weathering. Potassium is weathered out with a resultant lowering in the K content within the saprolite sample. This weathering has also resulted in the redistribution of Al, which can be seen in electron microprobe images of samples KIFE022 and KIFE048 (Figures 3.6 and 3.8). Continued weathering results in the removal of clays (kaolinites and smectites) leading to a decreased proportion of clay minerals at the top of the weathering profile. Instead, Fe-oxide indurated materials and quartz are the dominant constituents in the samples from these areas. The quartz grains in the samples of weathered bedrock display undulose extinction, suggesting a metamorphic origin. This is consistent with the protolith material being weathered bedrock, which in this area is the metasedimentary Kanmantoo Group. Samples KIFE018 and KIFE048 are different weathered bedrock samples and preserve

different relict fabrics probably due to the proximity to the shear zone associated with the Cygnet–Snelling Fault Zone. The samples with a well-defined fabric, particularly Sample KIFE018 where the quartz has formed veins, are from within the Cygnet–Snelling Fault Zone (Figure 3.1).

There have been several physical mechanisms suggested for the mobilisation of Fe within weathering profiles that subsequently form ferricretes, including those proposed Bourman (2006) and Muller and Bocquier (1986). Bourman (2006) suggests that ferruginous mottling is related to groundwater movement and *in situ* processes, with the transformation of hematite to goethite a result of dissolution and re-precipitation within contemporary soil environments. Muller and Bocquier (1986) propose a more detailed hypothesis, where the progression of weathering corresponds to structural changes in which Fe percentages increase and micas are replaced by Fe-kaolinites, resulting in new textures. Structural and mineralogical changes within the ferricretes are the result of the accumulation of Fe from an extraneous source combined with the weathering of micas and feldspars to form kaolinite. These two mechanisms explain what is observed at the microscopic level within the ferricretes on Kangaroo Island. The ferricrete is initially formed from the weathering of bedrock, which in this case is the meta-sedimentary Kanmantoo Group or the sedimentary Kangaroo Island Group. The parent rocks begin with quartz, mica and plagioclase, dominate mineral assemblages typical of a metasedimentary rock. These minerals are then altered to form kaolinites and smectite minerals as part of the weathering process. Groundwater is the mechanism by which the movement and transfer of Fe and the Fe-oxide alteration and induration of the weathered rocks occurs. Less resistant minerals are removed and replaced entirely by Fe-oxide indurated materials (Figures 3.5–3.10). The resistant nature of quartz means that it remains a dominant mineral throughout the different samples and levels of weathering.

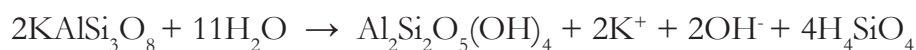
The chemical process that underpins these physical processes is ferrolysis. Brinkman (1970)

introduced the term ferrollysis to describe the formation of a particular type of soil, which contained clay decomposition and interlayering in seasonally wet, acidic soils (Brinkman, 1970; Van Ranst and De Coninck, 2002). The hydrolysis of Fe is also relevant to the formation of ferricretes, and Mann (1983) used equation 3.1 to describe the mobilisation and precipitation of iron for laterite in the Yilgarn Craton.



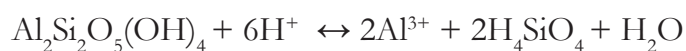
Equation 3.1: Simplified ferrollysis equation, where the oxidation and hydrolysis of ferrous iron can equate to an increase in the acidity of the subsurface Mann, (1983).

The oxidation and hydrolysis of ferrous iron (Fe^{2+}) results in an increase in the acidity of the subsurface (Mann, 1983). The acid lowering of pH impacts on the concentration of Al by resulting in increased weathering of sheet silicates (kaolinite) to form quartz clay saprolite as a concurrent process to the ferrollysis of Fe. Equation 3.2 describes the weathering of feldspar to form kaolinite (Mann, 1983).



Equation 3.2: The weathering of feldspar to kaolinite from Mann, (1983).

The breakdown of feldspars results in an increase in the proportion of kaolinite, which readily breaks down in acidic environments. As seen from Equation 3.1, the ferrollysis of ferrous iron results in the production of acid, and the process of the breakdown of kaolinite is summarised in Equation 3.3.



Equation 3.3: Breakdown of kaolinite to silicic acid, water and Al cations.

From Ambrosi et al., (1986).

The breakdown of the kaolinite releases Al cations, which results not just in a dilution factor of the Al and Si within the ferricretes as they form, but the active movement of Al. This movement of Al, and presumably other ions, in solution, can then be incorporated into the Fe-oxides. This process is observed in the electron microprobe maps, where Al is precipitated within the iron oxides, suggesting that Al is mobile (Figures 3.8 and 3.10, 3.11). As the breakdown of kaolinite also produces acid and both Fe and Al are further mobilised by acidic environments, the two processes can cause a continuous cycle (Mann, 1983).

This new work better establishes the relationship between the weathered bedrock and the saprolite. We conclude that simple ferruginous materials on Kangaroo Island were formed from the same protoliths, the Kanmantoo and Kangaroo Island Groups. The effects of weathering were more prevalent than those of erosion, enabling the landscape and weathered products to remain *'in situ'*.

3.4.2. Stage II – Reworked / Complex Ferricretes

The second classification given to ferricretes on Kangaroo Island is 'complex' or reworked ferricretes. These are further divided into pisoliths, nodules, vermiform and slabby ferricretes. The formation and the origins of pisoliths has been a long debated topic, with studies conducted on numerous different ferruginous materials (Aleva, 1994; Anand, 2002; Bourman, 1989a, 1993b; Bourman and Conacher, 1998; Norton, 1973; Schellmann, 1994; Stephens, 1971; Taylor et al., 1992; Twidale, 1983). The hypotheses of Nahon (1991) and Taylor and Eggleton (2008) as to the formation of ferricretes best apply to the samples examined here. Nahon (1991) suggests the movement of elements and their precipitation into finer grained matrix of the regolith as the primary means of forming the cores of pisoliths. Taylor and Eggleton (2008) suggest that nodules and pisoliths can vary greatly and one means by which pisoliths and nodules can be classified is according to their internal characteristics as the external features can have little relationship with these internal features. It is generally suggested that pisoliths cannot have formed where they now lie. Instead they

are the result of local overland transport after their release from the ferruginised zone of a weathering profile. The pisolith, nodule and vermiform maps presented in Figures 3.11–3.13 show the different textures that the complex ferricretes can exhibit.

The electron microprobe images of KIFE062 (nodular ferricrete) and KIFE012 (vermiform ferricrete) support suggestions that there are at least two, but possibly more, phases of development involved in the formation of the pisoliths (Figures 3.9, 3.11–3.13), similar to the weathering of bedrock discussed above. The first is the beginning of the weathering process and the breakdown of feldspars and micas, described above. This is followed by the mobilisation of Fe through ferrolysis. In samples KIFE02 and KIFE012, this is recorded by the accumulation of Fe in the core of the pisoliths, and to some extent the rinds, but not in the outer rind or the matrix. This suggests that there is probably another separate stage where accumulated Al on the outside cutans of the pisolith and within the matrix was mobile. Sample KIFE105 has an exceedingly hematite-rich matrix and pisoliths and is suggested to be an extreme end member, where a localised influx of Fe-oxide has completely overprinted any remaining Al or clays leaving only the quartz. The images of sample KIFE062 (Figure 3.9) show the edge of an individual pisolith. The images show the growth of initial pisolith, the edges of which are higher in Al than Fe. Iron and K delineate the second and third rinds, both of which are amorphous and relatively smooth, the third appears to be discontinuous. The outer rind has inclusions of high K and Ca and low amounts of Fe. These high levels of K and Ca demonstrate the possibility of the cations in solutions being re-precipitated as a K-rich clay phase. The precipitation of clay is most likely to occur at the surface when the material has been moved out of the ferrolysis environment. In this case, this is consistent with the occurrence of the K- and Ca-rich phase on the outer edges of the pisoliths, when the pisolith was at the surface and under pH neutral conditions, which were conducive to the re-precipitation of the cations in solution.

The pisoliths in this study are similar to those described in Milnes et al. (1987). The

ferruginous pisoliths have core materials reflecting a variety of sources and the cutans record a long history of development. Clasts of ferruginised bedrock may be encapsulated in cutans composed of ferruginised soil materials. Laminated deposits of goethite on the outsides of pisoliths incorporate single grains or lenses of quartz between the layers which confirms the accretionary nature of the cutans of the pisoliths (Milnes et al., 1987).

The electron microprobe maps show that the various ferricrete samples record different stages of the overall weathering process. Bedrock is weathered and feldspars and micas are replaced, shown in samples KIFE062 and KIFE102. Iron begins to be mobilised through the system, through ferrololysis, with small amounts accumulating within weathered samples when encountering reducing conditions. Sample KIFE048 demonstrates the beginning stages of the pisolith formation, showing areas with less quartz, and the overprinting by the iron oxides.

Maps of the edges of several pisoliths show the high concentration of Al, particularly within the cutan and the matrix, suggestive of the movement of Al in solution during ferrololysis. The Fe-oxide is only visible within the pisoliths, suggesting that they were indurated prior to the pisoliths being incorporated into the matrix. There are also inclusions of K and Ca with the pisolith cutans, again suggestive of another stage of formation under different conditions. Figure 3.12 demonstrates an individual pisolith at a smaller scale, where Al is dominant within the matrix and the cutans, with Fe-oxide only appearing within the pisoliths and as thin layers within the cutans.

Sample KIFE062 is the end product of several stages of weathering, demonstrating iron overprinting and erosion of the matrix within which the pisolith was originally contained. KIFE062 is a 'typical' representative of the majority of this field area, as it displays similar relationships (in hand sample) to most pisolith or nodules. An extreme example of the weathering system is represented by KIFE105, which appears to be comprised entirely

of Fe and quartz and there is very little Al left within the pisolith apart from a small amount along the edges of the cutans (Figure 3.8).

The vermiform sample, KIFE102, a transported ferricrete, represents the end point of the process. It contains a mix of different pisoliths of different origins, as seen in Figures 3.11–3.13, cemented in a matrix of quartz and Al. Given its classification and landscape setting, this highlights the importance of the knowledge of the landscape to be able to correctly identify and interpret data from different sample media.

3.4.3. Stage III - Mobilisation of indicator/economic elements

The SEM images of sample KIFE019 show native Cu in voids within the iron oxide matrix (Figure 3.7). This suggests that the Cu has been subject to movement in solution through the system. The Cu occurs as discrete crystals rather than in a dendritic or tendril like form within the SEM images (Figure 3.7), suggesting it has been weathered and transported rather than ‘grown’ in that area. Sample KIFE019 was taken within a few hundred meters of the Bonaventura prospect, so there is a known source of Cu mineralisation. This is the only sample where the native Cu was found, suggesting that Cu will only appear in geochemical samples that are close to the source of the mineralisation. Thus ferricrete can be both a good and a bad indicator of proximity to mineralisation. If high values are returned there is a likelihood an anomaly is close by, but if the sampling density is too low, possible anomalies can be easily missed.

3.5. Conclusions

3.5.1. *In situ* or transported?

The implications for mineral exploration

The micro analysis of the different ferricrete morphologies, suggests that they are formed both *in situ* and from transported materials, depending on the type of ferricrete. The weathered bedrock and saprolite are obviously weathered products of the underlying bedrock that have been subsequently overprinted by iron oxides. The origin of the complex, or reworked ferricretes is more challenging to determine particularly as the centres of pisoliths can have different origins, with rinds containing quartz grains, incorporated at a later date. Pisolith geochemistry can be useful, if viewed as a composite signal of an area, rather than a discreet point. However, the utility of this approach depends on an understanding and whether the landscape setting a pisolith was likely to have travelled locally, via gravity flow, or from a wider area. Samples of vermiform ferricretes, such as KIFE012, containing a mix of different pisoliths are best treated with care, as it is difficult to determine where they are likely to be derived from.

Further investigation is necessary to determine the exact sampling density appropriate for the use of ferricrete for mineral exploration. Sample KIFE019 is evidence of the ability of ferricrete to record metal anomalies in close proximity to a mineral deposit. However, the sampling density required to identify economic targets is still unclear and forms the subject of the next chapter.

Chapter 4

Geochemical Survey of the ferruginous
materials of Kangaroo Island

Foreword

This chapter investigates the whole rock geochemistry of the different types of ferricretes, already discussed in Chapters 2 and 3, collected as a part of a geochemical survey for mineral exploration. This survey was undertaken to facilitate a better understanding of the formation of the ferruginous materials on Kangaroo Island and how these may be used for geochemical mineral exploration. The geochemical expression of the ferricretes studied reflects different landscape settings and the progression from weathered bedrock through to indurated saprolite and transported material. The physical expressions of the processes involved in the formation of ferricretes in the landscape and in microanalysis have already been discussed in Chapter 2 and 3. It is hoped that through the addition of the whole rock geochemical data we are further able to clarify and explain the processes and mechanisms, as well as gain a better understanding of the capabilities of ferricrete as a sample medium for mineral exploration.

4.1. Introduction

“The primary purpose of geochemistry is to determine quantitatively the chemical composition of the Earth and its parts, and to discover the laws that control the distribution of the individual elements”
(Goldschmidt, 1937).

Applied geochemistry is the application of geochemical knowledge to societal benefits, in this case for the discovery of mineral deposits (Garrett et al., 2008; Reimann et al., 2010), here through the use of geochemical mapping. Geochemical mapping has been widely used since the 1960s and has developed from early geochemical prospectors panning for alluvial gold or tin to the current geochemical surveys that utilise a range of sampling media at varying survey densities (Garrett et al., 2008).

As iron is one of the most abundant elements on Earth, and iron oxides are a highly abundant product of weathering on the Earth’s surface, iron oxides are potentially a highly useful sampling media for geochemical exploration (McQueen, 2005). Iron oxides also have the ability to incorporate trace elements either in their structure or via adsorption (Aleva, 1994; McQueen, 2005; Scott, 2009). This provides the possibility for iron oxide weathering products, e.g. ferruginous materials, to host trace element or economic metal enrichments transferred from the underlying basement rock and therefore makes them useful for mineral exploration (McQueen, 2005; McQueen and Munro, 2003; Scott, 2009). There have been numerous studies investigating the chemical and physical mechanisms that are involved in the formation of ferruginous materials (Chapters 1–3). These studies have shown that the formation of ferruginous materials can involve numerous mechanisms within an open system, including the lateral and vertical transport of iron associated cations, pathfinder and trace elements, particularly in groundwater through hydrolysis and ferrollysis (Bourman, 1989, 1993a, 1993b; Mann, 1983; Milnes et al., 1987). This open system behaviour in the formation of ferruginous materials means that it is particularly important for mineral exploration purposes to understand which processes are at work and where the chemical

signatures contained within the ferruginous materials are likely to be sourced from. Ferricrete material has previously been used in geochemical surveys in Western Australia and areas of eastern Australia (Anand et al. 2002, 2016; Anand and Butt, 2010; Anand and Paine, 2002; Cohen et al., 1998; Cornelius et al., 2006, 2008; McQueen, 2005; McQueen and Munro, 2003; Taylor and Eggleton, 2008; Taylor et al., 2008). A geochemical atlas of the Yilgarn Craton completed by Cornelius et al. (2008) has shown that a low density sampling program of ferruginous materials can display regional and craton scale geochemical patterns. The survey by Cornelius (2008) provided a stimulus for 'greenfields' exploration in the region.

This study presents a regional scale geochemical survey of ferruginous material from Kangaroo Island. Kangaroo Island is an excellent place to study the formation and utility of ferruginous material for mineral exploration as it has a widespread distribution of ferruginous material, ease of access and the bedrock is relatively homogenous and well constrained. This survey involved 204 samples over an area of 4 405 km² with an average density of 1 sample point every 20 km² (Figure 4.1). Data collected were used to examine how sampling at this density can be used to identify the underlying geochemical processes of ferruginous material formation and assess the viability of ferruginous materials as a mineral exploration sample media.

Having previously identified three main aspects of the formation of the ferricretes through microanalysis, the work in this chapter is largely focused on identifying those processes through whole-rock geochemistry. The identified stages of formation were:

- 1) Breakdown and weathering of feldspars and the re-mobilisation of iron and aluminium to form 'simple' ferricretes.
- 2) The formation of the 'complex' ferricretes, which includes wetting and drying cycles to create the cutans of pisoliths.
- 3) The mobilisation of key indicator/trace/economic elements.

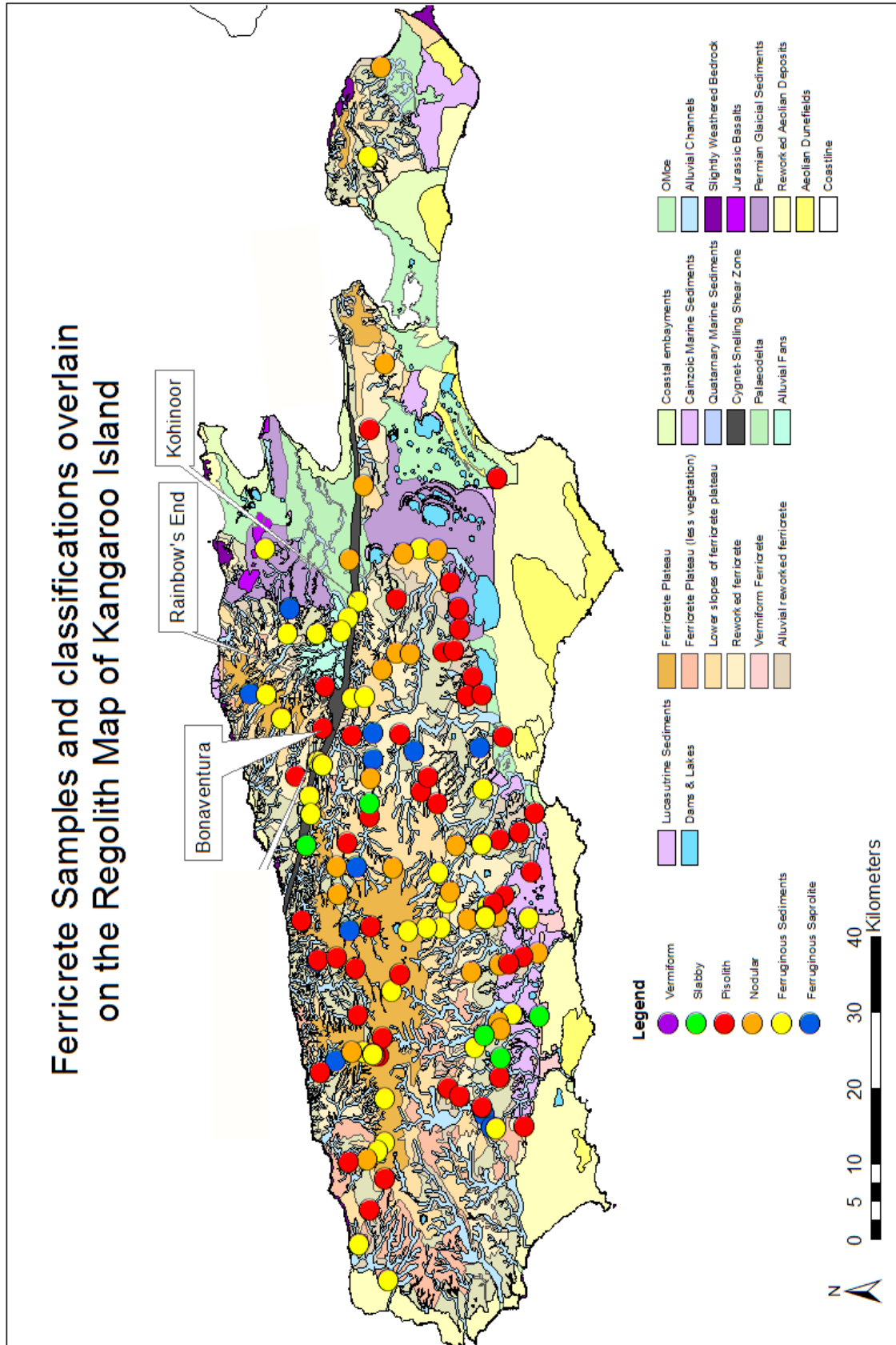


Figure 4.1: Ferricrete sample points and associated classifications, based on morphology and landscape setting (see Chapter 2). The points are overlain on the regolith map of Kangaroo Island. The three mineralisation sites are labelled, and the Cygnet-Snelling Fault is in dark grey.

The other key aim of the geochemical analysis is to examine the validity of the morphological classifications of the ferricretes, and whether these classifications translate into the geochemical results.

4.2. Background

Geochemical surveying has become a widely employed technique since the 1960s (Darnley, 1990, 1997; Reimann et al., 2005, 2009, 2010). The data are employed for a variety of different uses, particularly for mineral exploration, but also for environmental monitoring, including the fields of geo-health and medicine (Thornton and Plant, 1980; Friske et al., 2013; Morrison et al., 2014). There are, however, some limitations associated with geochemical surveys. These issues are dominated by three main aspects – survey size and associated sampling density; appropriate sampling media; and the background or baseline levels applied when analysing the data.

The following definitions of survey sizes for geochemical mapping are used by Reimann et al. (2010):

Global scale: >50 million km² — sample density of <1 site/5000 km²

Continental scale: 0.5–50 million km² — sample density between 1 site/5000 km² and 1 site/500 km²

Regional scale: 500–500 000 km² — sample density between 1 site/500 km² and 1 site/km²

Local scale: 0.5–500 km² — sample density between 1 site/km² and >100 sites/km²

Detailed Scale: <0.5 km² — sample density >100 sites/km²

Low density, continental or regional surveys are commonly carried out in order to identify areas for further study, as well as to create a regional framework for future work (Garrett et al., 2008). There have been a large number of continental and regional (usually co-

ordinated by a specific country) scale surveys completed, including surveys conducted in Europe, the US and China (Demetriades, 2010; Garrett et al., 2008; Gustavsson et al., 1994; Lax and Selinus, 2005). The ‘correct’ survey size and sampling density commonly varies from practitioner to practitioner but will inevitably depend upon the purpose of the study. Continental sized surveys with low densities are likely to display a dominant signal of the underlying geology and the regolith (Cohen et al., 2012a, 2012b). Features relating to mineralisation or anthropogenic impact are difficult to pinpoint at the larger scale using low density surveys. Regional mapping at higher densities is required to detect major sources of contamination or specific mineral deposits, rather than mineral districts (Cohen et al., 2012b; Cornelius et al., 2008; Reimann et al., 2010). In this study a regional scale sample density has been used in order to further explore various aspects of the sample media, as well as to establish a regional scale dataset which can be used as a base for further study.

The sample media used in a survey depends on the dominant soil or regolith material, which is directly related to the survey size as well as the purpose of the survey. The ideal sample media is one that is able to be kept consistent throughout the survey and can either be a type of regolith, such as ferricrete, carbonate or glacial till, or a specific soil horizon (Demetriades, 2010; Gustavsson et al., 1994; Lax and Selinus, 2005; Salminen and Tarvainen, 1997). In Europe, continental and regional scale surveys have used a combination of glacial till and specific soil horizons to provide a consistent sampling medium (Demetriades A., 2010; Gustavsson et al., 1994; Lax and Selinus, 2005). In the high density (1 site/1 km²) the geochemical survey of Cyprus, two sample types were collected; a composite top soil (0-25cm) and sub soil (50-75 cm), resulting in a grid of over 5000 sample sites (Cohen et al., 2012b). For the Kangaroo Island survey we have chosen ferruginous material as the sampling medium, as it covers a large portion of the survey area, and by sampling the materials that appear at the surface, it allows for landscape processes to be further examined.

Geochemical mapping makes use of the spatial distribution of data to identify patterns that indicate a change of lithology or a geochemical anomaly such as a mineral deposit. Although statistical approaches are vital to identify meaningful anomalies, simple statistical application of concepts such as a baseline or background to an entire dataset can produce erroneous results. Darnley (1997) raised the issue of background and threshold filters, where extreme values in the tails of a statistical distribution are not actually part of the same distribution. Subsequently these values can be defined as values belonging to a different population because they originate from another process or source, in which case the mean ± 2 standard deviations (2SD) can produce a relevant threshold estimate. Such a definition has the benefit of identifying geochemical anomalies related to mineral deposits, as the deposits most likely formed from different processes to the majority of lithologies in a survey and hence do not lie within the 2SD window of the remainder of the population. However, if multiple 'normal distributions' are generated by a range of geological or sampling bias processes within a single survey then simple statistical indicators generated for the resultant distribution may work to disguise geochemical anomalies associated with targets such as mineral deposits. This requires the combined use of statistical methods and thorough interrogation of the data for sampling or geological biases. The terms geochemical baseline and geochemical background provide a variety of meanings in different studies, however here we use the following definitions from Garrett et al. (2008) and Reimann et al. (2005). The geochemical background is defined as a range within which most observations fall, with the geochemical background having an average value that may be used as a baseline (Darnley, 1997; Reimann et al., 2009, 2010). A single value for a baseline cannot be used for all geochemical surveys, as backgrounds and baselines will vary in different environments across the Earth's surface (Darnley, 1997; Reimann et al., 2010). They will also change between different locations and potentially also with the number of samples taken in each area in low sampling density surveys (Garrett et al., 2008). The survey conducted on Kangaroo Island is being viewed as a discrete dataset, and the background and baseline levels are being determined from the survey, rather than from an external generalisation.

4.3. Methods

4.3.1. Sampling procedures and geochemical analysis

The sampling program for the geochemical survey of ferricrete on Kangaroo Island was undertaken in conjunction with biogeochemical surveys and conducted over two field seasons, March and April 2012 and April 2013. The surveys were designed along the predominantly north–south road network on Kangaroo Island (Figure 4.1). Ferricrete (where available) was sampled at approximately 2 km intervals north–south, and the roads are approximately 10 km apart east–west, equating to a sample density of approximately 1 sample every 20 km². This sample density is only an approximation as a large portion of the western area of the island is included in the Flinders Chase National Park and could not be sampled due to access difficulties. Samples were collected as far from the road as possible at each site to minimise contamination from the road base, which is predominately Fe-oxide transported from other parts of the island.

Samples were taken at three of the known mineralisation areas that form case studies in the biogeochemical data (Figure 4.1; Chapter 5). These known mineralisation areas are historically worked, but currently economically unviable, and include silver-lead-zinc (Rainbow's End), copper-gold (Kohinoor) and copper, gold, silver and zinc (Bonaventura) prospects (Crooks, 1991).

The sampling program was based on the work of Cornelius et al. (2006), where 'lateritic gravel', that is pisoliths and nodules that form the upper part of the lateritic residuum, were preferentially sampled. In this study, a similar method was employed, sampling the ferruginous materials found at the surface. This was not limited to the pisoliths but included a mix of ferruginised materials, in order to gain a full understanding of the different ferruginous regolith types on Kangaroo Island and their various chemical signatures. Ferruginous materials were collected as a consolidated sample over an area of 2–3 m². Samples equated to a sample mass of approximately 1–1.5 kg and were placed into plastic

sample bags in the field.

Samples were photographed and composite sub-samples of 100–150 g were taken in the laboratory and shipped for analysis. Samples were washed with de-ionised water to remove any remnants of soil or organic matter, but they were not crushed or sieved prior to being shipped for analysis so so they contained a variety of coarse material. Analyses were conducted at ACME Laboratories (now Bureau Veritas Upstream), Vancouver, Canada, where the samples were pulverised to $250 \mu\text{m} \geq 85\%$, and analysed for major elements using whole rock XRF analysis and for trace elements using ICP-MS, for a suite of 57 elements. Table 1 contains the detection limits for the elements analysed. Duplication and standards included blind duplicates at rate of 1 in 10 samples, through splitting a 300 g

Element	Method	Detection limit
SiO ₂	LF700/4X	0.01%
Al ₃ O ₃	LF700/4X	0.01%
Fe ₂ O ₃	LF700/4X	0.01%
CaO	LF700/4X	0.01%
MgO	LF700/4X	0.01%
Na ₂ O	LF700/4X	0.01%
K ₂ O	LF700/4X	0.01%
MnO	LF700/4X	0.01%
TiO ₂	LF700/4X	0.01%
P ₂ O ₅	LF700/4X	0.01%
Cr ₂ O ₃	LF700/4X	0.00%
Ba	LF700/4X	0.01%
LOI	LF700/4X	-5.11%
Ba	LF100/4B	1 ppm
Be	LF100/4B	1 ppm
Co	LF100/4B	0.2 ppm
Cs	LF100/4B	0.1 ppm
Ga	LF100/4B	0.5 ppm
Hf	LF100/4B	0.1 pm
Nb	LF100/4B	0.1 ppm
Rb	LF100/4B	0.1 ppm
Sn	LF100/4B	1 ppm
Ta	LF100/4B	0.1 ppm
Th	LF100/4B	0.2 ppm
U	LF100/4B	0.1 ppm
Au	AQ200/1DX	0.5 ppb
Hg	AQ200/1DX	0.01 ppm
Tl	AQ200/1DX	0.1 ppm
Se	AQ200/1DX	0.5 ppm

Element	Method	Detection limit
V	LF100/4B	8 ppm
W	LF100/4B	0.5 ppm
Zr	LF100/4B	0.1 ppm
Y	LF100/4B	0.1 ppm
La	LF100/4B	0.1 ppm
Ce	LF100/4B	0.1 ppm
Pr	LF100/4B	0.02 ppm
Nd	LF100/4B	0.3 ppm
Sm	LF100/4B	0.05 ppm
Eu	LF100/4B	0.02 ppm
Gd	LF100/4B	0.05 ppm
Tb	LF100/4B	0.01 ppm
Dy	LF100/4B	0.05 ppm
Ho	LF100/4B	0.02 ppm
Er	LF100/4B	0.03 ppm
Tm	LF100/4B	0.01 ppm
Yb	LF100/4B	0.05 ppm
Lu	LF100/4B	0.01 ppm
Mo	AQ200/1DX	0.1 ppm
Cu	AQ200/1DX	0.1 ppm
Pb	AQ200/1DX	0.1 ppm
Zn	AQ200/1DX	1 ppm
Ni	AQ200/1DX	0.1 ppm
As	AQ200/1DX	0.5 ppm
Cd	AQ200/1DX	0.1 ppm
Sb	AQ200/1DX	0.1 ppm
Bi	AQ200/1DX	0.1 ppm
Ag	AQ200/1DX	0.1 ppm

Table 4.1: Detection limits at ACME Laboratories (Bureau Veritas Upstream) for the different elements. This table includes the methods of analysis for the different elements.

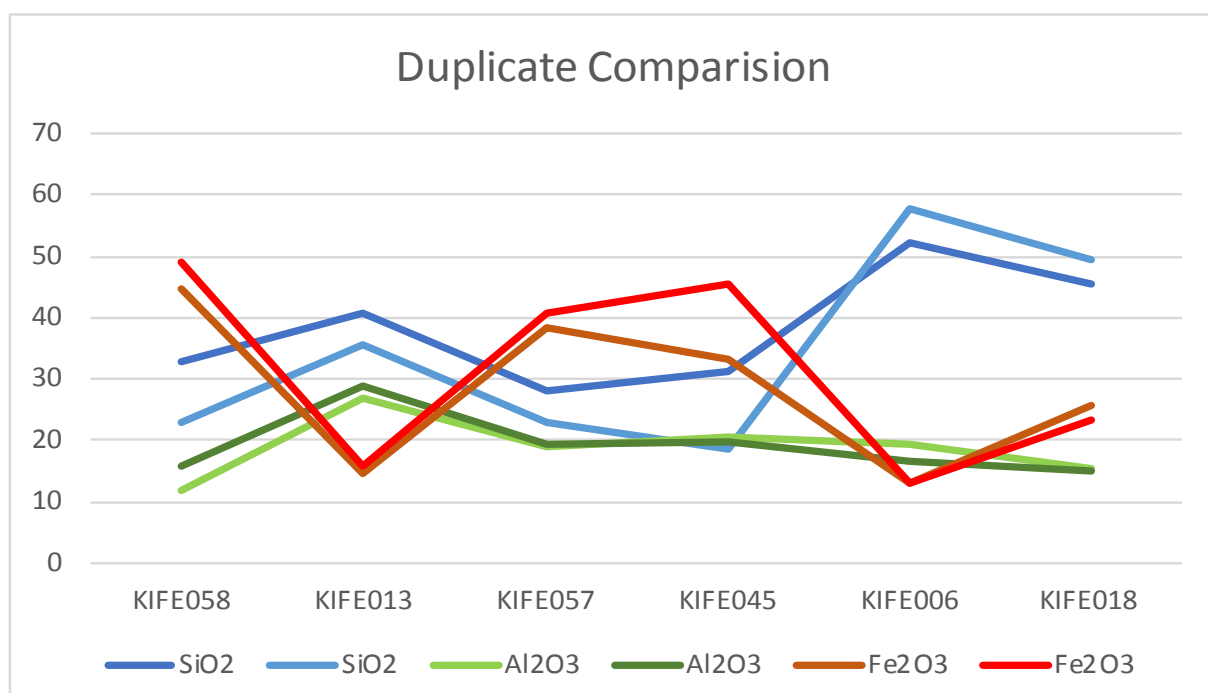


Figure 4.2: Ferricrete in-field duplicates, which display a high degree of variability due to the coarse fractions.

sub-sample of a ferricrete sample with one duplicate being renamed. Due to the coarse materials used in these fractions, the sample variability is quite high (Figure 4.2). Laboratory duplicates created by splitting of solutions at the analysis stage and in-house (ACME) standards, displayed acceptable sample variability and analytical accuracy respectively.

4.3.2. Data treatment

External standard deviation on the in-house ACME standards ranged from 150% (2SD) for element concentrations at or within uncertainty of detection limits down to 2.5% (2SD) with most elements in the range of ~15% (2SD). Figure 4.2 displays the high degree of variability between the in field duplicates, this trend in the major elements is repeated in the trace elements.

A further filter of data quality was used over and above the applied laboratory detection limit. For each element, the maximum external standard deviation (2SD in percent) observed in the in-house standards was added to the detection limit. Any data within this 2SD level of the detection limit (including rounding to the appropriate significant figures)

were discarded to ensure that only data that could be reliably considered to accurately represent the concentrations in the samples were used for data analysis. Some elements display ‘striped’ data in cumulative probability plots which reflect discretisation of the data due to rounding of low concentration values and do not indicate unreliable data.

There were several elements that returned limited results from the geochemical analysis, including: Ag, with only one sample above detection limits; Cd, with seven samples at detection limits (all 0.1 ppm); Tl, with only five samples above detection limits. These elements have been included in the maps in Appendix B, but will not be considered further in the discussion. A number of other elements display discretisation due to rounding including Be, Hg, MnO, Sb and Ta, however as these elements do have a large number of values, they remain in the dataset for consideration.

First pass data analysis used univariate statistics generated with IoGAS (version 6.1) statistical software (Appendix B). The results are presented spatially using ArcGIS (version

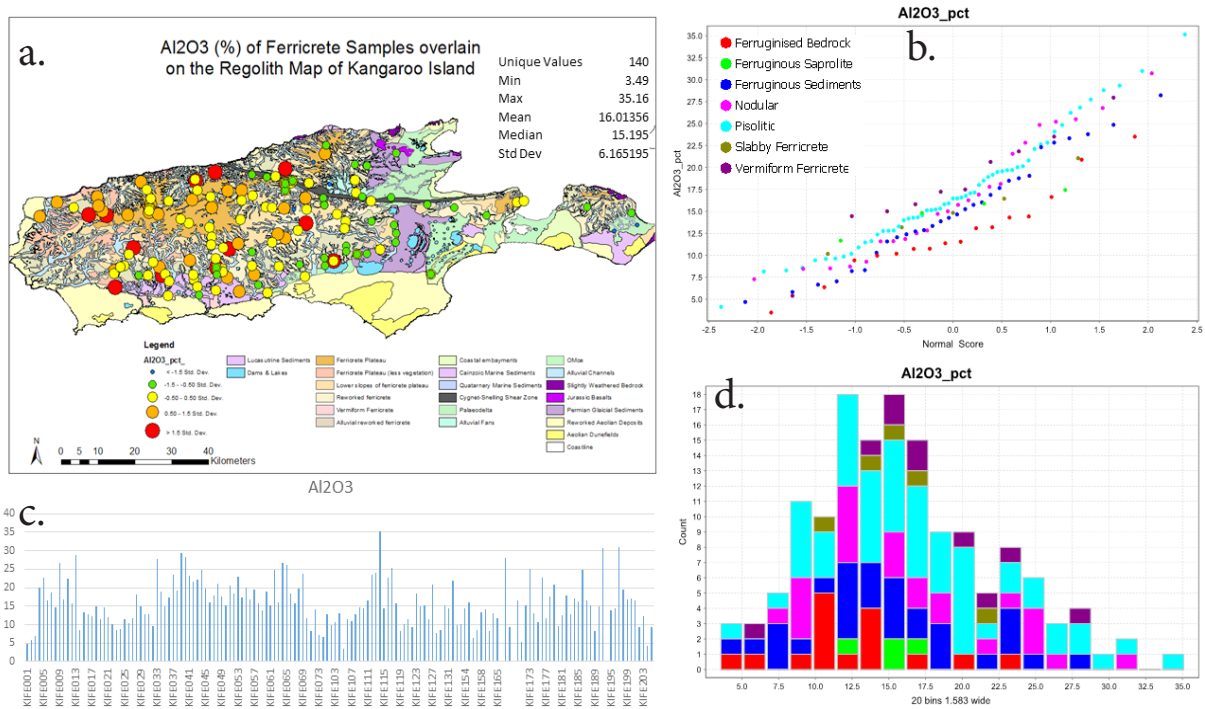


Figure 4.3: First pass data analysis of each of the elements which include: a) map of sample points which are ordered by standard deviation; b) normal probability plots; c) stacked histogram with different species differentiated between; and d) bar charts of samples, to check for periodicity within the samples.

10.3.1) generated maps with concentrations and standard deviations plotted (Appendix B, Figure 4.3). Exploration targets can be broadly defined as ‘Of Interest’ when element concentration values are greater than 1.5–2.5 standard deviations above the median. Data are also displayed on stacked normal probability plots for the geochemical data, with the different ferricrete classifications separated out (Figure 4.3b). This method was also employed to make the data from the ferricrete easily comparable to the data from the biogeochemical surveys. The plots used have element concentration on the ordinate axis and the ‘normal’ score on the abscissa. The ‘normal’ score is an approximation of the means or medians of the order statistics, allowing the data to be assessed in respect to being a ‘normal’ distribution. Ferricrete data are also plotted on logged stacked histograms (Figure 4.3d). The combination of these methods of presentation allows for data to be compared while taking into account the different morphological classifications of the ferricrete.

Multivariate plots were also used to examine the relationships of different elements to each other and to assess element mobility and concentration change due to mass loss or preservation in the rocks. Elements broadly considered to be geochemically immobile (e.g. Zr and Ti) are used to assess volume change in the rocks and also the mobility of other elements, in particular those of economic importance. To assist with this, data from this study are compared to data previously collected by De Pretis (2008) on the unweathered basement Kanmantoo Group on Kangaroo Island. These values allowed for bedrock and the weathered ferruginous material to be compared.

Major element behaviour during weathering was assessed using ternary plots and the Chemical Index of Alteration (CIA), defined by the equation below:

$$\text{CIA} = 100 * [(\text{Al}_2\text{O}_3) / (\text{Al}_2\text{O}_3 + \text{CaO} + \text{Na}_2\text{O} + \text{K}_2\text{O})]$$

The CIA allows for a comparison between fresh bedrock and weathered products, identifying the amount of according to the concentrations of Al_2O_3 , CaO, Na_2O and K_2O (McLennan et al., 2003; Nesbitt and Young, 1982).

There are multiple different weathering indices that have been produced, a comprehensive assessment of these can be found in (Price and Velbel, 2003). Major weathering indices, Table 4.2, including Parker's Weathering Index (1970), Harnois' Chemical Weathering Index (1988) and Nesbitt and Young's Chemical Index of Alteration (1982) were assessed as possible means of evaluating the behaviour of major elements in this system. The CIA and the CIW assume Al to be an immobile element, however, we have already established the Al is mobile in this system. In order to assess another index that did not rely on the immobility of Al, the WR of Chittleborough (1991) (Table 4.2) was also examined.

Table 4.2: Different weathering indices assessed for using in examining the major element behaviours.

Chemical Index of Weathering (Harnois 1988)	$CIW = 100 * [Al_2O_3 / (Al_2O_3 + CaO + Na_2O)]$
Chemical Index of Alteration (Nesbitt & Young 1982)	$CIA = 100 * [(Al_2O_3) / (Al_2O_3 + CaO + Na_2O + K_2O)]$
Weathering Index (Parker 1970)	$WI = 100 * [(2Na_2O/0.35 + (MgO/0.9) + 2K_2O/0.25) + (CaO/0.7)]$
Weathering Ratio (Chittleborough, 1991)	$WR = [(CaO + MgO + Na_2O) / ZrO_2]$

From comparison of plots, it was found the CIW, CIA and WI all returned similar trends and results for major elements. Figure 4.4 displays the trends for the WR, compared with a few plots of the CIA, which does not follow the exact trends as displayed by the other indices. However, this index assumes that Zr is an immobile element, while in this system it is mobile. This index also 'clumps' much of the data together, making comparisons of the weathering rates between the different types of ferricretes difficult. As a result of these examinations it was decided that the CIA would be the weathering index used.

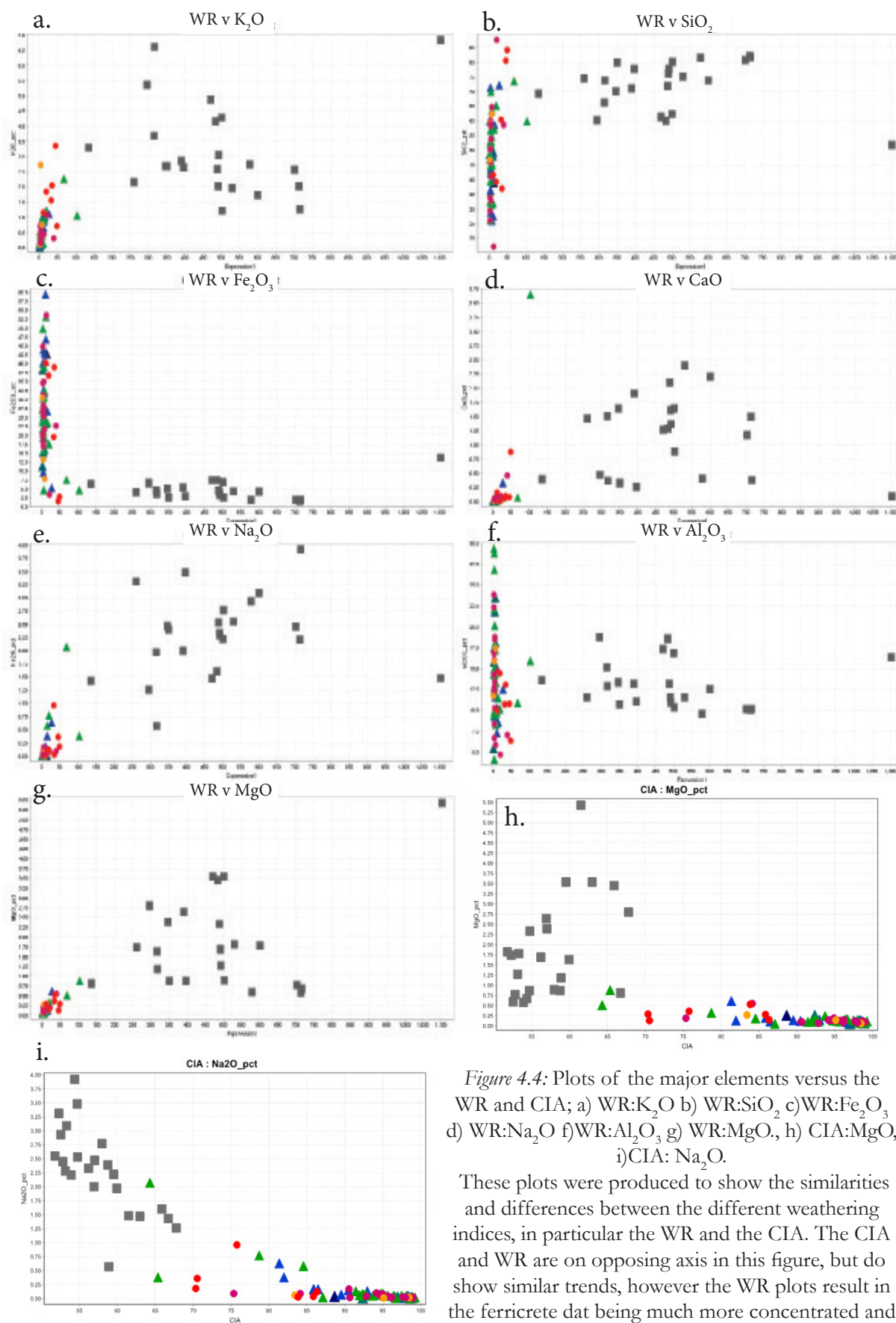


Figure 4.4: Plots of the major elements versus the WR and CIA; a) WR: K_2O b) WR: SiO_2 c)WR: Fe_2O_3 d) WR: Na_2O f)WR: Al_2O_3 g) WR:MgO, h) CIA:MgO, i)CIA: Na_2O .

These plots were produced to show the similarities and differences between the different weathering indices, in particular the WR and the CIA. The CIA and WR are on opposing axis in this figure, but do show similar trends, however the WR plots result in the ferricrete dat being much more concentrated and clumped in a certain part of the graph.

4.4. Results

Data tables are contained in Appendix A, while maps and plots for all elements analysed are in Appendix B.

4.4.1. Major Element Geochemistry

Samples of ferruginous material are dominated by SiO_2 , Al_2O_3 and Fe_2O_3 . A stacked bar chart of the main chemical components of the samples was produced (Figure 4.5), with the unweathered Kanmantoo Group samples included on the left for comparison. All samples were ordered on the y axis by the CIA, defined by Equation 4.1. The decrease in SiO_2 concentration can clearly be seen, with similar or increased Al_2O_3 concentrations, a broad increase in Fe_2O_3 concentrations and a significant increase in the LOI values within the more weathered samples as the remaining elements are removed from the samples. The variation of these major components highlights their mobility during weathering processes,

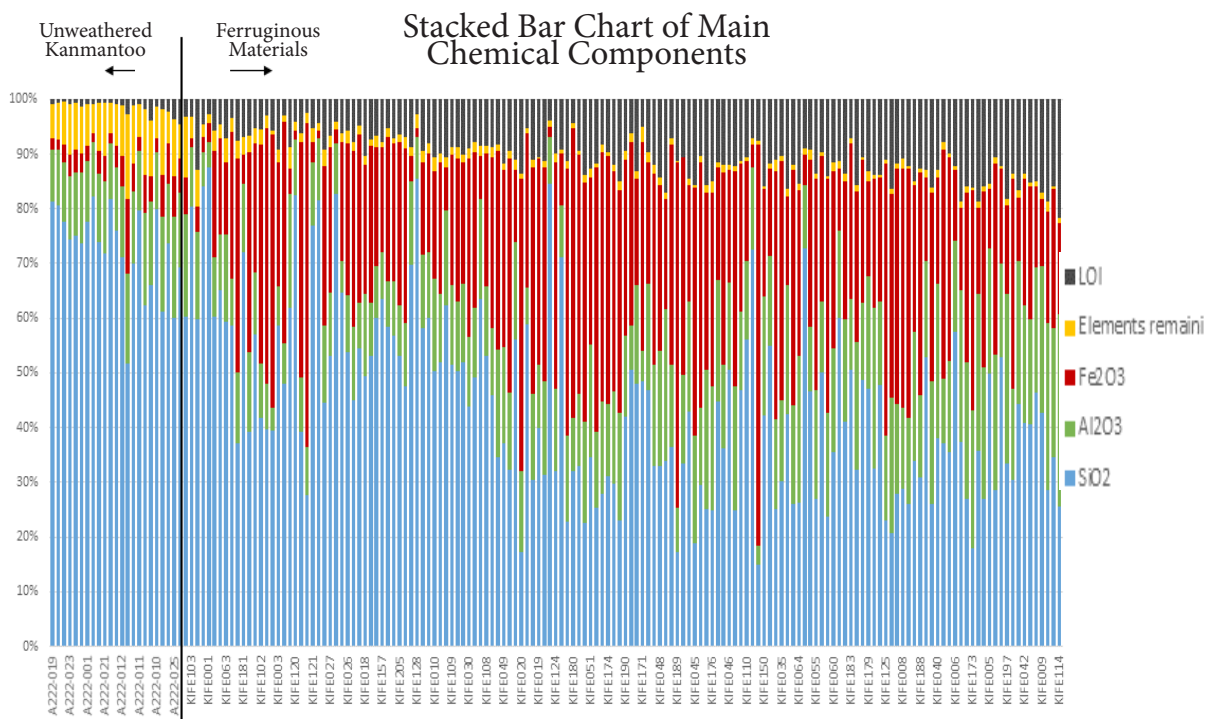


Figure 4.5: A stacked bar chart of the main chemical components SiO_2 , Al_2O_3 , Fe_2O_3 , and the remaining elements and LOI of the samples. Samples are ordered on the y axis by CIA. The Kanmantoo samples are presented on the left for comparison; the ferricrete samples are presented to the right.

as observed in the electron microprobe maps in Chapter 3. Therefore an assessment of mass loss or preservation using immobile trace elements is necessary.

The major elements in the ferricretes, Al_2O_3 , SiO_2 and Fe_2O_3 , have been plotted on a ternary diagram and are compared with the values for the Kanmantoo Group from De Pretis (2008; Figure 4.6). The range in which the unweathered Kanmantoo Group samples sit is used as a starting point for the composition of the parent rocks (Figure 4.6). The majority of the ferricrete samples do not fall within this range. Most of the ferruginised samples display an increase in Fe_2O_3 and an overall depletion in SiO_2 . Aluminium oxide in the ferricretes is very variable but is different from the Kanmantoo Group data and displays either an increase in concentrations or depletion.

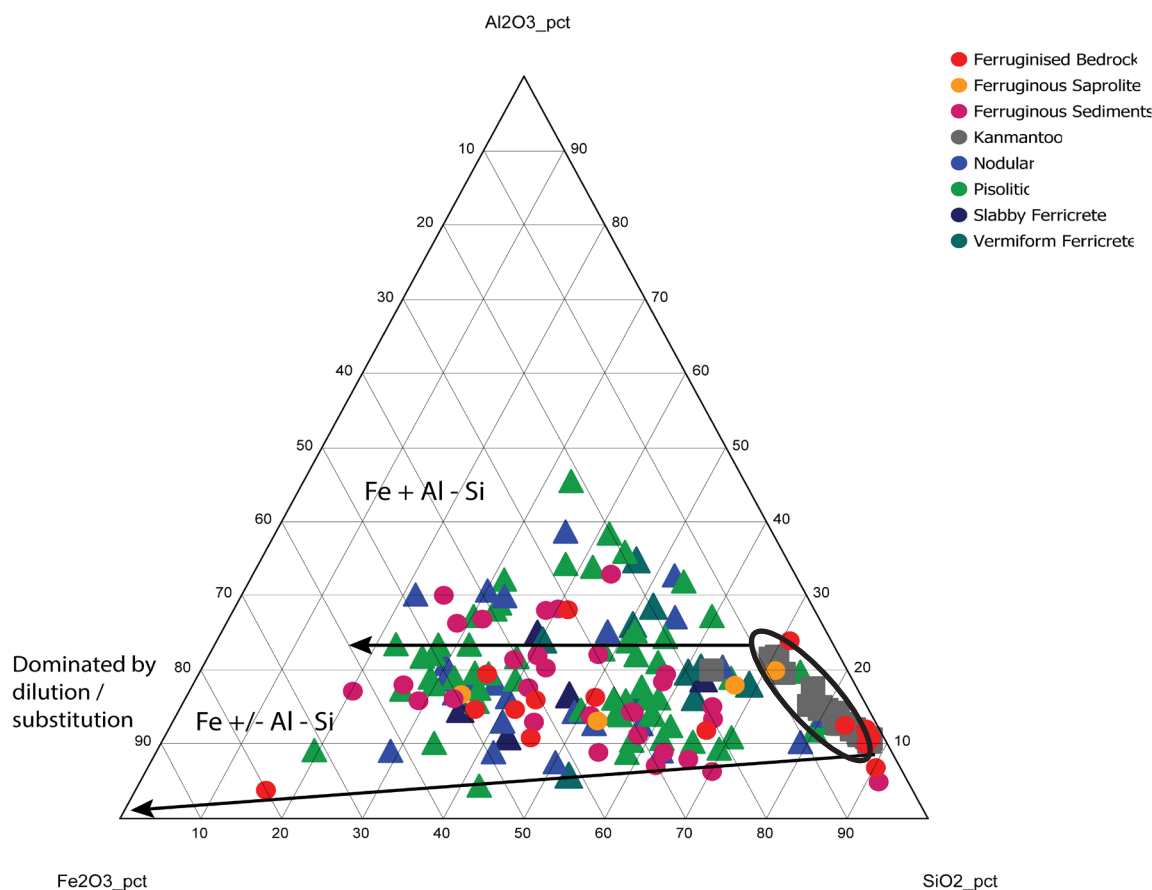


Figure 4.6: Ternary plot of SiO_2 - Al_2O_3 - Fe_2O_3 , with all ferricrete samples, as well as previously sampled Kanmantoo data plotted. The range of the unweathered Kanmantoo rocks is highlighted within the black ellipse, while the possible depletion or enrichment of Al_2O_3 (black arrow) highlight the different weathering trends that can occur.

SiO_2 , Fe_2O_3 , Al_2O_3 , Na_2O , MgO and K_2O are plotted against calculated CIA values (Figure 4.7). These plots show similar trends to the ternary diagrams, with the ferricrete samples displaying depletion in SiO_2 and enrichment in Fe_2O_3 relative to the Kanmantoo Group metasediments. The Al_2O_3 versus CIA ratio is variable, with no consistent trend between the ferricrete and the Kanmantoo Group, or with the ferricrete categories. The amounts of NaO , K_2O and MgO decrease with increasing CIA values (i.e. increased weathering).

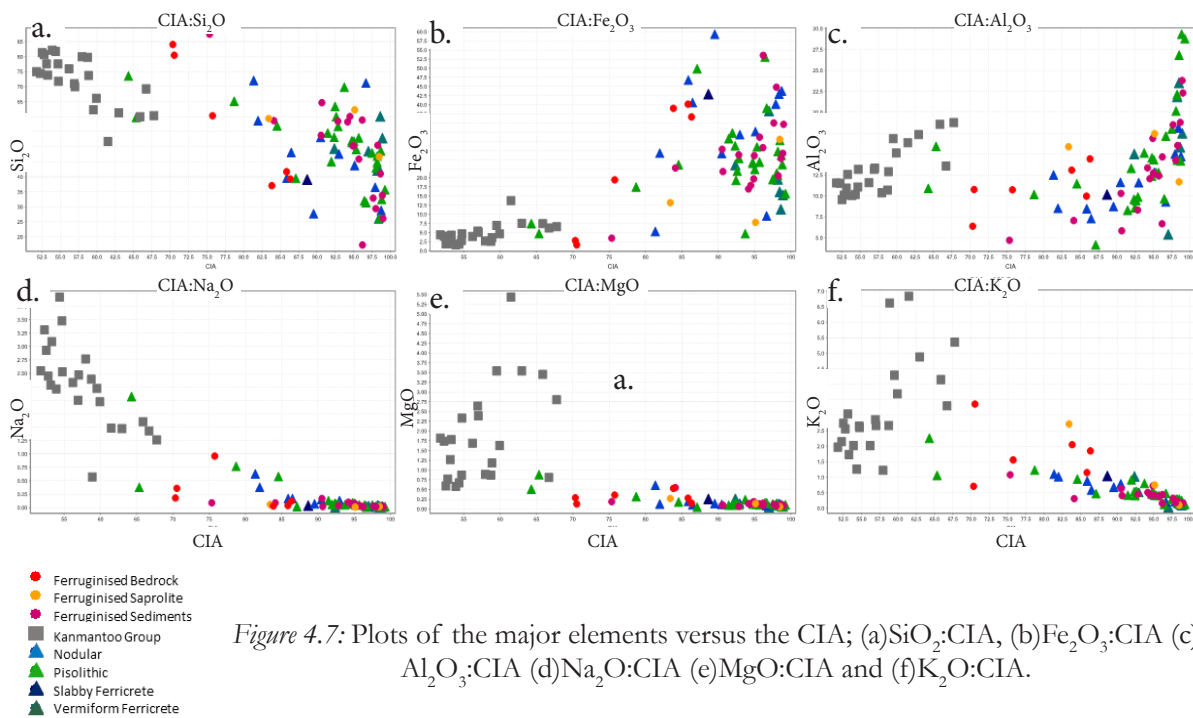


Figure 4.7: Plots of the major elements versus the CIA; (a) SiO_2 :CIA, (b) Fe_2O_3 :CIA (c) Al_2O_3 :CIA (d) Na_2O :CIA (e) MgO :CIA and (f) K_2O :CIA.

4.4.2. Trace Elements

Trace element loss or gain during alteration and weathering processes are often considered against ‘immobile’ elements in order to ascertain the behaviour of each element and determine the role, if any, of mass loss or gain in the rock. Elements that are generally considered immobile (TiO_2 , Nb and Zr) are plotted in Figure 4.8. The linear correlation between TiO_2 and Nb suggests they are immobile, as evidenced by a broadly consistent ratio between the two elements (Figure 4.8a). The overlapping range of concentrations of ferruginous materials to the range observed in unweathered Kanmantoo Group rocks also suggests immobility. Zirconium shows a broadly linear trend with TiO_2 in ferruginous

materials, but this trend is for the most part elevated above the concentrations present in the Kanmantoo Group rocks. The locations of the Kanmantoo Group samples do not exactly correspond to the locations of the ferruginous materials samples, and so it is unclear whether this represents introduction of Zr during the weathering process or simply the heterogeneity of the protolith. Due to this uncertainty, Zr is not considered to be immobile in this study and hence TiO_2 and Nb are used as the immobile reference elements.

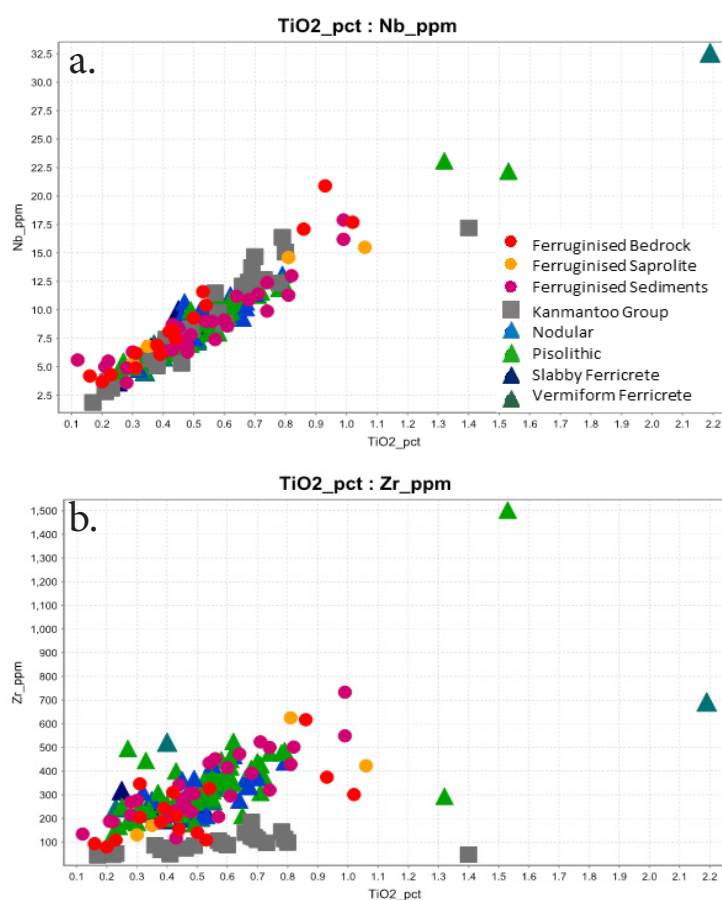


Figure 4.8: Plots TiO_2 versus Nb and Zr.

The trace elements are grouped into four categories based upon their behaviour relative to Fe_2O_3 (Figure 4.9). The four main categories are:

1. Strong, positive linear relationship with Fe_2O_3 , namely V which is the only element to show this behaviour (Figure 4.9a).
2. Weak positive correlation, such as As (Figure 4.9b) but also U and Th.
3. Strong depletions with increasing Fe_2O_3 , such as Rb (Figure 4.9c) Sr, Ba.

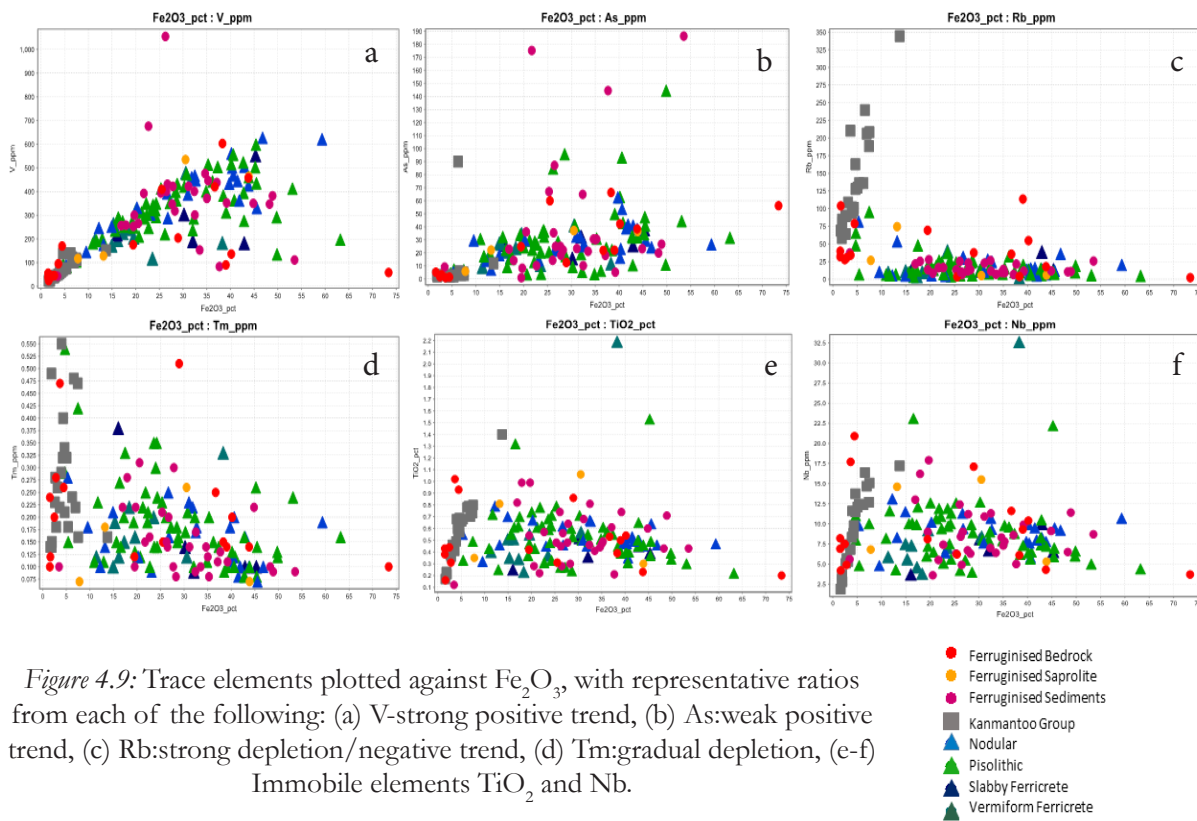


Figure 4.9: Trace elements plotted against Fe_2O_3 , with representative ratios from each of the following: (a) V:strong positive trend, (b) As:weak positive trend, (c) Rb:strong depletion/negative trend, (d) Tm:gradual depletion, (e-f) Immobile elements TiO_2 and Nb.

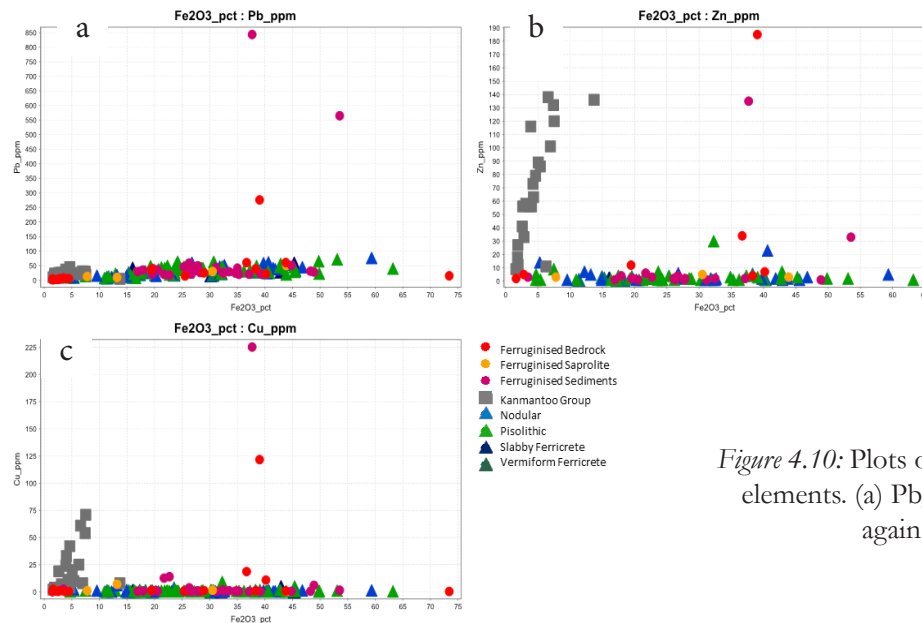


Figure 4.10: Plots of depleted economic elements. (a) Pb, (b) Zn, and (c) Cu against Fe_2O_3 .

4. Gradual depletion of the elements with increasing Fe_2O_3 as observed for the rare earth elements (REEs, Figure 4.9d)

The immobile elements, TiO_2 (Figure 4.9e) and Nb (Figure 4.9c), are displayed relative to Fe_2O_3 .

Economic elements Cu, Pb and Zn are plotted in Figure 4.10 and display similar trend of

depletion to the third group of trace elements (Rb, Figure 4.9c). In each of the outlined categories there are localised elevated levels associated with distinct geographical trends and/or proximal to mineralisation or the Cygnet-Snelling Fault Zone (Figure 4.11).

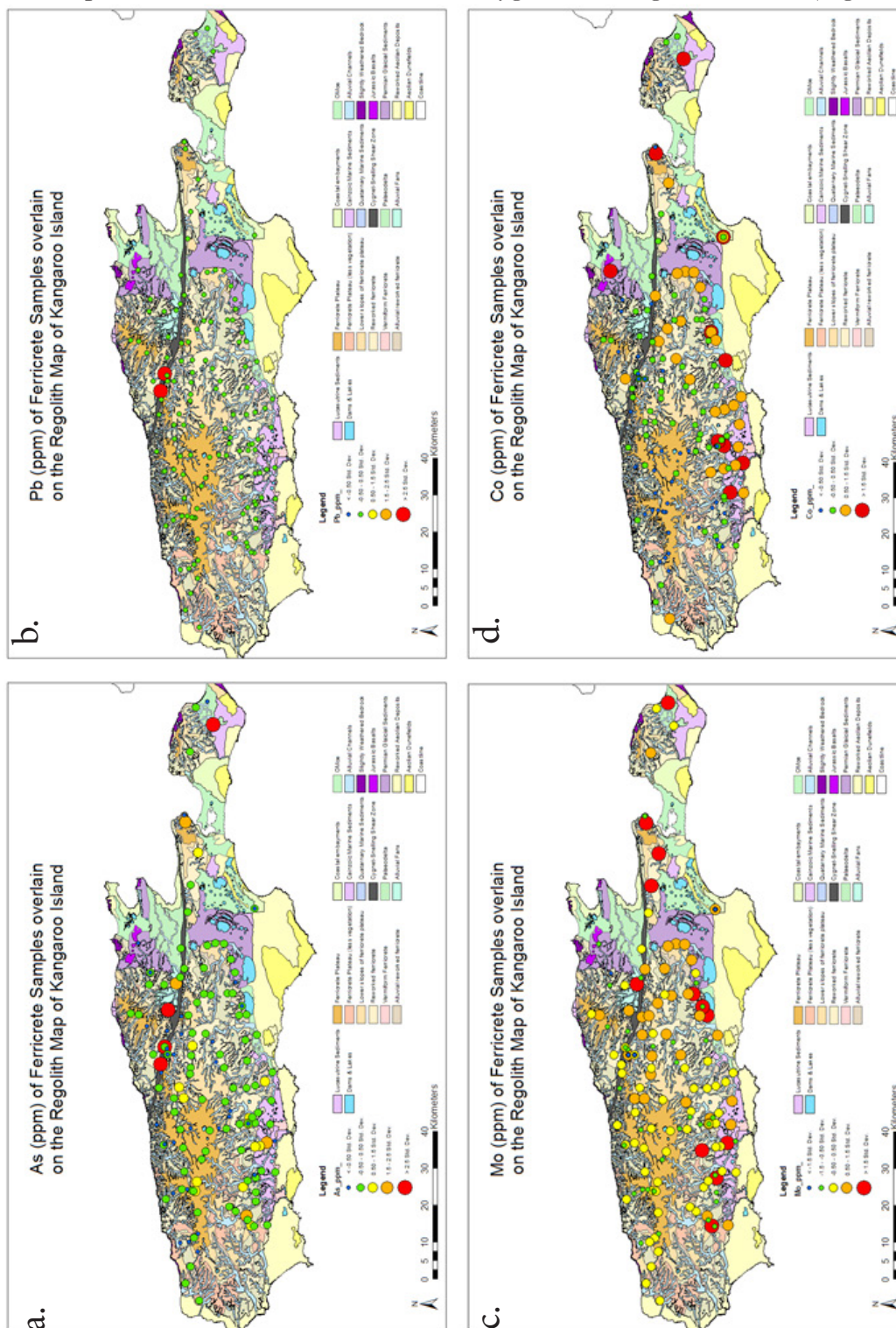


Figure 4.11: Kangaroo Island regolith-landform map, with the ferricrete sample points illustrating elevated levels of economic elements on the Cygnet-Snelling Fault Zone in a and b. Images c and d display the elements that have a particular geographic correlation, in this case with the edges of the ferricrete plateau.

4.5. Discussion

The microanalysis of ferricretes, presented in Chapter 3, determined three main stages in the formation of the ferricretes on Kangaroo Island:

1. Breakdown and weathering of feldspars and the re-mobilisation of iron and aluminium to form 'simple' ferricretes.
2. The formation of the 'complex' ferricretes, which includes wetting and drying cycles to create the cutans of pisoliths.
3. The mobilisation of key indicator/trace/economic elements

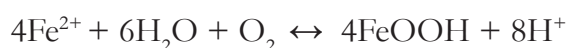
The above points highlight the physically observable processes, however, these need to be confirmed on the larger scale by geochemical data from across the survey area. As a result of the whole rock geochemical data collected in this study, other important factors in the formation and understanding of ferricretes have been identified and are discussed in detail below. These factors are:

1. The breakdown and weathering of feldspars and plagioclase.
2. The depletion of SiO_2 , an increase in Fe_2O_3 and variable mobility of Al_2O_3
3. Determination of mobile and immobile elements
4. The possible mobilisation of key indicator/trace/economic elements (Pb, As, Cu, Bi, Sb) all centred along the Cygnet–Snelling Fault Zone.
5. The range and variability of the chemistry displayed by the ferruginous materials which make it exceptionally difficult to determine chemical classifications.

4.5.1. The breakdown and weathering of primary material and the mobility of the major elements

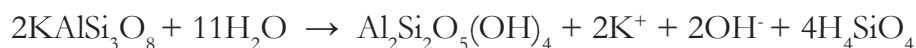
The general behaviour of SiO_2 , Al_2O_3 and Fe_2O_3 during weathering and ferruginisation of Kanmantoo Group rocks is readily assessed from the bar chart in Figure 3. Microanalysis of the different materials determined that the Kanmantoo Group was the most likely parent

material of the ferricretes on Kangaroo Island (Chapter 3). The bar chart clearly shows the mobility of SiO_2 and Fe_2O_3 during weathering, with a decrease in the concentration of SiO_2 , increase in the concentration Fe_2O_3 and an increased proportion of material that was subject to LOI relative to the Kanmantoo Group. The Al_2O_3 percentage is variable, with some samples displaying an increase from the proportions seen in the unweathered Kanmantoo, whereas other samples have similar concentrations. The mobilisation of Fe_2O_3 seen here can be explained through the chemical process of ferrollysis. The concept of ferrollysis was introduced by Brinkman (1970) to describe the formation of a particular type of soil, with clay decomposition and interlayering in seasonally wet, acidic soils (Brinkman, 1970; Van Ranst and De Coninck, 2002). Mann (1983) used the following simplified ferrollysis equation to describe the mobilisation and precipitation of Fe for laterite in the Yilgarn block.



Equation 4.2: Simplified ferrollysis equation, where the oxidation and hydrolysis of ferrous iron can equate to an increase in the acidity of the subsurface Mann, (1983).

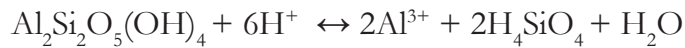
This explains the oxidation and hydrolysis of ferrous iron (Fe^{2+}) and results in increase in the acidity of the subsurface (Mann, 1983). This acidity and lowering of pH will impact on the concentration of Al, due to the increased weathering of kaolinite. This is due to the weathering of sheet silicates to form quartz clay saprolite as a concurrent process to ferrollysis. Equation 3 describes the weathering of feldspar to form kaolinite (Mann, 1983).



Equation 4.3: The weathering of feldspar to kaolinite equation, from Mann, (1983).

This breakdown of feldspars results in an increase of kaolinite, which will then readily breakdown in acidic environments. As seen from Equation 2, the ferrollysis of ferrous

iron results in the production of acid, and the process of the breakdown of kaolinite is summarised in equation 4.4.



Equation 4.4: Breakdown of kaolinite to silicic acid, water and Al cations, from Ambrosi et al., (1986).

The breakdown of the kaolinite releases Al cations, which results not just in a dilution of Al and Si with the introduction of Fe, but the active movement of Al and Si out of the system. This movement of Al, and presumably other ions, in solution can then be incorporated into the Fe-oxides. As the breakdown of kaolinite also produces acid, the two processes can cause a continuous cycle, as both Fe and Al are further mobilised by acidic environments, and the mobilisation reaction itself produces more acid (Mann, 1983).

The breakdown of kaolinite that is part of the process of ferrollysis and mobilisation of Al ions is also demonstrated by the Chemical Index of Alteration (CIA), which is used as a measure of the degree of weathering of a material (Equation 4.1). The CIA is plotted against major elements including Al_2O_3 , SiO_2 and Fe_2O_3 in Figure 4.7. This figure clearly shows the depletion of SiO_2 and enrichment of Fe_2O_3 as the samples become more weathered and the variable nature of the Al_2O_3 . The concentration of Al_2O_3 increases only at very high levels of weathering, suggesting that prior to this point the increasing CIA is largely a function of removal of CaO, Na_2O and K_2O from the system, potentially accompanied by some loss in total abundance of Al_2O_3 . In highly weathered samples Al_2O_3 is added to the system. This is consistent with the evidence provided in Chapter 3, where Al_2O_3 enrichment occurred at the rims of the pisoliths. This suggests that the breakdown of the kaolinite and mobilisation of Al occurs well after the introduction of Fe has commenced.

4.5.2. Mobile and Immobile elements

The mobilisation of the major element oxides Al_2O_3 , Fe_2O_3 and SiO_2 is obvious from

the ternary plot shown in Figure 6 as well as in the comparison to the CIA (Figure 4.7). Elements that have previously been interpreted as immobile during weathering, including REE, Zr and TiO_2 were also examined (Barnes et al., 2014). The graphs in Figure 4.8 show that TiO_2 and Nb can be considered immobile. However, Zr appears to show a systematic increase in the weathered material compared to the unweathered Kanmantoo Group rocks. The weathering process generally decreases the density of the parent material (i.e. mass loss) which could account for an increased concentration of an immobile element such as Zr. However, as TiO_2 and Nb show similar concentration ranges between the protolith and weathered samples, it is unlikely that sufficient mass loss occurred to enrich Zr to this extent. This leaves the possibilities that the protolith material is heterogenous and/or that Zr was introduced into the system. The Kanmantoo Group is not a homogenous lithological unit, and this is likely to be reflected in the geochemistry of the regolith. From previous geochemical surveys, the natural concentration of elements will vary dependent upon the parent material and the subsequent soil forming processes (Cohen et al., 2012a, 2012b). However, given the size of the enrichment over the majority of protolith samples, it also seems likely that some Zr mobility and introduction was experienced during the weathering process. Further detailed studies on small-scale, *in-situ* weathering profiles would need to be undertaken to establish the relative roles of protolith heterogeneity and Zr enrichment. The large ion lithophile elements (LILE; Rb, Sr, K_2O) show a gradual depletion trend with increasing ferruginisation. These elements are incorporated into the lattice of feldspar group minerals and/or micas and their gradual depletion can be interpreted to effectively mirror the breakdown of these major minerals. These cations therefore have similar major mineral phase-controlled behaviour as Al_2O_3 , but lack the final enrichment in highly ferruginised samples as demonstrated by Al_2O_3 , that is presumably the result of precipitation of Al_2O_3 on features such as pisoliths (Chapter 3). The high field strength elements (Zr, Nb, Hf, REE, Th, U and Ta) show variable behaviour, perhaps reflecting their variable host phases within the protolith. Niobium appears to be immobile, REEs tend to show mobilisation and progressive depletion, Zr shows enrichment and Th and U show strong enrichments.

Rare Earth Elements are likely to be predominantly contained within accessory minerals such as zircon, apatite, xenotime, allanite and monazite which are often resistant minerals during surficial processes. The gradual depletion may reflect the gradual breakdown of these minerals with very high degrees of ferruginisation. The Zr enrichment suggests that zircon is not breaking down and/or any breakdown of zircon does not include removal of the Zr from the system, and indeed more Zr appears to be introduced into the system. Uranium, and to a lesser extent Th, is highly mobile in oxidising environments. Hence it is reasonable that U would be mobile in the acidic oxidising conditions present during ferruginisation, with U being introduced external to the sampled rocks.

The behaviour of V in this study is near unique when compared to the other elements, showing a strong correlation to the concentration of Fe_2O_3 in the weathering products (Figure 4.9a). Vanadium has previously been demonstrated to fill a structural position in Fe oxides (Gehring et al. 1994; Schwertmann and Pfab 1996; Taylor and Giles 1970) and the behaviour observed here is consistent with this.

4.5.3. Behaviour of the economic elements

The economic metals (e.g. Cu, Pb, Zn, W) generally show strong depletion with increasing Fe_2O_3 and are largely found in the third category outlined above. Unlike the REES or LILEs which show gradual depletion, the economic metals appear to be depleted and mobilised out of the protolith as soon as weathering commences. This behaviour is arguably broadly consistent with the mineral host of the metals being sulphide minerals that are easily and rapidly degraded by oxidising and acidic conditions, which occur during the ferrolysis process. Localised elevated levels that occur proximal to mineralisation, (Cu, Pb, Zn and As) as highlighted in Figures 4.11 and 4.12. These proximal highs may either be due to extremely high initial values or a multiple-step process.

At a location such as Bonaventura, Cu, Pb and Zn may be leached from the rocks but are

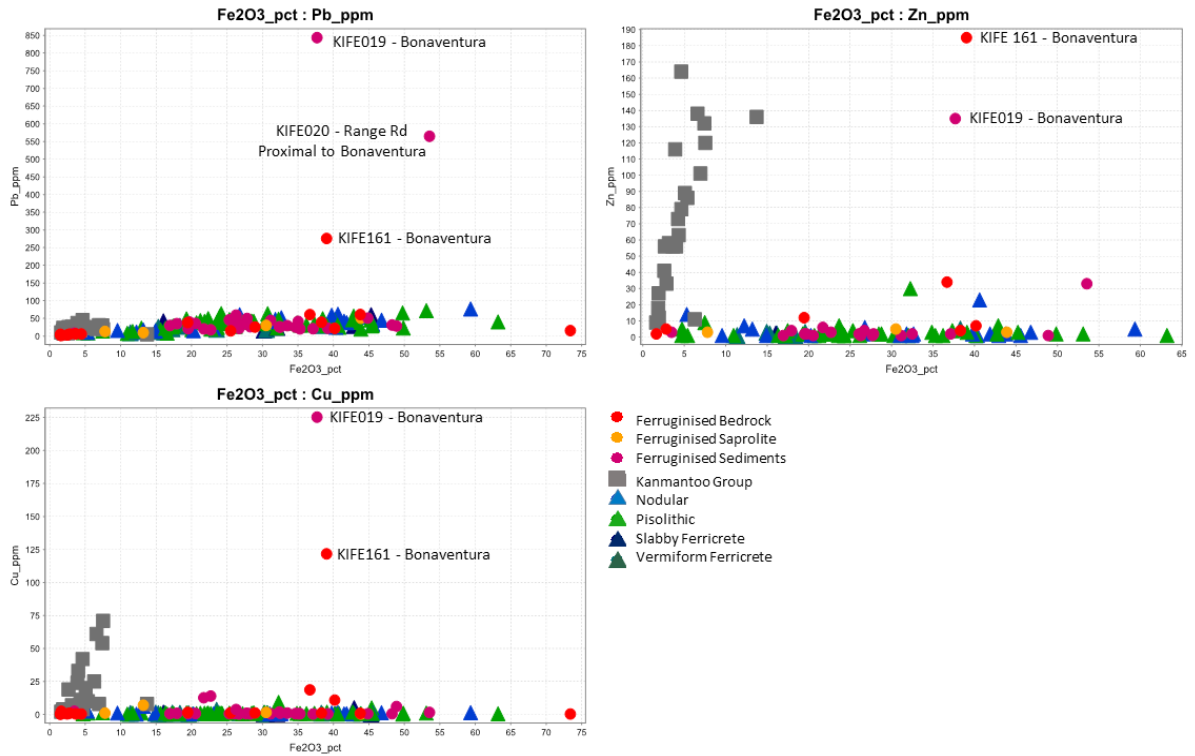


Figure 4.12: Plots of depleted economic elements, Pb, Zn, and Cu against Fe_2O_3 . The mineralised sites are highlighted and show elevated concentrations of economic elements.

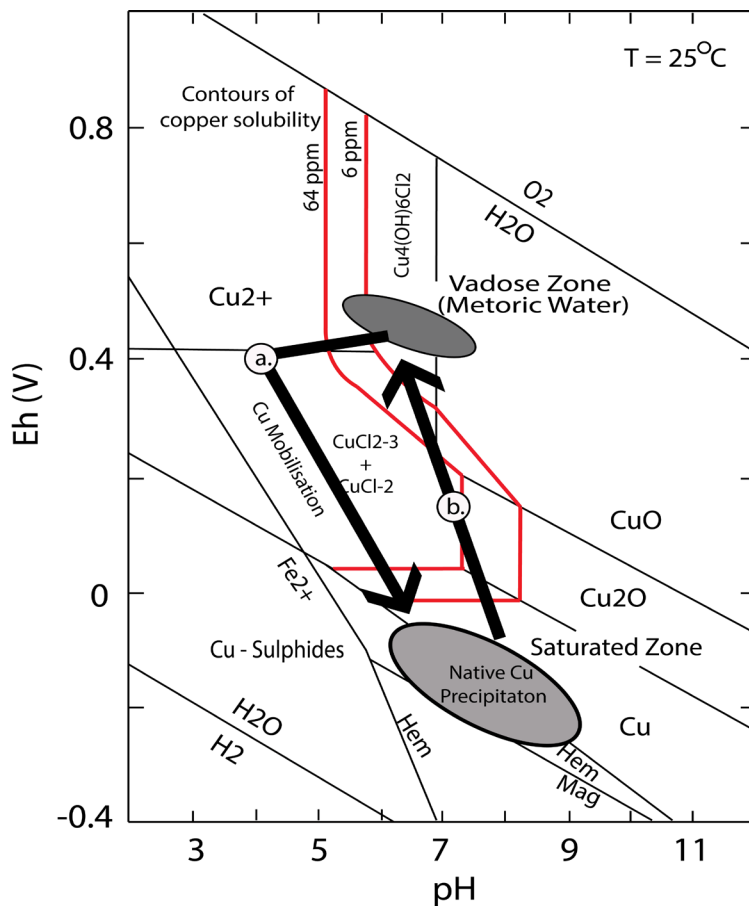


Figure 4.13: Eh-pH diagram which demonstrates the different conditions at which Cu will be soluble in groundwater and precipitate out of groundwater, from Brown, (2009). Pathway a. is the process of ferrollysis, and a rise in groundwater; pathway b. is fallig groundwater and the increasing influence of meteoric water.

then overprinted by the mineral system anomaly. The acid weathering system mobilises these elements, but they can be dropped out when the system returns to more neutral conditions, as demonstrated by the Eh–pH diagram in Figure 4.13. Neutral conditions can occur via movement of the materials towards the surface through erosion, leading to a greater influence of meteoric water on the materials, rather than acidic groundwater. A cyclic changing of groundwater sources and conditions is indicated by the cyclic growth of pisoliths, and hence a similar process may control the localised concentration of economic metals in the regolith above mineralisation. The reintroduction of the economic metals (or at least the remobilisation) is consistent with the findings of Chapter 3.

As there is no direct relationship between Fe concentrations and the economic minerals, and the economic metals are commonly highly depleted in the ferruginous materials, it raises the question as to whether these materials make a good sampling media. Although the ferruginous materials are generally depleted in economic elements, they do record enrichment in areas where there is known mineralisation. This means mineralised sites do stand out well against the non-mineralised, background locations. However, the samples must be taken within a reasonable proximity to the mineralisation to yield anomalous concentrations. At the sampling density used in this survey, exploration targets are quite small with little surrounding vector indicators. Using a smaller survey size may provide much better results in this regard. Therefore, using ferricretes for regional geochemical surveys may miss anomalies if the sample density is too large, or the mineral system too small.

4.5.4. Geochemical classification of ferricretes

Previous authors, such as Bourman (1989) and Schellmann (1981), have attempted to use geochemistry to better classify ferricretes. These classification schemes are plotted in the ternary diagram in Figure 4.14. The datasets used by Bourman (1989) and Schellmann (1981) do not display the same extent of variability that is present in the ferricrete results

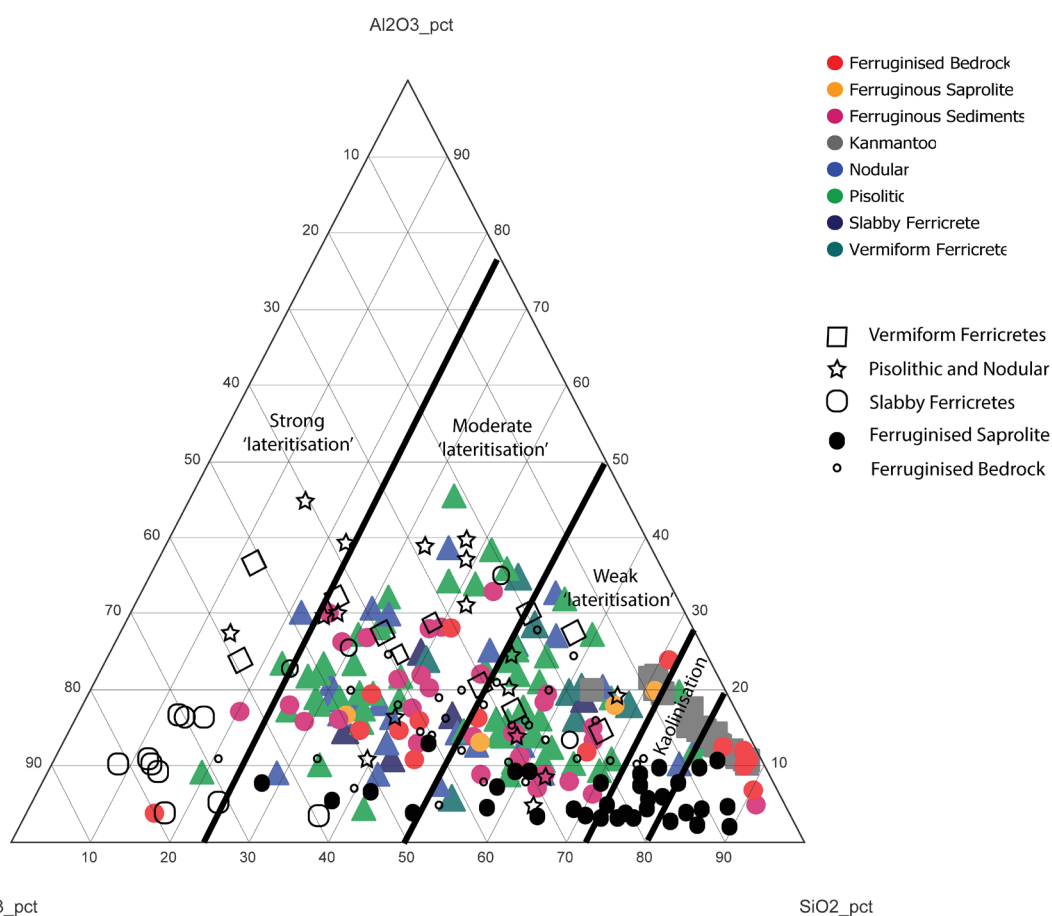


Figure 4.14: Ternary diagram of SiO_2 , Al_2O_3 , Fe_2O_3 , overlain with different classification systems. The black shapes are the classification system employed by Bourman (1989), and is the classification system used in this thesis. The classification system of Schellmann (1981), dividing samples by their degree of 'lateritisation' is also overlain.

analysed in this study. The morphology of the ferricretes, classified in hand sample, is not reflected in distinct geochemical compositions. There are clearly some samples that have been misclassified in hand-sample, such as sample KIFE105, which, although having landscape features suggesting it was an exceptionally ferruginised saprolite, contains Fe_2O_3 and Al_2O_3 contents that are more consistent with the classification of a complex ferricrete. However, despite the potential for some hand-specimen misclassification it is still not possible to correlate the ferricrete chemistry with the actual morphology. As there are no distinct geochemical features lending themselves to classifications, the best way in which to classify ferricretes is through the continued use of the morphology, where the landscape setting and form of the ferricrete is the primary means of classification and in a large respect determines the sampling media.

4.5.4. Geochemical Mapping

The maps produced in Figure 4.11 highlight a number of spatially meaningful patterns in the dataset. The economic elements (Cu, Pb and Zn) show highs centred on the Cygnet–Snelling Fault Zone and known mineralisation (Figure 4.11a, b). Elevated levels of (Co, Cs and Mo) occur in some samples along the edges of the main ferricrete plateau. However, these highs are not reflected within the ferricrete morphologies and they are considered to represent the possible leaching of mobile elements at groundwater table discharge points. The processes and results reflected in the geochemistry of the ferricretes suggest that regardless of the leaching of elements early within the weathering process, in certain circumstances ferruginous materials can be of use for mineral exploration.

The survey size and associated sampling density was appropriate for this study, as it was able to display differences within the sampling media, and pinpoint areas of known mineralisation. Previous studies (Gustavsson et al., 1994; Salminen and Tarvainen, 1997) have sampled soils. However, in terms of efficiency and time, sampling the ferruginous materials for this type of regional survey is perhaps the best option. Soil sampling in this area would have been difficult, as there is a limited soil profile on the island. The ferruginous materials display a signal over areas of known mineralisation, extensively cover the survey area and are easily sampled and therefore were an appropriate sample media in this survey. Soil sampling may be more appropriate for areas where a smaller density survey is being undertaken, such as a local-scale survey.

4.5.5. Implications for mineral exploration

Ferruginous materials can be useful as a sampling media for mineral exploration. This survey showed that samples surveyed over areas of known mineralisation returned results with elevated levels of economic elements. However, the limitation of these materials in a larger, regional scale survey is that the signals and indicators of mineralisation can be easily missed if the samples are not taken in the immediate vicinity of mineralisation. This is due to the

lack of an alteration halo or dispersion patterns with the geochemical materials. Overall, the geochemistry of the ferruginous materials can be useful, if viewed as a composite signal of an area rather than a discrete point. This will depend in some part on the landscape setting of the sampled material, as if the material is likely to have been transported any great distance, i.e. a pisolith from the main plateau, then it will be unlikely to provide a signal of that area. Samples of vermiform ferricretes that contain a mix of different pisoliths are best treated with care, as it would be difficult to determine where any anomalies had actually derived from. Ferruginised bedrock or saprolite samples presumably contain signals for the movement of groundwater in the immediate vicinity, and as a consequence are perhaps the most reliable of the ferruginous materials.

4.6. Conclusions

The primary purposes for this study were to investigate the processes involved in the formation of the ferricrete and to investigate aspects of geochemical mapping and the possible geochemical classifications of the ferricrete. Classification of the ferricretes on the basis of the geochemical data was not possible due to a lack of definable geochemical characteristics associated with ferricrete morphology. The geochemical evidence in this survey supports the findings of the microanalysis in the previous chapter. The influence of ferrolysis in the depletion and enrichment of principal components continued to be seen within the geochemical data. The geochemistry has also demonstrated the depletion of trace elements and the re-introduction of the economic elements that were thought to be occurring from the micro analysis, but, apart from Cu, were not able to be imaged. We have established that the ferruginous materials were the appropriate sample media for the geochemical mapping of Kangaroo Island, due to abundance, distribution and ease of access. The regional sampling den was appropriate for this type of first pass survey and was able to distinguish signal of mineralisation and determine some of the processes that are operating to form the ferruginous material

Chapter 5

Biogeochemical Surveys of Kangaroo Island

Foreword

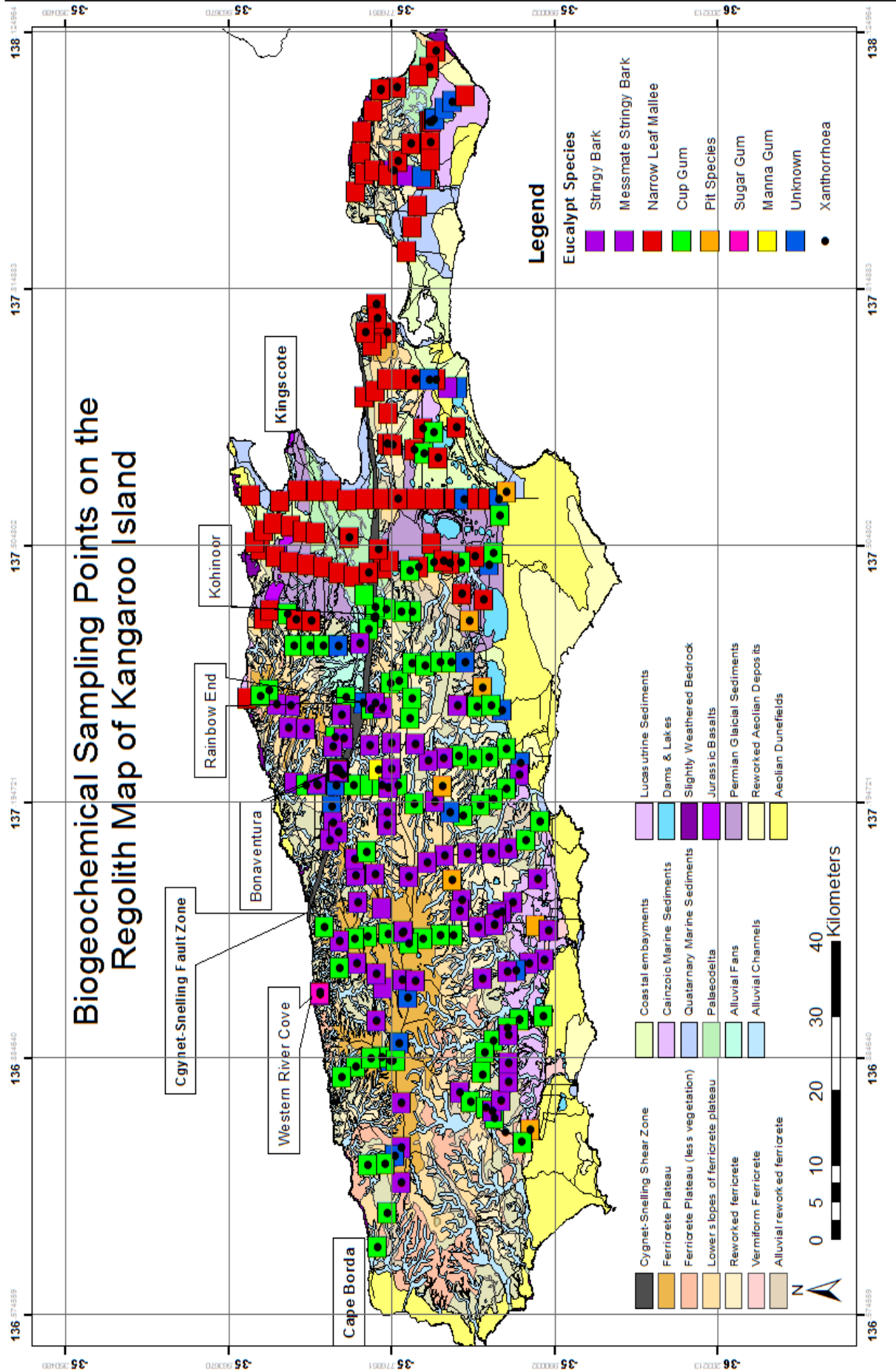
Biogeochemical surveys were undertaken in conjunction with the regional scale geochemical survey of ferruginous materials on Kangaroo Island. The aim of these surveys was to explore the possibilities of using biogeochemistry as a tool for mineral exploration under cover, as well as producing a database for the direct spatial comparison of geochemical and biogeochemical results. In all cases, biogeochemical samples were taken as close to the ferruginous geochemical samples as possible to minimise spatial variation between the different samples.

Two biogeochemical surveys were conducted, Figure 5.1. The first survey used xanthorrhoea, or grass trees, due to their widespread coverage across the island. The second survey utilised several eucalypt species. The two biogeochemical surveys could then be directly compared, and any differences noted and investigated in the context of varying depths of bedrock geology and regolith types of the different plant species. The two surveys identified that the xanthorrhoea biogeochemistry reflects the upper parts of the regolith, whereas the eucalypt biogeochemistry reflects an expression from deeper in the subsurface and the bedrock.

5.1. Introduction

Biogeochemistry is the study of the concentrations of chemical elements in vegetation, with the aim of gaining more information regarding the geology and chemistry of the substrate. It is based on the assumption that elements of interest in the bedrock, and thus overlying soil, will be accumulated in plants growing within the soil and as a consequence anomalous levels of an element in vegetation equates to anomalous levels within the soil (Brooks, 1972). Biogeochemistry was used extensively in the former Soviet Union from the 1930s (Brooks, 1972), however it has only gained traction within Western countries such as the US, UK, Canada and Australia since the 1960s (Brooks et al., 1995). It has proved to be particularly useful in areas of transported regolith and glacial cover where bedrock is not easily accessible. Within the last few decades this method has increasingly been used for mineral exploration in Australia (Arne et al., 1999; Cohen et al., 2010; Hodkinson et al., 2015; Lottermoser et al., 2008; Reid and Hill, 2010, 2013; Reid et al., 2008). Biogeochemistry particularly is a relatively low cost method in terms of time, human resources and minimal environmental impact, especially in comparison to drill rigs.

Biogeochemistry has been shown to be effective in arid areas (Hodkinson et al., 2015; Lintern, 2007; Reid and Hill, 2010, 2013; Reid et al., 2008, 2009), where plants have deep root systems with ‘sinker’ or tap roots accessing the underlying groundwater, illustrated in a cartoon in Figure 5.2 (Anand et al., 2016; Canadell, 1995, 1996). The Mediterranean climate of southern Australia, with seasonal hot dry summers and cool, wet winters, makes it an ideal place to study the effectiveness of using different plant species as a means of mineral exploration. In particular, eucalypt species have been shown to have a deep tap root that allows for foliage to be used as a proxy for the elemental characteristics of the underlying groundwater and lithology (Figure 5.2; Arne et al., 1999; Hill, 2004; Hodkinson et al., 2015; Hulme and Hill, 2004, 2005; Mitchell et al., 2015; Reid and Hill, 2010)). Non-essential elements, such as the economic metallic elements, have been shown to be taken up by plants and stored, rather than excreted (Brooks et al., 1995; Dunn, 2011). Previous studies



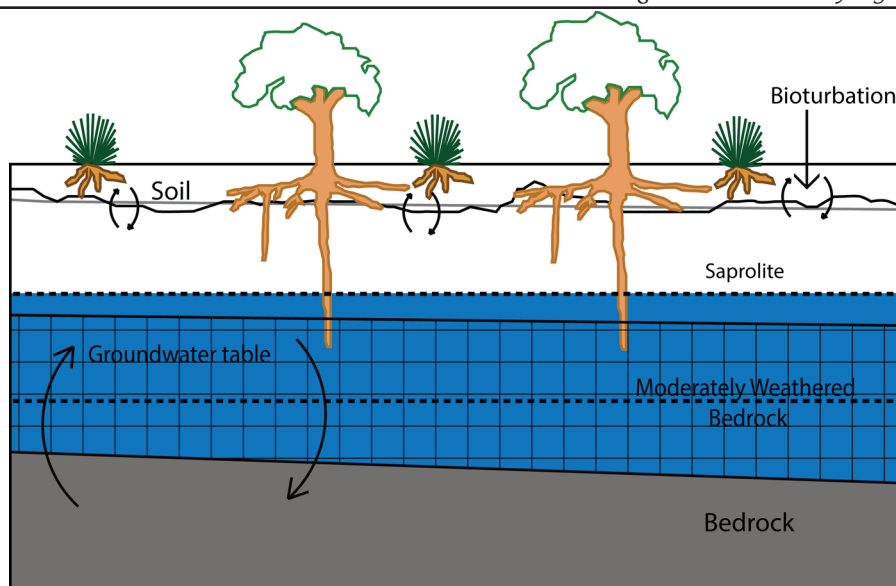


Figure 5.2: Schematic cross section of the biogeochemical system, adapted from Anand et al. (2016), showing the deeper root systems, in particular the ‘tap’ root of the eucalypt trees, compared to the xanthorrhoea. The influence of bioturbation within the upper layers of the saprolite and the soil profiles are also highlighted.

Figure 5.1 (Opposite Page): Map of Kangaroo Island with biogeochemical sampling points, showing the four mineralised case study areas and the Cygnet Snelling Fault Zone, overlain on the regolith map of the island from Chapter 2. Kingscote and Cape Borda are noted as this is where rainfall measurements are taken from. The biogeochemical sampling points are differentiated between the main species of eucalypt sample by coloured squares (the corresponding species to colour is noted in the legend) and the xanthorrhoea are marked by the small black dots.

in Australia using biogeochemistry for mineral exploration tended to be based in arid and semi-arid areas and sample media included eucalypt, acacia and melaleuca species as well as spinifex grasses, which have been shown to have a root system penetrating up to 30 m in poor soils (Cohen et al., 1998; Hulme and Hill, 2004; Lintern et al., 1997; Lottermoser et al., 2008; Reid and Hill, 2010, 2013; Reid et al., 2008). Studies using eucalypt species for biogeochemistry have utilised river red gums, particularly along creeks and other ephemeral waterways (Hulme and Hill, 2003, 2004, 2005; Mitchell et al., 2015), as well as other eucalypt species that were locally abundant in the study areas (Arne et al., 1999; Lintern, 1997, 2007).

Kangaroo Island provides an ideal area to perform a survey (Figure 5.1) to test biogeochemical methods on a regional scale due to its small population, limited anthropogenic pollution, widespread coverage of native vegetation and known mineralisation occurrences.

There were a number of aims in this survey, which were; to compare the biogeochemical signature in areas of known mineralisation to those that are ‘background’; to examine the

zonation of mineral signatures in this landscape setting; and to examine the potential of biogeochemical surveys to help in the characterisation of the regolith and landscape evolution. Ideally a biogeochemical study would utilise a single plant species, however, there is no single species of deep rooting plant that is sufficiently widespread or consistently distributed across Kangaroo Island. As a consequence, the five most prevalent and wide ranging of the Eucalyptus species and a single species of grass tree were used as sample media. The Kangaroo Island narrow leaf mallee (*Eucalyptus cneorifolia*) was the most commonly sampled species in the coastal regions with sandy soils, whereas cup gums (*Eucalyptus cosmophylla*) and stringy barks (*Eucalyptus baxteri* & *E. obliqua*) were the most commonly sampled species on the ferruginous upland areas of the island. Sugar (*Eucalyptus cladocalyx*) and manna (*Eucalyptus viminalis*) gums were also sampled in some areas, particularly around the mineralised zones. There was only one species of the xanthorrhoea sampled, *Xanthorrhoea semiplana*, which has a wide distribution across the island, no preferred soil type, and a vertical root extension of up to 3 m, dependent of the species (Canadell, 1995; Borsboom, 2005).

5.2. Background

The ever-increasing precision of instrumentation has allowed for low-level (ppb) concentrations of elements in plant material to be determined, and this has been integral to the advancement of the biogeochemical method being used for mineral exploration through cover (Brooks, 1972, 1995). Despite these advances, many elements still remain at or below detection limits in plant material. This is a limiting factor when considering biogeochemistry for some types of mineral deposits and mineral exploration, particularly if pathfinder elements are hoping to be utilised. This includes elements (Sb, W, Al, V, Ti, Pt, Be, Ag and Au) which either through low uptake by plants or through limited mobility in the subsurface can have limited results in biogeochemical surveys.

The effectiveness of biogeochemistry as an exploration technique is controlled by a number of basic process and factors that may interact in a complex manner. The ultimate control on

the use of biogeochemistry is the uptake (absorption) and transport of elements within a plant as a result of enzymatic processes (Kabata-Pendias, 2001). These elements are largely made available through the soil, although airborne uptake can and does occur (Kabata-Pendias, 2001). Consequently, the concentrations of elements within plants are controlled largely by soil factors including pH, Eh, water regime, clay content, organic matter content, mycorrhizae and the concentration of other trace elements (Kabata-Pendias, 2001). The movement of water through a system, as well as its pH and Eh, are key factors in the weathering system, as previously discussed in Chapters 3 and 4. The movement and interaction of water within a system will release ions that then become available for uptake by plants. The pH and Eh of a solution also affects the mobility and thus availability of elements for uptake. The proportion of clay and organic matter in the soil will affect the capacity of plants to remove ions from the soil, as the ions preferentially adsorb onto clay and humus which have higher cation exchange capacity (Brooks, 1972, 1995). The cation capacity of clays will also increase with the additional of organic matter, as it increases the surface area of the clays. The cation exchange capacity of humus increases with an increase in pH, and overall humus has a greater capacity to host cations than clays (Brooks, 1972). Mycorrhizae and bacteria play an important role in making elements in the soil available for the plants to access (Brooks, 1972; Kabata-Pendias, 2001), including through the fixing and the mobilisation of elements. Bacteria are known to play an important role in the breakdown of minerals, some of which can produce acids or corrosive agents to break down minerals including calcite, magnesite and feldspars (Brooks, 1972, 1995; Kabata-Pendias, 2001). The concentration of elements within the soil may also impact on the plants if one element has the ability to inhibit or stimulate the adsorption of other elements within plants (Kabata-Pendias, 2001). Interactions between elements may be both antagonistic (when the combination of elements is less effective than when independent) and synergistic (when the combination of the elements makes the elements more effective) (Kabata-Pendias, 2001). These relationships will vary between different plants, but commonly Fe, Mn, Cu and Zn are known to be antagonistic elements (Kabata-Pendias, 2001). Therefore, ideally

biogeochemical surveys would be accompanied by soil pH measurements at each site and estimates of the soil's clay and organic matter content to assess these factors. However, as the surface or near-surface soil composition potentially has limited relevance to the soil composition surrounding the plant roots (which can be many metres below the surface), obtaining the relevant information may become time consuming and/or extremely difficult.

As different species of plants have different trace element requirements, or are able to better survive with deficits or excesses of elements, the effectiveness of using biogeochemistry for mineral exploration varies. The trace element levels in plants are explained through the processes of accumulation and exclusion (Kabata-Pendias, 2001). Accumulation, where the plant uptakes an element and stores it, is largely reflective of the concentration of the specific element in the soil (Kabata-Pendias, 2001). Some plants, however, will hyper-accumulate elements, whereas in other cases over-accumulation of an element can result in toxicity to the plant (Kabata-Pendias, 2001). The exclusion of elements can occur through anti-uptake physiological barriers or due to an uneven chemical gradient (Brooks, 1972, 1995; Kabata-Pendias, 2001). The deficiency of an element, whether through exclusion or via deficiency within the soil, may be detrimental to the plant. The biogeochemical method is of limited utility if the subsurface material that the plant roots are in contact with is too far removed or disconnected from the mineralisation-hosting bedrock, as would be the case in regions with thick (>50 m) sedimentary cover.

Although the biogeochemical method has been shown to work well in numerous cases (Brooks, 1972, 1973, 1977, 1995; Dunn, 1986; Lottermoser et al., 2008), there are certain limitations on the effectiveness of using biogeochemistry as an exploration tool. These include climate, species variation, poor repeatability, insufficient analytical sensitivity and susceptibility to contamination (Arne et al., 1999; Brooks et al., 1995; Dunn, 2011; Lintern et al., 1997; Mitchell et al., 2015).

Southern Australia's Mediterranean climate is subject to seasonal rainfall which arguably aids in the viability of the biogeochemical method. With little rain falling during the dry summer months, the trees are forced to take water from the groundwater table, which has, in turn, interacted with the underlying bedrock. In species such as the eucalypts, this promotes the development of deep tap roots that penetrate the near-surface regolith and thus the trees provide a snapshot of the chemistry of the groundwater and bedrock (Canadell et al., 1996; Kabata-Pendias, 2001). Another characteristic of plants in southern Australia that aids their use as biogeochemical sample media is that they have roots with significant vertical extension, allowing for maximum availability of soil resources, moisture and nutrients. Dual root systems (i.e. shallow horizontal as well as vertical roots) enables the deeper roots to supply moisture to surficial roots, which remain active and exploit nutrient availability during periods of soil moisture (Canadell, 1995, 1996). Moisture and nutrient content of the soil will influence root form and distribution (Canadell, 1995, 1996; Kabata-Pendias, 2001). Localised, high moisture near-surface soil profiles (e.g. clay-rich soils in topographic depressions) may lead to greater development of shallow root systems, which limits plant communication with mineralised bedrock. Root morphology is also strongly influenced by soil or weathered bedrock properties, such as hardness, porosity, bedrock depth and degree of weathering (Kabata-Pendias, 2001).

An important consideration in the design of biogeochemical surveys, and a variable that can be controlled or addressed by the researcher, is seasonal variation. In the Northern Hemisphere it is well documented that the greatest concentrations of trace elements in plants occurs during the warmer months, i.e. spring to summer, and this corresponds to the peak growing season and a higher rate of plant activity (Dunn, 1981, 1989, 2011; Dunn and Scagel, 1989). In other regions, rainfall is the more significant variable. In these regions it is best to sample at the end of a significant dry spell, to ensure the sampled plant material is in maximum contact with the long-term, non-seasonal groundwater. The reasoning for this is demonstrated by Lintern (2007), who conducted a biogeochemical survey on the

Eyre Peninsula in the Southern Gawler Craton with repeated sampling of *Melaleuca* in April and September. Samples from April recorded higher concentrations than in September for the vast majority of elements. Of note, Ca, Mg and Na recorded double the mean concentrations in April when compared to September (Lintern, 2007). In southern Australia, April typically marks the end of the dry summer months and hence this is the ideal time to sample plant material to optimise the likelihood that their trace element compositions reflect the chemistry of the potentially mineralised bedrock. By comparison, in tropical northern Australia sampling should be conducted at the end of August before the summer monsoonal season. For studies that cover a broad area, there is also the influence of larger climate variations such as the El Nino and La Nina southern oscillation climate patterns (Mitchell et al., 2015), which may affect the sample media if surveys are conducted over a significant time period, or after long time periods have elapsed. The timeframes often employed in research and exploration do not necessarily allow for optimal sampling, for example, sampling may only be possible during a wet climate period, such as La Nina in southern Australia. This issue can be partly circumvented by acknowledging the influence of climate in the dataset and by using approaches such as applying lower thresholds for element concentrations considered anomalous.

5.3. Methods

The biogeochemical survey was preceded by a review of the dominant vegetation types on Kangaroo Island as documented in the literature (Berkinshaw, 2009; Brooker, 2004; Davies, 2002; Henschke, 1997) and from field observations. A number of different species considered suitable for a survey were determined to be present with their distribution largely dependent on different soil types. This included Kangaroo Island narrow leaf mallee (*Eucalyptus cneorifolia*) in the sandy soils which dominate the Dudley Peninsula and south coast; cup gums (*Eucalyptus cosmophylla*) and stringybarks (*Eucalyptus baxteri* and *E. obliqua*) on the main areas of the ferricrete plateau, with isolated populations of manna gums (*Eucalyptus viminalis*) in the northern areas of the island. Sugar gums (*Eucalyptus*

cladocalyx) were sampled at a number of the mineralisation case study sites as these were the only eucalypts growing in the immediate vicinity of the mineralisation occurrence. An unidentified species of eucalypt was sampled around the edges of some of the ‘ferricrete pits’, where the top soil had been disturbed to allow for the ferruginous material to be taken up and used as road base. This disturbance has resulted in the establishment of a monoculture of a single type of eucalypt species that is not commonly found on the island, and which were unable to be positively identified due to hybridisation.

Due to the inconsistent distribution of the eucalypt species on the island, xanthorrhoea (*Xanthorrhoea semiplana*) were sampled as an alternative species. This species has a wide and relatively consistent coverage across the island, allowing for the analysis of biogeochemical data for a single species across a large portion of the island.

5.3.1. Mineral workings on Kangaroo Island

There has been a history of small mineral workings on the island (Belperio, 1992, 1995; Mansfield, 1947), including Cu, Au, Ag, Pb and Zn mineralisation (Belperio, 1995; Flottmann, 1995; Jago and Gatehouse, 2009; Northcote, 1946). The signature of mineralised zones on Kangaroo Island was determined by using four case studies at sites of known mineralisation. These case studies were conducted at Bonaventura (BV), Kohinoor (Kh), Western River Cove (WRC) and Rainbow’s End (RE) prospects (Figure 1). These are all historically worked, but currently economically unviable, Ag-Pb-Zn (WRC and RE), Cu-Au (Kh) and Cu-Au-Ag-Zn (BV) prospects (Crooks, 1991a). These case studies have been used to examine the expression of underlying mineralisation within biogeochemical results, and what sample spacing is preferable for a regional scale survey. The most comprehensive case study was undertaken at BV, which at the time of sampling was part of a modern exploration tenement held by Monax Mineral Exploration. Bonaventura is a historical prospect of Cu-Au-Ag-Zn (Crooks, 1991b), located on the Cygnet–Snelling Fault Zone. The prospect straddles the Cygnet Creek, which has formed an incised gully and is heavily

vegetated. Kohinoor is a historic Cu-Au prospect along the Cygnet–Snelling Fault Zone (Crooks, 1991b). The area in which the historic workings are situated is currently being revegetated, and much of the vegetation in the area is relatively immature. Western River Cove is a historic Ag-Pb prospect (Crooks, 1991a) to the west of the Cygnet–Snelling Fault Zone, and is located outside of the ~ 30 km zone of the three previous prospects (Figure 1). The landscape has been cleared in this area, and is very steep due to the proximity to the northern coastal edge of the island (~ 900 m to the north). Rainbows End is a historic Pb-Ag deposit (Crooks, 1991b) on the Cygnet–Snelling Fault Zone, situated within an area currently under pine plantation. The terrain is rough and steep and much of the native vegetation has been cleared, which made finding appropriate sampling media difficult. As a consequence, limited samples were taken at this site and this is the area with the least coverage. Sample media were not able to be restricted to eucalypt species or xanthorrhoea, so in this case a casuarina (thought to be *Allocasuarina verticillata*) growing on the edge of a worked pit was sampled.

5.3.2. Sampling Procedures

The sampling programs for the biogeochemical vegetation surveys on Kangaroo Island were adapted from Dunn (2011) and Hill (2002). Three sampling programs were conducted over two field seasons, with several sites sampled each year to allow for an examination of temporal variation. Sampling was conducted in a reconnaissance survey in March 2012, with the main programs occurring in mid-April 2012 and 2013. The rainfall measurements in the three months preceding sampling were 25.3 mm (Jan–Mar 2012) and 41 mm (Jan–Mar 2013) at Kingscote, with 50.6 mm (Jan–Mar 2012) and 39.4 mm (Jan–Mar 2013) falling at Cape Borda (Table 5.1). Both of the sampling seasons experienced significant periods of rainfall during the sampling, from 30 mm to 40 mm at Kingscote and 45 mm to 49 mm at Cape Borda.

The survey was designed along the predominately north–south road network on Kangaroo

Table 5.1: Rainfall data for the three months prior to sampling and during the biogeochemical sampling periods. Data collated from the Bureau of Meteorology.

Kingscote	2012 (mm)	2013 (mm)	Average (1877- 2016)	Cape Borda	2012 (mm)	2013 (mm)	Average (1867 - 2007)
January	1.5	5.8	14.7	January	14.0	6.0	15.4
February	5.3	7.6	17.2	February	17.8	2.0	16.9
March	18.5	27.6	18.5	March	18.8	31.4	23.7
Total in prior 3 months to sampling	25.3	41	50.4	Total in prior 3 months to sampling	50.6	39.4	56
Rain during sampling period	(22nd – 26th April) 43.6	(16th – 28th April) 30.4	n/a	Rain during sampling period	(22nd – 26th April) 49.6	(16th – 28th April) 45.1	n/a
Total April rainfall	43.9	30.6	35.1	Total April rainfall	51.0	51.5	45.2

Island (Figure 5.1), with vegetation sampled at approximately 2 km intervals north–south, with the roads being approximately 10 km apart east–west. The majority of the roads have native vegetation belts running along them between 5 m to 10 m wide. Samples were collected as far away from the road as possible, to minimise dust contamination from the road. Whenever possible, leaves were taken from a number of points around the tree canopy to allow for natural variation. This natural variation can be the result of differing amounts of sunlight, prevailing wind direction or the effects of other vegetation (Dunn, 2011). Larger, more mature trees were preferentially chosen as they were likely to have a deeper root system. A large, mature xanthorrhoea was sampled next to the eucalyptus tree were possible, otherwise the largest xanthorrhoea within a 20 m area of the eucalypt was sampled. Xanthorrhoea were also sampled from around the circumference of the plant to allow for natural variation. At a number of locations, multiple species of eucalypt were sampled to allow for inter-species correlation and assessment of variation in element concentrations from the same location.

In the vicinity of the four mineralised sites, there were often no appropriate eucalypt species

to sample at the distances prescribed by the survey size. In these cases, eucalypts, and in one case a casuarina, were opportunistically sampled based on their proximity to survey sample points and ease of access rather than for species.

5.3.3. Geochemical analysis and data treatment

The collected plant material equated to a sample size of approximately 300 g in calico bags prior to removal of twigs and small branches, with only leaf matter used for analysis. Samples were allowed to air dry while in the field, and when returned to the laboratory, were oven dried for 2–3 days at 60 °C to prevent mould and rot. Samples were then repacked in paper envelopes and shipped to ACME Laboratories for analysis. Analyses were conducted at ACME Laboratories (now Bureau Veritas Upstream), Vancouver, Canada, where the samples were dried and milled with a final sample size of ~100 g. A 1 g split was digested in a two-step procedure using HNO₃ and Aqua Regia. Analysis of the digested material was done by ICP-MS for ultra-low detection limits of a suite of 53 elements. Analytical runs included blind duplicates created from splitting samples in the field, laboratory duplicates created by splitting of solutions at the analysis stage and in-house (ACME) standards. External standard deviation on the in-house ACME standards ranged from 50% (2SD) for element concentrations at or within uncertainty of detection limits down to 2.5% (2SD) with most elements in the range of 4–15% (2SD). Duplicates were within uncertainty of each other. A number of elements were below detection limits in the in-house standards (Pd, Pt, In, W, Tl, Be and Re) and hence these elements are automatically excluded from further analysis due to an inability to assess their accuracy. A further filter of data quality was used over and above the applied laboratory detection limit. For each element, the maximum external standard deviation (2SD in percent) observed in the in-house standards was added to the detection limit. Any data within this 2SD level of the detection limit (including rounding to the appropriate significant figures) were discarded to ensure that only data that could be reliably considered to accurately represent the concentrations in the samples were used for data analysis. Some elements displayed a ‘stripey’ quality when plotted on normal

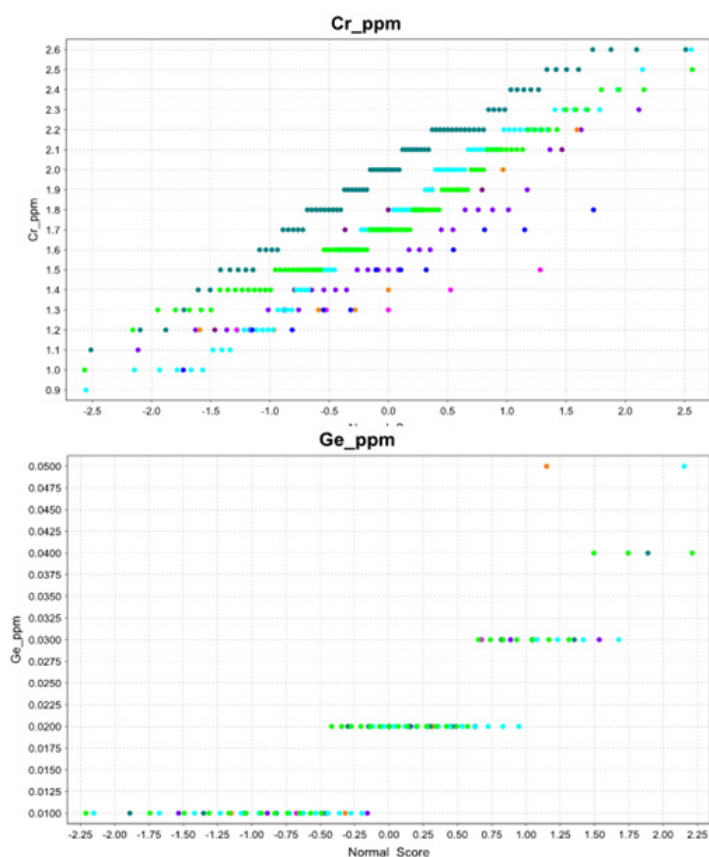


Figure 5.3: Elements that show discretisation due to rounding display as ‘striped’ data. Data are largely below detection limits, or when detected only have a limited number of unique values.

probability plots, this is attributed to discretisation due to rounding (Figure 5.3).

Data analysis used univariate statistics generated with IoGAS (version 6.1) statistical software (Dunn, 2011). The results are presented spatially using ArcGIS (version 10.3.1) generated maps with concentrations and standard deviations plotted (Figure 5.4). A commonly employed approach for assessing the spatial distribution of data in exploration biogeochemistry is to adopt the median concentration of an element within the survey area as the ‘background’ value of that element in the region (Dunn, 2011). Exploration targets are then defined relative to this background where element concentration values considered anomalous and are greater than 1.5–2.5 standard deviations above the median. To emulate this exploration workflow, the same approach to definition of ‘anomalous’ values has been employed within this study.

Data are also displayed on normal probability plots for both the eucalypts and xanthorrhoea geochemical data. The plots have element concentration on the ordinate axis and the

‘normal’ score on the abscissa. The ‘normal’ score is an approximation of the means or medians of the order statistics, allowing the data to be assessed in respect to being a ‘normal’ distribution. Eucalypt data are also plotted on logged stacked histograms (Figure 5.4). The combination of these methods of data presentation emulates the approach of industry exploration programs and allows data to be compared, taking into account species variation within the eucalypts. In this situation, the primary aim is to produce a first pass dataset that will narrow down a regional scale area to a smaller prospect scale area for

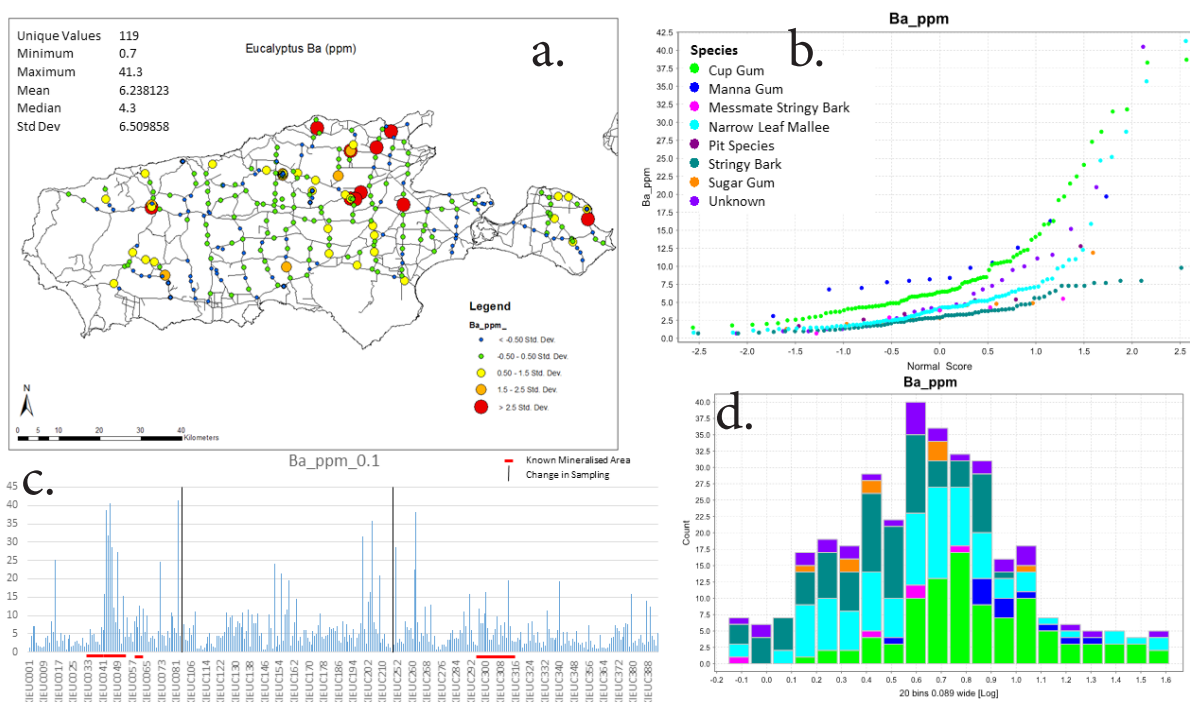


Figure 5.4: Data treatment for biogeochemical results, the example here showing results for Ba in eucalypt samples. Univariate statistics were used to determine the standard deviations, which were then plotted on ArcGIS a). Anomalous values are in red, and are from 1.5 to over 2.5 standard deviations. Image b) is normal probability plots and d) histograms, stacked according to the different eucalypt species. Plot c) is a histogram of the entire dataset was produced to examine any periodicity with the sample for laboratory bias, with the known mineralised zones highlighted by the red lines.

further exploration.

5.4. Results

All raw data are presented in Appendix A with all element maps and distributions presented in Appendices C (eucalypts) and D (xanthorrhoea). A number of elements were below detection limits in all samples. These were In, W and Be for eucalypt samples and Be, Ga, In, Nb, U, Sb, W, Tl and Pd for xanthorrhoea samples. Several elements returned values less

than the nominated 2SD threshold above the laboratory detection limit. In almost all cases these were elements whose reported values were at detection limit.

Elements that are known to be commonly affected by dust contamination, such as Zr and Al (Dunn, 2011), show a linear trend (Figure 5.5), suggesting the presence of dust contamination on the plant material. Iron, Th, V and Hf and Fe and Th in the eucalypt and xanthorrhoea, respectively, also show similar linear trends. These elements will not be considered further due to the likelihood of dust contamination.

The results are presented below by plant order in the first instance with reference made to the individual areas of known mineralisation. In the following, the essential nutrients to be considered are Na, Mg, P, S, Cl, K, Ca, Cu, and Zn (Dunn, 2011) with Fe, Mn and Sn removed from consideration for reasons described above. Copper and Zn are considered as

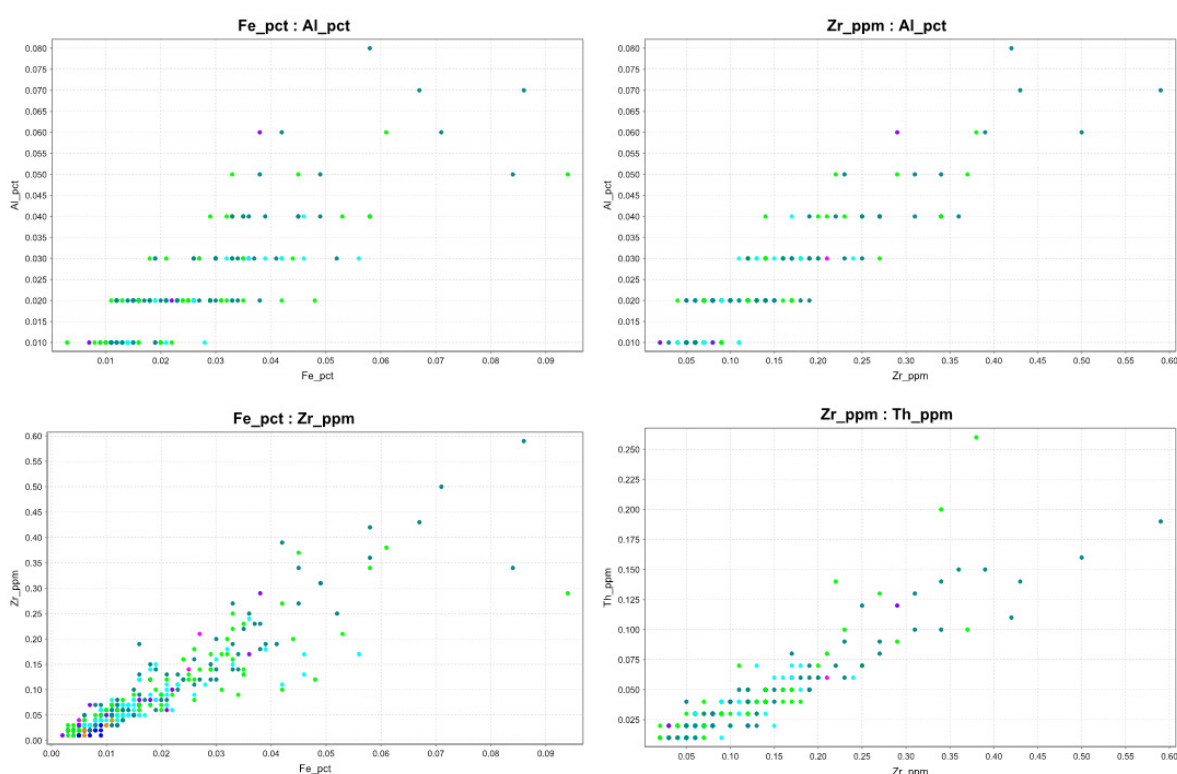


Figure 5.5: Data showing dust contamination from the eucalypt biogeochemical results. Elements commonly associated with dust contamination, such as Zr, Al, Th (Dunn, 2011), are plotted against one another, the linear trend suggesting dust contamination. Iron has also been included within this dataset due to the use of ferricrete as a road base in much of the survey area.

economic elements, as are Ag, Au, Ni and Pb. The elements Cd and Cs can also be used as proxies for Zn and Au respectively (Dunn, 2011), due to their similar atomic structure and proven associations in previous biogeochemical studies (Dunn, 2011). The use of proxies for these two elements is important due to the ‘nugget’ effect of Au and due to Zn being an essential element for plants (Dunn, 2011).

5.4.1. Eucalyptus Results

To assess temporal variation, elements were plotted in stacked graphs according to sampling program (Figure 5.6). There were three main trends displayed in this data, these are: elements that had the same trends for each of the sampling programs include As, Au, Hg, Mn, Zn, Cu, Li and La (Figure 5.6a); elements that follow the same trends but vary significantly at the higher end of the graphs are Hf, Sn, Y, Pb (Figure 5.6b); and elements that have significantly varying datasets, such as K, Ca, Rb, V, Fe, Na and Cr (Figure 5.6c).

The elements that will be considered more closely are the economic elements of Au, Ag, Cu, Pb and Zn (Figures 5.7–5.11); elements that can be used as proxies for economic elements, Cd and Cs (Figures 5.12, 5.13); the elements that were significantly higher in concentration within the xanthorrhoea, Ba, K, Sn and Rb (Figures 5.18–5.21); and elements that show a significant spatial variation that may represent a change in lithology, Ca, Na, Ni and Y (Figures 5.14–5.17).

Of the economic elements, both Au and Ag have datasets with a small number of unique values, with data displaying the ‘striped’ quality of values that are discretised due to rounding. The highest values for both elements were gained at the known mineralisation sites, RE and WRC, for Au and Ag respectively. A comparatively large number of eucalyptus samples returned results where Ag was above detection limits compared to the xanthorrhoea samples. The number of samples returning results above detection limits for Au were slightly more consistent between the two different surveys.

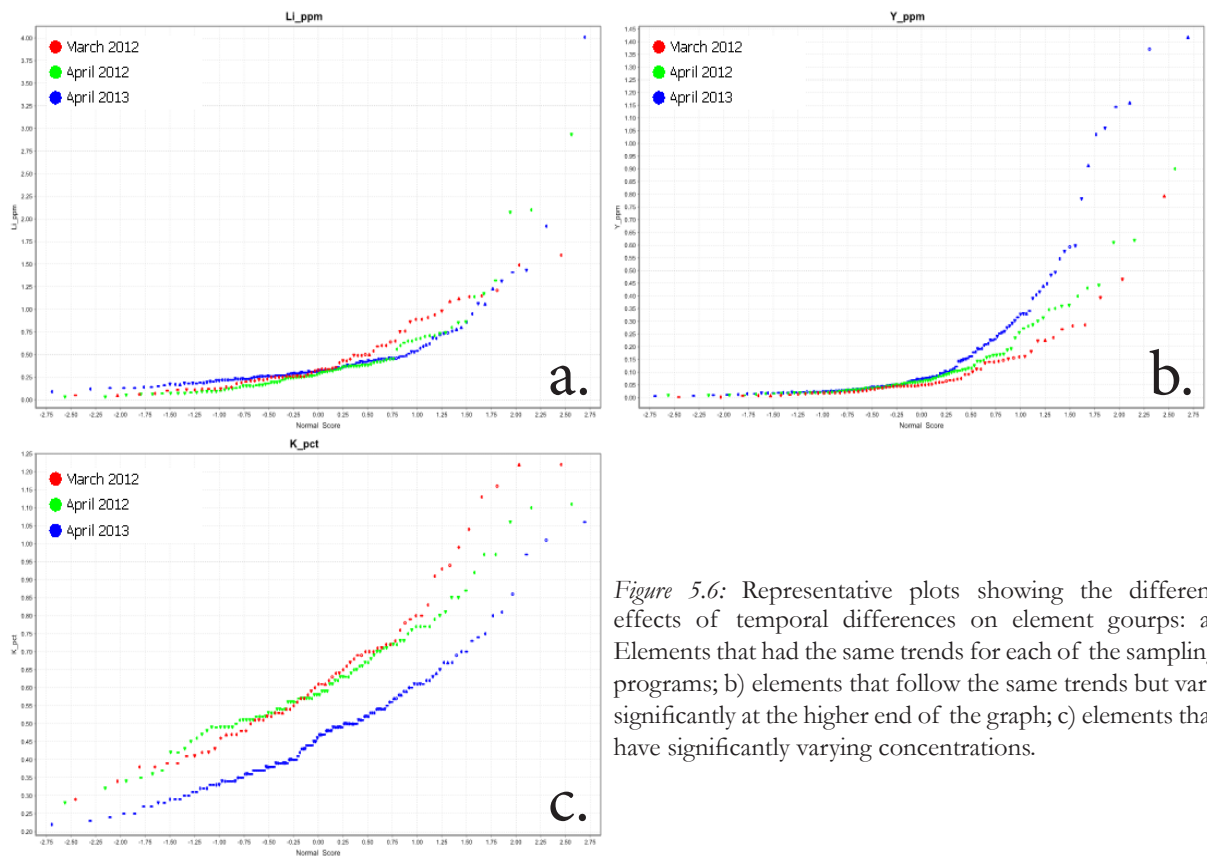
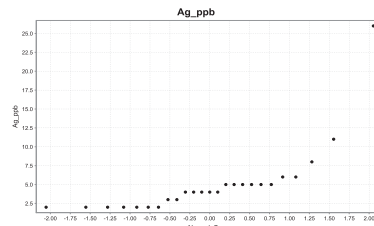
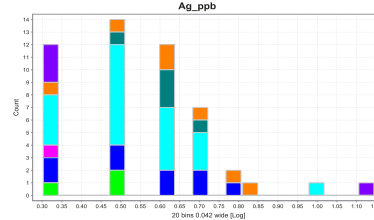
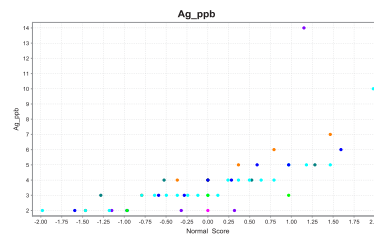
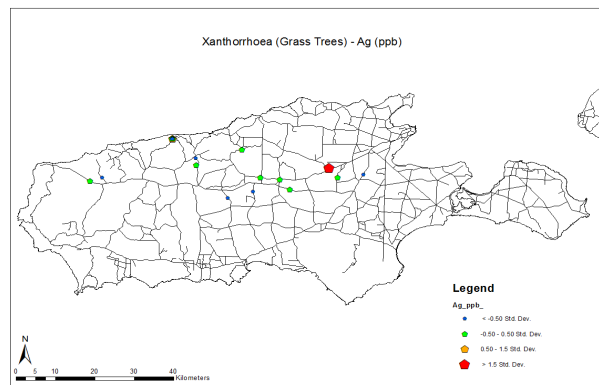
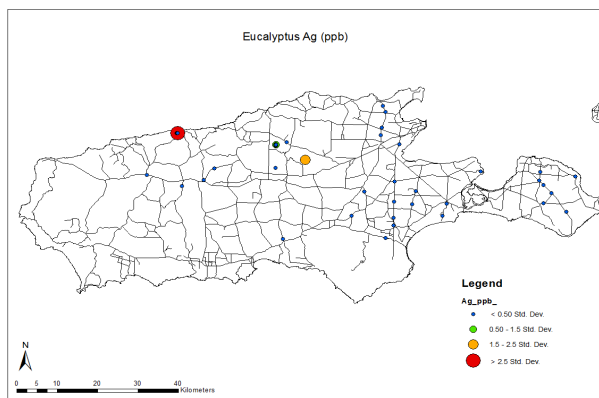


Figure 5.6: Representative plots showing the different effects of temporal differences on element gourps: a) Elements that had the same trends for each of the sampling programs; b) elements that follow the same trends but vary significantly at the higher end of the graph; c) elements that have significantly varying concentrations.



- Species**
- Cup Gum
 - Manna Gum
 - Messmate Stringy Bark
 - Narrow Leaf Mallee
 - Pit Species
 - Stringy Bark
 - Sugar Gum
 - Unknown

Figure 5.7: Data for Ag, a economic element, for eucalypt and xanthorrhoea data. Statistical graphs are included with the maps to gain a complete picture of the expression of the elements in the biogeochemistry of Kangaroo Island.

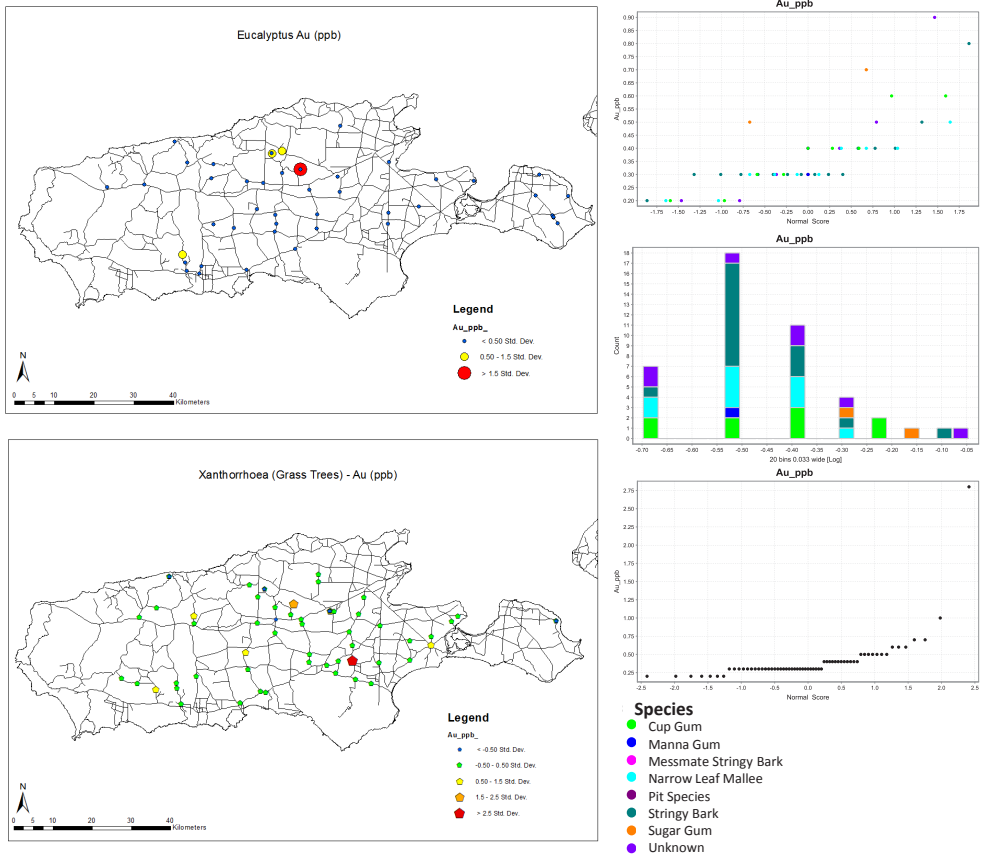


Figure 5.8: Data for Au, an economic element, for eucalypt and xanthorrhoea data. Statistical graphs are included with the maps to gain a complete picture of the expression of the elements in the biogeochemistry of Kangaroo Island.

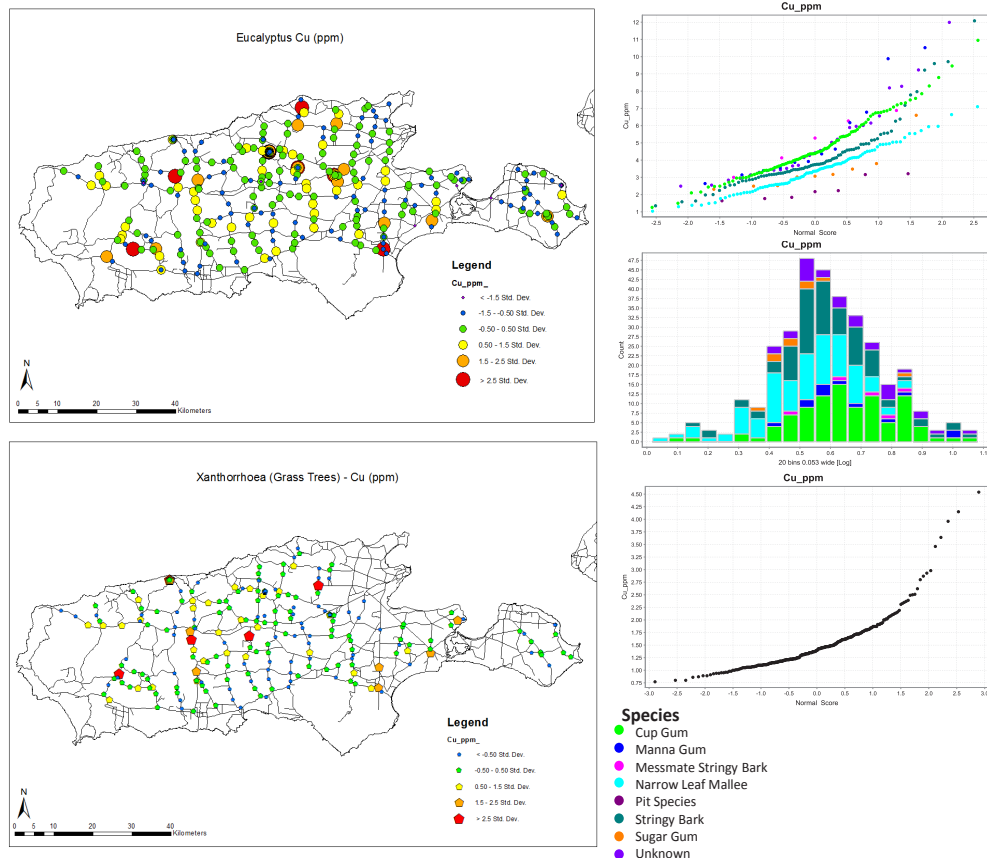
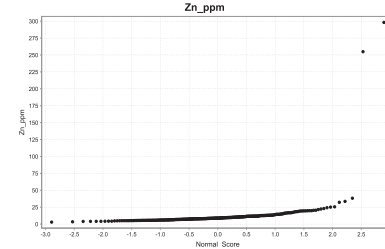
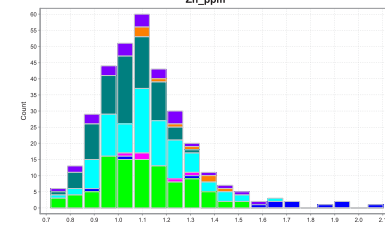
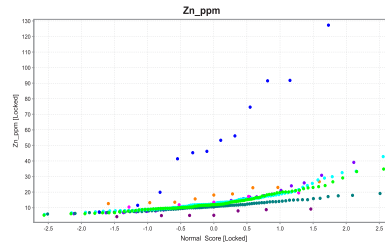
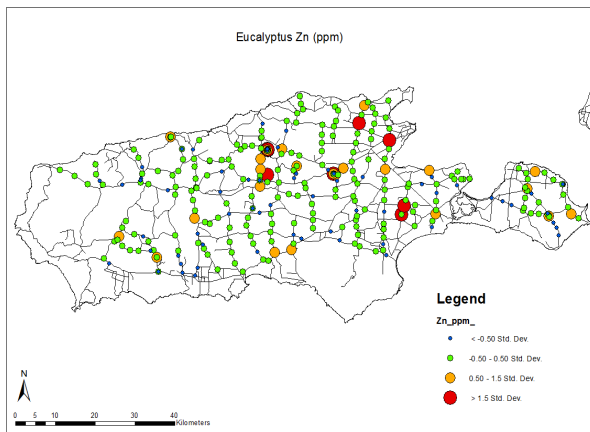
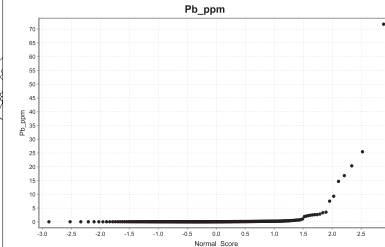
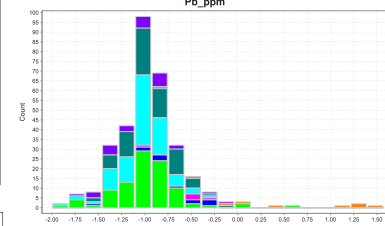
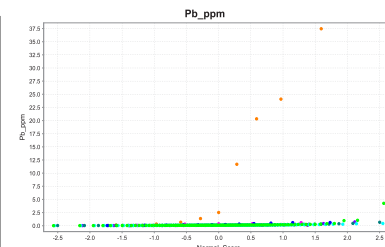
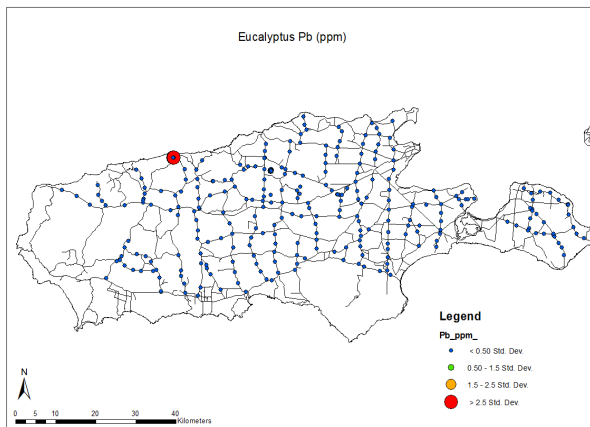
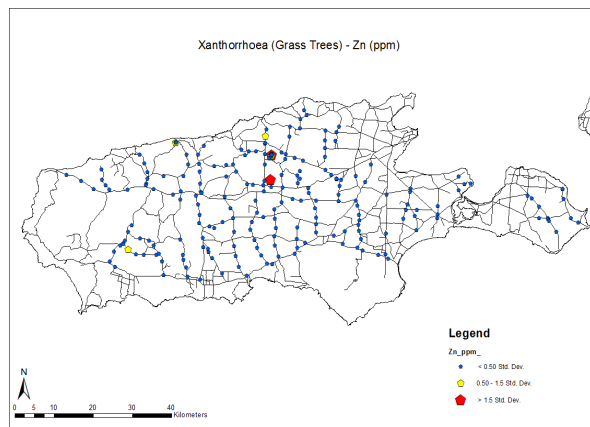


Figure 5.9: Data for Cu, an economic element, for eucalypt and xanthorrhoea data. Statistical graphs are included with the maps to gain a complete picture of the expression of the elements in the biogeochemistry of Kangaroo Island.



- Species**
- Cup Gum
 - Manna Gum
 - Messmate Stringy Bark
 - Narrow Leaf Mallee
 - Pit Species
 - Stringy Bark
 - Sugar Gum
 - Unknown



- Species**
- Cup Gum
 - Manna Gum
 - Messmate Stringy Bark
 - Narrow Leaf Mallee
 - Pit Species
 - Stringy Bark
 - Sugar Gum
 - Unknown

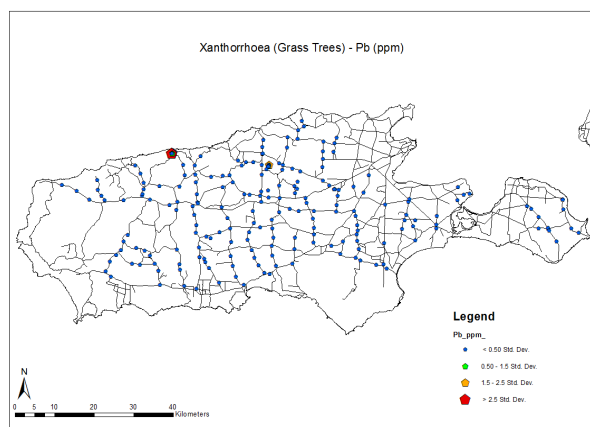
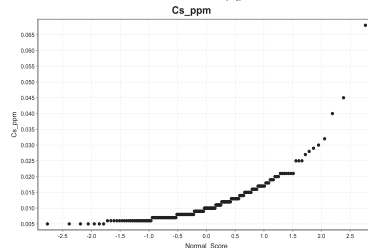
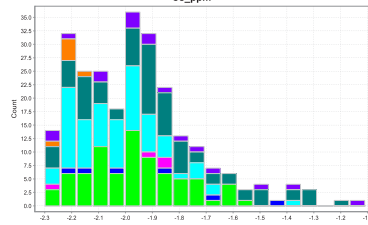
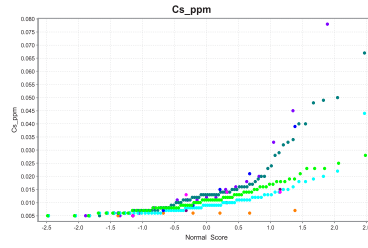
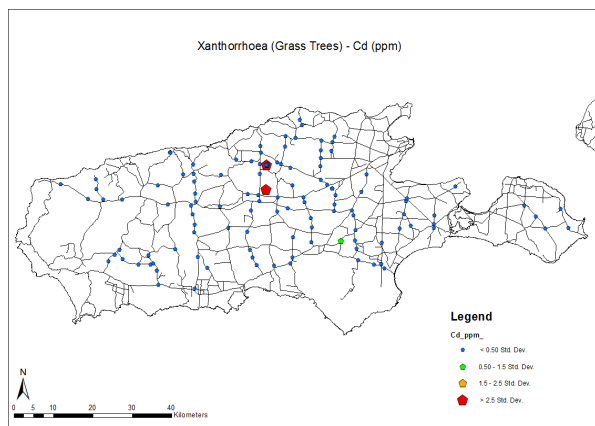
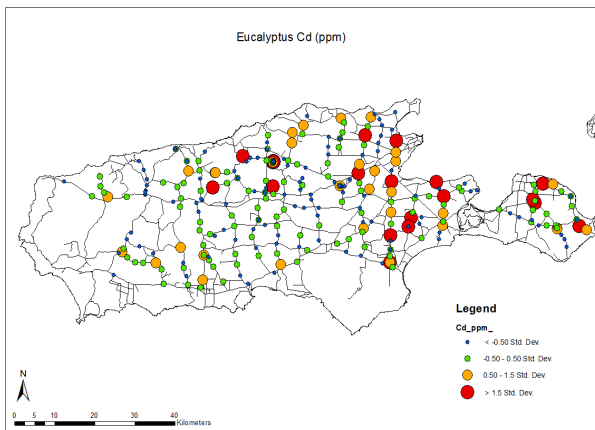
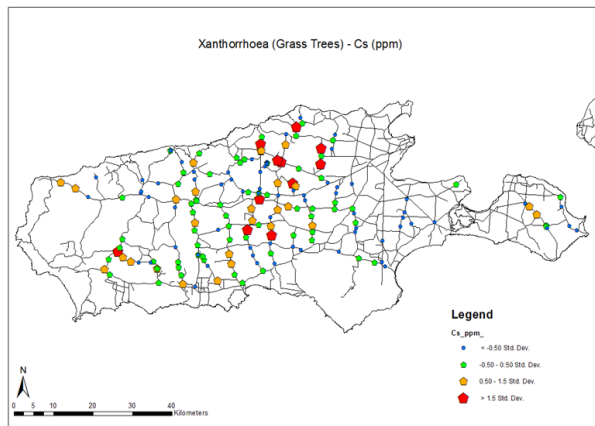
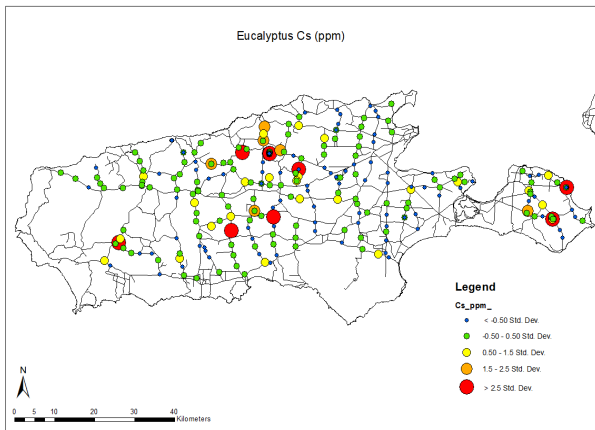
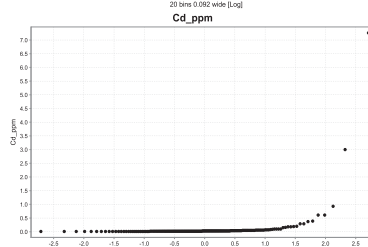
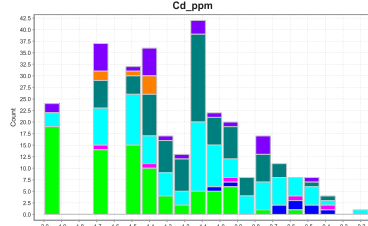
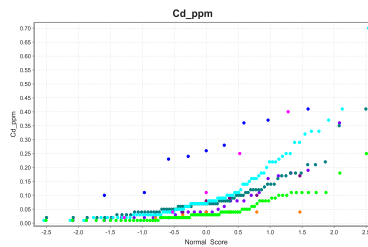


Figure 5.10: Data for Zn, a economic element, for eucalypt and xanthorrhoea data. Statistical graphs are included with the maps to gain a complete picture of the expression of the elements in the biogeochemistry of Kangaroo Island.

Figure 5.11: Data for Pb, a economic element, for eucalypt and xanthorrhoea data. Statistical graphs are included with the maps to gain a complete picture of the expression of the elements in the biogeochemistry of Kangaroo Island.



- Species**
- Cup Gum
 - Manna Gum
 - Messmate Stringy Bark
 - Narrow Leaf Mallee
 - Pit Species
 - Stringy Bark
 - Sugar Gum
 - Unknown



- Species**
- Cup Gum
 - Manna Gum
 - Messmate Stringy Bark
 - Narrow Leaf Mallee
 - Pit Species
 - Stringy Bark
 - Sugar Gum
 - Unknown

Figure 5.12: Data for Cs for eucalypt and xanthorrhoea data. Cs can be used as a proxy for Au. Statistical graphs are included with the maps to gain a complete picture of the expression of the elements in the biogeochemistry of Kangaroo Island.

Figure 5.13: Data for Cd for eucalypt and xanthorrhoea data. Cd can be used as a proxy for Zn. Statistical graphs are included with the maps to gain a complete picture of the expression of the elements in the biogeochemistry of Kangaroo Island.

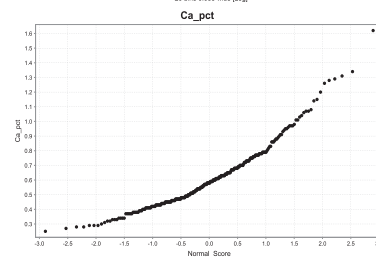
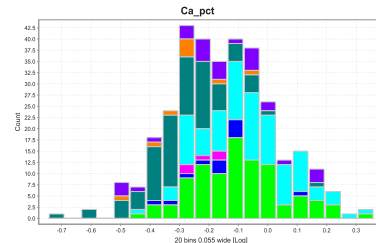
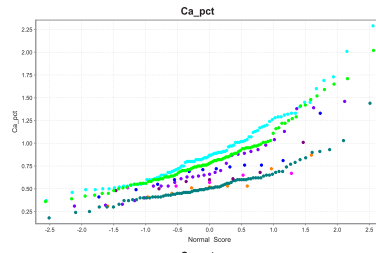
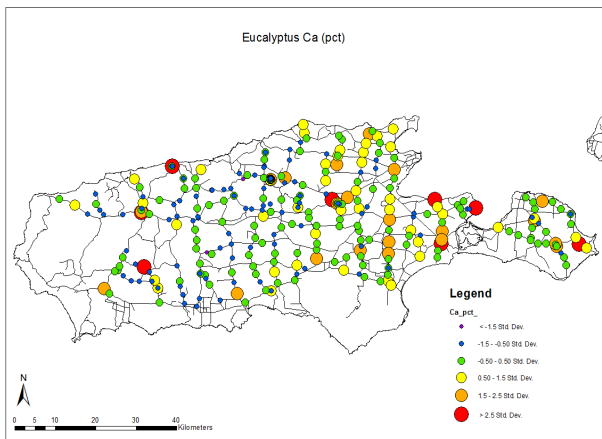
The data for Cu showed a normal distribution within the different eucalypt species, with no species having higher concentrations than any other. The highest values from the eucalypts were from sites of known mineralisation. The distribution of results above detection limits across the island was widespread, as would be expected from an essential element.

The data for Pb are skewed due to the exceptionally high results that were recorded at WRC for the eucalypts. This is seen in the high results obtained in the sugar gum samples (only sampled at mineralised sites) and on the maps (Figure 5.11), where the only anomalous points are at WRC and BV. The dataset has values above detection limits across the Island.

The Zn dataset has values above detection limits across the Island, as it is also an essential element. The eucalypt data contains numerous elevated concentrations of Zn, particularly within the manna gums, which have elevated levels up to 130 ppm.

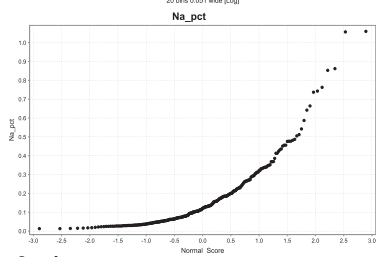
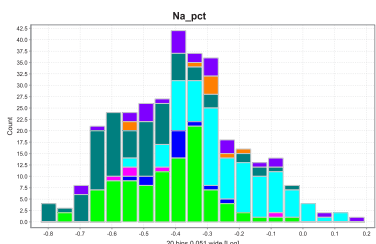
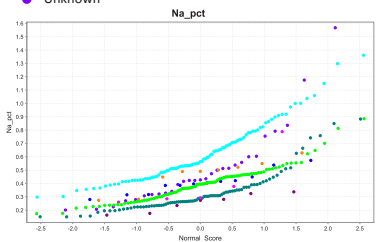
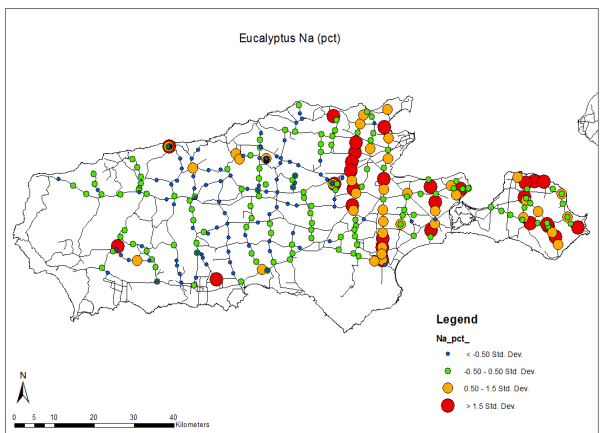
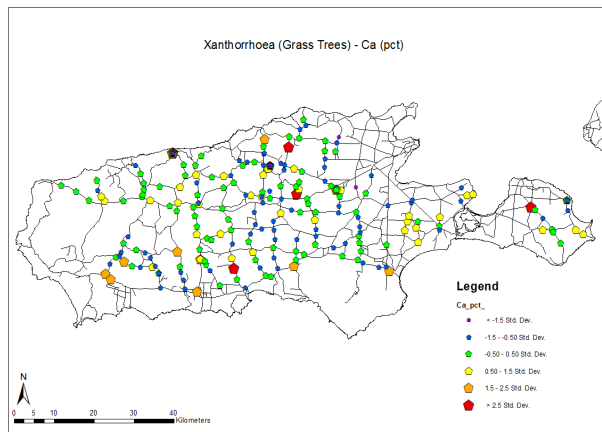
Proxies for essential elements that are also economic elements include Cd for Zn (Figure 5.12) and Cs for Au (Figure 5.13; Dunn, 2011). The histograms of the eucalypts are a skewed dataset, with the narrow leaf mallee containing slightly higher concentrations of Cd than the other eucalypt species, which is seen in the distribution of the anomalous points on the map (Figure 5.12). Caesium does not have an obvious relationship with Au as Cd does with Zn, however elevated concentrations still occur around the known mineralised sites (Figure 5.13). There is a trend of higher values in the central portion of the island, running north–south, perpendicular to the Cygnet–Snelling Fault Zone.

Four elements are singled out for examination due to their distinct spatial trends, including Ca, Na, Ni and Y. Sodium and Ni have the most distinct geographical trends and are associated with a particular eucalypt species, the narrow leaf mallee (Figures 5.15–5.16). Narrow leaf mallee were only sampled on the eastern parts of the island and Dudley Peninsula (Figure 5.1) as they grow in the sandy soils in and around the coastal lowlands. Calcium results for



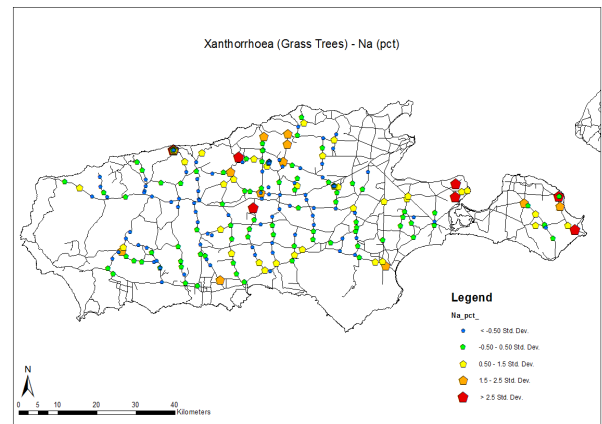
- Species**
- Cup Gum
 - Manna Gum
 - Messmate Stringy Bark
 - Narrow Leaf Mallee
 - Pit Species
 - Stringy Bark
 - Sugar Gum
 - Unknown

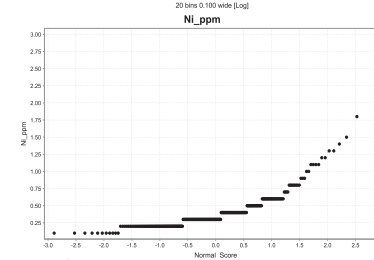
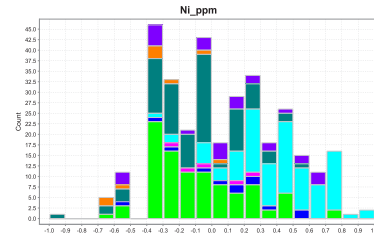
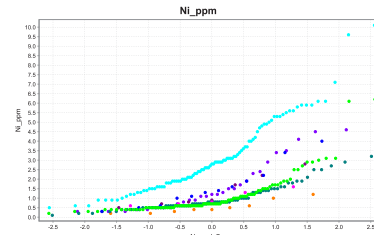
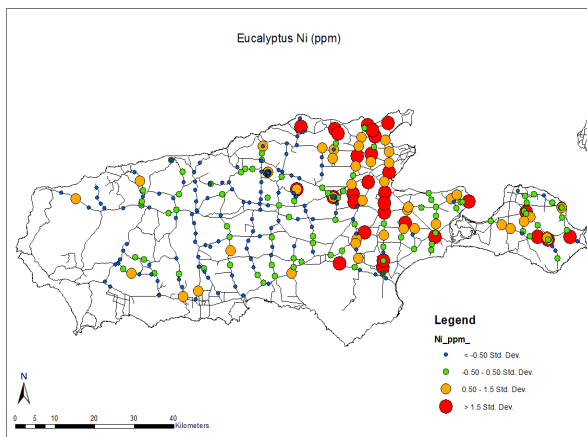
Figure 5.14: Eucalypt and xanthorrhoea data for Ca. Calcium shows particular geographical trends, particularly around the coastline. Statistical graphs are included with the maps to gain a complete picture of the expression of the elements in the biogeochemistry of Kangaroo Island.



- Species**
- Cup Gum
 - Manna Gum
 - Messmate Stringy Bark
 - Narrow Leaf Mallee
 - Pit Species
 - Stringy Bark
 - Sugar Gum
 - Unknown

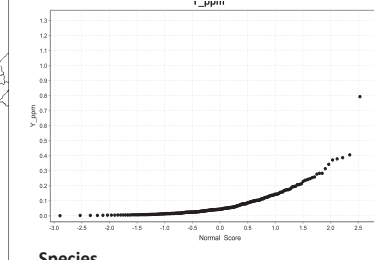
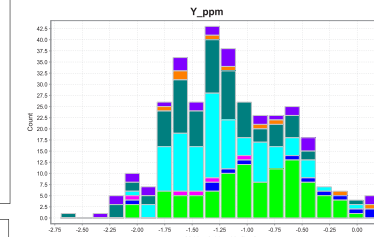
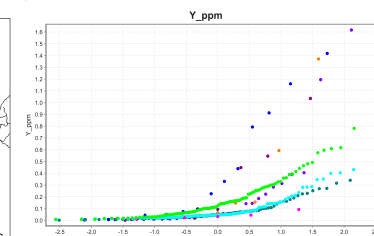
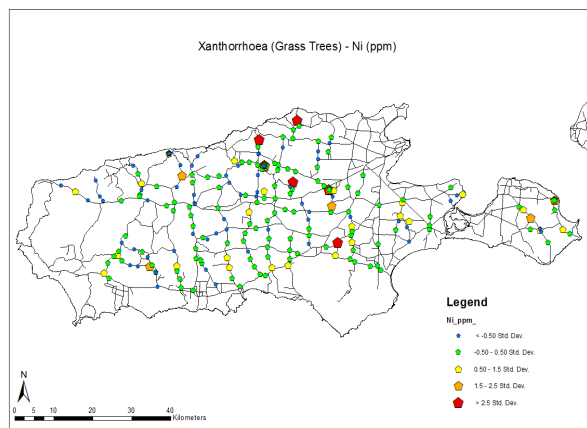
Figure 5.15: Eucalypt and xanthorrhoea data for Na. Sodium shows particular geographical trends. Statistical graphs are included with the maps to gain a complete picture of the expression of the elements in the biogeochemistry of Kangaroo Island.





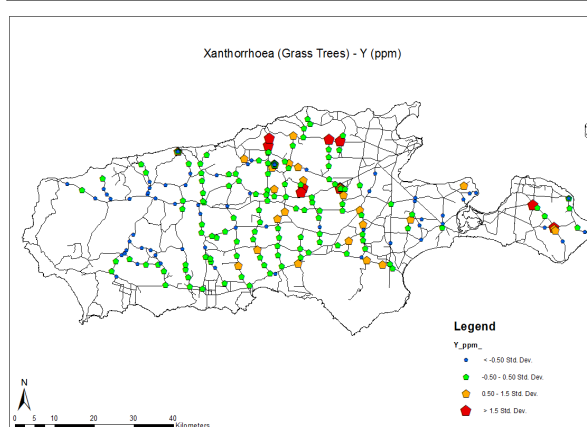
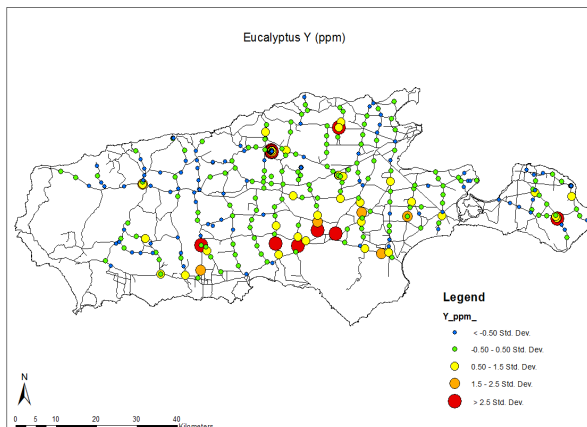
- Species**
- Cup Gum
 - Manna Gum
 - Messmate Stringy Bark
 - Narrow Leaf Mallee
 - Pit Species
 - Stringy Bark
 - Sugar Gum
 - Unknown

Figure 5.16: Eucalypt and xanthorrhoea data for Ni. Nickel shows particular geographical trends, as well as being an economic element. Statistical graphs are included with the maps to gain a complete picture of the expression of the elements in the biogeochemistry of Kangaroo Island.



- Species**
- Cup Gum
 - Manna Gum
 - Messmate Stringy Bark
 - Narrow Leaf Mallee
 - Pit Species
 - Stringy Bark
 - Sugar Gum
 - Unknown

Figure 5.17: Eucalypt and xanthorrhoea data for Y. Yttrium shows particular geographical trends. Statistical graphs are included with the maps to gain a complete picture of the expression of the elements in the biogeochemistry of Kangaroo Island.



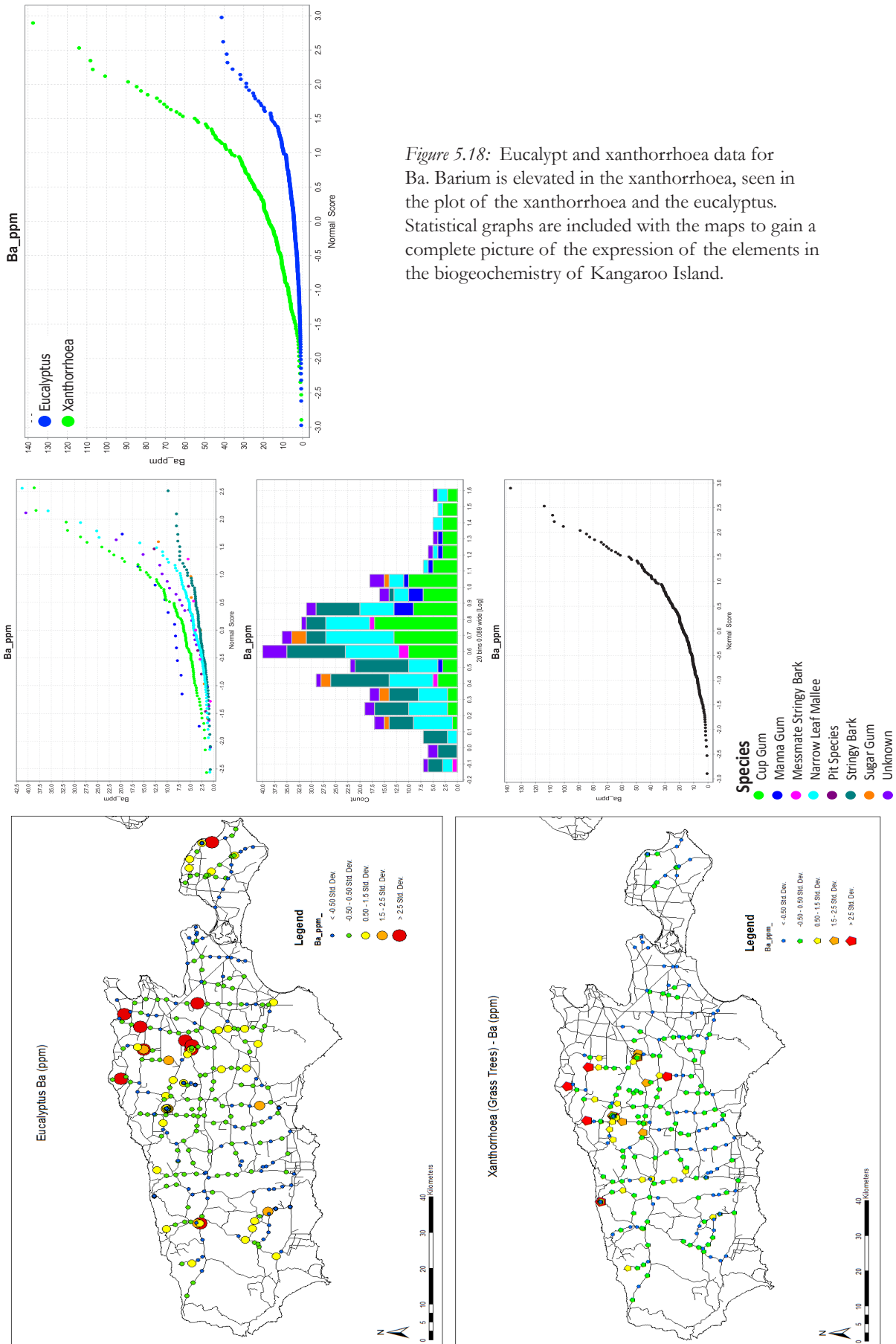
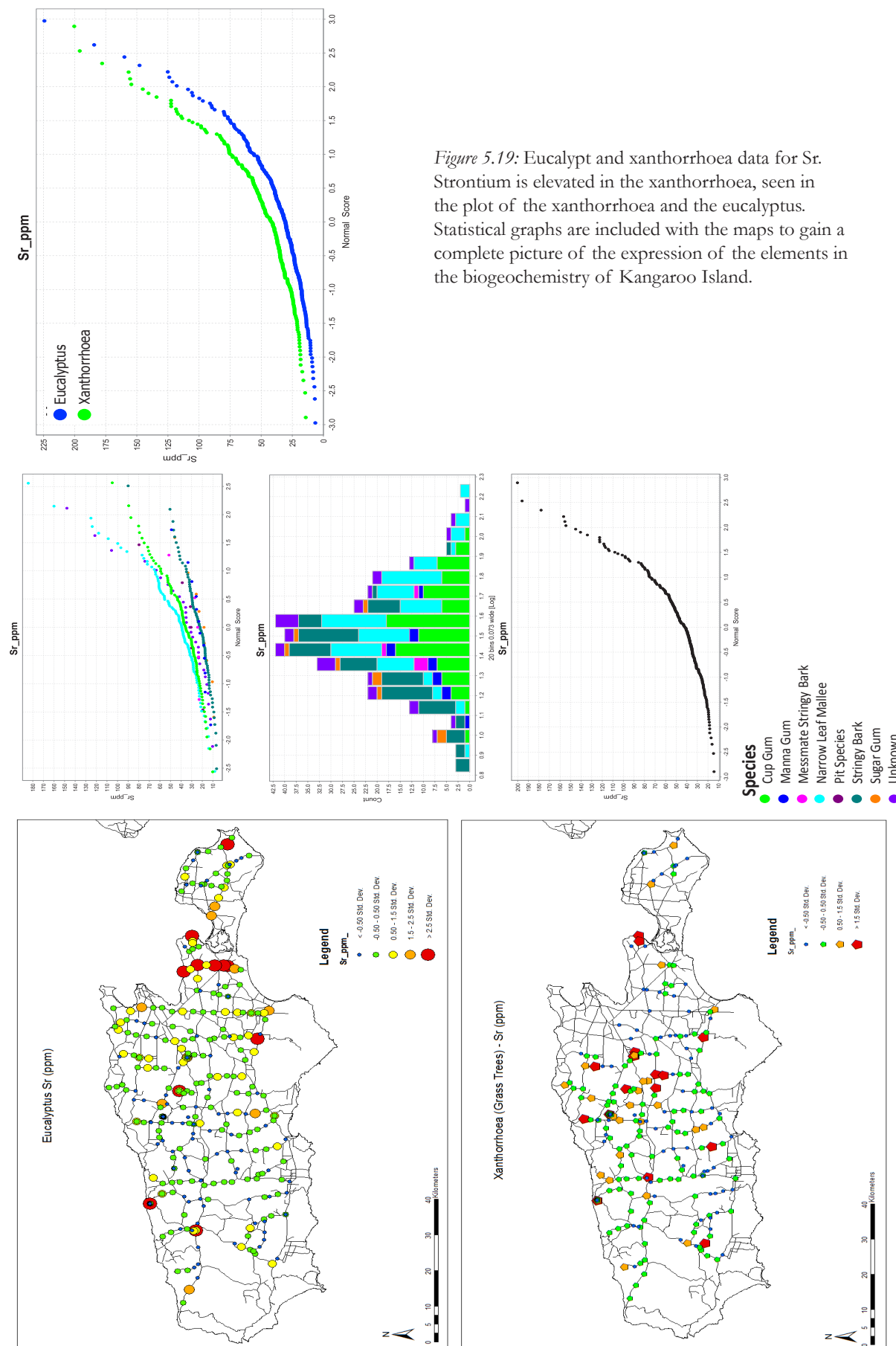


Figure 5.18: Eucalypt and xanthorrhoea data for Ba. Barium is elevated in the xanthorrhoea, seen in the plot of the xanthorrhoea and the eucalyptus. Statistical graphs are included with the maps to gain a complete picture of the expression of the elements in the biogeochemistry of Kangaroo Island.



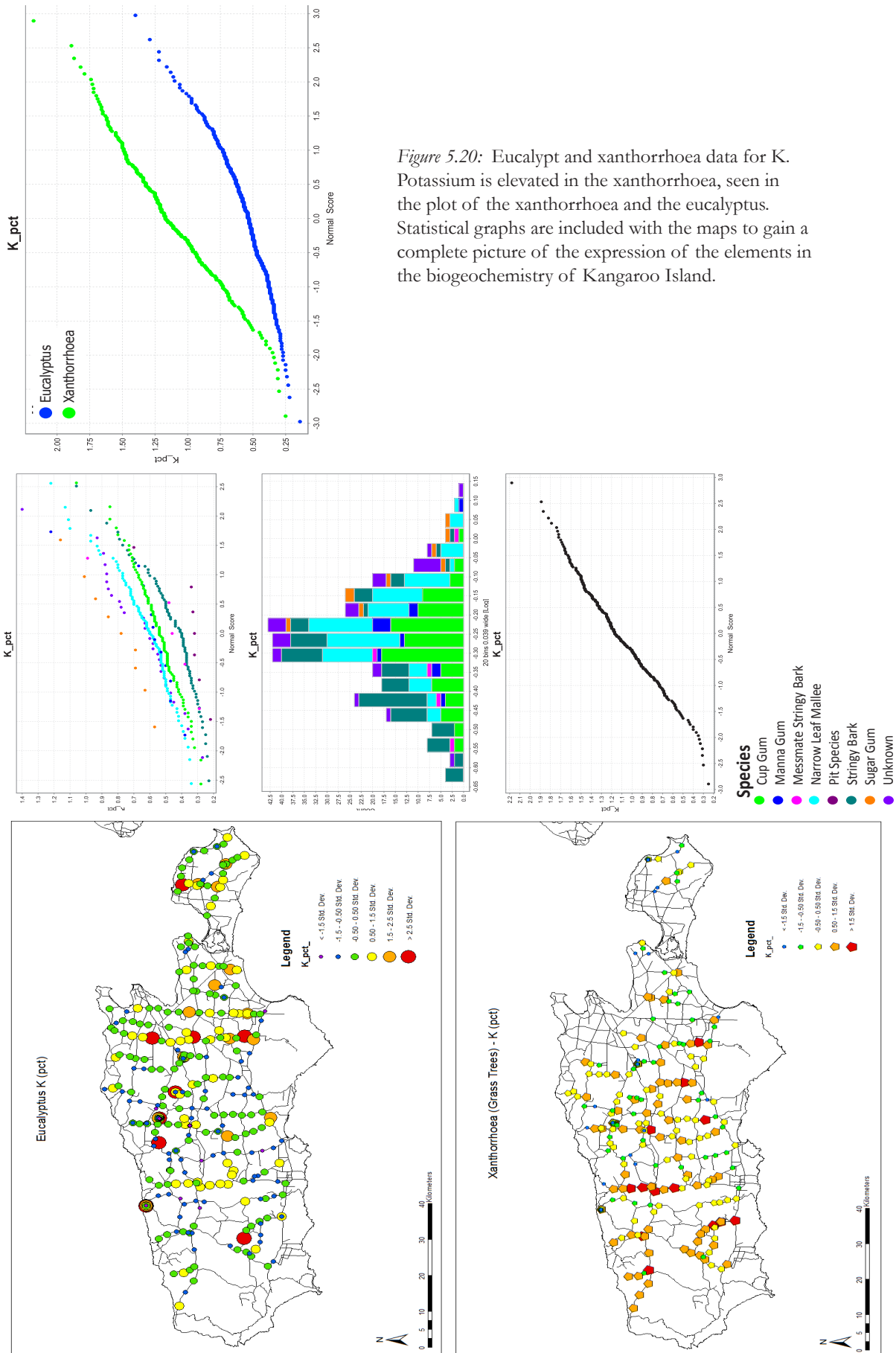
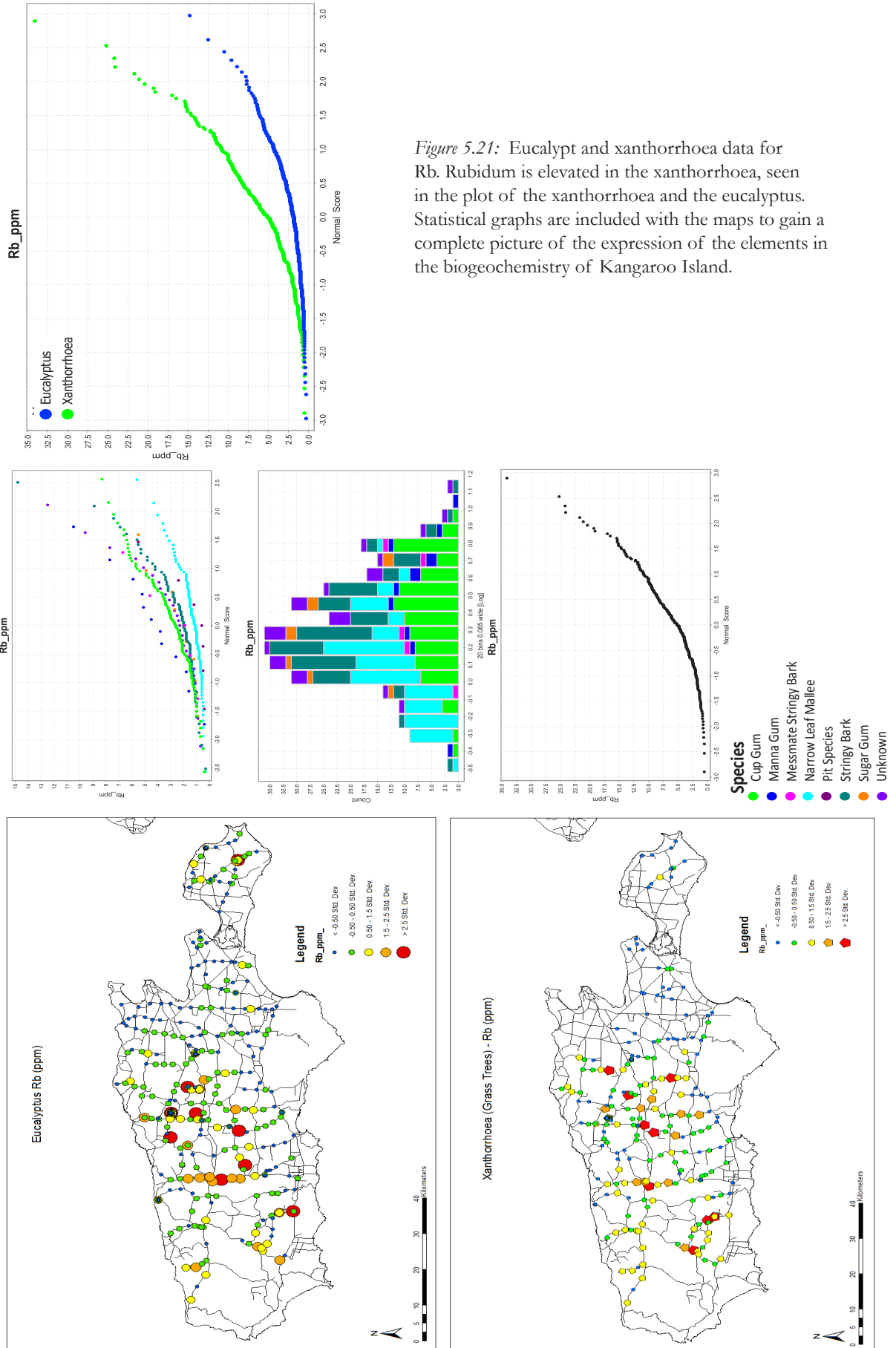


Figure 5.20: Eucalypt and xanthorrhoea data for K. Potassium is elevated in the xanthorrhoea, seen in the plot of the xanthorrhoea and the eucalyptus. Statistical graphs are included with the maps to gain a complete picture of the expression of the elements in the biogeochemistry of Kangaroo Island.



the eucalypts show a slight trend of elevated values towards the coast and a significant lack of elevated values on the main plateau (Figure 5.14). This is reflected in a lower response from the stringy barks in the species comparison than the narrow leaf mallee or the cup gum. Yttrium data has differing trends for the eucalypts and the xanthorrhoea (Figure 5.17). The eucalypts have significantly higher results in the manna gums, but also show a band of elevated concentrations running parallel to the southern coastline, with low levels elsewhere on the plateau.

Barium, Sr, K and Rb are examined due to their higher concentrations within the xanthorrhoea samples (Figures 5.18–5.21). Within the eucalypts, there are some spatial trends evident. Barium has higher concentrations to the north of the Cygnet–Snelling Fault Zone, while occurrences of elevated concentrations of Rb are more common to the south, on the ferricrete plateau. Potassium and Sr do not display any particular trend. Strontium values are quite high along one road. However, this is dismissed as possible contamination, due to different road surface materials, as the strike of the road crosses a number of different regolith and subsurface geology units.

5.4.2. Xanthorrhoea Results

For the xanthorrhoea samples, elements that had the same trends for each of the sampling programs (with some outliers) include Au, Ag, Cs, Ba, Sr, Y; elements that follow the same trends but vary significantly at the higher end of the graphs are Cu, Pb, Cd, Ni, Na, Zn (Figure 5.6a); and elements that have significantly varying datasets, are K, Ca, Rb (Figure 5.6c).

As with the eucalypt data, both Au and Ag have datasets with a small number of unique values, with data discretised due to rounding. Due to their importance as economic elements, these elements are still considered. The highest value of Au in the xanthorrhoea did not come from a known mineralised zone. Similarly, a number of the elevated values of Cu

returned for the xanthorrhoea were from areas outside of known mineralised zones. The Cu dataset returned results across the island, as is expected from an essential element. The data for Pb is skewed due to the exceptionally high results that were recorded at WRC. The majority of the values in the Zn dataset are over detection limits across the island, as it is also an essential element; however, the data are skewed due to two points of elevated Zn (250 ppm and 300 ppm) one of which is at BV.

Proxies for essential elements that are also economic elements include Cd for Zn and Cs for Au (Dunn, 2011). The Cd results from the xanthorrhoea (Figure 5.13) show the same trend as the Zn data (Figure 5.10). The two highest concentrations of Cd are in the same locations as the two elevated concentrations of Zn, which has again skewed the data. The concentrations of Cd are significantly higher in the xanthorrhoea (7 ppm) than the eucalypts (0.7 ppm). The relationships between Cs and Au is not as strong as the relationship between Cd and Zn; however, elevated concentrations of Cs are still focused on the known mineralised sites. Both datasets have a trend of higher values in the central portion of the Island, running north–south perpendicular to the Cygnet–Snelling Fault Zone.

There are four elements; Ba, Sr, K and Rb: where the majority of the data are at higher concentrations for the xanthorrhoea samples than for the eucalypts. The distribution of these datasets are normal and show no particular trends, beyond being much more elevated for the xanthorrhoea than for the eucalypt samples. K and Rb are also the only samples that displayed significant temporal variation with the xanthorrhoea samples, with the results from the April 2012 sampling program displaying elevated levels for both elements. This was not reflected in the Sr or Ba datasets.

Four elements (Ca, Na, Ni, Y) were examined due to their distinct spatial trends in the eucalypt samples. These elements do not show the same spatial patterns in the xanthorrhoea samples as in the eucalypts. Sodium and Ni have limited responses, as does Ca. Yttrium data

has differing trends for the eucalypts and the xanthorrhoea. The eucalypts show a band of elevated concentrations running parallel to the southern coastline, with low levels elsewhere on the plateau. The xanthorrhoea results contain low level concentrations on the plateau, but instead of showing elevated concentrations on the south coast, they show elevated levels in the north of the island.

5.4.3. Case studies in areas of known mineralisation

Bonaventura returned high values of Cu in the eucalypts; this was not expressed in the xanthorrhoea results. The elements that were in high concentrations in both species of vegetation were Cd, Co, Li, Zn, while Al, Cr, Th and Zr were at higher levels in adjacent areas (Table 5.2). Rainbow's End has the highest Au values in the survey at 3.6 ppb (median = 0.3 ppb). The site also had high values of Au, Mg and Sr in both the eucalypts and the xanthorrhoea, with Cr being elevated in the surrounding area for both media (Table 5.2). Samples of both eucalypt and xanthorrhoea were taken at Kohinoor, with Ba, Ce, La, Mn, Ni elevated in both species; and Ba, Cr, Hg elevated in adjacent areas (Table 5.2). Ag, Ca, La, Li, Na, P, Pb, Sr, Ti were high in both species at WRC. A lack of adequate vegetation and poor access resulted in a lesser number of samples in the immediate area of the historic prospect, however from the sample that was obtained outside the area of known mineralisation, Cr was again high in both species.

5.5. Discussion

The primary aim of most biogeochemical surveys is to provide a proxy to enable the characterisation of the chemistry of the underlying bedrock. This allows areas of economic mineralisation to be identified. In order to do this it is necessary to understand the causes of variation within plant chemistry particularly in regards to the landscape setting and differing species sampled.

5.5.1. Comparing Xanthorrhoea and Eucalypt Datasets

There are a number of differences to note in the elemental uptake between the eucalypts and the xanthorrhoea. The concentrations of Rb, Sr, K, and Ba are significantly higher in the xanthorrhoea than in the eucalypts (Figures 5.18-5.21), with the eucalypts being higher in B, Cu, Hg, Mn, Ni and Zn. A comparison of stacked normal probability plots and histograms (Figures 5.7-5.17), shows that some elements also have higher concentrations in a particular species of eucalypt. This includes higher concentrations of Na and Ni in the narrow leaf mallee; B and Ba in the cup gum; and Cd, Mn, Zn in the manna gum.

Of the elements enriched in the xanthorrhoea, Ba shows the greatest variation from the eucalypt concentrations, with a mean and maximum of 22.65 ppm and 140 ppm in the xanthorrhoea and 6.2 ppm and 42.5 ppm in the eucalypts. The distribution of both datasets are normal, with slightly higher results from the eucalypts in the northern area of the island. Rubidium was also found in significantly higher concentrations in the xanthorrhoea than in the eucalypts, with a mean and maximum of 6.46 ppm and 34.1 ppm in the xanthorrhoea compared to 2.51 ppm and 14.8 ppm in the eucalypts. The distributions of both datasets are again close to normal; however, in contrast to Ba higher values occur in the southern and central parts of the Island for both datasets. Unlike Rb and Ba, K and Sr do not have significantly higher maximum values in the xanthorrhoea compared to the eucalypts, but the mean values of each in the xanthorrhoea are greater than double that observed in the eucalypts. The mean values for K are 0.5% for the eucalypts and 1.1% for the xanthorrhoea, while Sr values are 37.6 ppm and 51.16 ppm for the eucalypts and xanthorrhoea respectively.

The elements that are consistently enriched in the xanthorrhoea are Group I and II lithophile elements that are considered to be quite mobile within the low temperature regolith environment (Scott, 2009). In many cases their mobility is associated with the weathering of feldspars into clays, in particular Sr from plagioclase and Ba, Rb and K from potassium feldspar (Kabata-Pendias, 2001; Scott, 2009) These elements show differences between the

three sampling periods, suggesting a strong influence of near-surface groundwater on the concentrations in plant materials. The xanthorrhoea, with shallower root systems, are likely to be tapping into 'enriched' zones or water sources of mobile elements in the near surface. By comparison, the deeper-rooted eucalypts are drawing water from the groundwater that is potentially in chemical equilibrium with the bedrock. The elements that are higher in the eucalypts include Cu, Hg, Mn, Ni and Zn and are all transition metallic elements. These could be present in the less weathered bedrock that the eucalypt roots are tapping into. The lower concentrations of these elements in the xanthorrhoea data may suggest that they are absent from the upper parts of the profile. This interpretation is also consistent with the differences in concentration observed in the xanthorrhoea compared to the eucalypts.

5.5.1.1. Significant spatial variation and the influence of species bias

Four elements are examined that show definite and defined trends or anomalies within the data that correlate to particular geographical areas. For three of the four elements (except Na), the concentrations of elements within the eucalypts are far higher than in the xanthorrhoea. These elements are used to examine possible species bias, as different species of plants will have different element requirements and as a consequence, different elemental signatures.

Sodium and Ni have the most distinct geographical trends, however these trends are associated with a particular eucalypt species, the narrow leaf mallee. This suggests that this species accumulates both Ni and Na to a greater extent than the other eucalypt species. The narrow leaf mallee was only sampled on the eastern parts of the island and Dudley Peninsula (Figure 5.1), as it grows in the sandy soils found in and around the coastal lowlands. This distribution accounts for the perceived spatial trends seen in the data when the eucalypt data are viewed as a single dataset. The geographical Ni anomaly, as an element of economic interest, is not considered to represent a real basement chemistry anomaly as no anomaly is observed within the xanthorrhoea dataset (Figures 5.15–5.16).

Calcium results for the eucalypts show a slight trend of elevated values towards the coast and a significant lack of elevated values on the main plateau. This is reflected in a lower response from the stringy barks in the species comparison than the narrow leaf mallee or the cup gum. These trends are much less distinct within the xanthorrhoea samples, but do still show similar trends to the eucalypt data. Given the prevalence of the Bridgewater Formation and other carbonate regolith in the coastal regions, the elevated Ca levels are attributed to regolith and location.

Yttrium data shows differing characteristics for the eucalypts and the xanthorrhoea. The eucalypts have significantly higher results in the manna gums associated with mineralisation, but also show a band of elevated concentrations running parallel to the southern coastline, with low levels elsewhere on the plateau. The xanthorrhoea results also show lower levels on the plateau. However they do not show the same elevated concentrations on the south coast, and instead show elevated areas in the north of the island that are not associated with mineralisation.

In order to examine these trends further, we looked at the elements with the most pronounced species differentiation (Na, Ni, and Pb) to determine whether there was an effect if the species were treated as different datasets (Figures 5.22–5.25). Only five of the species are considered here; cup gums, manna gums, narrow leaf mallee, sugar gums and stringy barks. All three elements showed significantly different spatial data when the statistics were limited to individual species, particularly for Na and Ni. This is likely to be due to the removal of geobotanical bias associated with the narrow leaf mallee. As a consequence, the lithological and landscape change is less apparent, but elevated points within the data are much more apparent and are a better representation of elevated signals within the system as a whole. The differences in the species are more apparent when considering the statistics, for example, the range of Ni in the cup gums is 0.2 ppm to 6.2 ppm, while the narrow leaf mallee is 0.5 ppm to 10.1 ppm. The Pb data were treated differently, as three of the species

(manna gum, narrow leaf mallee and stringy bark) all contained exceptionally low values. These were plotted up on the map using the manna gum standard deviation statistics. By separating the data into three different groups, a larger variation in the individual species datasets can be seen, providing a more useful spatial representation of the data than was originally produced due to the skew created by the high values of select species.

The higher concentrations of Ni and Na in the narrow leaf mallee are geobotanical indicators, in that they indicate a different lithology type in that area. The change in distribution of the narrow leaf mallee compared to the cup gum and stringy bark also supports a change in lithology type. There seems to be no preferred area for the cup gums or stringy barks on the central portion of the island. Ni is also enriched within the narrow leaf mallee, by removing that population from the larger set of statistics, the anomalous zones around the known areas of mineralisation become more distinct. This highlights the importance of considering the influence of a particular species on a given element within multi-species biogeochemical vegetation surveys. When elemental concentration bias is introduced by a particular species, treating the different species as different datasets (as has been done here) is a relatively straightforward method of examining these issues within the data. Within a large-scale, regional exploration survey, this method of separating the data by species may not be feasible for all elements, as it produces too many variables for routine consideration and for the majority of elements is unwarranted. However, for some elements it is vital for as demonstrated by the pronounced difference seen between species for elements such as Na and Ni.

A suggested workflow for large, multi-species biogeochemical surveys is:

1. Examination of the raw data with stacked normal probability plots and/or histograms differentiated according to species to allow for determination of clear inter-species biases in element concentrations. If no inter-species biases are observed for a given element then the dataset can be considered as a whole for identification of spatial variation

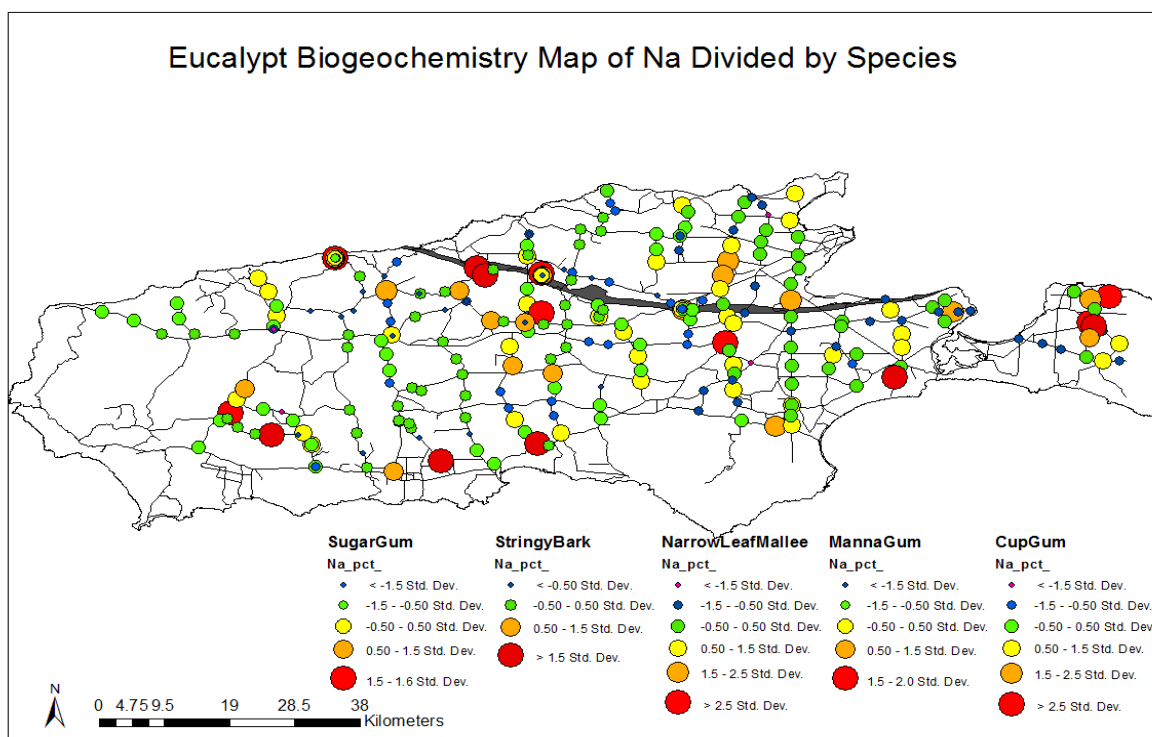


Figure 5.22: Eucalypt data for Na, but mapped by species statistics, rather than as a whole dataset. In this case, this has removed the geographical bias seen in Figure 15.

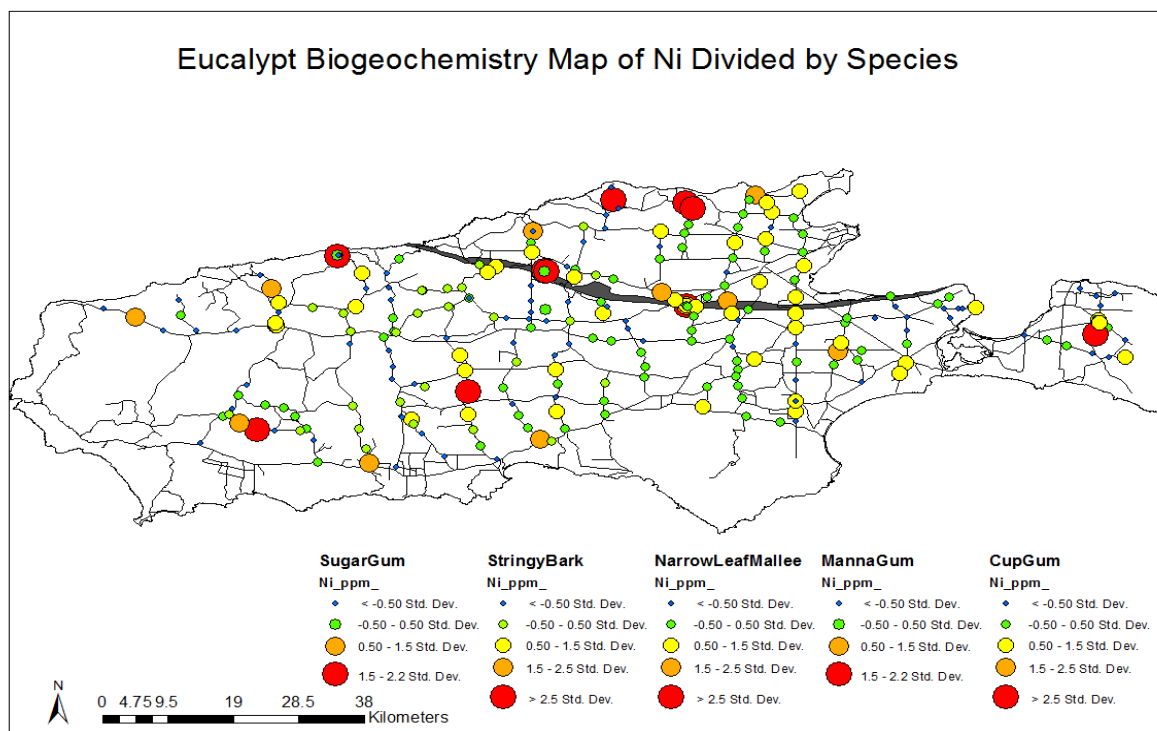


Figure 5.23: Eucalypt data for Ni, but mapped by species statistics, rather than as a whole dataset. In this case, this has removed the geographical bias seen in Figure 16, which was related to increased uptake of Ni by the narrow leaf mallee, a species with a particular distribution.

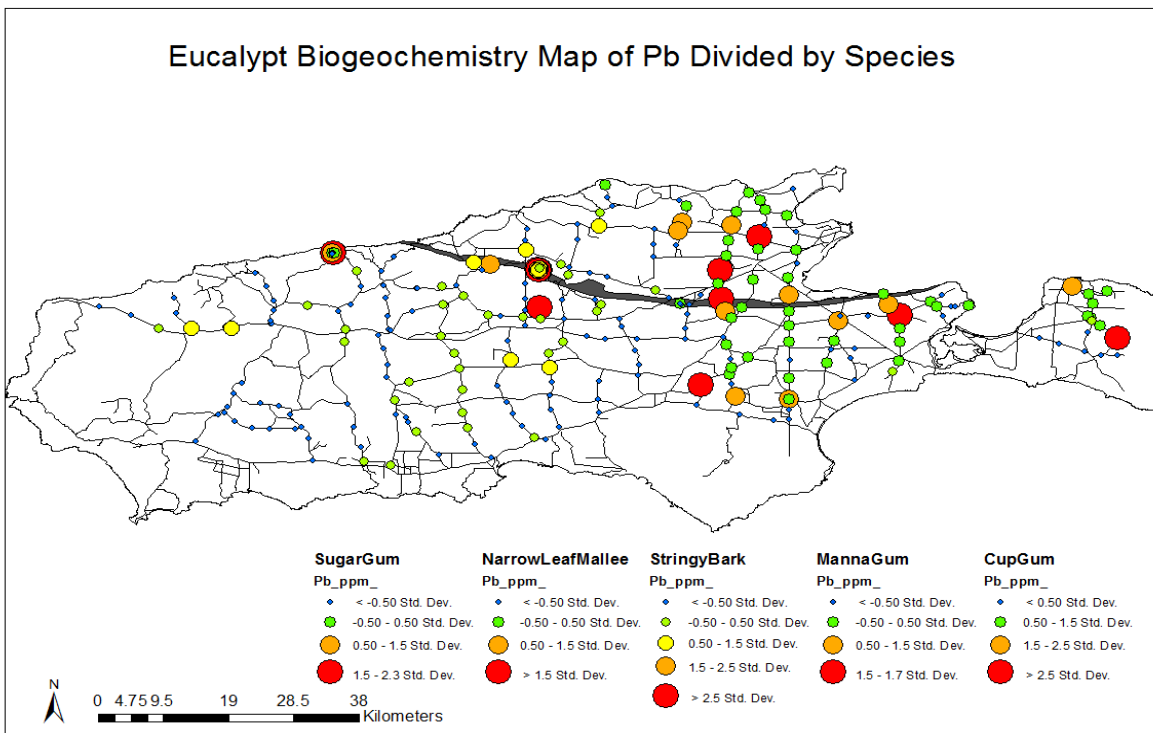


Figure 5.24: Eucalypt data for Pb, but mapped by species statistics, rather than as a whole dataset. In this case, this has removed the geographical bias seen in Figure 11, due to the very high levels of Pb in the WRC prospect.

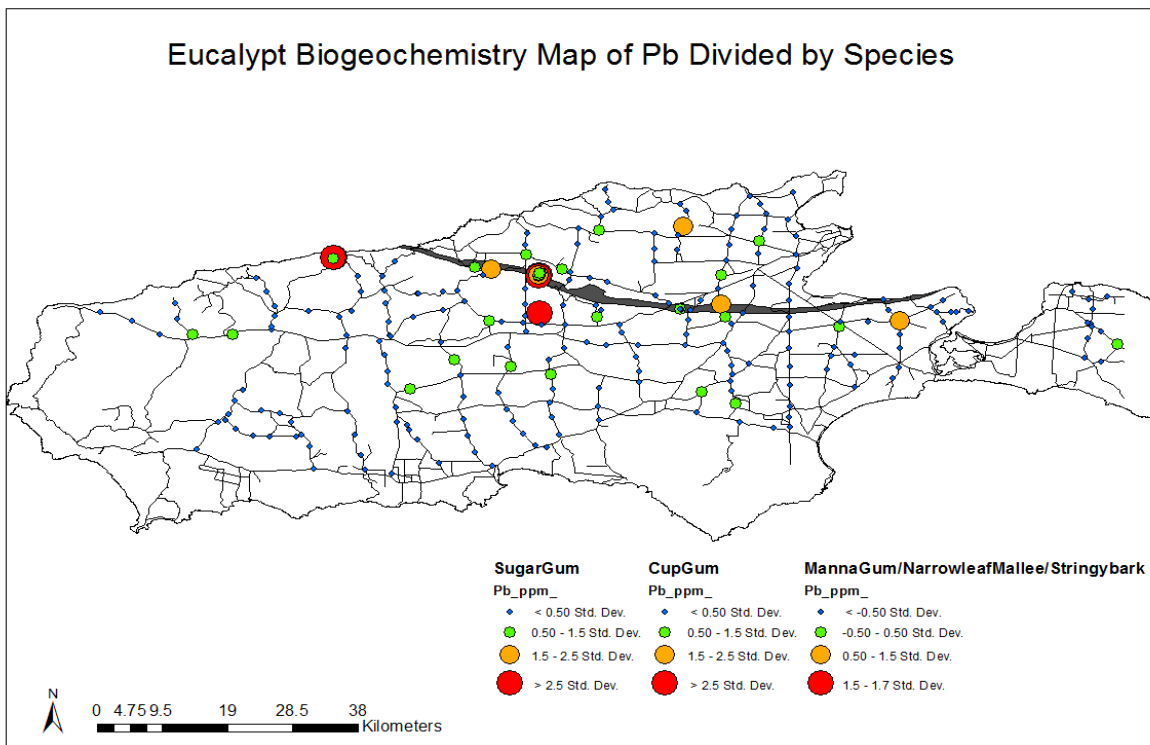


Figure 5.25: Eucalypt data for Pb, this time the species statistics are grouped. The manna gum, narrow leaf mallee and stringybark all returned quite low results, so were grouped together. This has removed the variety of elevated levels that were seen in Figure 23, however has highlighted the area around the Cygnet-Snelling Fault Zone.

and exploration target identification.

2. Where inter-species bias is identified, then the spatial distribution of each species can be considered for geobotanical influence.

- a) Assuming the geobotanical influence does not correlate with mineralisation then the species can be separated and plotted with separate statistics in order to see if anomalies are associated with mineralisation, as demonstrated above.
- b) If a geo-botanical distribution coincides with mineralisation, then a similar process should be followed, however the removal of just the species associated with mineralisation should be sufficient to remove the bias from the dataset. Any other occurrences of that species could be indicative of mineralisation, so should be examined closely.

In treating biogeochemical data, Dunn (2011) suggests the median levels of datasets be considered as the background level, in order to identify anomalously high values worth considering. This approach appears appropriate for most elements in this study. However, as discussed, in some cases data must be separated by species as consistently higher element concentrations can bias the median towards values higher than the true background. Such an effect would not be expected by extreme values reported from a single site, i.e. plants sampled around a mine, as their inclusion would not sufficiently modify the median value to falsely increase the background values and hide otherwise anomalous concentrations and sites.

Sampling over known mineralisation as part of any larger scale survey is recommended, to test and identify the biogeochemical response of the vegetation sampled to the mineralisation in the area. The incorporation of known mineralisation into every survey makes it easier to identify natural variation, elevated points and any geobotanical or species bias. If there is no known mineralisation in the area, then test sampling outside the tenement should be considered. If anomalies are returned outside of known mineralisation, then QA/QC

should be considered carefully and the data validated. In the case of a larger, regional scale survey, a smaller, more densely sampled survey would then be appropriate, as was conducted over known mineralised zones in this study.

5.5.2. Mineralised Zones

Four case studies were conducted over known mineralised areas, with both the biogeochemical datasets. Several elements were similarly elevated for both the eucalypts and the xanthorrhoea, such as Pb, Cd, Zn, Co, Li and Zn. These high values for both species are an indication that these elements are mobile up and down the soil profile. However, in a few cases the highest values for the element are from the xanthorrhoea in the mineralised zones (Pb, Cd, Zn) suggest that either these elements are being accumulated within the top of the soil profile, or by the plants themselves. Essential elements for plants include Ca, Cu, Fe, Mg, Mn, Mo, N, P, K, S and Zn. However, looking at the elements relative to each other within the system still gives a reasonable indication of what is anomalous and what is background. In this survey, the essential elements Ca, Cu, Fe, Mg, Mn, Mo and P showed elevated levels both in areas that are known to be mineralised and those that are not. As a consequence, these are elements that need to be treated with caution. When used in conjunction with other elements and data, they provide more evidence for a prospect, however when looked at in isolation, may provide false positives. Elements that have been suggested to be used as proxies for some of these essential, and economic elements, include Cd for Zn (Dunn, 2011). In comparing these two elements for eucalypt samples, there is certainly a correlation between areas that are high in Cd and those that are high in Zn, however this is not always the case.

Within the eucalypt samples at these sites, there are a number of elements that are at or near detection limits in the 'striped' graphs that have been dismissed. Of particular interest for mineral exploration is Tl; as the only places where Tl is detected is at Western River Cove, Bonaventura and Rainbow End deposits. Tl is known to be associated with Ag and

Pb (Kabata-Pendias, 2001) and the Pb levels where Tl is detected are very high. As a consequence, it is suggested that Tl could be used as a pathfinder for Ag–Pb deposits. However due to the lack of dispersion of Tl, it would most likely only occur when the presence of Pb and Ag is already known.

The extremely high anomalies of Pb, may be the result of partial exclusion of the metals by the plants (Brooks, 1972); this partial exclusion can result in either very high or very low levels. If the elements become too concentrated within a plant then this will prove fatal to the plant, and therefore anomalous values should not be expected. Aside from the paddock clearance, this may also have an influence on the lack of vegetation in the areas around Western River Cove, as the other sites were all quite heavily vegetated.

In regards to biogeochemical pathfinders and halos, the surveys were poorly designed to specifically consider this aspect. To fully explore the relationships of the elements moving towards a mineralised zone, there needed to be consistent sampling at regular intervals from the mineralised zone. Due to the sparse and variable nature of the vegetation, in part reflecting the variable landscape and underlying lithologies, this was not possible. However, from the sample sites that were located in proximity to the mineralised zones, Cr in particular is consistently elevated, for both types of biogeochemical samples. Other elements such as Al, Hg and Mg also appear frequently, but with no preference to a particular species. The natural variation present in vegetation also makes defining small-scale anomalies difficult. These factors make it difficult to say exactly what the ideal sampling density is for mineral exploration. The sampling programs in the mineralised case study areas suggest that sampling over a mineralised area does not guarantee elevated concentrations of elements within the biogeochemical survey.

5.6. Conclusions

In this study, biogeochemical surveys have been useful and provided additional information regarding the landscape system. The data from each of the biogeochemical sampling media, whilst interacting with the other media, does need to be analysed individually. In order to gain as more information, the use of a number of biogeochemical sample media may allow for different aspects of the subsurface to be expressed.

The sample media that is appropriate for the survey is primarily dependant on the objective element or purpose of the survey. Eucalypt species would be the most suitable sample media for a mineral exploration project targeting the traditional metallic commodities of Cu, Pb, Zn, Au and Ag. Whereas if sruvey purpose was environmental, in order to examine the upper levels of the soil and subsurface, the xanthorrhoea would be more suitable.

Sampling density is also dependent on the purpose of the survey. Large scale surveys, such as conducted here, are ideal for a 'first pass' exploration technique, as they will broadly identify areas that have a change in lithology. High-density, localised sampling can be variable, and it is perhaps best done in conjunction with other types of surveying, such as soil sampling. Consistency within the sampling media is paramount as the differences between the species can be quite significant. If the sample media are consistent then one aspect of variation that may affect the dataset is eliminated.

Despite the difficulties of collecting consistent, contaminant free biogeochemical samples, as well as the high rate of natural variability, biogeochemistry is recommended as a first pass, large scale exploration technique for mineral prospects, particularly in areas where bedrock is difficult to access. The use of the biogeochemistry at a prospect scale can also be of use, however this is dependent on a high number of factors including vegetation coverage, species consistency, sample variation and landscape inconsistencies, which make it difficult gain accurate, reliable results.

Element	N	Detection Limits	Unique Values	Mean	Standard Deviation	Minimum	50%	Maximum
Ag (ppb)	341	2 ppb		5.471	9.63288	2	4	70
Al (pct)	341	0.01%		0.02303	0.01354	0.01	0.02	0.08
As (ppm)	341	0.1 ppm	6	0.18046	0.077518	0.1	0.2	0.6
Au (ppb)	341	0.2 ppb	10	0.440426	0.494605	0.2	0.3	3.6
B (ppm)	341	1 ppm	68	30.422	17.621	8	26	131
Ba (ppm)	341	0.1 ppm	119	6.2381	6.5098	0.7	4.3	41.3
Be (ppm)	341	0.1 ppm	2	0.1	0	0.1	0.1	0.1
Bi (ppm)	341	0.02 ppm	12	0.054889	0.049446	0.02	0.04	0.3
Ca (%)	341	0.01%	116	0.766217	0.348266	0.18	3.17	3.17
Cd (ppm)	341	0.01 ppm	37	0.08686	0.090332	0.01	0.06	0.7
Ce (ppm)	341	0.01 ppm	113	0.505249	0.863242	0.02	0.2	9.2
Co(ppm)	341	0.01 ppm	35	0.0877	0.109	0.01	0.06	1.22
Cr (ppm)	341	0.1 ppm	19	1.7575	0.37727	0.9	1.7	2.6
Cs (ppm)	341	0.005 ppm	36	0.012788	0.009494	0.005	0.011	0.078
Cu (ppm)	341	0.01 ppm	265	4.22	1.8478	1.04	3.79	12.08
Fe (%)	341	0.00%	56	0.01726	0.0145	0.002	0.012	0.094
Ga (ppm)	341	0.1 ppm	3	0.12	0.04	0.1	0.1	0.2
Ge (ppm)	341	0.01 ppm	6	0.019038	0.009401	0.01	0.02	0.05
Hf (ppm)	341	0.001 ppm	21	0.00475	0.004336	0.001	0.003	0.031
Hg (ppm)	341	1 ppm	63	27.357	15.8906	2	24	101
In (ppm)	341	0.02 ppm	n/a	n/a	n/a	n/a	n/a	n/a
K (%)	341	0.01%	83	0.565	0.196	0.14	0.53	1.4
La (ppm)	341	0.01 ppm	82	0.2663	0.454	0.01	0.11	5.1
Li (ppm)	341	0.01 ppm	99	0.4307	0.432019	0.03	0.31	4.01
Mg (%)	341	0.00%	177	0.2241	0.068391	0.09	0.222	0.442
Mn (ppm)	341	1 ppm	168	116.6891	192.678	6	59	1956
Mo (ppm)	341	0.01 ppm	36	0.0775	0.2059	0.01	0.04	3.48
Na (%)	341	0.00%	262	0.456293	0.2216	0.15	0.413	1.567
Nb (ppm)	341	0.01 ppm	3	0.015	0.01	0.01	0.01	0.03
Ni (ppm)	341	0.1 ppm	58	1.68	1.5583	0.1	1.1	10.1
P (%)	341	0.00%	108	0.06969	0.034522	0.008	0.59	0.224
Pb (ppm)	341	0.01 ppm	57	0.6075	4.128	0.01	0.105	57.11
Pd (ppb)	341	2 ppb	3	2.667	1.1547	2	2	4
Pt (ppb)	341	1 ppb	6	1.8518	1.511	1	1	7
Rb (ppm)	341	0.1 ppm	72	2.5167	2.019	1.8	1.8	14.8
Re (ppb)	341	1 ppb	5	2.65	4.826	1	2	23
S (%)	341	0.01%	27	0.1432	0.0477	0.02	0.14	0.28
Sb (ppm)	341	0.02 ppm	3	0.03	0.2236	0.02	0.02	0.07
Sc (ppm)	341	0.1 ppm	6	0.241	0.0754	0.1	0.2	0.5
Se (ppm)	341	0.1 ppm	8	0.207	0.101	0.1	0.2	0.7
Sn (ppm)	341	0.02 ppm	10	0.03416	0.021717	0.02	0.025	0.11
Sr (ppm)	341	0.5 ppm	267	37.6305	26.33805	6.5	30.6	224.3
Ta (ppm)	341	0.001 ppm	3	0.001143	3.59E-04	0.001	0.001	0.002
Te (ppm)	341	0.02 ppm	5	0.03	0.0085	0.02	0.03	0.05
Th (ppm)	341	0.01 ppm	20	0.0393	0.0371	0.01	0.03	0.26
Ti (ppm)	341	1 ppm	13	3.4401	2.1351	1	3	13
Tl (ppm)	341	0.02 ppm	9	0.073636	0.0504	0.02	0.05	0.18
U (ppm)	341	0.01 ppm	10	0.025	0.0177	0.01	0.02	0.1
V (ppm)	341	2 ppm	20	8.523	4.8915	2	7	20
W (ppm)	341	0.1 ppm	n/a	n/a	n/a	n/a	n/a	n/a
Y (ppm)	341	0.001 ppm	186	0.1473	0.2277	0.002	0.06	1.617
Zn (ppm)	341	0.1 ppm	170	14.7413	11.61	4.2	11.9	127.3
Zr (ppm)	341	0.01 ppm	38	0.087552	0.086433	0.01	0.06	0.59

Table 5.2: Univariate statistics by element for eucalypt samples.

Element	N	Detection Limits	Unique Values	Mean	Standard Deviation	Minimum	50%	Maximum
Ag (ppb)	263	2 ppb	9	5.08	4.8	2	4	26
Al (pct)	263	0.01%	4	0.0159	0.006277	0.01	0.01	0.03
As (ppm)	263	0.1 ppm	6	0.212	0.0946	0.1	0.2	0.5
Au (ppb)	263	0.2 ppb	9	0.407	0.3375	0.2	0.3	2.8
B (ppm)	263	1 ppm	16	5.988	3.1142	3	5	34
Ba (ppm)	263	0.1 ppm	199	22.65	20.7719	0.6	17.1	137.5
Be (ppm)	263	0.1 ppm	n/a	n/a	n/a	n/a	n/a	n/a
Bi (ppm)	263	0.02 ppm	10	0.0552	0.04	0.02	0.04	0.14
Ca (%)	263	0.01%	83	0.6168	0.2219	0.25	0.58	1.65
Cd (ppm)	263	0.01 ppm	23	0.1263	0.6459	0.01	0.03	7.26
Ce (ppm)	263	0.01 ppm	81	0.3601	0.6292	0.01	0.19	7.1
Co(ppm)	263	0.01 ppm	19	0.0404	0.0376	0.01	0.03	0.3
Cr (ppm)	263	0.1 ppm	20	1.6748	0.3957	0.3	1.6	2.6
Cs (ppm)	263	0.005 ppm	27	0.012	0.0077	0.005	0.01	0.068
Cu (ppm)	263	0.01 ppm	123	1.5086	0.527	0.77	1.4	4.54
Fe (%)	263	0.00%	32	0.0105	0.0075	0.001	0.008	0.045
Ga (ppm)	263	0.1 ppm	n/a	n/a	n/a	n/a	n/a	n/a
Ge (ppm)	263	0.01 ppm	7	0.0217	0.0117	0.01	0.02	0.06
Hf (ppm)	263	0.001 ppm	12	0.0029	0.002	0.001	0.002	0.011
Hg (ppm)	263	1 ppm	26	9.7374	4.4417	1	9	29
In (ppm)	263	0.02 ppm	n/a	n/a	n/a	n/a	n/a	n/a
K (%)	263	0.01%	125	1.1214	0.3603	0.25	1.17	2.18
La (ppm)	263	0.01 ppm	63	0.2026	0.3432	0.01	0.11	4.29
Li (ppm)	263	0.01 ppm	33	0.0896	0.0695	0.01	0.07	0.51
Mg (%)	263	0.00%	149	0.182	0.063	0.066	0.17	0.452
Mn (ppm)	263	1 ppm	94	44.9467	43.8203	3	31	280
Mo (ppm)	263	0.01 ppm	23	0.0582	0.048	0.01	0.05	0.39
Na (%)	263	0.00%	185	0.177	0.1765	0.013	0.121	1.06
Nb (ppm)	263	0.01 ppm	n/a	n/a	n/a	n/a	n/a	n/a
Ni (ppm)	263	0.1 ppm	18	0.4162	0.3057	0.1	0.3	3
P (%)	263	0.00%	38	0.0312	0.0114	0.019	0.029	0.141
Pb (ppm)	263	0.01 ppm	60	0.8486	5.1334	0.01	0.07	71.78
Pd (ppb)	263	2 ppb	n/a	n/a	n/a	n/a	n/a	n/a
Pt (ppb)	263	1 ppb	3	1.2	0.4103	1	1	2
Rb (ppm)	263	0.1 ppm	117	6.4676	5.0596	0.5	5.1	34.1
Re (ppb)	263	1 ppb	4	2.8571	6.3833	1	1	25
S (%)	263	0.01%	28	0.1046	0.0508	0.01	0.1	0.32
Sb (ppm)	263	0.02 ppm	n/a	n/a	n/a	n/a	n/a	n/a
Sc (ppm)	263	0.1 ppm	6	0.2525	0.0743	0.1	0.2	0.5
Se (ppm)	263	0.1 ppm	6	0.1797	0.084	0.1	0.2	0.5
Sn (ppm)	263	0.02 ppm	6	0.0321	0.0127	0.02	0.03	0.06
Sr (ppm)	263	0.5 ppm	217	51.16	31.054	14.2	41.8	200.3
Ta (ppm)	263	0.001 ppm	3	0.0011	3.52E-04	0.001	0.001	0.002
Te (ppm)	263	0.02 ppm	3	0.0228	0.0048	0.02	0.02	0.03
Th (ppm)	263	0.01 ppm	11	0.0262	0.018	0.01	0.02	0.1
Ti (ppm)	263	1 ppm	7	2.0109	0.9102	1	2	8
Tl (ppm)	263	0.02 ppm	n/a	n/a	n/a	n/a	n/a	n/a
U (ppm)	263	0.01 ppm	n/a	n/a	n/a	n/a	n/a	n/a
V (ppm)	263	2 ppm	17	8.4545	3.9227	2	9	17
W (ppm)	263	0.1 ppm	n/a	n/a	n/a	n/a	n/a	n/a
Y (ppm)	263	0.001 ppm	139	0.0813	0.1179	0.001	0.044	1.328
Zn (ppm)	263	0.1 ppm	120	12.142	23.795	2.9	8.8	298.1
Zr (ppm)	263	0.01 ppm	22	0.0494	0.0425	0.01	0.04	0.22

Table 5.3: Univariate statistics by element for xanthorrhoea samples.

Chapter 6

The Landscape Evolution of Kangaroo Island:
Integrating Datasets

6.1. Introduction

This thesis aimed to bring together field observations, petrography, geochemistry and biogeochemistry to characterise the landscape evolution of Kangaroo Island and further investigate the use of regolith and biogeochemical systems for mineral exploration. The following interlinked interpretations are considered to be the primary findings and conclusions from these studies.

1. Ferricrete and ferruginous materials on Kangaroo Island are the result of an extended period of formation, and have been largely in place since the Eocene.
2. Identification of *in situ* and transported ferricretes is best done through identifying different morphologies in hand specimen.
3. The mobilisation of major, trace and economic elements potentially limits the use of many of the weathered materials for mineral exploration.
4. The interaction of biogeochemical systems with the regolith and landscape mean they are a suitable sampling material for mineral exploration.

Each of these points will be further discussed below, bringing together ideas and concepts that have been raised and discussed separately in the individual chapters within the thesis.

6.2. Ferricrete on Kangaroo Island: the result of continuous formation but largely in place since the Eocene

The initiation of ferricrete formation on Kangaroo Island, established through relative age constraints, occurred during the Eocene–Oligocene. This regolith system was possibly initiated by tectonic movement and uplift along the Cygnet–Snelling Fault Zone, as part of regional scale tectonic reactivation of pre-existing structures. The establishment of relative age constraints on ferricrete formation indicates they are long-lived within the landscape but have been continually reworked and reformed.

One of the striking aspects of the landscape evolution on Kangaroo Island is the long-lived nature of the ferricrete landscape surface. Arguably, science and general opinion regarding landscape evolution is still influenced heavily by the concepts taken from the Northern hemisphere, in which landforms and landscapes are young, due to widespread Quaternary glaciation. However, the semi-arid climates that operate in southern Australia, including on Kangaroo Island, typically have slow erosion rates helping to preserve landscape features such as the studied ferricrete. Similar weathering rates are widely acknowledged from elsewhere in the world but the lack of widespread Quaternary glaciation makes this much more demonstrable in the Southern Hemisphere (Gale, 1992). The small and slow variation in climate in southeast Australia during the Mesozoic and Cenozoic, in contrast to the increase in denudation and abrupt climate shifts globally, also helps to maintain a near steady-state weathering system within these extremely long time scales (Bourman, 1989; Taylor et al., 1992).

The self-preserving nature of the ferricretes, and thus the plateau, is also a major contributor to the long lived nature of the landscape. Indurated iron oxides are significantly more robust than highly weathered saprolite or non-indurated soil profiles. This means they do not readily erode, and even when physically eroded will often be continually reworked, and remain as a primary part of the landscape. This behavior also highlights the on-going

nature of the regolith forming process, as exemplified by the vermiform ferricretes.

It is acknowledged that these conclusions have been reached through the relative dating of the landscape and landscape processes, rather than any absolute dating. At this point it is exceptionally difficult to date regolith materials, particularly as they are often continually reworked, so signatures of formation are overprinted and become mixed. In addition, many of the methods used for dating landscape evolution processes (e.g. optically stimulated luminescence (OSL)) are only able to constrain the age of the last exposure at the land surface. Such approaches will not work for regolith materials formed *in situ* (i.e. the majority of the ferricrete) but do hold potential to determine the most recent age of mobilisation and reworking of the vermiform ferricretes. The provision of an absolute date for the initiation of ferruginisation and the beginning of that aspect of landscape evolution would allow for improved correlation of episodes of ferricrete formation and reworking to global and local climate and sea-level changes.

6.3. Identification of *in situ* and transported ferricrete formation

Petrography and micro-analytical geochemical data were able to demonstrate that ferruginous materials on Kangaroo Island formed from the weathering of the underlying bedrock; the Cambrian Kanmantoo and the Kangaroo Island Group metasedimentary rocks. In the studied weathered bedrock and saprolite samples it was apparent that the preserved fabric and mineralogy indicated the protolith material was the Kanmantoo Group metasedimentary rocks. Field observations of weathering profiles indicated that the complex ferricretes also had a direct relationship to the weathered bedrock, suggesting that the pisoliths are a direct relation of the weathered bedrock. The rounded nature of the pisolith concretions are the result of the repetition of groundwater conditions causing cyclic deposition of aluminium and iron around a central core of highly weathered bedrock material. In contrast, the vermiform ferricretes are formed by reworking of transported regolith and ferricrete materials. It is perhaps not surprising that a significant amount of

transported and reworked ferricrete material exists – the marble-like nature of the pisoliths means they are easily transported. As a consequence the ferricrete materials can be actively redistributed and spread throughout the landscape during weathering and erosion after their initial formation. As will be discussed, correctly identifying transported versus ferricrete material has important ramifications for mineral exploration applications.

As the ferruginous materials are dominantly formed from the underlying bedrock, there is the need to understand the bedrock as a starting point for the materials that follow. As a metasedimentary group comprised of 8 sub-units, the Kanmantoo Group is heterogeneous and so the likelihood of derived regolith materials being homogenous is quite slim. A means by which this is described is by Phillips (2003), who uses the theories of non-linearity and complexity to explain geomorphic systems. Through this, even very small changes can result in very large differences, i.e. small variations in bedrock mineralogy or fabric will result in significant differences in the regolith product. For regolith materials formed over extremely long time periods (e.g. the Kangaroo Island ferricretes) these differences are exacerbated to produce dramatically varying products (e.g. the *in situ* versus vermiform ferricretes). The lack of easily discernible geochemical indicators between *in situ* and reworked ferricretes on Kangaroo Island highlights that more research is required in order to quantify means by which these changes can be measured. For regolith materials used as exploration media, the ability to adjust the geochemical baseline levels reflecting variation within the protolith material would greatly enhance the quality and reliability of detectable geochemical anomalies.

6.4. The mobilisation of major, trace and economic elements: A potentially limiting factor the use of weathered materials in mineral exploration

Electron microprobe maps and geochemical analysis have highlighted the significant mobility of the majority of the elements within the landscape system on Kangaroo Island. The mobility of elements is interpreted to be due to the acidic environment present within the subsurface, caused through the ferrolysis reactions and processes during weathering. The weathering of sheet silicates and the introduction of water into the system in the form of groundwater leads to perfect conditions for ferrolysis, which then acidifies the subsurface environment. This acidic environment aids the further breakdown of minerals and mobilisation of their constituent elements out of the protolith. The mobilised elements are then precipitated either when the local chemical conditions change or the elements are transported to a differing chemical environment (e.g. more or less oxidising, or differing pH levels). The mobility of the elements in this system was particularly highlighted by major elements such as SiO_2 , Fe_2O_3 and Al_2O_3 . The depletion of numerous trace and economic elements from the protolith system was demonstrated to occur relatively early during the weathering process. However, economic elements such as Cu do show elevated levels proximal to mineralisation, indicating the continued movement and mobilisation of elements may still preserve some indicators of anomalous values within the underlying bedrock, depending on the chemical conditions of the system.

Due to the early mobilisation of economic elements during the weathering process, weathered bedrock and saprolite are not going to be useful for mineral exploration unless secondary enrichment occurs. The potential for some preservation of initial chemical indicators is demonstrated by the presence of native copper observed in KIFE019, this is likely to occur when the breakdown of sulphide minerals releases more Cu than can be accommodated by the surrounding groundwater and it remains '*in situ*'. Where the leached economic elements are taken into solution in groundwater these elements will be transported to the discharge points of the groundwater table, resulting in elevated levels of an element, i.e. supergene

enrichment (Butt, 2005; Lowell and Guilbert, 1970; Mathur et al., 2005). This behaviour is also likely seen in the geochemical maps of Mo and Co in Chapter 4. Both elements display elevated levels around the edges of the plateau. These possible signals may be more apparent within a higher density, smaller survey.

Another limiting factor on the use of ferricretes as a sampling media for geochemical exploration is the survey size and sample density. As the ferricretes appear not to display any geochemical alteration halos or dispersion trends, samples need to be taken close to the source of the mineral signature. This equates to requiring small, high density geochemical surveys, which are appropriate for prospect or local scale surveys, but less so to large scale, regional scale surveys at lower densities.

The integration of the geochemical results and a study of the hydrogeology and hydrogeochemistry of the area would allow for further improvement in understanding of the landscape and the landscape processes. A thorough knowledge of the hydrogeology would allow for the direction of groundwater flow and movement to be determined and this would enable the prediction of any 'downstream plumes' of economic elements from sites of mineralisation and/or the back-projection of mineralisation from groundwater discharge sites that are associated with enriched levels of elements such as Cu or Pb.

When coupled with higher sampling densities and hydrogeology studies there are multiple statistical methods which could be applied to the geochemical data in order to further elucidate any potential sites of mineralisation. This includes partial least squares regression analysis (PLSR), (Lax and Selinus, 2005) and the MAD (Median absolute derivation) method, which results in the lowest threshold, i.e. most number of samples that are elevated (Reimann et al., 2005).

6.5. The interaction of biogeochemical systems with the regolith and landscape: A suitable sampling material for mineral exploration

The biogeochemical surveys were successful in highlighting areas of mineralisation, with a greater dispersion halo than observed in the ferruginous materials. The biogeochemical surveys also helped to provide further information into the processes involved in the landscape.

Of the two biogeochemical surveys, if the aim is to conduct a mineral exploration survey then the eucalypts returned the best results. The eucalypts are interpreted to source groundwater from the weathering zone in the bedrock and effectively pick up elements as they are leached, which accounts for the greater dispersion halo observed within the biogeochemical results. While displaying a high degree of variability, even over areas of known mineralisation, this dataset was better for picking up signals at a larger scale than the ferricrete. However, there can also be difficulties in biogeochemical surveys, particularly when it comes to inter-species variations, which can be quite marked. This makes large, regional scale surveys difficult, as there is a high possibility that there will not be a consistent vegetation species available for sampling across the entire area. This results in a data set in which different species need to be compared and potentially excluded in order to correctly identify meaningful chemical anomalies. The xanthorrhoea, overall, was less successful in taking up elements of interest, most likely to do with its shallower root system. The shallower root system is likely to tap into the already leached saprolite or groundwater that has only been recently recharged by rainwater (diluting any chemical signature of the underlying bedrock).

The shallower root system of the xanthorrhoea allows for the investigation of the mobility of certain elements in the subsurface. The increased uptake of Ba, K, Sr and Na, in the xanthorrhoea is consistent with the release of these elements during weathering of feldspars and clays in the upper subsurface. These elements are also likely to be mobile in the environments created by the ferrollysis process on the island. Further research could be

conducted to see if xanthorrhoea surveys at high sampling density are able to characterise the variation within subsurface environments related to seasonal variation in groundwater levels and recharge and/or the spatial variation in subsurface chemical conditions (e.g. stage of weathering). An interesting aspect to consider is the use plants such as xanthorrhoea for environmental contamination monitoring. As it has a shallow root system it will be much more sensitive to human-induced contamination of groundwater and may therefore be better suited to biogeochemical surveys targeting environmental contamination mapping rather than economic mineralisation.

6.6. Final Remarks

This work provides a landscape context and framework for the use of regolith and plant materials in exploration on Kangaroo Island. Regolith field observations and the production of the regolith–landform map have placed more constraints on the ferricrete and plateau formation and also on the formation of the landscape and the landscape history of the island.

This work has demonstrated the complex and interlinked nature of the controls that impact on weathering processes and the formation of the regolith. Ferricretes and ferruginous materials are an exceedingly complex materials with both *in situ* and transported materials present on Kangaroo Island. Despite this complexity the ferricrete materials have been demonstrated to be useful for mineral exploration, and although potentially only providing small target areas, they do highlight areas of mineralisation. Conversely, and maybe surprisingly, the underlying weathered bedrock potentially has less use for mineral exploration as the economic metals have been readily mobilised out of the bedrock during the weathering processes on Kangaroo Island.

The biogeochemical surveys proved to be successful exploration techniques. Of the

two surveys, the eucalypts were the most successful in regards to displaying economic mineralisation signatures of the underlying bedrock. However, inter-species variations with the eucalypts makes large scale surveys difficult as further filtering or consideration is required to compare different species within the data set. The xanthorrhoea data are interpreted to provide information on processes and subsurface chemistry in the upper part of the subsurface. This means they can be highly influenced by rainfall events and climatic variation potentially requiring sampling within short time periods to ensure comparability of data across the entire survey region.

This thesis has been able to demonstrate the potential usefulness as well as challenges associated with ferricrete and vegetation for biogeochemical and geochemical sampling for mineral exploration. In further examining these materials a contribution has been made to furthering the understanding of the landscape evolution of Kangaroo Island, building on previous work, and providing a basis for future work.

References

ALEVA, G.J.J., 1994. Laterites: concepts, geology, morphology and chemistry. International Soil Reference and Information Centre (ISRIC).

ALLEY, N., BOURMAN, R., MILNES, A.R., 2013. Late Paleozoic Troubridge Basin sediments on Kangaroo Island, South Australia.

ALLEY, N.F., 1977. Age and origin of laterite and silcrete duricrusts and their relationship to episodic tectonism in the mid-north of South Australia. *Journal of the Geological Society of Australia* 24, 107-116.

AMBROSI, J.P., NAHON, D., HERBILLON, A.J., 1986. The epigenetic replacement of kaolinite by hematite in laterite — petrographic evidence and the mechanisms involved. *Geoderma* 37, 283-294.

ANAND, R.R., 2016. Regolith-landform processes and geochemical exploration for base metal deposits in regolith-dominated terrains of the Mt Isa region, northwest Queensland, Australia. *Ore Geology Reviews* 73, Part 3, 451-474.

ANAND, R.R., ASPANDIAR, M.F., NOBLE, R.R.P., 2016. A review of metal transfer mechanisms through transported cover with emphasis on the vadose zone within the Australian regolith. *Ore Geology Reviews* 73, Part 3, 394-416.

ANAND, R.R., BUTT, C.R.M., 2010. A guide for mineral exploration through the regolith in the Yilgarn Craton, Western Australia. *Australian Journal of Earth Sciences* 57, 1015-1114.

ANAND, R.R., PAINE, M., 2002. Regolith geology of the Yilgarn Craton, Western Australia: implications for exploration. *Australian Journal of Earth Sciences* 49, 3-162.

ANAND, R.R., PAINE, M.D., SMITH, R.E., 2002. Gensis, classification and atlas of ferruginous materials, Yilgarn Craton

ANDERSON, S.P., DIETRICH, W.E., BRIMHALL, G.H., 2002. Weathering profiles, mass-balance analysis, and rates of solute loss: Linkages between weathering and erosion in a small, steep catchment. *Geological Society of America Bulletin* 114, 1143-1158.

ARNE, D.C., STOTT, J.E., WALDRON, H.M., 1999. Biogeochemistry of the Ballarat East goldfield, Victoria, Australia. *Journal of Geochemical Exploration* 67, 1-14.

BANKS, E.W., SIMMONS, C.T., LOVE, A.J., SHAND, P., 2011. Assessing spatial and temporal connectivity between surface water and groundwater in a regional catchment: Implications for regional scale water quantity and quality. *Journal of Hydrology* 404, 30-49.

BARNES, S.J., FISHER, L.A., ANAND, R., UEMOTO, T., 2014. Mapping bedrock lithologies through *in situ* regolith using retained element ratios: a case study from the Agnew-Lawlers area, Western Australia. *Australian Journal of Earth Sciences* 61, 269-285.

BARNETT, S., 1977. The hydrogeology of Kangaroo Island. *Mineral Resources Review*, South Australia 141, 77-81.

BARRON, E.J., 1987. Cretaceous plate tectonic reconstructions. *Palaeogeography, Palaeoclimatology, Palaeoecology* 59, 3-29.

BAUER, F.H., 1959. The regional geography of Kangaroo Island, South Australia. Australian National University.

BELPERIO, A.P., 1995A. A Guide to the Geology of Kangaroo Island in: Department of Mines and Energy, G.S. (Ed.), Adelaide.

BELPERIO, A.P., 1995B. The Quarternary, in: Drexel, J.F, Priess, W.V. (Ed.), The Geology of south Australia. Vol. 2, The Phanerozoic. Geological Survey of South Australia, South Australia

BELPERIO, A.P., & FLINT, R. B. , 1992. The Geological and Geomorphological Framework of Kangaroo Island in: Department of Mines and Energy, G.S. (Ed.). Department of Mines and Energy Adelaide, South Australia p. 16

BELPERIO, A.P., HARVEY, N., BOURMAN, R.P., 2002. Spatial and temporal variability in the Holocene sea-level record of the South Australian coastline. *Sedimentary Geology* 150, 153-169.

BELPERIO, A.P., MURRAY-WALLACE, C.V., CANN, J.H., 1995. The last interglacial shoreline in southern Australia: Morphostratigraphic variations in a temperate carbonate setting. *Quaternary International* 26, 7-19.

BELTON, D.X., BROWN, R.W., KOHN, B.P., FINK, D., FARLEY, K.A., 2004. Quantitative resolution of the debate over antiquity of the central Australian landscape: implications for the tectonic and geomorphic stability of cratonic interiors. *Earth Planet. Sci. Lett.* 219, 21-34.

BERGER, V.I., SINGER, DONALD A., BLISS, JAMES D., AND MORING, BARRY C., 2011. Ni-Co laterite deposits of the world: U.S. Geological Survey Open-File Report 2011-1058. U.S. Geological Survey, U.S. Geological Survey, Menlo Park, California. .

BERKINSHAW, T., 2009. The complete guide to the vegetation of temperate South Australia : mangroves to mallee. Greening Australia South Australia Pasadena, S. Aust.

BEVERSKOG, B., PUIGDOMENECH, I., 1996. Revised pourbaix diagrams for iron at 25–300 °C. *Corrosion Science* 38, 2121-2135.

BIERMAN, P., STEIG, E.J., 1996. Estimating rates of denudation using cosmogenic isotope abundences in sediment., *Earth Surface Processes and Landforms* 21, 125-139.

BIERMAN, P.R., CAFFEE, M., 2001. Slow Rates of Rock Surface Erosion and Sediment Production across the Namib Desert and Escarpment, Southern Africa. *American Journal of Science* 301, 326-358.

BIERMAN, P.R., CAFFEE, M., 2002. Cosmogenic exposure and erosion history of Australian bedrock landforms. *Geological Society of America Bulletin* 114, 787-803.

BIRD, M.I., ANDREW, A.S., CHIVAS, A.R., LOCK, D.E., 1989. An isotopic study of surficial alunite in Australia: 1. Hydrogen and sulphur isotopes. *Geochimica et Cosmochimica Acta* 53, 3223-3237.

BIRD, M.I., CHIVAS, A.R., 1988. Oxygen isotope dating of the Australian regolith. *Nature* 331, 513-516.

BIRD, M.I., CHIVAS, A.R., 1989. Stable-isotope geochronology of the Australian regolith. *Geochimica et Cosmochimica Acta* 53, 3239-3256.

BIRD, M.I., CHIVAS, A.R., 1993. Geomorphic and palaeoclimatic implications of an oxygen isotope chronology for Australian deeply weathered profiles. *Australian Journal of Earth Sciences* 40, 345-358.

BISHOP, P., 1985. Southeast Australian late Mesozoic and Cenozoic denudation rates: A test for late Tertiary increases in continental denudation. *Geology* 13, 479-482.

BISHOP, P., 2007. Long-term landscape evolution: linking tectonics and surface processes. *Earth Surface Processes and Landforms* 32, 329-365.

BISHOP, P., YOUNG, R.W., MCDUGALL, I., 1985. Stream Profile Change and Longterm Landscape Evolution: Early Miocene and Modern Rivers of the East Australian Highland Crest, Central New South Wales, Australia. *The Journal of Geology* 93, 455-474.

BOGER, S.D., MILLER, J.M., 2004. Terminal suturing of Gondwana and the onset of the Ross–Delamerian Orogeny: the cause and effect of an Early Cambrian reconfiguration of plate motions. *Earth Planet. Sci. Lett.* 219, 35-48.

BOGGS, S., KWON, Y.-I., GOLES, G.G., RUSK, B.G., KRINSLEY, D., SEYEDOLALI, A., 2002. Is Quartz Cathodoluminescence Color a Reliable Provenance Tool? A Quantitative Examination. *Journal of Sedimentary Research* 72, 408-415.

BÖLVIKEN, B., STOKKE, P.R., FEDER, J., JÖSSANG, T., 1992. The fractal nature of geochemical landscapes. *Journal of Geochemical Exploration* 43, 91-109.

BONNET, S., CRAVE, A., 2003. Landscape response to climate change: Insights from experimental modeling and implications for tectonic versus climatic uplift of topography. *Geology* 31, 123-126.

BORSBOOM, A.C. (2005) Xanthorrhoea: A review of current knowledge with a focus on *X. johnsonii* and *X. latifolia*, two Queensland protected plants-in-trade. Environmental Protection Agency, Queensland.

BOURMAN, ALLEY, 1999. Permian glaciated bedrock surfaces and associated sediments on Kangaroo Island, South Australia: implications for local Gondwanan ice-mass dynamics. *Australian Journal of Earth Sciences* 46, 523.

BOURMAN, R., 1993A. Modes of ferricrete genesis: evidence from southeastern Australia. *Zeitschrift für Geomorphologie* 37, 77-77.

BOURMAN, R., 1995. A review of laterite studies in southern South Australia. *Trans. R. Soc. S. Aust.* 119, 1-28.

BOURMAN, R., ALLEY, N., 1990. Stratigraphy and environments of deposition at Hallett Cove during the Late Palaeozoic. Department of Mines and Energy, South Australia, *Mines and Energy Review* 46, 69-82.

BOURMAN, R., ALLEY, N., 1995. Late Palaeozoic glaciogene sediments at King Point southeastern Troubridge Basin, South Australia. *Geological Survey of South Australia Quarterly Geological Notes* 46, 2-7.

BOURMAN, R.P., 1989A. Investigations of ferricretes and weathered zones in parts of southern and southeastern Australia : a reassessment of the 'Laterite' concept Department of Soil Science Univeristy of Adelaide, Adelaide, South Australia

BOURMAN, R.P., 1993B. Perennial problems in the study of laterite - a review *Australian Journal of Earth Sciences* 40, 387-401.

BOURMAN, R.P., 2006. A composite regolith profile at Ceduna, South Australia. *Trans. R. Soc. S. Aust.* 130, 197-205.

BOURMAN, R.P., 2007. Deep regolith weathering on the summit surface of the southern Mount Lofty Ranges, south Australia: A contribution to the 'Laterite' debate. *Geogr. Res.* 45, 291-299.

BOURMAN, R.P., BUCKMAN, S., PILLANS, B., WILLIAMS, M.A.J., WILLIAMS, F., 2010. Traces from the past: the Cenozoic regolith and intraplate neotectonic history of the Gun Emplacement, a ferricreted bench on the western margin of the Mt Lofty Ranges, South Australia. *Australian Journal of Earth Sciences* 57, 577-595.

BOURMAN, R.P., CONACHER, A.J., 1998. Genesis of 'Lateritic' duricrusts in Western Australia. *Quaternary International* 51-52, 45-46.

- BOURMAN, R.P., OLLIER, C.D., 2002. A critique of the Schellmann definition and classification of 'laterite'. *CATENA* 47, 117-131.
- BOURMAN, R.P., PILLANS, B., 1997. The use of the geomagnetic polarity time scale in elucidating pleistocene landscape evolution: An example from South Australia. *South African Geographical Journal* 79, 75-82.
- BOURMAN, R.P.L., J M, 1989B. Timing, extent and character of Late Cenozoic faulting on the eastern margin of the Mt. Lofty Ranges, South Australia *Trans. R. Soc. S. Aust.* 113.
- BOVE, M.A., AYUSO, R.A., DE VIVO, B., LIMA, A., ALBANESE, S., 2011. Geochemical and isotopic study of soils and waters from an Italian contaminated site: Agro Aversano (Campania). *Journal of Geochemical Exploration* 109, 38-50.
- BOWLER, J., 1982. Aridity in the late Tertiary and Quaternary of Australia. Evolution of the flora and fauna of arid Australia, 35-45.
- BOWLER, J.M., 1976. Aridity in Australia: Age, origins and expression in aeolian landforms and sediments. *Earth-Science Reviews* 12, 279-310.
- BRIFFA, K.R., 2000. Annual climate variability in the Holocene: interpreting the message of ancient trees. *Quaternary Science Reviews* 19, 87-105.
- BRINKMAN, R., 1970. Ferrollysis, a hydromorphic soil forming process. *Geoderma* 3, 199-206.
- BROCK, E., 1971. The denudation chronology of the Fleurieu Peninsula, South Australia. *Trans. R. Soc. S. Aust.* 95, 85-94.
- BROOKER, M.I.H., 2004. Field guide to eucalypts Vol 2, South-western and southern Australia 2nd Edition ed. Blooming Books, Melbourne, Australia.
- BROOKS, R.R., 1972. Geobotany and biogeochemistry in mineral exploration.
- BROOKS, R.R., 1973. Biogeochemical Parameters and Their Significance for Mineral Exploration. *Journal of Applied Ecology* 10, 825-836.
- BROOKS, R.R., DUNN, C.E., HALL, G.E., 1995. Biological systems in mineral exploration and processing. Ellis Horwood Ltd.
- BROOKS, R.R., LEE, J., REEVES, R.D., JAFFRE, T., 1977. Detection of nickeliferous rocks by analysis of herbarium specimens of indicator plants. *Journal of Geochemical Exploration* 7 49-7.
- BROWN, A.C., 2009. A process-based approach to estimating the copper derived from red beds in the sediment-hosted stratiform copper deposit model. *Economic Geology* 104, 857-868.
- BRYANT, E., 1992. Last interglacial and Holocene trends in sea-level maxima around Australia: Implications for modern rates. *Marine Geology* 108, 209-217.

BUCHANAN, F.H., 1807. A journey from Madras through the countries of Mysore, Canara, and Malabar, performed under the orders of the most noble the marquis Wellesley, governor general of India. Cadell.

BURKE, B.C., HEIMSATH, A.M., DIXON, J.L., CHAPPELL, J., YOO, K., 2009. Weathering the escarpment: chemical and physical rates and processes, south-eastern Australia. *Earth Surface Processes and Landforms* 34, 768-785.

BURKE, B.C., HEIMSATH, A.M., WHITE, A.F., 2007. Coupling chemical weathering with soil production across soil-mantled landscapes. *Earth Surface Processes and Landforms* 32, 853-873.

BUTT, C., BRISTOW, A., 2013. Relief inversion in the geomorphological evolution of sub-Saharan West Africa. *Geomorphology* 185, 16-26.

BUTT, C.R.M., ROBERTSON, I. D. M., SCOTT, K. M., CORNELIUS, M. , 2005. Regolith Expression of Australian Ore Systems: A compilation of exploration case histories with conceptual dispersion, process and exploration models CRC LEME, Perth, p. 431.

CALLEN, R., 1977. Late cainozoic environments of part of Northeastern South Australia. *Journal of the Geological Society of Australia* 24, 151-169.

CAMPBELL, A.S., SCHWERTMANN, U., STANJEK, H., FRIEDL, J., KYEK, A., CAMPBELL, P.A., 2002. Si Incorporation into Hematite by Heating Si–Ferrihydrite. *Langmuir* 18, 7804-7809.

CANADELL, J., JACKSON, R.B., EHLERINGER, J.B., MOONEY, H.A., SALA, O.E., SCHULZE, E.-D., 1996. Maximum rooting depth of vegetation types at the global scale. *Oecologia* 108, 583-595.

CANADELL, J., ZEDLER, P. H. , 1995. Underground Structures of Woody Plants in Mediterranean Ecosystems of Australia, California and Chile in: Kalin Arroyo, M.T., Zedler, P. H. Fox, M. D. (Ed.), *Ecology and biogeography of Mediterranean ecosystems in Chile, California, and Australia* Springer-Verlag New York

CARRANZA, E.J.M., 2011. Geochemical sampling for geological–environmental studies. *Journal of Geochemical Exploration* 111, 57-58.

CÉLÉRIER, J., SANDIFORD, M., HANSEN, D.L., QUIGLEY, M., 2005. Modes of active intraplate deformation, Flinders Ranges, Australia. *Tectonics* 24, TC6006.

CHENG, Q., AGTERBERG, F.P., BALLANTYNE, S.B., 1994. The separation of geochemical anomalies from background by fractal methods. *Journal of Geochemical Exploration* 51, 109-130.

CHEITRI, M.K., SAWIDIS, T., KARATAGLIS, S., 1997. Lichens as a Tool for Biogeochemical Prospecting. *Ecotoxicology and Environmental Safety* 38, 322-335.

CHITTLEBOROUGH, D.J., 1991. Indices of weathering for soils and palaeosols formed on silicate rocks. *Australian Journal of Earth Sciences* 38, 115-120.

- CLARKE, G.L., POWELL, R., 1989. Basement-cover interaction in the Adelaide Foldbelt, South Australia: the development of an arcuate foldbelt. *Tectonophysics* 158, 209-226.
- CLARKE, J.D.A., PAIN, C.F., 2009. Australian Cenozoic continental sediments. *Australian Journal of Earth Sciences* 56, S1-S4.
- COBLENTZ, D.D., SANDIFORD, M., RICHARDSON, R.M., ZHOU, S., HILLIS, R., 1995. The origins of the intraplate stress field in continental Australia. *Earth Planet. Sci. Lett.* 133, 299-309.
- COCKBURN, H.A.P., BROWN, R.W., SUMMERFIELD, M.A., SEIDL, M.A., 2000. Quantifying passive margin denudation and landscape development using a combined fission-track thermochronology and cosmogenic isotope analysis approach. *Earth Planet. Sci. Lett.* 179, 429-435.
- COHEN, D.R., HOFFMAN, E.L., NICHOL, I., 1987. Biogeochemistry: A geochemical method for gold exploration in the Canadian Shield. *Journal of Geochemical Exploration* 29, 49-73.
- COHEN, D.R., KELLEY, D.L., ANAND, R., COKER, W.B., 2010. Major advances in exploration geochemistry, 1998–2007. *Geochemistry: Exploration, Environment, Analysis* 10, 3-16.
- COHEN, D.R., RUTHERFORD, N.F., MORISSEAU, E., CHRISTOFOROU, I., ZISSIMOS, A.M., 2012A. Anthropogenic versus lithological influences on soil geochemical patterns in Cyprus. *Geochemistry: Exploration, Environment, Analysis* 12, 349-360.
- COHEN, D.R., RUTHERFORD, N.F., MORISSEAU, E., ZISSIMOS, A.M., 2012B. Geochemical patterns in the soils of Cyprus. *Science of The Total Environment*.
- COHEN, D.R., SHEN, X.C., DUNLOP, A.C., RUTHERFORD, N.F., 1998. A comparison of selective extraction soil geochemistry and biogeochemistry in the Cobar area, New South Wales. *Journal of Geochemical Exploration* 61, 173-189.
- COOPER, H.M., 1953. *The Unknown Coast: Being the explorations of Captain Matthew Flinders, R.N., along the shores of South Australia 1802.* The Advertiser Printing Office, Adelaide.
- CORNELIUS, M., MORRIS, P.A., CORNELIUS, A., LEME, C., Scientific, C., 2006. *Laterite Geochemical Database for the Southwest Yilgarn Craton Western Australia.* CRC LEME.
- CORNELIUS, M., ROBERTSON, I.D.M., CORNELIUS, A.J., MORRIS, P.A., 2008. Geochemical mapping of the deeply weathered western Yilgarn Craton of Western Australia, using laterite geochemistry. *Geochem.-Explor. Environ. Anal.* 8, 241-254.
- COVELL, S., EMILI, A., ACQUAVITA, A., KORON, N., FAGANELI, J., 2011. Benthic biogeochemical cycling of mercury in two contaminated northern Adriatic coastal lagoons. *Cont. Shelf Res.* 31, 1777-1789.
- COVENTRY, R., TAYLOR, R., FITZPATRICK, R., 1983. Pedological significance of the gravels in some red and grey earths of central north Queensland. *Soil Research* 21, 219-240.

- CROOKS, A.F., 1991A. Mineral Occurances of Kangaroo Island, in: Energy, D.o.M.a. (Ed.), Adelaide, South Australia
- CROOKS, A.F., 1991B. Mineral Occurances of Kangaroo Island: A minedep database pilot project in: Energy, D.o.M.a. (Ed.), Adelaide, South Australia
- DAILY, B., MILNES, A.R., 1972. Significance of basal Cambrian metasediments of andalusite grade, Dudley Peninsula, Kangaroo Island, South Australia. *Search Sydney* 3, 89-90.
- DAILY, B., MILNES, A.R., 1973. Stratigraphy, structure and metamorphism of the Kanmantoo Group (Cambrian) in its type section east of Tunkalilla Beach, South Australia. *Trans. R. Soc. S. Aust.* 97, 213-242.
- DAILY, B., MOORE, P.S., RUST, B.R., 1980. Terrestrial-marine transition in the Cambrian rocks of Kangaroo Island, South Australia. *Sedimentology* 27, 379-399.
- DAILY, B., TWIDALE, C.R., MILNES, A.R., 1974. The age of the lateritized summit surface on Kangaroo Island and adjacent areas of South Australia. *Journal of the Geological Society of Australia* 21, 387-392.
- DARNLEY, A.G., 1990. International geochemical mapping: a new global project. *Journal of Geochemical Exploration* 39, 1-13.
- DARNLEY, A.G., 1997. A global geochemical reference network: the foundation for geochemical baselines. *Journal of Geochemical Exploration* 60, 1-5.
- DAVIES, M., TWIDALE, C.R., TYLER, M. J., , 2002. *The Natural History of Kangaroo Island* 2nd Edition ed. Royal Society of South Australia Adelaide, South Australia
- DAVIS, W.M., 1899. The Geographical Cycle. *The Geographical Journal* 14, 481-504.
- DE OLIVEIRA, S.M.B., PESSEDA, L.C.R., FAVARO, D.I.T., BABINSKI, M., 2012. A 2400-year record of trace metal loading in lake sediments of Lagoa Vermelha, southeastern Brazil. *J. South Am. Earth Sci.* 33, 1-7.
- DE PRETIS, D.G., 2008. Application of lithogeochemistry to identify stratigraphic units and provenance of the Kanmantoo Group, Kangaroo Island., *Geology and Geophysics; Department of Earth Sciences University of Adelaide*
- DE VIVO, B., BONI, M., MARCELLO, A., DI BONITO, M., RUSSO, A., 1997. Baseline geochemical mapping of Sardinia (Italy). *Journal of Geochemical Exploration* 60, 77-90.
- DEMETRIADES A., R.C., BIRKE M. SALMINEN R., DE VOS W., TARVAINEN T. AND THE EUROGEO SURVEYS GEOCHEMISTRY EXPERT GROUP, 2010. Geochemical Atlases of Europe produced by the EuroGeoSurveys Geochemistry Expert Group: State of progress and potential uses. *Bulletin of the Geological Society of Greece Proceedings of the 12th International Congress*, 2350-2360.

DETHIER, D.P., LAZARUS, E.D., 2006. Geomorphic inferences from regolith thickness, chemical denudation and CRN erosion rates near the glacial limit, Boulder Creek catchment and vicinity, Colorado. *Geomorphology* 75, 384-399.

DICKINSON, J., WALLACE, M., HOLDGATE, G., DANIELS, J., GALLAGHER, S., THOMAS, L., 2001. Neogene tectonics in SE Australia: implications for petroleum systems. *APPEA Journal* 41, 37-52.

DICKINSON, J.A., WALLACE, M.W., HOLDGATE, G.R., GALLAGHER, S.J., THOMAS, L., 2002. Origin and Timing of the Miocene-Pliocene Unconformity in Southeast Australia. *Journal of Sedimentary Research* 72, 288-303.

DIETSCH, C., DORTCH, J.M., REYNHOUT, S.A., OWEN, L.A., CAFFEE, M.W., 2014. Very slow erosion rates and landscape preservation across the southwestern slope of the Ladakh Range, India. *Earth Surface Processes and Landforms*, n/a-n/a.

DIXON, J.L., HEIMSATH, A.M., AMUNDSON, R., 2009. The critical role of climate and saprolite weathering in landscape evolution. *Earth Surface Processes and Landforms* 34, 1507-1521.

DOSSETO, A., TURNER, S.P., CHAPPELL, J., 2008. The evolution of weathering profiles through time: New insights from uranium-series isotopes. *Earth Planet. Sci. Lett.* 274, 359-371.

DREXEL, J.F., PRIESS, W.V., 1995. *The Geology of South Australia, Vol. 2, The Phanerozoic.* Geological Survey of South Australia, Bulletin 54

DUNN, C.E., 1974. Identification of sedimentary cycles through Fourier analysis of geochemical data. *Chemical Geology* 13, 217-232.

DUNN, C.E., 1981. The biogeochemical expression of deeply buried uranium mineralisation in Saskatchewan, Canada. *Journal of Geochemical Exploration* 15, 437-452.

DUNN, C.E., 1986. Biogeochemistry as an aid to exploration for gold, platinum and palladium in the northern forests of Saskatchewan, Canada. *Journal of Geochemical Exploration* 25, 21-40.

DUNN, C.E., 2011. *Biogeochemistry in mineral exploration.* Elsevier.

DUNN, C.E., HALL, G.E.M., HOFFMAN, E., 1989. Platinum group metals in common plants of northern forests: developments in analytical methods, and the application of biogeochemistry to exploration strategies. *Journal of Geochemical Exploration* 32, 211-222.

DUNN, C.E., SCAGEL, R.K., 1989. Tree-top sampling from a helicopter - a new approach to gold exploration. *Journal of Geochemical Exploration* 34, 255-270.

EGGLETON, R., TAYLOR, G., 1998. Selected thoughts on laterite, *New Approaches to an Old Continent: Proceedings of the 3rd Australian Regolith Conference*, pp. 209-226.

EGGLETON, R.A., 2001. The Regolith Glossary, 1st ed. Cooperative Research Centre for Landscape Evolution and Mineral Exploration Canberra, p. 144.

ENGLAND, P., MOLNAR, P., 1990. Surface uplift, uplift of rocks, and exhumation of rocks. *Geology* 18, 1173-1177.

EUSTERHUES, K., RENNERT, T., KNICKER, H., KOGEL-KNABNER, I., TOTSCHKE, K.U., SCHWERTMANN, U., 2011. Fractionation of Organic Matter Due to Reaction with Ferrihydrite: Coprecipitation versus Adsorption. *Environmental Science & Technology* 45, 527-533.

EUSTERHUES, K., RENNERT, T., KNICKER, H., KÖGEL-KNABNER, I., TOTSCHKE, K.U., SCHWERTMANN, U., 2010. Fractionation of Organic Matter Due to Reaction with Ferrihydrite: Coprecipitation versus Adsorption. *Environmental Science & Technology* 45, 527-533.

EUSTERHUES, K., WAGNER, F.E., HÄUSLER, W., HANZLIK, M., KNICKER, H., TOTSCHKE, K.U., KÖGEL-KNABNER, I., SCHWERTMANN, U., 2008. Characterization of Ferrihydrite-Soil Organic Matter Coprecipitates by X-ray Diffraction and Mössbauer Spectroscopy. *Environmental Science & Technology* 42, 7891-7897.

FAIRCLOUGH, M.C., 2008. KINGSCOTE SPECIAL map sheet, Geological Atlas 1:250 000 Series, 2nd Edition ed. South Australian Geological Survey South Australia, pp. Geological Atlas 1:250 000 Series, sheet SH 253-216.

FARMER, V.C., MILNES, A.R., 1990. Podzol to laterite; a possible genetic sequence. *Sciences Geologiques Memoire* 85, 149-154.

FENSHAM, R.J., 2008. A protocol for assessing applications to selectively clear vegetation in Australia. *Land Use Policy* 25, 249-258.

FIRMAN, J.B., 1988. Soil evolution: Evidence from southern australia. *Earth-Science Reviews* 25, 373-386.

FIRMAN, J.B., 1994. Paleosols in laterite and silcrete profiles Evidence from the South East Margin of the Australian Precambrian Shield. *Earth-Science Reviews* 36, 149-179.

FLINT, D.J., 1976. Heavy mineral rich sediments within the Kanmantoo Group, Kangaroo Island. *Quarterly Geological Notes South Australia Geological Survey* 59, 11-13.

FLINT, D.J., 1978. Deep sea fan sedimentation of the Kanmantoo Group, Kangaroo Island. *Trans. R. Soc. S. Aust.* 102, 203-222.

FLINT, D.J., GRADY, A.E., 1979. Structural geology of Kanmantoo Group metasediments between West Bay and Breakneck River, Kangaroo Island. *Trans. R. Soc. S. Aust.* 103, 1-2.

FLOTTMANN, T., JAMES, P., 1997. Influence of basin architecture on the style of inversion and fold-thrust belt tectonics—the southern Adelaide Fold-Thrust Belt, South Australia. *Journal of Structural Geology* 19, 1093-1110.

FLOTTMANN, T., 1995. The structure of Kangaroo Island, South Australia: strain and kinematic partitioning during Delamerian basin and platform reactivation. *Australian Journal of Earth Sciences* 42, 35-49.

FLÖTTMANN, T., COCKSHELL, C.D., 1996. Palaeozoic basins of southern South Australia: New insights into their structural history from regional seismic data. *Australian Journal of Earth Sciences* 43, 45-55.

FLOTTMANN, T., HAINES, P., JAGO, J., JAMES, P., BELPERIO, A., GUM, J., 1998. Formation and reactivation of the Cambrian Kanmantoo Trough, SE Australia: implications for early Palaeozoic tectonics at eastern Gondwana's plate margin. *Journal of the Geological Society* 155, 525-539.

FLOTTMANN, T., HAINES, P.W., CLOCKSELL, C.C., PREISS, W.V., 1998. Reassessment of the seismic stratigraphy of the Early Palaeozoic Stransbury Basin. *Australian Journal of Earth Sciences* 45, 547.

FODEN, J., SONG, S.H., TURNER, S., ELBURG, M., SMITH, P.B., VAN DER STELDT, B., VAN PENGLIS, D., 2002. Geochemical evolution of lithospheric mantle beneath S.E. South Australia. *Chemical Geology* 182, 663-695.

FODEN, J.D., ELBURG, M.A., TURNER, S.P., SANDIFORD, M., O'CALLAGHAN, J., MITCHELL, S., 2002. Granite production in the Delamerian Orogen, South Australia. *Journal of the Geological Society* 159, 557-575.

FORBES, M.S., KOHN, M.J., BESTLAND, E.A., WELLS, R.T., 2010. Late Pleistocene environmental change interpreted from $\delta^{13}\text{C}$ and $\delta^{18}\text{O}$ of tooth enamel from the Black Creek Swamp Megafauna site, Kangaroo Island, South Australia. *Palaeogeography, Palaeoclimatology, Palaeoecology* 291, 319-327.

FORTESCUE, J.A.C., 1992. Landscape geochemistry: retrospect and prospect—1990. *Applied Geochemistry* 7, 1-53.

FRIED, A.W., SMITH, N., 1992. Timescales and the role of inheritance in long-term landscape evolution, northern New England, Australia. *Earth Surface Processes and Landforms* 17, 375-385.

FRISKE, P.W.B., RENCZ, A.N., FORD, K.L., KETTLES, I.M., GARRETT, R.G., GRUNSKY, E.C., MCNEIL, R.J., KLASSEN, R.A., 2013. Overview of the Canadian component of the North American Soil Geochemical Landscapes Project with recommendations for acquiring soil geochemical data for environmental and human health risk assessments. *Geochemistry: Exploration, Environment, Analysis* 13, 267-283.

GALE, S.J., 1992. Long-term landscape evolution in Australia. *Earth Surface Processes and Landforms* 17, 323-343.

GARRETT, R.G., REIMANN, C., SMITH, D.B., XIE, X., 2008. From geochemical prospecting to international geochemical mapping: A historical overview. *Geochemistry: Exploration, Environment, Analysis* 8, 205-217.

GEHRING, A.U., FRY, I.V., LUSTER, J., SPOSITO, G., 1993a. The chemical form of vanadium (IV) in kaolinite. *Clays and Clay Minerals* 41, 662-667.

GEHRING, A.U., FRY, I.V., LUSTER, J., SPOSITO, G., 1994. Vanadium in sepiolite: A redox-indicator for an ancient closed brine System in the Madrid Basin, central Spain. *Geochimica et Cosmochimica Acta* 58, 3345-3351.

GEHRING, A.U., LUSTER, J., SPOSITO, G., FRY, I.V., 1993b. Vanadium (IV) in a Multimineral Lateritic Saprolite: A Thermoanalytical and Spectroscopic Study. *Soil Sci. Soc. Am. J.* 57, 868-873.

GISLASON, S.R., OELKERS, E.H., EIRIKSDOTTIR, E.S., KARDJILOV, M.I., GISLADOTTIR, G., SIGFUSSON, B., SNORRASON, A., ELEFSEN, S., HARDARDOTTIR, J., TORSSANDER, P., OSKARSSON, N., 2009. Direct evidence of the feedback between climate and weathering. *Earth Planet. Sci. Lett.* 277, 213-222.

GLASAUER, S., FRIEDL, J., SCHWERTMANN, U., 1999. Properties of Goethites Prepared under Acidic and Basic Conditions in the Presence of Silicate. *Journal of Colloid and Interface Science* 216, 106-115.

GLENIE, R.C., SCHOFIELD, J.C., WARD, W.T., 1968. Tertiary sea levels in Australia and New Zealand. *Palaeogeography, Palaeoclimatology, Palaeoecology* 5, 141-163.

GOLDSCHMIDT, V.M., 1937. The principles of distribution of chemical elements in minerals and rocks. The seventh Hugo Muller Lecture, delivered before the Chemical Society on March 17th, 1937. *Journal of the Chemical Society (Resumed)*, 655-673.

GUSTAVSSON, N., LAMPIO, E., NILSSON, B., NORBLAD, G., ROS, F., SALMINEN, R., 1994. Geochemical maps of Finland and Sweden. *Journal of Geochemical Exploration* 51, 143-160.

HACHMANN, W., TIETZ, G., 1998. Chemical Mapping of Weathering Stages in Laterites, in: Love, G., Nicholson, W.A.P., Armigliato, A. (Eds.), *Modern Developments and Applications in Microbeam Analysis*. Springer Vienna, pp. 237-246.

HAINES, P.W., FLÖTTMANN, T., 1998. Delamerian Orogeny and potential foreland sedimentation: A review of age and stratigraphic constraints. *Australian Journal of Earth Sciences* 45, 559-570.

HAINES, P.W., JAGO, J.B., GUM, J.C., 2001. Turbidite deposition in the Cambrian Kanmantoo Group, South Australia. *Australian Journal of Earth Sciences* 48, 465-478.

- HARNOIS, L., 1988. The CIW index: a new chemical index of weathering. *Sedimentary Geology* 55, 319-322.
- HAQ, B.U., 1988. Mesozoic and Cenozoic chronostratigraphy and cycles of sea-level change
- HAQ, B.U., SCHUTTER, S.R., 2008. A chronology of Paleozoic sea-level changes. *Science* 322, 64-68.
- HENSCHKE, C.J., 1997. Dryland Salinity management on Kangaroo Island in: Australia, P.I.S. (Ed.), Adelaide pp. 1-32.
- HILL, L., 2002. Branching out into biogeochemical surveys: a guide to vegetation sampling. *Regolith and landscapes in eastern Australia*. CRC LEME, 50-53.
- HILL, S., 2004. Biogeochemical sampling media for regional-to prospect-scale mineral exploration in regolith-dominated terrains of the Curnamona Province and adjacent areas in western NSW and eastern SA, *Regolith*, pp. 128-133.
- HODKINSON, I.P., DUNN, C.E., WALDRON, H.M., SCARLETT, R., VOSE, C.P., 2015. Biogeochemical exploration using *Triodia pungens* in the Tanami Desert, Australia. *Geochemistry: Exploration, Environment, Analysis* 15, 179-192.
- HULME, K., HILL, S., 2003. River red gums as a biogeochemical sampling medium in mineral exploration and environmental chemistry programs in the Curnamona Craton and adjacent regions of NSW and SA. *Advances in Regolith* 2003, 205-210.
- HULME, K., HILL, S., 2004. Seasonal element variations of *Eucalyptus camaldulensis* biogeochemistry and implications for mineral exploration: an example from Teilita, Curnamona Province, western NSW, *Regolith*. Citeseer, pp. 151-156.
- HULME, K., HILL, S., 2005. River red gum biogeochemistry associations with substrate: bedrock penetrators or stream sediment amalgamators, *Regolith*, pp. 146-151.
- HUNT, P.A., MITCHELL, P.B., PATON, T.R., 1977. "Laterite profiles" and "lateritic ironstones" on the hawkesbury sandstone, Australia. *Geoderma* 19, 105-121.
- IRELAND, T.R., FLÖTTMANN, T., FANNING, C.M., GIBSON, G.M., PREISS, W.V., 1998. Development of the early Paleozoic Pacific margin of Gondwana from detrital-zircon ages across the Delamerian orogen. *Geology* 26, 243-246.
- ISTANBULLUOGLU, E., BRAS, R.L., 2005. Vegetation-modulated landscape evolution: Effects of vegetation on landscape processes, drainage density, and topography. *Journal of Geophysical Research: Earth Surface* 110, F02012.

JACOBSON, A.D., BLUM, J.D., CHAMBERLAIN, C.P., CRAW, D., KOONS, P.O., 2003. Climatic and tectonic controls on chemical weathering in the New Zealand Southern Alps. *Geochimica et Cosmochimica Acta* 67, 29-46

JAGO, J.B., GATEHOUSE, C.G., 2009. The Type Section of the Cambrian Backstairs Passage Formation, Kanmantoo Group, South Australia. *Trans. R. Soc. S. Aust.* 133, 150-163.

JAGO, J.B., GUM, J.C., BURTT, A.C., HAINES, P.W., 2003. Stratigraphy of the Kanmantoo Group: A critical element of the Adelaide Fold Belt and the Palaeo-Pacific plate margin, Eastern Gondwana. *Australian Journal of Earth Sciences* 50, 343-363.

JAMES, N.P., BONE, Y., 1991. Origin of a cool- water, Oligocene-Miocene deep shelf limestone, Eucla Platform, southern Australia. *Sedimentology* 38, 323-341.

JENKINS, R.J.F., SANDIFORD, M., 1992. Observations on the tectonic evolution of the southern Adelaide Fold Belt. *Tectonophysics* 214, 27-36.

KABATA-PENDIAS, A., 2001. Trace elements in soils and plants 3rd Edition ed. CRC Press

KENNEDY, W.Q., 1962. Some Theoretical Factors in Geomorphological Analysis. *Geological Magazine* 99, 304-312.

KLOOTWIJK, C.T., 1980. Early palaeozoic palaeomagnetism in Australia I. Cambrian results from the Flinders Ranges, South Australia II. Late Early Cambrian results from Kangaroo Island, South Australia III. Middle to early-Late Cambrian results from the Amadeus Basin, Northern Territory. *Tectonophysics* 64, 249-332.

KOHN, B., GLEADOW, A., BROWN, R., GALLAGHER, K., O'SULLIVAN, P., FOSTER, D., 2002. Shaping the Australian crust over the last 300 million years: insights from fission track thermotectonic imaging and denudation studies of key terranes. *Australian Journal of Earth Sciences* 49, 697-717.

KOOI, H., BEAUMONT, C., 1996. Large-scale geomorphology: Classical concepts reconciled and integrated with contemporary ideas via a surface processes model. *Journal of Geophysical Research: Solid Earth* 101, 3361-3386.

LAMBECK, K., NAKADA, M., 1990. Late Pleistocene and Holocene sea-level change along the Australian coast. *Palaeogeography, Palaeoclimatology, Palaeoecology* 89, 143-176.

LAMPLUGH, G., 1902. Calcrete. *Geological Magazine (Decade IV)* 9, 575-575.

LARIOS, R., FERNÁNDEZ-MARTÍNEZ, R., LEHECHO, I., RUCANDIO, I., 2012. A methodological approach to evaluate arsenic speciation and bioaccumulation in different plant species from two highly polluted mining areas. *Science of The Total Environment* 414, 600-607.

LAX, K., SELINUS, O., 2005. Geochemical mapping at the Geological Survey of Sweden. *Geochemistry: Exploration, Environment, Analysis* 5, 337-346.

- LAMBECK, K., NAKADA, M., 1990. Late Pleistocene and Holocene sea-level change along the Australian coast. *Palaeogeography, Palaeoclimatology, Palaeoecology* 89, 143-176.
- LAMPLUGH, G., 1902. Calcrete. *Geological Magazine (Decade IV)* 9, 575-575.
- LARIOS, R., FERNÁNDEZ-MARTÍNEZ, R., LEHECHO, I., RUCANDIO, I., 2012. A methodological approach to evaluate arsenic speciation and bioaccumulation in different plant species from two highly polluted mining areas. *Science of The Total Environment* 414, 600-607.
- LEBEDEVA, M.I., FLETCHER, R.C., BALASHOV, V.N., BRANTLEY, S.L., 2007. A reactive diffusion model describing transformation of bedrock to saprolite. *Chemical Geology* 244, 624-645.
- LEE, K.E., CHON, H.T., JUNG, M.C., 2008. Contamination level and distribution patterns of Hg in soil, sediment, dust and sludge from various anthropogenic sources in Korea. *Mineralogical Magazine* 72, 445-449.
- LIMA DA COSTA, M., 1993. Gold distribution in lateritic profiles in South America, Africa, and Australia: applications to geochemical exploration in tropical regions. *Journal of Geochemical Exploration* 47, 143-163.
- LINDENMAYER, D.B., CUNNINGHAM, R.B., DONNELLY, C.F., TANTON, M.T., NIX, H.A., 1993. The abundance and development of cavities in Eucalyptus trees: a case study in the montane forests of Victoria, southeastern Australia. *Forest Ecology and Management* 60, 77-104.
- LINDSAY, J.M., 1983. Late Eocene to Late Oligocene age of the Kingscote Limestone, Kangaroo Island, SA. *Trans. R. Soc. S. Aust.* 107, 127-128.
- LINTERN, M., HOUGH, R., RYAN, C., 2012. Experimental studies on the gold-in-calcrete anomaly at Edoldeh Tank Gold Prospect, Gawler Craton, South Australia. *Journal of Geochemical Exploration* 112, 189-205.
- LINTERN, M.J., 2007. Vegetation controls on the formation of gold anomalies in calcrete and other materials at the Barns Gold Prospect, Eyre Peninsula, South Australia. *Geochemistry: Exploration, Environment, Analysis* 7, 249-266.
- LINTERN, M.J., BUTT, C.R.M., SCOTT, K.M., 1997. Gold in vegetation and soil — three case studies from the goldfields of southern Western Australia. *Journal of Geochemical Exploration*
- LIS, J., PASIECZNA, A., STRZELECKI, R., WOLKOWICZ, S., LEWANDOWSKI, P., 1997. Geochemical and radioactivity mapping in Poland. *Journal of Geochemical Exploration* 60, 39-53.
- LJUNG, K., BJÖRCK, S., HAMMARLUND, D., BARNEKOW, L., 2006. Late Holocene multi-proxy records of environmental change on the South Atlantic island Tristan da Cunha. *Palaeogeography, Palaeoclimatology, Palaeoecology* 241, 539-560.

LONERAGAN, J., NICHOLAS, D., 1975. The availability and absorption of trace elements in soil-plant systems and their relation to movement and concentrations of trace elements in plants. Academic Press, New York.

LOTTERMOSER, B.G., ASHLEY, P.M., MUNKSGAARD, N.C., 2008. Biogeochemistry of Pb–Zn gossans, northwest Queensland, Australia: Implications for mineral exploration and mine site rehabilitation. *Applied Geochemistry* 23, 723-742.

LOWELL, J.D., GUILBERT, J.M., 1970. Lateral and vertical alteration-mineralization zoning in porphyry ore deposits. *Economic Geology* 65, 373-408.

LYONS, W.B., WAYNE, D.M., WARWICK, J.J., DOYLE, G.A., 1998. The Hg geochemistry of a geothermal stream, Steamboat Creek, Nevada: natural vs. anthropogenic influences. *Environmental Geology* 34, 143-150.

MA, Y., RATE, A.W., 2009. Formation of trace element biogeochemical anomalies in surface soils: the role of biota. *Geochemistry: Exploration, Environment, Analysis* 9, 353-367.

MACPHAIL, M., 2007. Australian Palaeoclimates: Cretaceous to Tertiary. A review of palaeobotanical and related evidence to the year 2000. , p. 266.

MAJZLAN, J., NAVROTSKY, A., SCHWERTMANN, U., 2004. Thermodynamics of iron oxides: Part III. Enthalpies of formation and stability of ferrihydrite (Fe(OH)₃), schwertmannite (FeO(OH)_{3/4}(SO₄)_{1/8}), and ε-Fe₂O₃. *Geochimica et Cosmochimica Acta* 68, 1049-1059.

MANN, A.W., 1983. Hydrogeochemistry and weathering on the Yilgarn Block, Western Australia—ferrolysis and heavy metals in continental brines. *Geochimica et Cosmochimica Acta* 47, 181-190.

MANSFIELD, L.L., 1947. THORIUM : Kangaroo Island Prospecting in: Mines, D.o. (Ed.), Adelaide.

MARSHAK, S., FLÖTTMANN, T., 1996. Structure and origin of the Fleurieu and Nackara Arcs in the Adelaide fold-thrust belt, South Australia: Salient and recess development in the Delamerian Orogen. *Journal of Structural Geology* 18, 891-908.

MARTENS, D.M., 1993. Hydrologic inferences from tree-ring studies on the Hawkesbury River, Sydney, Australia. *Geomorphology* 8, 147-164.

MARTIN, H.A., 1991. Tertiary stratigraphic palynology and palaeoclimatic of the inland river systems in New South Wales Geological Society of Australia Special Publication 18; The Cainozoic in Australia: A re-appraisal of the evidence 18, 181-194.

MARTIN, H., 2006. Cenozoic climatic change and the development of the arid vegetation in Australia. *Journal of Arid Environments* 66, 533-563.

- MASSIMO, S., 2006. Geochemical mapping using a geomorphologic approach based on catchments. *Journal of Geochemical Exploration* 90, 183-196.
- MATHUR, R., RUIZ, J., TITTLE, S., LIERMANN, L., BUSS, H., BRANTLEY, S., 2005. Cu isotopic fractionation in the supergene environment with and without bacteria. *Geochimica et Cosmochimica Acta* 69, 5233-5246.
- MATMON, A., BIERMAN, P., ENZEL, Y., 2002. Pattern and tempo of great escarpment erosion. *Geology* 30, 1135-1138.
- MAUD, R.R., 1972. *Geology, geomorphology, and soils of Central County Hindmarsh (Mount Compass - Milang), South Australia*, Melbourne.
- MCGOWRAN, B., BEECROFT, A., 1986. Neritic, southern extratropical foraminifera and the terminal eocene event. *Palaeogeography, Palaeoclimatology, Palaeoecology* 55, 23-34.
- MCGOWRAN, B., 1989. The later Eocene transgressions in southern Australia. *Alcheringa: An Australasian Journal of Palaeontology* 13, 45-68.
- MCINNES, B.I.A., DUNN, C.E., CAMERON, E.M., KAMEKO, L., 1996. Biogeochemical exploration for gold in tropical rain forest regions of Papua New Guinea. *Journal of Geochemical Exploration* 57, 227-243.
- MCLENNAN, S.M., BOCK, B., HEMMING, S.R., HUROWITZ, J.A., LEV, S.M., MCDANIEL, D.K., 2003. The roles of provenance and sedimentary processes in the geochemistry of sedimentary rocks, in: Lentz, D. (Ed.), *Geochemistry of sediments and sedimentary rocks: evolutionary considerations to mineral deposit-forming environments* pp. 7-38.
- MCQUEEN, K.G., 2005. Towards understanding the ferruginous component of the regolith in: Anand, R., Morris, P. (Ed.), 2005 *Minerals Exploration Seminar CRC LEME*, WA School of Mines, Conference Centre, Kalgoorlie p. 87.
- MCQUEEN, K.G., MUNRO, D.C., 2003. Weathering-controlled fractionation of ore and pathfinder elements at Cobar, NSW. *Advances in Regolith. CRC LEME*, 296-300.
- MELCHIORRE, E.B., WILLIAMS, P.A., ROSE, T.P., TALYN, B.C., 2006. Biogenic nitrogen from termite mounds and the origin of gerhardite at the Great Australia Mine, Cloncurry, Queensland, Australia *The Canadian Mineralogist* 44, 1447-1455.
- MESHARAM, R.R., RANDIVE, K.R., 2011. Geochemical study of laterites of the Jamnagar district, Gujarat, India: Implications on parent rock, mineralogy and tectonics. *J. Asian Earth Sci.* 42, 1271-1287.
- MIGOŃ, P., LIDMAR-BERGSTRÖM, K., 2001. Weathering mantles and their significance for geomorphological evolution of central and northern Europe since the Mesozoic. *Earth-Science Reviews* 56, 285-324.

MILLER, K.G., KOMINZ, M.A., BROWNING, J.V., WRIGHT, J.D., MOUNTAIN, G.S., KATZ, M.E., SUGARMAN, P.J., CRAMER, B.S., CHRISTIE-BLICK, N., PEKAR, S.F., 2005. The Phanerozoic record of global sea-level change. *science* 310, 1293-1298.

MILLER, K.G., MOUNTAIN, G.S., BROWNING, J.V., KOMINZ, M., SUGARMAN, P.J., CHRISTIE BLICK, N., KATZ, M.E., WRIGHT, J.D., 1998. Cenozoic global sea level, sequences, and the New Jersey transect: results from coastal plain and continental slope drilling. *Reviews of Geophysics* 36, 569-601.

MILLOT, R., GAILLARDET, J., DUPRÉ, B., ALLÈGRE, C.J., 2002. The global control of silicate weathering rates and the coupling with physical erosion: new insights from rivers of the Canadian Shield. *Earth Planet. Sci. Lett.* 196, 83-98.

MILNES, A., BOURMAN, R., 1972. A Late Palaeozoic glaciated granite surface at Port Elliot, South Australia. *Trans. R. Soc. S. Aust.* 96, 149-155.

MILNES, A.R., 1986. The Encounter Bay Granites and their relationship to the Cambrian Kanmantoo Group., Geological Society of Australia, Adelaide, South Australia, Australia.

MILNES, A.R., 1990. The Encounter Bay Granites, Fleurieu Peninsula and Kangaroo Island. Special Publication Geological Society of Australia 16, 421-449.

MILNES, A.R., BOURMAN, R.P., FITZPATRICK, R.W., 1987. Petrology and mineralogy of 'laterites' in southern and eastern Australia and southern Africa. *Chemical Geology* 60, 237-250.

MILNES, A.R., BOURMAN, R.P., NORTHCOTE, K.H., 1985. Field relationships of ferricretes and weathered zones in South Australia - A contribution to laterite studies in Australia *Australian Journal of Soil Research* 23, 441-465.

MILNES, A.R., COOPER, B.J., COOPER, J.A., 1982. The Jurassic Wisanger Basalt of Kangaroo Island, South Australia. *Trans. R. Soc. S. Aust.* 106, 1-13.

MILNES, A.R., LUDBROOK, N.H., LINDSAY, J.M., COOPER, B.J., 1983. The succession of Cenozoic marine sediments on Kangaroo Island South Australia *Trans. R. Soc. S. Aust.* 107, 1-36.

MITCHELL, C., HILL, S.M., GILES, D., HULME, K., 2015. El Niño–La Niña cycles and biogeochemical sampling: variability of element concentrations within *E. camaldulensis* leaves in semi-arid Australia. *Geochemistry: Exploration, Environment, Analysis* 15, 350-360.

MOKHTARI, A.R., COHEN, D.R., GATEHOUSE, S.G., 2009. Geochemical effects of deeply buried Cu-Au mineralization on transported regolith in an arid terrain. *Geochemistry Exploration Environment Analysis* 9, 227-236.

MORRIS, B.J., 1977. Mineral Sands, Morrison Beach, Kangaroo Island in: Mines, D.o. (Ed.). Geological Survey, Adelaide, South Australia pp. 1-7.

- MORRIS, B.J., 1988. Review of Lead-Zinc Mineralisation in South Australia, Kanmantoo Trough in: Department of Mines and Energy, S.A. (Ed.), Adelaide, South Australia
- MORRIS, P.A., 2013. Fine fraction regolith chemistry from the East Wongatha area, Western Australia: tracing bedrock and mineralization through thick cover. *Geochemistry: Exploration, Environment, Analysis* 13, 21-40.
- MORRISON, S., FORDYCE, F.M., SCOTT, E.M., 2014. An initial assessment of spatial relationships between respiratory cases, soil metal content, air quality and deprivation indicators in Glasgow, Scotland, UK: relevance to the environmental justice agenda. *Environmental Geochemistry and Health* 36, 319-332.
- MULLER, J.-P., BOCQUIER, G., 1986. Dissolution of kaolinites and accumulation of iron oxides in lateritic-ferruginous nodules: Mineralogical and microstructural transformations. *Geoderma* 37, 113-136.
- MÜLLER, R.D., DYKSTERHUIS, S., REY, P., 2012. Australian paleo-stress fields and tectonic reactivation over the past 100 Ma. *Australian Journal of Earth Sciences* 59, 13-28.
- MURRAY-WALLACE, C.V., 2002. Pleistocene coastal stratigraphy, sea-level highstands and neotectonism of the southern Australian passive continental margin—a review. *Journal of Quaternary Science* 17, 469-489.
- MURRAY-WALLACE, C.V., BELPERIO, A.P., 1991. The last interglacial shoreline in Australia — A review. *Quaternary Science Reviews* 10, 441-461.
- NAHON, D., JANOT, C., KARPOFF, A.M., PAQUET, H., TARDY, Y., 1977. Mineralogy, petrography and structures of iron crusts (ferricretes) developed on sandstones in the western part of Senegal. *Geoderma* 19, 263-277.
- NAHON, D.B., 1991. Introduction to the petrology of soils and chemical weathering. John Wiley and Sons, Inc.
- NASH, D.J., MCLAREN, S.J., 2011. *Geochemical sediments and landscapes*. John Wiley & Sons.
- NESBITT, H.W., YOUNG, G.M., 1984. Prediction of some weathering trends of plutonic and volcanic rocks based on thermodynamic and kinetic considerations. *Geochimica et Cosmochimica Acta* 48, 1523-1534.
- NEVES, M.O., FIGUEIREDO, V.R., ABREU, M.M., 2012. Transfer of U, Al and Mn in the water–soil–plant (*Solanum tuberosum* L.) system near a former uranium mining area (Cunha Baixa, Portugal) and implications to human health. *Science of The Total Environment* 416, 156-163.
- NORTHCOTE, K., 1946. A fossil soil from Kangaroo Island, South Australia. *Trans. Royal Soc. S. Aust* 70, 294-296.

- NORTHCOTE, K.H., TUCKER, B.M., 1948. A Soil Survey of the Hundred of Seddon and Part of the Hundred of MacGillivray, Kangaroo Island, South Australia:(including Also Portions of the Hundreds of Cassini and Duncan). Council for Scientific and Industrial Research.
- NORTON, S.A., 1973. Laterite and Bauxite Formation. *Economic Geology* 68, 353-361.
- ÓDOR, L., HORVÁTH, I., FÜGEDI, U., 1997. Low-density geochemical mapping in Hungary. *Journal of Geochemical Exploration* 60, 55-66.
- OLLIER, C.D., 1988. The regolith in Australia. *Earth-Science Reviews* 25, 355-361.
- OLLIER, C.D., 1995. *Regolith, soils and landforms*. John Wiley, New York.
- OLLIER, C.D., 1995. Tectonics and landscape evolution in southeast Australia. *Geomorphology* 12, 37-44.
- OLLIER, C.D., GALLOWAY, R.W., 1990. The laterite profile, ferricrete and unconformity. *CATENA* 17, 97-109.
- OLLIER, C.D., PAIN, C.F., 1997. Equating the basal unconformity with the palaeoplain: a model for passive margins. *Geomorphology* 19, 1-15.
- OVERTON, B., 2007. *Salt, Gypsum and Charcoal Industries on Kangaroo Island 1803 to 1992*. Environmental Realist, Australia.
- PAIN, C.F., OLLIER, C.D., 1995. Inversion of relief — a component of landscape evolution. *Geomorphology* 12, 151-165.
- PARKER A.J, 1986. Tectonic development and metallogeny of the Kanmantoo Trough in South Australia. *Ore Geology Reviews* 1, 203-212.
- PARKER, A., 1970. An index of weathering for silicate rocks. *Geological Magazine* 107, 501-504.
- PATON, T.R., WILLIAMS, M.A.J., 1972. The concept of laterite. *Annals of the Association of American Geographers* 62, 42-56.
- PAVICH, M.J., 1989. Regolith residence time and the concept of surface age of the Piedmont “Peneplain”. *Geomorphology* 2, 181-196.
- PETRONIO, B.M., CARDELLICCHIO, N., CALACE, N., PIETROLETTI, M., PIETRANTONIO, M., CALIANDRO, L., 2012. Spatial and Temporal Heavy Metal Concentration (Cu, Pb, Zn, Hg, Fe, Mn, Hg) in Sediments of the Mar Piccolo in Taranto (Ionian Sea, Italy). *Water Air Soil Pollut.* 223, 863-875.
- PHILLIPS, J.D., 2001. Inherited vs. acquired complexity in east Texas weathering profiles. *Geomorphology* 40, 1-14.

- PHILLIPS, J.D., 2002. Erosion, isostatic response, and the missing peneplains. *Geomorphology* 45, 225-241.
- PHILLIPS, J.D., 2003. Sources of nonlinearity and complexity in geomorphic systems. *Progress in Physical Geography* 27, 1-23.
- PHILLIPS, J.D., 2005. Weathering instability and landscape evolution. *Geomorphology* 67, 255-272.
- PILLANS, B., 1997. Soil development at snail's pace: evidence from a 6 Ma soil chronosequence on basalt in north Queensland, Australia. *Geoderma* 80, 117-128.
- PILLANS, B., 2003. Subdividing the Pleistocene using the Matuyama–Brunhes boundary (MBB): an Australasian perspective. *Quaternary Science Reviews* 22, 1569-1577.
- PILLANS, B., BOURMAN, R., 2001. Mid Pleistocene arid shift in southern Australia, dated by magnetostratigraphy. *Soil Research* 39, 89-98.
- PRATAS, J., PRASAD, M.N.V., FREITAS, H., CONDE, L., 2005. Plants growing in abandoned mines of Portugal are useful for biogeochemical exploration of arsenic, antimony, tungsten and mine reclamation. *Journal of Geochemical Exploration* 85, 99-107.
- PREISS, W.V., 2000. The Adelaide Geosyncline of South Australia and its significance in Neoproterozoic continental reconstruction. *Precambrian Research* 100, 21-63.
- PRICE, J.R., VELBEL, M.A., 2003. Chemical weathering indices applied to weathering profiles developed on heterogeneous felsic metamorphic parent rocks. *Chemical Geology* 202, 397-416.
- RAYMO, M.E., RUDDIMAN, W.F., 1992. Tectonic forcing of late Cenozoic climate. *Nature* 359, 117-122.
- REID, N., HILL, S.M., 2010. Biogeochemical sampling for mineral exploration in arid terrains: Tanami Gold Province, Australia. *Journal of Geochemical Exploration* 104, 105-117.
- REID, N., HILL, S.M., 2013. Spinifex biogeochemistry across arid Australia: Mineral exploration potential and chromium accumulation. *Applied Geochemistry* 29, 92-101.
- REID, N., HILL, S.M., LEWIS, D.M., 2008. Spinifex biogeochemical expressions of buried gold mineralisation: The great mineral exploration penetrator of transported regolith. *Applied Geochemistry* 23, 76-84.
- REID, N., HILL, S.M., LEWIS, D.M., 2009. Biogeochemical expression of buried gold mineralisation in semi-arid northern Australia: penetration of transported cover at the Titania Gold Prospect, Tanami Desert, Australia. *Geochemistry: Exploration, Environment, Analysis* 9, 267-273.

- REIMANN, C., FILZMOSER, P., GARRETT, R.G., 2005. Background and threshold: Critical comparison of methods of determination. *Science of The Total Environment* 346, 1-16.
- REIMANN, C., MATSCHULLAT, J., BIRKE, M., SALMINEN, R., 2010. Antimony in the environment: Lessons from geochemical mapping. *Applied Geochemistry* 25, 175-198.
- REIMANN, C., DE CARITAT, P., TEAM, G.P., TEAM, N.P., 2012. New soil composition data for Europe and Australia: demonstrating comparability, identifying continental-scale processes and learning lessons for global geochemical mapping. *Sci Total Environ* 416, 239-252.
- REIMANN, C., MATSCHULLAT, J., BIRKE, M., SALMINEN, R., 2009. Arsenic distribution in the environment: The effects of scale. *Applied Geochemistry* 24, 1147-1167.
- REIMANN, C., MATSCHULLAT, J., BIRKE, M., SALMINEN, R., 2010. Antimony in the environment: Lessons from geochemical mapping. *Applied Geochemistry* 25, 175-198.
- REISENAUER, H.M., TABIKH, A.A., STOUT, P.R., 1962. Molybdenum Reactions With Soils and the Hydrous Oxides of Iron, Aluminum, and Titanium¹. *Soil Sci. Soc. Am. J.* 26, 23-27.
- RIEBE, C.S., KIRCHNER, J.W., GRANGER, D.E., FINKEL, R.C., 2001. Strong tectonic and weak climatic control of long-term chemical weathering rates. *Geology* 29, 511-514.
- RIEBE, C.S., KIRCHNER, J.W., FINKEL, R.C., 2003. Long-term rates of chemical weathering and physical erosion from cosmogenic nuclides and geochemical mass balance. *Geochimica et Cosmochimica Acta* 67, 4411-4427.
- RUSK, B.G., LOWERS, H.A., REED, M.H., 2008. Trace elements in hydrothermal quartz: Relationships to cathodoluminescent textures and insights into vein formation. *Geology* 36, 547-550.
- RUSK, B.G., REED, M.H., DILLES, J.H., KENT, A.J.R., 2006. Intensity of quartz cathodoluminescence and trace-element content in quartz from the porphyry copper deposit at Butte, Montana. *American Mineralogist* 91, 1300-1312.
- SALMINEN, R., TARVAINEN, T., 1997. The problem of defining geochemical baselines. A case study of selected elements and geological materials in Finland. *Journal of Geochemical Exploration* 60, 91-98.
- SANDIFORD, M., 2007. The tilting continent: A new constraint on the dynamic topographic field from Australia. *Earth Planet. Sci. Lett.* 261, 152-163.
- SANDIFORD, M., QUIGLEY, M., DE BROEKERT, P., JAKICA, S., 2009. Tectonic framework for the Cenozoic cratonic basins of Australia. *Australian Journal of Earth Sciences* 56, S5-S18.
- SANDIFORD, M., WALLACE, M., COBLENTZ, D., 2004. Origin of the in situ stress field in south-eastern Australia. *Basin Research* 16, 325-338.

SHELLMANN, W., 1981. Considerations on the definition and classification of laterites. Lateritisation processes. Proc. international seminar, Trivandrum, India, 1979, 1-10.

SHELLMANN, W., 1989. Allochthonous surface alteration of Ni-laterites. *Chemical Geology* 74, 351-364.

SHELLMANN, W., 1994. Geochemical differentiation in laterite and bauxite formation. *CATENA* 21, 131-143.

SHELLMANN, W., 1995. Microprobe analysis of the Al-Fe-Si variation in laterites. *Chemie der Erde - Geochemistry* 55, 97-108.

SHELLMANN, W., 2003. Discussion of "A critique of the Schellmann definition and classification of laterite" by R.P. Bourman and C.D. Ollier (*Catena* 47, 117-131). *CATENA* 52, 77-79.

SCHMIDT, P.W., CURREY, D.T., OLLIER, C.D., 1976. Sub-basaltic weathering, damsites, palaeomagnetism, and the age of lateritization. *Journal of the Geological Society of Australia* 23, 367-370.

SCHMIDT, P.W., EMBLETON, B.J.J., 1976. Palaeomagnetic results from sediments of the Perth Basin, Western Australia, and their bearing on the timing of regional lateritisation. *Palaeogeography, Palaeoclimatology, Palaeoecology* 19, 257-273.

SCHUSTER, P.F., KRABBENHOFT, D.P., NAFTZ, D.L., CECIL, L.D., OLSON, M.L., DEWILD, J.F., SUSONG, D.D., GREEN, J.R., ABBOTT, M.L., 2002. Atmospheric mercury deposition during the last 270 years: A glacial ice core record of natural and anthropogenic sources. *Environmental Science & Technology* 36, 2303-2310.

SCHWARZ, T., GERMANN, K., 1993. Ferricretes as a source of continental oolitic ironstones in northern Sudan. *Chemical Geology* 107, 259-265.

SCHWERTMANN, U., FRIEDL, J., PFAB, G., GEHRING, A.U., 1995. Iron substitution in soil and synthetic anatase. *Clays and Clay Minerals* 43, 599-606.

SCHWERTMANN, U., FRIEDL, J., STANJEK, H., SCHULZE, D.G., 2000a. The effect of Al on Fe oxides. XIX. Formation of Al-substituted hematite from ferrihydrite at 25 degrees C and pH 4 to 7. *Clays and Clay Minerals* 48, 159-172.

SCHWERTMANN, U., FRIEDL, J., STANJEK, H., SCHULZE, D.G., 2000b. The effect of clay minerals on the formation of goethite and hematite from ferrihydrite after 16 years' ageing at 25 degrees C and pH 4-7. *Clay Minerals* 35, 613-623.

SCHWERTMANN, U., PFAB, G., 1994. Structural vanadium in synthetic goethite. *Geochimica et Cosmochimica Acta* 58, 4349-4352.

- SCHWERTMANN, U., PFAB, G., 1996. Structural vanadium and chromium in lateritic iron oxides: Genetic implications. *Geochimica et Cosmochimica Acta* 60, 4279-4283.
- SCOTese, C.R., GAHAGAN, L.M., LARSON, R.L., 1988. Plate tectonic reconstructions of the Cretaceous and Cenozoic ocean basins. *Tectonophysics* 155, 27-48.
- SCOTT, K., AND PAIN, COLIN., , 2009. *Regolith Science*.
- SEVIN, B., RICORDEL-PROGNON, C., QUESNEL, F., CLUZEL, D., LESIMPLE, S., MAURIZOT, P., 2012. First palaeomagnetic dating of ferricrete in New Caledonia: new insight on the morphogenesis and palaeoweathering of Grande Terre'. *Terr. Nova* 24, 77-85.
- SHAND, P., JAMES-SMITH, J., LOVE, A.J., NILSEN, T., THOMAS, D. , 2006. Hydrogeochemistry of surface waters and groundwater, Kangaroo Island in: Department of Water, L.a.B.C. (Ed.) , Adelaide
- SHOTYK, W., GOODSITE, M.E., ROOS-BARRACLOUGH, F., FREL, R., HEINEMEIER, J., ASMUND, G., LOHSE, C., HANSEN, T.S., 2003. Anthropogenic contributions to atmospheric Hg, Pb and As accumulation recorded by peat cores from southern Greenland and Denmark dated using the 14C "bomb pulse curve". *Geochimica et Cosmochimica Acta* 67, 3991-4011.
- SIMMS, M.J., 2004. Tortoises and hares: dissolution, erosion and isostasy in landscape evolution. *Earth Surface Processes and Landforms* 29, 477-494.
- SINGH, B., GILKES, R.J., 1992. Properties and distribution of iron oxides and their association with minor elements in the soils of south-western Australia. *Journal of Soil Science* 43, 77-98.
- SIVARAJASINGHAM, S., ALEXANDER, L.T., CADY, J.G., CLINE, M.G., 1962. Laterite, in: Norman, A.G. (Ed.), *Advances in Agronomy*. Academic Press, pp. 1-60.
- SMITH, R.E., PERDRIX, J.L., 1983. Pisolithic laterite geochemistry in the Golden Grove massive sulphide district, Western Australia. *Journal of Geochemical Exploration* 18, 131-164.
- SOLOMON, M., GROVES, D.I., 2000. The geology and origin of Australia's mineral deposits.
- SPADONI, M., 2006. Geochemical mapping using a geomorphologic approach based on catchments. *Journal of Geochemical Exploration* 90, 183-196.
- STEPHENS, C.G., 1971. Laterite and silcrete in Australia: A study of the genetic relationships of laterite and silcrete and their companion materials, and their collective significance in the formation of the weathered mantle, soils, relief and drainage of the Australian continent. *Geoderma* 5, 5-52.
- STEWART, A.J., BLAKE, D.H., OLLIER, C.D., 1986. Cambrian River Terraces and Ridgetops in Central Australia: Oldest Persisting Landforms? *Science* 233, 758-761.

- STOFFEL, M., 2008. Dating past geomorphic processes with tangential rows of traumatic resin ducts. *Dendrochronologia* 26, 53-60.
- STRIEWSKI, B., MAYR, C., FLENLEY, J., NAUMANN, R., TURNER, G., LÜCKE, A., 2009. Multi-proxy evidence of late Holocene human-induced environmental changes at Lake Pupuke, Auckland (New Zealand). *Quaternary International* 202, 69-93.
- SUNDERLAND, E.M., CHMURA, G.L., 2000. An inventory of historical mercury emissions in Maritime Canada: implications for present and future contamination. *Science of The Total Environment* 256, 39-57.
- TARDY, Y., NAHON, D., 1985. Geochemistry of laterites, stability of Al-goethite, Al-hematite, and Fe (super 3+) -kaolinite in bauxites and ferricretes; an approach to the mechanism of concretion formation. *American Journal of Science* 285, 865-903.
- TAYLOR, R.M., GILES, J.B., 1970. The association of Vanadium and Molybdenum with Iron oxides in soils. *Journal of Soil Science* 21, 203-215.
- TAYLOR, G., EGGLETON, R.A., 2008. Genesis of pisoliths and of the Weipa Bauxite deposit, northern Australia. *Australian Journal of Earth Sciences* 55, S87-S103.
- TAYLOR, G., EGGLETON, R.A., FOSTER, L.D., TILLEY, D.B., LE GLEUHER, M., MORGAN, C.M., 2008. Nature of the Weipa Bauxite deposit, northern Australia. *Australian Journal of Earth Sciences* 55, S45-S70.
- TAYLOR, G., EGGLETON, R.A., HOLZHAUER, C.C., MACONACHIE, L.A., GORDON, M., BROWN, M.C., MCQUEEN, K.G., 1992. Cool climate lateritic and bauxitic weathering *Journal of Geology* 100, 669-677.
- THEOBALD, P.K., EPPINGER, R.G., TURNER, R.L., SHIQUAN, S., 1991. The effect of scale on the interpretation of geochemical anomalies. *Journal of Geochemical Exploration* 40, 9-23.
- THORNTON, I., PLANT, J., 1980. Regional geochemical mapping and health in the United Kingdom. *Journal of the Geological Society* 137, 575-586.
- TOKAREV, V., SANDIFORD, M., GOSTIN, V., 1999. Landscape evolution in the Mount Lofty Ranges: implications for regolith development, New approaches to an old continent, 3rd Australian Regolith Conference Proceedings, Regolith, pp. 127-134.
- TROLARD, F., BOURRIE, G., JEANROY, E., HERBILLON, A.J., MARTIN, H., 1995. Trace metals in natural iron oxides from laterites: A study using selective kinetic extraction. *Geochimica et Cosmochimica Acta* 59, 1285-1297.

TROLARD, F., TARDY, Y., 1987. The stabilities of gibbsite, boehmite, aluminous goethites and aluminous hematites in bauxites, ferricretes and laterites as a function of water activity, temperature and particle size. *Geochimica et Cosmochimica Acta* 51, 945-957.

TUCKER, G.E., HANCOCK, G.R., 2010. Modelling landscape evolution. *Earth Surface Processes and Landforms* 35, 28-50. TWIDALE, C., 1983. Australian laterites and silcretes: ages and significance. *Revue de géologie dynamique et de géographie physique* 24, 35-45.

TURNER, S., FODEN, J., SANDIFORD, M., BRUCE, D., 1993. Sm-Nd isotopic evidence for the provenance of sediments from the Adelaide Fold Belt and southeastern Australia with implications for episodic crustal addition. *Geochimica et Cosmochimica Acta* 57, 1837-1856.

TWIDALE, C.R., 1976. On the survival of paleoforms. *American Journal of Science* 276, 77-95.

TWIDALE, C.R., 1981. Granitic Inselbergs: Domed, Block-Strewn and Castellated. *The Geographical Journal* 147, 54-71.

TWIDALE, C.R., 1998. Antiquity of landforms: An 'extremely unlikely' concept vindicated. *Australian Journal of Earth Sciences* 45, 657-668.

TWIDALE, C., 1983. Australian laterites and silcretes: ages and significance. *Revue de géologie dynamique et de géographie physique* 24, 35-45.

TWIDALE, C., BOURNE, J.A., 1975. Geomorphological evolution of part of the eastern Mount Lofty Ranges, South Australia. *Trans. R. Soc. S. Aust.* 99, 197-209.

TWIDALE, C.R., 1994. Gondwanan (Late Jurassic and Cretaceous) palaeosurfaces of the Australian craton. *Palaeogeography, Palaeoclimatology, Palaeoecology* 112, 157-186.

TWIDALE, C.R., 1997. The great age of some Australian landforms: examples of, and possible explanations for, landscape longevity. *Geological Society, London, Special Publications* 120, 13-23.

TWIDALE, C.R., 2000. Early Mesozoic (?Triassic) Landscapes in Australia: Evidence, Argument, and Implications. *The Journal of Geology* 108, 537-552.

TWIDALE, C.R., CAMPBELL, E.M., 1995. Pre-Quaternary landforms in the low latitude context: the example of Australia. *Geomorphology* 12, 17-35.

TWIDALE, C.R., BOURNE, J.A., 1998. The use of duricrusts and topographic relationships in geomorphological correlation: conclusions based in Australian experience. *CATENA* 33, 105-122.

TWIDALE, C.R., BOURNE, J. A. , 2002. *The Land Surface in: Davies, M., Twidale, C.R., Tyler, M. J., (Ed.), Natural History of Kangaroo Island 2nd Edition ed. Royal Society of South Australia Richmond, South Australia*

- VAN RANST, E., DE CONINCK, F., 2002. Evaluation of ferrollysis in soil formation. *European Journal of Soil Science* 53, 513-520.
- VON BLANCKENBURG, F., 2006. The control mechanisms of erosion and weathering at basin scale from cosmogenic nuclides in river sediment. *Earth Planet. Sci. Lett.* 242, 224-239.
- VON DER BORCH, C.C., 1980. Evolution of late proterozoic to early paleozoic Adelaide foldbelt, Australia: Comparisons with postpermian rifts and passive margins. *Tectonophysics* 70, 115-134.
- VRANA, K., RAPANT, S., BODIŠ, D., MARSINA, K., MAŇKOVSKÁ, B., ČURLÍK, J., ŠEFČÍK, P., DANIEL, J., LUČIVJANSKÝ, L., LEXA, J., PRAMUKA, S., 1997. Geochemical Atlas of the Slovak Republic at a scale of 1:1,000,000. *Journal of Geochemical Exploration* 60, 7-37.
- WANG, X., XIE, X., CHENG, Z., LIU, D., 1999. Delineation of regional geochemical anomalies penetrating through thick cover in concealed terrains — a case history from the Olympic Dam deposit, Australia. *Journal of Geochemical Exploration* 66, 85-97.
- WARD, D.J., LAMONT, B.B., BURROWS, C.L., 2001. Grasstrees reveal contrasting fire regimes in eucalypt forest before and after European settlement of southwestern Australia. *Forest Ecology and Management* 150, 323-329.
- WARD, W.T., 1965. Eustatic and Climatic History of the Adelaide Area South Australia. *The Journal of Geology* 73, 592-602.
- WASSON, R., 1982. Landform development in Australia, in: Barker, W.R.a.G., P.J.M. (Ed.), *Evolution of the flora and fauna of arid Australia*. Frewville, S. Aust : Peacock Publications in association with Australian Systematic Botany Society and ANZAAS, South Australian Division p. 392.
- WATCHMAN, A.L., TWIDALE, C.R., 2002. Relative and 'absolute' dating of land surfaces. *Earth-Science Reviews* 58, 1-49.
- WATT, G.R., WRIGHT, P., GALLOWAY, S., MCLEAN, C., 1997. Cathodoluminescence and trace element zoning in quartz phenocrysts and xenocrysts. *Geochimica et Cosmochimica Acta* 61, 4337-4348.
- WEEKS, R.A., 1956. Paramagnetic Resonance of Lattice Defects in Irradiated Quartz. *Journal of Applied Physics* 27, 1376-1381.
- WEST, A.J., GALY, A., BICKLE, M., 2005. Tectonic and climatic controls on silicate weathering. *Earth Planet. Sci. Lett.* 235, 211-228.
- WHITE, A.F., BLUM, A.E., 1995. Effects of climate on chemical weathering in watersheds. *Geochimica et Cosmochimica Acta* 59, 1729-1747.

WHITE, A.F., BLUM, A.E., SCHULZ, M.S., VIVIT, D.V., STONESTROM, D.A., LARSEN, M., MURPHY, S.F., EBERL, D., 1998. Chemical Weathering in a Tropical Watershed, Luquillo Mountains, Puerto Rico: I. Long-Term Versus Short-Term Weathering Fluxes. *Geochimica et Cosmochimica Acta* 62, 209-226.

WHITE, A.F., BULLEN, T.D., SCHULZ, M.S., BLUM, A.E., HUNTINGTON, T.G., PETERS, N.E., 2001. Differential rates of feldspar weathering in granitic regoliths. *Geochimica et Cosmochimica Acta* 65, 847-869.

WHITE, W.M., 2013. *Geochemistry*. Wiley, Somerset, NJ, USA.

WILFORD, J., 2012. A weathering intensity index for the Australian continent using airborne gamma-ray spectrometry and digital terrain analysis. *Geoderma* 183–184, 124-142.

WILFORD, J., THOMAS, M., 2013. Predicting regolith thickness in the complex weathering setting of the central Mt Lofty Ranges, South Australia. *Geoderma* 206, 1-13.

WILLETT, S.D., 1999. Orogeny and orography: The effects of erosion on the structure of mountain belts. *Journal of Geophysical Research: Solid Earth* 104, 28957-28981.

WILLGOOSE, G., 2005. Mathematical modeling of whole landscape evolution *Annual Review of Earth & Planetary Sciences* 33, 443-459.

WRIGHT, V.P., SLOAN, R.J., VALERO GARCÉS, B., GARVIE, L.A.J., 1992. Groundwater ferricretes from the Silurian of Ireland and Permian of the Spanish Pyrenees. *Sedimentary Geology* 77, 37-49.

XUEJING, X., XUZHAN, M., TIANXIANG, R., 1997. Geochemical mapping in China. *Journal of Geochemical Exploration* 60, 99-113.

YOUNG, R., MCDUGALL, I., 1993. Long-Term Landscape Evolution: Early Miocene and Modern Rivers in Southern New South Wales, Australia. *The Journal of Geology* 101, 35-49.

YOUNG, R.W., 1983. The Tempo of Geomorphological Change: Evidence from Southeastern Australia. *The Journal of Geology* 91, 221-230.

Appendices

Appendix A:
Geochemical and
Biogeochemical
Data Tables

Geochemical Data Tables

Samples	Easting	Northing	Ferricrete Classification	Zone	Wgt Method	LOI %	SiO ₂ %	Al ₂ O ₃ %	Fe ₂ O ₃ %	CaO %	MgO %	Na ₂ O %	K ₂ O %	TiO ₂ %	P ₂ O ₅ %
KIFE001	235504	6033047	Ferruginous Sediments	54H	Dect. Limit	-5.11	0.1	0.01	0.01	0.01	0.01	0.01	0.01	0.01	0.01
KIFE002	230484	6031218	Ferruginous Sediments	54H	0.21	2.64	87.5	4.7	3.46	0.1	0.19	0.09	1.08	0.12	<0.01
KIFE003	724992	6052722	Ferruginous Sediments	53H	0.21	6.27	64.7	5.83	21.71	0.06	0.55	0.09	0.41	0.22	0.05
KIFE004	689539	6017705	Pisolitic	53H	0.21	9.19	58.7	7.05	22.69	0.46	0.15	0.02	0.31	0.57	0.02
KIFE005	687032	6021325	Pisolitic	53H	0.21	14.51	43	20.15	21.24	0.02	0.08	0.03	0.28	0.61	0.02
KIFE006	686067	6022817	Pisolitic	53H	0.21	12.14	57.6	16.49	12.93	0.02	0.07	<0.01	0.1	0.25	0.02
KIFE007	685858	6023638	Ferruginous Sediments	53H	0.22	13.58	41	18.78	25.32	0.02	0.12	0.02	0.17	0.48	0.02
KIFE008	684538	6026351	Nodular	53H	0.21	10.88	28.8	14.72	43.79	0.03	0.06	0.02	0.09	0.45	0.03
KIFE009	687468	6028692	Nodular	53H	0.21	17.12	42.7	26.77	12.22	0.01	0.07	<0.01	0.07	0.79	0.01
KIFE010	686326	6029086	Ferruginous Sediments	53H	0.21	10.59	50.3	16.88	19.71	0.03	0.19	0.03	0.72	0.99	0.04
KIFE011	689629	6030098	Ferruginous Sediments	53H	0.21	16.2	26.1	22.31	34.64	0.01	0.09	0.01	0.17	0.44	0.02
KIFE012	684675	6024014	Vermiform Ferricrete	53H	0.22	11.25	60.1	15.82	11.37	0.02	0.1	0.01	0.15	0.4	0.02
KIFE013	662244	6019233	Pisolitic	53H	0.22	18.66	35.7	28.8	15.64	0.02	0.11	0.02	0.13	0.55	0.02
KIFE014	723525	6041318	Nodular	53H	0.21	3.46	58.7	8.52	26.77	0.06	0.13	0.38	1.02	0.46	0.03
KIFE015	719099	6040427	Ferruginous Sediments	53H	0.21	9.38	58.3	13.35	16.94	0.05	0.14	0.1	0.51	0.82	0.02
KIFE016	708613	6041461	Ferruginous Sediments	53H	0.22	8.64	50.3	12.73	26.07	0.04	0.13	0.08	0.42	0.74	0.02
KIFE017	708764	6039652	Ferruginous Sediments	53H	0.21	8.7	45.9	12.4	31.14	0.03	0.13	0.04	0.39	0.68	0.03
KIFE018	701534	6045597	Vermiform Ferricrete	53H	0.21	10.28	49.4	15.02	23.53	0.04	0.26	0.01	1.03	0.37	0.03
KIFE019	701940	6046202	Ferruginous Sediments	53H	0.21	10.53	39.9	11.58	37.68	0.03	0.12	<0.01	0.31	0.21	0.11
KIFE020	698173	6047316	Ferruginous Sediments	53H	0.21	13.61	17.3	14.66	53.54	0.03	0.15	0.02	0.44	0.43	0.1
KIFE021	696304	6047229	Ferruginous Sediments	53H	0.22	8.08	60.1	12.06	17.92	0.05	0.14	0.08	0.43	0.99	0.02
KIFE022	692989	6047936	Slabby Ferricrete	53H	0.2	6.24	39.1	10.17	42.92	0.04	0.26	0.04	1.04	0.45	0.02
KIFE023	731496	6039213	Nodular	53H	0.18	2.92	39.6	8.47	46.78	0.07	0.2	0.17	0.88	0.46	0.03
KIFE024	234134	6036021	Nodular	54H	0.18	2.47	27.7	8.73	59.34	0.08	0.14	0.07	0.68	0.47	0.04
KIFE025	724232	6029535	Nodular	53H	0.18	6.79	47.6	11.59	31.81	0.05	0.15	0.13	0.51	0.45	0.03
KIFE026	724419	6031878	Ferruginous Sediments	53H	0.19	5.74	53.8	10.3	27.82	0.05	0.1	0.17	0.63	0.64	0.03
KIFE027	723981	6034153	Nodular	53H	0.17	6.67	53.1	11.62	26.65	0.05	0.12	0.15	0.79	0.62	0.02
KIFE028	711574	6037252	Nodular	53H	0.18	12.03	26	18.13	42.93	0.03	0.14	0.04	0.16	0.5	0.03
KIFE029	713432	6035281	Nodular	53H	0.2	7.08	36.5	15.01	40.21	0.03	0.1	0.01	0.22	0.52	0.02
KIFE030	713171	6033475	Nodular	53H	0.21	8.95	43.8	12.83	32.65	0.04	0.14	0.07	0.42	0.66	0.02
KIFE031	713412	6028940	Pisolitic	53H	0.2	7.69	49.1	12.78	28.45	0.04	0.12	0.05	0.42	0.6	0.02
KIFE032	713401	6027571	Pisolitic	53H	0.2	7.31	53.2	9.6	28.77	0.04	0.13	0.08	0.53	0.53	0.02
KIFE033	666483	6029399	Pisolitic	53H	0.01	17.04	34	27.74	20.05	<0.01	0.09	<0.01	0.52	0.74	0.01
KIFE034	665504	6027794	Pisolitic	53H	0.21	14.03	23.7	18.92	42.78	0.01	0.07	<0.01	0.2	0.45	0.01
KIFE035	663568	6024498	Ferruginous Saprolite	53H	0.22	10.44	30.1	14.82	43.89	0.01	0.05	<0.01	0.17	0.3	0.01
KIFE036	662030	6022925	Vermiform Ferricrete	53H	0.16	12.19	52.8	17.24	17.28	<0.01	0.03	<0.01	0.07	0.34	0.02
KIFE037	649853	6041631	Vermiform Ferricrete	53H	0.21	16.47	42.5	23.52	16.16	0.03	0.11	0.02	0.25	0.51	0.02
KIFE038	653587	6040165	Pisolitic	53H	0.2	15.09	40.7	19.18	24.27	<0.01	0.03	<0.01	0.06	0.33	0.02
KIFE039	656833	6038127	Pisolitic	53H	0.33	13.82	32.5	29.33	23.66	0.02	0.1	0.02	0.25	0.59	0.03
KIFE040	660713	6038011	Ferruginous Sediments	53H	0.18	12.96	38	28.22	19.51	0.02	0.09	<0.01	0.21	0.54	0.02
KIFE041	659824	6039012	Ferruginous Sediments	53H	0.29	15.68	32.2	23.33	27.69	0.02	0.09	<0.01	0.22	0.48	0.03
KIFE042	658961	6040465	Nodular	53H	0.2	13.57	40.8	21.56	23.1	<0.01	0.05	<0.01	0.07	0.45	0.02
KIFE043	658771	6042877	Pisolitic	53H	0.21	11.55	44.8	22.12	20.69	0.02	0.09	0.02	0.3	0.43	0.02

Sample	Easting	Northing	Ferricrete Classification	Zone	Wgt	LOI	SiO2	Al2O3	Fe2O3	CaO	MgO	Na2O	K2O	TiO2	P2O5
KIFE044	665470	6037969	Ferruginous Sediments	53H	0.23	16.28	20.7	24.86	37.12	<0.01	0.05	<0.01	0.22	0.61	0.02
KIFE045	670138	6038556	Pisolitic	53H	0.3	15.65	18.8	19.71	45.39	<0.01	0.06	<0.01	0.3	0.37	0.01
KIFE046	674233	6020625	Ferruginous Sediments	53H	0.21	11.92	50.5	16.03	20.54	0.01	0.07	0.01	0.22	0.28	0.02
KIFE047	673362	6022408	Nodular	53H	0.21	11	56	17.81	13.2	0.01	0.4	<0.01	0.6	0.46	0.02
KIFE048	672088	6024411	Slabby Ferricrete	53H	0.22	14.33	33	21.06	30.2	0.01	0.1	<0.01	0.4	0.52	0.02
KIFE050	670104	6039096	Ferruginous Sediments	53H	0.2	11.69	37.1	17.67	32.37	0.02	0.09	<0.01	0.59	0.46	0.02
KIFE051	670221	6039473	Vermiform Ferricrete	53H	0.21	13.76	47.7	15.23	22.72	<0.01	0.06	<0.01	0.13	0.31	0.01
KIFE052	670221	6039473	Pisolitic	53H	0.22	12.61	34.6	20.64	30.58	<0.01	0.09	<0.01	0.44	0.57	0.02
KIFE053	670539	6040691	Ferruginous Sediments	53H	0.22	13.79	22.5	18.52	43.87	<0.01	0.08	<0.01	0.4	0.46	0.02
KIFE054	669664	6044450	Ferruginous Saprolite	53H	0.22	12.21	24.8	22.84	39.2	0.01	0.08	<0.01	0.32	0.74	0.03
KIFE055	668459	6046461	Pisolitic	53H	0.19	10.68	62.3	17.44	7.79	0.02	0.14	0.01	0.75	0.35	0.02
KIFE056	670537	6042204	Nodular	53H	0.21	13.54	26.9	20.03	38.49	0.01	0.08	<0.01	0.22	0.45	0.01
KIFE057	672089	6038131	Pisolitic	53H	0.21	8.15	27.9	16.92	45.56	0.02	0.09	<0.01	0.33	0.64	0.02
KIFE058	677015	6036757	Ferruginous Sediments	53H	0.2	14.91	23.1	19.58	40.81	<0.01	0.09	<0.01	0.39	0.4	0.02
KIFE059	683685	6029949	Ferruginous Sediments	53H	0.22	11.19	22.8	15.75	48.89	<0.01	0.06	<0.01	0.39	0.71	0.02
KIFE060	683772	6031864	Ferruginous Sediments	53H	0.22	11.73	25.4	13.88	48.26	<0.01	0.07	<0.01	0.28	0.43	0.02
KIFE061	683364	6034390	Ferruginous Sediments	53H	0.22	11.44	35.4	19.06	32.48	0.01	0.08	<0.01	0.2	0.81	0.02
KIFE062	683972	6039476	Pisolitic	53H	0.21	12.08	36.2	15.27	35.28	<0.01	0.06	<0.01	0.21	0.49	0.02
KIFE063	683737	6042352	Ferruginous Saprolite	53H	0.21	10.5	28.5	24.84	34.85	0.01	0.05	<0.01	0.11	0.51	0.03
KIFE064	684900	6048700	Pisolitic	53H	0.19	7.18	59.4	15.88	13.19	0.01	0.27	0.06	2.72	0.81	0.03
KIFE065	700461	6049237	Pisolitic	53H	0.21	15.33	26.2	26.83	30.27	0.03	0.1	0.02	0.29	0.71	0.02
KIFE066	698420	6023909	Ferruginous Sediments	53H	0.21	16.59	44.2	26.23	11.69	0.02	0.09	<0.01	0.08	0.72	0.02
KIFE067	697076	6030163	Pisolitic	53H	0.21	11.95	32.9	18.5	35.02	0.02	0.12	0.03	0.32	0.47	0.02
KIFE068	698357	6032393	Pisolitic	53H	0.21	12.24	26	15.82	45.48	0.02	0.07	<0.01	0.12	0.49	0.02
KIFE069	709308	6052961	Ferruginous Sediments	53H	0.21	8.25	34.6	19.7	36.2	0.03	0.14	<0.01	0.68	0.57	0.02
KIFE070	709523	6055111	Ferruginous Saprolite	53H	0.21	14.87	33.8	23.79	26.7	0.02	0.09	0.03	0.16	0.56	0.02
KIFE071	715741	6049998	Ferruginous Sediments	53H	0.21	6.26	50.5	8.21	33.5	0.06	0.07	<0.01	0.1	1.06	0.02
KIFE072	715655	6046018	Ferruginous Sediments	53H	0.21	10.37	29.4	14.27	44.83	0.03	0.08	0.02	0.18	0.6	0.02
KIFE073	744525	6036101	Nodular	53H	0.2	2.95	48.1	7.29	40.62	0.11	0.11	0.17	0.59	0.35	0.05
KIFE100	717233	6041637	Ferruginous Sediments	53H	0.22	5.23	58.9	6.67	28.27	0.03	0.09	0.02	0.16	0.3	<0.01
KIFE101	715854	6042738	Ferruginous Sediments	53H	0.2	9.63	50.2	12.87	26.47	0.02	0.04	<0.01	0.12	0.28	0.02
KIFE102	718428	6049605	Ferruginised Bedrock	53H	0.19	5.49	41.7	9.97	40.18	0.16	0.28	0.04	1.15	0.54	0.04
KIFE103	718428	6049605	Ferruginised Bedrock	53H	0.19	3.28	80.5	10.76	1.62	0.08	0.13	0.36	3.36	0.16	<0.01
KIFE104	704812	6038620	Ferruginised Bedrock	53H	0.18	9.38	32.9	13.2	43.78	0.02	0.11	<0.01	0.28	0.23	0.02
KIFE105	702046	6038660	Ferruginised Bedrock	53H	0.18	7.62	14.8	3.49	73.4	<0.01	0.01	<0.01	0.03	0.2	0.23
KIFE106	717944	6026798	Pisolitic	53H	0.18	5.3	57	11.47	23.58	0.05	0.18	<0.01	0.94	0.68	0.03
KIFE107	715737	6026658	Pisolitic	53H	0.21	2.3	73.6	10.91	7.47	0.07	0.51	2.07	2.26	0.49	0.04
KIFE108	710538	6025147	Pisolitic	53H	0.19	8.47	53	12.8	24.31	0.02	0.11	0.05	0.41	0.71	0.02
KIFE109	704032	6021198	Pisolitic	53H	0.05	8.66	51.4	14.56	23.97	0.04	0.13	0.09	0.52	0.48	0.03
KIFE110	684459	6018128	Vermiform Ferricrete	53H	0.19	10.6	56	14.46	18.35	0.02	0.08	<0.01	0.18	0.23	0.02
KIFE111	673931	6016908	Slabby Ferricrete	53H	0.22	11.73	54.9	16.45	16.03	0.01	0.07	<0.01	0.2	0.25	0.02
KIFE112	662178	6023646	Ferruginised Bedrock	53H	0.21	15.79	34.6	23.51	25.5	<0.01	0.03	<0.01	0.05	0.31	0.01
KIFE113	679628	6041604	Pisolitic	53H	0.22	16.01	27	24.09	32.03	0.01	0.06	<0.01	0.12	0.55	0.02
KIFE114	680529	6046587	Pisolitic	53H	0.23	21.59	25.6	35.16	16.56	<0.01	0.02	<0.01	0.08	1.32	0.02
KIFE115	680403	6046850	Ferruginised Bedrock	53H	0.24	6.62	39.3	14.43	36.68	0.01	0.15	0.12	1.85	0.53	0.03

Sample	Easting	Northing	Ferricrete Classification	Zone	Wgt	LOI	SiO2	Al2O3	Fe2O3	CaO	MgO	Na2O	K2O	TiO2	P2O5
KIFE116	687572	6043745	Nodular	53H	0.25	14.86	46.4	22.83	14.91	<0.01	0.04	<0.01	0.07	0.7	0.02
KIFE117	690596	6043937	Nodular	53H	0.23	15.56	25	25.5	32.47	0.01	0.1	<0.01	0.39	0.67	0.03
KIFE118	690199	6036277	Nodular	53H	0.23	11	30.4	15.75	41.5	<0.01	0.1	<0.01	0.47	0.53	0.01
KIFE119	766788	6037631	Ferruginised Sediments	53H	0.24	5.34	58.5	8.32	26.27	0.04	0.07	0.04	0.45	0.45	0.01
KIFE120	700340	6043771	Ferruginised Bedrock	53H	0.21	4.05	82.5	10.19	1.51	<0.01	0.23	<0.01	1.17	0.38	0.02
KIFE121	700340	6043771	Ferruginised Bedrock	53H	0.18	5.18	76.9	11.55	3.65	<0.01	0.26	<0.01	1.03	1.02	0.02
KIFE122	700340	6043771	Ferruginised Bedrock	53H	0.23	4.14	82.6	9.43	2.46	<0.01	0.16	<0.01	0.78	0.44	<0.01
KIFE123	700340	6043771	Ferruginised Saprolite	53H	0.2	8.4	63.4	18.36	7.96	<0.01	0.19	0.02	0.66	0.73	<0.01
KIFE124	700340	6043771	Ferruginised Saprolite	53H	0.21	9.91	32.1	14.99	41.48	<0.01	0.11	<0.01	0.42	0.39	0.01
KIFE125	700340	6043771	Pisolitic	53H	0.22	10.95	23.1	15.32	49.76	0.01	0.05	<0.01	0.13	0.39	0.01
KIFE126	700381	6045457	Ferruginised Bedrock	53H	0.2	4.4	81.5	11.38	1.5	<0.01	0.2	<0.01	0.99	0.43	0.01
KIFE127	700381	6045457	Ferruginised Bedrock	53H	0.19	8.65	61.9	20.89	4.45	<0.01	0.72	0.04	2.43	0.93	0.01
KIFE128	700381	6045457	Ferruginised Saprolite	53H	0.2	2.61	85.4	7.84	1.6	0.16	0.8	0.16	0.11	0.35	<0.01
KIFE129	700381	6045457	Ferruginised Saprolite	53H	0.18	3.76	84.6	8.5	1.77	<0.01	0.1	0.01	0.23	0.55	<0.01
KIFE130	700381	6045457	Ferruginised Saprolite	53H	0.19	7.15	72.5	15.17	4.06	0.02	0.15	0.01	0.19	0.51	0.01
KIFE131	700381	6045457	Pisolitic	53H	0.2	11.2	46.9	14.28	27.2	0.02	0.08	0.02	0.17	0.27	0.02
KIFE150	645971	6037861	Vermiform Ferricrete	53H	0.11	15.81	42.12	21.84	19.57	0.04	0.1	0.04	0.23	0.55	0.02
KIFE151	719115	6035158	Pisolitic	53H	0.1	6.99	56.78	9.87	25.33	0.04	0.11	0.07	0.51	0.79	0.02
KIFE153	717943	6026808	Pisolitic	53H	0.11	4.56	65.18	10.17	17.47	0.06	0.32	0.77	1.23	0.7	0.03
KIFE154	720802	6027834	Pisolitic	53H	0.11	10.15	51.86	14.33	22.34	0.05	0.16	0.08	0.47	0.61	0.02
KIFE155	731840	6021196	Pisolitic	53H	0.11	12.89	59.81	15.93	4.72	3.65	0.88	0.38	1.06	0.58	0.01
KIFE156	731840	6021196	Ferruginised Bedrock	53H	0.13	4.62	84.06	6.38	2.8	0.88	0.29	0.18	0.71	0.31	<0.01
KIFE157	731840	6021196	Pisolitic	53H	0.11	7.75	63.43	8.59	19.28	0.07	0.14	0.07	0.41	0.37	0.02
KIFE158	752793	6039501	Pisolitic	53H	0.11	7.89	45.07	13.3	32.26	0.02	0.11	0.06	0.92	0.49	0.03
KIFE159	751267	6039333	Pisolitic	53H	0.11	10.67	48.64	14.19	26.16	0.02	0.07	0.01	0.12	0.27	0.03
KIFE160	737517	6038253	Pisolitic	53H	0.11	4.85	54.59	8.29	30.73	0.05	0.1	0.13	0.42	0.5	0.02
KIFE161	701964	6046152	Ferruginised Bedrock	53H	0.11	7.52	37.05	13.09	39.03	0.1	0.53	0.03	2.05	0.5	0.06
KIFE165	684654	6023952	Pisolitic	53H	0.1	9.05	72.8	11.62	5.41	0.02	0.06	<0.01	0.11	0.33	0.01
KIFE166	x	x	x	x	x	x	x	x	x	x	x	x	x	x	x
KIFE167	684646	6024036	Vermiform Ferricrete	53H	0.12	18.65	37.28	27.96	14.94	0.02	0.11	<0.01	0.18	0.51	0.02
KIFE168	684793	6022152	Nodular	53H	0.11	9.2	71.25	9.28	9.55	0.03	0.09	0.03	0.21	0.32	<0.01
KIFE169	x	x	x	x	x	x	x	x	x	x	x	x	x	x	x
KIFE170	680838	6044131	Pisolitic	53H	0.09	11.77	27.83	16.58	42.86	0.01	0.05	<0.01	0.14	0.65	<0.01
KIFE171	706714	6050896	Vermiform Ferricrete	53H	0.1	4.93	48.53	5.4	38.29	0.04	0.05	0.03	0.04	2.19	0.04
KIFE172	705549	6045464	Pisolitic	53H	0.11	8.77	69.86	15.14	4.69	0.02	0.24	0.05	0.8	0.58	0.01
KIFE173	699982	6039027	Nodular	53H	0.11	16.03	17.95	25.21	40.36	0.03	0.08	<0.01	0.11	0.47	0.02
KIFE174	697324	6039270	Slabby Ferricrete	53H	0.11	9.65	31.15	13.19	45.31	0.02	0.1	<0.01	0.25	0.39	0.01
KIFE175	702993	6024406	Ferruginised Bedrock	53H	0.11	5.75	60.34	10.73	19.45	0.06	0.36	0.96	1.56	0.42	0.02
KIFE176	699977	6031291	Pisolitic	53H	0.11	15.05	24.95	22.63	35.29	0.01	0.12	<0.01	0.33	0.61	0.02
KIFE177	692575	6027761	Nodular	53H	0.11	7.79	37.06	11.86	41.87	0.01	0.05	<0.01	0.08	0.49	0.02
KIFE178	692532	6024316	Vermiform Ferricrete	53H	0.1	12.97	52.87	17.5	15.3	0.02	0.07	0.02	0.11	0.35	0.02
KIFE179	692999	6021850	Pisolitic	53H	0.11	13.12	46.97	20.8	17.22	0.03	0.12	<0.01	0.17	0.62	0.01
KIFE180	693803	6019221	Pisolitic	53H	0.11	4.32	32.02	9.65	53.1	0.07	0.16	0.05	0.13	0.3	0.02
KIFE181	695762	6017171	Nodular	53H	0.12	6.85	72.08	12.51	5.29	0.33	0.61	0.63	1.1	0.55	0.02
KIFE182	680717	6016908	Pisolitic	53H	0.11	13.22	47.93	18.01	19.54	0.03	0.13	0.05	0.29	0.47	0.02
KIFE183	680334	6019079	Pisolitic	53H	0.11	7.21	50.6	12.83	28.6	0.02	0.06	<0.01	0.11	0.24	0.02

Sample	Easting	Northing	Ferricrete Classification	Zone	Wgt	LOI	SiO2	Al2O3	Fe2O3	CaO	MgO	Na2O	K2O	TiO2	P2O5
KIFE184	679663	6020983	Pisolitic	53H	0.11	12.01	29.62	17.07	40.17	0.01	0.09	<0.01	0.34	0.4	0.02
KIFE185	679580	6022229	Nodular	53H	0.11	10.49	33.34	16.28	39.75	0.02	0.09	<0.01	0.24	0.48	0.02
KIFE186	678880	6025908	Nodular	53H	0.12	15.97	27.04	24.85	31.02	<0.01	0.09	<0.01	0.17	0.5	0.02
KIFE187	678833	6035613	Pisolitic	53H	0.11	10.97	25.11	16.48	45.23	0.01	0.06	<0.01	0.2	1.53	0.04
KIFE188	664366	6024811	Pisolitic	53H	0.11	12.56	30.87	15.16	40.59	<0.01	0.05	<0.01	0.11	0.31	0.02
KIFE189	667559	6022358	Pisolitic	53H	0.12	11.36	17.21	8.16	63.21	0.01	0.06	<0.01	0.12	0.22	0.02
KIFE190	669607	6022205	Slabby Ferricrete	53H	0.12	9.45	42.07	14.84	32.06	<0.01	0.05	<0.01	0.29	0.36	0.01
KIFE191	672682	6022174	Nodular	53H	0.11	18.66	28.46	30.72	20.26	0.01	0.06	<0.01	0.08	0.67	0.01
KIFE192	x	x	x	x	x	x	x	x	x	x	x	x	x	x	x
KIFE193	x	x	x	x	x	x	x	x	x	x	x	x	x	x	x
KIFE194	x	x	x	x	x	x	x	x	x	x	x	x	x	x	x
KIFE195	674543	6041379	Pisolitic	53H	0.12	9.36	32.36	14	42.72	<0.01	0.11	<0.01	0.47	0.5	0.02
KIFE196	702846	6033214	Ferruginised Bedrock	53H	0.16	9.09	44.44	14.31	28.94	0.01	0.2	<0.01	1.24	0.86	0.04
KIFE197	704689	6034979	Pisolitic	53H	0.11	18.25	33.37	30.99	16.31	0.02	0.1	<0.01	0.11	0.61	0.02
KIFE198	704695	6041585	Pisolitic	53H	0.11	9.64	46.82	19.48	22.21	0.03	0.12	<0.01	0.35	0.62	0.02
KIFE199	695890	6039376	Pisolitic	53H	0.11	9.96	35.42	16.78	37.32	0.01	0.08	<0.01	0.12	0.55	0.02
KIFE200	693052	6042412	Pisolitic	53H	0.12	11.22	31.42	17.15	39.09	0.02	0.16	0.01	0.48	0.39	0.03
KIFE201	690545	6041216	Ferruginised Bedrock	53H	0.11	13.54	30.51	16.64	38.31	0.01	0.05	<0.01	0.05	0.39	0.03
KIFE202	708539	6025993	Pisolitic	53H	0.11	6.74	60.02	9.44	21.82	0.03	0.11	0.05	0.55	0.78	0.02
KIFE203	708624	6023892	Pisolitic	53H	0.11	9.79	51.99	12.37	24.18	0.03	0.15	0.07	0.46	0.62	0.02
KIFE204	710064	6045006	Pisolitic	53H	0.12	5.67	39.49	4.14	49.85	0.03	0.05	0.02	0.47	0.34	0.14
			Mean			10.319073	44.55841	15.912848	27.7007947	0.0752066	0.137682	0.1266667	0.462715	0.5276159	0.0253191
			Median			10.49	42.7	15.16	27.2	0.02	0.1	0.04	0.3	0.49	0.02
			Minimum			2.3	14.8	3.49	1.5	0.01	0.01	0.01	0.03	0.12	0.01
			Maximum			21.59	87.5	35.16	73.4	3.65	0.88	2.07	3.36	2.19	0.23
			Standard Deviation			4.0717286	16.6273	6.1320958	14.2435899	0.3408203	0.134543	0.2802256	0.517534	0.2472535	0.0238613

Sample Method	Cr2O3 % 4X	SUM % 4X	TOT/C % 2A Leco	TOT/S % 2A Leco	Ba ppm 4B	Be ppm 4B	Co ppm 4B	Cs ppm 4B	Ga ppm 4B	Hf ppm 4B	Nb ppm 4B	Rb ppm 4B	Sn ppm 4B	Sr ppm 4B	Ta ppm 4B	Th ppm 4B	U ppm 4B
Dect. Limit																	
KIFE001	0.001	0.01	0.02	0.02	1	1	0.2	0.1	0.5	0.1	0.1	0.1	1	0.5	0.1	0.2	0.1
KIFE002	0.005	99.91	0.04	<0.02	257	2	3.1	1	3.8	3.5	5.6	37.3	1	38.3	0.3	9.3	0.7
KIFE003	0.041	99.43	0.16	0.03	85	2	11.5	0.6	5.4	5	5.5	16.4	<1	15.1	0.4	12	1.9
KIFE004	0.019	99.68	0.09	0.03	649	<1	11.9	0.9	9.2	6	7.4	16.5	1	51.2	0.6	13.9	1.1
KIFE005	0.034	99.99	0.32	0.1	88	7	7.5	2.7	20	9.1	10.6	19	3	23.2	0.6	18.2	3.1
KIFE006	0.02	99.65	0.34	<0.02	23	2	4.2	0.7	19.8	10.8	8.2	6.4	3	11.5	0.3	34.2	2.9
KIFE007	0.024	99.51	0.27	0.06	31	3	8.4	2.1	23.8	6.8	6.3	13.2	3	17.3	0.4	30.3	4.5
KIFE008	0.042	98.86	0.32	0.04	27	3	4.4	1.9	21.7	5.4	7.8	6.9	2	20.9	0.4	31.7	2.8
KIFE009	0.021	99.78	0.36	0.04	25	<1	2.6	1	28.4	11.2	13.1	5.4	3	10.4	0.9	38.9	5.1
KIFE010	0.036	99.55	0.59	0.03	320	1	2.5	1	22	21.3	17.9	27.8	2	33.3	1	132.5	5.9
KIFE011	0.035	100.03	0.23	0.08	71	3	4.2	1.2	28.7	8.8	8.3	9.6	1	17.5	0.5	107.5	6.5
KIFE012	0.013	99.22	0.47	0.03	37	1	2.2	1.3	22.8	13.1	5.9	9.4	2	13	0.4	8.8	1.6
KIFE013	0.03	99.65	0.46	0.03	29	<1	3.8	1.5	23.8	8.8	10	9.5	2	14.5	0.5	24.1	3.4
KIFE014	0.024	99.6	0.13	<0.02	312	<1	4.5	1.1	15.7	7.9	9.4	31.6	2	33.4	0.9	22	1.6
KIFE015	0.019	99.61	0.23	<0.02	131	1	6.3	1.8	17.4	14.5	13	21.7	2	26.2	1	18	2.5
KIFE016	0.023	99.16	0.34	0.02	118	3	4.6	2.6	27	12.8	12.4	25.3	3	24.5	1	19.8	2.3
KIFE017	0.03	99.39	0.29	0.03	108	1	5.4	2.5	23.3	9.5	10.9	22.9	2	22.8	0.8	36.4	3.1
KIFE018	0.016	100.01	0.36	0.04	333	<1	2.1	1	14.1	5.7	7	40	1	12.9	0.5	55.2	2.4
KIFE019	0.014	100.55	0.23	0.05	93	7	3.8	1.3	10.2	4.7	5	21.5	1	23.6	0.3	23.6	3.4
KIFE020	0.019	100.31	0.28	0.06	122	3	2.8	2.1	19.2	3.5	8.7	25.7	3	20.2	0.6	26	3.4
KIFE021	0.032	99.87	0.41	0.03	109	<1	3.2	3	21.5	13.7	16.2	25.4	2	22.1	1.2	19.8	3.1
KIFE022	0.036	100.31	0.25	0.04	297	<1	0.7	0.6	15.2	5.3	10	38.6	2	12.9	0.5	34.6	1.6
KIFE023	0.049	99.61	0.14	<0.02	311	<1	3.4	1.5	37.4	8.1	9.2	36	3	26.4	0.5	54.9	1.2
KIFE024	0.091	99.8	0.11	<0.02	364	<1	3.7	0.6	39.3	6.6	10.7	20.2	2	31.7	0.5	69.8	2.1
KIFE025	0.036	99.1	0.16	<0.02	138	3	5.9	1.9	21.5	9.8	7.8	27.8	1	25.4	0.5	35.2	3.6
KIFE026	0.031	99.29	0.18	<0.02	181	<1	6.2	1.4	23.5	12.7	11.2	23	<1	26.7	0.9	21.5	2.6
KIFE027	0.036	99.8	0.17	<0.02	200	<1	5.7	1.7	21.3	11.4	11.3	29.3	3	31.5	0.7	31.1	3.2
KIFE028	0.039	100.04	0.14	0.06	41	4	7.8	1.8	32	7.3	8.3	13.8	2	17.6	0.5	51.7	4.5
KIFE029	0.041	99.75	0.2	<0.02	79	10	4.2	1.5	31.9	8.7	9.9	13.5	2	17.3	1	53.6	3.1
KIFE030	0.029	99.57	0.21	0.03	112	<1	6.4	2	22.8	9.7	9.3	24.7	1	21.8	0.7	24.6	3
KIFE031	0.033	99.29	0.22	<0.02	119	2	5.2	1.7	25.8	11.2	9.9	23.7	1	22.8	0.7	17.5	1.8
KIFE032	0.018	100.23	0.26	0.03	128	<1	3.8	1.6	23.8	10.4	8.9	25.4	<1	19.5	0.8	9.9	1.6
KIFE033	0.045	100.23	0.33	0.03	110	<1	1.8	0.8	31	14.1	12.6	20.3	3	9.4	0.8	159.5	6.3
KIFE034	0.03	100.22	0.3	0.11	62	<1	2.4	0.7	21.2	8.3	7.4	9.4	<1	12.8	0.5	74.7	4.1
KIFE035	0.033	99.84	0.18	0.08	26	<1	0.3	0.8	13.7	3.8	5.3	6	1	5.1	0.4	49.7	2.9
KIFE036	0.024	100.01	0.38	0.1	14	4	1.8	0.5	16.5	7.5	4.6	4	<1	9.5	0.4	20.3	4
KIFE037	0.022	99.6	0.56	0.09	58	<1	3.8	1.7	23.1	5.5	7.3	12.4	2	19.1	0.7	8.9	2
KIFE038	0.02	99.65	0.35	0.1	16	3	2.7	0.6	22.3	7.2	5.6	4.3	<1	9.5	0.2	19	3.7
KIFE039	0.043	100.33	0.64	0.07	67	<1	1.2	1.6	29.7	11.3	9.7	13.9	2	14.3	0.7	87.5	4.3
KIFE040	0.046	99.61	0.71	0.15	59	<1	1	1.2	28.9	13.8	9	13.4	1	9.2	0.8	127.3	3.8
KIFE041	0.031	99.76	0.61	0.09	66	2	1.5	1.2	22.3	9.5	6.7	11.8	1	13.1	0.6	80.4	5.1
KIFE042	0.03	99.65	0.51	0.11	18	<1	1.9	0.7	22.4	9.1	6.4	4.8	<1	9	0.6	39.9	6.3
KIFE043	0.032	100.07	0.37	0.08	97	<1	3.1	1.3	17.8	7.6	6.5	13.3	<1	10.6	0.7	41.1	3.5

Sample	Cr2O3	SUM	TOT/C	TOT/S	Ba	Be	Co	Cs	Ga	Hf	Nb	Rb	Sn	Sr	Ta	Th	U
KIFE044	0.029	99.87	0.46	0.13	78	<1	0.7	0.5	26	9.7	8.6	6.7	1	9.5	0.8	69.2	3.9
KIFE045	0.038	100.29	0.33	0.16	66	3	1.1	0.4	39.8	9.1	5.9	9.4	<1	4.4	0.4	108.5	5.4
KIFE046	0.022	99.64	0.25	0.09	49	5	9	0.7	13.6	6.4	3.6	8.6	<1	12.4	0.3	24.3	5.2
KIFE047	0.033	99.52	0.51	0.07	103	3	3.5	5.8	17.1	8	8.3	53.7	2	14.2	0.8	60.5	2.6
KIFE048	0.043	99.68	0.54	0.09	60	<1	1.8	0.7	28.5	7.2	8.1	12	2	7.5	0.7	74.2	2.8
KIFE049	0.043	100.02	0.33	0.11	62	1	1.6	0.8	21.1	7.6	7	26.5	1	15	0.6	104.7	3.5
KIFE050	0.022	99.89	0.73	0.15	37	<1	1	0.9	14.1	7	5.1	7.4	<1	7	0.3	26.9	2.6
KIFE051	0.039	99.59	0.21	0.14	142	<1	1.4	1.1	29.9	11	8.4	15.7	2	9	0.8	148.5	5.1
KIFE052	0.039	99.6	0.31	0.14	129	2	1.7	0.5	32.8	8.6	7.2	11.6	2	6.7	0.5	138.2	5.8
KIFE053	0.024	100.27	0.61	0.13	116	<1	1	0.8	25.2	9.1	9.9	11.4	3	15.4	0.8	88.2	5.2
KIFE054	0.014	99.51	0.62	0.09	205	<1	1.3	0.7	15.7	4.9	6.8	26.7	2	8.6	0.6	36.7	1.7
KIFE055	0.035	99.78	0.26	0.11	54	<1	2.8	1.8	29	6.5	6.2	9.7	2	9.1	0.6	55.6	4.4
KIFE056	0.027	99.64	0.38	0.06	120	<1	1	1.1	20.9	7.5	9.5	11.8	2	10.2	0.7	54.2	2.7
KIFE057	0.025	99.35	0.39	0.14	88	2	1.4	0.9	20.9	8.5	6.5	12.7	1	6.3	0.5	85.1	4.3
KIFE058	0.06	99.85	0.26	0.14	124	<1	1.4	0.4	30.8	15.5	11.4	10.9	2	7.1	0.9	108.6	4.6
KIFE059	0.036	100.08	0.16	0.13	103	5	2.6	1.3	20.9	7.3	6.5	10.5	1	8.2	0.6	105	4.4
KIFE060	0.039	99.46	0.32	0.08	63	<1	2.2	1.3	27.5	12.5	11.3	11.4	3	12.6	0.9	62.1	4.5
KIFE061	0.025	99.62	0.32	0.12	77	2	2.1	0.8	29.7	7.7	7.8	9.2	1	7.4	0.6	61	3.6
KIFE062	0.042	99.36	0.43	0.08	41	<1	2	1.4	36.2	7.7	7.9	7.7	2	8	0.6	73	5.9
KIFE063	0.025	99.62	0.31	0.05	476	<1	1.1	1.5	16.6	16.1	14.6	74.5	3	40.9	1.3	91	3.4
KIFE064	0.058	99.85	0.43	0.09	99	<1	3.3	1.4	44.8	9	12.7	12.5	5	13.1	0.9	79.8	5.4
KIFE065	0.022	99.62	0.29	0.1	23	<1	5.3	0.8	25.2	10.4	11.6	5.6	2	10.9	0.9	37.9	5.1
KIFE066	0.046	99.4	0.23	0.08	105	2	4.5	2.1	22	6.7	7.3	14	1	11.6	0.5	86.2	4.7
KIFE067	0.032	100.28	0.26	0.11	42	<1	4.3	1.1	22.6	7.2	7	7.9	2	8.5	0.7	43	3.9
KIFE068	0.053	100.25	0.35	0.05	93	2	3.3	2.7	32.3	11	9.6	32.6	3	11.3	1	81.9	4.7
KIFE069	0.026	100.01	0.39	0.1	31	<1	2.4	1.2	31.7	13.1	9	9.3	2	12.5	0.8	86.9	4.8
KIFE070	0.032	99.28	0.11	0.08	19	<1	2.8	0.6	46.5	12.8	15.5	5.1	4	12.5	1.4	73.7	2.8
KIFE071	0.016	99.1	0.19	0.02	23	2	1.7	1.4	12.7	6.4	6.4	7	<1	7.8	0.7	23.1	1.5
KIFE072	0.034	99.82	0.16	0.05	25	<1	2.7	1.9	20.5	11.2	9.1	11.9	3	5.3	0.7	76.7	5.1
KIFE073	0.028	100.41	0.09	<0.02	151	<1	6.1	0.5	14.3	8.2	5.8	15.2	<1	35.1	0.5	20.7	1.4
KIFE100	0.029	99.73	0.13	0.03	36	<1	2.1	1	17.9	6.6	6.3	13.6	<1	10.9	0.4	63.1	1
KIFE101	0.02	99.66	0.22	0.05	27	<1	4.4	0.6	14.5	8.2	4.9	6.5	1	9.5	0.4	34.8	5.4
KIFE102	0.019	99.56	0.36	<0.02	210	<1	1.6	3.8	12.2	8.7	10.4	54.7	3	27	0.9	36.4	2.2
KIFE103	0.005	100.31	0.11	<0.02	592	<1	0.5	2.3	8.9	3	4.2	103.9	1	56.5	0.4	6.4	0.7
KIFE104	0.031	99.91	0.18	0.06	68	<1	3.7	2.1	17.1	3.1	4.3	17.8	<1	12.9	0.4	37.1	4.5
KIFE105	0.009	99.84	0.16	0.05	9	<1	2.1	0.5	6.4	2.3	3.7	2.3	<1	3.2	0.3	4.8	1.2
KIFE106	0.037	99.86	0.17	0.02	219	<1	4	2.1	26.4	11.1	11.9	37.3	3	36.4	1	41.7	2.2
KIFE107	0.017	99.76	0.08	<0.02	480	<1	4.5	1.7	13.3	7	10	95.2	3	69.5	0.7	18.7	2.8
KIFE108	0.022	99.88	0.2	0.04	110	5	6.4	1.9	19.6	10.5	11.3	21.5	2	24.7	1.6	21	3.2
KIFE109	0.025	99.92	0.21	0.03	145	<1	8.7	1.7	19.6	8.2	7.5	25.5	1	29.1	0.8	16	2.8
KIFE110	0.02	99.99	0.29	0.08	43	5	6.7	0.9	11.4	6	3.8	9.9	<1	13	0.3	12.3	2.6
KIFE111	0.02	99.71	0.32	0.09	56	<1	7.4	1.1	13	8.8	3.7	11	<1	13	0.4	21.2	4.4
KIFE112	0.02	99.82	0.22	0.1	12	<1	2.5	0.6	24	11.3	6.2	3.7	3	8.4	0.5	93.2	6.8
KIFE113	0.027	99.88	0.47	0.06	36	<1	1.9	1.3	22.6	8.4	8	8	2	11.6	0.6	47.9	4.6
KIFE114	0.026	100.33	0.34	0.07	28	<1	1.7	0.8	48.8	7.9	23.1	3.3	6	7.2	1.6	34.5	4.5
KIFE115	0.049	99.77	0.23	0.08	572	<1	0.4	0.4	22	3.5	11.6	35.4	3	21.6	0.9	47.4	2.3

Sample	Cr2O3	SUM	TOT/C	TOT/S	Ba	Be	Co	Cs	Ga	Hf	Nb	Rb	Sn	Sr	Ta	Th	U
KIFE116	0.021	99.84	0.3	0.05	21	<1	2.9	1.1	25.2	9.7	11.5	5.2	2	11.8	0.8	29.4	4.9
KIFE117	0.033	99.73	0.25	0.05	151	5	3	1.4	37.7	9.6	10.7	15.1	2	32.8	0.8	93	6.3
KIFE118	0.024	99.76	0.16	0.1	177	3	2.8	1.2	25	6.2	9.5	16	2	9.2	0.9	50.5	6
KIFE119	0.037	99.55	0.09	0.03	221	<1	1.9	0.4	20.3	7.1	8.4	10.2	2	12.3	0.7	41.3	1.6
KIFE120	0.004	100.12	0.03	<0.02	393	<1	0.4	0.7	14.6	4.8	6.9	39.7	1	20.3	0.6	8.7	0.9
KIFE121	0.013	99.6	0.13	<0.02	334	3	0.9	1.3	33.4	8.6	17.7	34.1	4	30.7	1.4	18.5	1.5
KIFE122	0.007	100.02	0.05	<0.02	254	3	0.7	1	20	4.8	7.5	27.7	3	11.6	0.5	10.9	0.6
KIFE123	0.015	99.75	0.11	0.04	190	9	2.7	3.3	29.1	7	11.3	30.6	4	14.7	0.9	27.1	1.7
KIFE124	0.021	99.41	0.13	0.09	113	<1	1.6	2.3	21.3	4.3	6.5	23.4	2	5.7	0.5	56.6	2.6
KIFE125	0.021	99.68	0.21	0.07	29	3	2.6	1.7	21.9	5.8	6	9.9	2	5.6	0.6	76.3	4.6
KIFE126	0.008	100.5	0.07	<0.02	384	3	1.6	0.9	15.1	6	8.2	32	2	23.1	0.7	15	1.7
KIFE127	0.024	100.1	0.14	0.02	794	<1	3.5	2.2	30.5	9.6	20.9	78.8	5	17.3	2.5	37.2	4.2
KIFE128	0.007	99.02	0.02	<0.02	40	1	2.4	0.3	11.7	8.7	9	4	7	65.1	1.2	9.2	1.1
KIFE129	0.012	99.51	0.05	<0.02	67	1	0.9	0.6	12.5	22.3	8.9	10.7	2	13.7	0.7	17.6	1.6
KIFE130	0.01	99.74	0.05	<0.02	45	<1	2.5	1.2	16.1	13.7	10.9	13.9	3	15.5	1.7	18	2.2
KIFE131	0.03	100.17	0.36	0.03	46	4	3.5	1.3	17.7	13.4	5.5	11.1	1	8	0.6	50.6	5.3
KIFE150	0.018	100.35	0.55	0.07	70	3	5.5	1.9	20.1	6.8	9.2	13.1	2	22.1	0.6	12.1	1.8
KIFE151	0.018	100.55	0.17	0.03	128	2	4.3	2	21.7	11.9	12.6	23.8	2	24.6	0.9	10.9	1.9
KIFE153	0.018	100.55	0.25	0.03	250	1	4.8	1.8	21.2	11.6	12.1	47.9	2	33.4	0.9	25.3	2.1
KIFE154	0.019	100.12	0.25	0.03	118	5	7.6	1.6	17.3	11.5	9.4	23.9	2	23.9	0.7	16.5	2.1
KIFE155	0.011	99.97	0.78	<0.02	320	3	19.7	5	16.4	8.8	8	65.8	2	142.6	0.6	18	1.4
KIFE156	0.003	100.25	0.18	<0.02	122	<1	3.7	1.8	6.8	5.1	4.9	30.3	<1	39.8	0.4	5.8	0.7
KIFE157	0.008	100.16	0.2	<0.02	103	2	6.2	0.8	11	7.6	6	15.7	<1	21.4	0.4	8	2
KIFE158	0.045	100.24	0.34	0.05	343	<1	0.6	0.2	20.9	4.6	9	17.1	3	9	0.8	49.3	1.9
KIFE159	0.015	100.2	0.27	0.04	35	3	12.1	0.7	12.7	5.3	4.2	5.6	<1	8.1	0.3	28.5	5.9
KIFE160	0.016	99.71	0.14	<0.02	101	2	4.9	1	15.1	7.3	8	15.8	1	24.3	0.5	16	1.5
KIFE161	0.008	100.01	0.39	0.02	369	3	2.4	3.7	16	4	9.3	113.6	3	16.8	0.7	14.2	2.6
KIFE165	0.008	99.43	0.42	0.03	23	1	2.5	0.6	10.7	11.4	4.8	6.9	1	11.3	0.4	7.8	1.5
KIFE166	x	x	x	x	x	x	x	x	x	x	x	x	x	x	x	x	x
KIFE167	0.023	99.71	0.52	0.04	36	2	3.1	1.2	20.3	7.5	7.5	11.4	2	17.4	0.5	14	2
KIFE168	0.011	99.99	0.87	0.04	69	2	8.9	0.9	13.5	7.7	4.8	10.4	1	12.4	0.4	6.1	0.7
KIFE169	x	x	x	x	x	x	x	x	x	x	x	x	x	x	x	x	x
KIFE170	0.017	99.92	0.18	0.08	40	2	2.7	1.1	26.3	5.3	10.5	6	3	3.7	0.8	59.9	3.4
KIFE171	0.022	99.57	0.18	0.06	14	<1	1.3	0.2	66.6	19.4	32.6	2.2	8	11.3	2.6	106.2	4.4
KIFE172	0.008	100.21	0.69	0.02	216	<1	1.8	1.8	15.8	11.5	11	48	3	11.8	0.9	20.8	1.9
KIFE173	0.018	100.29	0.27	0.07	34	<1	3.6	1.1	26.7	7.4	7.6	7.5	2	8.3	0.6	60.2	3.9
KIFE174	0.031	100.14	0.18	0.12	74	2	3	1.6	21.5	5	6.5	13.1	2	9.4	0.5	39.3	2.6
KIFE175	0.014	99.72	0.13	0.02	482	3	3.6	3.1	15.8	7.8	8.1	69.3	2	44.2	0.6	43.7	1.9
KIFE176	0.039	99.07	0.2	0.06	80	2	5.5	1.9	34	11.3	9.8	15.8	3	12.8	0.7	93.3	6.8
KIFE177	0.023	99.27	0.24	0.06	25	<1	2.5	1	23.7	9.8	8	5.3	2	5.8	0.5	71.5	3.5
KIFE178	0.017	99.26	0.37	0.1	28	3	6.1	1.1	14.7	6.2	5.6	8.2	1	12	0.4	14.8	3
KIFE179	0.021	99.1	0.29	0.04	44	2	6.7	1.5	25.5	9.1	9.9	12.7	2	17.1	0.7	20.7	3.5
KIFE180	0.018	99.87	0.06	0.03	36	3	6.7	0.7	13.4	4.8	5	5.8	1	15	0.3	21.6	2.4
KIFE181	0.009	100.04	0.49	0.02	250	4	8.3	4.9	15.1	10.5	9.8	81.8	2	67.8	0.7	13.3	2
KIFE182	0.015	99.73	0.5	0.04	75	2	6.3	2	18.6	5.9	7.2	18	2	19.9	0.5	9	1.7
KIFE183	0.019	99.73	0.26	0.04	36	3	7.2	0.8	12.8	4.9	4	5.4	<1	9	0.4	32.7	4.3

Sample	Cr2O3	SUM	TOT/C	TOT/S	Ba	Be	Co	Cs	Ga	Hf	Nb	Rb	Sn	Sr	Ta	Th	U
KIFE184	0.022	99.75	0.2	0.07	117	<1	2.5	1.3	22.6	7.1	6.4	13.4	2	10.5	0.5	65.2	4.5
KIFE185	0.032	100.74	0.17	0.05	73	3	7.6	2.3	19	8	7.8	13.5	2	11.4	0.6	27.3	3.2
KIFE186	0.026	99.67	0.18	0.06	44	3	6.8	1.4	30.7	8.3	7.6	11	3	10.3	0.6	85.1	10.1
KIFE187	0.046	99.66	0.24	0.08	79	<1	3.1	1.1	20	39.8	22.2	10.7	3	18.5	1.8	112.5	10.3
KIFE188	0.027	99.67	0.32	0.12	33	1	2.5	1.4	17.1	7.1	5.6	6.3	3	8.7	0.5	49.9	3.6
KIFE189	0.012	100.36	0.17	0.1	40	2	3.9	0.6	8.7	3.4	4.4	4.6	1	5.3	0.4	25.2	3.2
KIFE190	0.026	99.15	0.23	0.05	63	<1	1.3	0.7	17.5	5.8	6.7	11.9	2	2.7	0.6	75.9	1.9
KIFE191	0.025	98.93	0.32	0.05	20	<1	4.6	0.9	37	9.4	10.2	5.6	3	8.3	0.8	47.8	5.7
KIFE192	x	x	x	x	x	x	x	x	x	x	x	x	x	x	x	x	x
KIFE193	x	x	x	x	x	x	x	x	x	x	x	x	x	x	x	x	x
KIFE194	x	x	x	x	x	x	x	x	x	x	x	x	x	x	x	x	x
KIFE195	0.043	99.58	0.19	0.08	187	<1	1.4	0.9	31.8	8.5	8.3	15	3	5.6	0.6	82.5	4.4
KIFE196	0.016	99.17	0.27	0.06	361	1	2.6	0.5	20.3	16.4	17.1	37.5	4	26.2	1.6	76	4.2
KIFE197	0.027	99.79	0.27	0.08	29	2	5.9	1.7	25.2	10.8	10.1	10.3	3	10.4	0.8	46.8	6.3
KIFE198	0.03	99.33	0.38	0.03	108	4	4.6	1.9	24.7	13.1	10.9	19.7	2	17.8	0.9	73.8	5.7
KIFE199	0.041	100.29	0.24	0.06	55	2	2.7	1.2	35.6	10.6	8.8	10.4	3	9.7	0.8	79.5	3.7
KIFE200	0.017	100	0.19	0.07	143	3	4.3	1.1	17.6	7	7.3	20.2	2	9.7	0.6	49.3	6.4
KIFE201	0.011	99.55	0.37	0.09	14	2	4.7	0.6	15	6.3	6.1	4	1	5.9	0.5	25.1	7.9
KIFE202	0.012	99.6	0.17	0.03	142	1	4.2	1.8	14.3	12.1	11.9	26.2	2	21.8	0.9	12.1	2
KIFE203	0.017	99.71	0.25	0.04	141	3	6.3	1.7	16.6	13.2	10	23.7	2	21	0.9	15.9	2.5
KIFE204	0.003	100.25	0.24	0.02	119	11	5	1.1	6.5	5.6	6.6	19.2	<1	16.8	0.5	7.3	1.2
Sample	Cr2O3	SUM	TOT/C	TOT/S	Ba	Be	Co	Cs	Ga	Hf	Nb	Rb	Sn	Sr	Ta	Th	U
Mean	0.0259338	99.793245	0.28615894	0.06698413	129.45033	2.95	3.7860927	1.380132	21.778146	8.870861	8.870199	20.084768	2.259843	17.982119	0.704636	45.61656	3.429139
Median	0.024	99.76	0.25	0.06	80	3	3.1	1.2	21.1	8.2	8.2	13.4	2	12.9	0.6	36.4	3.2
Minimum	0.003	98.86	0.02	0.02	9	1	0.3	0.2	3.8	2.3	3.6	2.2	1	2.7	0.2	4.8	0.6
Maximum	0.091	100.74	0.87	0.16	794	11	19.7	5.8	66.6	39.8	32.6	113.6	8	142.6	2.6	159.5	10.3
Standard Deviation	0.0129309	0.3647932	0.160149351	0.03551382	137.08565	1.895364	2.7013093	0.873462	8.9765979	4.237697	3.923617	19.188086	1.142349	15.756739	0.361541	33.54895	1.781445

Sample Method	V ppm	W ppm	Zr ppm	Y ppm	La ppm	Ce ppm	Pr ppm	Nd ppm	Sm ppm	Eu ppm	Gd ppm	Tb ppm	Dy ppm	Ho ppm	Er ppm	Tm ppm	Yb ppm	Lu ppm
	4B	4B	4B	4B	4B	4B	4B	4B	4B	4B	4B	4B	4B	4B	4B	4B	4B	4B
Dect. Limit	8	0.5	0.1	0.1	0.1	0.1	0.02	0.3	0.05	0.02	0.05	0.01	0.05	0.02	0.03	0.01	0.05	0.01
KIFE001	43	<0.5	133.9	3.7	5	10.2	1.09	3.3	0.84	0.26	0.8	0.15	0.77	0.14	0.51	0.1	0.59	0.11
KIFE002	392	1.1	185.1	7.3	16.4	16.4	1.98	8.6	1.82	0.44	1.69	0.32	1.51	0.39	1.11	0.15	1.16	0.17
KIFE003	676	<0.5	206.7	11.8	14.5	17.7	3.19	13.7	2.17	0.47	2.09	0.32	2.13	0.43	1.01	0.16	1.14	0.16
KIFE004	312	1	326.7	11.5	11.9	23.4	2.49	10.2	1.75	0.33	1.72	0.31	1.99	0.49	1.54	0.22	1.68	0.23
KIFE005	181	0.9	400.1	6.5	4.1	36	0.84	3	0.63	0.11	0.64	0.13	1.04	0.2	0.75	0.11	1.07	0.14
KIFE006	201	<0.5	250.1	6	5.3	14	1.21	5.5	0.98	0.26	1.09	0.21	1.18	0.25	0.85	0.11	0.96	0.12
KIFE007	394	1	228.2	9	10.9	19.3	2.06	7.9	1.72	0.44	1.6	0.32	2.24	0.39	1.25	0.21	1.78	0.18
KIFE008	426	1.2	216.4	7	9.6	16.4	1.63	4.1	1.29	0.19	0.87	0.17	1.3	0.22	0.89	0.1	0.8	0.11
KIFE009	246	1.5	438.2	6.7	4.4	10.7	0.76	2	0.73	0.14	0.73	0.15	1.17	0.22	0.89	0.1	1	0.15
KIFE010	300	1.1	733	11.5	50.8	110.4	9.94	34	5.79	0.96	4.18	0.74	3.8	0.64	1.7	0.22	2.06	0.29
KIFE011	476	1	341.4	7	17.1	35.8	3.26	10.1	1.88	0.34	1.37	0.26	1.55	0.34	1.04	0.14	1.27	0.18
KIFE012	194	0.9	521.7	6.9	5.1	10.2	1.05	4	0.73	0.15	0.77	0.14	1.25	0.27	0.95	0.12	0.99	0.14
KIFE013	235	1.3	316.5	8.2	7.5	16.4	1.42	4.7	1.13	0.19	1.11	0.2	1.28	0.4	1.07	0.15	1.4	0.21
KIFE014	288	1.1	288.9	8.9	11.1	21.5	2.46	7.7	1.78	0.32	1.52	0.28	1.78	0.36	1.09	0.16	1.4	0.16
KIFE015	256	1.7	501.5	12	10.7	24.3	2.23	9.1	1.45	0.26	1.6	0.3	1.9	0.39	1.4	0.22	1.97	0.26
KIFE016	406	1.3	499.4	10.2	8.3	16.8	1.76	5.9	1.21	0.22	1.44	0.25	1.49	0.38	1.1	0.15	1.1	0.19
KIFE017	422	1.9	391.3	9.7	10.7	23.7	2.25	9.2	1.48	0.28	1.58	0.27	1.84	0.32	1.33	0.14	1.27	0.2
KIFE018	117	1.2	207.9	13.5	15.7	23.9	2.8	10.6	2.05	0.38	1.72	0.3	1.88	0.45	1.49	0.2	1.48	0.22
KIFE019	83	0.5	187.8	10	37.1	57.7	7.79	26.2	4.5	0.86	3.03	0.49	2.52	0.41	1.2	0.13	1.07	0.12
KIFE020	111	0.9	117.9	6.5	17.6	26.6	2.64	9.1	1.34	0.29	1.07	0.19	1.65	0.23	0.74	0.09	0.74	0.09
KIFE021	258	1.7	548.7	17.5	15.5	34.2	3.32	9.3	2.07	0.38	2.17	0.42	3.12	0.61	2.06	0.28	2.19	0.35
KIFE022	182	1.4	202	6.2	18.1	32.3	3.6	12.7	2.16	0.31	1.36	0.18	1.6	0.21	0.75	0.1	1.05	0.12
KIFE023	627	0.8	277.8	6.1	4.2	8.4	0.89	2.5	0.75	0.15	0.91	0.16	0.86	0.23	0.87	0.1	0.87	0.11
KIFE024	621	1	202.5	11.5	10	21.9	2.34	9.7	1.64	0.28	1.67	0.28	1.87	0.45	1.52	0.19	1.31	0.19
KIFE025	460	1.2	362.5	11.4	12.7	25.1	2.81	10.5	2.13	0.42	2.06	0.33	1.97	0.46	1.39	0.22	1.49	0.2
KIFE026	422	1.1	472.4	14.9	14.1	31.2	3.08	10.1	2.24	0.38	2.01	0.39	2.36	0.52	1.66	0.25	1.58	0.3
KIFE027	392	0.5	465.9	14.5	14.3	29	3.01	13.8	2.27	0.42	2.17	0.37	2.63	0.56	1.88	0.25	1.58	0.3
KIFE028	505	1.3	217.5	9.2	8.4	15.6	2.09	9.3	1.86	0.39	1.57	0.26	1.92	0.35	0.99	0.16	1.27	0.18
KIFE029	561	1.6	314.1	7.5	7.3	12.3	1.13	4.4	0.97	0.17	0.96	0.17	1.33	0.35	1.01	0.11	0.9	0.14
KIFE030	448	1.9	366.8	10.5	11.9	21	2.22	8.8	1.82	0.31	1.52	0.3	1.81	0.42	1.55	0.18	1.51	0.2
KIFE031	400	1.4	391.4	10.4	9.9	19.6	2.14	7.3	1.41	0.22	1.44	0.26	1.5	0.47	1.26	0.18	1.16	0.19
KIFE032	432	1.3	378.1	11.4	8.7	18.8	1.94	6.1	1.36	0.27	1.36	0.26	1.64	0.37	1.44	0.16	1.3	0.2
KIFE033	322	0.8	476.9	7.5	9.2	127.4	1.43	4.1	0.99	0.17	0.92	0.19	1.16	0.29	0.98	0.12	0.88	0.14
KIFE034	395	0.9	265.6	8.8	8.3	14.9	1.39	3.1	0.97	0.15	0.96	0.21	1.32	0.34	1.2	0.16	1.21	0.15
KIFE035	464	1.1	130.4	2.9	4.4	8.1	0.63	2.6	0.39	0.11	0.43	0.09	0.54	0.14	0.44	0.07	0.54	0.07
KIFE036	224	1.2	254.5	5.5	3.4	10.9	0.86	3.2	0.9	0.22	0.91	0.18	1.07	0.27	0.68	0.15	0.8	0.16
KIFE037	195	0.9	205	5.5	7	13.5	1.41	5.3	0.73	0.18	1.03	0.16	0.86	0.18	0.79	0.12	0.71	0.13
KIFE038	293	0.7	241.2	5	4.6	10.2	1.06	4.3	1.17	0.22	0.82	0.19	1.3	0.23	0.71	0.14	0.85	0.13
KIFE039	343	1.2	381.5	6.5	5.4	35	1.11	5.1	0.83	0.21	1.06	0.17	1.34	0.22	0.67	0.14	0.88	0.13
KIFE040	253	1.4	434.5	5.7	5.4	36.9	1.15	3.3	0.82	0.21	1.05	0.17	0.89	0.24	0.63	0.1	0.74	0.14
KIFE041	347	1	306.9	4.2	16	31.6	2.62	6.6	1.11	0.21	0.99	0.16	0.87	0.19	0.61	0.1	0.64	0.11
KIFE042	303	1.3	278.1	4.4	3.6	7.8	0.77	2.2	0.72	0.17	0.6	0.14	0.93	0.21	0.62	0.09	0.78	0.11
KIFE043	210	0.9	280.1	6.3	5.9	13.8	1.28	4.7	0.99	0.22	0.95	0.2	1.2	0.25	0.73	0.12	0.95	0.14

Sample	V	W	Zr	Y	La	Ce	Pr	Nd	Sm	Eu	Gd	Tb	Dy	Ho	Er	Tm	Yb	Lu
KIFE044	438	1.1	294.7	4.1	9.8	19.8	1.72	4.1	0.76	0.15	0.66	0.13	0.79	0.2	0.66	0.11	0.69	0.11
KIFE045	598	0.9	288.9	4.2	1.6	5.2	0.36	1.9	0.31	0.09	0.37	0.08	0.63	0.15	0.55	0.08	0.63	0.09
KIFE046	266	0.7	213.9	10.3	6.1	31.3	2.43	11.7	3.34	0.68	2.42	0.5	3.05	0.66	1.79	0.31	2.07	0.31
KIFE047	175	0.9	247.1	7.7	23.1	37.9	2.56	8.9	1.67	0.33	1.6	0.26	1.68	0.35	0.96	0.14	1.06	0.15
KIFE048	303	1	246.7	7.6	3.7	10.9	0.68	2	0.6	0.13	0.82	0.17	1.2	0.35	0.83	0.04	1.13	0.17
KIFE049	401	1.2	254.4	4.1	11.3	23.2	1.87	6.6	1.17	0.19	0.86	0.15	0.92	0.21	0.64	0.09	0.82	0.1
KIFE050	247	0.7	247.7	4.1	2.7	6.3	0.65	1.6	0.55	0.11	0.61	0.12	0.86	0.21	0.55	0.1	0.69	0.1
KIFE051	479	1.2	332.4	5.4	5.3	10.1	0.8	3	0.6	0.1	0.59	0.11	0.87	0.21	0.61	0.12	0.8	0.12
KIFE052	461	1.1	274.1	4.9	3.5	9.2	0.59	2.6	0.43	0.14	0.54	0.11	0.91	0.24	0.68	0.1	0.72	0.09
KIFE053	352	1.1	319.7	5.9	14.6	29.7	2.99	11.3	1.74	0.31	1.24	0.2	1.2	0.23	0.69	0.11	0.86	0.15
KIFE054	117	0.9	170.2	4.1	9.4	15.2	1.05	2.7	0.58	0.12	0.73	0.11	0.71	0.19	0.36	0.07	0.68	0.09
KIFE055	383	1.6	217.5	4.2	3.2	10.2	0.84	3.5	0.71	0.16	0.71	0.15	0.93	0.2	0.64	0.09	0.89	0.12
KIFE056	331	1.2	277.2	3.9	6.3	9.9	0.89	2.8	0.43	0.06	0.47	0.08	0.62	0.15	0.44	0.07	0.51	0.08
KIFE057	363	1.1	262.9	6.3	3.9	9.4	0.82	3.8	0.59	0.17	0.65	0.15	1.15	0.32	0.68	0.12	0.83	0.13
KIFE058	382	1.3	523.3	4.1	4.9	10.2	0.97	2.9	0.74	0.14	0.52	0.11	0.96	0.17	0.53	0.09	0.63	0.14
KIFE059	347	1.2	234.3	4.6	8.5	19.1	1.83	4.6	1.52	0.23	0.96	0.17	0.96	0.24	0.67	0.1	0.73	0.09
KIFE060	301	1.9	428.3	7.9	9.5	20.7	1.83	5.3	1.19	0.23	1.12	0.21	1.24	0.32	0.85	0.17	1.09	0.19
KIFE061	446	1	304.3	4.4	3.3	7.3	0.68	2.3	0.59	0.11	0.68	0.11	0.59	0.15	0.6	0.08	0.66	0.09
KIFE062	401	1.5	312.6	5.2	4.7	11.4	1.17	4.7	0.99	0.23	0.84	0.18	1.2	0.22	0.77	0.11	0.88	0.11
KIFE063	128	1.2	624.9	8.8	26.4	51.7	4.03	11	1.74	0.25	1.5	0.22	1.2	0.25	1.1	0.18	1.38	0.23
KIFE064	421	2.1	309.3	8.3	5.2	21.3	1.07	3.7	0.82	0.21	1.03	0.22	1.55	0.36	1.02	0.17	1.09	0.17
KIFE065	193	1.6	378	12	7.6	39	1.78	5.9	1.45	0.34	1.79	0.33	2.1	0.51	1.67	0.23	1.81	0.24
KIFE066	371	1	235.2	5.2	6.4	12.9	1.33	5.4	1.17	0.26	1.03	0.17	1.2	0.24	0.67	0.12	0.85	0.13
KIFE067	435	1.2	269.4	7.1	5.1	10	1.1	4.7	0.94	0.24	0.93	0.19	1.38	0.29	0.88	0.14	1.06	0.15
KIFE068	443	1.7	374.8	8.2	5.7	17.1	1.52	6.2	1.44	0.27	1.21	0.22	1.4	0.32	0.81	0.15	1.18	0.17
KIFE069	431	1.5	452.3	9.7	9.1	20.5	2.16	6.3	1.63	0.27	1.36	0.28	1.49	0.41	1.24	0.2	1.43	0.25
KIFE070	535	3.8	422.4	13.5	9.5	17.9	2.19	9.4	1.42	0.32	1.58	0.32	2.26	0.55	1.45	0.26	1.83	0.29
KIFE071	153	3	205.6	4.9	4.9	8.8	0.99	3.7	0.76	0.15	0.64	0.14	0.98	0.24	0.55	0.1	0.88	0.12
KIFE072	350	2.2	414	10.1	8.7	17.1	1.96	8	1.52	0.28	1.34	0.3	1.73	0.46	1.31	0.22	1.39	0.23
KIFE073	468	1.9	278.9	9.7	10.1	24.7	2.71	9	2.16	0.44	2.09	0.35	1.76	0.37	1.28	0.2	1.41	0.18
KIFE100	318	0.7	276.1	4.1	4.2	6.9	0.79	3	0.66	0.15	0.6	0.12	0.71	0.24	0.7	0.08	0.56	0.1
KIFE101	401	0.8	268.7	6.1	5.3	21.2	1.35	5.7	1.24	0.3	1.13	0.22	1.2	0.3	0.76	0.14	0.87	0.16
KIFE102	136	2.3	326.3	10.9	5.5	9.2	1.07	4	0.95	0.26	1.21	0.25	1.75	0.37	1.29	0.2	1.36	0.24
KIFE103	24	1.4	93.3	6.2	4.6	7.2	0.69	1.8	0.47	0.19	0.59	0.12	0.87	0.26	0.54	0.12	1.01	0.14
KIFE104	458	0.9	108.7	6.2	13.8	22.6	2.62	8.9	1.68	0.39	1.23	0.23	1.34	0.25	0.75	0.14	0.98	0.12
KIFE105	58	0.6	79.5	3.6	3.4	9.9	1.16	5.8	1.15	0.28	0.94	0.16	1	0.2	0.45	0.1	0.49	0.12
KIFE106	330	1.7	411.6	18.9	25.1	50	5.34	20.2	3.42	0.63	3.4	0.56	3.13	0.7	2.06	0.35	2.32	0.35
KIFE107	105	1	288.8	26.5	54.5	106.8	11.13	36.9	6.51	1.2	5.09	0.81	4.41	1	2.56	0.42	2.37	0.41
KIFE108	350	1.3	427.2	12	11.9	23.1	2.66	9	1.78	0.33	1.71	0.32	1.83	0.49	1.4	0.24	1.5	0.28
KIFE109	324	0.9	301.6	16	13.8	28	3.13	10	2.31	0.43	2.14	0.43	2.77	0.64	2.11	0.3	2.16	0.33
KIFE110	242	0.5	244.2	9.1	6.8	14.4	1.97	8.5	1.97	0.46	1.68	0.33	1.58	0.38	1.11	0.22	1.22	0.19
KIFE111	218	0.6	317.5	14.8	7.2	28.6	3.38	13	4.2	1.01	3.61	0.69	4.07	0.81	2.18	0.38	2.49	0.38
KIFE112	409	1.6	346	6.9	3.5	13.1	0.87	2.8	0.96	0.17	0.71	0.13	1.19	0.29	0.86	0.15	1.02	0.16
KIFE113	238	1.4	284.4	5.9	4.7	13.6	0.91	3.1	0.7	0.18	0.6	0.13	0.85	0.21	0.8	0.1	0.69	0.12
KIFE114	279	3.5	293.2	6.8	3	7.9	0.62	2.8	0.54	0.15	0.52	0.15	0.99	0.26	0.76	0.14	1.04	0.16
KIFE115	420	2.4	109.2	11.9	4.2	6.4	0.67	1.6	0.51	0.14	0.67	0.2	1.59	0.41	1.35	0.25	1.45	0.25

Sample	V	W	Zr	Y	La	Ce	Pr	Nd	Sm	Eu	Gd	Tb	Dy	Ho	Er	Tm	Yb	Lu
KIFE116	252	2.1	372.7	8.7	4.8	17.3	1	2.8	0.98	0.24	0.97	0.21	1.55	0.32	1.16	0.21	1.55	0.25
KIFE117	467	1.7	342.9	7.2	15.3	31	2.98	10.4	1.9	0.4	1.76	0.28	1.66	0.37	1.03	0.17	1.08	0.17
KIFE118	445	1.3	212.2	4.5	5.9	9.7	0.91	3.2	0.76	0.19	0.67	0.14	0.86	0.2	0.61	0.08	0.73	0.13
KIFE119	1055	1.3	281.3	10.5	8.4	18.3	2.05	6.7	1.69	0.23	1.37	0.25	1.91	0.34	1.13	0.15	1.41	0.18
KIFE120	38	0.9	184.8	14.7	24	39.4	3.8	13.9	2.44	0.49	2.27	0.4	2.5	0.51	1.65	0.24	1.08	0.21
KIFE121	95	1.7	300.7	28.4	30.4	37.7	3.55	11.2	2.3	0.58	3.25	0.64	4.78	1.12	3.3	0.47	3.06	0.46
KIFE122	43	1.2	153.5	12.8	11.3	18.5	1.99	6.1	1.55	0.44	1.82	0.33	2.2	0.45	1.43	0.2	1.34	0.19
KIFE123	141	1.5	262.4	14.4	10.1	16.9	1.99	9.4	1.57	0.39	1.87	0.35	2.2	0.59	1.4	0.25	1.68	0.29
KIFE124	230	1.2	145.7	7.9	4.6	7.8	1.13	4.1	0.89	0.22	1.05	0.22	1.2	0.3	0.94	0.16	1.01	0.16
KIFE125	292	1.1	199.8	6.4	3.8	11.1	0.91	3.2	0.76	0.2	0.92	0.19	1.31	0.27	0.8	0.13	0.78	0.13
KIFE126	55	1.1	210.8	6.6	7.3	9.4	0.93	2.3	0.9	0.13	0.8	0.17	1.06	0.26	0.82	0.1	0.88	0.15
KIFE127	170	3.5	373.9	12.1	9.2	17.6	1.96	7.7	1.38	0.23	1.36	0.23	1.72	0.44	1.37	0.26	1.96	0.27
KIFE128	52	1.5	327.7	5.3	7.8	12.4	1.2	3.6	0.74	0.14	0.73	0.12	0.8	0.22	0.76	0.11	0.86	0.14
KIFE129	83	1.1	843	10.4	19.7	26.9	2.48	8.1	1.31	0.21	1.25	0.21	1.59	0.38	1.21	0.2	1.38	0.23
KIFE130	90	1.3	579.4	9.8	13.8	20.5	2.08	6.8	1.36	0.18	1.53	0.26	1.78	0.39	1.3	0.19	1.37	0.22
KIFE131	352	1.6	495.4	9.6	6.2	16.9	1.35	4.6	1	0.2	1.06	0.21	1.57	0.33	0.97	0.18	1.24	0.22
KIFE150	206	1	274.8	9.1	7.1	13.1	1.45	5.1	0.93	0.21	0.99	0.2	1.34	0.31	0.98	0.16	1.08	0.18
KIFE151	413	1.6	486.6	12.4	14.3	24	2.7	9.5	1.78	0.35	1.75	0.32	2.08	0.44	1.44	0.23	1.58	0.26
KIFE153	251	1.2	439.1	19.7	31	57.3	6.33	22.8	3.94	0.7	3.39	0.55	3.25	0.69	2	0.33	2.01	0.34
KIFE154	302	1.2	448.6	10.9	10.7	21.2	2.42	8.6	1.65	0.32	1.56	0.28	1.81	0.38	1.23	0.21	1.4	0.23
KIFE155	86	1.1	351.7	25.7	19.1	44.4	4.92	19.3	4.71	0.99	4.73	0.87	5.44	1.13	3.47	0.54	3.39	0.56
KIFE156	45	0.5	204.9	16.4	12.3	23.7	3.25	12.8	2.51	0.53	2.37	0.42	2.7	0.57	1.77	0.28	1.71	0.28
KIFE157	274	1	309.4	10	11.1	21.7	2.73	10.1	1.98	0.34	1.7	0.3	1.77	0.37	1.19	0.19	1.3	0.2
KIFE158	287	2.4	176.9	11	1.5	2	0.27	1.2	0.32	0.1	0.65	0.17	1.52	0.4	1.24	0.2	1.49	0.23
KIFE159	220	0.7	187.2	11.5	11	32.4	2.89	11.1	2.21	0.46	2.06	0.37	2.23	0.47	1.26	0.2	1.32	0.21
KIFE160	473	1.4	305.8	10.2	11.7	23.6	3.1	11.3	2.29	0.48	1.86	0.33	2	0.41	1.26	0.21	1.33	0.22
KIFE161	90	1.5	140.4	7.5	17	31.3	3.63	13.1	2.44	0.49	1.91	0.26	1.54	0.29	0.83	0.14	1	0.15
KIFE165	81	0.8	444.6	6.8	5.8	13.7	1.39	5.2	1.28	0.28	1.14	0.22	1.42	0.27	0.8	0.15	1	0.17
KIFE166	x	x	x	x	x	x	x	x	x	x	x	x	x	x	x	x	x	x
KIFE167	172	0.9	284.1	5.5	5.3	9.8	0.93	3.2	0.66	0.13	0.67	0.13	0.92	0.19	0.64	0.1	0.73	0.13
KIFE168	145	0.8	310.7	8.1	5.7	10.3	1.47	6.1	1.37	0.3	1.3	0.25	1.58	0.33	1.06	0.18	1.19	0.19
KIFE169	x	x	x	x	x	x	x	x	x	x	x	x	x	x	x	x	x	x
KIFE170	276	1.3	211.4	3.8	2.3	4.7	0.51	2.1	0.55	0.12	0.49	0.1	0.64	0.15	0.51	0.08	0.56	0.09
KIFE171	183	4.9	691.7	14.9	4	8.9	0.89	3.6	0.92	0.24	1.14	0.29	2.21	0.55	1.84	0.33	2.5	0.41
KIFE172	94	1.6	447.4	18.2	22	40.7	4.49	15	2.84	0.61	2.76	0.49	3.13	0.62	1.88	0.29	1.88	0.29
KIFE173	501	1.1	274	6.8	4.6	9.7	1.09	4.1	0.99	0.23	0.88	0.17	1.18	0.25	0.81	0.12	0.89	0.15
KIFE174	553	0.9	195.1	5.4	7.7	10.5	1.34	4.5	0.89	0.2	0.81	0.13	0.91	0.17	0.59	0.1	0.69	0.11
KIFE175	175	0.9	310.1	5.9	17.7	23.8	2.46	7.1	1.21	0.29	1.07	0.2	1.19	0.23	0.67	0.12	0.83	0.14
KIFE176	514	1.6	417.2	10.2	10.4	27.1	2.02	6.9	1.49	0.32	1.51	0.28	1.89	0.42	1.31	0.2	1.53	0.26
KIFE177	362	1.2	368.7	4.7	3.1	10.6	0.69	2.5	0.51	0.13	0.59	0.11	0.75	0.18	0.61	0.1	0.75	0.12
KIFE178	263	0.8	224.1	8	5.1	11.6	1.57	6.4	1.7	0.41	1.57	0.32	1.87	0.37	1.14	0.19	1.39	0.2
KIFE179	274	1.6	349	10.1	7.3	15.8	1.56	5.8	1.13	0.25	1.25	0.24	1.7	0.35	1.19	0.2	1.32	0.21
KIFE180	412	0.8	182.4	13.2	18	53.2	6.17	23	4.28	0.92	3.32	0.5	2.93	0.56	1.61	0.24	1.56	0.23
KIFE181	89	1.5	427.5	16.9	23.3	45.4	5.15	19.3	3.62	0.76	3.06	0.5	2.98	0.62	1.8	0.28	1.94	0.32
KIFE182	249	1.5	244.8	7.2	8.4	16.1	1.72	6.4	1.25	0.2	1.04	0.2	1.22	0.28	0.82	0.13	0.93	0.15
KIFE183	363	0.7	166.5	7.4	7.1	21.6	1.83	7.1	1.5	0.35	1.47	0.25	1.62	0.33	0.9	0.15	0.96	0.16

Sample	V	W	Zr	Y	La	Ce	Pr	Nd	Sm	Eu	Gd	Tb	Dy	Ho	Er	Tm	Yb	Lu
KIFE184	516	1	244.6	7.3	10.8	25.3	1.78	6	1.19	0.27	1.18	0.2	1.3	0.29	0.85	0.13	0.96	0.14
KIFE185	434	1.2	307.5	8.8	7.9	20.1	1.97	7.8	1.61	0.3	1.41	0.25	1.52	0.31	1.06	0.18	1.1	0.19
KIFE186	387	1.1	283.5	11.1	9.6	33.5	2.45	9.3	2.06	0.46	1.81	0.34	2.19	0.49	1.44	0.23	1.65	0.25
KIFE187	503	1.6	1502.3	10.3	16.9	31.9	3.46	11.9	1.97	0.31	1.64	0.28	1.89	0.43	1.36	0.26	1.9	0.33
KIFE188	556	3.5	250.4	4.3	7.3	10.9	1.17	4.2	0.87	0.19	0.7	0.13	0.85	0.17	0.53	0.1	0.69	0.11
KIFE189	197	0.6	133	7.9	8.4	15.8	1.77	6.4	1.36	0.29	1.15	0.22	1.43	0.31	0.92	0.16	1.05	0.15
KIFE190	191	0.8	200.6	4.7	1	3.3	0.25	1	0.21	0.06	0.28	0.08	0.58	0.16	0.54	0.09	0.61	0.1
KIFE191	332	1.5	334.6	5.2	3.4	13.2	0.78	3.2	0.68	0.16	0.73	0.14	0.94	0.23	0.61	0.12	0.89	0.14
KIFE192	x	x	x	x	x	x	x	x	x	x	x	x	x	x	x	x	x	x
KIFE193	x	x	x	x	x	x	x	x	x	x	x	x	x	x	x	x	x	x
KIFE194	x	x	x	x	x	x	x	x	x	x	x	x	x	x	x	x	x	x
KIFE195	523	1.4	281.9	4.3	3.3	6.5	0.71	2.7	0.65	0.16	0.56	0.11	0.75	0.17	0.49	0.08	0.54	0.1
KIFE196	204	1.4	617	30.6	21.6	39.6	4.56	16.2	3.21	0.66	3.6	0.71	5.1	1.07	3.17	0.51	3.31	0.49
KIFE197	290	1.4	370.8	13.1	8.2	28.7	2.19	8.1	1.97	0.46	1.92	0.36	2.39	0.5	1.45	0.27	1.77	0.26
KIFE198	350	1.2	481.9	9	11.5	33.8	2.4	8.6	1.78	0.36	1.6	0.27	1.79	0.37	1.11	0.19	1.39	0.22
KIFE199	504	1.4	370.5	7.1	4.4	10.1	1.01	3.8	0.91	0.21	0.91	0.19	1.24	0.28	0.84	0.14	1.02	0.16
KIFE200	312	1.2	259.1	4.6	4.1	8.2	0.87	3.5	0.75	0.18	0.69	0.13	0.88	0.2	0.57	0.1	0.79	0.12
KIFE201	603	0.9	243	6.6	5.2	12.5	1.63	6.5	1.54	0.34	1.25	0.24	1.45	0.29	0.87	0.15	1.03	0.16
KIFE202	287	1.6	477.9	13.3	10.9	21.1	2.48	8.9	1.73	0.32	1.61	0.32	2.06	0.46	1.47	0.25	1.65	0.28
KIFE203	322	1.9	525.2	19.1	11.7	22.9	2.64	9.5	1.98	0.34	2.08	0.39	2.67	0.65	2.08	0.35	2.37	0.37
KIFE204	135	0.8	237.4	6.5	6.1	11.8	1.29	4.9	0.96	0.23	0.98	0.18	1.08	0.23	0.7	0.12	0.86	0.14

Sample	V	W	Zr	Y	La	Ce	Pr	Nd	Sm	Eu	Gd	Tb	Dy	Ho	Er	Tm	Yb	Lu
Mean	313.2715	1.322297	323.3146	9.40132	10.05894	21.89801	2.06457	7.380132	1.4972848	0.30543	1.3912583	0.256159	1.645467	0.360861	1.1013245	0.1735099	1.2291391	0.19
Median	312	1.2	288.9	7.9	8.2	17.7	1.77	6.1	1.29	0.26	1.18	0.22	1.495	0.32	0.98	0.15	1.08	0.17
Minimum	24	0.5	79.5	2.9	1	2	0.25	1	0.21	0.06	0.28	0.08	0.54	0.14	0.36	0.07	0.49	0.07
Maximum	1055	4.9	1502.3	30.6	54.5	127.4	11.13	36.9	6.51	1.2	5.09	0.87	5.44	1.13	3.47	0.54	3.39	0.56
Standard Deviation	159.2509	0.634262	159.9127	4.7907	7.96336	17.52884	1.58231	5.567489	1.0036725	0.194435	0.8326242	0.142276	0.862973	0.181655	0.5353001	0.0845789	0.5362785	0.0853698

Sample Method	MnO % 4X	Ba % 4X	Ag ppm 1DX	Cd ppm 1DX	Se ppm 1DX	Tl ppm 1DX	Hg ppm 1DX	Bi ppm 1DX	Sb ppm 1DX	Au ppb 1DX	As ppm 1DX	Ni ppm 1DX	Zn ppm 1DX	Pb ppm 1DX	Cu ppm 1DX	Mn ppm 1DX
Dect. Limit	0.1	0.1	0.1	0.1	0.5	0.1	0.01	0.1	0.1	0.5	0.5	0.1	1	0.1	0.1	0.1
KIFE001	<0.01	0.02	<0.1	<0.1	0.8	<0.1	<0.01	<0.1	0.2	1.9	9.2	2.6	3	8	2.5	6.1
KIFE002	0.02	0.01	<0.1	<0.1	1.4	<0.1	0.02	0.1	2.5	15.2	175.2	16.2	6	20.3	12.7	2.6
KIFE003	<0.01	0.06	<0.1	<0.1	1.2	<0.1	<0.01	<0.1	<0.1	487.8	10.2	10.4	3	17.7	14	0.7
KIFE004	<0.01	<0.01	<0.1	<0.1	<0.5	<0.1	0.08	0.5	0.1	9.6	29.5	13.4	1	44	1	3.8
KIFE005	<0.01	<0.01	<0.1	<0.1	<0.5	<0.1	0.08	0.3	0.2	61.6	30.6	9.1	1	7.6	0.3	2.9
KIFE006	<0.01	<0.01	<0.1	<0.1	1.2	<0.1	0.12	0.2	0.1	6.1	19.3	13.7	<1	22.5	1.2	1.8
KIFE007	<0.01	<0.01	<0.1	<0.1	1.2	<0.1	0.08	0.5	0.3	2.5	67	15.5	<1	45.8	0.7	4.7
KIFE008	<0.01	<0.01	<0.1	<0.1	2.7	<0.1	0.03	0.4	0.1	1.9	38.3	4.8	2	53.7	0.3	1.6
KIFE009	<0.01	<0.01	<0.1	<0.1	<0.5	<0.1	0.02	0.4	0.2	1.7	14	4.4	7	11.1	0.3	2.3
KIFE010	0.01	0.04	<0.1	<0.1	0.6	<0.1	<0.01	0.4	0.3	1.1	8.3	3.4	2	39.5	1.1	1.1
KIFE011	<0.01	0.01	<0.1	<0.1	0.5	<0.1	0.02	0.7	0.4	6.9	30.6	3.8	<1	25.5	0.7	4.4
KIFE012	<0.01	<0.01	<0.1	<0.1	0.5	<0.1	<0.01	0.2	<0.1	1.6	9.2	18.2	1	9.4	0.8	2.1
KIFE013	<0.01	<0.01	<0.1	<0.1	<0.5	<0.1	0.07	0.4	0.1	13.4	32.2	15.1	<1	16.9	0.7	4.3
KIFE014	<0.01	0.03	<0.1	<0.1	<0.5	<0.1	<0.01	0.5	0.6	1.1	24.7	11.8	6	60.1	1.1	3.4
KIFE015	<0.01	0.02	<0.1	<0.1	0.7	<0.1	0.04	0.4	0.2	8.3	22.9	10.3	1	29.8	0.7	3.8
KIFE016	<0.01	<0.01	<0.1	<0.1	<0.5	<0.1	<0.01	0.7	0.3	1	14.3	9.8	2	36.9	0.7	4.2
KIFE017	<0.01	0.01	<0.1	<0.1	<0.5	<0.1	0.02	0.8	0.3	3.7	23.3	8.7	1	44	0.6	4.2
KIFE018	<0.01	0.03	<0.1	<0.1	2.1	<0.1	<0.01	0.3	0.1	2.4	10.8	2	<1	19	3.3	1.3
KIFE019	<0.01	0.01	<0.1	<0.1	1.8	<0.1	0.01	9.5	1.2	<0.5	144.4	5.3	135	843.5	225.3	2.4
KIFE020	<0.01	0.02	<0.1	<0.1	4.8	<0.1	0.1	0.3	0.3	1.1	186.2	2.2	33	564.8	1.6	2.1
KIFE021	<0.01	0.01	<0.1	<0.1	<0.5	<0.1	<0.01	0.6	0.2	1.7	14.2	10.6	4	29.8	0.9	2.2
KIFE022	<0.01	0.03	<0.1	<0.1	0.6	<0.1	0.02	0.7	0.2	<0.5	25.7	1.3	4	45	4.5	0.7
KIFE023	0.01	0.03	<0.1	<0.1	<0.5	<0.1	<0.01	1.1	0.8	2.3	24.4	11.5	3	76.7	1.4	3.5
KIFE024	0.01	0.03	<0.1	<0.1	<0.5	<0.1	<0.01	1.5	0.7	0.8	26.5	19.3	5	47.4	1.4	2.5
KIFE025	<0.01	0.01	<0.1	<0.1	<0.5	<0.1	<0.01	0.7	0.5	0.7	32.7	12.9	2	49.8	0.8	4.4
KIFE026	<0.01	0.02	<0.1	<0.1	<0.5	<0.1	0.01	0.6	0.3	1.3	18.2	11.6	2	46.1	0.9	4.6
KIFE027	<0.01	0.02	<0.1	<0.1	<0.5	<0.1	<0.01	0.6	0.3	<0.5	21.8	10.8	2	44.2	0.8	4.3
KIFE028	<0.01	<0.01	<0.1	<0.1	1	<0.1	0.02	0.9	0.3	<0.5	40.9	7.3	1	45.1	0.9	5
KIFE029	<0.01	<0.01	<0.1	<0.1	<0.5	<0.1	<0.01	0.6	0.3	<0.5	16.3	6.5	<1	51.8	0.6	2.8
KIFE030	<0.01	0.01	<0.1	<0.1	<0.5	<0.1	0.03	0.6	0.3	193.7	26.7	9	2	42.3	0.8	5.4
KIFE031	<0.01	0.01	<0.1	<0.1	<0.5	<0.1	0.01	0.6	0.2	<0.5	20.2	11	2	41.6	0.8	4.1
KIFE032	<0.01	0.01	<0.1	<0.1	<0.5	<0.1	<0.01	0.7	0.3	4.9	17.6	9.3	2	18.5	1.3	6.6
KIFE033	0.02	0.02	<0.1	<0.1	0.9	<0.1	0.02	0.7	0.6	12.8	24.4	3.2	<1	39	0.3	2.9
KIFE034	<0.01	<0.01	<0.1	<0.1	0.5	<0.1	0.07	0.7	0.2	0.6	31.9	4.1	<1	50.6	0.4	3.3
KIFE035	<0.01	<0.01	0.2	<0.1	1	<0.1	0.01	0.4	0.2	5	36.4	1.4	3	20.7	0.4	1.7
KIFE036	<0.01	<0.01	<0.1	<0.1	1.3	<0.1	0.1	0.3	0.1	5.4	16.6	5.8	1	11.3	1.1	1.9
KIFE037	<0.01	<0.01	<0.1	<0.1	0.6	<0.1	0.02	0.2	<0.1	2.4	20.9	24	2	35.8	0.8	2.7
KIFE038	<0.01	<0.01	<0.1	<0.1	2.1	<0.1	<0.01	0.3	0.2	<0.5	32.5	8.3	1	24.5	0.7	2.4
KIFE039	<0.01	0.01	<0.1	<0.1	<0.5	<0.1	<0.01	0.7	0.3	<0.5	4	6.1	7	21.2	0.5	2.2
KIFE040	<0.01	0.01	<0.1	<0.1	<0.5	<0.1	<0.01	0.5	0.2	<0.5	1	5.3	2	34.3	0.7	1.1
KIFE041	<0.01	<0.01	<0.1	<0.1	<0.5	<0.1	0.02	0.7	0.2	<0.5	25	4.3	1	22.7	0.5	3.7
KIFE042	<0.01	<0.01	<0.1	<0.1	<0.5	<0.1	0.04	0.5	0.1	<0.5	14.5	5.1	<1	37.7	0.5	2.6
KIFE043	<0.01	0.01	<0.1	<0.1	<0.5	<0.1	0.03	0.4	0.1	<0.5	3.5	14.3	1	37.7	0.7	1.6

Sample	Mo	Cu	Pb	Zn	Ni	As	Au	Sb	Bi	Hg	Tl	Se	Cd	Ag	Ba	MnO
KIFE044	2.1	0.4	20.9	2	2.3	18.1	<0.5	0.2	0.8	0.02	<0.1	<0.5	<0.1	<0.1	0.01	0.01
KIFE045	2.1	5.1	29.1	<1	2.6	47.4	2.5	0.5	2.1	0.02	<0.1	1.9	<0.1	<0.1	<0.01	<0.01
KIFE046	3	0.8	35.6	1	13.3	36.1	<0.5	0.2	0.4	0.14	<0.1	1.5	0.1	<0.1	0.01	<0.01
KIFE047	0.7	6.3	17	5	13.3	7.1	<0.5	0.2	0.2	0.02	0.5	<0.5	<0.1	<0.1	0.02	0.01
KIFE048	2.5	0.7	16.8	<1	3.5	15.8	<0.5	0.2	0.5	0.03	<0.1	1.3	<0.1	<0.1	<0.01	<0.01
KIFE049	2.7	1.9	26.4	<1	4	64.9	3.1	0.4	0.4	0.06	<0.1	1	<0.1	<0.1	<0.01	<0.01
KIFE050	1.6	0.7	19.9	<1	5.5	26.6	<0.5	0.1	0.5	0.13	<0.1	2.5	<0.1	<0.1	<0.01	<0.01
KIFE051	2.7	0.7	18.6	<1	2.9	41.1	<0.5	0.4	1.8	0.05	<0.1	1.6	<0.1	<0.1	0.01	<0.01
KIFE052	2.3	0.7	20	<1	2.9	32.1	<0.5	0.3	1.9	0.01	<0.1	<0.5	<0.1	<0.1	0.02	<0.01
KIFE053	1.3	0.5	22.3	<1	3.4	5.2	1.1	0.3	0.9	<0.01	<0.1	<0.5	<0.1	<0.1	0.02	<0.01
KIFE054	0.5	1.1	13.2	3	4.7	5.9	<0.5	0.1	0.1	<0.01	<0.1	<0.5	<0.1	<0.1	0.02	<0.01
KIFE055	3	0.5	49.2	<1	4.3	22.2	2.2	0.2	0.7	0.02	<0.1	1.3	0.1	<0.1	<0.01	<0.01
KIFE056	1.8	1	33.2	1	2.1	29.6	5.3	0.2	0.4	<0.01	<0.1	0.5	<0.1	<0.1	0.02	<0.01
KIFE057	2.5	0.6	25	<1	3.3	43.1	<0.5	0.3	1	0.03	<0.1	1.7	<0.1	<0.1	0.01	<0.01
KIFE058	2	6.1	28.4	1	3.2	26.7	<0.5	0.4	1.7	<0.01	<0.1	<0.5	<0.1	<0.1	0.01	0.01
KIFE059	2.6	0.6	31.2	<1	2.1	19.9	<0.5	0.1	0.5	0.01	<0.1	<0.5	<0.1	<0.1	0.01	<0.01
KIFE060	1.7	1	25.2	2	5.8	10.2	<0.5	0.2	0.6	<0.01	<0.1	<0.5	<0.1	<0.1	0.01	<0.01
KIFE061	2.4	0.6	20.4	<1	3	30.6	<0.5	0.3	0.9	0.02	<0.1	<0.5	<0.1	<0.1	0.01	<0.01
KIFE062	2.5	0.9	36.8	3	6.2	3.8	<0.5	0.2	0.6	0.03	<0.1	<0.5	<0.1	<0.1	<0.01	<0.01
KIFE063	1	7.1	9.6	<1	2.4	22.2	<0.5	1.1	0.2	0.01	<0.1	1.1	<0.1	<0.1	0.05	0.03
KIFE064	3.1	1.7	35.2	1	6	9.3	<0.5	0.5	0.8	0.04	<0.1	<0.5	<0.1	<0.1	0.01	0.01
KIFE065	2.4	1	12.9	<1	8.9	17.4	<0.5	0.1	0.3	0.07	<0.1	1.1	<0.1	<0.1	<0.01	<0.01
KIFE066	2.4	0.6	41.4	<1	5.7	30.2	<0.5	0.1	0.4	0.02	<0.1	3.8	<0.1	<0.1	0.01	<0.01
KIFE067	2.6	0.7	30.3	<1	6	41	<0.5	0.2	0.6	<0.01	<0.1	1.1	<0.1	<0.1	<0.01	<0.01
KIFE068	1.9	0.7	31.4	1	8.3	6.2	10.7	0.8	0.7	<0.01	<0.1	<0.5	<0.1	<0.1	0.01	<0.01
KIFE069	4.7	0.4	21.6	4	5.3	25	2.4	0.3	0.6	0.02	<0.1	0.6	<0.1	<0.1	<0.01	<0.01
KIFE070	2.9	1.6	30.1	5	3.3	37.1	2.4	0.4	0.7	0.04	<0.1	4.6	0.1	<0.1	<0.01	<0.01
KIFE071	1.7	1.1	29.4	<1	3.1	21.2	0.7	0.2	0.4	0.03	<0.1	2	<0.1	<0.1	<0.01	<0.01
KIFE072	3.3	0.6	50.9	<1	3.6	23.2	1.2	0.2	0.5	0.02	<0.1	3.5	<0.1	<0.1	<0.01	<0.01
KIFE073	6.3	1.5	61.9	23	27.6	53.7	2.5	0.6	0.5	<0.01	<0.1	<0.5	<0.1	<0.1	0.02	0.02
KIFE100	1.7	0.5	26.3	<1	1.3	22.2	0.8	0.3	0.5	0.02	<0.1	4.2	<0.1	<0.1	<0.01	<0.01
KIFE101	6.8	1.1	39.1	<1	6.3	87.1	<0.5	0.9	0.4	0.05	<0.1	1.6	<0.1	<0.1	<0.01	<0.01
KIFE102	0.3	10.9	21.6	7	4.5	42.2	<0.5	0.4	0.8	<0.01	<0.1	1.4	<0.1	<0.1	0.02	<0.01
KIFE103	<0.1	2.5	1.6	2	0.8	5.2	0.5	0.1	<0.1	<0.01	<0.1	<0.5	<0.1	<0.1	0.06	<0.01
KIFE104	3.1	0.9	60.9	<1	2.2	38.4	<0.5	0.3	0.4	0.04	<0.1	4.6	<0.1	<0.1	<0.01	<0.01
KIFE105	1.5	0.4	15.4	<1	2.7	56.2	<0.5	0.2	<0.1	<0.01	<0.1	<0.5	<0.1	<0.1	<0.01	<0.01
KIFE106	3.5	1	39.8	1	8	20.5	<0.5	0.5	0.5	0.05	<0.1	2	<0.1	<0.1	0.03	<0.01
KIFE107	1.2	1.3	14.7	9	13.2	6.8	<0.5	0.2	0.2	0.01	0.3	<0.5	<0.1	<0.1	0.05	0.01
KIFE108	5.8	0.7	51.5	1	10.1	36.4	<0.5	0.3	0.5	0.06	<0.1	1.1	<0.1	<0.1	0.01	<0.01
KIFE109	4.9	1	55.8	2	15.1	35.7	<0.5	0.1	0.4	0.05	<0.1	0.5	<0.1	<0.1	0.02	<0.01
KIFE110	4.1	0.9	27.9	1	12.1	23.8	<0.5	0.1	0.2	0.08	<0.1	0.7	<0.1	<0.1	<0.01	<0.01
KIFE111	3	1.1	40.6	2	16.7	26.2	0.5	0.1	0.3	0.36	<0.1	1.4	<0.1	<0.1	<0.01	<0.01
KIFE112	6.8	1.3	14.8	<1	3.6	60	<0.5	0.4	1	0.1	<0.1	0.8	<0.1	<0.1	<0.01	<0.01
KIFE113	2.9	0.7	23.1	1	5.6	19	<0.5	0.3	0.4	0.04	<0.1	0.5	<0.1	<0.1	<0.01	<0.01
KIFE114	2.1	0.4	8.3	<1	4	9.2	<0.5	0.1	0.5	0.03	<0.1	1.1	<0.1	<0.1	<0.01	<0.01
KIFE115	0.4	18.7	60.7	34	0.9	21.9	<0.5	0.3	0.5	<0.01	<0.1	2.9	<0.1	<0.1	0.06	<0.01

Biogeochemical Data Tables
Eucalypts

Table with columns: Sample, Sampling Time, Zone, Easting, Northing, Species, Mo ppm, Cu ppm, Pb ppm, Zn ppm, Ag ppb, Ni ppm, Co ppm, Mn ppm, As ppm, U ppm, Au ppb, Sr ppm, Cd ppm, Sb ppm, Bi ppm, Ca %, P %, La ppm. Rows list various KIEUC samples from 160 to 210.

Sample	Sampling Time	Zone	Easting	Northing	Species	Mo ppm	Cu ppm	Pb ppm	Zn ppm	Ag ppb	Ni ppm	Co ppm	Mn ppm	As ppm	U ppm	Au ppb	Sr ppm	Cd ppm	Sb ppm	Bi ppm	Ca %	P %	La ppm
KIEUC352	Apr-13	53H	680334	6019079	SB	0.02	2.93	0.06	8.2	<2	0.9	0.02	90	<0.1	0.02	0.3	33.8	0.04	<0.02	<0.02	0.5	0.037	0.02
KIEUC353	Apr-13	53H	679663	6020983	Unknown	0.04	3.39	0.18	7.9	<2	0.9	0.07	90	0.2	0.02	0.9	10.3	0.05	<0.02	<0.02	0.37	0.044	0.07
KIEUC354	Apr-13	53H	679580	6022229	SB	<0.01	2	0.06	15.1	<2	1.2	0.04	38	<0.1	0.02	<0.2	26.9	0.04	<0.02	<0.02	0.65	0.042	0.03
KIEUC355	Apr-13	53H	678880	6025908	SB	0.01	3.5	0.05	14.9	<2	0.7	0.03	71	<0.1	<0.01	<0.2	8.2	0.14	<0.02	<0.02	0.46	0.063	0.01
KIEUC356	Apr-13	53H	678833	6035613	SB	<0.01	3.24	0.11	12.9	5	0.6	0.08	93	<0.1	0.01	<0.2	41.4	0.05	<0.02	<0.02	1.03	0.04	0.13
KIEUC357	Apr-13	53H	664366	6024811	SB	<0.01	5.56	0.05	11.9	<2	0.8	0.05	41	<0.1	0.02	<0.2	30.2	0.22	<0.02	<0.02	0.82	0.088	0.08
KIEUC358	Apr-13	53H	665566	6023456	SB	<0.01	3.19	0.06	12.8	<2	1.9	0.03	20	0.3	<0.01	<0.2	16.7	0.06	<0.02	<0.02	0.5	0.062	0.04
KIEUC359	Apr-13	53H	667559	6022358	SB	0.03	9.71	0.07	15.8	<2	3.2	0.04	168	0.2	0.01	<0.2	16.1	0.07	<0.02	<0.02	0.52	0.058	0.05
KIEUC360	Apr-13	53H	669607	6022205	SB	<0.01	3.84	0.04	10.4	<2	0.5	0.05	48	<0.1	0.01	<0.2	17.3	0.11	<0.02	<0.02	0.46	0.051	0.03
KIEUC361	Apr-13	53H	672682	6022174	SB	<0.01	3.45	0.09	6.9	<2	0.9	0.03	43	<0.1	0.03	<0.2	12.4	0.18	<0.02	<0.02	0.51	0.041	0.03
KIEUC362	Apr-13	53H	674637	6017192	CG	<0.01	3.28	0.07	8.9	<2	0.7	0.12	14	<0.1	0.03	<0.2	27.6	0.09	<0.02	<0.02	0.75	0.048	0.44
KIEUC363	Apr-13	53H	683859	6016252	SB	0.03	3.11	0.11	7.9	<2	0.5	0.11	8	<0.1	<0.01	0.3	6.5	0.08	<0.02	<0.02	0.37	0.048	0.21
KIEUC364	Apr-13	53H	684655	6024042	SB	0.02	4.69	0.09	11.6	<2	0.5	0.04	27	<0.1	0.03	<0.2	31.3	0.07	<0.02	<0.02	0.59	0.04	0.48
KIEUC365	Apr-13	53H	691699	6033540	SB	0.03	3.25	0.2	14.2	<2	1.4	0.06	79	0.1	0.02	<0.2	8.8	0.06	<0.02	<0.02	0.41	0.049	0.06
KIEUC366	Apr-13	53H	677722	6049446	SG	0.07	2.52	2.52	12.6	5	0.2	0.02	20	<0.1	<0.01	<0.2	9.1	<0.01	<0.02	<0.02	0.31	0.148	0.05
KIEUC367	Apr-13	53H	677684	6049445	SG	0.08	3.17	24.08	18.8	6	0.2	0.06	129	<0.1	<0.01	<0.2	18.4	0.04	<0.02	<0.02	0.52	0.122	0.08
KIEUC368	Apr-13	53H	674543	6041379	SB	<0.01	3	0.1	13.8	<2	0.8	0.03	62	0.1	0.01	<0.2	32.2	0.1	<0.02	<0.02	0.77	0.038	0.04
KIEUC369	Apr-13	53H	702846	6033214	SB	0.02	4.59	0.12	6.8	<2	0.6	0.06	50	<0.1	0.01	<0.2	18.5	0.05	<0.02	<0.02	0.4	0.048	0.13
KIEUC370	Apr-13	53H	704689	6034979	SB	0.02	4.95	0.1	11	<2	0.4	0.06	36	0.2	0.07	<0.2	38.7	0.12	<0.02	<0.02	0.68	0.063	0.23
KIEUC371	Apr-13	53H	704695	6041585	SB	0.01	4.92	0.08	10.3	<2	0.6	0.07	31	<0.1	0.05	0.2	35.1	0.09	<0.02	<0.02	0.62	0.064	0.18
KIEUC372	Apr-13	53H	702063	6038634	SB	0.02	4.11	0.11	9.9	<2	0.6	0.06	88	<0.1	0.02	<0.2	29.2	0.07	<0.02	<0.02	0.79	0.042	0.06
KIEUC373	Apr-13	53H	695890	6039376	SB	0.04	3.59	0.18	15.1	<2	0.8	0.03	54	0.3	0.07	0.4	24.4	0.12	<0.02	<0.02	0.43	0.076	0.05
KIEUC374	Apr-13	53H	693052	6042412	SB	0.02	4.62	0.11	9.9	<2	0.4	0.05	187	<0.1	0.03	<0.2	25.9	0.1	<0.02	<0.02	0.61	0.052	0.09
KIEUC375	Apr-13	53H	693052	6042412	CG	0.02	4.33	0.07	10.5	<2	0.6	0.06	22	<0.1	0.01	<0.2	25	0.03	<0.02	<0.02	0.55	0.064	0.11
KIEUC376	Apr-13	53H	690545	6041216	SB	0.02	2.24	0.11	8.4	<2	1	0.03	58	<0.1	0.04	<0.2	24.1	0.12	<0.02	<0.02	0.6	0.106	0.08
KIEUC377	Apr-13	53H	686885	6040251	SB	0.01	2.88	0.07	11.7	4	0.7	0.06	55	<0.1	0.02	0.4	22	0.35	<0.02	<0.02	0.66	0.059	0.09
KIEUC378	Apr-13	53H	694252	6037185	SB	0.02	4.46	0.03	9.4	4	0.7	0.03	63	<0.1	<0.01	<0.2	10.3	0.04	<0.02	<0.02	0.4	0.062	0.02
KIEUC379	Apr-13	53H	670145	6038581	CG	0.03	1.26	0.15	10.2	2	1.8	0.16	381	<0.1	0.07	0.3	76.9	0.02	<0.02	<0.02	1.42	0.052	0.33
KIEUC380	Apr-13	53H	726514	6032105	NLM	0.19	2.4	0.12	13.6	<2	5.6	0.06	276	<0.1	<0.01	<0.2	28.4	0.02	<0.02	<0.02	0.6	0.068	0.13
KIEUC381	Apr-13	53H	724523	6030514	NLM	0.06	4.93	0.09	12	<2	3.7	0.13	169	<0.1	<0.01	<0.2	8.3	0.15	<0.02	<0.02	0.37	0.064	0.28
KIEUC382	Apr-13	53H	710531	6025164	Pit Species	0.03	1.84	0.05	5	<2	1.7	0.1	54	<0.1	<0.01	<0.2	26.1	0.1	<0.02	<0.02	0.48	0.033	0.4
KIEUC383	Apr-13	53H	708539	6025993	CG	0.05	3.46	0.2	6.7	<2	1	0.08	34	<0.1	<0.01	<0.2	33	0.01	<0.02	<0.02	0.96	0.035	0.46
KIEUC384	Apr-13	53H	708724	6028827	SB	0.03	3.15	0.09	9.7	<2	0.8	0.1	49	<0.1	<0.01	<0.2	34.9	0.13	<0.02	<0.02	0.62	0.055	0.09
KIEUC385	Apr-13	53H	709277	6040724	SB	0.03	3.52	0.11	7.5	<2	0.5	0.14	35	<0.1	<0.01	<0.2	29.5	0.07	<0.02	<0.02	0.56	0.043	0.09
KIEUC386	Apr-13	53H	708624	6023892	CG	0.06	3.88	0.08	10.4	<2	1.1	0.15	17	0.1	<0.01	<0.2	12.7	<0.01	<0.02	<0.02	0.42	0.048	1.12
KIEUC387	Apr-13	53H	717310	6041561	CG	0.2	3.85	0.13	6.7	<2	2	0.09	47	<0.1	0.02	<0.2	66	0.02	<0.02	<0.02	1.71	0.048	0.35
KIEUC388	Apr-13	53H	715782	6042796	SB	0.1	3.78	0.11	10.5	<2	1.9	0.05	106	0.2	<0.01	<0.2	12.2	0.08	<0.02	<0.02	0.46	0.055	0.08
KIEUC389	Apr-13	53H	710064	6045006	CG	0.02	4.49	0.05	9.5	<2	0.8	0.03	51	0.1	<0.01	<0.2	35.8	0.03	<0.02	<0.02	0.83	0.04	0.04
KIEUC390	Apr-13	53H	708035	6045704	SB	0.01	5.49	0.07	14.8	<2	0.8	0.02	58	0.1	<0.01	<0.2	17.4	0.07	<0.02	<0.02	0.44	0.07	0.07
KIEUC391	Apr-13	53H	704699	6047048	SB	0.04	4.61	0.18	7.5	4	0.5	0.1	35	0.1	0.01	0.8	40.9	0.04	<0.02	<0.02	0.6	0.039	0.06
KIEUC392	Apr-13	53H	700588	6049377	SB	0.04	2.71	0.22	10.3	<2	1.3	0.12	59	<0.1	0.03	<0.2	17.4	0.07	<0.02	<0.02	0.45	0.059	0.14
KIEUC393	Apr-13	53H	718431	6049800	NLM	0.03	4.52	0.06	19.6	<2	3	0.05	38	0.1	0.03	<0.2	60.5	0.05	<0.02	<0.02	1.45	0.113	0.14

Sample	Cr ppm	Mg %	Ba ppm	Ti ppm	B ppm	Na %	K %	Sc ppm	Ti ppm	S %	Hg ppb	Se ppm	Te ppm	Cs ppm	Ge ppm	Rb ppm	Sn ppm	Y ppm	Ce ppm	Li ppm	W ppm	Be ppm	Pd ppb	Pt ppb	Re ppb
KIEUC001	1	0.156	1.2	4	16	0.709	0.42	0.2	<0.02	0.11	19	0.3	<0.02	<0.005	<0.01	1	0.03	1VE	1VE	1VE	1VE	1VE	1	1	<1
KIEUC002	1.2	0.263	4.5	5	38	1	0.83	0.2	<0.02	0.25	36	0.3	<0.02	0.009	<0.01	1.6	<0.02	0.033	0.14	0.32	<0.1	<0.1	<1	2	<1
KIEUC003	1.3	0.442	7.1	9	35	0.495	0.53	0.2	<0.02	0.18	56	0.2	<0.02	0.007	<0.01	0.9	<0.02	0.236	1.01	1.49	<0.1	<0.1	<1	<1	<1
KIEUC004	1.4	0.359	7.2	3	35	0.415	0.55	0.2	<0.02	0.21	59	0.1	<0.02	0.012	<0.01	2.7	0.02	0.16	0.42	0.28	<0.1	<0.1	<1	<1	<1
KIEUC005	1.3	0.255	2.5	4	22	0.51	0.58	0.2	<0.02	0.2	34	0.2	<0.02	0.006	<0.01	0.6	<0.02	0.06	0.31	0.54	<0.1	<0.1	<2	2	<1
KIEUC006	1.5	0.112	1.8	6	17	0.54	0.72	0.3	<0.02	0.19	13	0.2	<0.02	0.009	<0.01	2	<0.02	0.023	0.1	0.12	<0.1	<0.1	<2	<1	<1
KIEUC007	1.4	0.211	1.5	4	25	0.381	0.61	0.3	<0.02	0.21	38	0.2	<0.02	<0.005	<0.01	1.4	<0.02	0.019	0.05	0.3	<0.1	<0.1	<2	6	<1
KIEUC008	1.8	0.157	1.3	5	39	0.424	0.76	0.3	<0.02	0.23	43	0.3	<0.02	<0.005	<0.01	1.5	<0.02	0.018	0.06	0.89	<0.1	<0.1	<2	1	<1
KIEUC009	1.2	0.134	1.4	3	31	0.513	0.64	0.2	<0.02	0.21	38	0.2	<0.02	<0.005	0.02	0.8	<0.02	0.008	0.04	0.6	<0.1	<0.1	<2	1	<1
KIEUC010	1.6	0.332	4	12	28	0.644	0.7	0.3	<0.02	0.18	21	<0.1	<0.02	0.012	0.01	1.2	0.02	0.143	0.5	0.91	<0.1	<0.1	2	2	<1
KIEUC011	1.6	0.365	4.4	5	30	0.918	0.38	0.2	<0.02	0.16	41	0.2	<0.02	0.011	0.01	0.5	0.02	0.041	0.16	1.6	<0.1	<0.1	<2	4	<1
KIEUC012	1.4	0.211	2.5	4	28	0.765	0.54	0.3	<0.02	0.24	48	0.3	<0.02	0.009	0.02	0.7	<0.02	0.05	0.15	0.94	<0.1	<0.1	<2	2	<1
KIEUC013	1.5	0.293	8.3	6	21	0.614	0.57	0.2	<0.02	0.18	20	0.4	<0.02	<0.005	<0.01	0.7	<0.02	0.013	0.06	0.34	<0.1	<0.1	<2	<1	<1
KIEUC014	1.5	0.405	5.4	13	33	0.656	0.51	0.3	<0.02	0.22	59	0.3	<0.02	0.01	<0.01	0.7	0.02	0.05	0.17	1.14	<0.1	<0.1	<2	<1	<1
KIEUC015	1.5	0.205	25.2	6	23	0.499	0.8	0.3	<0.02	0.18	42	<0.1	<0.02	0.009	0.02	1.7	<0.02	0.038	0.16	0.26	<0.1	<0.1	<2	<1	<1
KIEUC016	1.3	0.291	3	6	24	0.919	0.68	0.4	<0.02	0.16	28	0.2	<0.02	0.011	<0.01	1.6	<0.02	0.044	0.3	0.21	<0.1	<0.1	<2	2	<1
KIEUC017	1.5	0.141	1.5	7	14	1.15	1.13	0.3	<0.02	0.11	10	<0.1	<0.02	0.016	0.01	3.1	<0.02	0.069	0.37	0.34	<0.1	<0.1	<2	<1	<1
KIEUC018	1.4	0.161	5.2	8	20	1.059	0.66	0.3	<0.02	0.09	15	0.4	<0.02	0.009	0.01	1.8	0.02	0.027	0.11	0.19	<0.1	<0.1	<2	<1	<1
KIEUC019	1.3	0.161	3.1	5	31	0.909	0.71	0.3	<0.02	0.14	30	0.2	<0.02	0.006	<0.01	1.6	<0.02	0.046	0.23	0.25	<0.1	<0.1	<2	<1	<1
KIEUC020	1.1	0.163	4.7	5	31	0.538	0.63	0.2	<0.02	0.14	26	0.2	<0.02	<0.005	0.02	1.2	<0.02	0.223	0.55	0.25	<0.1	<0.1	<2	<1	<1
KIEUC021	1.2	0.1	0.7	4	15	0.292	0.99	0.2	<0.02	0.06	11	0.2	<0.02	<0.005	0.01	1.5	0.02	0.009	0.03	0.06	<0.1	<0.1	<2	<1	<1
KIEUC022	1.2	0.137	3.7	5	21	0.423	0.87	0.2	<0.02	0.12	10	0.3	<0.02	0.006	<0.01	2.4	<0.02	0.011	0.04	0.06	<0.1	<0.1	<2	<1	<1
KIEUC023	1.1	0.33	4.7	4	20	0.883	0.69	0.2	<0.02	0.04	13	0.3	<0.02	0.016	<0.01	3.3	<0.02	0.14	0.41	0.26	<0.1	<0.1	<2	<1	1
KIEUC024	1.2	0.31	1.4	4	17	0.224	0.48	0.2	<0.02	0.06	31	<0.1	<0.02	0.007	<0.01	1.3	<0.02	0.06	0.14	0.34	<0.1	<0.1	<2	<1	<1
KIEUC025	1.2	0.204	1.8	2	24	0.341	0.39	0.2	<0.02	0.05	26	<0.1	<0.02	0.007	<0.01	1.4	<0.02	0.269	0.37	0.36	<0.1	<0.1	<2	<1	<1
KIEUC026	1.5	0.24	2.8	2	19	0.265	0.39	0.3	<0.02	0.07	36	0.2	<0.02	0.006	<0.01	1.5	<0.02	0.036	0.08	0.59	<0.1	<0.1	<2	<1	<1
KIEUC027	1.5	0.333	3	3	24	0.354	0.61	0.2	<0.02	0.08	9	0.2	<0.02	0.013	0.02	4.4	<0.02	0.002	0.03	0.11	<0.1	<0.1	<2	<1	<1
KIEUC028	1.5	0.266	2.3	3	17	0.268	0.8	0.2	<0.02	0.07	14	<0.1	<0.02	0.018	<0.01	8.9	<0.02	0.011	0.04	0.12	<0.1	<0.1	<2	<1	<1
KIEUC029	1.3	0.229	1.7	5	16	0.372	0.79	0.3	<0.02	0.12	10	<0.1	<0.02	<0.005	0.03	2.2	<0.02	0.007	0.02	0.05	<0.1	<0.1	<2	<1	<1
KIEUC030	1.2	0.167	3.9	3	11	0.274	0.7	0.2	<0.02	0.08	8	<0.1	<0.02	0.015	<0.01	5.5	<0.02	0.002	0.02	0.12	<0.1	<0.1	<2	<1	<1
KIEUC031	1.5	0.28	1.5	4	16	0.373	0.41	0.4	<0.02	0.07	16	0.1	<0.02	0.005	0.02	1.8	<0.02	0.068	0.23	0.2	<0.1	<0.1	<2	1	<1
KIEUC032	1.4	0.367	2.6	2	17	0.324	0.34	0.2	<0.02	0.07	17	0.2	<0.02	0.005	0.02	1.2	<0.02	0.018	0.04	0.14	<0.1	<0.1	<2	<1	<1
KIEUC033	<0.1	0.153	2.1	8	18	0.859	1.29	0.4	<0.02	0.02	7	0.2	<0.02	0.006	0.02	3.8	<0.02	0.013	0.07	0.38	<0.1	<0.1	<2	<1	<1
KIEUC034	1.1	0.188	6.2	3	12	0.304	0.14	0.1	0.03	0.06	6	0.1	0.03	<0.005	0.01	0.6	0.09	0.017	0.1	0.06	<0.1	<0.1	<2	<1	<1
KIEUC035	1.2	0.26	4.6	9	29	0.549	0.94	0.2	0.09	0.16	13	0.1	<0.02	0.007	0.02	1.1	0.07	0.147	0.5	0.33	<0.1	<0.1	<2	<1	<1
KIEUC036	1.3	0.236	4.9	8	34	0.49	0.69	0.2	0.05	0.14	22	<0.1	0.02	0.006	<0.01	1.2	0.03	0.045	0.34	0.64	<0.1	<0.1	<2	<1	1
KIEUC037	1.3	0.149	2.8	7	66	0.282	0.63	0.4	0.18	0.2	44	0.1	<0.02	<0.005	<0.01	0.9	0.05	0.065	0.47	1.21	<0.1	<0.1	<2	<1	<1
KIEUC038	1.2	0.251	2.8	11	24	0.629	1.16	0.3	0.05	0.23	12	0.2	<0.02	0.006	0.01	2.7	0.03	0.156	1.86	0.5	<0.1	<0.1	<2	<1	<1
KIEUC039	1.8	0.233	2	3	21	0.501	0.78	0.3	0.04	0.17	7	0.1	<0.02	<0.005	0.05	1.9	0.11	0.018	0.1	0.26	<0.1	<0.1	<2	<1	<1
KIEUC040	2	0.149	6.9	2	40	0.824	0.73	0.2	<0.02	0.22	43	<0.1	0.02	<0.005	0.01	0.6	0.08	0.024	0.1	0.89	<0.1	<0.1	<2	<1	<1
KIEUC041	2.2	0.33	6	3	26	0.668	0.7	0.5	<0.02	0.22	70	0.1	0.05	0.011	<0.01	1.4	0.07	0.112	0.25	0.25	<0.1	<0.1	<2	<1	<1
KIEUC042	1.7	0.241	15.8	2	30	0.622	0.71	0.3	<0.02	0.08	2	<0.1	<0.02	<0.005	0.04	4.2	0.08	0.135	1.13	0.26	<0.1	<0.1	<2	1	<1
KIEUC043	1.3	0.219	38.7	2	41	0.311	0.41	0.2	<0.02	0.23	27	0.2	<0.02	<0.005	<0.01	1.5	0.02	0.392	4.11	0.49	<0.1	<0.1	<2	1	<1
KIEUC044	1.3	0.162	31.8	4	63	0.457	0.43	0.3	<0.02	0.24	32	0.2	<0.02	0.007	<0.01	2.1	<0.02	0.161	1.74	0.86	<0.1	<0.1	<2	<1	<1
KIEUC045	1.3	0.253	40.5	3	23	0.558	0.54	0.3	<0.02	0.21	17	0.2	<0.02	<0.005	<0.01	2	0.02	0.391	5.42	0.48	<0.1	<0.1	<2	<1	<1

Sample	In ppm	Nb ppm	Ta ppm	Ga ppm	Fe %	Zr ppm	Th ppm	V ppm	Hf ppm	Al %
KIEUC001	0.02	0.01	0.001	0.1	0.001	0.01	1VE	2	0.001	0.01
KIEUC002	<0.02	<0.01	0.001	1VE	1VE	1VE	1VE	1VE	1VE	1VE
KIEUC003	<0.02	<0.01	<0.001	<0.1	0.006	0.04	<0.01	<2	<0.001	<0.01
KIEUC004	<0.02	<0.01	<0.001	<0.1	0.012	0.07	0.02	<2	0.002	0.01
KIEUC005	<0.02	<0.01	<0.001	<0.1	0.014	0.05	0.01	<2	0.002	<0.01
KIEUC006	<0.02	<0.01	<0.001	<0.1	0.014	0.07	0.02	<2	0.005	0.01
KIEUC007	<0.02	<0.01	<0.001	<0.1	0.007	0.03	0.01	<2	<0.001	<0.01
KIEUC008	<0.02	<0.01	<0.001	<0.1	0.012	0.06	0.02	<2	0.006	0.01
KIEUC009	<0.02	<0.01	<0.001	<0.1	0.008	0.03	<0.01	<2	0.002	<0.01
KIEUC010	<0.02	<0.01	<0.001	<0.1	0.014	0.05	0.01	<2	0.002	0.01
KIEUC011	<0.02	<0.01	<0.001	<0.1	0.019	0.15	0.02	2	0.002	0.03
KIEUC012	<0.02	<0.01	<0.001	<0.1	0.013	0.07	0.02	<2	0.001	0.02
KIEUC013	<0.02	<0.01	<0.001	<0.1	0.009	0.06	0.01	2	0.002	<0.01
KIEUC014	<0.02	<0.01	<0.001	<0.1	0.005	0.04	<0.01	3	<0.001	<0.01
KIEUC015	<0.02	<0.01	0.001	<0.1	0.016	0.12	0.03	4	0.008	0.02
KIEUC016	<0.02	<0.01	<0.001	<0.1	0.012	0.07	0.02	3	0.003	0.01
KIEUC017	<0.02	<0.01	<0.001	<0.1	0.021	0.11	0.03	2	0.006	0.01
KIEUC018	<0.02	<0.01	<0.001	<0.1	0.033	0.15	0.06	<2	0.006	0.02
KIEUC019	<0.02	<0.01	<0.001	<0.1	0.028	0.11	0.04	<2	0.006	0.01
KIEUC020	<0.02	<0.01	<0.001	<0.1	0.011	0.08	0.02	<2	<0.001	0.01
KIEUC021	<0.02	<0.01	<0.001	<0.1	0.005	0.03	<0.01	<2	<0.001	<0.01
KIEUC022	<0.02	<0.01	<0.001	<0.1	0.008	0.04	<0.01	<2	0.003	<0.01
KIEUC023	<0.02	<0.01	<0.001	<0.1	0.012	0.06	0.02	<2	<0.001	0.01
KIEUC024	<0.02	<0.01	<0.001	<0.1	0.011	0.07	0.02	<2	0.004	0.01
KIEUC025	<0.02	<0.01	<0.001	<0.1	0.009	0.07	0.02	<2	0.004	0.01
KIEUC026	<0.02	<0.01	<0.001	<0.1	0.006	0.05	<0.01	3	0.003	<0.01
KIEUC027	<0.02	<0.01	<0.001	<0.1	0.003	0.02	<0.01	4	0.001	<0.01
KIEUC028	<0.02	<0.01	<0.001	<0.1	0.008	0.07	0.02	5	0.005	<0.01
KIEUC029	<0.02	<0.01	<0.001	<0.1	0.005	0.03	0.01	6	0.001	<0.01
KIEUC030	<0.02	<0.01	<0.001	<0.1	0.003	0.02	<0.01	5	0.002	<0.01
KIEUC031	<0.02	<0.01	0.001	<0.1	0.016	0.19	0.05	5	0.006	0.02
KIEUC032	<0.02	<0.01	<0.001	<0.1	0.004	0.02	<0.01	5	<0.001	<0.01
KIEUC033	<0.02	<0.01	<0.001	<0.1	0.006	0.02	0.01	<2	0.004	<0.01
KIEUC034	<0.02	<0.01	0.001	<0.1	0.003	0.02	<0.01	<2	0.004	<0.01
KIEUC035	<0.02	<0.01	0.002	<0.1	0.008	0.03	0.02	<2	0.005	<0.01
KIEUC036	<0.02	<0.01	<0.001	<0.1	0.007	0.03	0.01	<2	0.002	<0.01
KIEUC037	<0.02	<0.01	<0.001	<0.1	0.005	0.03	0.02	2	0.003	<0.01
KIEUC038	<0.02	<0.01	<0.001	<0.1	0.006	0.03	0.01	2	0.001	<0.01
KIEUC039	<0.02	<0.01	0.001	<0.1	0.005	0.02	<0.01	<2	<0.001	<0.01
KIEUC040	<0.02	<0.01	<0.001	<0.1	0.009	0.05	<0.01	<2	<0.001	<0.01
KIEUC041	<0.02	<0.01	<0.001	<0.1	0.035	0.13	0.07	<2	0.002	0.03
KIEUC042	<0.02	<0.01	<0.001	<0.1	0.003	0.03	<0.01	<2	0.002	<0.01
KIEUC043	<0.02	<0.01	<0.001	<0.1	0.003	0.02	<0.01	2	<0.001	<0.01
KIEUC044	<0.02	<0.01	<0.001	<0.1	0.005	0.01	<0.01	3	<0.001	<0.01
KIEUC045	<0.02	<0.01	<0.001	<0.1	0.005	0.03	<0.01	3	0.003	<0.01

Sample	In ppm	Nb ppm	Ta ppm	Ga ppm	Fe %	Zr ppm	Th ppm	V ppm	Hf ppm	Al %
KIEUC110	<0.02	<0.01	<0.001	<0.1	0.01	0.05	0.01	<2	<0.001	<0.01
KIEUC111	<0.02	<0.01	<0.001	<0.1	0.008	0.04	<0.01	<2	0.001	<0.01
KIEUC112	<0.02	<0.01	<0.001	<0.1	0.004	0.02	<0.01	<2	<0.001	0.05
KIEUC113	<0.02	<0.01	<0.001	<0.1	0.004	0.01	<0.01	<2	<0.001	0.03
KIEUC114	<0.02	<0.01	<0.001	<0.1	0.011	0.03	<0.01	<2	<0.001	<0.01
KIEUC115	<0.02	<0.01	<0.001	<0.1	0.009	0.06	<0.01	<2	0.002	<0.01
KIEUC116	<0.02	<0.01	<0.001	<0.1	0.018	0.07	0.02	<2	<0.001	<0.01
KIEUC117	<0.02	<0.01	<0.001	<0.1	0.018	0.12	0.02	<2	0.003	<0.01
KIEUC118	<0.02	<0.01	<0.001	<0.1	0.02	0.09	0.01	<2	<0.001	<0.01
KIEUC119	<0.02	<0.01	<0.001	<0.1	0.01	0.04	<0.01	<2	0.001	<0.01
KIEUC120	<0.02	<0.01	<0.001	<0.1	0.006	0.03	<0.01	<2	<0.001	<0.01
KIEUC121	<0.02	<0.01	<0.001	<0.1	0.011	0.04	<0.01	<2	<0.001	<0.01
KIEUC122	<0.02	<0.01	<0.001	<0.1	0.008	0.04	<0.01	<2	<0.001	0.01
KIEUC123	<0.02	<0.01	<0.001	<0.1	0.005	0.02	<0.01	<2	<0.001	<0.01
KIEUC124	<0.02	<0.01	<0.001	0.1	0.039	0.18	0.07	<2	0.005	0.02
KIEUC125	<0.02	<0.01	<0.001	<0.1	0.006	0.03	<0.01	<2	<0.001	0.04
KIEUC126	<0.02	<0.01	<0.001	<0.1	0.021	0.09	0.03	<2	0.003	0.02
KIEUC127	<0.02	<0.01	<0.001	<0.1	0.021	0.07	0.03	<2	0.003	0.03
KIEUC128	<0.02	<0.01	<0.001	<0.1	0.03	0.16	0.06	<2	<0.001	0.02
KIEUC129	<0.02	<0.01	<0.001	<0.1	0.025	0.12	0.03	<2	0.004	0.02
KIEUC130	<0.02	<0.01	<0.001	<0.1	0.011	0.04	0.01	<2	<0.001	<0.01
KIEUC131	<0.02	<0.01	<0.001	<0.1	0.029	0.14	0.04	<2	0.008	0.02
KIEUC132	<0.02	<0.01	<0.001	<0.1	0.031	0.17	0.05	<2	<0.001	<0.01
KIEUC133	<0.02	<0.01	<0.001	<0.1	0.011	0.04	0.02	<2	<0.001	0.02
KIEUC134	<0.02	<0.01	<0.001	<0.1	0.012	0.05	0.02	<2	0.004	<0.01
KIEUC135	<0.02	<0.01	<0.001	<0.1	0.004	0.01	<0.01	<2	<0.001	<0.01
KIEUC136	<0.02	<0.01	<0.001	<0.1	0.026	0.08	0.03	<2	0.004	0.02
KIEUC137	<0.02	<0.01	<0.001	<0.1	0.021	0.06	0.02	<2	<0.001	0.04
KIEUC138	<0.02	<0.01	<0.001	<0.1	0.004	0.02	<0.01	<2	0.001	0.01
KIEUC139	<0.02	<0.01	<0.001	<0.1	0.006	0.02	0.01	<2	<0.001	0.02
KIEUC140	<0.02	<0.01	0.001	<0.1	0.012	0.06	0.03	<2	<0.001	0.02
KIEUC141	<0.02	<0.01	<0.001	<0.1	0.003	0.02	<0.01	<2	<0.001	0.02
KIEUC142	<0.02	<0.01	<0.001	<0.1	0.005	<0.01	<0.01	<2	<0.001	0.07
KIEUC143	<0.02	<0.01	<0.001	<0.1	0.005	0.14	0.05	<2	<0.001	0.03
KIEUC144	<0.02	<0.01	<0.001	<0.1	0.029	0.14	0.05	<2	0.003	0.04
KIEUC145	<0.02	<0.01	<0.001	<0.1	0.03	0.14	0.05	<2	<0.001	0.02
KIEUC146	<0.02	<0.01	<0.001	<0.1	0.01	0.06	0.03	<2	0.004	0.02
KIEUC147	<0.02	<0.01	<0.001	<0.1	0.006	0.03	0.02	<2	<0.001	<0.01
KIEUC148	<0.02	<0.01	<0.001	<0.1	0.003	<0.01	<0.01	<2	<0.001	<0.01
KIEUC149	<0.02	<0.01	<0.001	<0.1	0.003	<0.01	<0.01	<2	<0.001	<0.01
KIEUC150	<0.02	<0.01	<0.001	<0.1	0.045	0.27	0.09	<2	0.009	0.04
KIEUC151	<0.02	<0.01	<0.001	0.2	0.061	0.38	0.26	3	0.016	0.06
KIEUC152	<0.02	<0.01	<0.001	<0.1	0.006	0.04	0.01	<2	<0.001	<0.01
KIEUC153	<0.02	<0.01	<0.001	<0.1	0.006	0.03	<0.01	<2	<0.001	0.02
KIEUC154	<0.02	<0.01	<0.001	<0.1	0.008	0.05	0.01	<2	0.001	0.01
KIEUC155	<0.02	<0.01	<0.001	<0.1	0.005	0.02	<0.01	<2	<0.001	0.03
KIEUC156	<0.02	<0.01	<0.001	<0.1	0.005	0.02	<0.01	<2	<0.001	0.02
KIEUC157	<0.02	<0.01	<0.001	<0.1	0.003	0.02	0.02	<2	<0.001	0.02
KIEUC158	<0.02	<0.01	<0.001	<0.1	0.004	0.02	0.01	<2	<0.001	<0.01
KIEUC159	<0.02	<0.01	<0.001	<0.1	0.003	0.02	<0.01	<2	<0.001	0.02

Sample	In ppm	Nb ppm	Ta ppm	Ga ppm	Fe %	Zr ppm	Th ppm	V ppm	Hf ppm	Al %
KIEUC352	<0.02	<0.01	<0.001	<0.1	0.013	0.06	0.02	18	<0.001	0.01
KIEUC353	<0.02	<0.01	<0.001	0.1	0.038	0.29	0.12	20	0.011	0.06
KIEUC354	<0.02	<0.01	0.001	<0.1	0.011	0.06	<0.01	<2	<0.001	0.01
KIEUC355	<0.02	<0.01	<0.001	<0.1	0.011	0.05	0.01	3	0.005	0.01
KIEUC356	<0.02	<0.01	<0.001	<0.1	0.024	0.12	0.05	4	<0.001	<0.01
KIEUC357	<0.02	<0.01	<0.001	<0.1	0.015	0.05	0.04	10	0.005	0.02
KIEUC358	<0.02	<0.01	<0.001	<0.1	0.023	0.1	0.04	15	0.003	0.02
KIEUC359	<0.02	<0.01	<0.001	<0.1	0.021	0.08	0.02	17	0.005	0.02
KIEUC360	<0.02	<0.01	0.002	<0.1	0.011	0.05	<0.01	17	<0.001	0.01
KIEUC361	<0.02	<0.01	0.001	<0.1	0.011	0.05	0.01	14	<0.001	0.01
KIEUC362	<0.02	<0.01	<0.001	<0.1	0.012	0.05	0.03	12	0.001	<0.01
KIEUC363	<0.02	<0.01	<0.001	0.1	0.036	0.25	0.07	14	0.009	0.04
KIEUC364	<0.02	<0.01	<0.001	<0.1	0.016	0.13	0.03	16	0.005	0.02
KIEUC365	<0.02	<0.01	0.001	0.1	0.058	0.36	0.15	17	0.014	0.04
KIEUC366	<0.02	<0.01	0.001	<0.1	0.006	0.02	<0.01	11	0.001	<0.01
KIEUC367	<0.02	<0.01	<0.001	<0.1	0.011	0.04	<0.01	12	0.003	<0.01
KIEUC368	<0.02	<0.01	<0.001	<0.1	0.012	0.03	<0.01	11	<0.001	<0.01
KIEUC369	<0.02	<0.01	<0.001	0.1	0.037	0.23	0.09	15	0.008	0.03
KIEUC370	<0.02	<0.01	<0.001	<0.1	0.015	0.05	0.02	13	0.002	0.02
KIEUC371	<0.02	<0.01	<0.001	<0.1	0.014	0.06	0.01	15	<0.001	0.02
KIEUC372	<0.02	<0.01	<0.001	<0.1	0.033	0.19	0.06	15	0.01	0.03
KIEUC373	<0.02	0.01	0.002	0.1	0.084	0.34	0.14	14	0.015	0.05
KIEUC374	<0.02	<0.01	<0.001	<0.1	0.029	0.12	0.04	7	0.005	0.02
KIEUC375	<0.02	<0.01	<0.001	<0.1	0.02	0.06	0.03	9	<0.001	<0.01
KIEUC376	<0.02	<0.01	<0.001	<0.1	0.012	0.03	0.01	<2	<0.001	0.01
KIEUC377	<0.02	<0.01	<0.001	<0.1	0.015	0.05	0.02	3	<0.001	0.01
KIEUC378	<0.02	<0.01	<0.001	<0.1	0.013	0.04	0.01	9	0.002	<0.01
KIEUC379	<0.02	<0.01	0.001	0.1	0.058	0.34	0.2	3	0.007	0.04
KIEUC380	<0.02	<0.01	<0.001	<0.1	0.026	0.09	0.04	<2	0.004	0.02
KIEUC381	<0.02	<0.01	<0.001	<0.1	0.012	0.05	<0.01	4	<0.001	<0.01
KIEUC382	<0.02	<0.01	<0.001	<0.1	0.011	0.04	<0.01	8	0.001	<0.01
KIEUC383	<0.02	<0.01	<0.001	<0.1	0.048	0.12	0.03	7	0.004	0.02
KIEUC384	<0.02	<0.01	<0.001	<0.1	0.029	0.15	0.04	8	0.006	0.02
KIEUC385	<0.02	<0.01	<0.001	0.1	0.035	0.22	0.07	12	0.016	0.04
KIEUC386	<0.02	<0.01	<0.001	<0.1	0.016	0.07	0.01	14	0.003	0.02
KIEUC387	<0.02	<0.01	0.001	<0.1	0.035	0.13	0.04	5	0.006	0.02
KIEUC388	<0.02	<0.01	<0.001	<0.1	0.023	0.13	0.02	8	0.007	0.02
KIEUC389	<0.02	<0.01	<0.001	<0.1	0.034	0.09	0.03	<2	0.003	<0.01
KIEUC390	<0.02	<0.01	<0.001	<0.1	0.018	0.15	0.05	<2	0.007	0.02
KIEUC391	<0.02	<0.01	0.001	0.2	0.071	0.5	0.16	7	0.024	0.06
KIEUC392	<0.02	<0.01	<0.001	0.2	0.058	0.42	0.11	7	0.031	0.08
KIEUC393	<0.02	<0.01	<0.001	<0.1	0.022	0.06	0.03	<2	0.003	<0.01
Sample	In ppm	Nb ppm	Ta ppm	Ga ppm	Fe %	Zr ppm	Th ppm	V ppm	Hf ppm	Al %
Mean	n/a	0.015	0.00114	0.12	0.0173	0.08755	0.03937	8.5235	0.00475	0.02304
Median	n/a	0.01	0.001	0.1	0.012	0.06	0.03	7	0.003	0.02
Std. Dev.	n/a	0.007746	0.00035	0.03935	0.0146	0.08639	0.03709	4.8588	0.004324	0.01347
Min	0	0.01	0.001	0.1	0.002	0.01	0.01	2	0.001	0.01
Max	0	0.03	0.002	0.2	0.094	0.59	0.26	20	0.031	0.08

Biogeochemical Data Tables

Xanthorrhoea

Sample	Sampling Period	Zone	Eastings	Northing	Mo ppm	Cu ppm	Pb ppm	Zn ppm	Ag ppb	Ni ppm	Co ppm	Mn ppm	As ppm	Au ppb	Th ppm	Sr ppm	Cd ppm	Bi ppm	Ca %	P %	La ppm
KIXAN001	Mar-12	54H	238252	Dec. Limit	0.01	0.01	0.01	0.1	2	0.1	0.01	1	0.1	0.2	0.01	0.5	0.01	0.02	0.01	0.001	0.1
KIXAN002	Mar-12	54H	236356	Method	1VE	1VE	1VE	1VE	1VE	1VE	1VE	1VE	1VE	1VE	1VE	1VE	1VE	1VE	1VE	1VE	1VE
KIXAN003	Mar-12	54H	230484	6030613	0.1	1.66	0.15	7.5	<2	0.5	<0.01	7	<0.1	<0.2	<0.01	20.8	<0.01	<0.02	0.88	0.05	0.06
KIXAN004	Mar-12	53H	770188	6031489	0.01	1.4	0.48	4.1	<2	0.7	0.05	14	<0.1	<0.2	<0.01	72.9	0.04	<0.02	0.78	0.033	0.32
KIXAN005	Mar-12	53H	708012	6031218	0.1	1.45	0.07	10	<2	0.2	0.05	38	<0.1	<0.2	<0.01	54.1	<0.01	<0.02	0.63	0.025	0.48
KIXAN006	Mar-12	53H	702275	6031105	0.1	1.02	0.05	6.5	<2	0.4	0.03	10	<0.1	<0.2	<0.01	42	<0.01	<0.02	0.75	0.036	0.04
KIXAN007	Mar-12	53H	689539	6022456	0.05	1.2	0.12	8.4	<2	0.8	0.08	88	<0.1	<0.2	<0.01	38.5	0.02	<0.02	0.97	0.031	0.33
KIXAN008	Mar-12	53H	687032	6019885	0.39	1.08	0.07	4.9	<2	0.3	0.02	28	<0.1	0.3	<0.01	34.8	<0.01	<0.02	0.67	0.022	0.03
KIXAN009	Mar-12	53H	686067	6017705	0.01	1.72	0.03	14.4	<2	0.2	0.04	28	<0.1	<0.2	<0.01	58.8	<0.01	<0.02	0.66	0.024	0.18
KIXAN010	Mar-12	53H	685858	6021325	0.04	1.33	0.06	11.3	<2	0.1	<0.01	11	<0.1	<0.2	<0.01	18.3	0.01	<0.02	0.42	0.026	0.02
KIXAN011	Mar-12	53H	684538	6022817	<0.01	1.66	0.05	20.4	<2	0.3	0.01	40	<0.1	<0.2	<0.01	19.1	<0.01	<0.02	0.67	0.032	0.08
KIXAN012	Mar-12	53H	687663	6023638	0.06	0.98	0.07	4.1	<2	0.3	0.02	18	<0.1	<0.2	<0.01	32.3	<0.01	<0.02	0.59	0.019	0.07
KIXAN013	Mar-12	53H	686326	6026351	<0.01	2.39	0.04	16.1	<2	0.3	0.02	65	<0.1	<0.2	<0.01	57.1	<0.01	<0.02	0.58	0.039	0.04
KIXAN014	Mar-12	53H	687689	6029086	0.02	1.33	0.07	7.9	<2	0.2	<0.01	12	<0.1	<0.2	<0.01	32.6	<0.01	<0.02	0.51	0.029	0.1
KIXAN015	Mar-12	53H	684675	6029086	0.02	2.11	0.19	11.5	<2	0.3	0.02	55	0.1	<0.2	<0.01	51.5	<0.01	0.13	0.65	0.038	0.14
KIXAN016	Mar-12	53H	662244	6030098	0.02	1.45	0.1	11.1	<2	0.2	<0.01	52	0.1	<0.2	<0.01	48.8	<0.01	0.03	0.93	0.026	0.1
KIXAN017	Mar-12	53H	677710	6024014	0.06	2.16	0.52	10.6	<2	0.3	<0.01	61	0.1	0.5	0.04	47	0.01	0.12	1.07	0.039	0.12
KIXAN018	Mar-12	53H	677696	6019233	0.2	1.81	0.12	5.7	<2	0.3	0.01	11	<0.1	<0.2	<0.01	32	<0.01	0.03	0.96	0.032	0.03
KIXAN019	Mar-12	53H	677689	6049441	0.01	2.62	0.67	13.2	4	0.3	<0.01	16	0.2	<0.2	<0.01	26.9	0.02	<0.02	0.48	0.062	0.19
KIXAN020	Mar-12	53H	677675	6049435	0.04	3.96	0.27	20.5	4	0.2	0.01	50	<0.1	0.3	<0.01	46.8	0.1	<0.02	0.79	0.057	0.36
KIXAN021	Mar-12	53H	677663	6049437	0.02	2.8	2.62	17.6	<2	0.2	0.02	270	<0.1	0.5	0.01	53.5	0.07	<0.02	1.31	0.053	1.26
KIXAN022	Mar-12	53H	677622	6049430	0.04	3.46	2.4	38.2	<2	0.3	0.02	104	<0.1	<0.2	<0.01	85.7	0.07	<0.02	1.34	0.055	0.49
KIXAN023	Mar-12	53H	677628	6049415	0.05	1.91	2.23	33.6	3	0.8	0.01	91	<0.1	<0.2	<0.01	48.4	0.03	<0.02	0.62	0.141	0.19
KIXAN024	Mar-12	53H	677643	6049435	0.07	2.08	14.69	13	2	0.2	0.04	61	0.2	<0.2	0.02	54.8	0.03	<0.02	0.8	0.05	0.15
KIXAN025	Mar-12	53H	677758	6049437	0.05	2.14	0.39	15.1	<2	0.3	0.01	37	<0.1	<0.2	<0.01	75.8	0.02	<0.02	0.95	0.044	0.05
KIXAN026	Mar-12	53H	677763	6049455	0.02	1.71	7.52	11.6	<2	0.2	<0.01	18	<0.1	<0.2	0.02	28.9	0.02	<0.02	0.65	0.041	0.17
KIXAN027	Mar-12	53H	677747	6049462	0.02	1.63	71.78	12.7	8	<0.1	<0.01	133	<0.1	<0.2	0.01	27.1	0.19	<0.02	0.61	0.046	0.1
KIXAN028	Mar-12	53H	677747	6049458	0.07	3.64	2.1	13	6	0.5	0.02	16	0.2	<0.2	<0.01	14.7	<0.01	<0.02	0.25	0.071	0.02
KIXAN029	Mar-12	53H	677747	6049458	0.05	2.51	20.32	8	5	0.2	<0.01	22	<0.1	0.3	0.02	56.7	<0.01	<0.02	0.98	0.05	0.21
KIXAN030	Mar-12	53H	677747	6049458	0.05	2.13	16.78	4.2	5	0.2	0.02	19	<0.1	<0.2	0.02	48	<0.01	<0.02	0.81	0.03	0.22
KIXAN031	Mar-12	53H	677747	6049458	0.08	4.15	2.51	13.5	6	0.4	<0.01	27	<0.1	<0.2	<0.01	23.1	<0.01	<0.02	0.41	0.061	0.04
KIXAN032	Mar-12	53H	723525	6041318	0.07	1.06	0.11	5.3	<2	0.5	0.05	17	<0.1	<0.2	0.02	19.4	<0.01	<0.02	0.28	0.022	0.06
KIXAN033	Mar-12	53H	718671	6040563	0.01	1.37	0.07	12.9	<2	0.5	0.04	26	<0.1	<0.2	<0.01	69.1	<0.01	<0.02	0.9	0.036	0.44
KIXAN034	Mar-12	53H	718662	6040602	0.02	1.25	0.21	8.5	<2	0.9	0.04	51	<0.1	0.7	<0.01	177.9	0.01	<0.02	0.75	0.033	1.64
KIXAN035	Mar-12	53H	718660	6040611	<0.01	1.52	0.13	8.6	<2	0.6	0.04	19	<0.1	0.2	<0.01	156.6	<0.01	<0.02	1.03	0.026	0.79
KIXAN036	Mar-12	53H	718671	6040601	<0.01	1.34	0.1	7.2	<2	0.7	0.05	121	<0.1	<0.2	<0.01	114.4	0.02	<0.02	0.97	0.027	1.01
KIXAN037	Mar-12	53H	718642	6040604	0.01	1.06	0.09	13.2	<2	0.3	0.03	40	<0.1	<0.2	<0.01	154.4	<0.01	<0.02	0.78	0.02	1.17
KIXAN038	Mar-12	53H	718642	6040603	<0.01	1.22	0.03	6.6	<2	1.1	0.1	109	<0.1	0.3	<0.01	145.2	0.02	<0.02	0.63	0.029	0.56
KIXAN039	Mar-12	53H	718626	6040632	<0.01	1.44	0.11	10.4	<2	0.6	0.06	211	<0.1	<0.2	<0.01	98.4	0.02	<0.02	1.08	0.037	4.29
KIXAN040	Mar-12	53H	718605	6040631	0.02	1.87	0.12	19.8	<2	1.8	0.05	234	<0.1	0.2	<0.01	113.5	0.05	<0.02	1.01	0.043	0.97
KIXAN041	Mar-12	53H	709317	6042480	<0.01	1.24	0.1	5	<2	1.4	0.09	33	<0.1	1	<0.01	105.2	<0.01	<0.02	0.52	0.023	0.39

Sample	Sampling Period	Zone	Easting	Northing	Mo ppm	Cu ppm	Pb ppm	Zn ppm	Ag ppb	Ni ppm	Co ppm	Mn ppm	As ppm	Au ppb	Th ppm	Sr ppm	Cd ppm	Bi ppm	Ca %	P %	La ppm
KIXAN042	Mar-12	53H	708613	6041461	0.04	1.32	0.19	6.8	<2	0.2	0.02	26	<0.1	<0.2	<0.01	55.2	0.06	<0.02	0.68	0.031	0.07
KIXAN043	Mar-12	53H	708764	6039652	0.02	1.33	0.1	14	<2	0.3	0.03	124	<0.1	0.3	<0.01	93.8	<0.01	<0.02	1.62	0.027	0.63
KIXAN044	Mar-12	53H	701534	6045597	0.01	1.81	0.11	5.4	<2	0.3	0.02	21	<0.1	0.2	0.01	70.4	<0.01	<0.02	0.91	0.039	0.4
KIXAN045	Mar-12	53H	702091	6046326	0.02	1.22	0.14	298.1	<2	3	0.23	231	<0.1	<0.2	<0.01	32.9	7.26	<0.02	0.75	0.028	0.37
KIXAN046	Mar-12	53H	702082	6046328	0.02	1.66	0.18	19.3	<2	0.6	<0.01	61	<0.1	<0.2	<0.01	21	0.93	<0.02	0.43	0.026	0.07
KIXAN047	Mar-12	53H	702076	6046324	0.02	1.21	0.03	25.5	<2	0.4	0.01	166	<0.1	<0.2	<0.01	38.4	0.37	<0.02	0.67	0.026	0.65
KIXAN048	Mar-12	53H	701935	6046207	<0.01	1.09	0.33	9.1	<2	0.3	0.01	34	<0.1	<0.2	<0.01	32.7	0.01	<0.02	0.46	0.025	0.13
KIXAN049	Mar-12	53H	701944	6046264	0.01	1.1	2.83	19.8	<2	0.2	0.01	95	<0.1	<0.2	<0.01	60.4	0.29	<0.02	1.06	0.024	0.07
KIXAN050	Mar-12	53H	698133	6047346	0.01	1.78	0.34	6.9	<2	0.4	<0.01	85	<0.1	0.3	0.05	48.2	0.04	0.14	0.59	0.036	0.18
KIXAN051	Mar-12	53H	696303	6047265	0.02	1.18	0.13	9.5	<2	0.4	0.01	22	<0.1	<0.2	0.05	31.2	<0.01	0.04	0.38	0.023	0.08
KIXAN052	Mar-12	53H	694373	6047680	<0.01	1.82	0.12	10.2	<2	0.6	0.03	62	<0.1	<0.2	0.04	23.2	0.01	<0.02	0.38	0.037	0.28
KIXAN053	Mar-12	53H	731450	6036850	0.04	1.21	0.06	4.7	<2	0.3	0.02	12	<0.1	0.3	<0.01	22.3	<0.01	<0.02	0.42	0.023	0.1
KIXAN054	Mar-12	53H	739084	6033104	0.09	1.49	0.12	12.6	<2	0.6	0.01	29	<0.1	0.3	<0.01	36.2	<0.01	0.02	0.6	0.025	0.02
KIXAN055	Mar-12	54H	233785	6038464	<0.01	1.22	0.09	3.4	<2	0.3	0.03	17	<0.1	0.3	<0.01	62.4	<0.01	<0.02	0.79	0.022	0.16
KIXAN056	Mar-12	54H	234134	6036021	0.02	1.46	0.06	7.9	<2	0.5	0.11	15	<0.1	<0.2	0.01	18.7	0.03	<0.02	0.34	0.031	0.2
KIXAN080	Apr-12	53H	767278	6036572	0.02	1.65	0.15	8	<2	0.4	0.05	16	0.2	<0.2	<0.01	75.7	0.01	<0.02	1.29	0.05	0.91
KIXAN081	Apr-12	54H	230505	6030953	<0.01	1.62	0.08	8.4	<2	0.7	0.09	22	0.3	<0.2	<0.01	35.2	0.03	<0.02	0.65	0.046	0.28
KIXAN082	Apr-12	54H	230814	6030585	<0.01	1.25	0.07	6.2	<2	0.2	0.03	43	0.1	<0.2	<0.01	26.1	<0.01	<0.02	0.57	0.037	0.22
KIXAN083	Apr-12	54H	232823	6028034	0.02	1.06	0.06	5.9	<2	0.3	0.02	10	<0.1	<0.2	<0.01	26.3	<0.01	<0.02	0.7	0.034	0.02
KIXAN084	Apr-12	53H	744314	6031073	0.16	2.31	0.06	10.2	<2	0.4	0.02	14	<0.1	<0.2	<0.01	49.3	0.03	<0.02	0.41	0.039	0.1
KIXAN085	Apr-12	53H	731239	6027397	0.06	2.33	0.04	12.6	<2	0.3	0.02	38	0.1	0.3	0.01	22.9	0.05	<0.02	0.51	0.041	0.02
KIXAN086	Apr-12	53H	731104	6022306	0.06	2.35	0.08	13.8	<2	0.3	0.08	25	<0.1	<0.2	<0.01	38.7	0.02	<0.02	0.47	0.039	0.14
KIXAN087	Apr-12	53H	723957	6023898	0.02	1.45	0.04	8.7	<2	0.4	<0.01	51	<0.1	<0.2	<0.01	122.4	<0.01	<0.02	0.58	0.026	0.01
KIXAN088	Apr-12	53H	724843	6025993	0.02	2.02	0.07	7.2	<2	0.4	0.18	31	<0.1	<0.2	0.02	54.8	0.02	<0.02	0.51	0.032	0.16
KIXAN089	Apr-12	53H	724359	6028039	0.01	1.38	0.06	7.8	<2	0.6	0.17	108	<0.1	2.8	<0.01	33.6	0.02	<0.02	0.63	0.036	0.16
KIXAN090	Apr-12	53H	724232	6029535	0.04	1.01	0.06	7.9	<2	0.5	0.03	25	0.1	<0.2	<0.01	39.3	<0.01	<0.02	0.59	0.037	0.15
KIXAN091	Apr-12	53H	724419	6031878	0.02	1.65	0.1	10.1	<2	0.6	0.05	37	0.1	0.3	0.03	31	<0.01	<0.02	0.41	0.031	0.23
KIXAN092	Apr-12	53H	723981	6034153	0.02	1.54	0.07	6.8	<2	0.2	0.03	25	<0.1	<0.2	0.03	31	0.05	<0.02	0.47	0.035	0.1
KIXAN093	Apr-12	53H	723593	6035303	0.02	1.47	0.1	8.8	<2	0.5	0.05	28	0.4	0.4	0.03	52.9	0.01	0.04	0.58	0.03	0.25
KIXAN094	Apr-12	53H	711397	6038465	0.01	0.8	0.11	6.9	<2	<0.1	0.03	50	<0.1	0.5	0.03	82	0.01	<0.02	0.55	0.019	0.28
KIXAN095	Apr-12	53H	711574	6037252	0.02	1.15	0.05	13.1	<2	0.2	0.06	93	0.4	0.3	0.03	82.9	0.03	<0.02	0.54	0.028	0.22
KIXAN096	Apr-12	53H	713432	6035281	0.03	0.94	0.04	7.4	<2	0.2	0.01	23	0.3	<0.2	<0.01	195.9	<0.01	<0.02	0.61	0.026	0.12
KIXAN097	Apr-12	53H	713171	6033475	<0.01	1.14	0.03	8.1	<2	0.2	0.04	86	0.2	<0.2	<0.01	117.9	0.03	<0.02	0.73	0.03	0.18
KIXAN098	Apr-12	53H	713507	6031183	0.04	1.8	0.03	8.3	<2	0.4	0.04	20	0.2	<0.2	<0.01	32.9	0.02	<0.02	0.38	0.03	0.02
KIXAN099	Apr-12	53H	713428	6029618	0.02	1.21	0.05	5.6	<2	0.4	0.06	26	0.2	0.5	<0.01	49.8	<0.01	<0.02	0.39	0.033	0.13
KIXAN100	Apr-12	53H	713401	6027571	<0.01	1.43	0.04	11.5	<2	0.2	0.02	45	0.1	0.5	<0.01	51	0.03	<0.02	0.62	0.031	0.06
KIXAN101	Apr-12	53H	666483	6029399	0.02	1.11	0.06	8.9	<2	0.3	0.02	20	<0.1	<0.2	<0.01	25.2	<0.01	<0.02	0.49	0.022	0.07
KIXAN102	Apr-12	53H	665504	6027794	<0.01	1.77	0.04	10.8	<2	0.2	<0.01	30	0.2	<0.2	<0.01	76.1	<0.01	<0.02	0.65	0.027	<0.01
KIXAN103	Apr-12	53H	664764	6025670	0.02	2.93	0.03	8.1	<2	0.3	<0.01	25	0.2	<0.2	<0.01	35.2	0.06	<0.02	0.41	0.045	0.02
KIXAN104	Apr-12	53H	663568	6024498	0.16	1.56	0.01	16.7	<2	0.3	0.02	41	0.3	<0.2	<0.01	41.3	0.04	<0.02	0.72	0.027	0.03
KIXAN105	Apr-12	53H	662030	6022925	0.02	0.89	0.02	16.7	<2	0.3	0.03	47	0.1	<0.2	<0.01	50.1	0.02	<0.02	0.5	0.024	0.07
KIXAN106	Apr-12	53H	660937	6020529	0.02	1.46	0.01	14.7	<2	0.6	0.02	41	0.3	<0.2	<0.01	37.2	<0.01	<0.02	1.07	0.028	0.07
KIXAN107	Apr-12	53H	649853	6041631	0.04	1.16	0.05	6.1	<2	0.2	0.02	46	0.2	<0.2	<0.01	36.9	0.01	<0.02	0.61	0.034	0.01
KIXAN108	Apr-12	53H	653587	6040165	0.02	1.23	0.08	6.8	<2	0.7	0.03	17	0.4	<0.2	0.02	65.7	<0.01	<0.02	0.54	0.02	0.23
KIXAN109	Apr-12	53H	656833	6038127	<0.01	1.87	0.07	16	5	0.2	0.02	31	0.2	<0.2	0.02	44.8	0.03	<0.02	0.7	0.036	0.05
KIXAN110	Apr-12	53H	660713	6038011	<0.01	2.1	0.09	8.8	<2	0.2	<0.01	111	0.3	<0.2	<0.01	40.4	0.1	<0.02	0.88	0.03	0.03

Sample	Sampling Period	Zone	Easting	Northing	Mo ppm	Cu ppm	Pb ppm	Zn ppm	Ag ppb	Ni ppm	Co ppm	Mn ppm	As ppm	Au ppb	Th ppm	Sr ppm	Cd ppm	Bi ppm	Ca %	P %	La ppm
KIXAN111	Apr-12	53H	659824	6039012	<0.01	1.37	0.05	6	2	0.1	0.01	40	<0.1	<0.2	<0.01	62.8	<0.01	<0.02	0.78	0.029	0.05
KIXAN112	Apr-12	53H	658961	6040465	0.02	1.11	0.04	9	<2	<0.1	0.02	29	0.3	<0.2	<0.01	33.9	0.01	<0.02	0.49	0.029	<0.01
KIXAN113	Apr-12	53H	658771	6042877	<0.01	1.35	0.04	6.9	<2	0.2	0.02	24	0.4	<0.2	<0.01	79.6	0.02	<0.02	0.7	0.037	0.09
KIXAN114	Apr-12	53H	665470	6037969	<0.01	1.91	0.05	10.7	<2	0.3	<0.01	15	0.3	<0.2	0.01	51.7	0.01	<0.02	0.67	0.033	0.04
KIXAN115	Apr-12	53H	674637	6017214	<0.01	1.43	0.03	8.6	<2	0.2	0.02	32	0.2	<0.2	<0.01	52.6	0.02	<0.02	0.49	0.022	0.08
KIXAN116	Apr-12	53H	674233	6020625	<0.01	1.61	0.07	5.6	<2	0.2	0.03	32	0.2	0.6	<0.01	25.2	0.03	<0.02	0.6	0.028	0.08
KIXAN117	Apr-12	53H	674233	6020625	0.1	1.74	0.04	7.7	<2	0.3	0.02	33	0.3	<0.2	<0.01	35.2	0.02	<0.02	0.42	0.034	0.06
KIXAN118	Apr-12	53H	673362	6022408	0.02	1.87	0.03	8.8	<2	0.3	0.02	13	0.3	<0.2	<0.01	46.1	0.02	<0.02	0.33	0.027	0.05
KIXAN119	Apr-12	53H	672088	6024411	<0.01	1.77	0.07	10.6	<2	0.2	<0.01	25	<0.1	<0.2	<0.01	28.5	0.09	<0.02	0.43	0.032	0.02
KIXAN120	Apr-12	53H	670815	6025661	<0.01	1.48	0.04	6.4	<2	0.4	0.01	14	0.2	<0.2	<0.01	36.2	<0.01	<0.02	0.34	0.024	0.07
KIXAN121	Apr-12	53H	668600	6026200	0.03	1.45	0.07	6.8	<2	0.1	0.02	20	0.2	<0.2	<0.01	57.3	<0.01	<0.02	0.54	0.028	0.03
KIXAN122	Apr-12	53H	670104	6039096	0.02	0.96	0.05	5.8	<2	0.3	0.02	25	<0.1	0.3	<0.01	55.1	<0.01	<0.02	0.61	0.021	<0.01
KIXAN123	Apr-12	53H	670221	6039473	0.04	1.95	0.02	9.6	<2	0.5	0.01	42	0.2	<0.2	<0.01	34.3	<0.01	<0.02	0.55	0.03	<0.01
KIXAN124	Apr-12	53H	670539	6040691	0.02	0.98	0.05	7.8	<2	0.2	0.03	12	<0.1	<0.2	0.02	26.4	<0.01	<0.02	0.57	0.02	0.03
KIXAN125	Apr-12	53H	669664	6044450	<0.01	2.02	0.1	19.4	<2	0.3	0.04	28	0.3	<0.2	0.03	52.3	<0.01	<0.02	0.58	0.034	0.16
KIXAN126	Apr-12	53H	668459	6046461	0.03	1.6	0.08	8.4	<2	0.2	0.01	11	<0.1	<0.2	0.02	35.8	<0.01	<0.02	0.44	0.03	0.1
KIXAN127	Apr-12	53H	670537	6042204	<0.01	1.4	0.05	7.1	<2	0.6	0.01	62	0.2	<0.2	0.02	36.2	<0.01	<0.02	0.62	0.023	<0.01
KIXAN128	Apr-12	53H	672089	6038131	<0.01	1.52	0.05	8.9	<2	0.2	<0.01	15	<0.1	<0.2	<0.01	48.8	<0.01	0.09	0.77	0.023	0.03
KIXAN129	Apr-12	53H	677015	6036757	<0.01	1.39	0.04	7.8	<2	0.3	<0.01	24	<0.1	<0.2	<0.01	36.7	0.02	<0.02	0.52	0.023	0.08
KIXAN130	Apr-12	53H	683685	6029949	0.02	1.62	0.24	8.7	<2	0.2	<0.01	31	<0.1	<0.2	0.01	52.6	0.02	<0.02	0.86	0.036	0.08
KIXAN131	Apr-12	53H	683772	6031864	<0.01	2.05	0.09	9.2	<2	0.5	0.02	48	<0.1	<0.2	0.01	61.4	0.02	<0.02	0.72	0.034	0.15
KIXAN132	Apr-12	53H	683364	6034390	0.03	2.98	0.07	11.8	<2	0.5	<0.01	67	<0.1	<0.2	0.05	45.6	0.04	<0.02	0.69	0.033	0.02
KIXAN133	Apr-12	53H	682851	6036544	<0.01	2.5	0.28	9.3	<2	0.4	<0.01	19	<0.1	<0.2	<0.01	16.1	0.04	<0.02	0.62	0.034	0.02
KIXAN134	Apr-12	53H	684090	6037421	0.02	1.36	0.69	7.8	<2	0.2	0.02	19	0.1	0.4	0.06	23.2	0.08	<0.02	0.4	0.034	0.12
KIXAN135	Apr-12	53H	683972	6039476	0.01	1.17	0.19	10.5	<2	0.1	<0.01	31	<0.1	0.7	0.02	45.4	0.02	<0.02	0.68	0.024	0.17
KIXAN136	Apr-12	53H	683737	6042352	0.03	1.93	0.11	9.6	5	0.5	0.01	36	<0.1	<0.2	0.09	41.8	0.06	<0.02	0.48	0.029	0.13
KIXAN137	Apr-12	53H	683629	6044283	0.01	1.8	0.36	8.2	2	0.3	<0.01	65	0.1	<0.2	0.02	37	0.03	<0.02	0.73	0.035	0.05
KIXAN138	Apr-12	53H	683366	6046498	<0.01	1.63	0.27	12.8	<2	0.2	<0.01	54	<0.1	<0.2	0.01	70.1	0.05	<0.02	0.72	0.041	0.05
KIXAN139	Apr-12	53H	684900	6048700	0.03	1.23	0.37	6.3	<2	0.2	0.03	31	<0.1	<0.2	0.07	81.5	<0.01	<0.02	0.61	0.032	0.24
KIXAN140	Apr-12	53H	700777	6052678	0.04	1.58	0.58	7.8	<2	1.5	0.1	26	<0.1	<0.2	0.04	155.4	<0.01	<0.02	0.95	0.034	1.45
KIXAN141	Apr-12	53H	700497	6050989	0.03	1.43	0.23	32.2	<2	0.5	0.01	32	<0.1	<0.2	0.03	40.3	0.03	<0.02	0.56	0.033	0.75
KIXAN142	Apr-12	53H	700461	6049237	<0.01	0.95	0.21	8.8	<2	0.1	<0.01	10	<0.1	<0.2	<0.01	37.9	<0.01	<0.02	0.41	0.024	0.07
KIXAN143	Apr-12	53H	700386	6046668	0.01	1.31	0.19	5.7	<2	0.3	0.07	74	<0.1	<0.2	<0.01	34.7	0.05	<0.02	0.46	0.033	0.1
KIXAN144	Apr-12	53H	700348	6044156	0.01	1.69	0.2	12.6	<2	0.2	0.02	31	0.2	0.3	<0.01	68.2	0.04	<0.02	0.89	0.033	0.17
KIXAN145	Apr-12	53H	700223	6040101	0.03	1.16	0.16	10	<2	0.1	0.03	35	<0.1	<0.2	<0.01	35.8	<0.01	<0.02	0.54	0.032	0.1
KIXAN146	Apr-12	53H	700208	6037602	0.05	1.93	0.06	10.4	<2	0.3	0.03	14	<0.1	0.3	<0.01	25	0.03	<0.02	0.29	0.043	0.03
KIXAN147	Apr-12	53H	700938	6020105	0.04	1.26	0.18	5.6	<2	0.4	0.05	43	<0.1	0.3	0.03	48.9	<0.01	<0.02	0.68	0.021	0.05
KIXAN148	Apr-12	53H	699502	6021989	0.02	1.74	0.11	6.1	<2	0.4	0.02	25	<0.1	<0.2	<0.01	25.7	0.06	<0.02	0.34	0.038	0.04
KIXAN149	Apr-12	53H	698420	6023909	0.01	1.05	0.26	9.8	<2	0.3	0.05	29	<0.1	<0.2	0.02	95.5	0.01	<0.02	0.58	0.025	0.07
KIXAN150	Apr-12	53H	697733	6025777	0.01	1.47	0.22	12.7	<2	0.1	0.03	77	<0.1	0.3	0.02	77.2	0.02	<0.02	0.77	0.035	0.29
KIXAN151	Apr-12	53H	696730	6028306	0.01	1.18	0.22	5.5	<2	0.3	0.01	27	0.2	<0.2	0.02	53.4	<0.01	<0.02	0.55	0.032	0.16
KIXAN152	Apr-12	53H	697076	6030163	0.02	1.87	0.14	6.1	<2	0.3	<0.01	25	0.2	0.6	0.03	40.9	0.01	<0.02	0.45	0.028	0.18
KIXAN153	Apr-12	53H	698357	6032393	<0.01	1.47	0.17	7.6	<2	0.3	0.02	38	0.2	<0.2	0.02	37.2	<0.01	<0.02	0.44	0.029	0.06
KIXAN154	Apr-12	53H	698080	6035284	0.01	4.54	0.12	9.3	2	0.6	0.1	59	0.2	<0.2	0.05	25.5	0.2	<0.02	0.43	0.079	0.21
KIXAN155	Apr-12	53H	709308	6052961	0.02	1.91	0.19	11.8	<2	0.4	0.04	50	<0.1	<0.2	0.05	35.8	0.04	0.04	0.52	0.023	0.06

Sample	Sampling Period	Zone	Easting	Northing	Mo ppm	Cu ppm	Pb ppm	Zn ppm	Ag ppb	Ni ppm	Co ppm	Mn ppm	As ppm	Au ppb	Th ppm	Sr ppm	Cd ppm	Bi ppm	Ca %	P %	La ppm
KIXAN156	Apr-12	53H	709523	6055111	<0.01	1.19	0.15	22.3	<2	0.4	<0.01	8	0.1	<0.2	0.01	37.8	<0.01	<0.02	0.37	0.023	0.07
KIXAN157	Apr-12	53H	710989	6056082	0.06	1.68	0.18	9.7	<2	0.3	0.06	27	<0.1	<0.2	0.04	43.1	0.06	<0.02	0.42	0.032	0.14
KIXAN158	Apr-12	53H	710436	6057344	<0.01	0.89	0.16	7.3	<2	1.2	0.13	21	<0.1	<0.2	<0.01	80.2	0.03	<0.02	0.57	0.024	0.54
KIXAN159	Apr-12	53H	719249	6053309	0.04	1.43	0.07	9.7	<2	0.3	0.08	16	0.1	<0.2	<0.01	22	0.06	<0.02	0.28	0.03	0.06
KIXAN160	Apr-12	53H	718690	6051942	0.01	1.47	0.1	4.3	<2	0.2	0.03	27	0.3	<0.2	0.03	65.4	0.02	<0.02	0.47	0.028	0.71
KIXAN161	Apr-12	53H	715875	6052350	0.01	1.1	0.15	5.9	<2	0.5	0.06	30	<0.1	<0.2	0.01	75.7	0.02	<0.02	0.53	0.02	0.63
KIXAN162	Apr-12	53H	715741	6049998	0.01	0.77	0.22	9	<2	0.2	0.05	10	0.1	0.4	0.02	200.3	0.03	<0.02	0.64	0.029	0.11
KIXAN163	Apr-12	53H	715703	6048087	0.06	2.87	0.29	11.5	<2	0.1	0.07	68	<0.1	0.4	0.02	34.4	0.18	<0.02	0.44	0.04	0.06
KIXAN164	Apr-12	53H	715655	6046018	0.02	1.48	0.23	6.3	<2	0.3	0.05	16	<0.1	<0.2	0.01	35	0.03	<0.02	0.41	0.031	0.16
KIXAN165	Apr-12	53H	744472	6034076	0.03	1.72	0.09	7.1	<2	0.3	0.03	9	<0.1	0.3	<0.01	94.6	0.02	<0.02	0.73	0.035	0.04
KIXAN166	Apr-12	53H	744417	6032021	0.01	1.72	0.21	8.1	<2	0.3	<0.01	39	<0.1	0.6	<0.01	57	0.01	<0.02	0.56	0.033	<0.01
KIXAN200	Apr-13	53H	707439	6035795	0.12	1.29	0.12	9.8	5	0.5	0.03	37	<0.1	<0.2	0.02	37.3	0.01	0.03	0.49	0.026	0.09
KIXAN201	Apr-13	53H	709656	6035362	0.06	1.22	0.07	5.3	<2	0.4	0.07	44	<0.1	<0.2	0.02	98.1	<0.01	<0.02	0.68	0.02	0.15
KIXAN202	Apr-13	53H	719115	6035158	0.08	1.28	0.08	12.6	<2	0.3	0.01	16	<0.1	<0.2	0.03	43.7	0.03	<0.02	0.46	0.025	0.15
KIXAN203	Apr-13	53H	719181	6036782	0.04	1.47	0.04	8.5	<2	0.9	0.03	50	<0.1	<0.2	0.01	34	0.03	<0.02	0.48	0.031	0.13
KIXAN204	Apr-13	53H	719468	6038996	0.04	1.33	0.05	17.2	4	0.2	0.05	72	<0.1	<0.2	0.01	38.5	0.02	<0.02	0.67	0.029	0.37
KIXAN205	Apr-13	53H	719796	6040445	0.03	1.62	0.07	5.7	<2	0.6	0.04	32	<0.1	0.3	0.01	134.1	<0.01	<0.02	0.86	0.028	0.41
KIXAN206	Apr-13	53H	727374	6044091	0.05	1.1	0.02	6	<2	0.3	0.06	74	0.1	0.4	<0.01	24.6	0.02	<0.02	0.44	0.023	0.1
KIXAN207	Apr-13	53H	725982	6039822	0.09	1.15	0.02	5	2	0.4	0.03	28	<0.1	0.4	<0.01	28.6	0.04	<0.02	0.6	0.028	0.02
KIXAN208	Apr-13	53H	717943	6026808	0.03	1.47	0.03	8.3	<2	0.3	0.04	28	0.1	0.3	<0.01	14.2	<0.01	<0.02	0.37	0.024	0.05
KIXAN209	Apr-13	53H	720802	6027834	0.04	1.5	0.08	21.5	<2	1.3	0.2	156	<0.1	0.4	<0.01	23.8	0.61	<0.02	0.45	0.028	0.25
KIXAN210	Apr-13	53H	720183	6024778	0.08	1.11	0.03	6.4	<2	0.8	0.05	10	<0.1	0.3	<0.01	39.6	<0.01	<0.02	0.63	0.026	0.08
KIXAN211	Apr-13	53H	725240	6023230	0.07	1.73	0.23	7.1	<2	0.5	0.06	24	<0.1	0.3	0.02	37.6	0.02	<0.02	0.5	0.032	0.26
KIXAN212	Apr-13	53H	729236	6022112	0.1	2.19	0.05	8.2	<2	0.3	0.09	15	<0.1	0.4	0.02	19.2	0.03	<0.02	0.33	0.031	0.26
KIXAN213	Apr-13	53H	731840	6021196	0.15	0.96	0.05	7.8	<2	0.5	0.06	76	<0.1	<0.2	0.02	70.3	0.01	<0.02	1.14	0.022	0.12
KIXAN214	Apr-13	53H	749709	6037926	0.23	1.59	0.03	7.2	<2	0.2	0.03	8	<0.1	0.3	<0.01	31.2	<0.01	<0.02	0.47	0.093	0.03
KIXAN215	Apr-13	53H	752793	6039501	0.07	1.18	0.04	6.1	<2	0.6	0.02	6	<0.1	<0.2	<0.01	122.5	<0.01	<0.02	0.79	0.023	0.02
KIXAN216	Apr-13	53H	751267	6039333	0.11	2.37	0.05	11.4	<2	0.2	0.04	3	<0.1	0.3	0.01	118.5	<0.01	<0.02	0.83	0.036	0.07
KIXAN217	Apr-13	53H	749744	6041150	0.07	1.35	0.11	8.3	<2	0.3	0.08	25	0.3	<0.2	0.04	27.5	0.03	<0.02	0.43	0.026	0.23
KIXAN218	Apr-13	53H	737517	6038253	0.09	1.49	0.07	10.1	<2	0.3	0.03	11	<0.1	<0.2	<0.01	17	0.02	<0.02	0.32	0.032	0.02
KIXAN219	Apr-13	53H	737348	6037517	0.09	1.7	0.11	6	<2	0.8	0.07	50	0.1	<0.2	0.02	18.3	0.05	<0.02	0.45	0.031	0.04
KIXAN220	Apr-13	53H	736739	6034351	0.13	1.61	0.1	4.3	<2	0.6	0.04	39	<0.1	<0.2	0.02	23.3	0.02	<0.02	0.77	0.029	0.25
KIXAN221	Apr-13	53H	736325	6033038	0.09	1.1	0.04	8.8	<2	0.2	0.05	27	0.2	<0.2	0.02	46.4	<0.01	<0.02	0.94	0.024	0.49
KIXAN222	Apr-13	53H	735730	6030916	0.17	1.36	0.04	7	<2	0.4	0.05	37	<0.1	<0.2	0.03	27.8	0.04	<0.02	0.74	0.028	0.16
KIXAN223	Apr-13	53H	739017	6028163	0.3	1.16	0.03	5.4	<2	0.2	0.03	4	<0.1	0.4	<0.01	21.2	<0.01	<0.02	0.73	0.029	0.03
KIXAN224	Apr-13	53H	738551	6031588	0.12	2	0.04	9.5	<2	0.2	0.02	29	<0.1	<0.2	<0.01	42.5	0.03	<0.02	0.76	0.03	0.02
KIXAN225	Apr-13	53H	768329	6035878	0.09	1.14	0.18	6.8	<2	0.8	0.06	18	<0.1	<0.2	0.05	34.7	<0.01	<0.02	0.6	0.029	0.26
KIXAN226	Apr-13	53H	770224	6033876	0.09	1.49	0.07	7.9	<2	1	0.09	13	<0.1	<0.2	0.03	23.6	0.02	<0.02	0.29	0.041	0.2
KIXAN227	Apr-13	54H	233774	6038416	0.09	1.07	0.02	5.4	<2	1.1	0.03	16	<0.1	0.2	<0.01	42.9	<0.01	<0.02	0.64	0.021	0.04
KIXAN228	Apr-13	54H	233768	6038414	0.07	1.18	0.02	5	<2	0.4	0.05	12	<0.1	0.2	<0.01	32.5	<0.01	<0.02	0.52	0.025	0.03
KIXAN229	Apr-13	54H	233753	6038419	0.06	1.05	0.05	5.1	<2	0.6	0.03	19	<0.1	0.2	0.01	32.6	<0.01	<0.02	0.45	0.022	0.04
KIXAN230	Apr-13	54H	233731	6038400	0.08	1.05	0.09	5.7	<2	0.6	0.08	6	0.3	<0.2	0.04	55.9	<0.01	<0.02	0.83	0.028	0.13
KIXAN231	Apr-13	53H	702198	6046341	0.05	1.03	0.05	11.6	<2	0.6	0.02	47	<0.1	<0.2	<0.01	47.6	0.02	<0.02	0.3	0.023	0.19
KIXAN232	Apr-13	53H	702102	6046329	0.09	1.25	0.02	9.5	<2	0.6	0.03	146	<0.1	<0.2	<0.01	40	0.18	<0.02	0.51	0.024	0.03
KIXAN233	Apr-13	53H	702125	6046275	0.04	0.94	0.01	14.4	<2	0.2	0.01	139	<0.1	<0.2	<0.01	24.4	0.29	0.05	0.4	0.023	0.02

Sample	Sampling Period	Zone	Easting	Northing	Mo ppm	Cu ppm	Pb ppm	Zn ppm	Ag ppb	Ni ppm	Co ppm	Mn ppm	As ppm	Au ppb	Th ppm	Sr ppm	Cd ppm	Bi ppm	Ca %	P %	La ppm
KIXAN234	Apr-13	53H	702086	6046194	0.05	1.2	0.01	15.2	<2	1	0.03	280	0.3	0.4	<0.01	20.1	0.1	0.02	0.31	0.025	0.17
KIXAN235	Apr-13	53H	702013	6046170	0.04	1.14	0.46	8	<2	0.2	0.03	174	0.1	<0.2	<0.01	31.8	0.02	<0.02	0.45	0.026	0.04
KIXAN236	Apr-13	53H	701964	6046152	0.04	1.16	2.59	9.7	<2	0.3	0.03	31	0.1	0.2	<0.01	28.8	0.05	<0.02	0.47	0.021	0.05
KIXAN237	Apr-13	53H	701871	6046132	0.04	1.23	0.13	7.5	<2	0.6	0.02	28	0.3	<0.2	<0.01	40.6	<0.01	<0.02	0.38	0.029	0.23
KIXAN238	Apr-13	53H	702009	6046286	0.06	1.22	0.14	24.2	<2	0.2	0.02	114	0.1	<0.2	<0.01	34.7	<0.01	<0.02	0.48	0.025	0.15
KIXAN239	Apr-13	53H	702041	6046345	0.06	1.41	0.08	19.5	<2	1.3	0.23	241	<0.1	<0.2	<0.01	25.4	0.61	<0.02	0.48	0.027	0.29
KIXAN240	Apr-13	53H	702125	6046423	0.02	1.33	0.13	11.9	<2	0.9	0.02	31	<0.1	<0.2	<0.01	46.8	0.39	<0.02	0.43	0.035	0.64
KIXAN241	Apr-13	53H	702198	6046565	0.02	1.1	3.29	18.3	<2	0.4	0.02	36	0.2	<0.2	<0.01	83.2	0.03	<0.02	0.59	0.025	0.14
KIXAN242	Apr-13	53H	702198	6046565	0.06	1.12	0.03	13.2	<2	0.4	0.03	34	0.4	<0.2	<0.01	76.7	<0.01	<0.02	0.47	0.023	0.03
KIXAN243	Apr-13	53H	702147	6046570	0.05	0.8	9.3	7.5	<2	0.4	0.03	56	0.1	<0.2	<0.01	51.2	0.03	<0.02	0.43	0.024	0.34
KIXAN244	Apr-13	53H	702076	6046594	0.05	1.35	0.07	19.5	<2	0.8	0.02	21	<0.1	<0.2	<0.01	40.7	0.01	<0.02	0.34	0.027	0.34
KIXAN245	Apr-13	53H	702007	6046606	0.08	1.06	0.03	19.1	<2	0.6	0.06	37	<0.1	<0.2	<0.01	61.3	<0.01	<0.02	0.27	0.027	0.17
KIXAN246	Apr-13	53H	702040	6046531	0.08	0.86	0.06	12.5	<2	1.2	0.11	64	0.3	<0.2	<0.01	69.5	0.07	<0.02	0.37	0.025	0.59
KIXAN247	Apr-13	53H	702102	6046507	0.06	0.91	0.8	12.3	<2	0.6	0.03	50	<0.1	<0.2	<0.01	101.1	0.05	<0.02	0.87	0.02	0.24
KIXAN248	Apr-13	53H	702083	6046480	0.08	1.01	0.06	5.6	<2	0.3	0.05	95	0.2	<0.2	<0.01	56.4	0.1	<0.02	0.69	0.023	0.28
KIXAN249	Apr-13	53H	701942	6040422	0.1	1.12	0.64	254.8	<2	0.8	0.12	198	0.2	<0.2	<0.01	24.2	3	<0.02	0.5	0.025	0.41
KIXAN250	Apr-13	53H	701921	6046351	0.1	1.24	0.05	18.1	<2	0.5	0.03	30	0.4	<0.2	<0.01	30.8	0.03	<0.02	0.4	0.024	0.13
KIXAN251	Apr-13	53H	701982	6046315	0.09	0.87	0.07	23	<2	0.2	0.03	27	<0.1	<0.2	<0.01	64.6	0.01	<0.02	0.7	0.023	0.25
KIXAN252	Apr-13	53H	690177	6036271	0.1	1.8	0.04	7.3	<2	0.3	0.03	44	0.3	<0.2	0.01	39.1	0.01	<0.02	0.63	0.026	0.05
KIXAN253	Apr-13	53H	679882	6037553	0.09	1.08	0.14	8.8	<2	0.4	0.04	96	<0.1	<0.2	0.1	75	<0.01	<0.02	0.75	0.025	0.09
KIXAN254	Apr-13	53H	679633	6041301	0.09	1.23	0.05	6	<2	0.2	0.02	29	0.2	<0.2	0.01	60	<0.01	<0.02	0.79	0.026	0.06
KIXAN255	Apr-13	53H	680838	6044131	0.09	1.57	0.04	11.6	<2	1.1	0.02	10	0.5	<0.2	0.02	56.5	0.03	<0.02	0.58	0.031	0.03
KIXAN256	Apr-13	53H	680489	6046576	0.09	1.04	0.05	13	<2	0.2	0.03	20	0.2	<0.2	0.02	65.4	<0.01	<0.02	0.65	0.026	0.09
KIXAN257	Apr-13	53H	687505	6043739	0.11	1.84	0.06	9.6	<2	0.4	0.02	33	0.2	<0.2	0.03	60.3	<0.01	<0.02	0.7	0.03	0.06
KIXAN258	Apr-13	53H	690537	6043954	0.12	1.71	0.11	10.9	<2	0.4	0.03	19	<0.1	<0.2	0.08	76.4	0.02	<0.02	0.73	0.03	0.13
KIXAN259	Apr-13	53H	692264	6044119	0.09	1.32	0.05	14.4	<2	0.2	0.04	62	0.2	<0.2	0.02	46.9	<0.01	<0.02	0.46	0.031	0.15
KIXAN260	Apr-13	53H	695291	6046454	0.1	1.58	0.04	9.5	3	0.2	0.04	31	0.4	<0.2	<0.01	64.9	<0.01	<0.02	0.64	0.029	0.03
KIXAN261	Apr-13	53H	706811	6053367	0.08	1.49	0.05	11.5	<2	0.4	0.03	61	<0.1	<0.2	0.01	39.6	0.05	<0.02	0.56	0.025	0.21
KIXAN262	Apr-13	53H	706714	6050896	0.08	1.57	0.07	3.9	<2	0.2	0.04	42	<0.1	<0.2	0.01	73.7	0.02	<0.02	1.26	0.026	0.24
KIXAN263	Apr-13	53H	705692	6046648	0.08	1.85	0.04	5.5	<2	0.3	0.05	30	0.2	<0.2	0.02	54	0.01	<0.02	0.47	0.036	0.27
KIXAN264	Apr-13	53H	705549	6045464	0.08	1.57	0.04	11.8	<2	0.3	0.02	21	0.3	<0.2	<0.01	55.9	<0.01	<0.02	0.44	0.031	0.1
KIXAN265	Apr-13	53H	699982	6039027	0.08	1.46	0.06	5.1	<2	0.2	0.04	11	<0.1	<0.2	0.03	75.9	<0.01	<0.02	0.77	0.033	0.16
KIXAN266	Apr-13	53H	699982	6039027	0.08	1.3	0.05	11.1	4	0.2	0.03	44	0.2	<0.2	<0.01	29.1	0.02	<0.02	0.45	0.025	0.07
KIXAN267	Apr-13	53H	697324	6039270	0.08	1.37	0.08	9.7	<2	0.4	0.07	50	0.2	<0.2	0.01	56.1	0.02	<0.02	0.91	0.026	0.24
KIXAN268	Apr-13	53H	704871	6038561	0.09	1.31	0.05	12.5	4	0.3	0.03	12	<0.1	0.2	<0.01	37.6	0.02	0.07	0.37	0.021	0.05
KIXAN269	Apr-13	53H	703851	6021808	0.04	1.54	0.06	11.7	<2	0.8	0.3	124	<0.1	<0.2	0.01	30.7	0.16	<0.02	0.42	0.032	0.29
KIXAN270	Apr-13	53H	702993	6024406	0.08	1.15	0.05	10.9	<2	0.4	0.03	44	<0.1	<0.2	0.03	48.7	<0.01	<0.02	0.48	0.026	0.07
KIXAN271	Apr-13	53H	702850	6026743	0.04	1.07	0.05	7.2	<2	0.5	0.02	25	<0.1	<0.2	0.01	30.9	<0.01	<0.02	0.57	0.033	0.08
KIXAN272	Apr-13	53H	703187	6028743	0.03	1.15	0.03	9.8	<2	0.5	0.06	28	<0.1	<0.2	0.01	53.5	<0.01	<0.02	0.33	0.026	0.09
KIXAN273	Apr-13	53H	702985	6030988	0.05	1.31	0.08	11.7	<2	0.2	0.03	33	<0.1	<0.2	0.05	43	<0.01	<0.02	0.39	0.026	0.13
KIXAN274	Apr-13	53H	699977	6031291	0.06	1.35	0.03	8.5	<2	0.4	0.01	35	<0.1	<0.2	<0.01	39.2	<0.01	<0.02	0.46	0.024	0.05
KIXAN275	Apr-13	53H	692346	6031061	0.05	1.84	0.05	16.7	<2	0.2	0.03	36	<0.1	<0.2	0.07	34.7	0.02	<0.02	0.57	0.039	0.07
KIXAN276	Apr-13	53H	692575	6027761	0.05	1.37	0.04	8	<2	0.4	0.01	37	0.2	<0.2	0.04	20.8	<0.01	<0.02	0.45	0.032	0.07
KIXAN277	Apr-13	53H	692532	6024316	0.05	1.56	0.04	8	<2	0.6	0.02	21	<0.1	<0.2	0.02	38.4	<0.01	<0.02	0.77	0.024	0.1
KIXAN278	Apr-13	53H	692999	6021850	0.05	1	0.07	4.8	<2	0.6	0.05	22	<0.1	<0.2	0.02	116.9	<0.01	<0.02	1.2	0.023	0.3

Sample	Sampling Period	Zone	Eastings	Northing	Mo ppm	Cu ppm	Pb ppm	Zn ppm	Ag ppb	Ni ppm	Co ppm	Mn ppm	As ppm	Au ppb	Th ppm	Sr ppm	Cd ppm	Bi ppm	Ca %	P %	La ppm
KIXAN279	Apr-13	53H	693803	6019221	0.08	1.21	0.03	10.5	<2	0.4	0.04	32	<0.1	<0.2	0.02	45.6	<0.01	<0.02	0.68	0.025	0.09
KIXAN281	Apr-13	53H	695762	6017171	0.06	1.2	0.06	11.5	<2	0.3	0.04	56	<0.1	0.3	0.04	33.9	<0.01	<0.02	0.47	0.026	0.22
KIXAN282	Apr-13	53H	680717	6016908	0.06	1.11	0.04	5	<2	0.3	0.03	54	<0.1	0.3	<0.01	21.2	<0.01	<0.02	0.49	0.026	0.12
KIXAN283	Apr-13	53H	680334	6019079	0.05	1.21	<0.01	5.5	<2	0.4	0.02	53	<0.1	<0.2	<0.01	35.1	<0.01	<0.02	0.45	0.027	0.08
KIXAN284	Apr-13	53H	679663	6020983	0.06	1.44	0.05	11.7	<2	0.5	0.03	42	<0.1	0.5	0.02	19.5	<0.01	<0.02	0.46	0.026	0.16
KIXAN285	Apr-13	53H	679580	6022229	0.06	1.48	0.02	10.7	<2	0.6	0.01	25	<0.1	0.4	<0.01	24.2	<0.01	<0.02	0.63	0.025	0.09
KIXAN286	Apr-13	53H	678880	6025908	0.05	1.07	0.01	7.6	<2	0.1	0.02	17	<0.1	<0.2	<0.01	38	0.04	<0.02	0.97	0.025	0.05
KIXAN287	Apr-13	53H	678833	6035613	0.06	1.17	0.02	11.8	<2	0.3	<0.01	17	<0.1	<0.2	0.01	31	<0.01	<0.02	0.54	0.024	0.07
KIXAN288	Apr-13	53H	664366	6024811	0.07	1.21	<0.01	4	<2	0.6	<0.01	9	0.3	<0.2	<0.01	40.6	<0.01	<0.02	0.29	0.027	0.04
KIXAN289	Apr-13	53H	665568	6023456	0.18	1.65	<0.01	25.1	<2	0.5	0.03	42	<0.1	0.5	<0.01	122.5	0.02	<0.02	1.04	0.038	0.11
KIXAN290	Apr-13	53H	667559	6022358	0.08	1.32	0.03	5.5	<2	0.2	0.01	45	<0.1	<0.2	<0.01	42.8	<0.01	<0.02	0.6	0.022	0.04
KIXAN291	Apr-13	53H	669607	6022205	0.09	2.07	0.02	11.8	<2	0.2	<0.01	31	<0.1	0.3	<0.01	28.9	0.02	<0.02	0.5	0.03	0.07
KIXAN292	Apr-13	53H	672682	6022174	0.09	1.35	<0.01	18.5	<2	1.1	0.03	21	0.2	<0.2	<0.01	24.3	0.02	<0.02	0.82	0.029	0.09
KIXAN293	Apr-13	53H	683859	6016252	0.08	1.61	0.03	8.8	<2	0.4	0.04	27	<0.1	<0.2	<0.01	37.1	0.02	<0.02	1.01	0.028	0.33
KIXAN294	Apr-13	53H	684655	6024042	0.09	1.72	0.03	14.4	<2	0.4	0.02	40	0.1	<0.2	<0.01	34.9	<0.01	<0.02	0.76	0.036	0.09
KIXAN295	Apr-13	53H	691699	6033540	0.2	1.1	0.09	5.8	2	0.1	0.02	41	0.2	<0.2	0.08	19.6	<0.01	<0.02	0.65	0.032	0.15
KIXAN296	Apr-13	53H	677752	6049450	0.12	1.61	3.53	10.2	5	0.3	0.01	22	<0.1	<0.2	<0.01	47.8	<0.01	<0.02	0.53	0.035	0.09
KIXAN297	Apr-13	53H	677752	6049450	0.1	1.38	25.46	8.1	11	0.1	<0.01	69	<0.1	0.2	<0.01	18.5	0.15	<0.02	0.38	0.037	0.06
KIXAN298	Apr-13	53H	677709	6049449	0.09	2	1.94	14.8	2	<0.1	0.02	7	0.2	<0.2	<0.01	79.5	<0.01	<0.02	1.15	0.041	0.55
KIXAN299	Apr-13	53H	674543	6041379	0.09	1.44	0.05	9.3	<2	0.4	<0.01	17	<0.1	0.3	<0.01	49.1	0.03	<0.02	0.59	0.028	0.08
KIXAN300	Apr-13	53H	702846	6033214	0.12	1.3	0.05	8.6	<2	0.4	0.02	27	<0.1	<0.2	0.06	33.3	<0.01	<0.02	0.43	0.023	0.23
KIXAN301	Apr-13	53H	704689	6034979	0.11	1.15	0.02	7.1	<2	0.3	0.03	59	<0.1	0.3	<0.01	72.9	0.01	<0.02	0.76	0.028	0.22
KIXAN302	Apr-13	53H	704695	6041585	0.11	1.5	0.1	10.4	<2	0.3	0.02	23	<0.1	0.3	0.01	68.6	<0.01	<0.02	0.7	0.029	0.28
KIXAN303	Apr-13	53H	702063	6038634	0.05	1.31	0.02	7.8	<2	0.3	0.02	31	<0.1	<0.2	0.04	36.9	<0.01	0.05	0.64	0.027	0.11
KIXAN304	Apr-13	53H	695890	6039376	0.03	1.79	0.03	16.4	<2	0.2	0.03	21	<0.1	<0.2	0.03	60.4	<0.01	0.02	0.48	0.033	0.07
KIXAN305	Apr-13	53H	693052	6042412	0.02	1.52	0.01	7	<2	0.2	0.03	62	<0.1	<0.2	0.02	39.3	<0.01	<0.02	0.54	0.036	0.1
KIXAN306	Apr-13	53H	690545	6041216	0.01	1.5	0.02	11.7	<2	0.3	0.04	51	<0.1	<0.2	0.01	46.7	<0.01	<0.02	0.61	0.03	0.09
KIXAN307	Apr-13	53H	684252	6037185	0.04	1.06	0.03	5.1	<2	0.2	0.02	85	<0.1	<0.2	0.01	108.1	<0.01	<0.02	0.79	0.029	0.18
KIXAN308	Apr-13	53H	724523	6030514	0.14	1.11	0.04	6.7	<2	0.3	0.01	31	<0.1	<0.2	0.02	21.5	0.01	<0.02	0.37	0.026	0.02
KIXAN309	Apr-13	53H	710592	6025146	0.03	1.25	<0.01	9.1	<2	0.4	0.04	48	<0.1	<0.2	<0.01	51.4	<0.01	<0.02	0.55	0.034	0.16
KIXAN310	Apr-13	53H	708539	6025993	0.05	0.95	0.11	2.9	<2	0.4	0.05	36	0.2	<0.2	0.03	56.7	<0.01	<0.02	0.71	0.027	0.25
KIXAN311	Apr-13	53H	708724	6028827	0.06	1.23	0.01	5.6	<2	0.3	0.03	54	<0.1	<0.2	<0.01	35.4	0.01	<0.02	0.45	0.027	0.12
KIXAN312	Apr-13	53H	709277	6040724	0.06	1.13	0.04	10	<2	0.4	0.04	60	<0.1	<0.2	0.02	50.3	<0.01	<0.02	0.86	0.03	0.46
KIXAN313	Apr-13	53H	708624	6023892	0.05	1.18	<0.01	6.4	<2	0.4	0.04	24	<0.1	<0.2	<0.01	51.5	0.01	<0.02	0.53	0.026	0.15
KIXAN314	Apr-13	53H	717310	6041561	0.02	1.22	0.05	7.5	26	0.4	0.05	31	<0.1	<0.2	0.03	35.8	0.01	0.02	0.63	0.023	0.06
KIXAN315	Apr-13	53H	715782	6042796	0.04	0.93	0.02	6.1	<2	0.3	0.06	17	0.1	<0.2	0.01	39.4	0.02	<0.02	0.47	0.021	0.08
KIXAN316	Apr-13	53H	710064	6045006	0.05	1.75	0.02	5.7	<2	0.4	0.03	43	0.1	<0.2	0.01	60.1	<0.01	<0.02	0.51	0.03	0.03
KIXAN317	Apr-13	53H	708035	6045704	0.06	1.64	0.04	7.6	<2	0.3	0.03	52	<0.1	<0.2	0.03	37.8	0.02	<0.02	0.78	0.033	0.47
KIXAN318	Apr-13	53H	704699	6047048	0.07	1.19	0.03	6	<2	0.3	0.03	18	<0.1	<0.2	0.04	50.6	0.01	<0.02	0.39	0.025	0.04
KIXAN319	Apr-13	53H	700588	6049377	0.06	1.72	0.07	8.5	<2	0.2	0.04	26	0.1	<0.2	0.01	31.7	0.02	<0.02	0.32	0.03	0.05
KIXAN320	Apr-13	53H	718431	6049800	0.04	1	0.02	10.7	<2	0.4	0.04	16	<0.1	<0.2	<0.01	47.1	0.01	<0.02	0.68	0.029	0.43

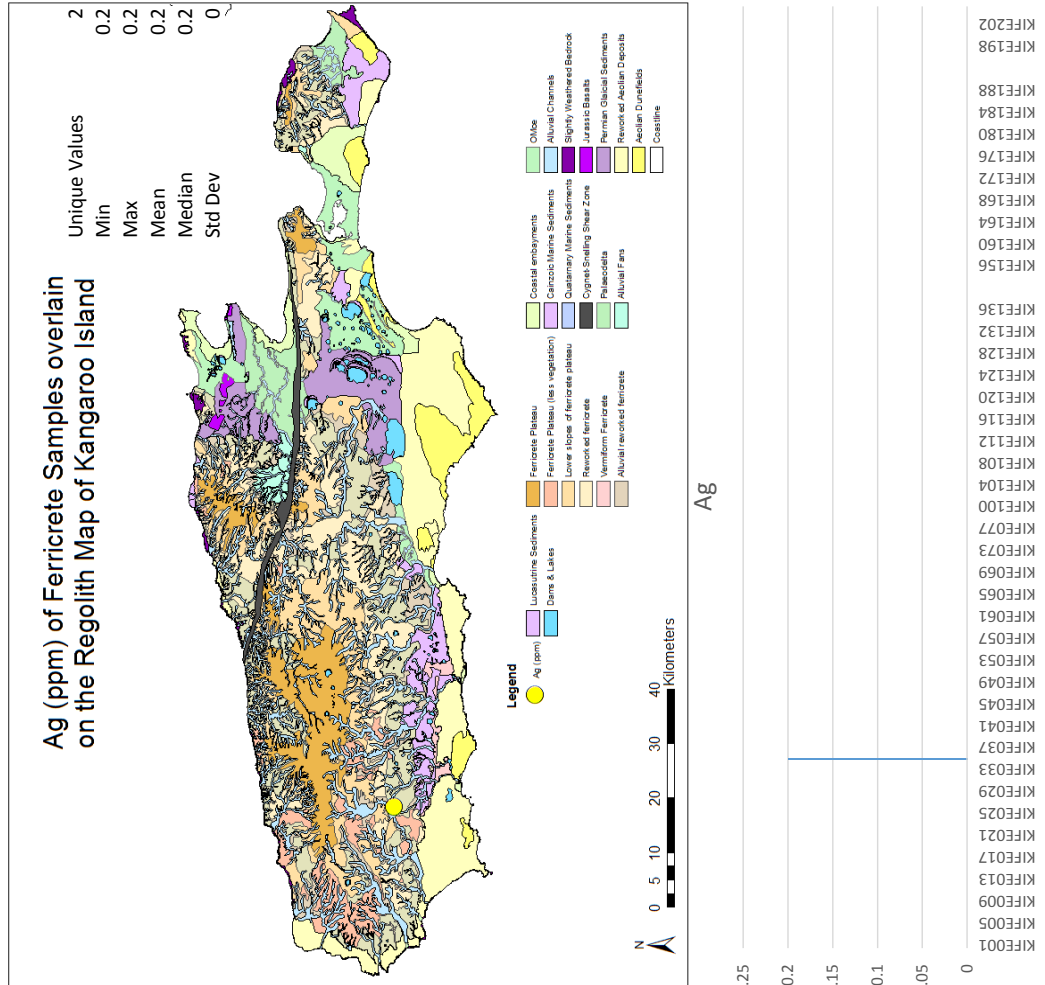
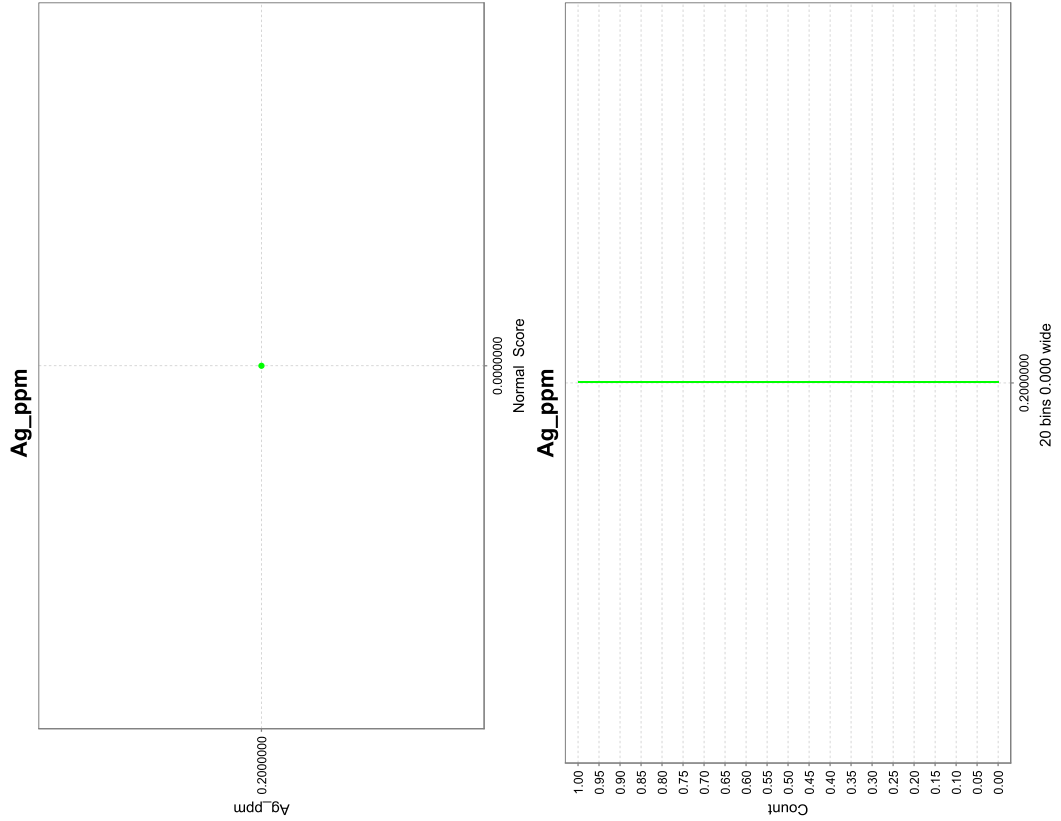
Mo ppm	Cu ppm	Pb ppm	Zn ppm	Ag ppb	Ni ppm	Co ppm	Mn ppm	As ppm	Au ppb	Th ppm	Sr ppm	Cd ppm	Bi ppm	Ca %	P %	La ppm
Mean	0.058202	1.50863	0.8486	12.143	5.08	0.4162	0.04044	44.94677	0.21222	0.02624	51.1601	0.12638	8.4545	0.61684	0.03125	0.20261
Median	0.05	1.4	0.07	8.8	4	0.3	0.03	31	0.2	0.02	41.8	0.03	9	0.58	0.029	0.11
Std Dev.	0.047911	0.52601	5.1234	23.7499	4.7491	0.3051	0.03754	43.73691	0.09408	0.01796	30.9957	0.64381	3.9049	0.22153	0.01139	0.34259

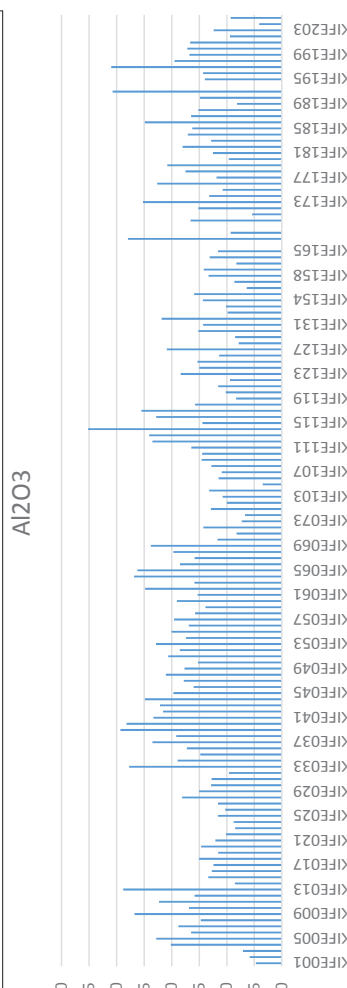
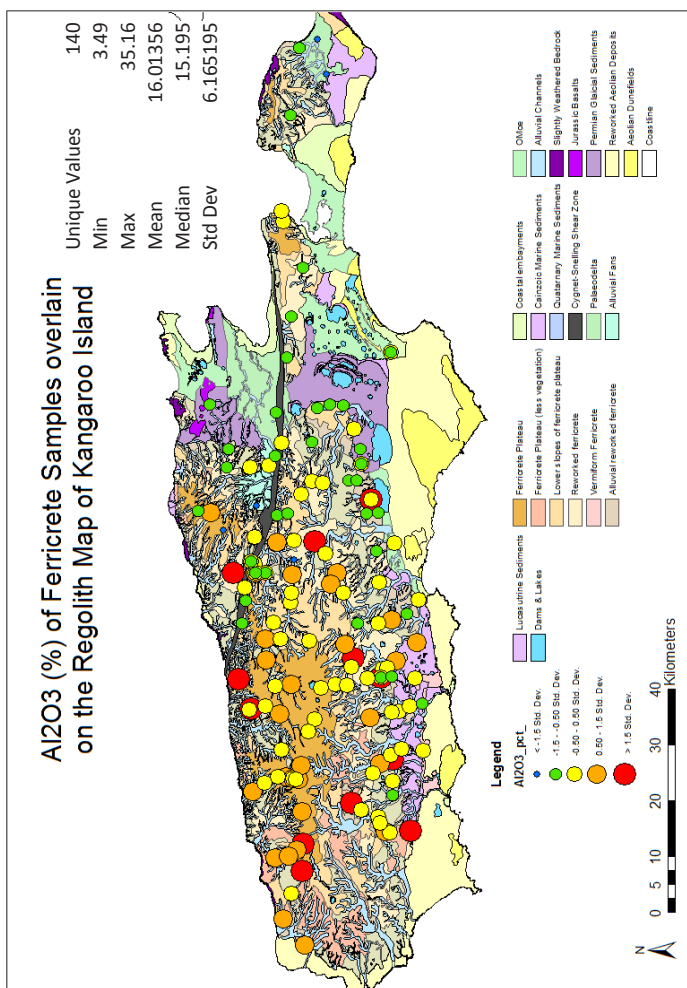
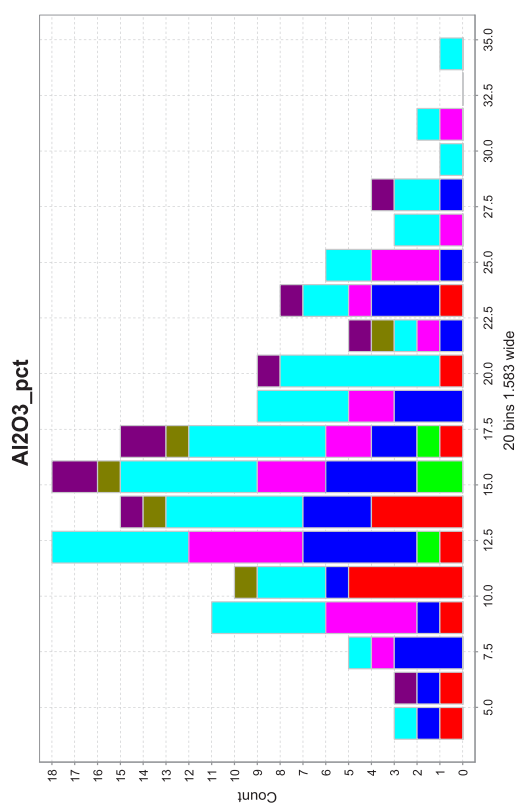
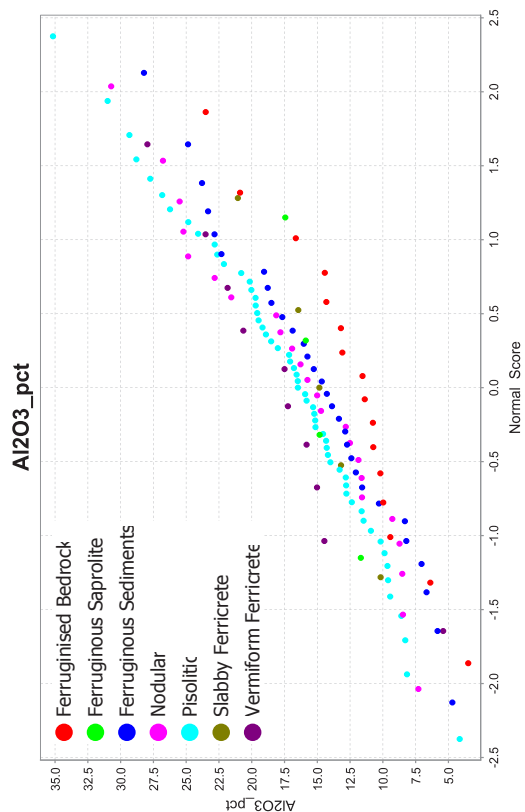
Sample	Cr ppm	Mg %	Ba ppm	Ti ppm	B ppm	Na %	K %	Sc ppm	S %	Hg ppb	Se ppm	Cs ppm	Ge ppm	Rb ppm	Y ppm	Ce ppm	Li ppm	Te pm	Sn ppm	Ta ppm	Al %	Zr ppm	Hf ppm	
Dect. Limit	0.1	0.001	0.1	1	1	0.001	1	0.1	1	1	0.1	0.005	0.01	0.1	0.001	0.01	0.01	0.02	0.02	0.001	0.01	0.001	0.001	
Method	1VE	1VE	1VE	1VE	1VE	1VE	1VE	1VE	1VE	1VE	1VE	1VE	1VE	1VE	1VE	1VE	1VE	1VE	1VE	1VE	1VE	1VE	1VE	1VE
KIXAN001	1.1	0.105	9.7	3	8	0.664	0.66	0.3	0.14	13	0.2	0.006	0.03	1.6	0.021	0.11	0.13	<0.02	<0.02	<0.001	<0.01	0.04	<0.001	
KIXAN002	1.1	0.258	10.5	3	9	0.349	0.53	0.2	0.13	13	<0.1	0.005	<0.01	0.8	0.104	0.45	0.37	<0.02	<0.02	<0.001	<0.01	0.03	<0.001	
KIXAN003	1.2	0.255	14.6	2	7	0.201	0.64	0.3	0.13	14	0.2	0.01	<0.01	1.7	0.379	1.16	0.08	<0.02	<0.02	<0.001	<0.01	0.05	<0.001	
KIXAN004	1.2	0.246	10	3	6	0.436	0.78	0.2	0.12	8	0.1	<0.005	<0.01	1.3	0.018	0.07	0.18	<0.02	<0.02	<0.001	<0.01	0.03	<0.001	
KIXAN005	1.1	0.152	11.5	2	7	0.24	1.21	0.2	0.14	12	0.3	<0.005	0.04	3	0.169	0.48	0.11	<0.02	<0.02	<0.001	<0.01	0.02	<0.001	
KIXAN006	1.1	0.095	18.3	2	6	0.014	1.16	0.2	0.11	3	0.1	<0.005	<0.01	2	0.006	0.03	0.06	<0.02	<0.02	<0.001	<0.01	0.03	<0.001	
KIXAN007	1.3	0.178	19.3	2	5	0.512	0.93	0.2	0.13	7	0.3	0.017	0.01	4.2	0.122	0.08	0.08	<0.02	<0.02	<0.001	<0.01	0.05	<0.001	
KIXAN008	1.2	0.168	4	2	4	0.013	1.39	0.3	0.12	6	<0.1	0.007	0.03	6.8	0.011	0.03	0.04	<0.02	<0.02	<0.001	<0.01	0.01	<0.001	
KIXAN009	0.3	0.133	1.8	2	4	0.083	1.31	0.2	0.08	7	0.1	0.014	0.02	7.7	0.051	0.19	0.08	<0.02	<0.02	<0.001	<0.01	0.02	0.002	
KIXAN010	0.9	0.228	9.1	1	4	0.136	1.17	0.2	0.09	7	0.2	0.013	<0.01	6.1	0.043	0.15	0.08	<0.02	<0.02	<0.001	<0.01	0.02	<0.001	
KIXAN011	0.9	0.158	14.7	2	5	0.052	1.41	0.2	0.11	6	0.2	0.014	0.01	9.8	0.013	0.04	0.03	<0.02	<0.02	<0.001	<0.01	0.02	<0.001	
KIXAN012	1.1	0.145	17.6	2	6	0.069	1.5	0.2	0.1	6	0.1	<0.005	0.03	8	0.042	0.14	0.04	<0.02	<0.02	<0.001	<0.01	0.02	<0.001	
KIXAN013	1	0.138	39.4	3	4	0.038	1.18	0.2	0.13	13	0.2	<0.005	<0.01	3	0.031	0.15	<0.01	<0.02	0.05	0.001	<0.01	0.03	<0.001	
KIXAN014	1.3	0.253	30.6	2	7	0.386	0.87	0.3	0.18	12	0.2	0.006	0.01	4.8	0.032	0.24	0.07	<0.02	0.03	<0.001	<0.01	0.03	0.003	
KIXAN015	1.2	0.154	14.1	3	5	0.224	1.06	0.2	0.15	11	0.1	0.007	<0.01	3.6	0.053	0.2	0.08	<0.02	0.05	<0.001	0.02	0.11	0.01	
KIXAN016	1.1	0.123	1.8	2	4	0.13	1.32	0.2	0.16	12	0.1	0.012	<0.01	10	0.016	0.06	0.04	<0.02	0.04	<0.001	<0.01	0.02	<0.001	
KIXAN017	1.2	0.165	5.1	4	8	0.348	1.11	0.2	0.19	7	0.3	<0.005	<0.01	2.7	0.056	0.41	0.27	<0.02	0.02	<0.001	<0.01	0.01	0.003	
KIXAN018	1.3	0.136	15.2	3	11	0.036	1.34	0.2	0.22	6	0.3	<0.005	<0.01	3.5	0.056	0.41	0.07	<0.02	<0.02	<0.001	<0.01	<0.01	<0.001	
KIXAN019	1.2	0.263	20.1	4	26	0.305	0.65	0.2	0.26	11	0.2	<0.005	<0.01	0.7	0.156	1.35	0.51	<0.02	<0.02	<0.001	<0.01	0.04	0.003	
KIXAN020	1.2	0.255	44.8	3	16	0.114	1	0.3	0.32	4	0.2	<0.005	0.03	2	0.103	0.64	0.11	<0.02	0.03	<0.001	<0.01	0.02	0.001	
KIXAN021	1.2	0.268	29.2	3	10	0.063	1.55	0.2	0.21	6	0.2	<0.005	<0.01	3.9	0.028	0.2	0.02	<0.02	0.03	<0.001	<0.01	0.01	<0.001	
KIXAN022	1.3	0.128	100.7	3	6	0.104	0.7	0.2	0.23	6	0.3	<0.005	<0.01	1.1	0.044	0.37	0.17	<0.02	<0.02	<0.001	<0.01	0.01	0.001	
KIXAN023	1.3	0.288	14.3	8	8	0.251	1.28	0.2	0.27	10	0.2	<0.005	<0.01	2.2	0.027	0.26	0.39	<0.02	<0.02	<0.001	<0.01	0.02	0.001	
KIXAN024	1.4	0.357	7.1	5	34	1.057	0.37	0.3	0.32	15	0.5	0.009	<0.01	0.6	0.037	0.25	0.36	<0.02	<0.02	<0.001	0.01	0.06	0.002	
KIXAN025	1.3	0.244	27.2	3	12	0.189	0.87	0.3	0.2	6	0.2	<0.005	<0.01	0.9	0.01	0.06	0.18	<0.02	<0.02	<0.001	<0.01	0.02	<0.001	
KIXAN026	1.4	0.266	16.9	3	9	0.482	0.51	0.4	0.2	10	0.2	<0.005	<0.01	0.6	0.194	0.31	0.17	<0.02	<0.02	<0.001	<0.01	0.04	0.003	
KIXAN027	1.3	0.197	19.7	3	5	0.332	1.17	0.3	0.18	10	0.1	<0.005	0.01	3	0.057	0.19	0.14	<0.02	<0.02	<0.001	<0.01	0.03	0.002	
KIXAN028	1.4	0.137	2.2	4	6	0.21	1.17	0.3	0.23	8	0.2	<0.005	<0.01	2.5	0.005	0.03	0.07	<0.02	<0.02	<0.001	<0.01	0.01	0.002	
KIXAN029	1.3	0.347	6.7	5	13	0.853	0.31	0.2	0.23	8	0.2	0.008	<0.01	0.5	0.058	0.33	0.27	<0.02	<0.02	<0.001	0.01	0.05	<0.001	
KIXAN030	1.2	0.327	6	3	16	1.06	0.31	0.3	0.25	23	0.3	0.007	<0.01	0.5	0.059	0.35	0.25	<0.02	<0.02	<0.001	0.01	0.06	0.001	
KIXAN031	1.5	0.17	3.4	4	6	0.323	1.13	0.3	0.12	4	0.2	<0.005	<0.01	2.5	0.01	0.06	0.13	<0.02	<0.02	<0.001	<0.01	0.02	0.002	
KIXAN032	1.4	0.132	15.3	2	5	0.101	1.12	0.3	<0.01	7	0.2	0.006	<0.01	2.9	0.025	0.12	0.07	<0.02	<0.02	<0.001	<0.01	0.06	0.002	
KIXAN033	1.2	0.261	53.2	2	6	0.054	1.02	0.2	0.06	6	0.1	<0.005	<0.01	4.5	0.103	0.76	0.06	<0.02	<0.02	<0.001	<0.01	0.02	0.001	
KIXAN034	1.4	0.191	107	2	4	0.166	0.81	0.3	0.12	8	0.1	<0.005	<0.01	3.1	0.406	3.34	0.04	<0.02	<0.02	<0.001	<0.01	0.02	0.001	
KIXAN035	1.2	0.15	108.2	2	4	0.127	1.33	0.2	0.08	9	0.3	<0.005	<0.01	5.5	0.147	1.61	0.03	<0.02	<0.02	<0.001	<0.01	0.02	0.001	
KIXAN036	1.3	0.134	48.9	2	7	0.156	0.97	0.2	0.08	7	0.1	<0.005	<0.01	2.5	0.283	2.08	0.07	<0.02	<0.02	<0.001	<0.01	0.01	0.001	
KIXAN037	1.5	0.105	53.9	2	6	0.323	0.58	0.2	0.13	12	0.2	<0.005	<0.01	1.7	0.259	2.15	0.06	0.03	<0.02	<0.001	<0.01	0.03	<0.001	
KIXAN038	1.2	0.134	69.2	2	6	0.096	1.21	0.3	0.04	11	0.2	<0.005	0.01	5.5	0.132	1.35	0.07	<0.02	<0.02	<0.001	<0.01	0.02	<0.001	
KIXAN039	1.1	0.297	72.7	2	12	0.079	1.12	0.2	0.15	13	0.2	<0.005	<0.01	2.2	1.328	7.1	0.05	<0.02	<0.02	<0.001	<0.01	0.02	0.004	
KIXAN040	1.1	0.452	24.2	2	10	0.075	1.18	0.2	0.15	8	<0.1	<0.005	0.01	7.5	0.229	1.61	0.09	<0.02	<0.02	<0.001	<0.01	<0.01	<0.001	
KIXAN041	1.3	0.443	13	2	6	0.221	0.82	0.3	0.06	13	0.2	<0.005	<0.01	1.1	0.239	0.65	0.08	<0.02	<0.02	<0.001	<0.01	0.02	<0.001	

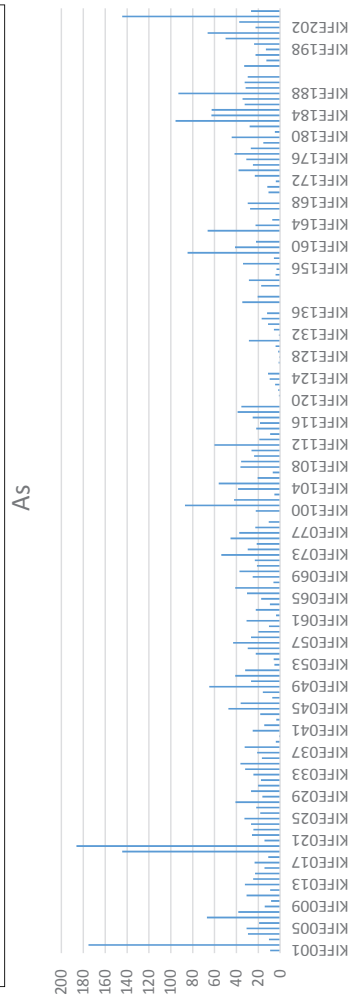
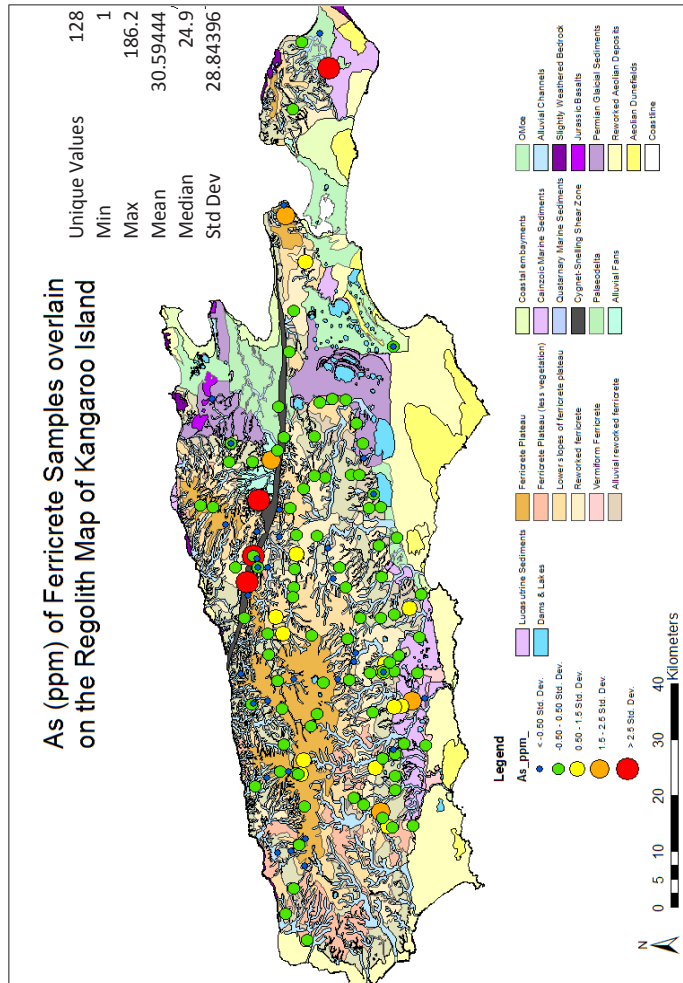
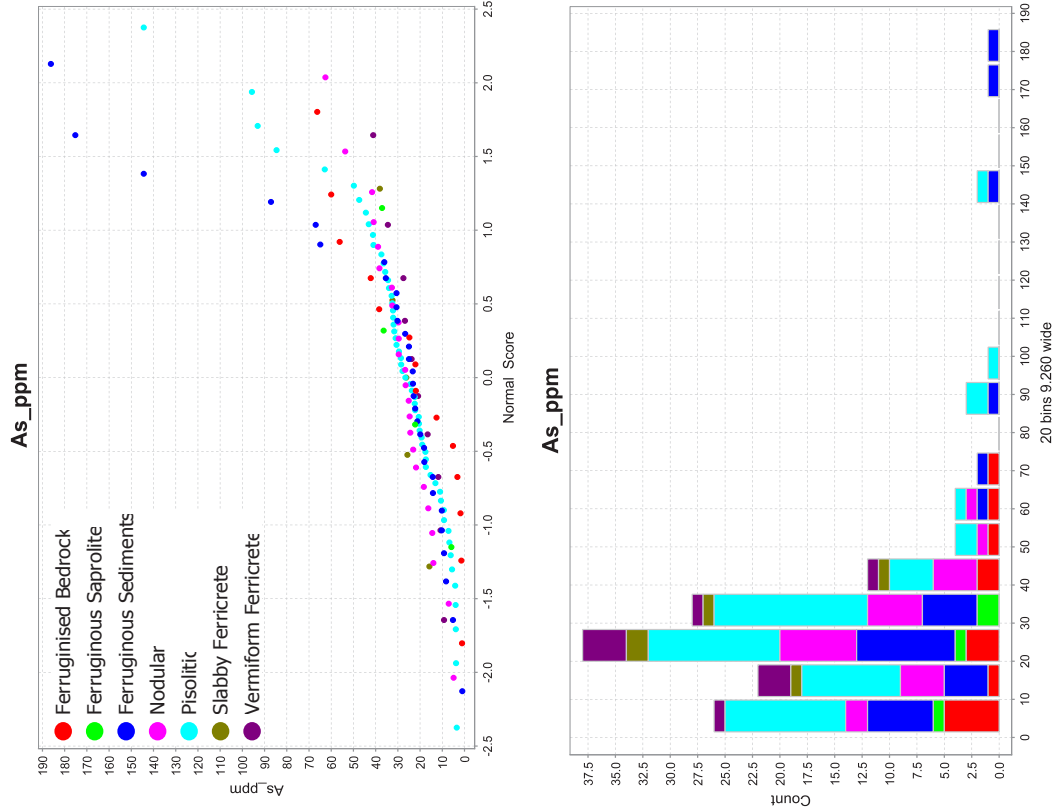
Sample	Cr ppm	Mg %	Ba ppm	Ti ppm	B ppm	Na %	K %	Sc ppm	S %	Hg ppb	Se ppm	Cs ppm	Ge ppm	Rb ppm	Y ppm	Ce ppm	Li ppm	Te pm	Sn ppm	Ta ppm	Al %	Zr ppm	Hf ppm
KIXAN111	1.4	0.129	26.5	2	4	0.159	0.69	0.3	0.07	14	0.2	<0.005	0.02	2.7	0.01	0.08	0.11	<0.02	<0.02	<0.001	<0.01	0.02	<0.001
KIXAN112	1.4	0.145	18.5	1	4	0.025	1.42	0.2	0.04	6	<0.1	<0.005	0.06	11.8	0.001	<0.01	0.01	<0.02	<0.02	<0.001	<0.01	<0.01	<0.001
KIXAN113	1.4	0.118	43.6	2	4	0.029	1.62	0.3	0.1	7	0.1	0.007	0.01	9.5	0.032	0.14	0.04	<0.02	<0.02	<0.001	<0.01	<0.01	0.001
KIXAN114	1.4	0.211	17.9	2	3	0.164	1.51	0.3	0.05	6	0.1	0.009	0.04	9	0.016	0.06	0.11	<0.02	<0.02	<0.001	<0.01	0.04	0.003
KIXAN115	1.4	0.119	13.6	1	5	0.048	1.87	0.3	0.03	12	0.3	0.01	0.04	11.4	0.044	0.09	0.11	<0.02	<0.02	<0.001	<0.01	0.02	<0.001
KIXAN116	1.3	0.175	6.4	1	4	0.038	1.48	0.3	0.03	12	<0.1	0.021	0.01	19.1	0.043	0.24	0.05	<0.02	<0.02	<0.001	<0.01	0.01	0.001
KIXAN117	1.2	0.16	19.7	2	4	0.111	1.68	0.4	0.03	11	<0.1	0.015	0.04	13.6	0.025	0.09	<0.01	<0.02	<0.02	<0.001	<0.01	0.02	<0.001
KIXAN118	1.3	0.168	46.2	1	3	0.015	1.79	0.2	0.02	6	<0.1	0.012	0.02	34.1	0.014	0.03	0.03	<0.02	<0.02	<0.001	<0.01	0.01	<0.001
KIXAN119	1.2	0.138	14	2	4	0.192	1.61	0.4	0.08	5	<0.1	<0.005	0.03	6.2	0.012	0.09	0.05	<0.02	<0.02	<0.001	<0.01	0.03	<0.001
KIXAN120	1.2	0.136	2.1	1	4	0.053	1.46	0.4	0.04	9	0.1	<0.005	0.02	10.8	0.01	0.07	<0.01	<0.02	<0.02	<0.001	<0.01	<0.01	<0.001
KIXAN121	1.5	0.257	5.6	1	4	0.048	1.66	0.3	0.05	8	0.1	<0.005	0.03	8.8	0.008	0.02	0.02	<0.02	<0.02	<0.001	<0.01	0.01	<0.001
KIXAN122	1.6	0.128	28.1	1	3	0.022	1.48	0.4	0.04	6	<0.1	0.007	0.03	9.3	0.004	0.01	0.03	<0.02	<0.02	<0.001	<0.01	0.02	<0.001
KIXAN123	1.2	0.155	12.9	1	3	0.072	1.72	0.3	0.04	5	<0.1	0.006	0.03	13.1	0.003	<0.01	0.04	<0.02	<0.02	<0.001	<0.01	0.01	<0.001
KIXAN124	1.4	0.084	11.1	1	5	0.056	1.22	0.3	0.07	6	<0.1	<0.005	0.02	7.4	0.007	0.06	0.04	<0.02	<0.02	<0.001	<0.01	0.02	<0.001
KIXAN125	1.4	0.109	16.1	2	4	0.2	1.29	0.4	0.08	11	0.2	<0.005	0.03	11.5	0.028	0.16	<0.01	<0.02	<0.02	<0.001	0.01	0.05	0.003
KIXAN126	1.3	0.158	11.3	2	4	0.185	1.47	0.2	0.05	9	<0.1	<0.005	0.03	4.2	0.044	0.16	0.05	<0.02	<0.02	<0.001	0.02	0.06	<0.001
KIXAN127	1.6	0.116	9	2	4	0.044	1.42	0.2	0.02	11	0.2	0.008	0.02	10	0.006	0.03	0.02	<0.02	<0.02	<0.001	<0.01	0.04	<0.001
KIXAN128	1.5	0.127	13.3	1	4	0.072	1.61	0.2	0.12	17	0.2	0.007	0.03	11.6	0.008	0.07	0.08	<0.02	0.03	<0.001	<0.01	<0.01	<0.001
KIXAN129	1.6	0.152	9.8	1	4	0.063	1.04	0.3	0.11	10	0.1	<0.005	0.03	5.1	0.015	0.11	<0.01	<0.02	<0.02	<0.001	<0.01	0.01	<0.001
KIXAN130	1.4	0.18	8	2	4	0.13	1.23	0.3	0.09	8	0.2	0.01	0.02	8.1	0.04	0.12	0.04	<0.02	<0.02	<0.001	<0.01	0.03	<0.001
KIXAN131	1.3	0.156	37	2	4	0.048	1.69	0.2	0.12	11	0.3	0.016	0.01	15.1	0.039	0.26	<0.01	<0.02	<0.02	<0.001	<0.01	0.04	<0.001
KIXAN132	1.5	0.167	15.3	2	4	0.064	1.6	0.2	0.15	17	0.2	0.012	0.02	14	0.011	0.05	0.1	<0.02	<0.02	<0.001	0.01	0.07	0.002
KIXAN133	1.4	0.134	19.5	2	4	0.079	1.89	0.4	0.08	3	<0.1	0.011	0.02	24.2	0.008	0.04	0.03	<0.02	0.02	<0.001	<0.01	0.03	<0.001
KIXAN134	1.7	0.177	11.8	3	4	0.077	1.32	0.4	0.08	11	<0.1	0.015	0.02	15.1	0.08	0.27	0.09	<0.02	<0.02	<0.001	0.01	0.17	0.002
KIXAN135	1.3	0.1	41.8	2	4	0.062	1.82	0.3	0.09	13	<0.1	0.018	<0.01	15.4	0.058	0.23	0.08	<0.02	<0.02	<0.001	<0.01	0.06	0.001
KIXAN136	1.7	0.193	10.2	3	3	0.036	1.73	0.4	0.09	12	0.2	0.007	<0.01	9.1	0.041	0.24	0.01	<0.02	<0.02	<0.001	0.02	0.12	0.005
KIXAN137	1.3	0.091	27.3	2	4	0.112	1.49	0.2	0.15	14	0.2	0.005	0.05	8.6	0.026	0.13	0.07	<0.02	<0.02	<0.001	<0.01	0.04	<0.001
KIXAN138	1.6	0.136	20	2	4	0.026	1.5	0.4	0.11	12	0.2	0.017	0.03	10.9	0.033	0.05	0.06	<0.02	<0.02	<0.001	<0.01	0.03	0.001
KIXAN139	1.7	0.148	19.8	3	6	0.295	0.57	0.2	0.15	12	0.2	0.011	0.01	1.4	0.073	0.37	0.11	<0.02	0.03	<0.001	0.03	0.19	0.005
KIXAN140	1.7	0.347	114	3	7	0.456	0.44	0.3	0.14	12	0.2	0.012	0.01	2	0.372	2.75	0.09	<0.02	<0.02	<0.001	0.01	0.09	<0.001
KIXAN141	1.6	0.293	7.2	2	6	0.133	1.38	0.2	0.11	9	0.2	0.029	0.01	6.2	0.793	3.54	0.07	<0.02	<0.02	<0.001	0.01	0.09	0.001
KIXAN142	1.5	0.175	19.6	2	3	0.176	1.45	0.2	0.08	12	0.1	0.021	0.04	13.8	0.04	0.1	0.07	<0.02	<0.02	<0.001	0.01	0.04	<0.001
KIXAN143	1.3	0.141	44.3	2	5	0.139	1.18	0.2	0.11	19	0.2	<0.005	0.02	6.9	0.042	0.22	0.04	<0.02	<0.02	<0.001	<0.01	0.02	<0.001
KIXAN144	1.4	0.218	67.2	2	7	0.052	1.4	0.2	0.08	5	0.1	0.005	0.03	9.3	0.101	0.27	0.06	<0.02	<0.02	<0.001	<0.01	0.01	<0.001
KIXAN145	1.3	0.193	31.6	2	4	0.096	1.32	0.3	0.08	11	0.1	0.007	0.03	8.1	0.053	0.2	0.05	<0.02	<0.02	<0.001	<0.01	0.02	<0.001
KIXAN146	1.3	0.124	11.5	2	5	0.062	2.18	0.2	0.09	9	<0.1	0.028	0.03	24.1	0.024	0.04	0.02	<0.02	<0.02	<0.001	<0.01	<0.01	<0.001
KIXAN147	1.8	0.155	6.6	2	4	0.293	0.84	0.3	0.07	14	0.5	0.009	<0.01	2.4	0.04	0.2	0.1	<0.02	<0.02	<0.001	0.02	0.11	0.008
KIXAN148	1.3	0.168	12.7	2	5	0.368	1.47	0.2	0.04	11	0.3	0.008	<0.01	7.4	0.024	0.09	0.09	<0.02	<0.02	<0.001	<0.01	0.02	<0.001
KIXAN149	1.7	0.201	9	2	6	0.065	1.2	0.2	0.06	9	0.2	0.008	0.01	7.2	0.041	0.11	0.03	<0.02	<0.02	<0.001	<0.01	0.06	0.003
KIXAN150	1.6	0.189	10.2	2	6	0.033	1.25	0.2	0.17	10	0.2	0.006	<0.01	6.5	0.17	0.71	0.07	<0.02	<0.02	<0.001	<0.01	0.05	0.002
KIXAN151	1.3	0.188	26.8	2	4	0.154	1.16	0.2	0.08	10	0.1	0.01	0.03	3.7	0.071	0.21	0.05	<0.02	<0.02	<0.001	0.01	0.05	0.002
KIXAN152	1.5	0.174	12.4	2	4	0.093	1.63	0.2	0.09	13	0.2	0.025	0.02	14.7	0.084	0.38	0.07	<0.02	<0.02	<0.001	<0.01	0.08	0.004
KIXAN153	1.6	0.16	17.8	2	5	0.196	1.29	0.2	0.1	12	0.2	0.019	0.01	8.1	0.042	0.12	0.09	<0.02	<0.02	<0.001	<0.01	0.05	0.002
KIXAN154	1.3	0.23	12.1	4	7	0.743	1.53	0.1	0.07	2	0.3	0.016	0.02	20.4	0.086	0.5	0.16	<0.02	<0.02	<0.001	<0.01	0.06	0.001
KIXAN155	1.7	0.253	9.6	3	3	0.158	1.46	0.2	0.08	12	<0.1	0.01	<0.01	7.1	0.026	0.14	0.03	<0.02	<0.02	<0.001	0.02	0.16	0.004

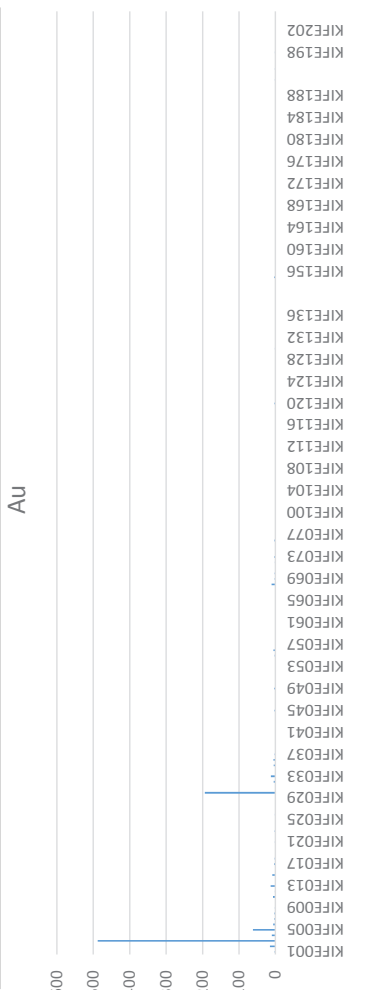
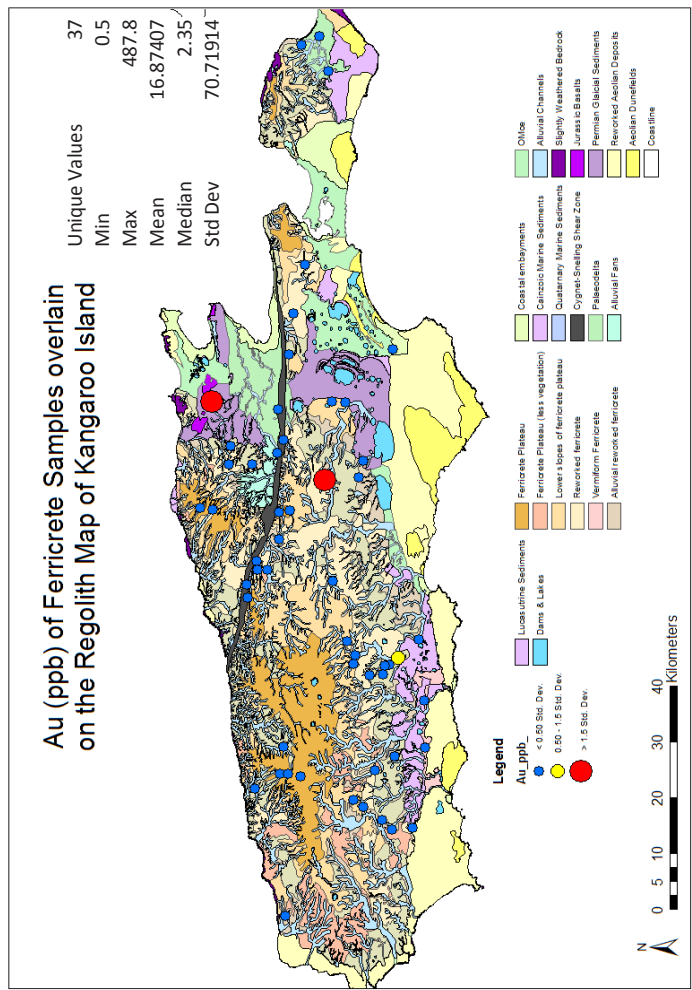
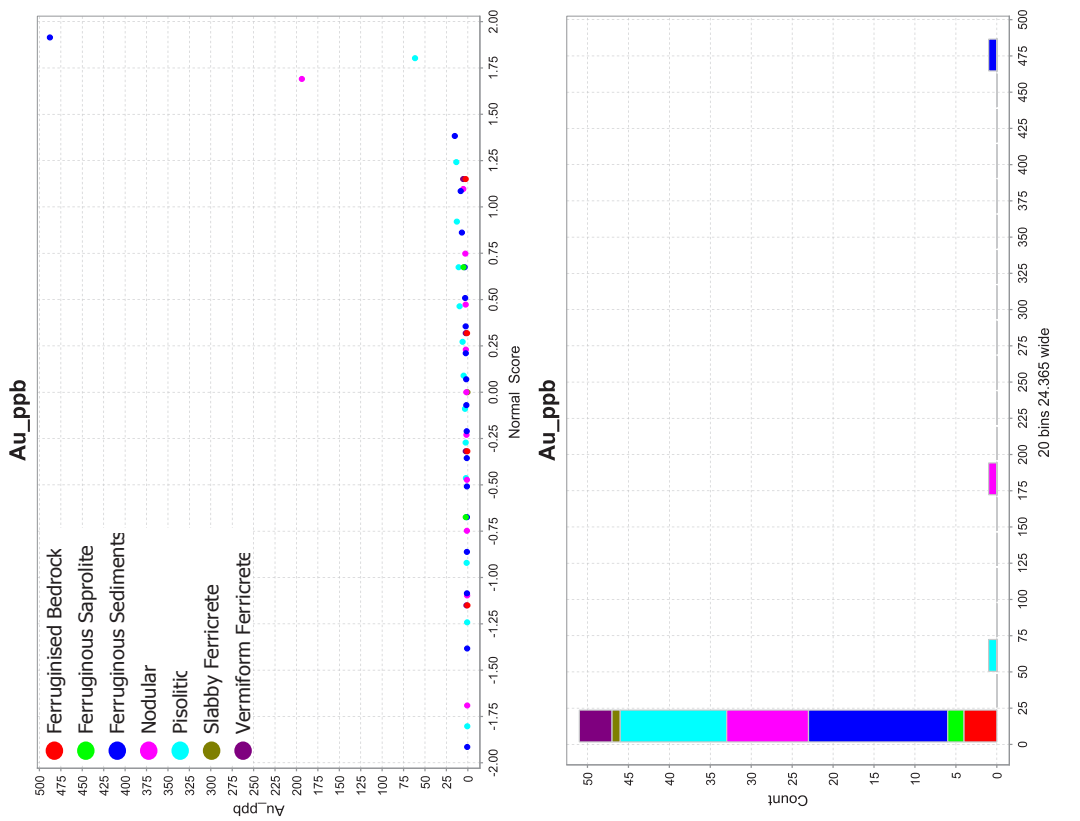
Sample	Cr ppm	Mg %	Ba ppm	Ti ppm	B ppm	Na %	K %	Sc ppm	S %	Hg ppb	Se ppm	Cs ppm	Ge ppm	Rb ppm	Y ppm	Ce ppm	Li ppm	Te pm	Sn ppm	Ta ppm	Al %	Zr ppm	Hf ppm
KIXAN156	1.4	0.12	23	1	5	0.084	1.25	0.2	0.08	5	0.2	0.04	0.02	10	0.043	0.12	<0.01	<0.02	<0.001	<0.001	<0.01	0.02	0.003
KIXAN157	1.7	0.268	6.4	2	5	0.423	1.07	0.1	0.08	11	0.2	0.013	0.01	10	0.08	0.35	0.13	<0.02	<0.001	<0.001	0.02	0.08	0.005
KIXAN158	1.6	0.239	137.5	1	8	0.142	1.15	0.2	0.04	11	0.1	0.008	<0.01	7.5	0.122	1.18	0.12	<0.02	<0.001	<0.001	<0.01	0.01	<0.001
KIXAN159	1.4	0.179	8.8	2	4	0.073	1.65	0.4	0.05	5	0.1	0.008	0.02	12.9	0.041	0.12	0.01	<0.02	<0.001	<0.001	<0.01	0.01	<0.001
KIXAN160	1.6	0.253	28.7	2	6	0.292	0.97	0.3	0.07	20	0.2	0.01	0.04	4.8	0.283	1.61	0.07	<0.02	<0.001	<0.001	0.01	0.05	0.002
KIXAN161	1.5	0.216	82.4	1	5	0.042	1.08	0.2	0.03	12	0.3	<0.005	<0.01	6.4	0.314	1.42	0.02	<0.02	<0.001	<0.001	<0.01	0.03	<0.001
KIXAN162	1.5	0.238	49.4	2	4	0.215	1.02	0.3	0.02	6	<0.1	0.045	<0.01	8.3	0.065	0.19	0.06	<0.02	<0.001	<0.001	0.01	0.05	0.002
KIXAN163	1.7	0.197	15	2	4	0.304	1.11	0.4	0.1	11	0.2	0.009	<0.01	9.8	0.032	0.14	0.06	<0.02	<0.001	<0.001	0.01	0.07	0.003
KIXAN164	1.7	0.144	24.7	2	5	0.07	1.66	0.3	0.08	7	0.1	0.025	0.02	19.3	0.078	0.32	0.03	<0.02	<0.001	<0.001	<0.01	0.05	0.005
KIXAN165	1.5	0.085	1.7	2	6	0.185	0.94	0.2	0.19	13	0.2	<0.005	<0.01	1.1	0.016	0.07	0.14	<0.02	<0.001	<0.001	<0.01	0.02	<0.001
KIXAN166	1.5	0.138	1.7	2	5	0.032	1.25	0.3	0.1	8	<0.1	0.008	0.05	4.2	0.005	0.01	0.09	<0.02	<0.001	<0.001	<0.01	<0.01	0.003
KIXAN200	1.6	0.181	30.9	1	4	0.027	1.5	0.2	0.04	9	<0.1	0.02	<0.01	17	0.051	0.19	0.05	<0.02	<0.001	<0.001	<0.01	0.07	0.005
KIXAN201	1.8	0.188	27.7	1	5	0.095	1.21	0.4	0.08	8	<0.1	0.015	<0.01	9.5	0.113	0.26	0.09	<0.02	<0.001	<0.001	<0.01	0.07	<0.001
KIXAN202	1.9	0.122	30.7	1	4	0.044	1.58	0.3	0.12	11	0.1	0.012	0.02	8.6	0.068	0.29	0.07	<0.02	<0.001	<0.001	0.01	0.08	<0.001
KIXAN203	1.9	0.137	13	<1	6	0.146	0.89	0.3	0.09	14	<0.1	0.009	<0.01	4.7	0.041	0.25	0.1	<0.02	<0.001	<0.001	<0.01	0.06	0.002
KIXAN204	1.9	0.153	4.9	<1	6	0.162	0.91	0.2	0.16	13	<0.1	0.005	<0.01	2.5	0.174	0.79	0.09	<0.02	<0.001	<0.001	<0.01	0.05	<0.001
KIXAN205	1.9	0.246	74.3	<1	6	0.369	0.4	0.2	0.16	17	<0.1	0.007	<0.01	1.6	0.078	0.86	0.18	<0.02	<0.001	<0.001	<0.01	0.05	<0.001
KIXAN206	2	0.148	9	<1	4	0.048	1.13	0.2	0.13	8	0.1	<0.005	<0.01	1.7	0.012	0.1	0.04	<0.02	<0.001	<0.001	<0.01	0.01	<0.001
KIXAN207	1.9	0.131	18.1	<1	7	0.185	1.36	0.2	0.15	12	<0.1	<0.005	0.02	1.6	0.003	0.03	0.08	<0.02	<0.001	<0.001	<0.01	0.01	<0.001
KIXAN208	2.2	0.111	13.4	<1	4	0.102	1.1	0.3	0.17	13	<0.1	<0.005	<0.01	4.6	0.038	0.1	0.04	<0.02	<0.001	<0.001	<0.01	0.02	<0.001
KIXAN209	2.1	0.155	21.7	<1	4	0.027	1.17	0.2	0.16	13	<0.1	<0.005	0.02	10.9	0.174	0.21	0.05	<0.02	<0.001	<0.001	<0.01	<0.01	<0.001
KIXAN210	2.2	0.129	19	<1	4	0.083	1.05	0.4	0.14	13	<0.1	0.006	<0.01	3.8	0.025	0.1	0.07	<0.02	<0.001	<0.001	<0.01	0.04	<0.001
KIXAN211	2.2	0.184	17.2	1	7	0.106	0.9	0.3	0.13	19	<0.1	0.009	0.01	4	0.181	0.24	0.09	<0.02	<0.001	<0.001	0.01	0.07	<0.001
KIXAN212	2.1	0.131	2.3	<1	7	0.352	0.82	0.3	0.15	13	<0.1	0.01	<0.01	4.5	0.21	0.55	0.11	<0.02	<0.001	<0.001	0.01	0.05	<0.001
KIXAN213	2.1	0.113	6.5	1	10	0.451	0.34	0.3	0.13	15	0.2	0.007	0.01	0.8	0.035	0.15	0.15	<0.02	<0.001	<0.001	0.02	0.06	0.003
KIXAN214	2.2	0.16	1.3	1	6	0.763	0.56	0.3	0.17	4	<0.1	<0.005	<0.01	1.1	0.008	0.06	0.11	<0.02	<0.001	<0.001	<0.01	0.03	<0.001
KIXAN215	2.1	0.191	1.1	<1	6	0.268	1.48	0.3	0.13	6	0.1	<0.005	<0.01	2.4	0.007	0.04	0.08	<0.02	<0.001	<0.001	<0.01	0.04	0.001
KIXAN216	2.1	0.083	0.7	<1	7	0.272	0.91	0.3	0.22	8	<0.1	<0.005	<0.01	3	0.017	0.07	0.05	<0.02	<0.001	<0.001	<0.01	0.03	<0.001
KIXAN217	2.1	0.173	10.4	2	10	0.737	0.35	0.3	0.14	20	<0.1	0.013	<0.01	0.7	0.157	0.52	0.21	<0.02	<0.001	<0.001	0.03	0.15	0.005
KIXAN218	2	0.175	3.5	<1	7	0.314	1.34	0.1	0.15	4	0.1	<0.005	<0.01	3.1	0.009	0.05	0.07	<0.02	<0.001	<0.001	<0.01	0.04	<0.001
KIXAN219	2.2	0.192	14.6	1	6	0.334	1.36	0.2	0.15	18	0.2	0.006	<0.01	3.6	0.017	0.08	0.16	<0.02	<0.001	<0.001	0.01	0.05	0.001
KIXAN220	2	0.099	14.8	2	7	0.225	1.36	0.3	0.15	11	<0.1	0.006	<0.01	2.5	0.082	0.14	0.11	<0.02	<0.001	<0.001	0.01	0.07	0.003
KIXAN221	2	0.07	13.3	<1	7	0.157	0.59	0.2	0.12	10	<0.1	0.007	<0.01	1.3	0.177	0.3	0.17	<0.02	<0.001	<0.001	0.01	0.06	0.001
KIXAN222	2	0.139	13.4	1	6	0.214	0.83	0.3	0.15	17	0.1	0.007	<0.01	2.1	0.113	0.18	0.11	<0.02	<0.001	0.002	0.02	0.08	0.003
KIXAN223	1.6	0.084	4.5	<1	5	0.23	0.73	0.3	0.02	10	<0.1	<0.005	<0.01	1.3	0.009	0.05	0.08	<0.02	<0.001	<0.001	<0.01	0.03	<0.001
KIXAN224	1.7	0.166	24.3	<1	9	0.114	0.92	0.2	0.09	9	<0.1	0.008	<0.01	3.6	0.001	0.05	0.12	<0.02	<0.001	<0.001	<0.01	0.03	<0.001
KIXAN225	2.2	0.114	12.9	3	6	0.093	0.5	0.3	0.1	17	0.1	0.017	<0.01	2.1	0.063	0.42	0.1	<0.02	<0.001	<0.001	0.01	0.09	0.002
KIXAN226	2.1	0.249	7.1	2	6	0.431	1.34	0.2	0.12	6	<0.1	0.021	<0.01	12.2	0.124	0.45	0.13	<0.02	<0.001	<0.001	0.01	0.07	0.002
KIXAN227	2.1	0.15	11.2	<1	7	0.124	0.85	0.4	0.15	13	<0.1	<0.005	0.01	1.6	0.023	0.09	0.08	<0.02	<0.001	<0.001	<0.01	0.02	<0.001
KIXAN228	2	0.189	10.6	<1	6	0.105	1.05	0.2	0.15	7	0.1	<0.005	0.02	3.6	0.019	0.06	0.04	<0.02	<0.001	<0.001	<0.01	0.02	<0.001
KIXAN229	2.2	0.177	20.2	<1	6	0.181	0.54	0.4	0.15	13	0.1	<0.005	<0.01	1.2	0.031	0.08	0.09	<0.02	<0.001	<0.001	<0.01	0.03	<0.001
KIXAN230	2.5	0.278	18.5	2	14	0.642	0.25	0.3	0.18	9	0.2	0.013	<0.01	0.7	0.099	0.3	0.24	<0.02	<0.001	<0.001	0.02	0.12	0.006
KIXAN231	2.1	0.147	36.1	<1	4	0.042	1.02	0.3	0.15	3	0.2	<0.005	<0.01	4.4	0.096	0.33	0.01	<0.02	<0.001	<0.001	<0.01	<0.01	0.002
KIXAN232	2	0.232	10.9	<1	5	0.046	1.38	0.2	0.15	7	0.1	<0.005	0.01	5.5	0.006	0.06	0.02	<0.02	<0.001	<0.001	<0.01	<0.01	<0.001
KIXAN233	1.2	0.195	17.1	<1	4	0.017	1.07	0.2	0.05	3	<0.1	<0.005	<0.01	7.4	0.007	0.03	0.03	<0.02	<0.001	<0.001	<0.01	<0.01	<0.001

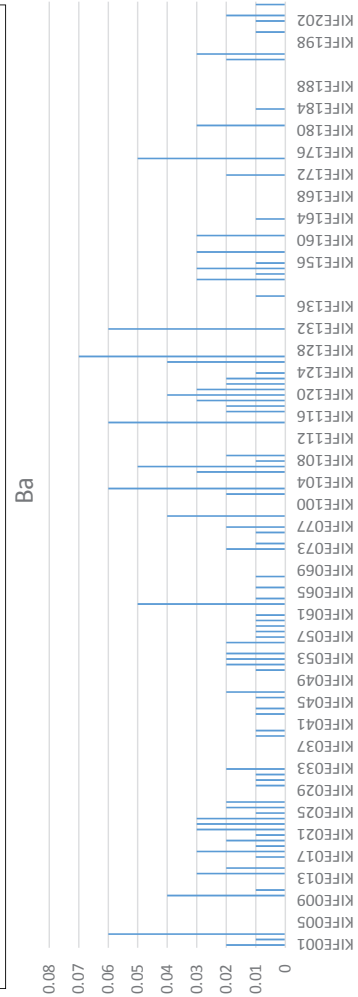
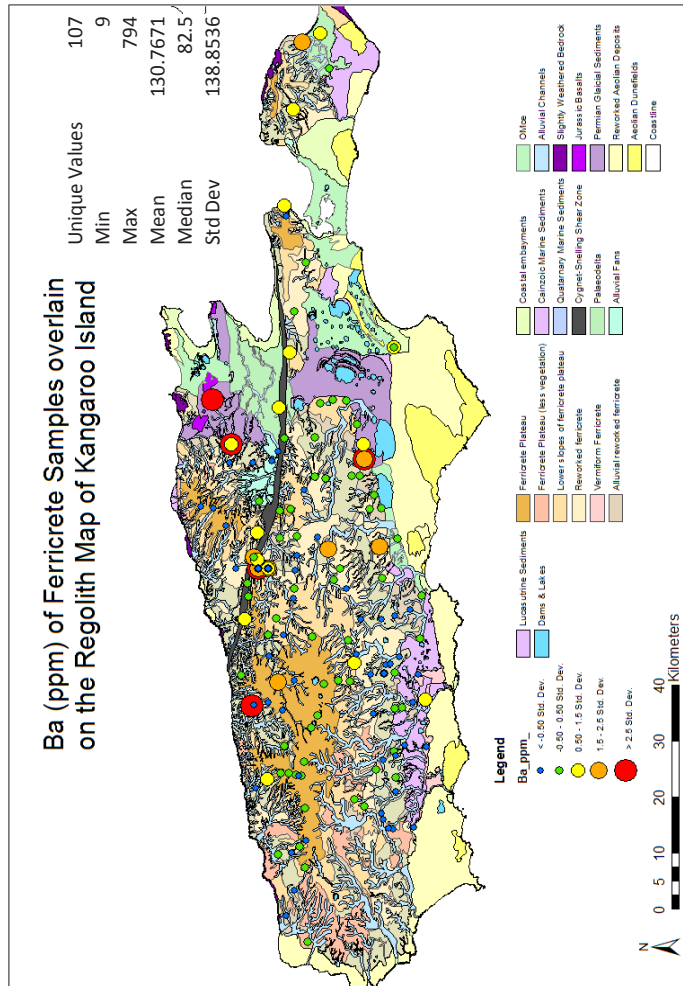
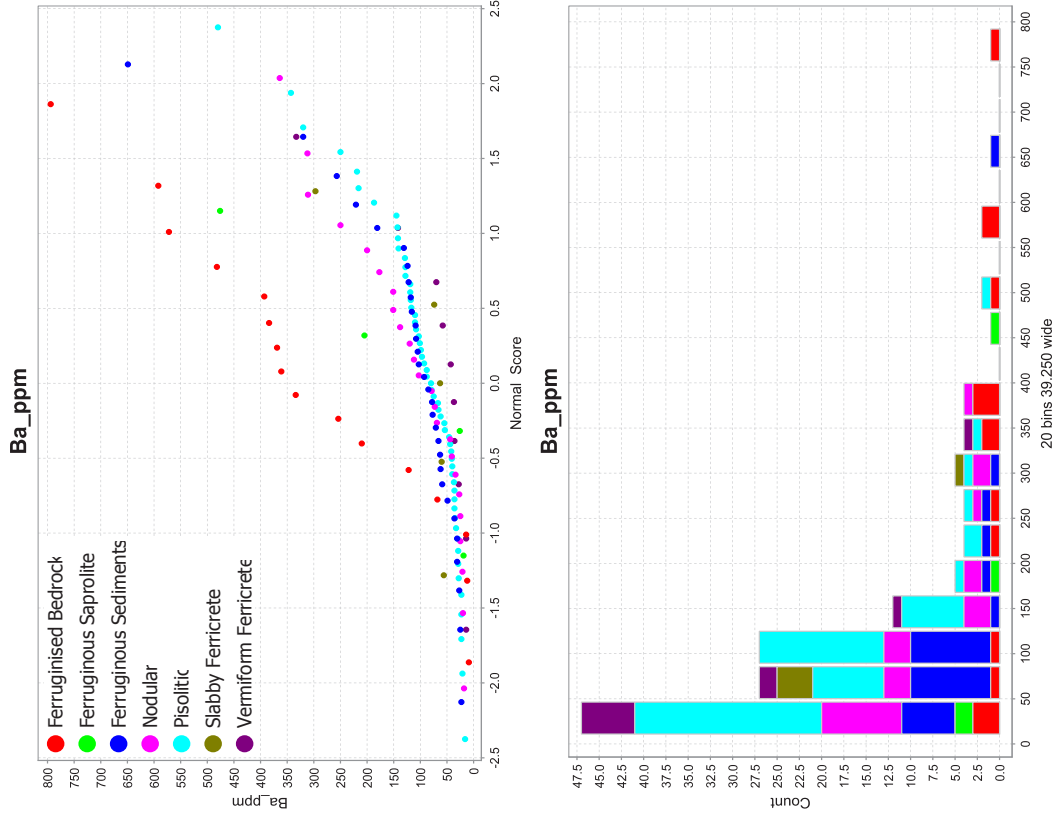
Appendix B: Ferricrete Maps and Graphs

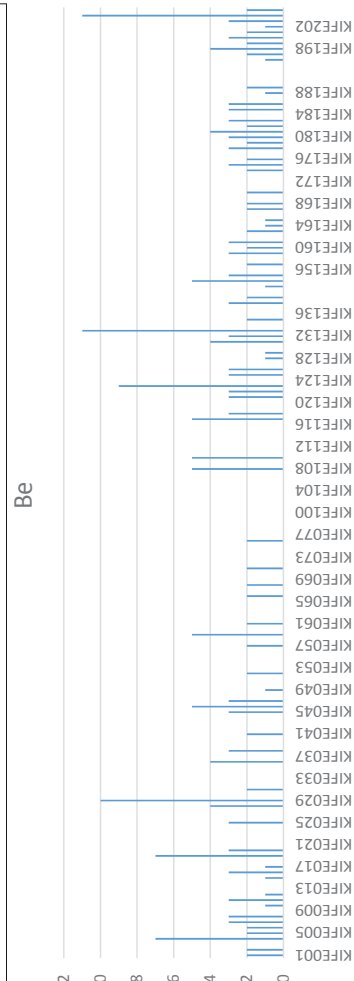
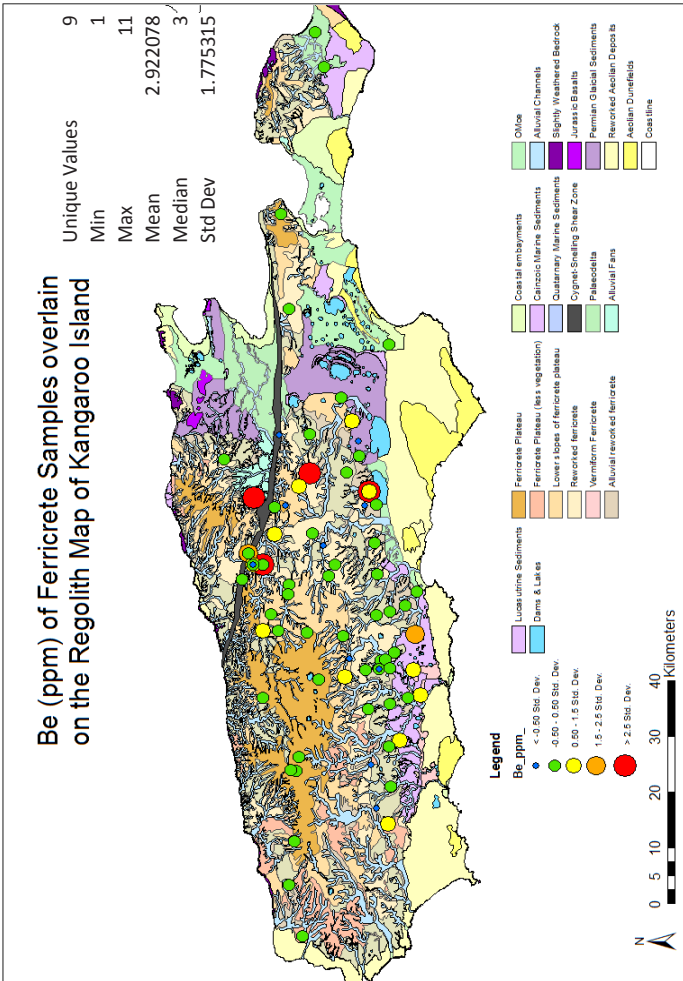
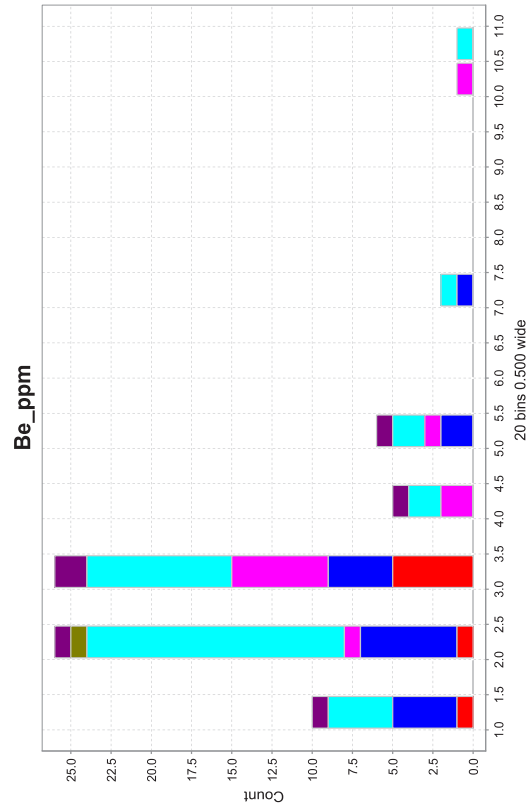
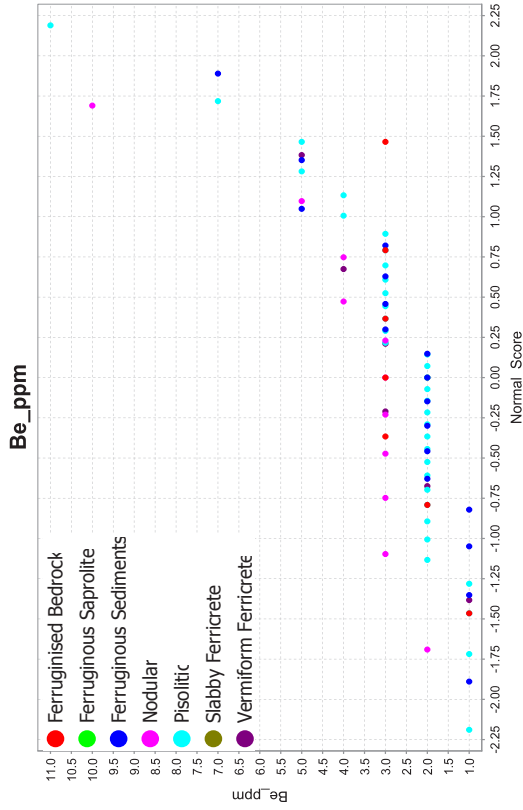


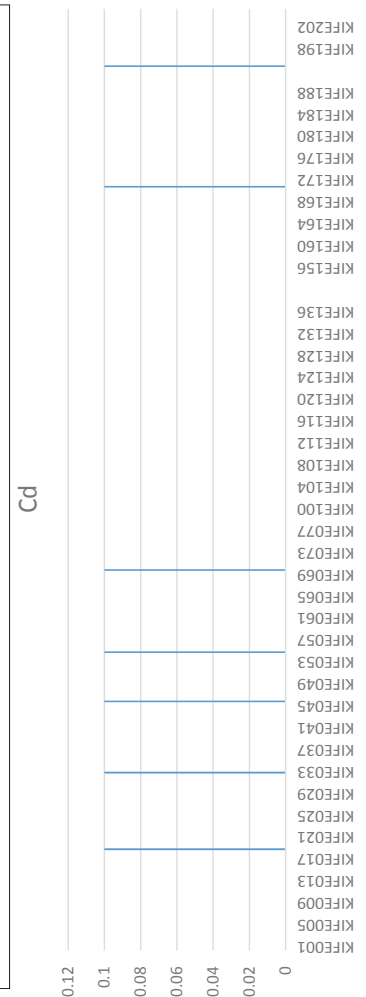
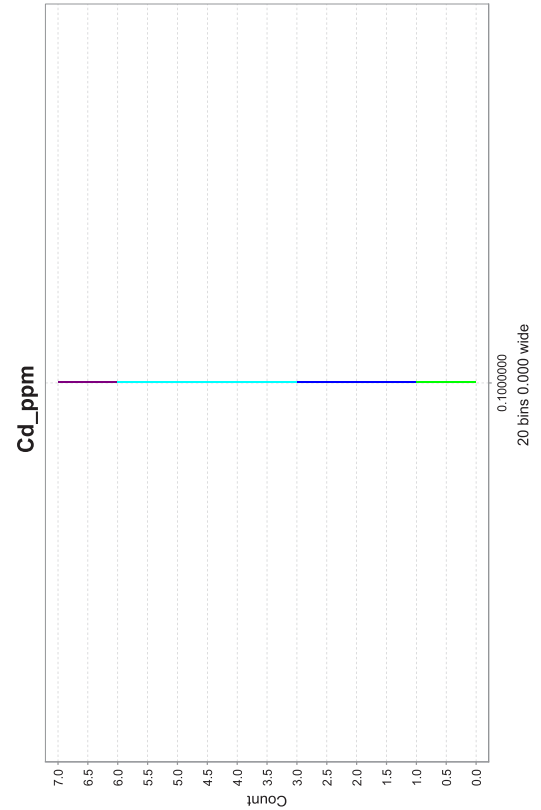
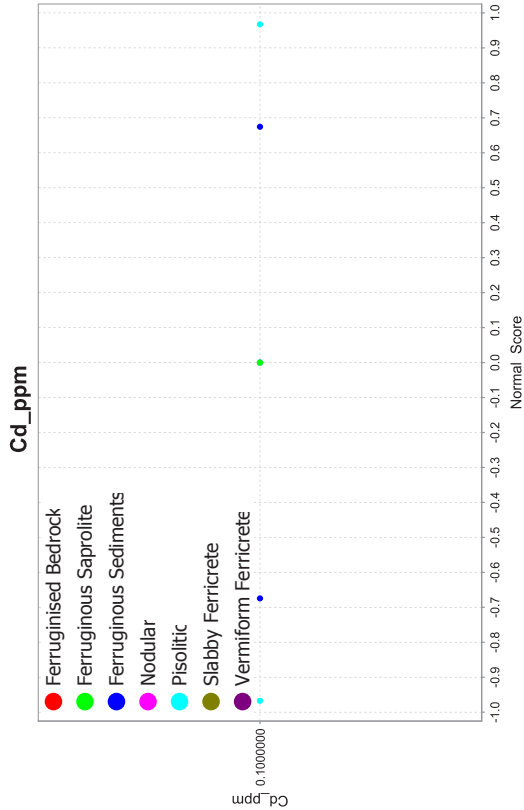
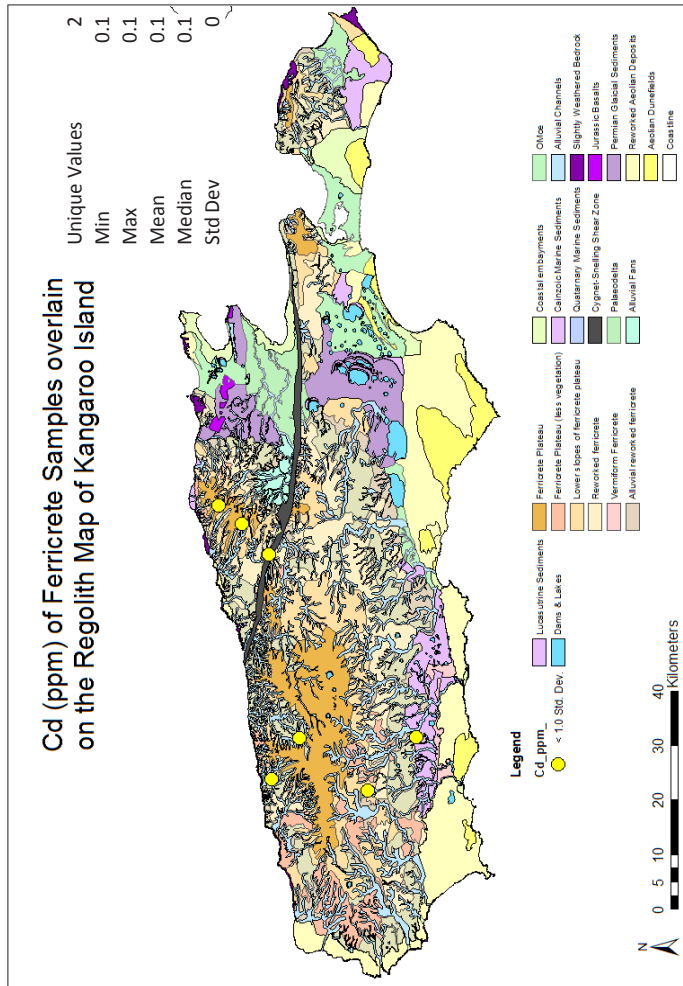


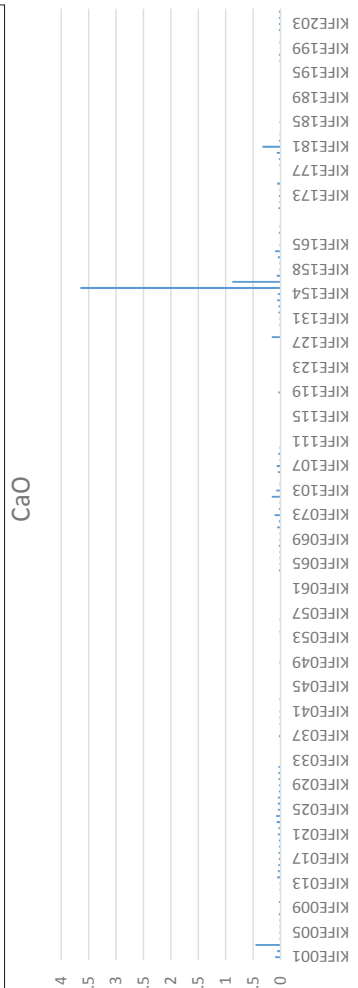
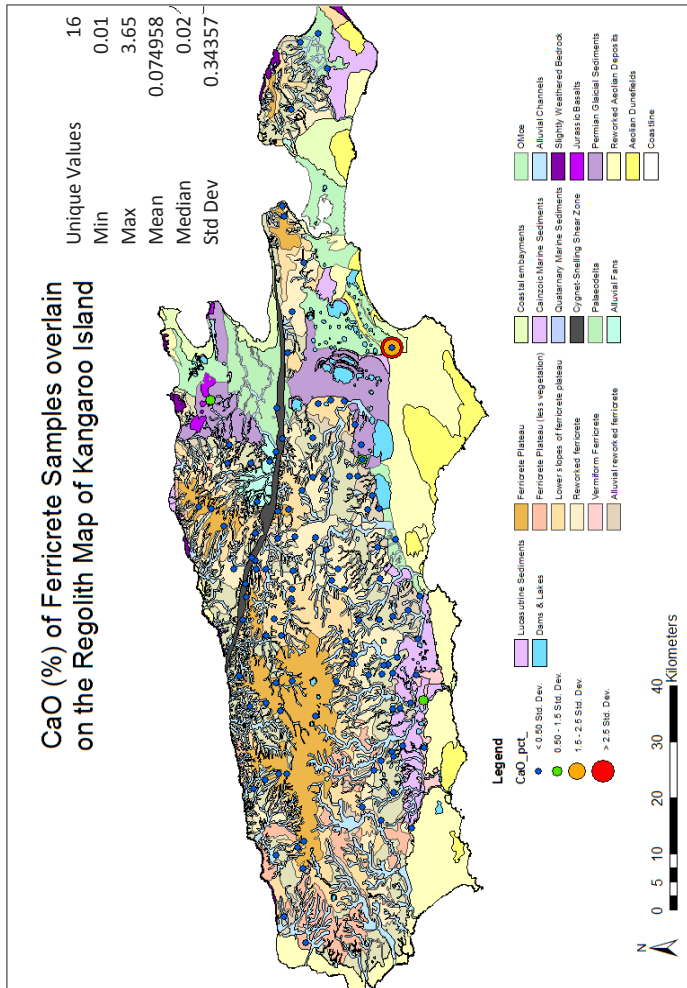
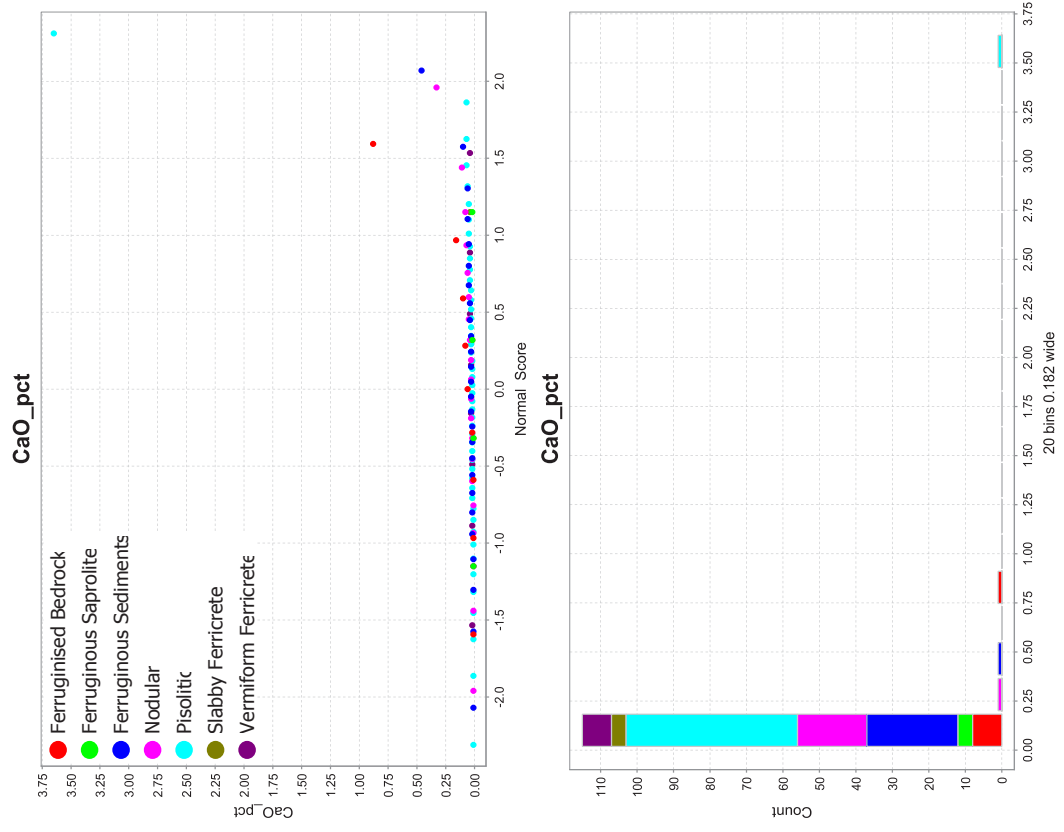


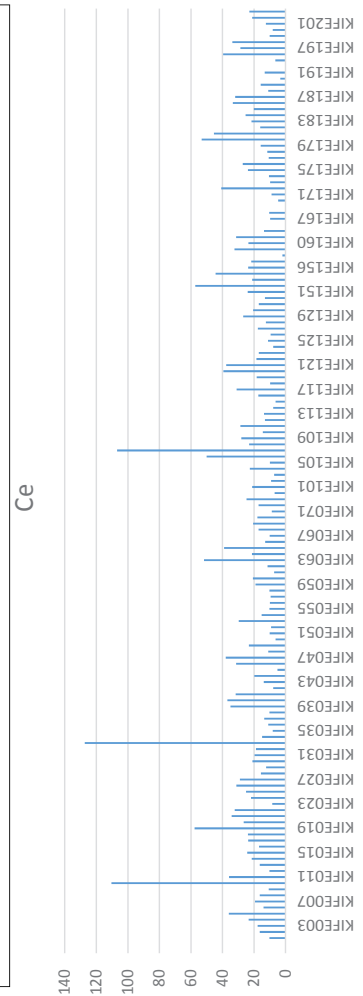
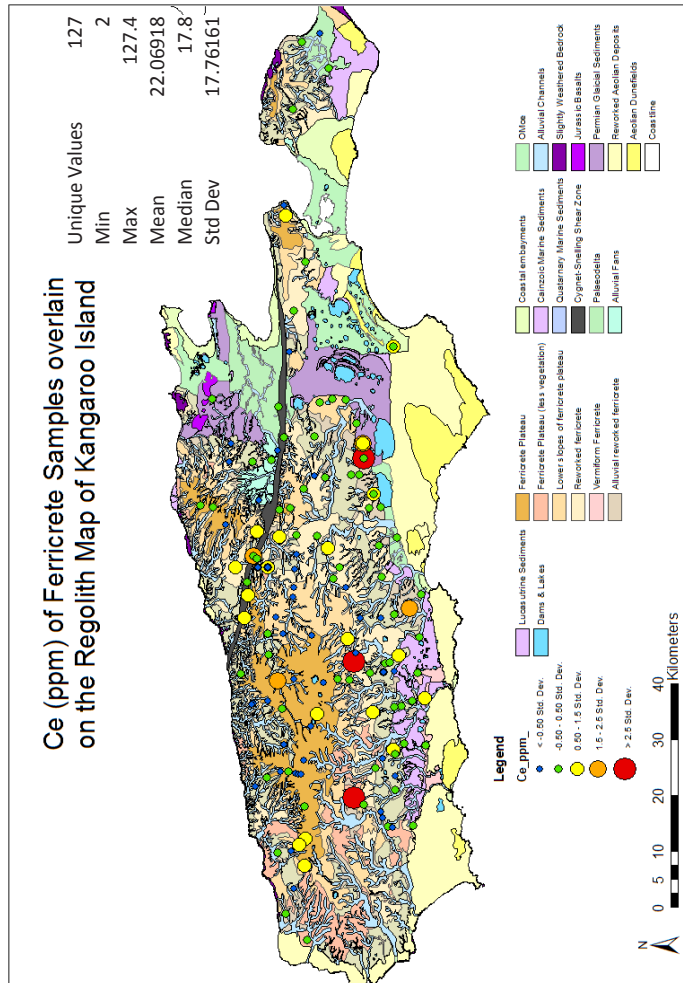
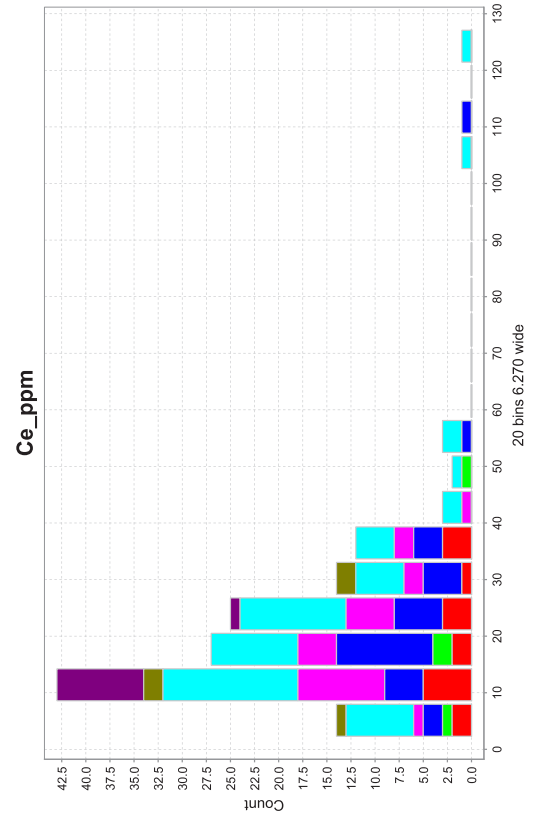
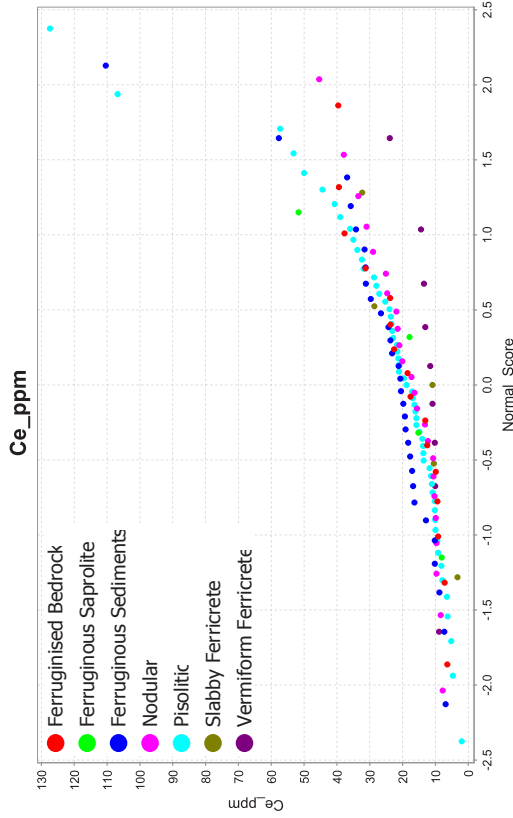


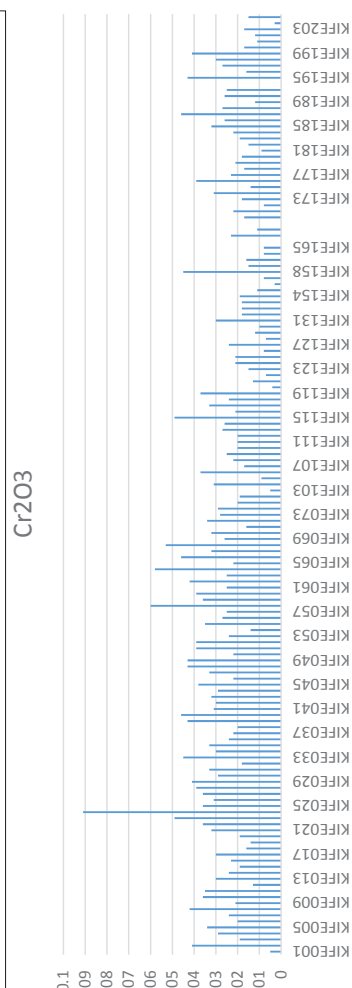
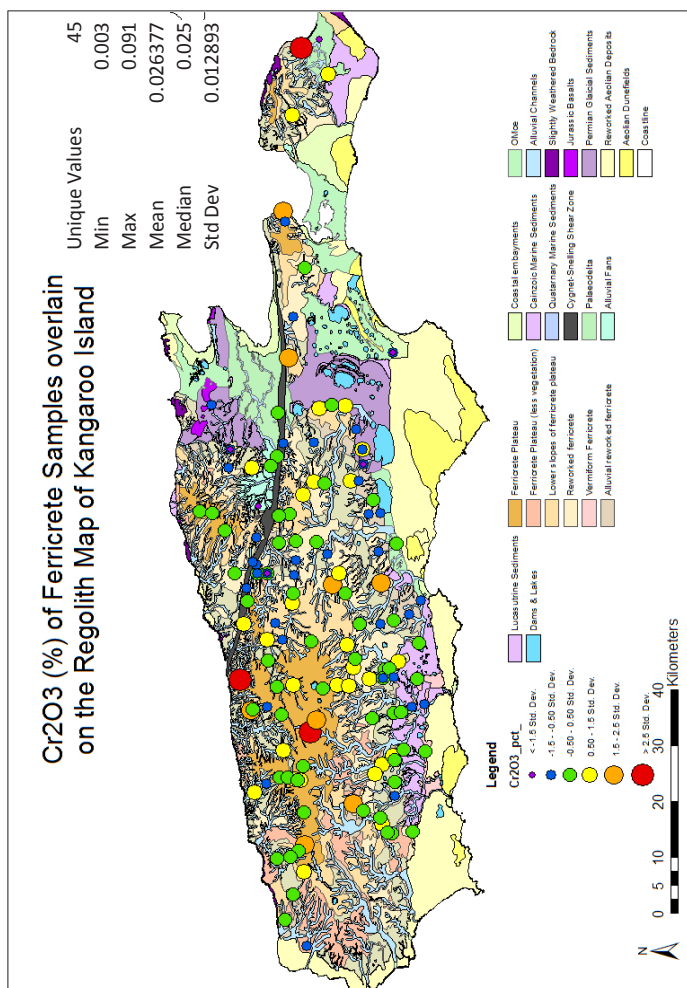
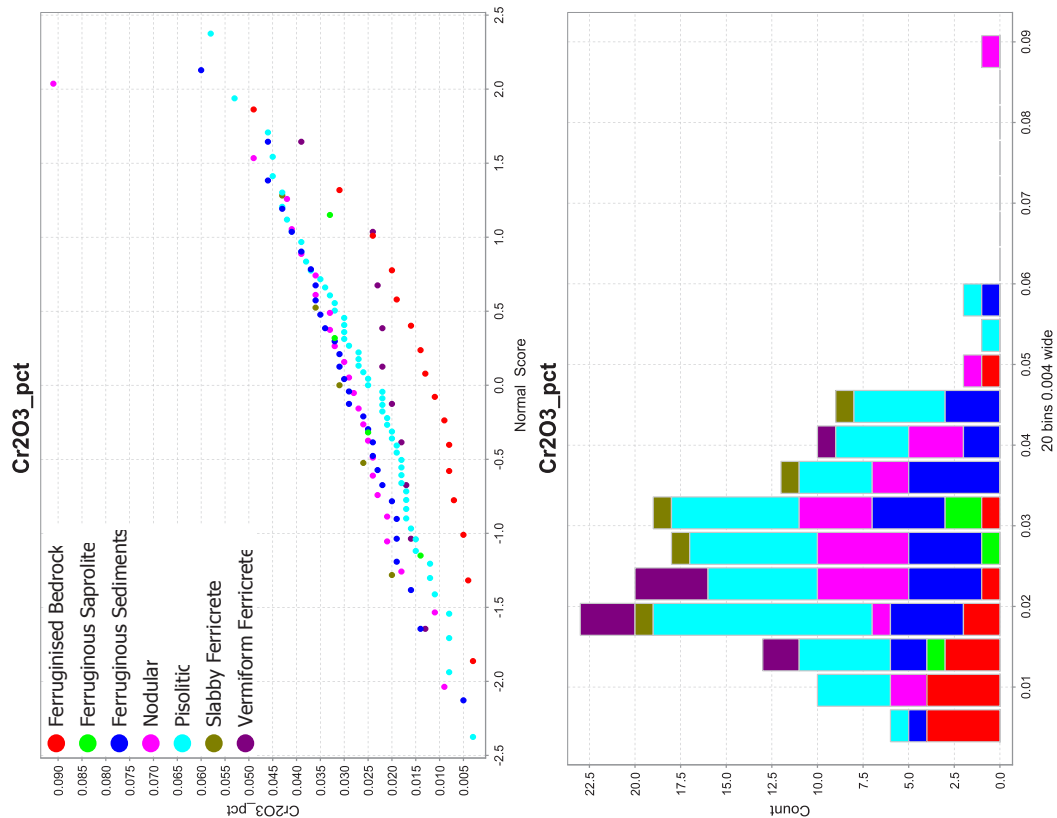


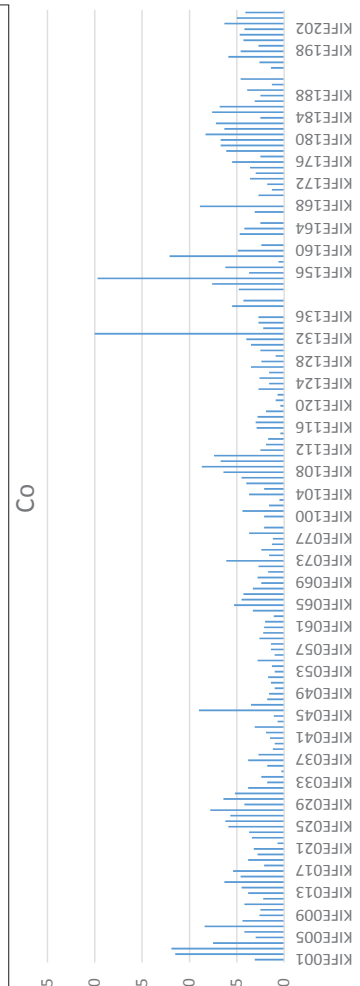
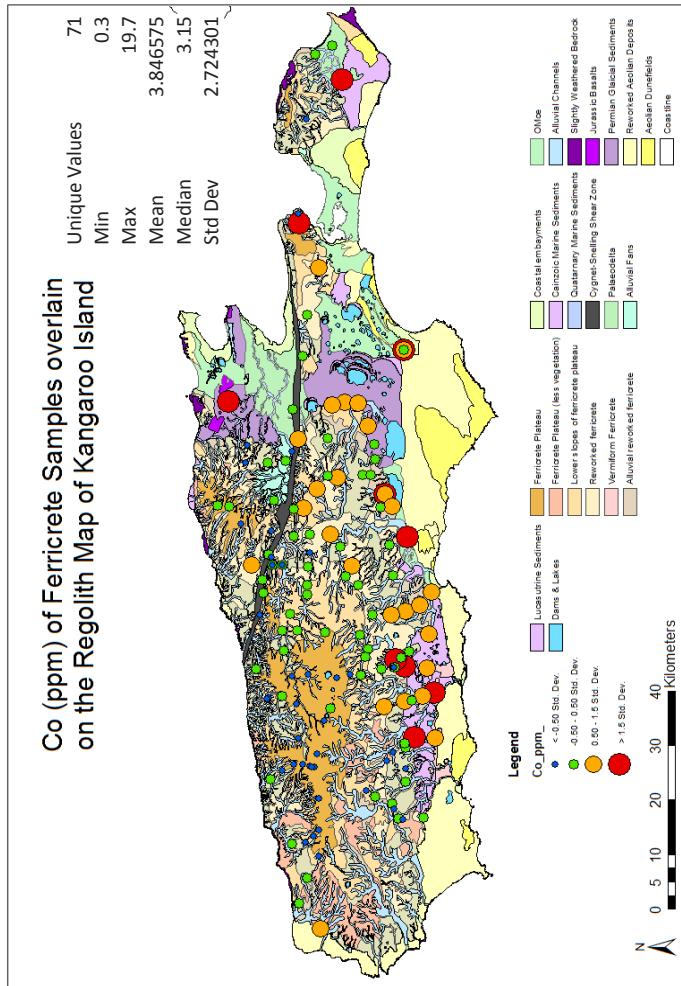
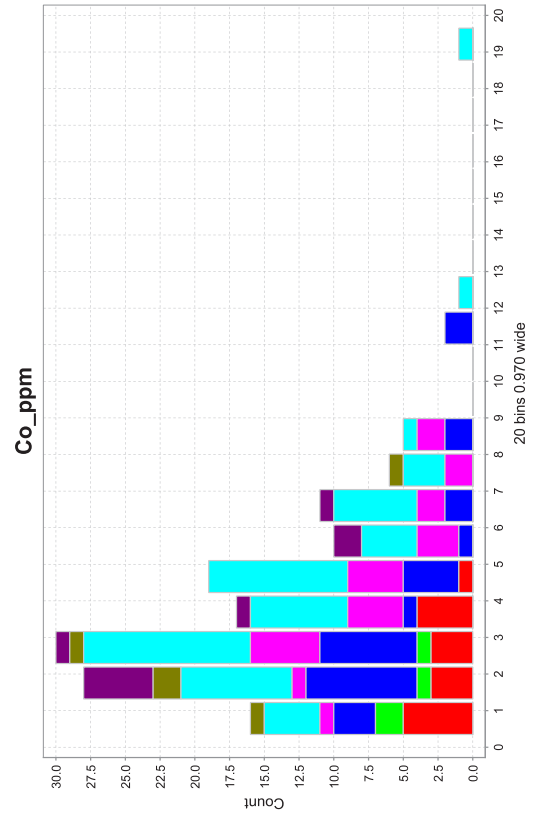
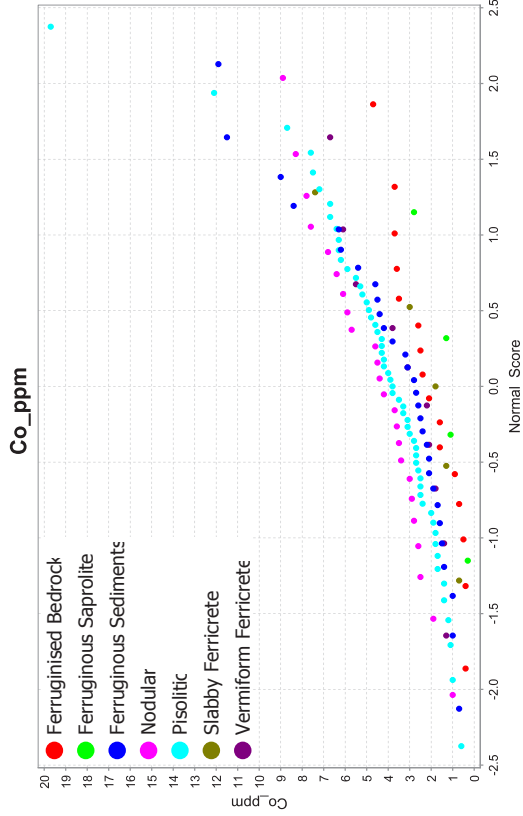


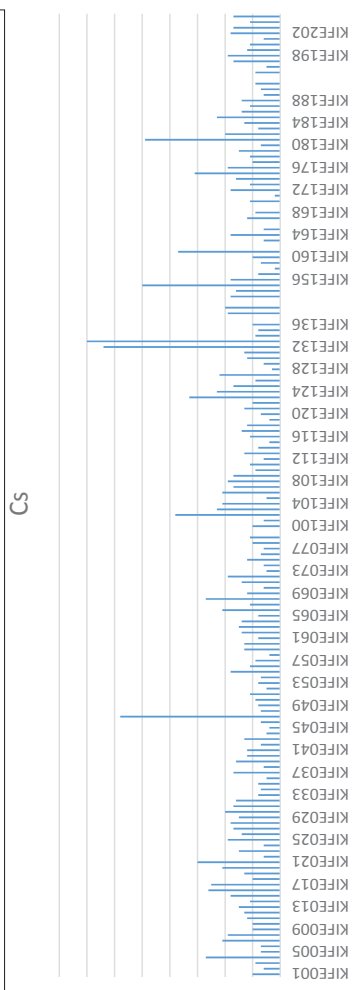
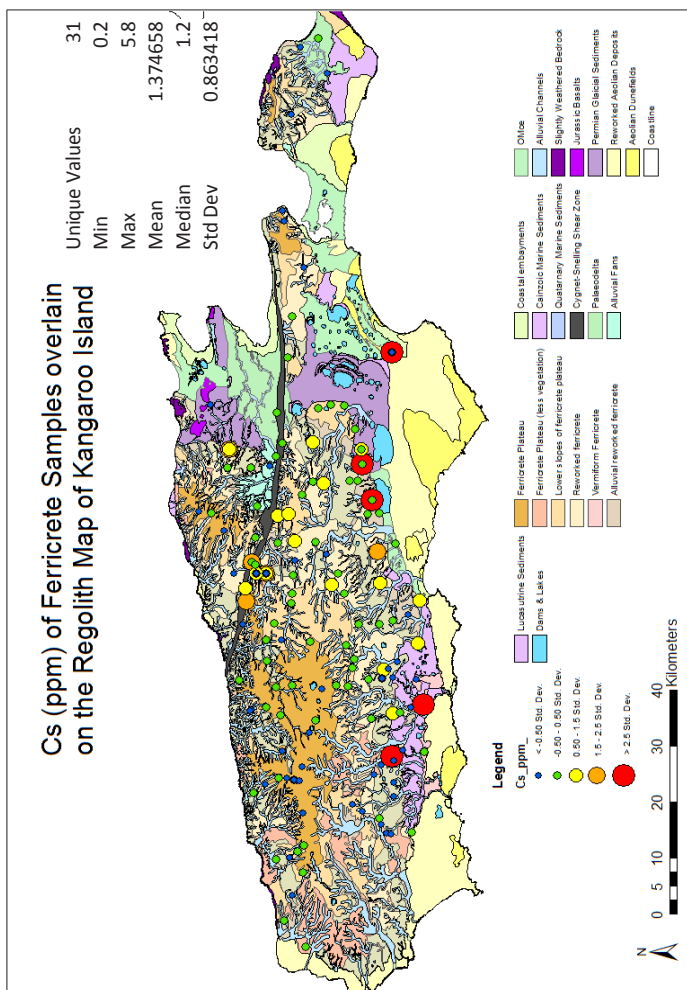
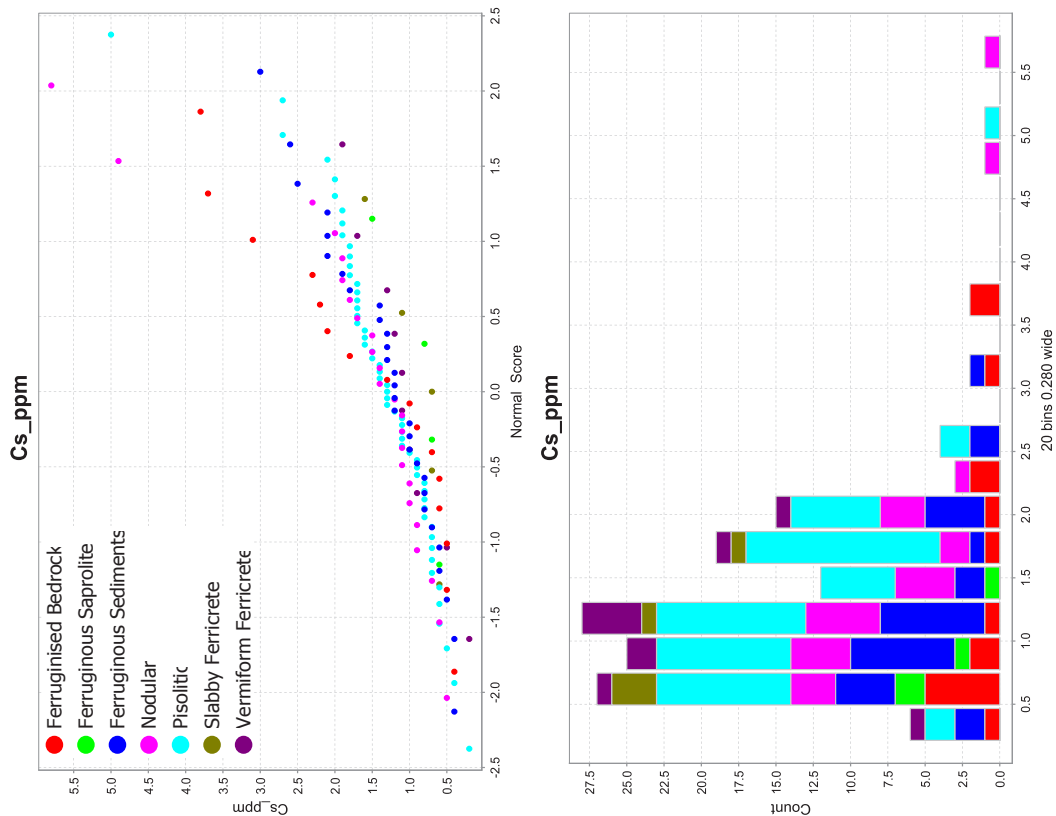


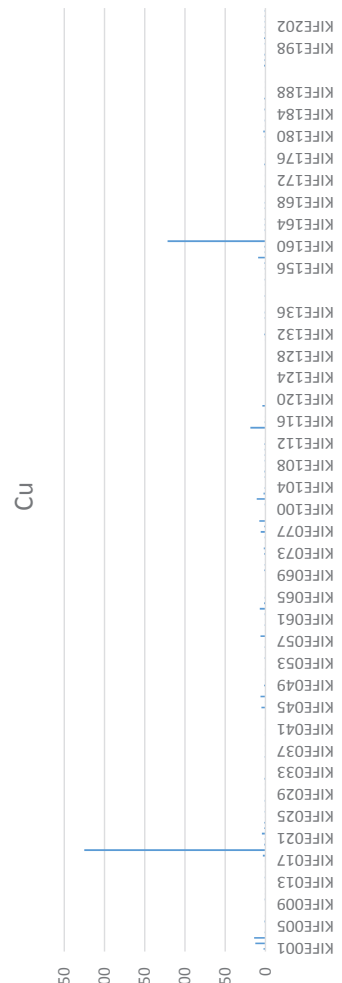
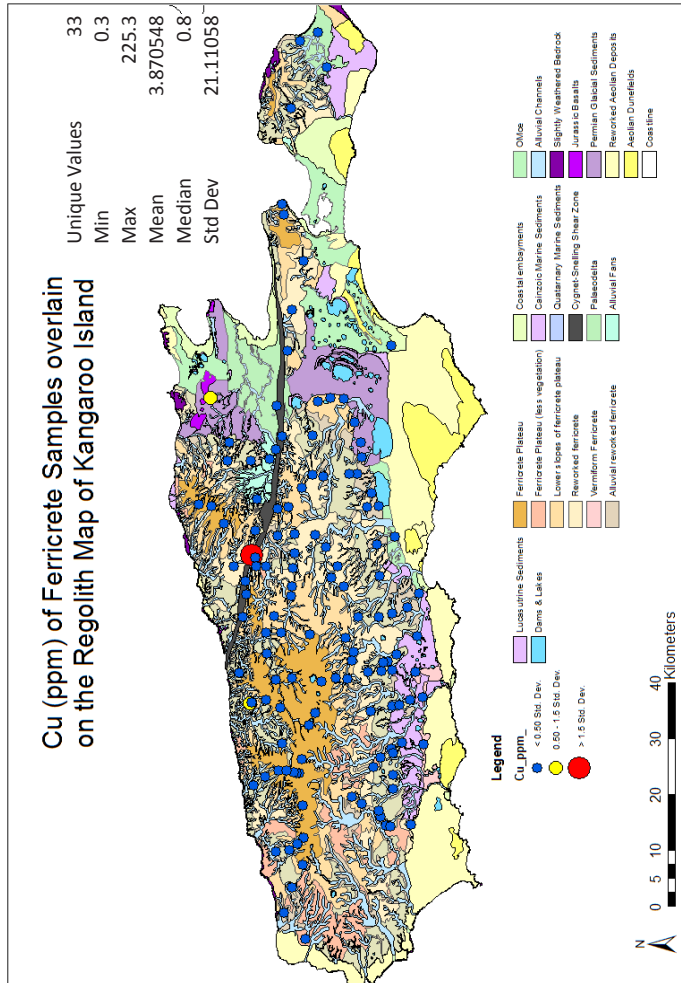
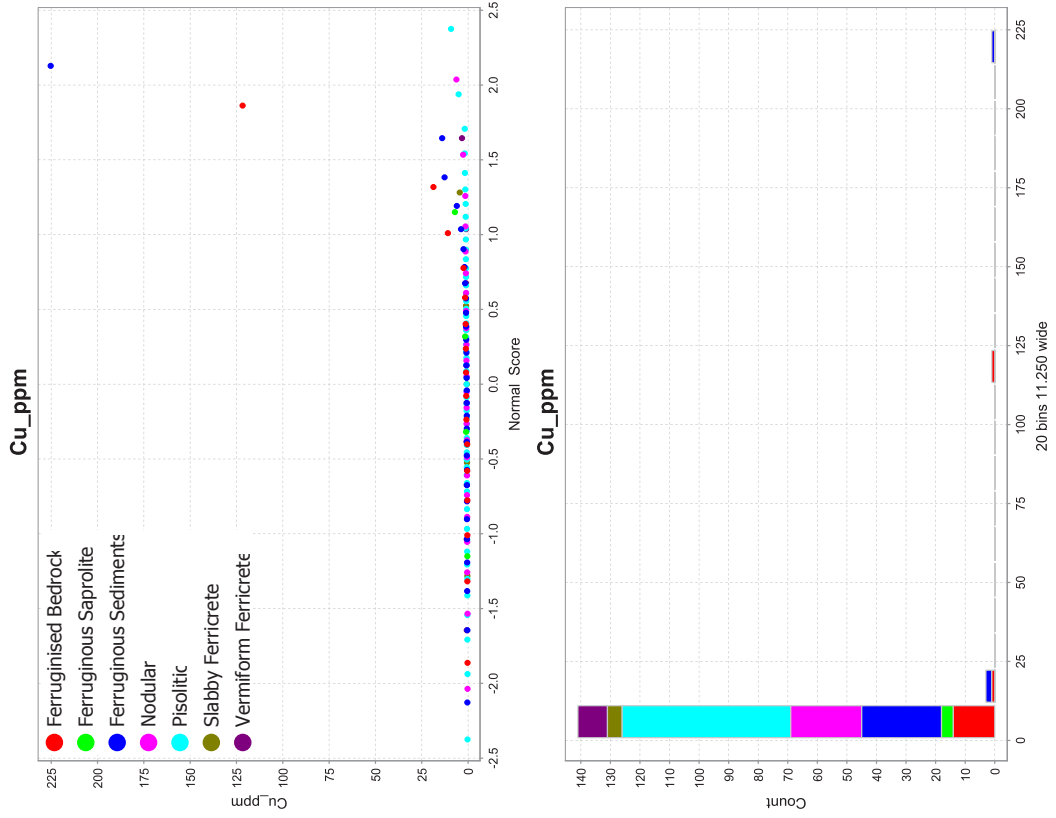


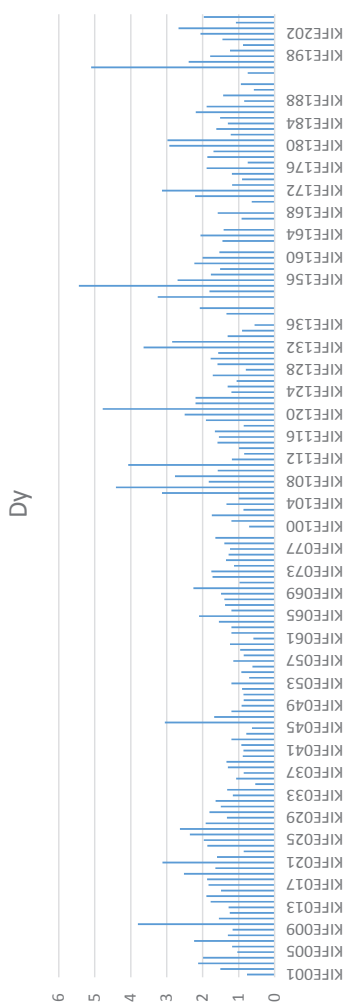
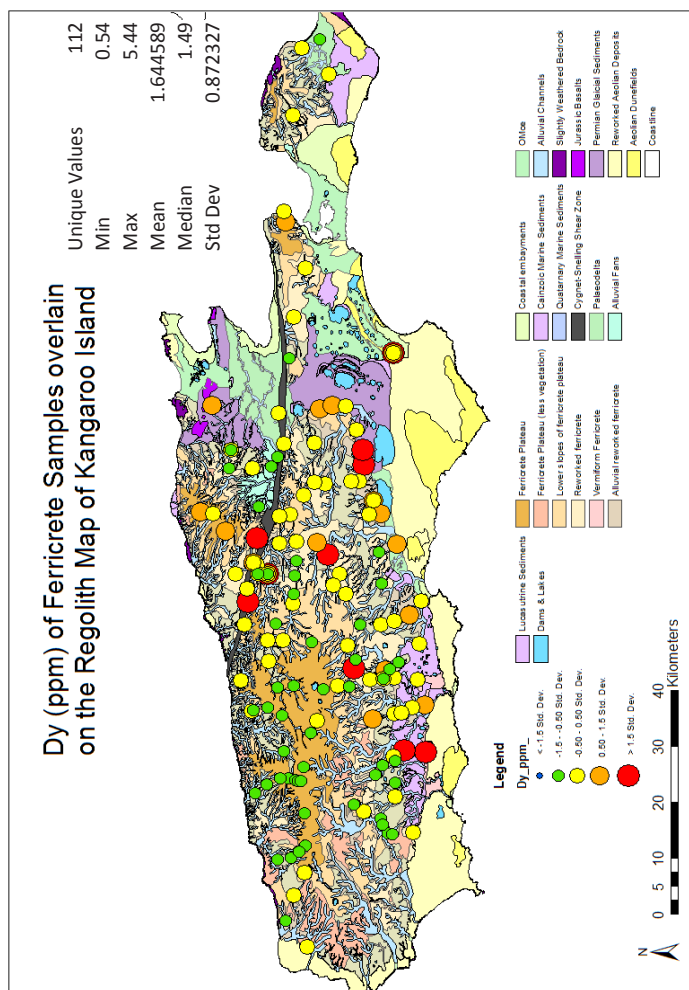
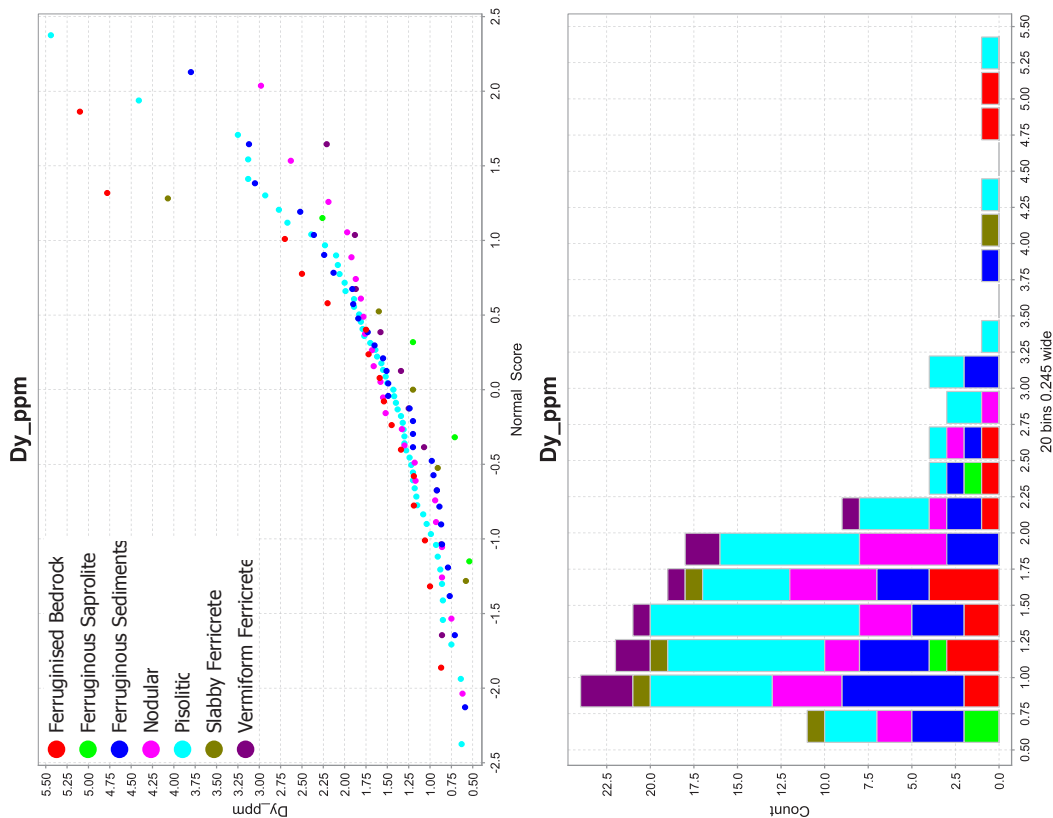


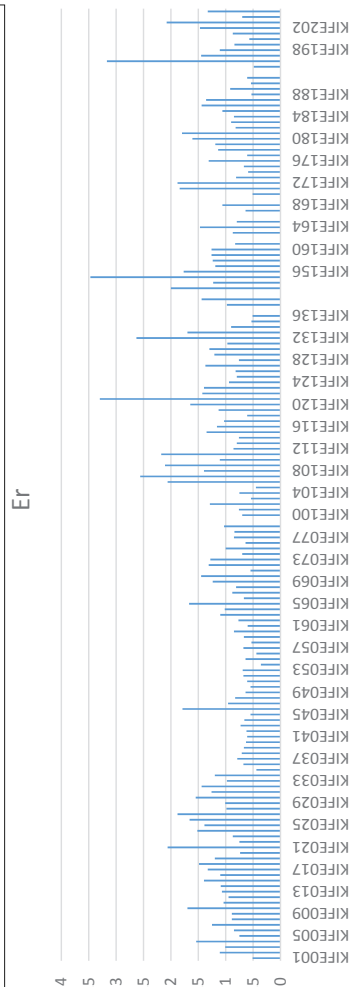
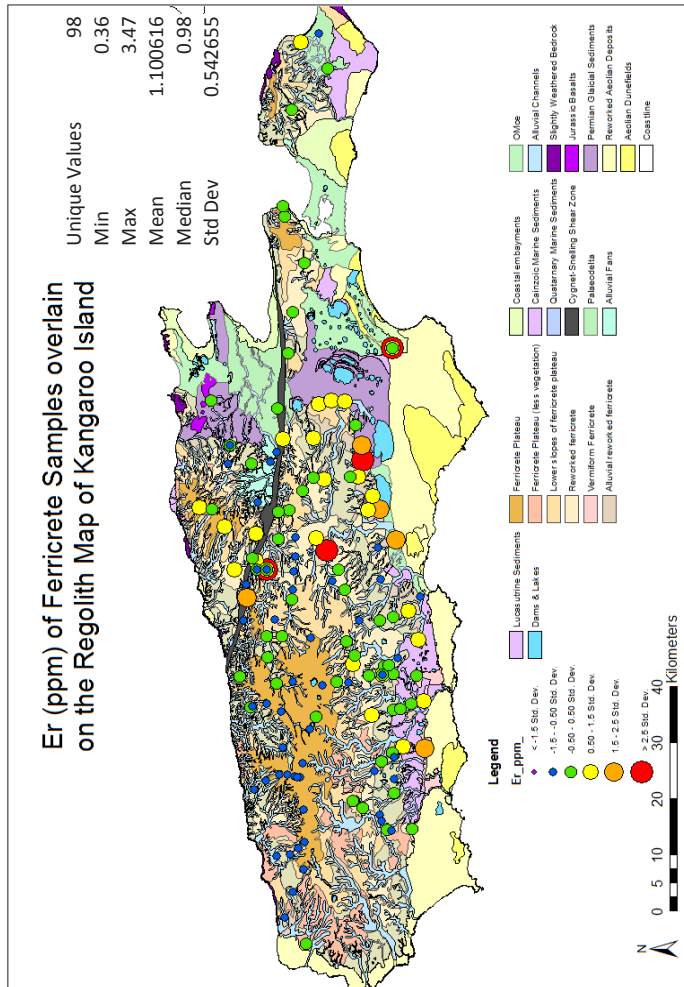
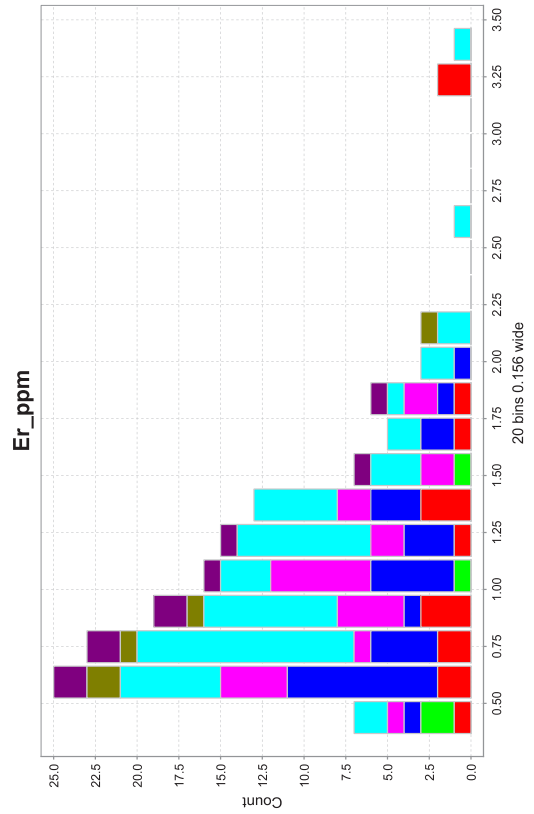
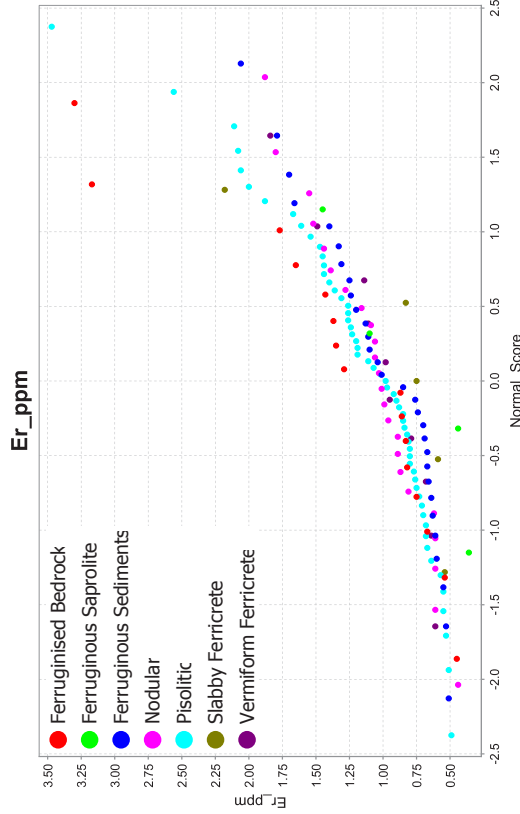


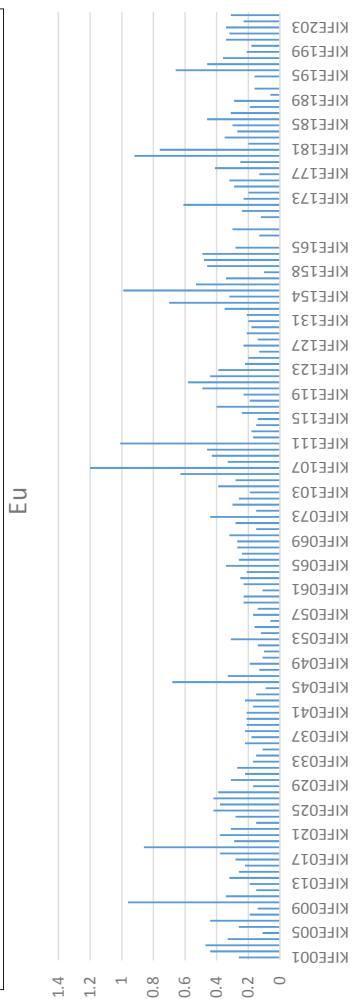
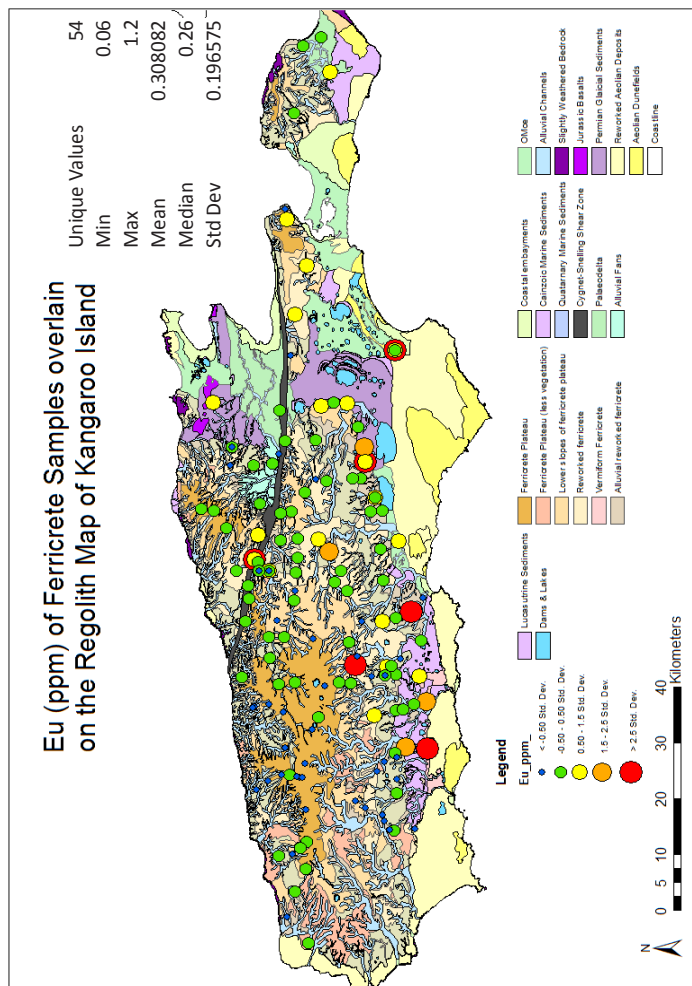
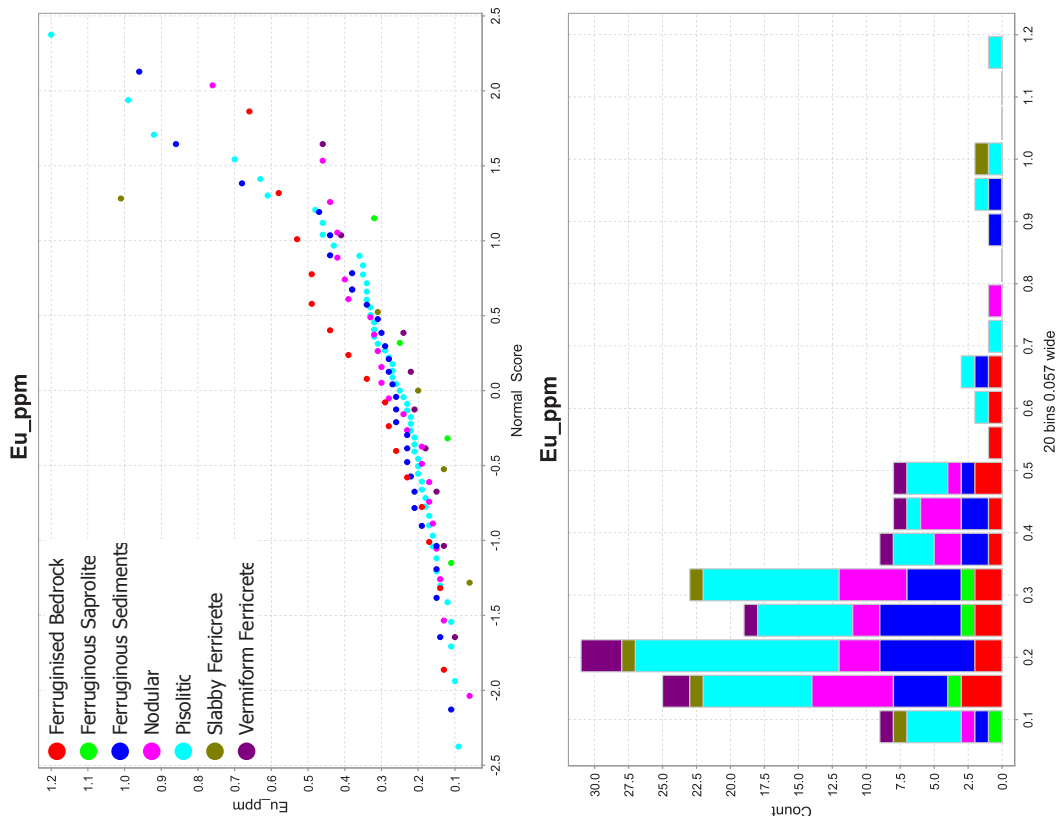


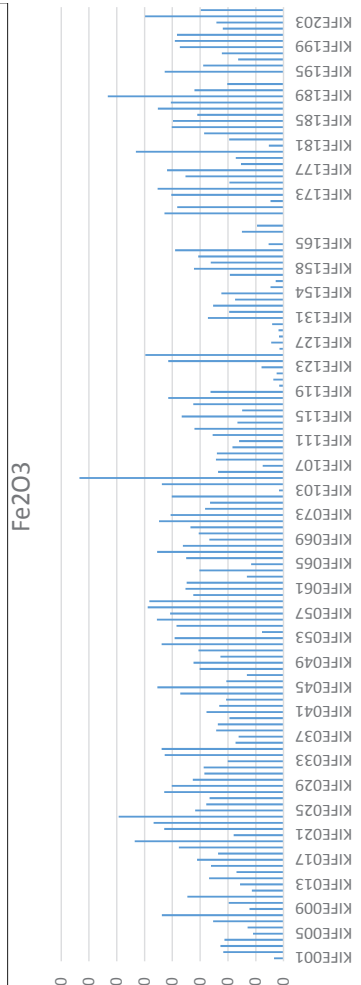
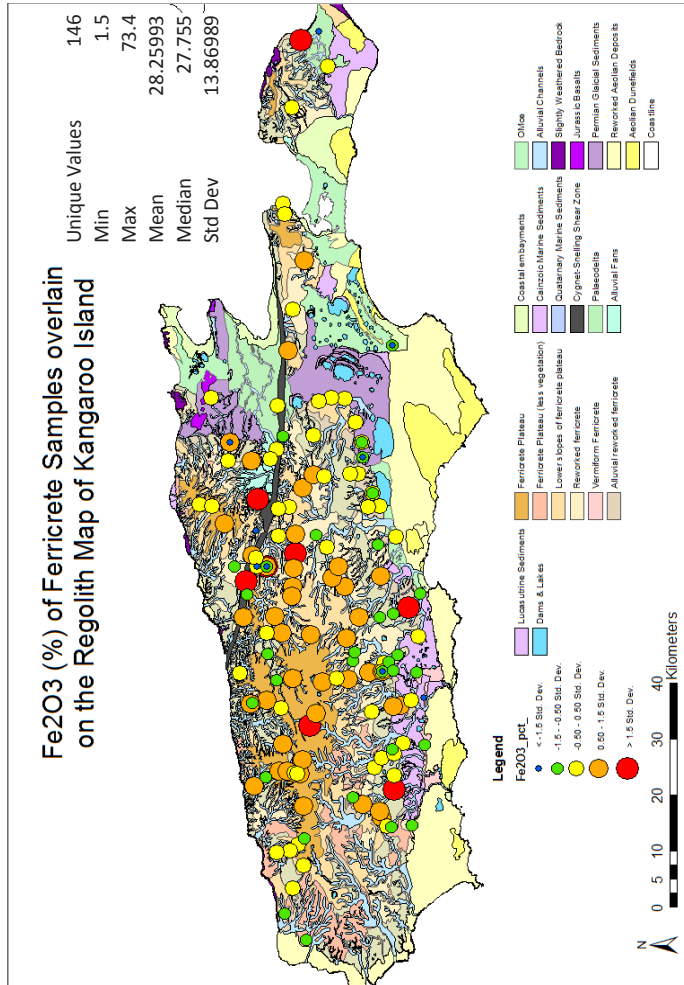
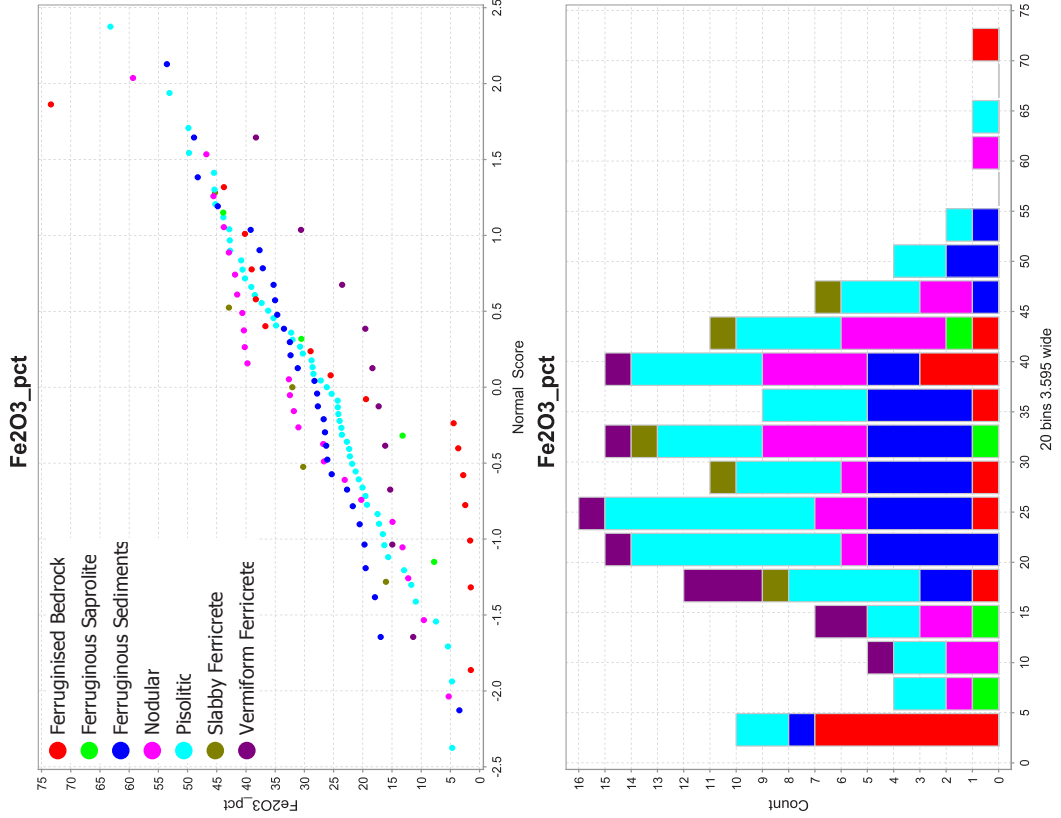


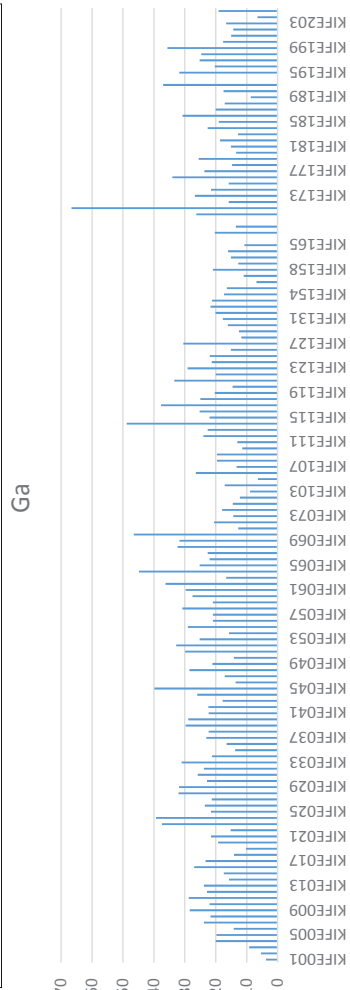
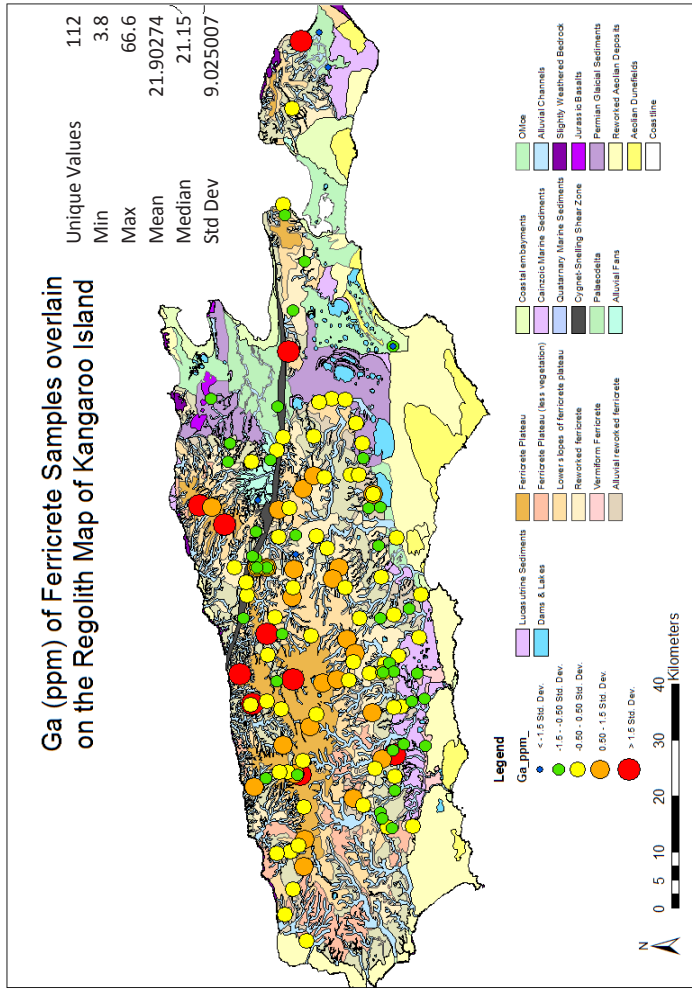
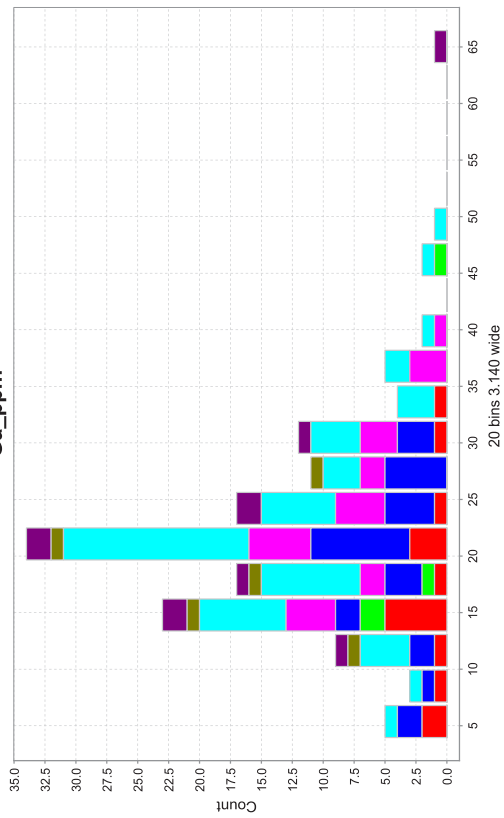
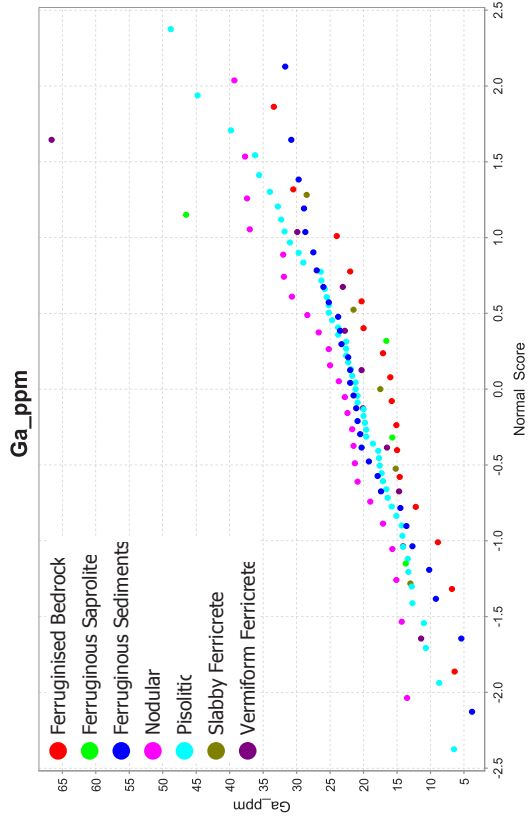


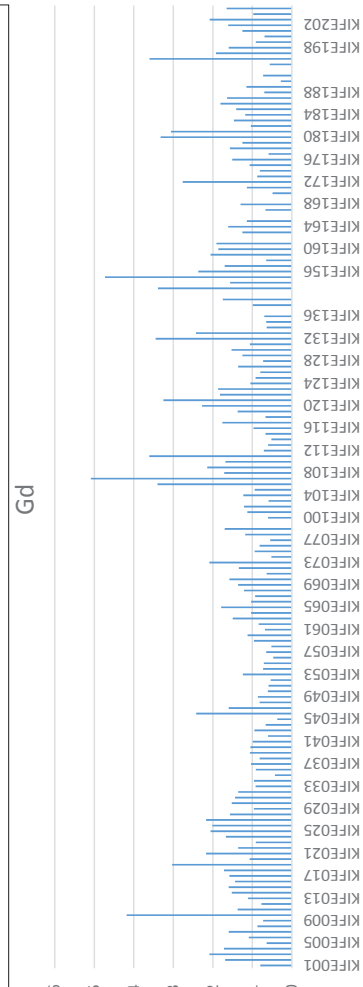
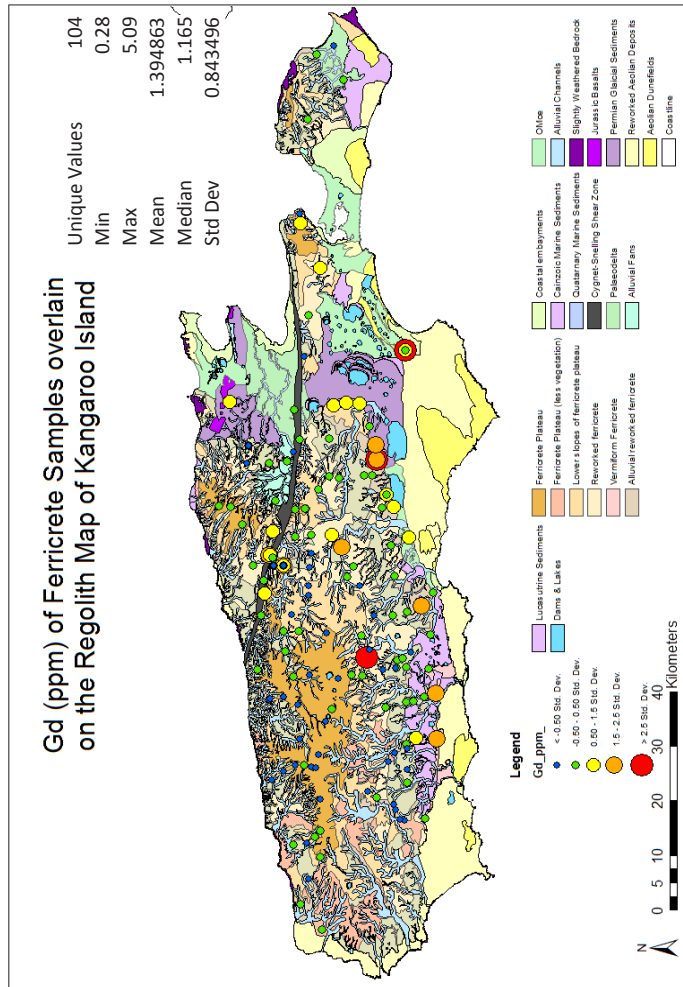
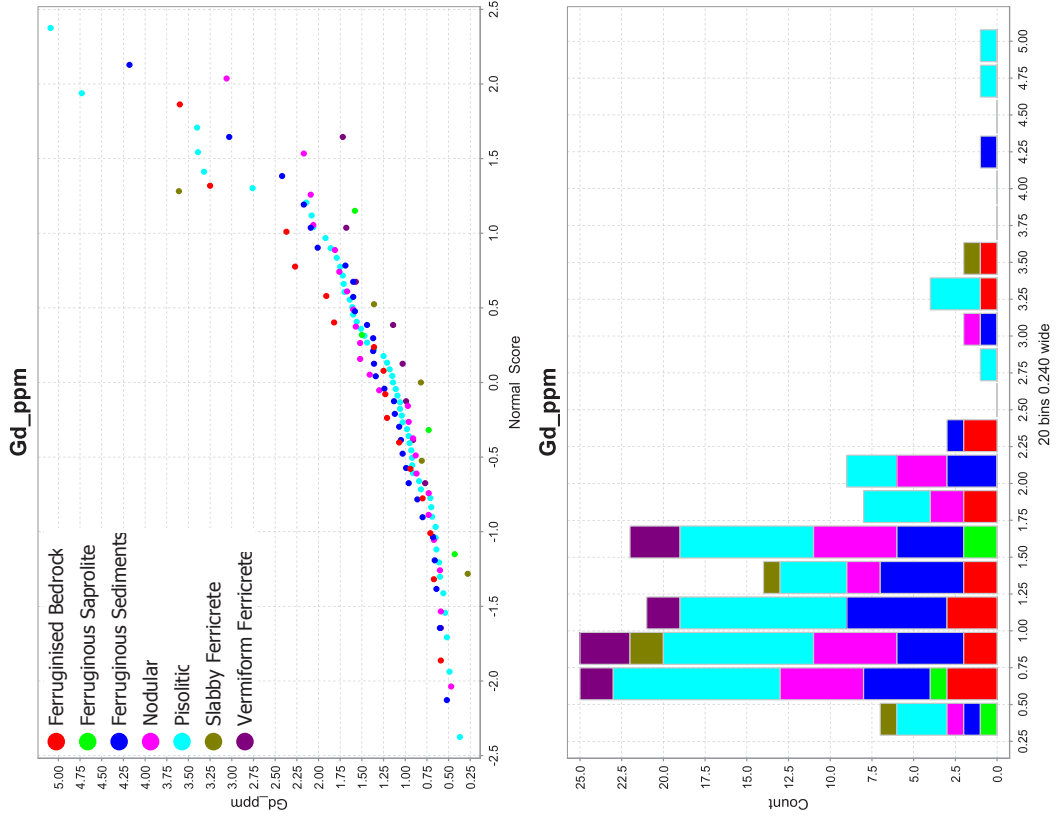


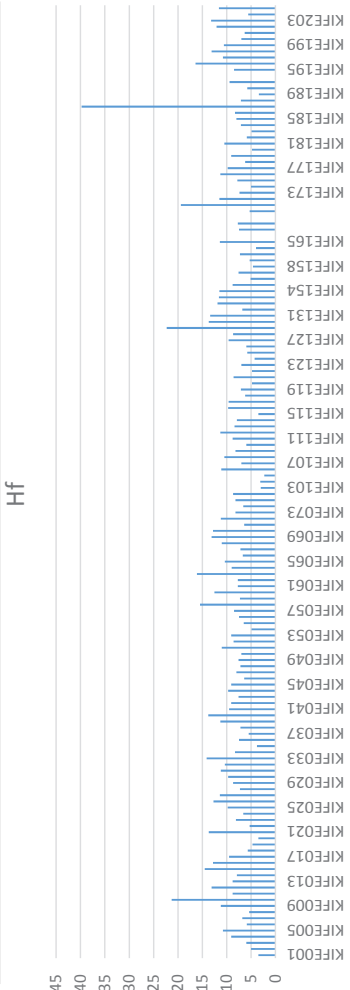
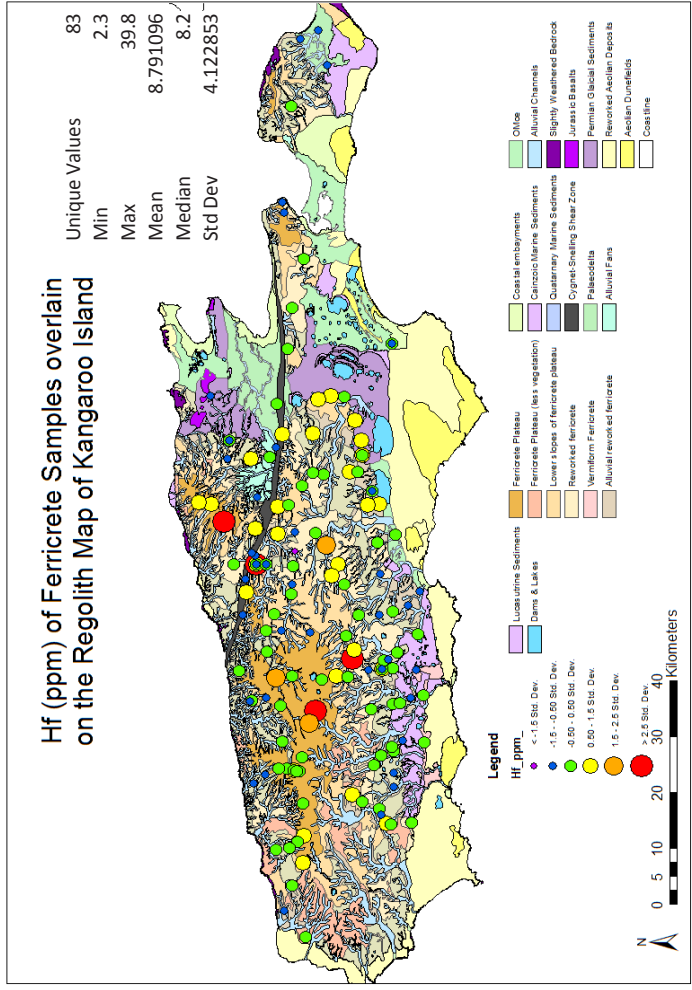
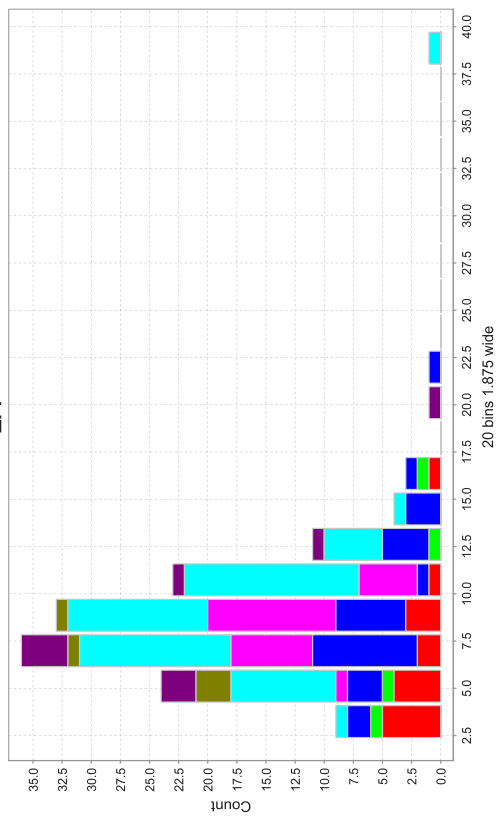
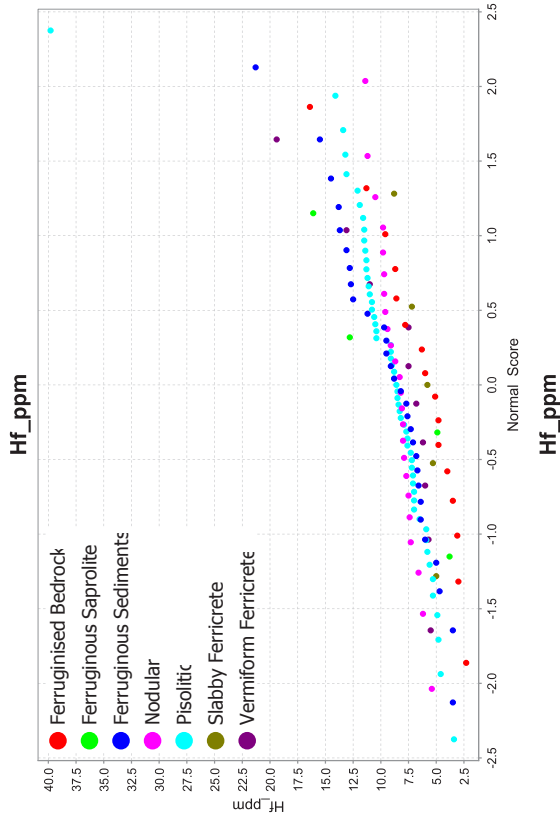


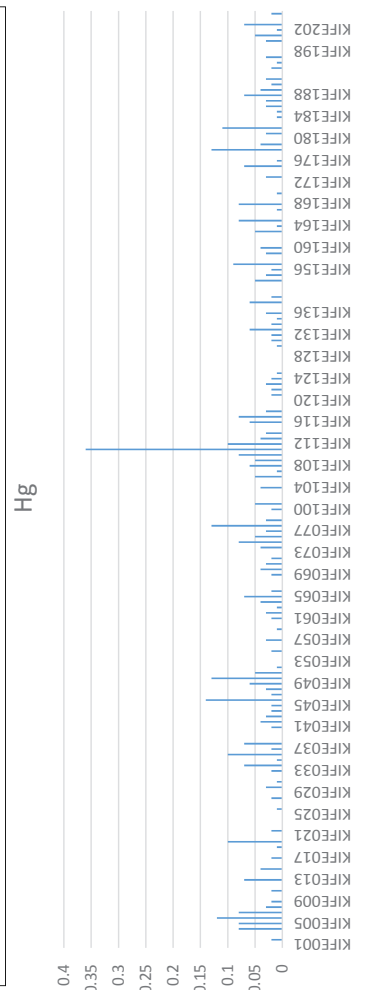
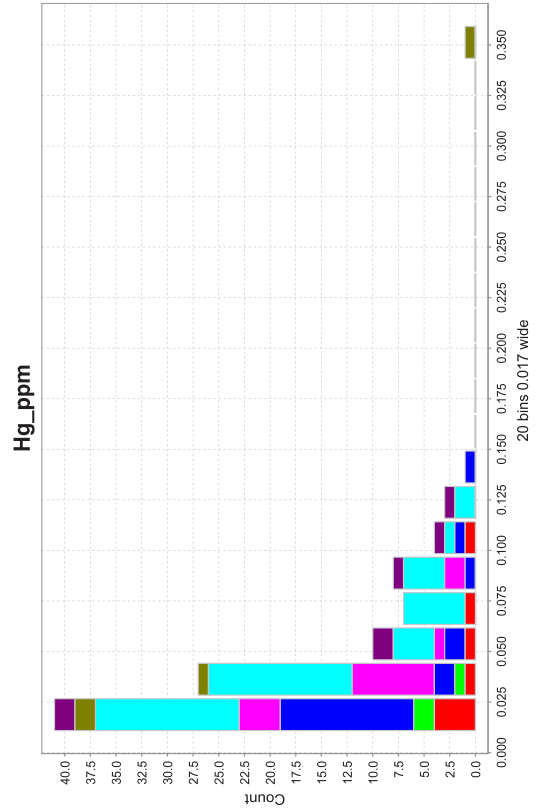
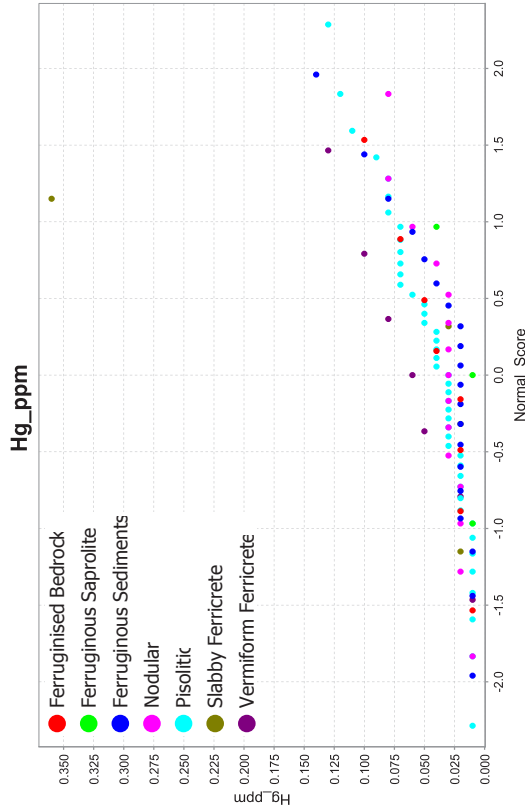
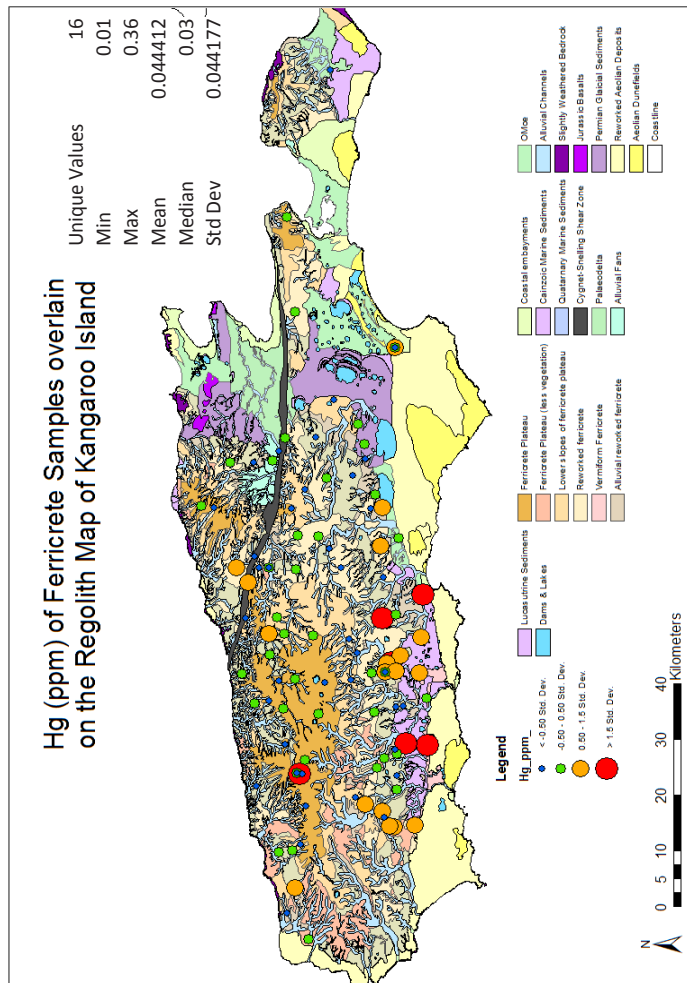


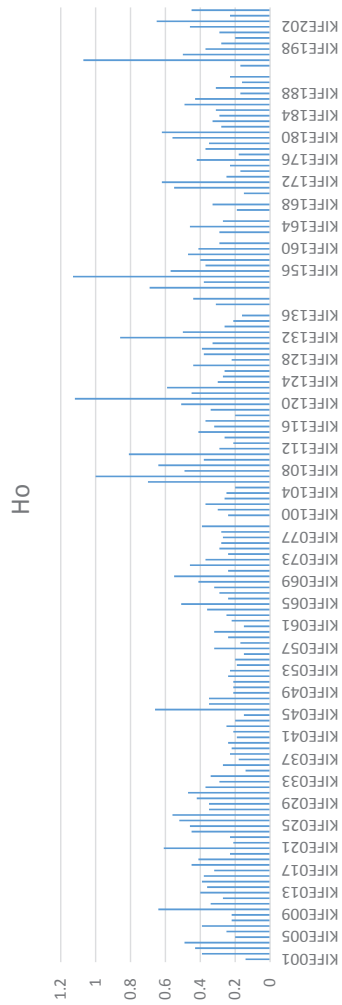
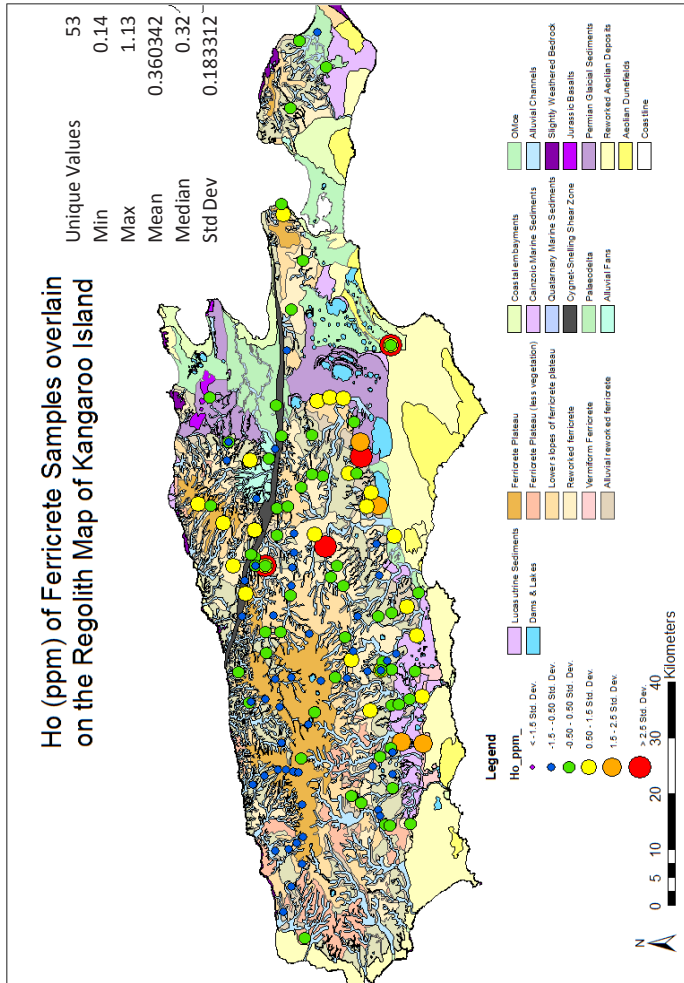
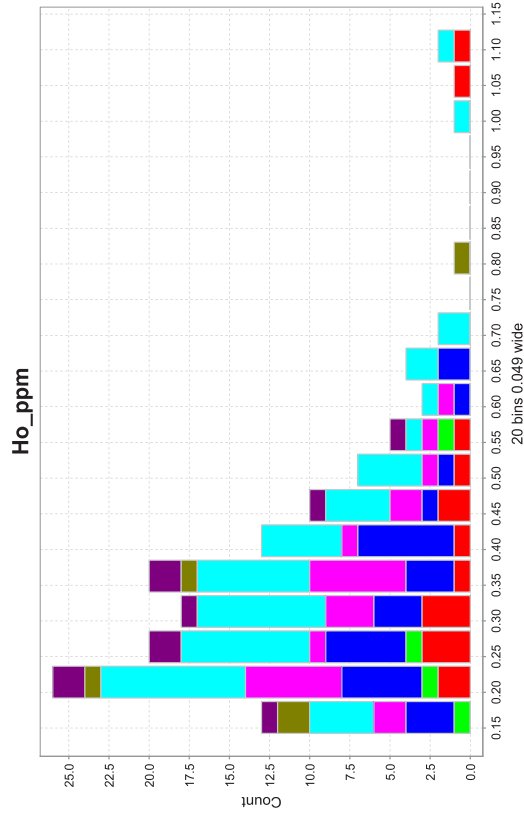
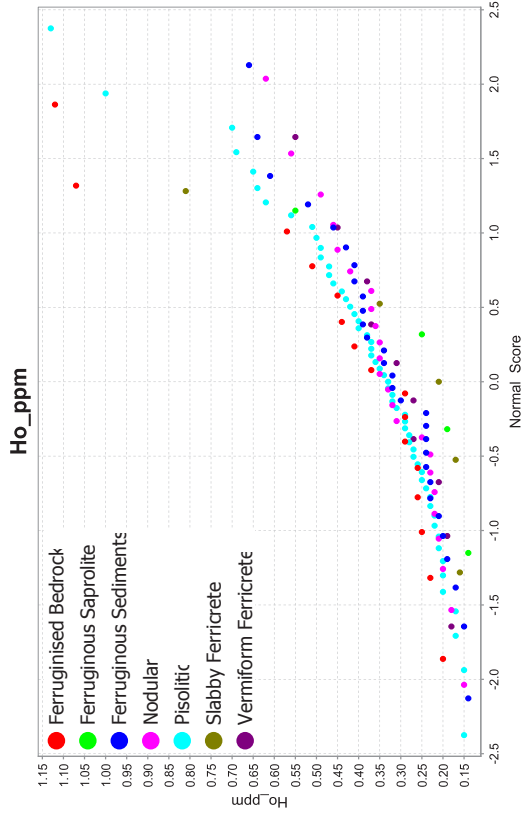


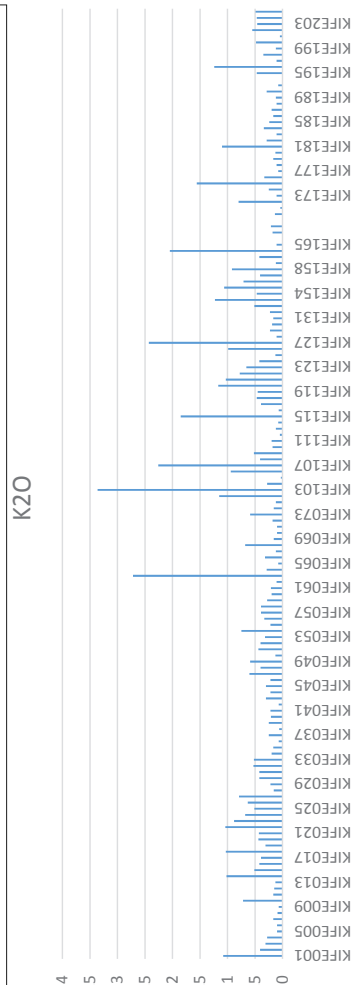
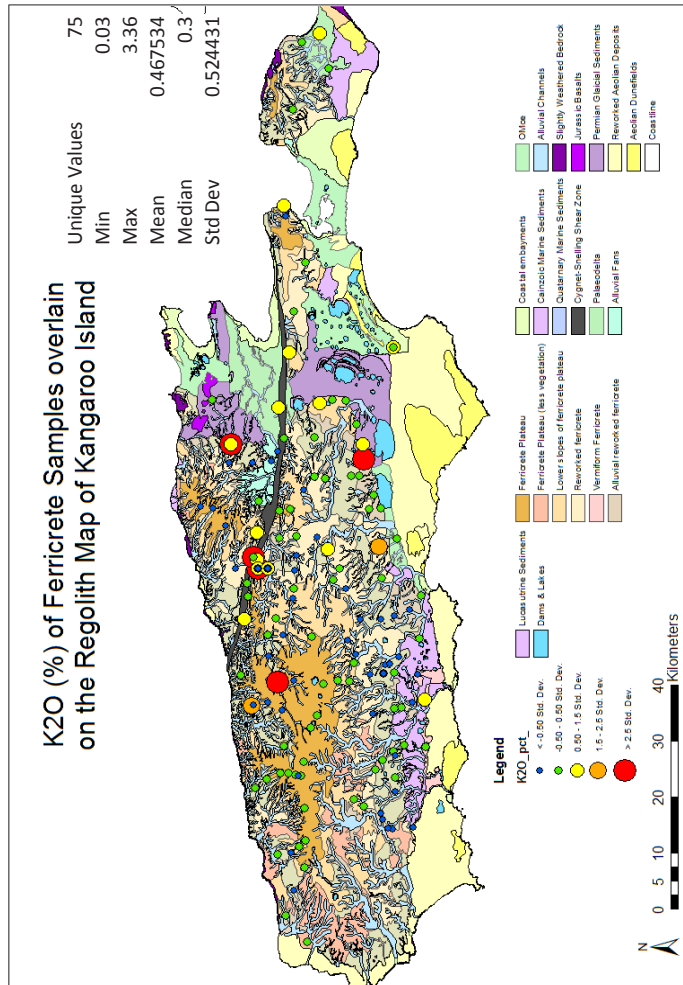
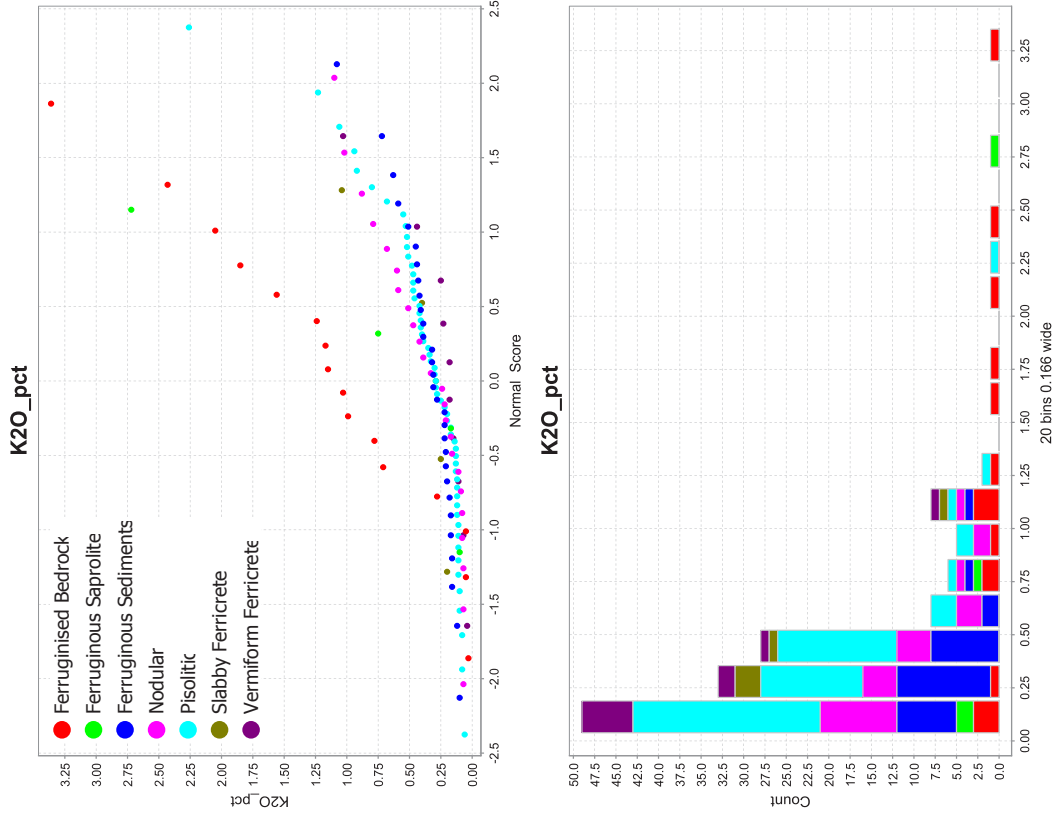


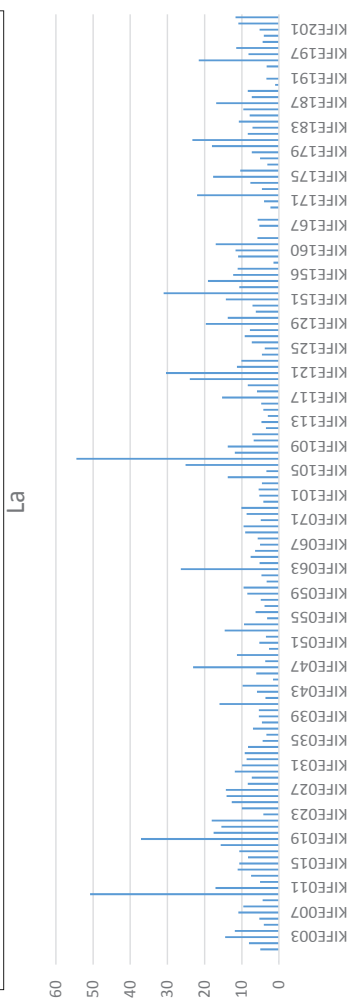
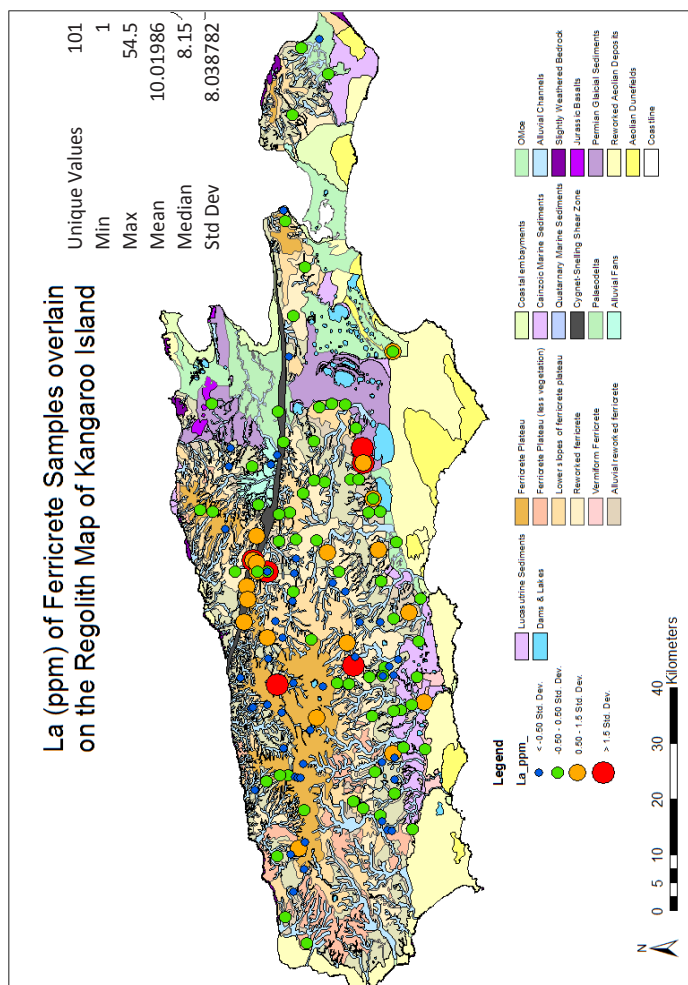
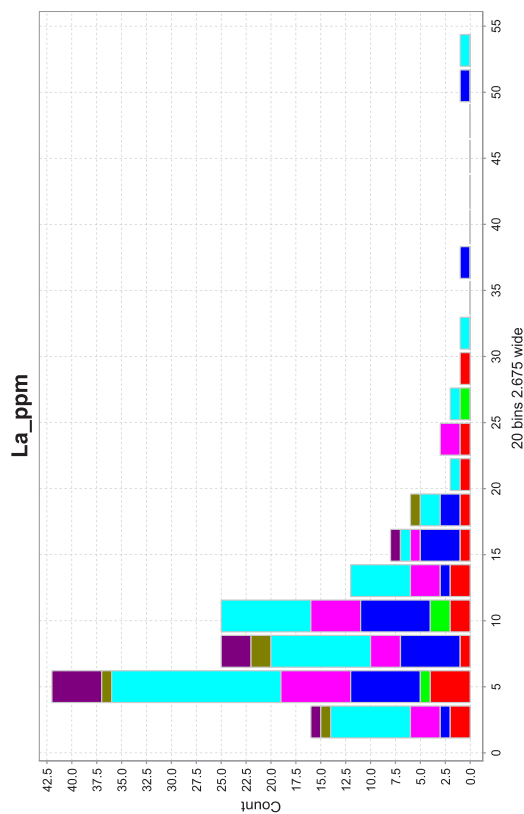
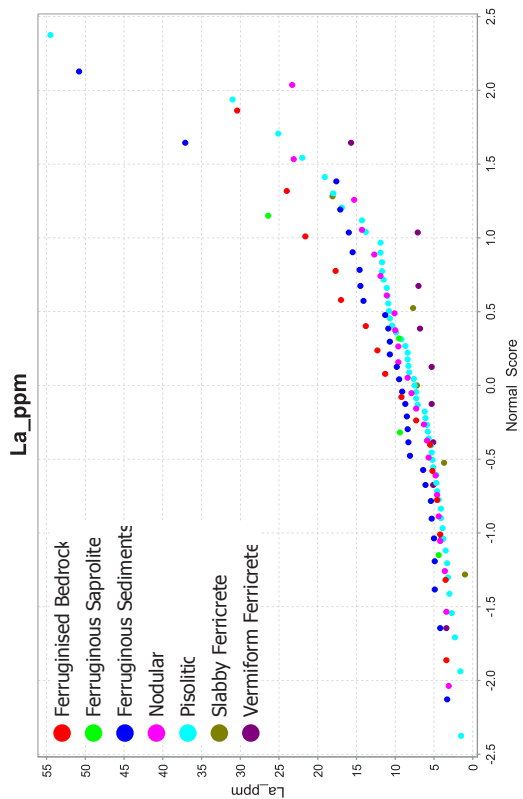


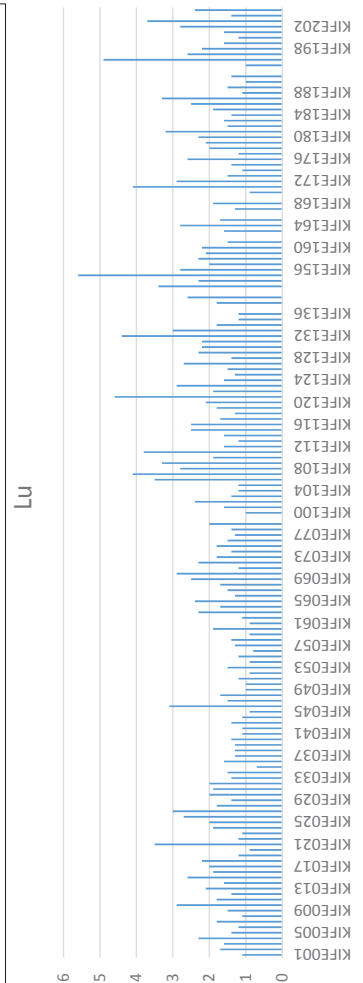
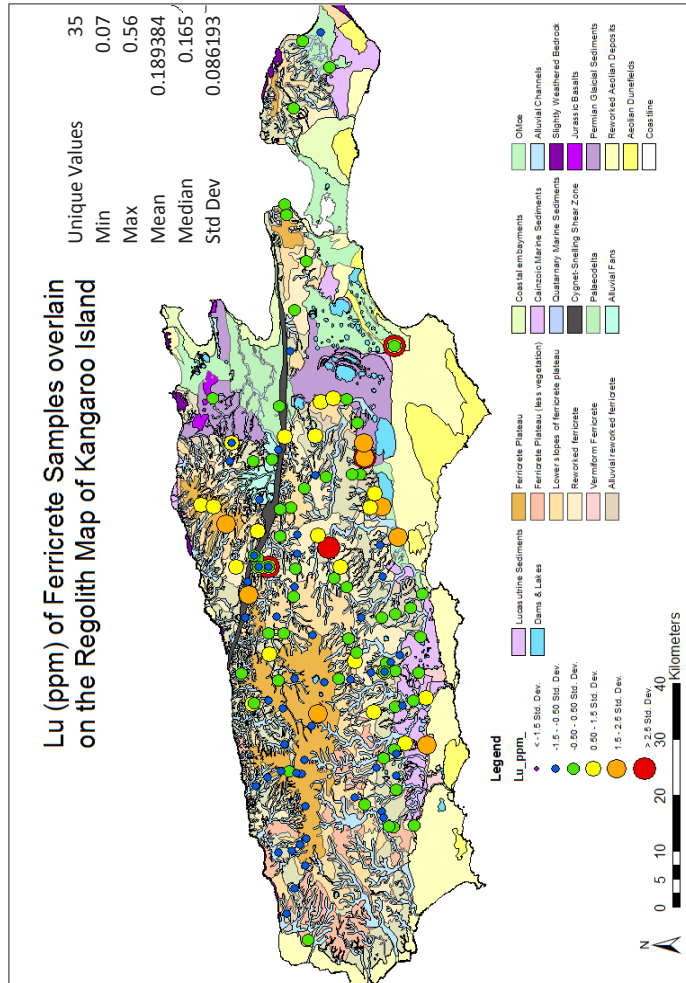
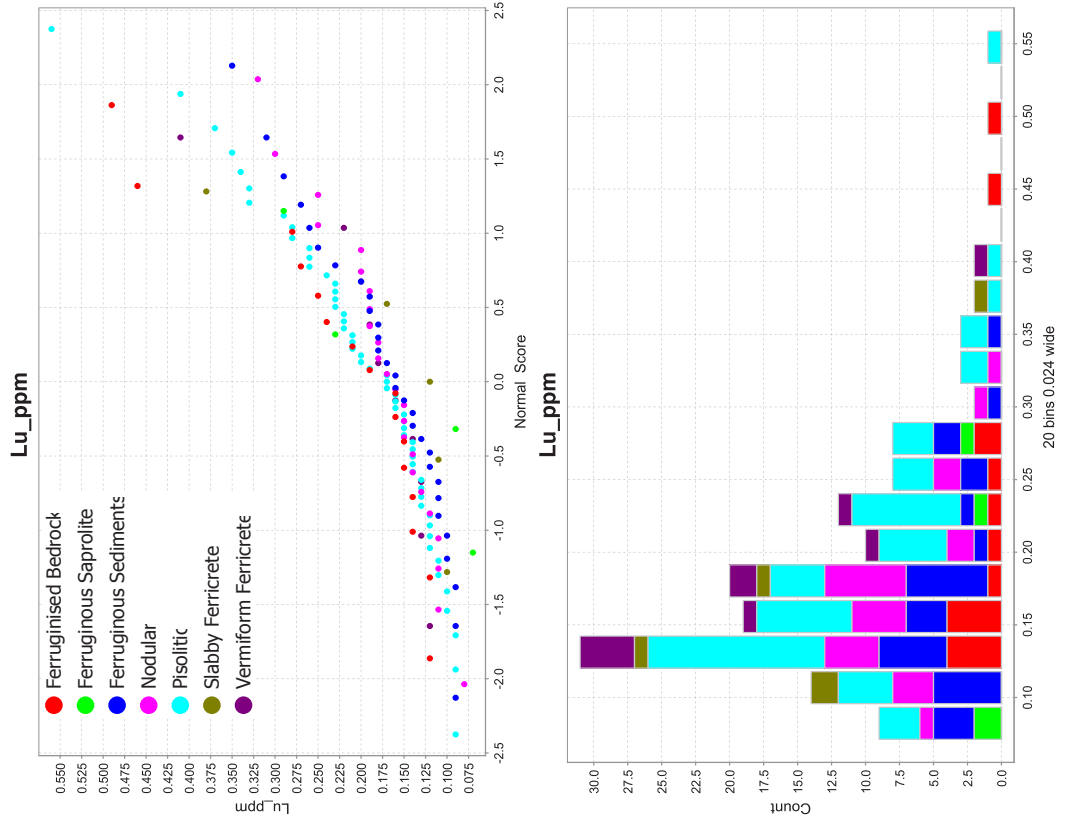


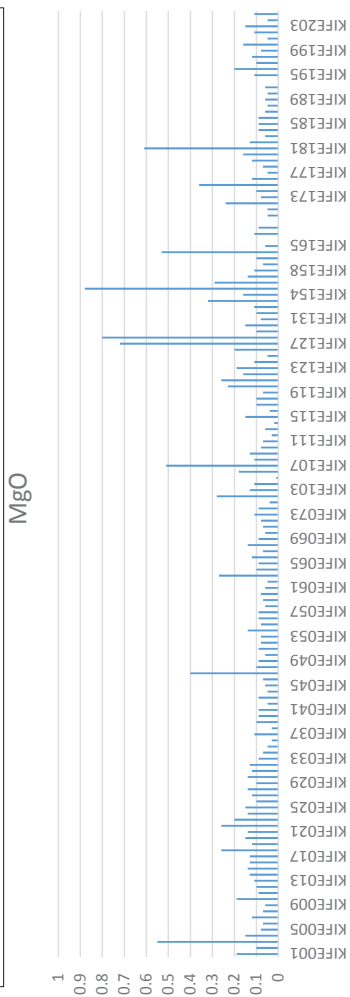
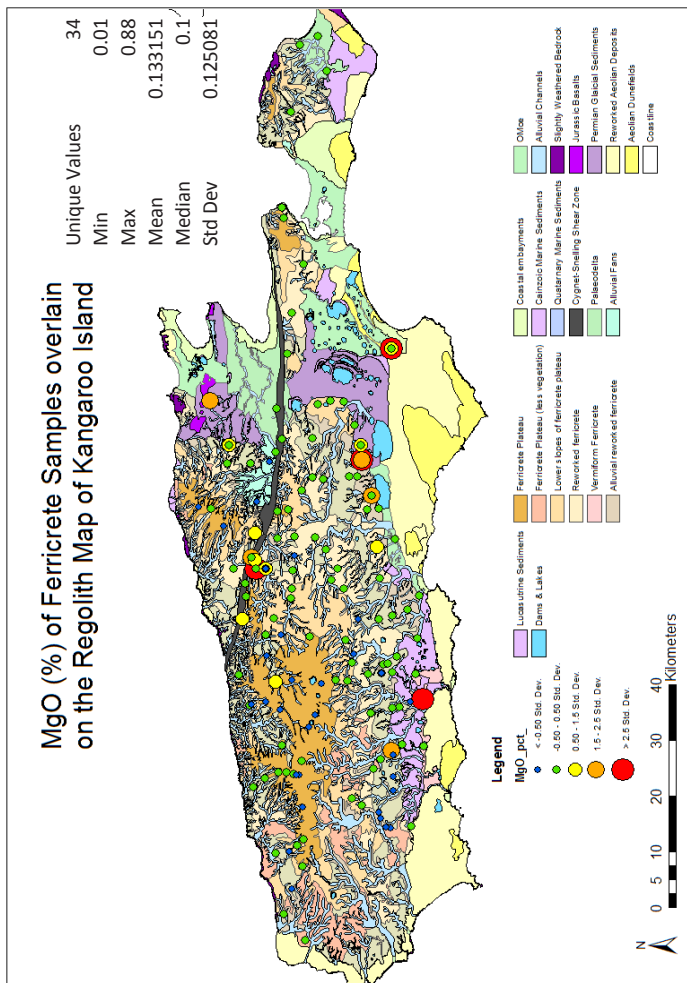
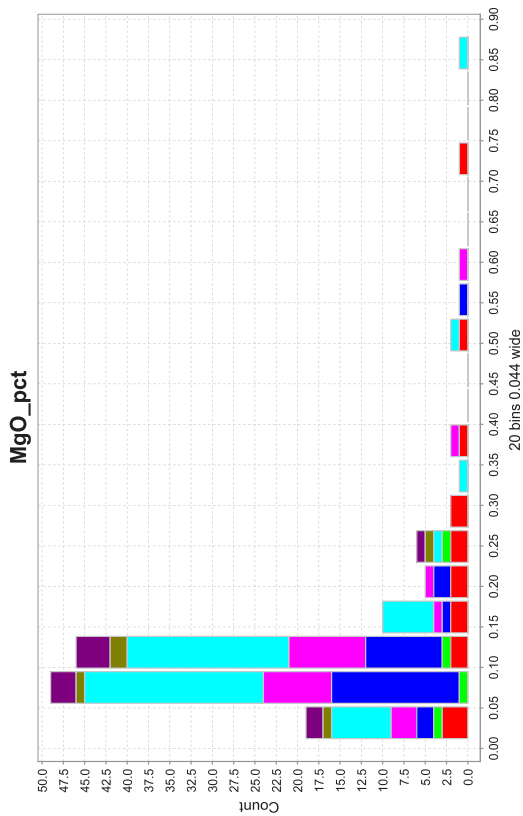
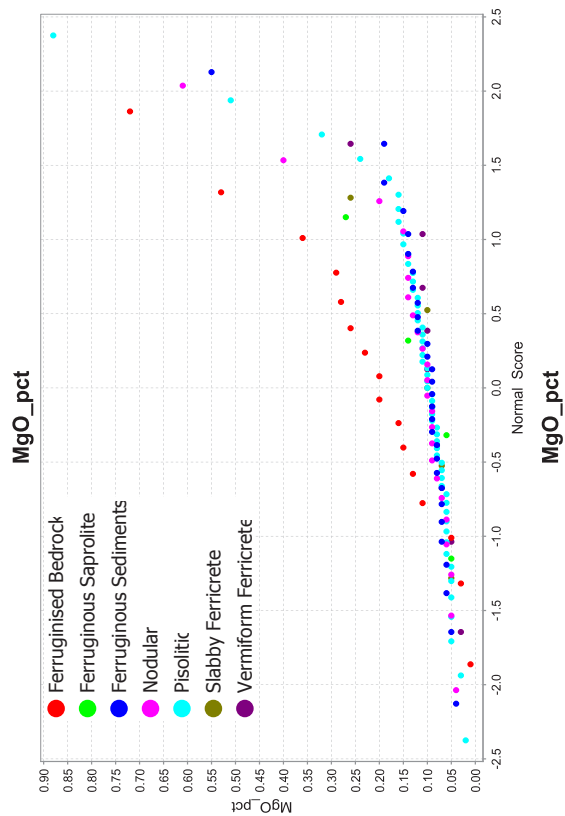


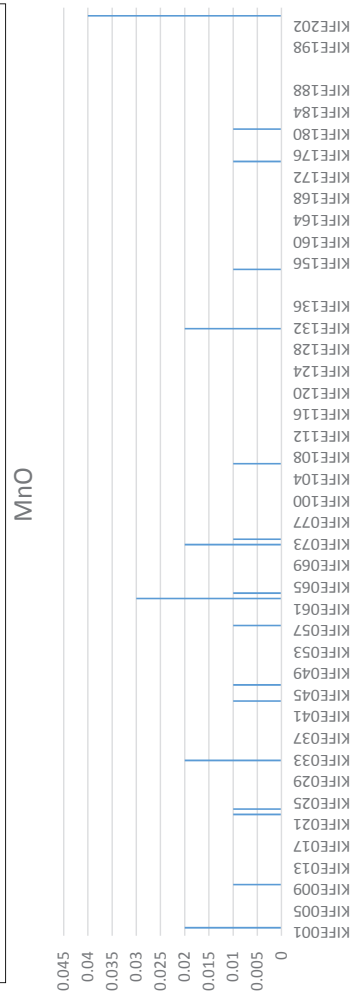
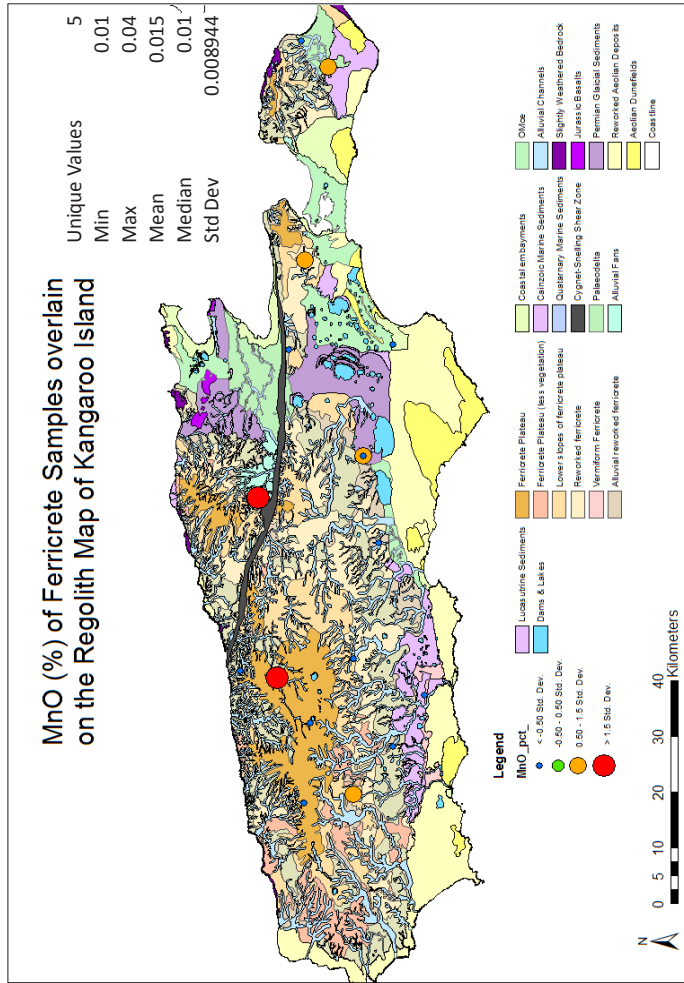
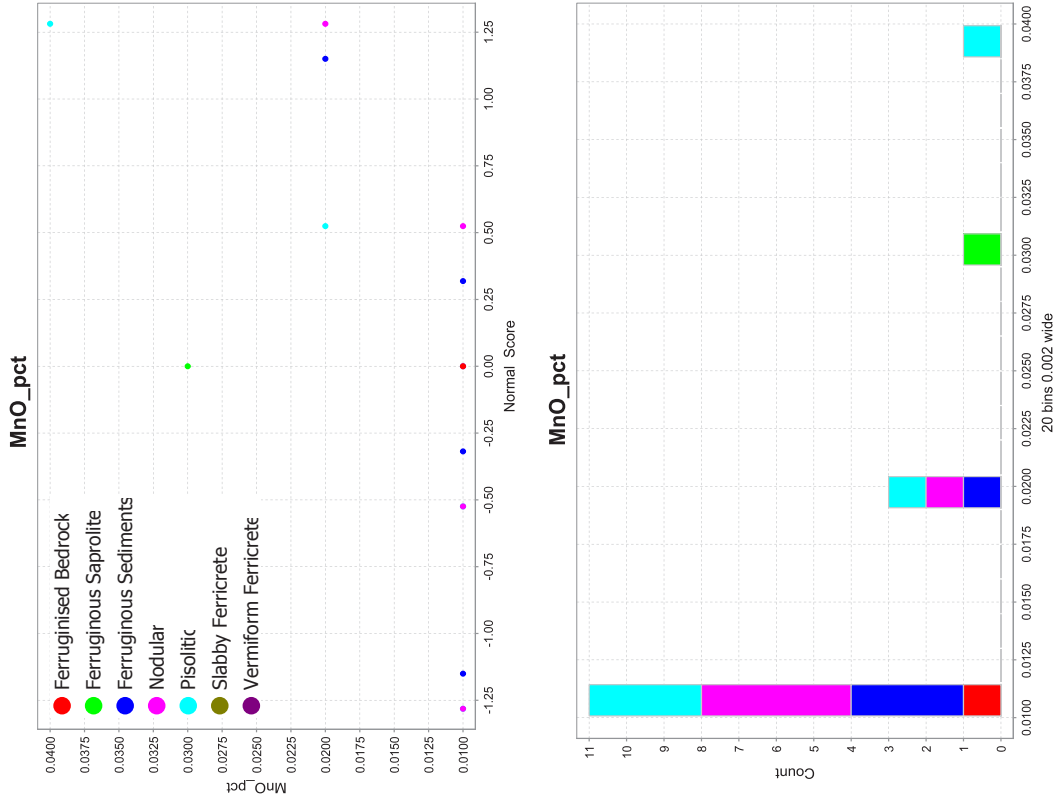


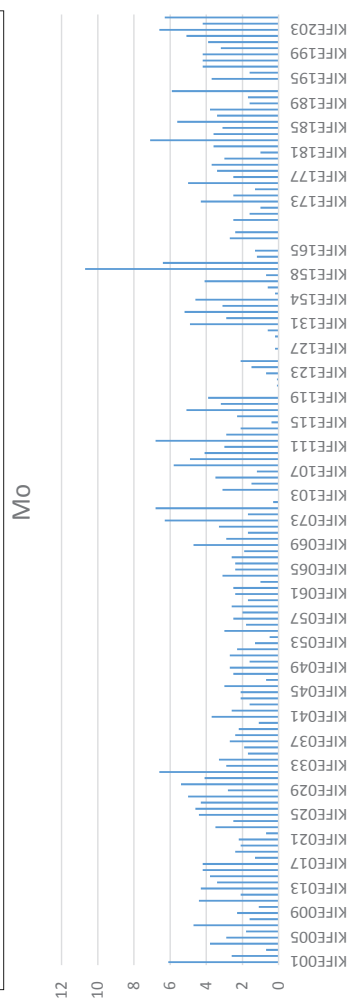
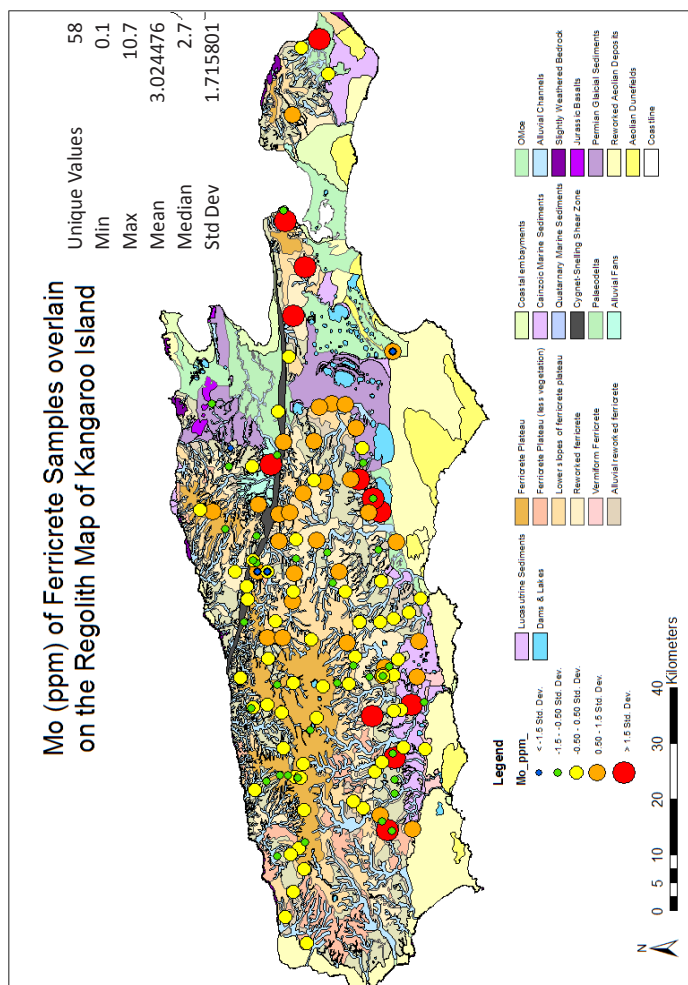
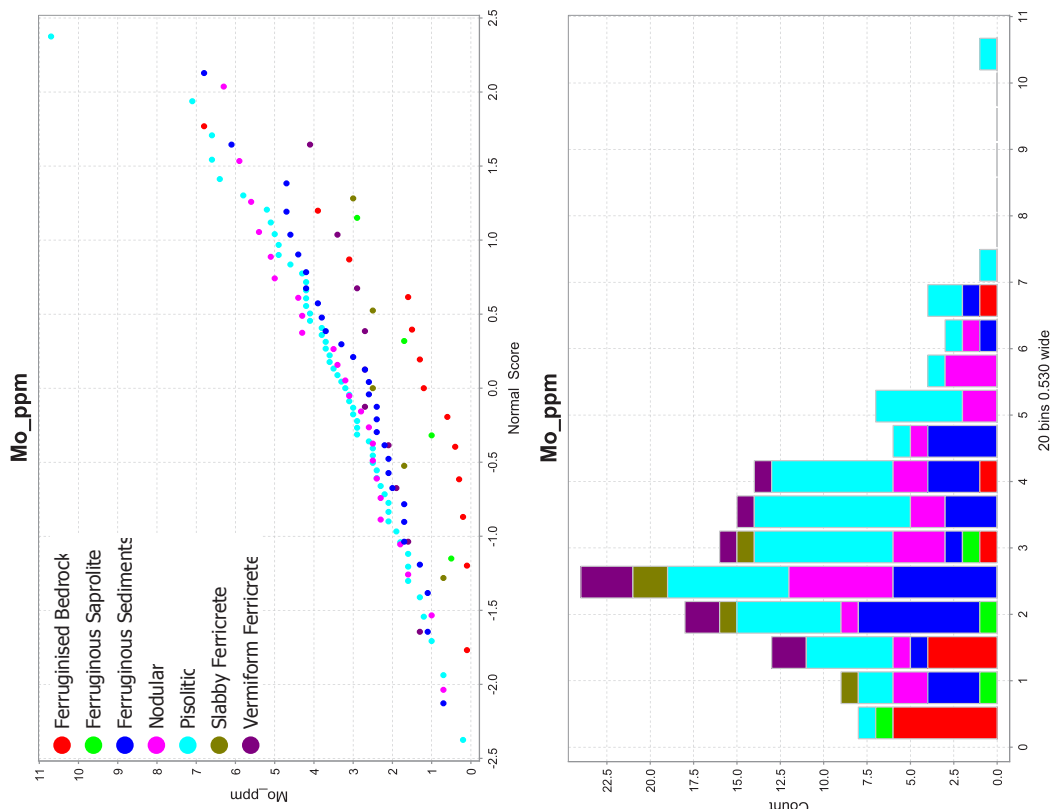


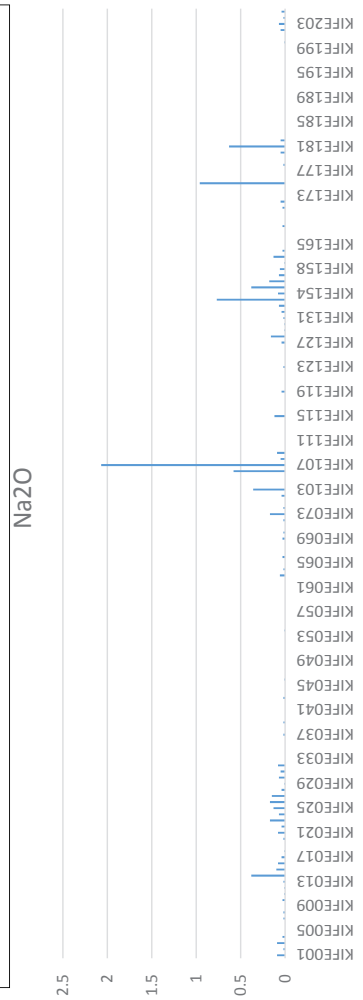
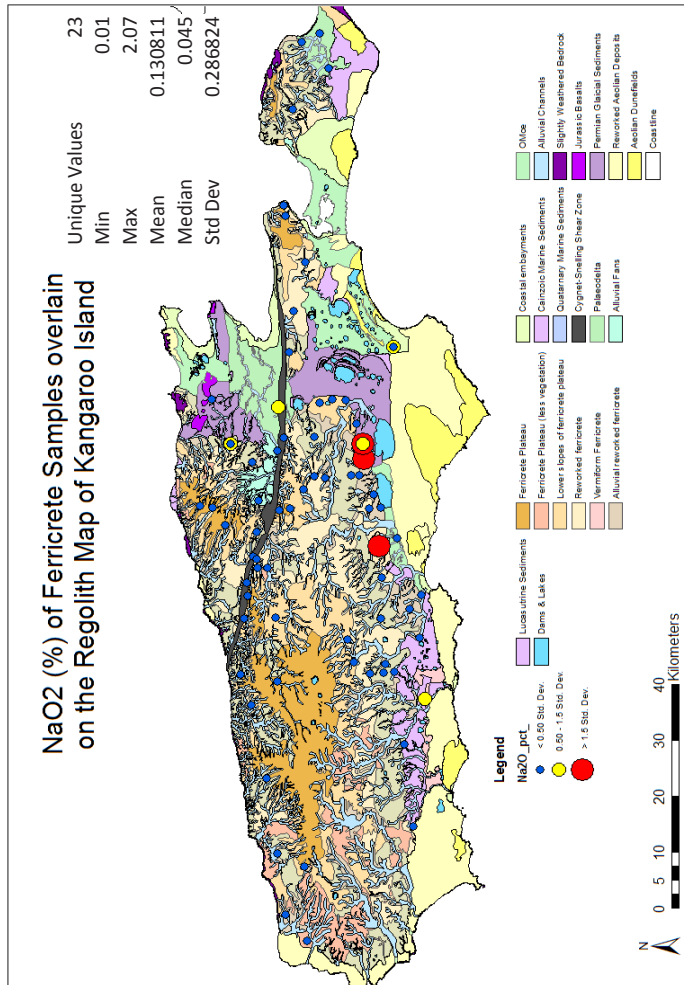
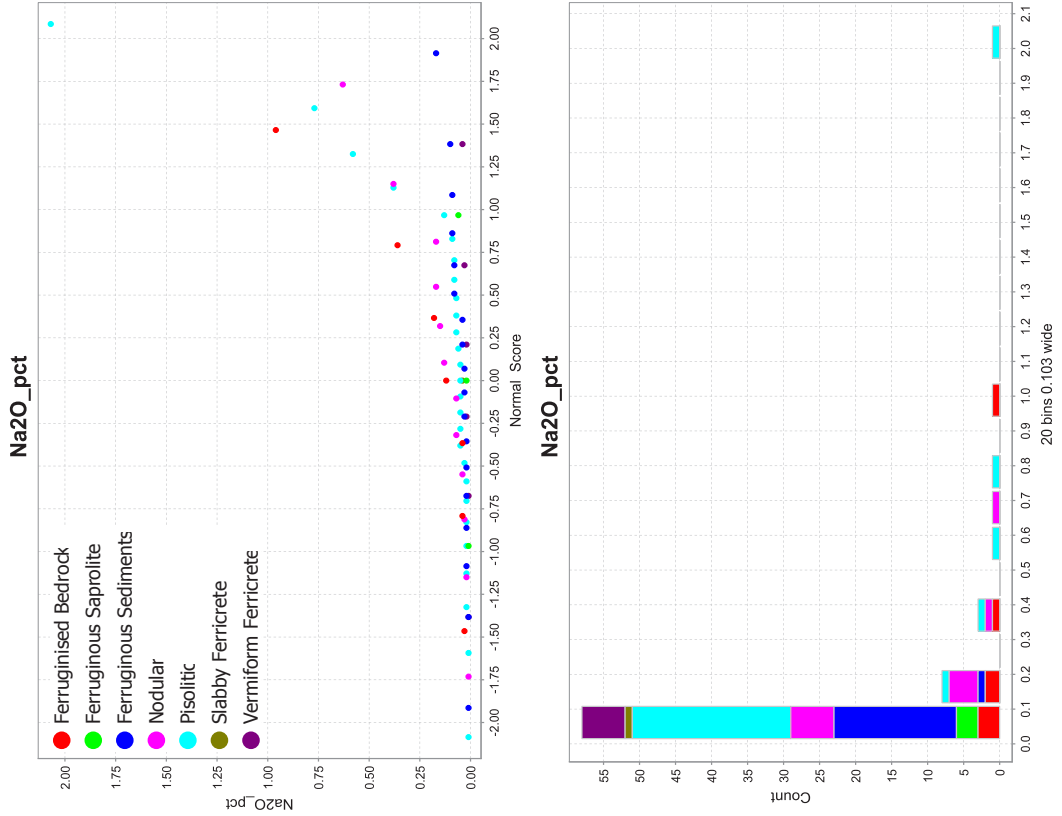


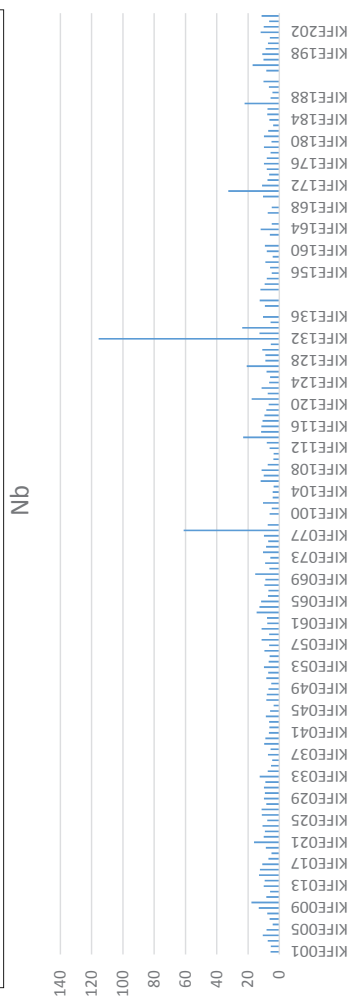
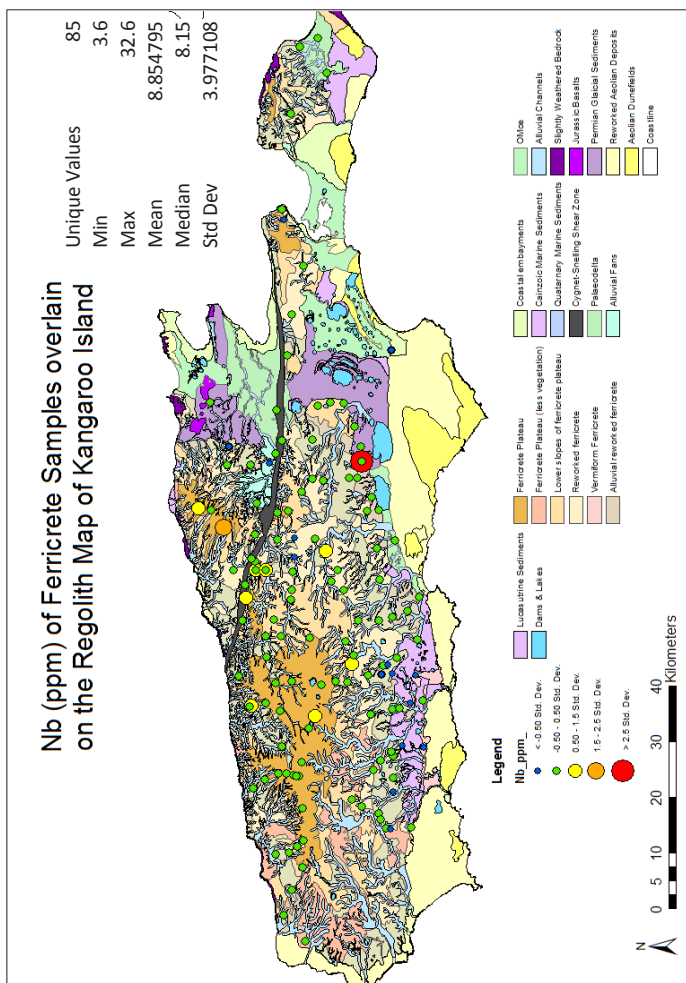
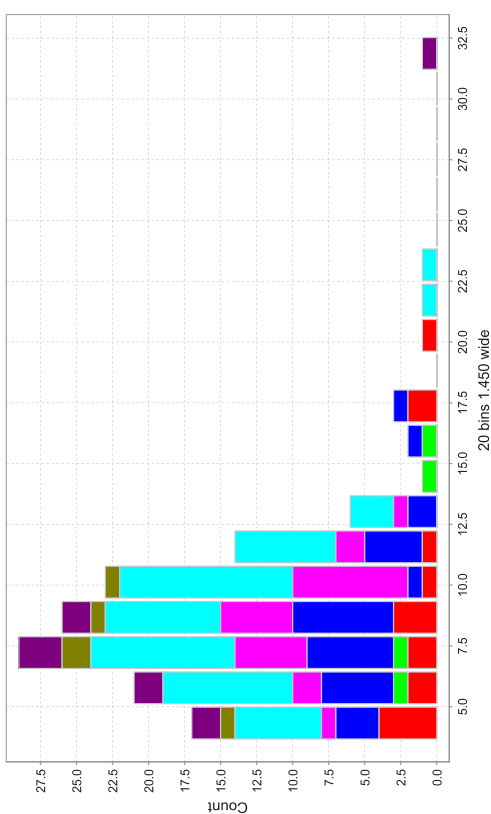
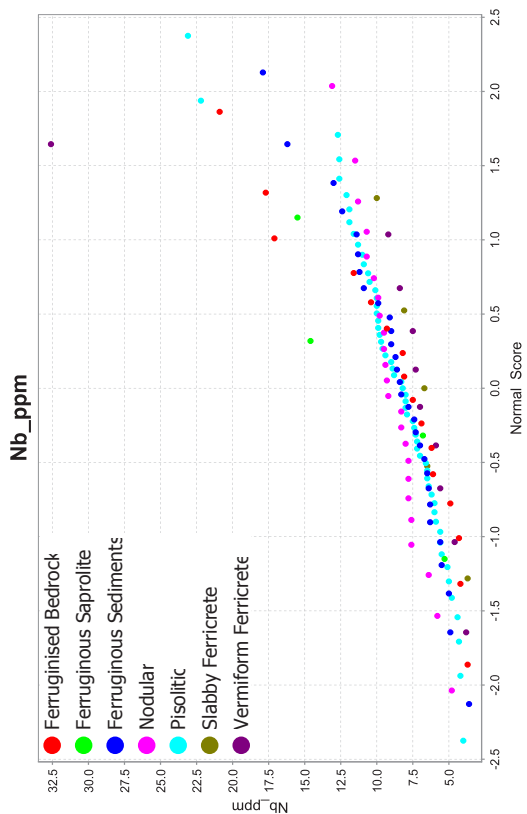


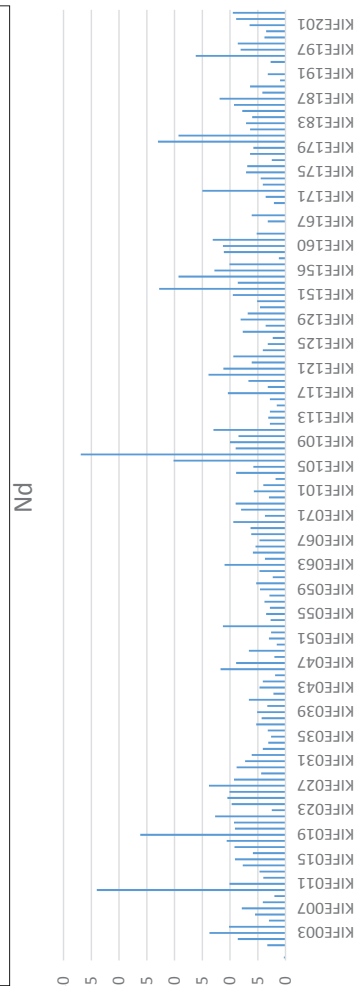
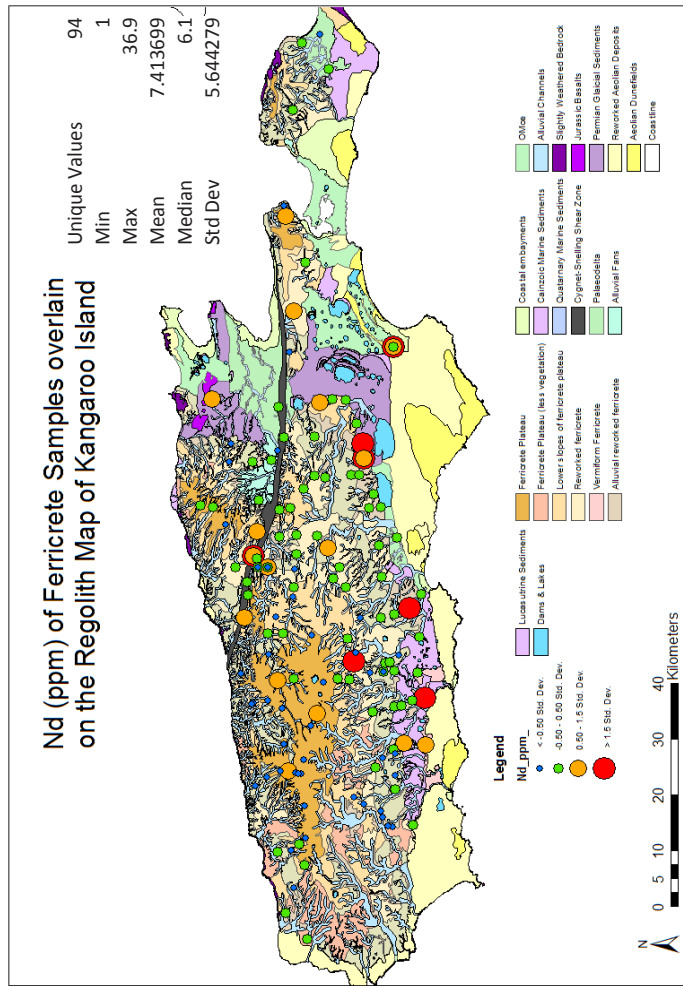
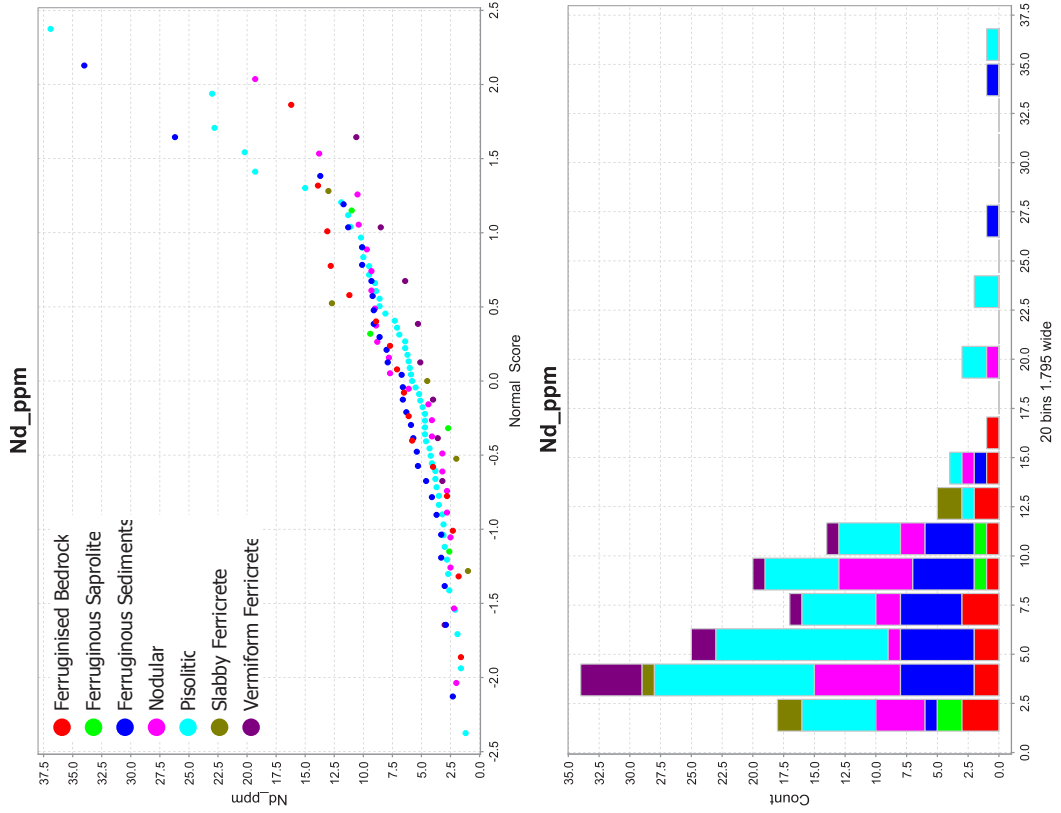


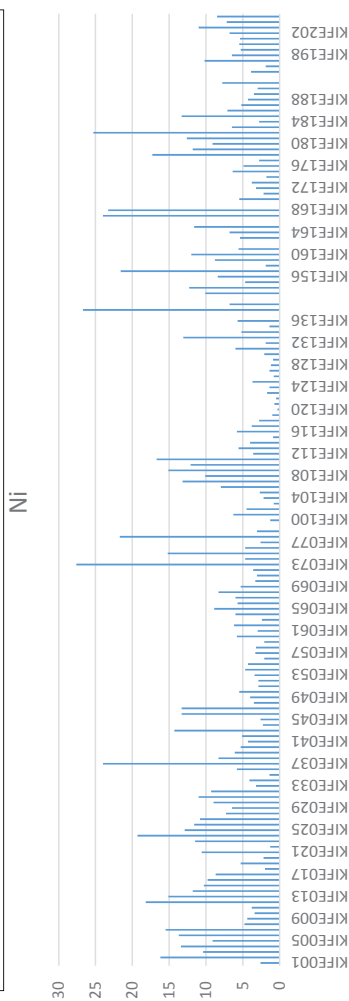
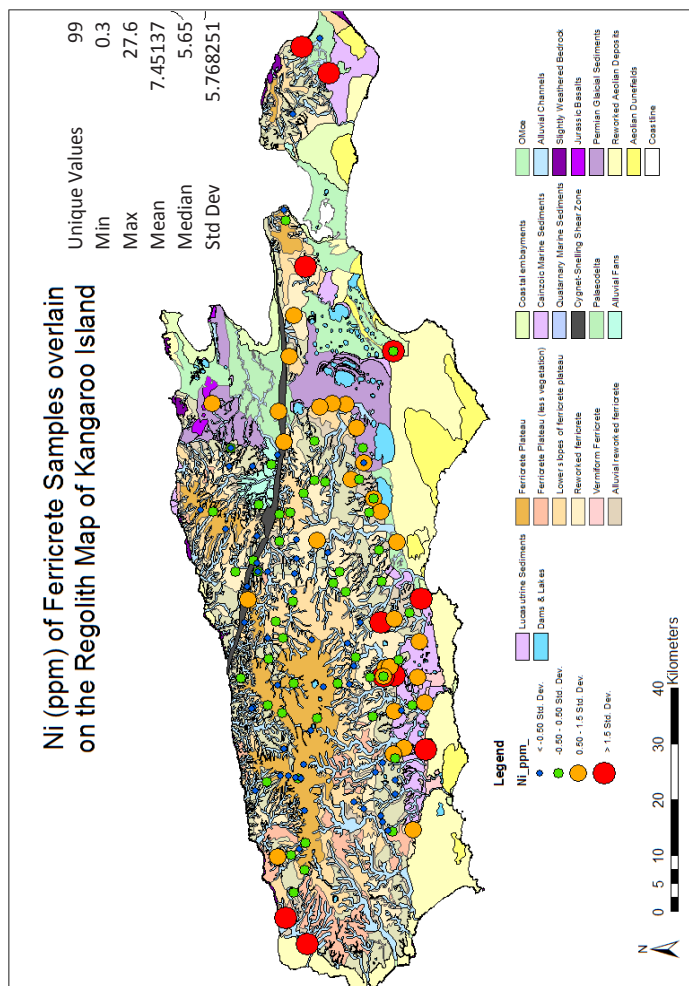
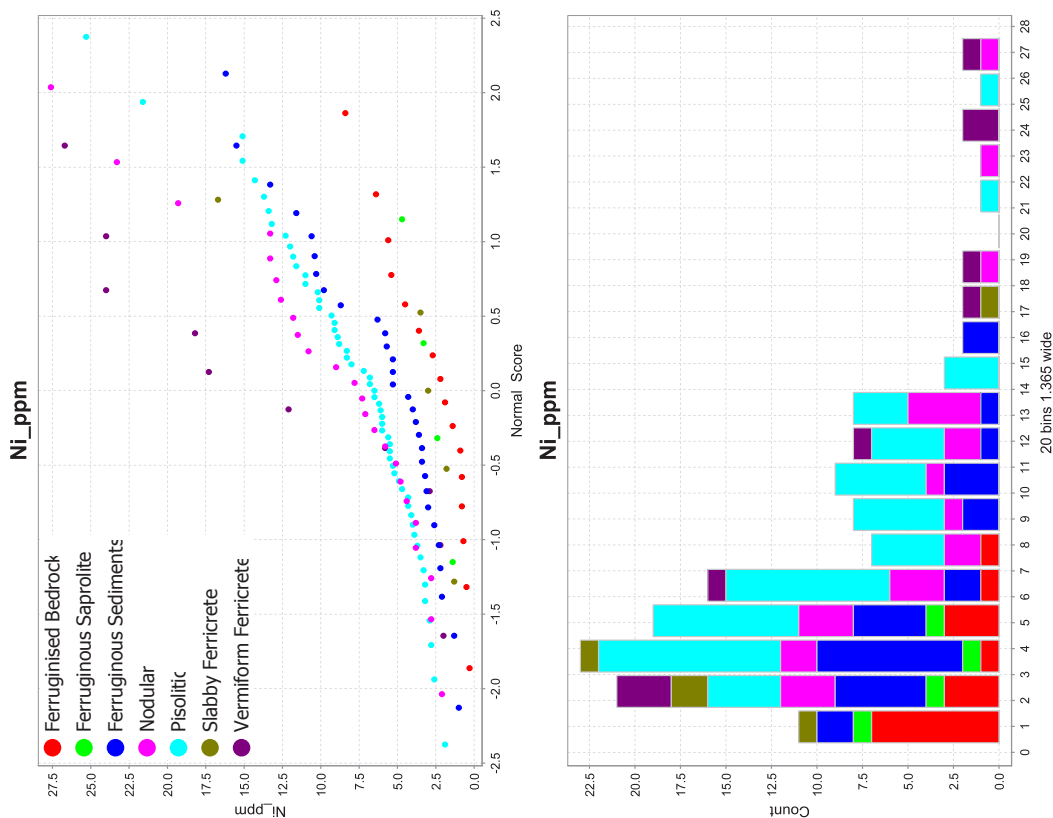


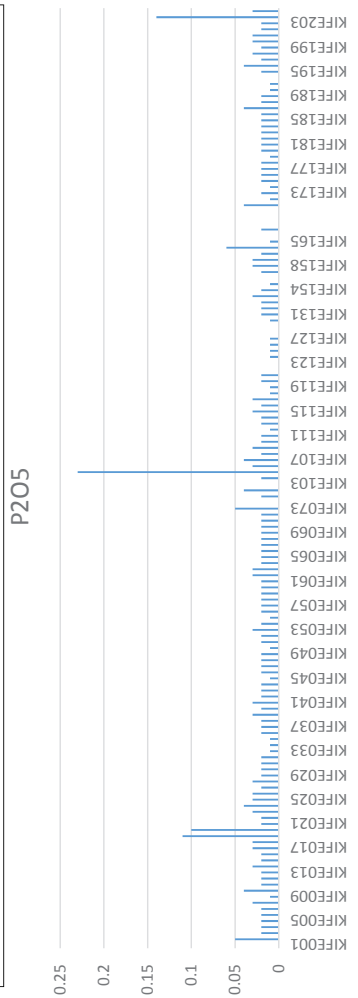
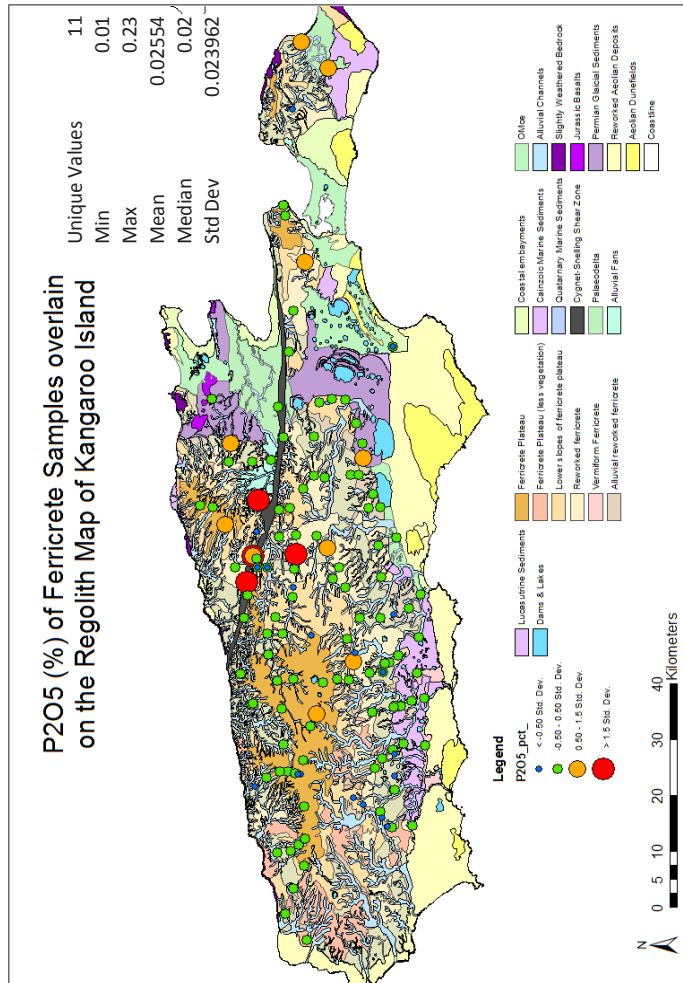
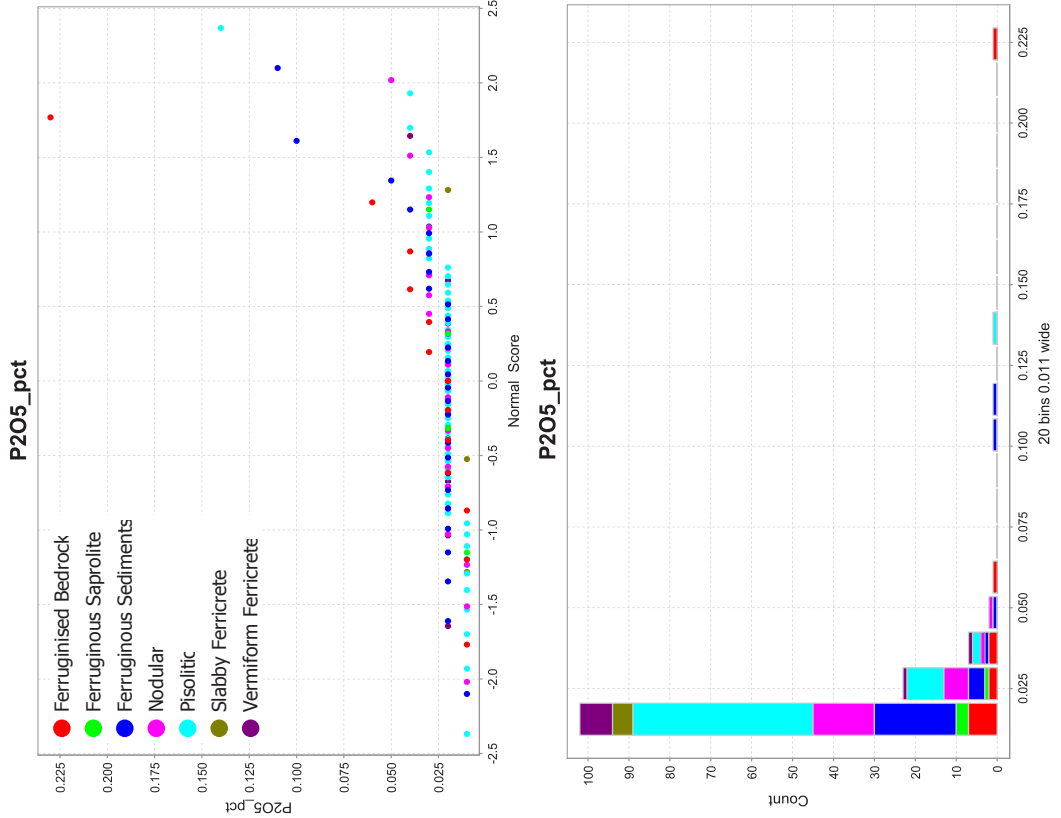


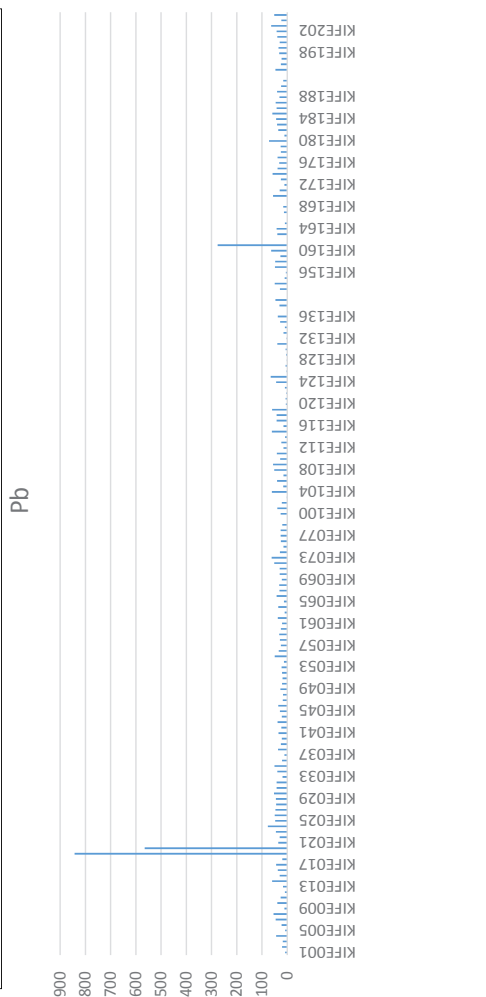
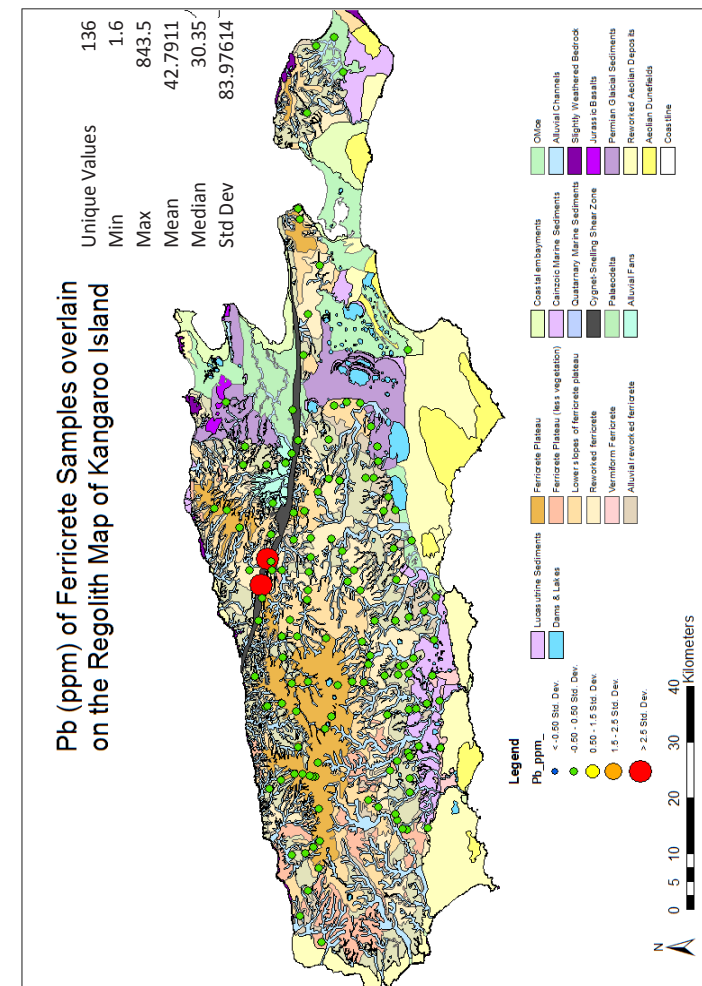
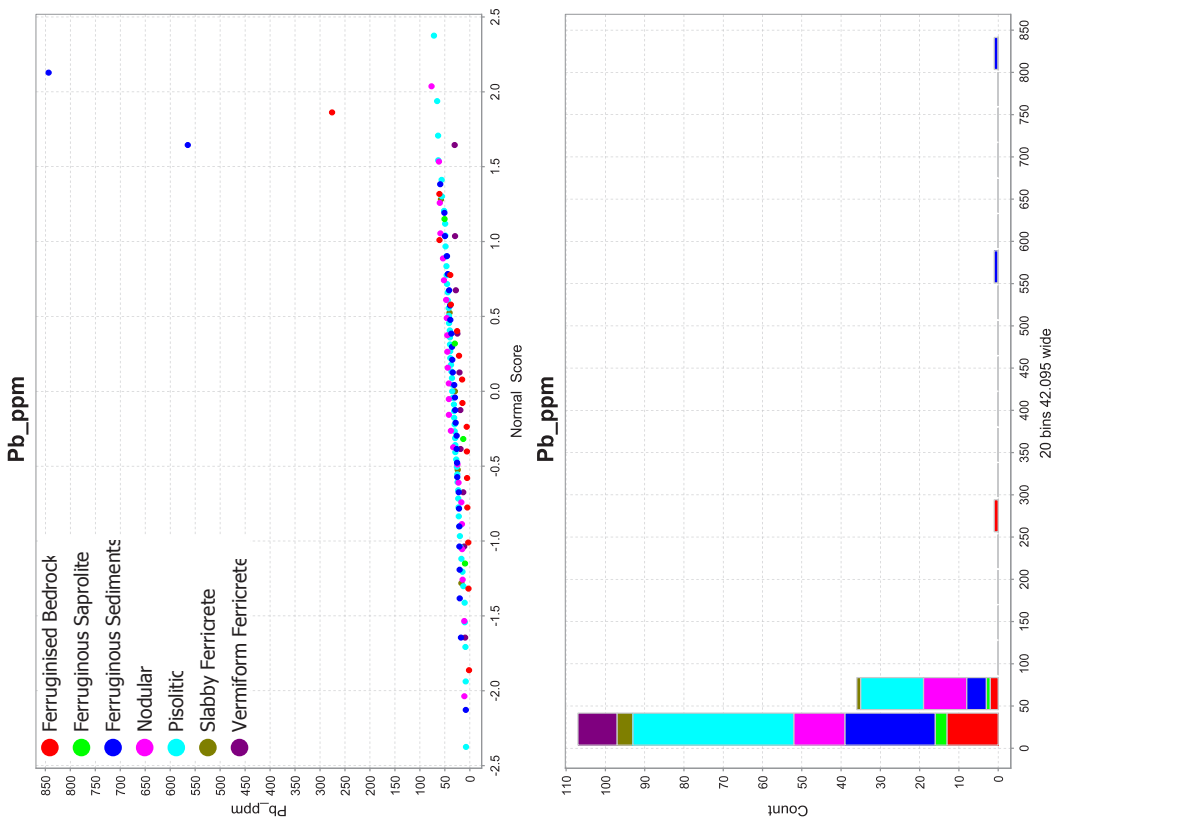


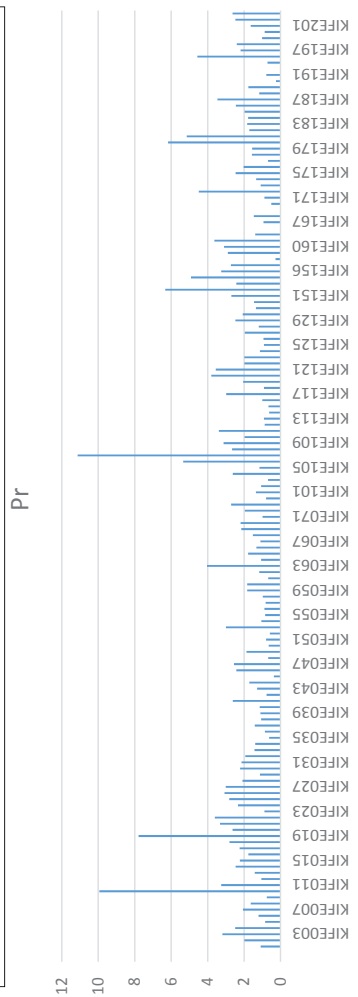
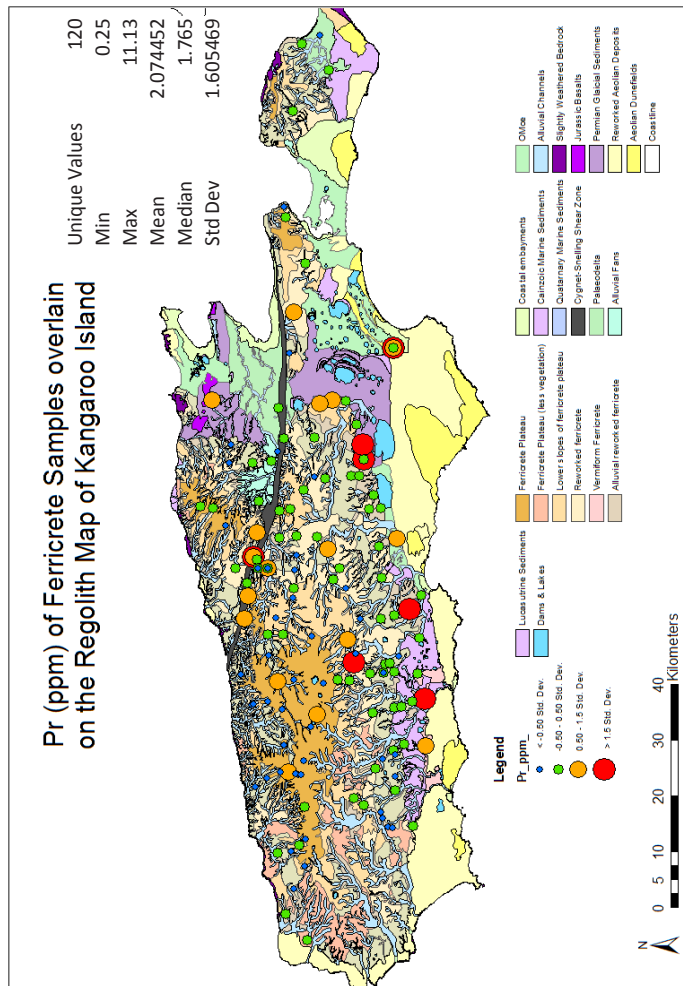
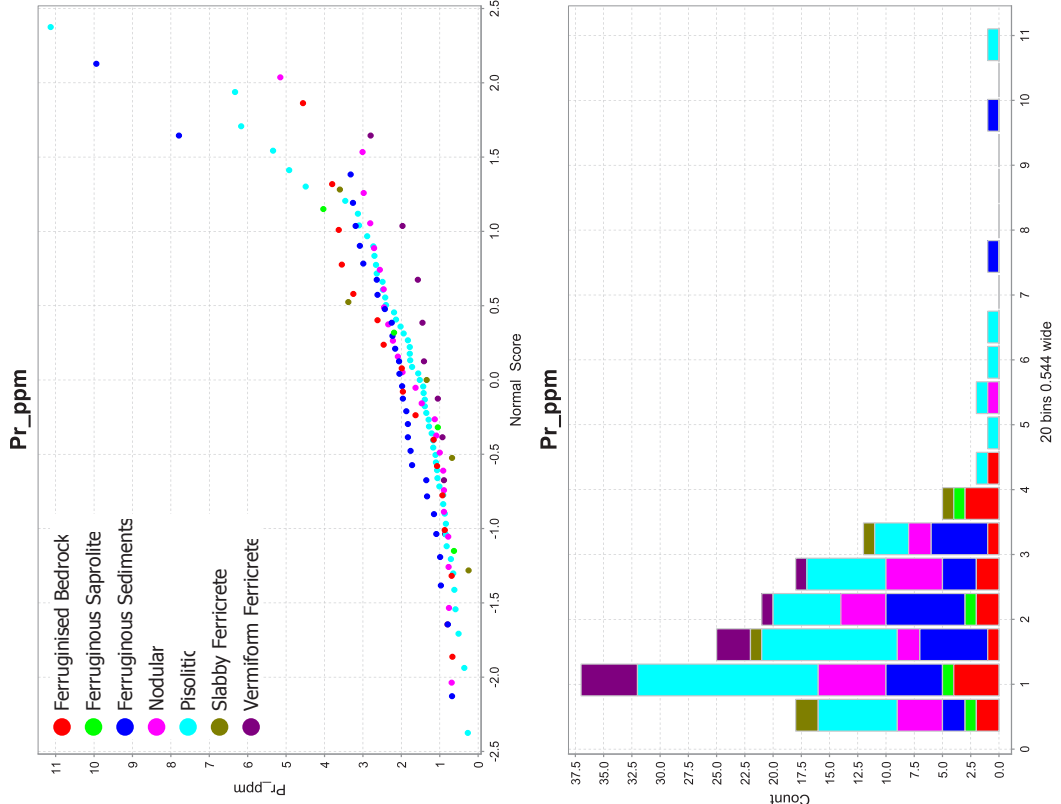


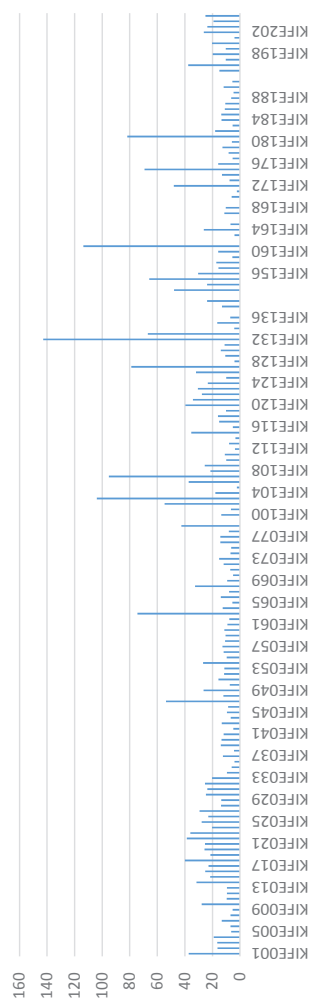
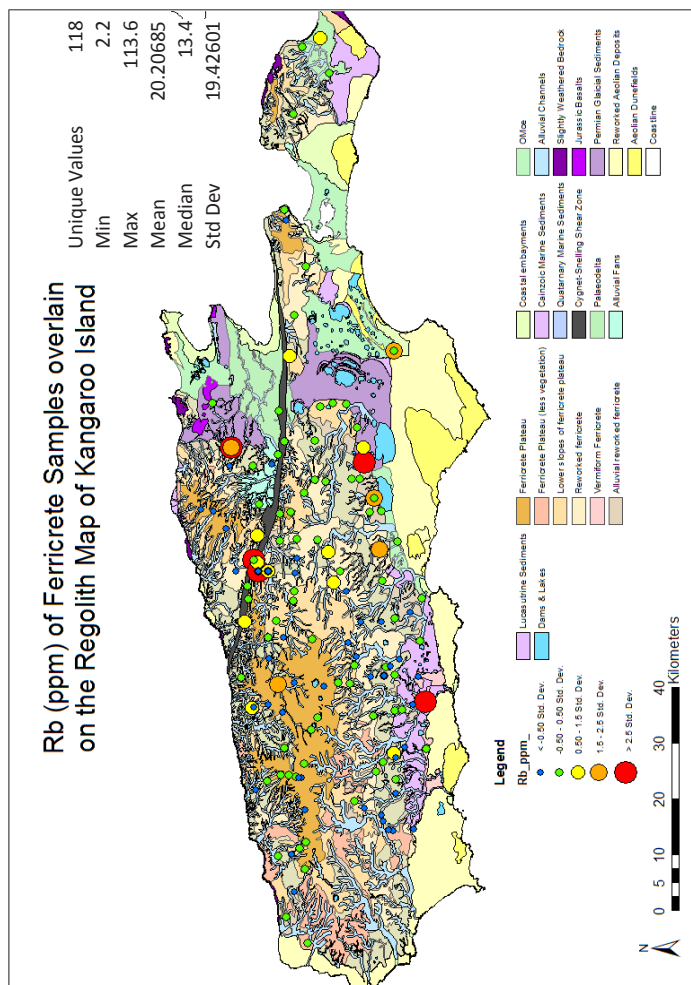
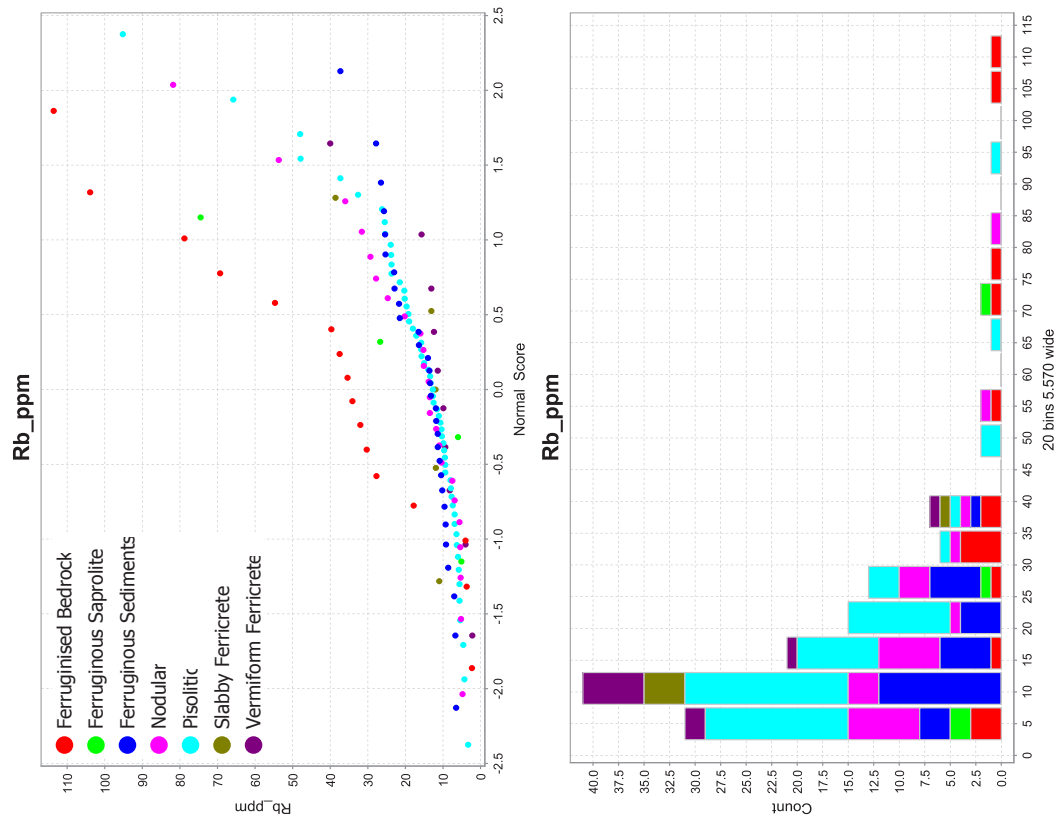


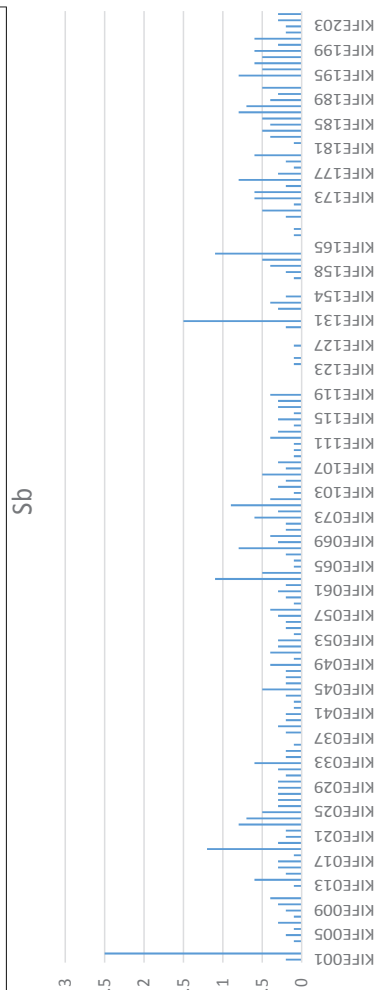
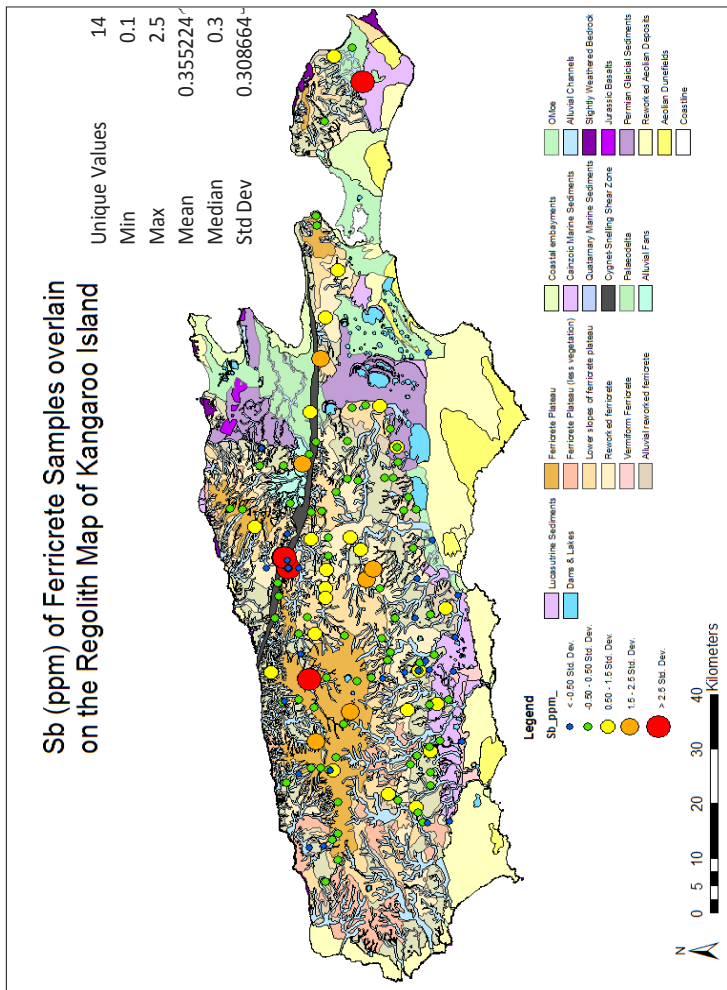
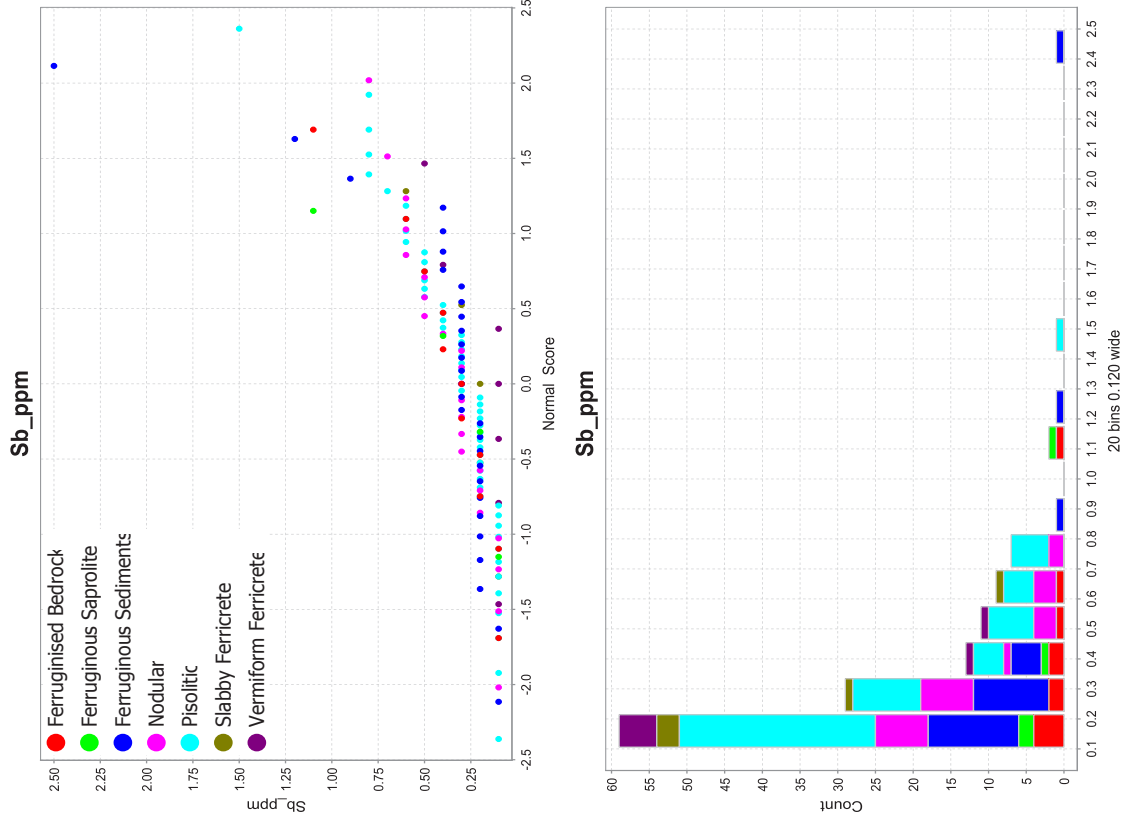


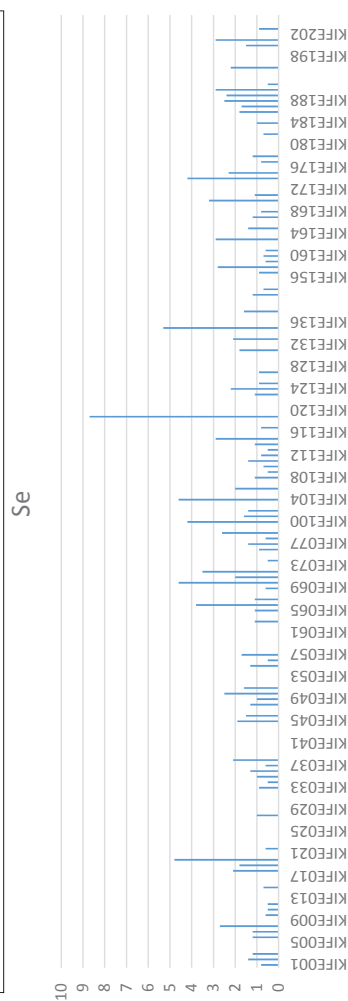
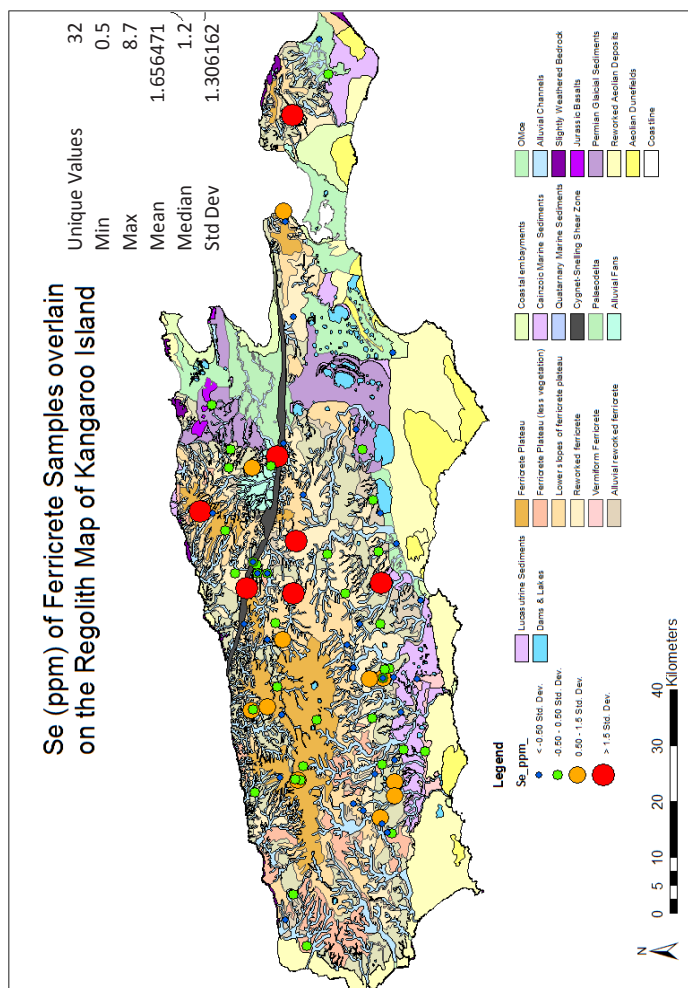
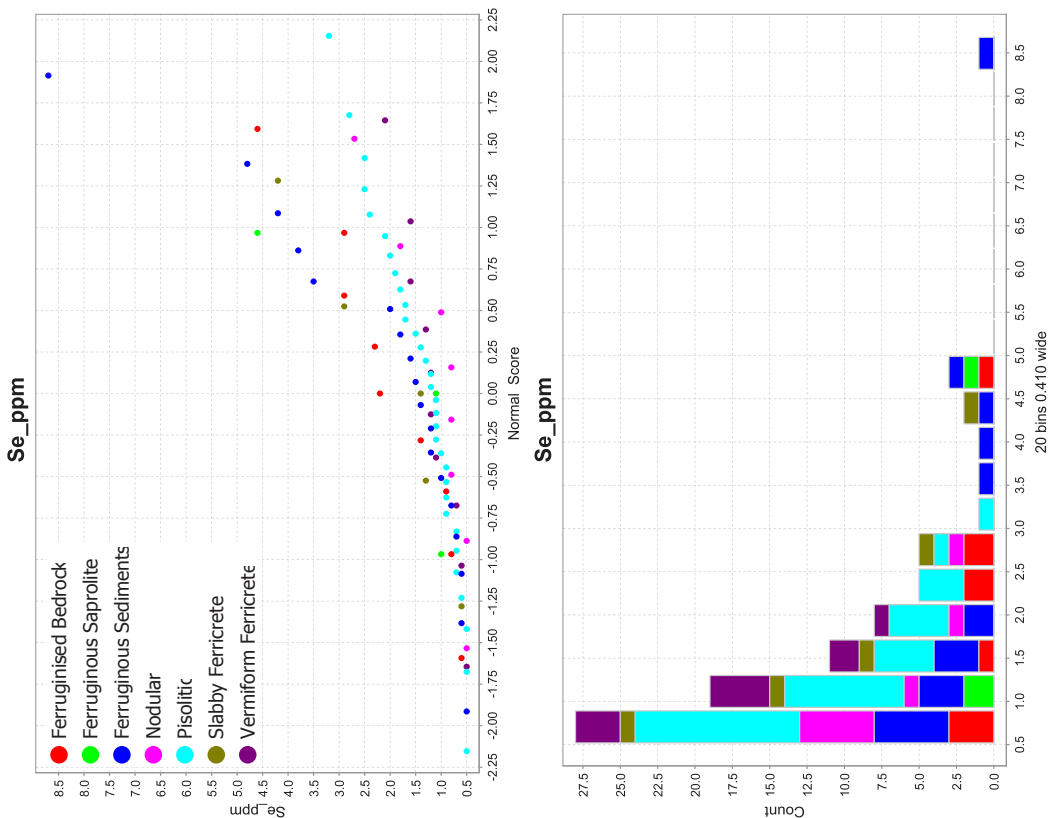


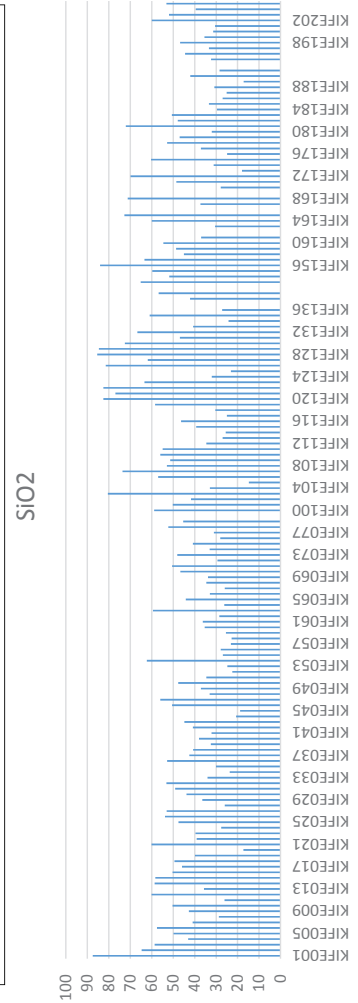
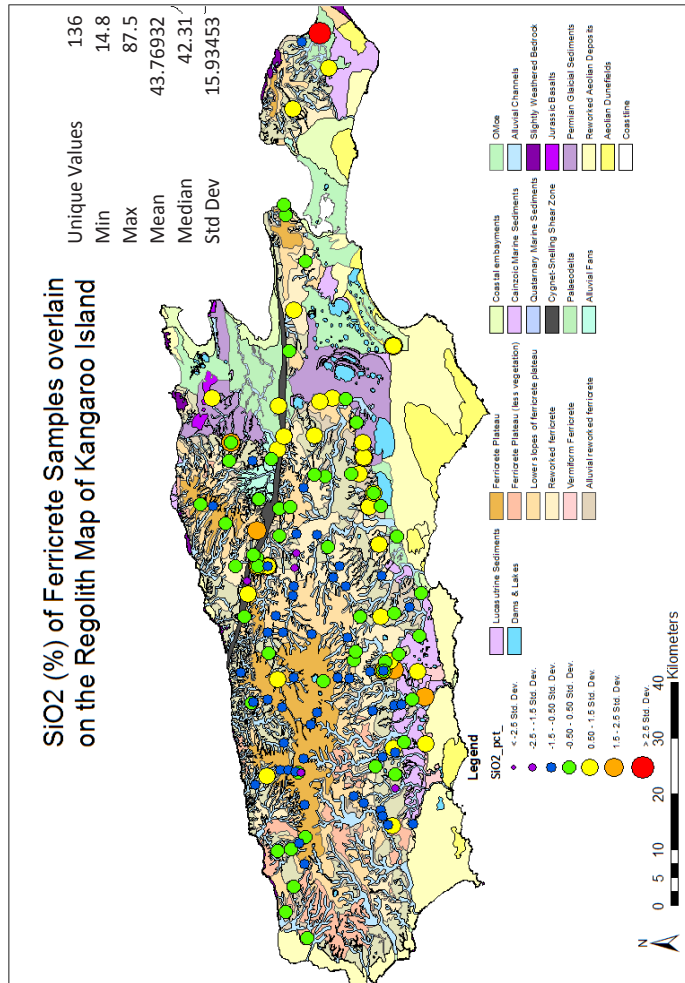
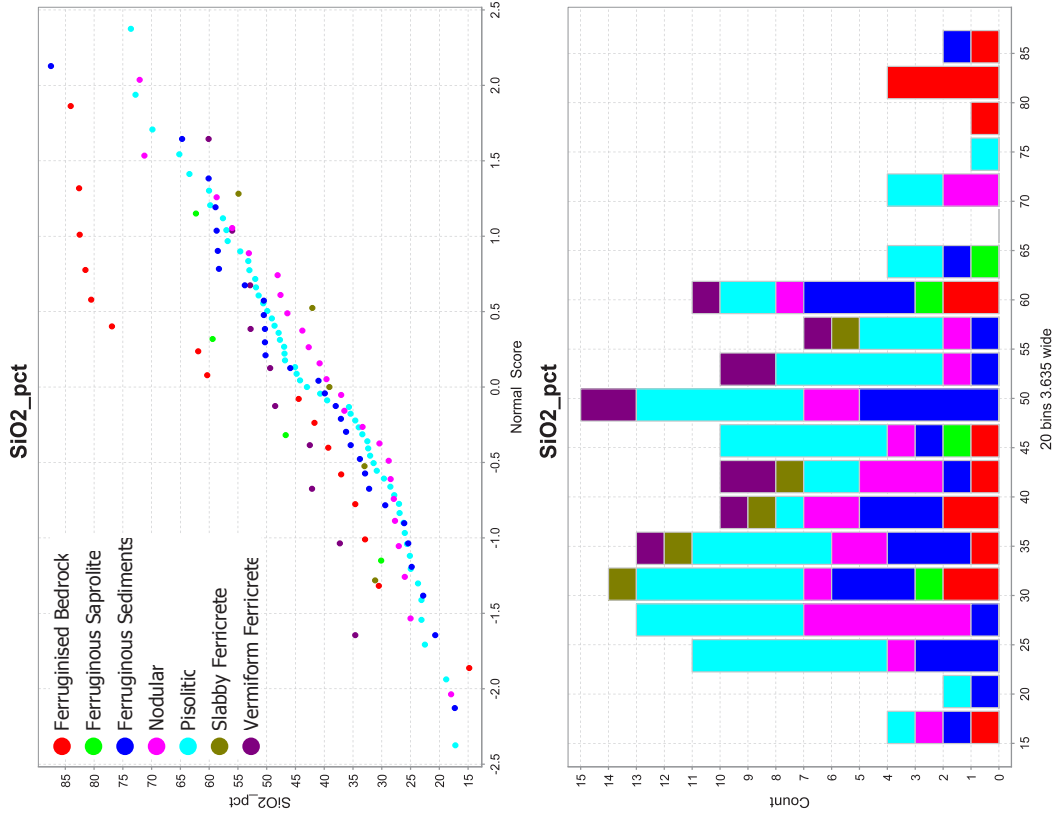


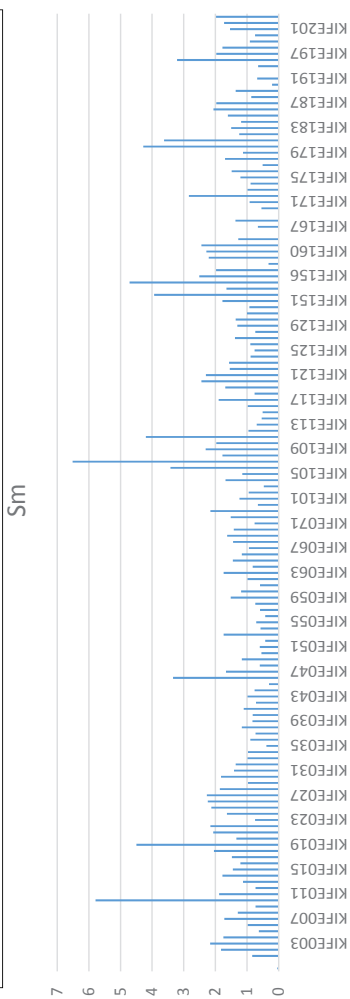
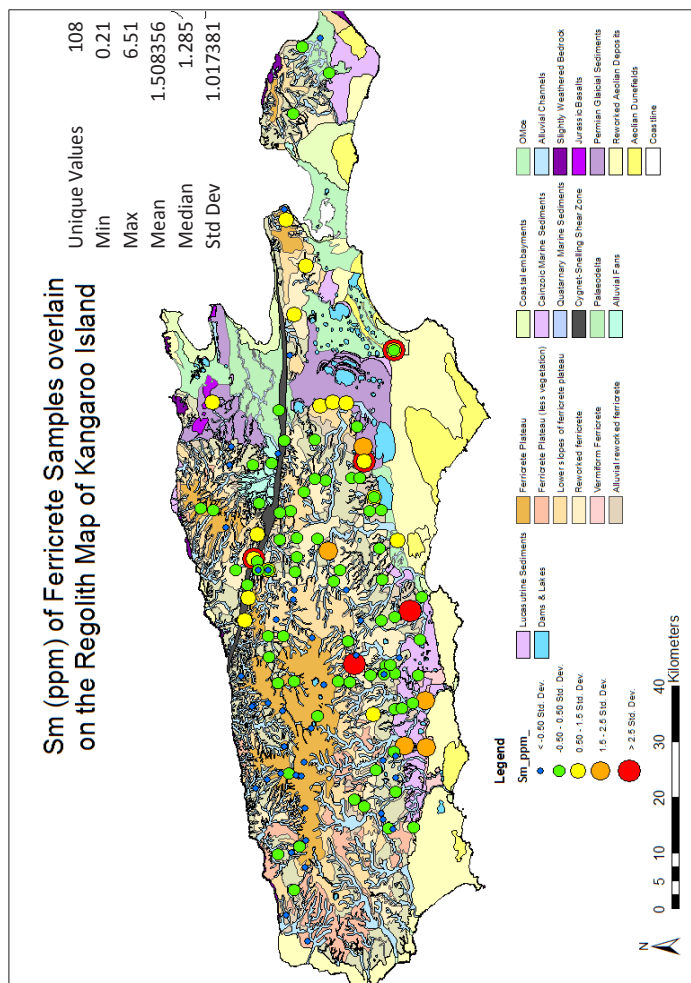
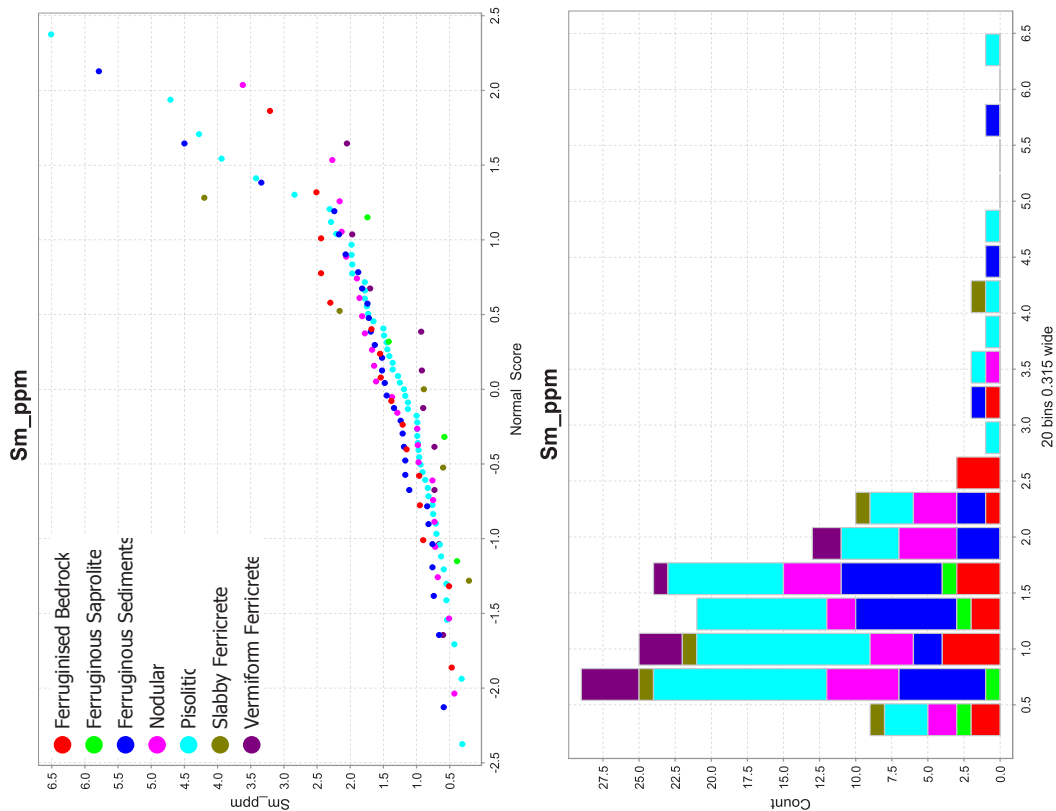


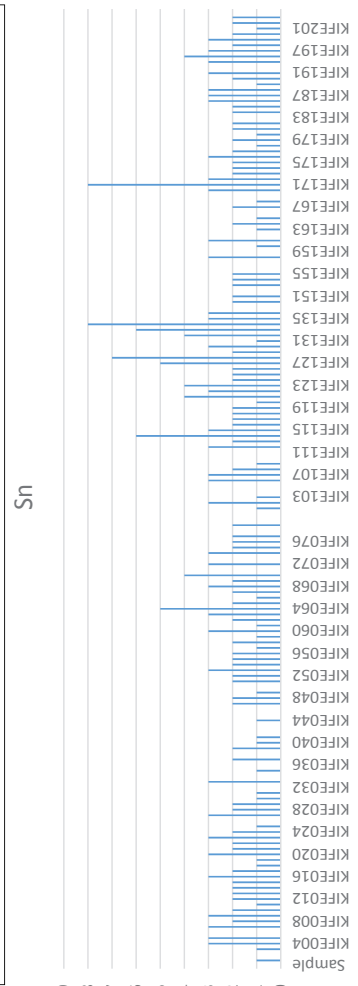
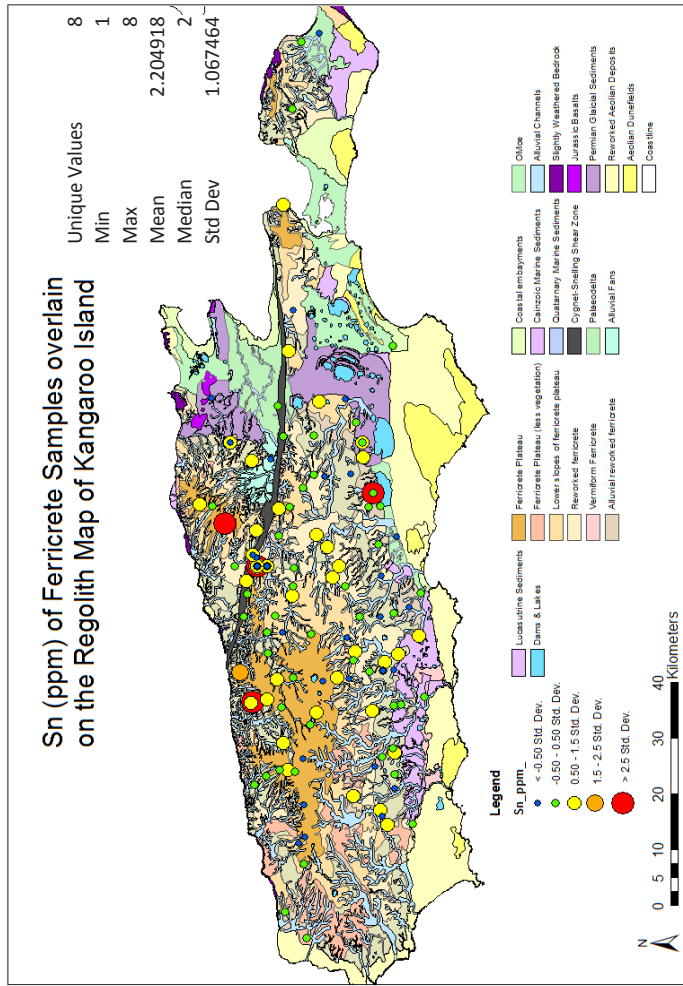
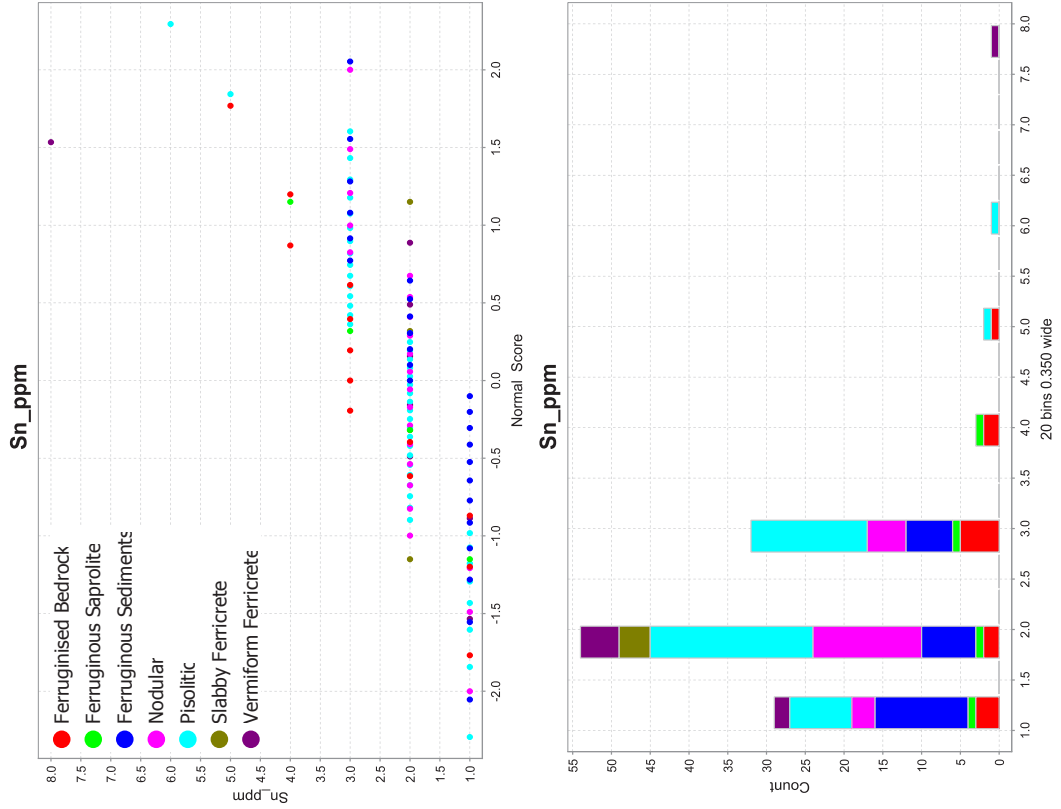


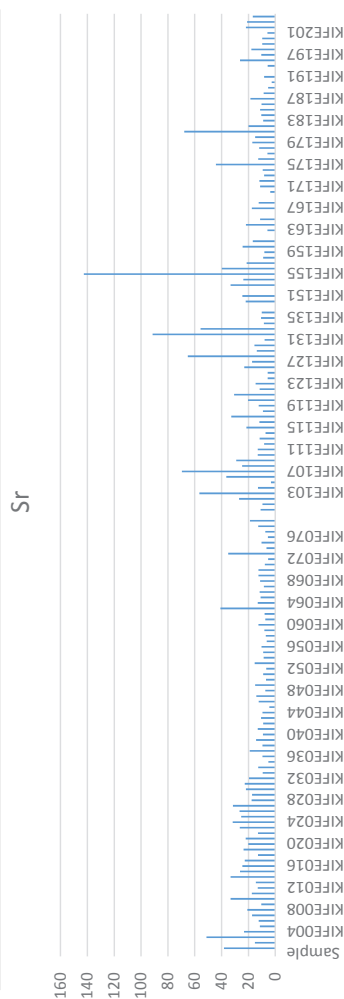
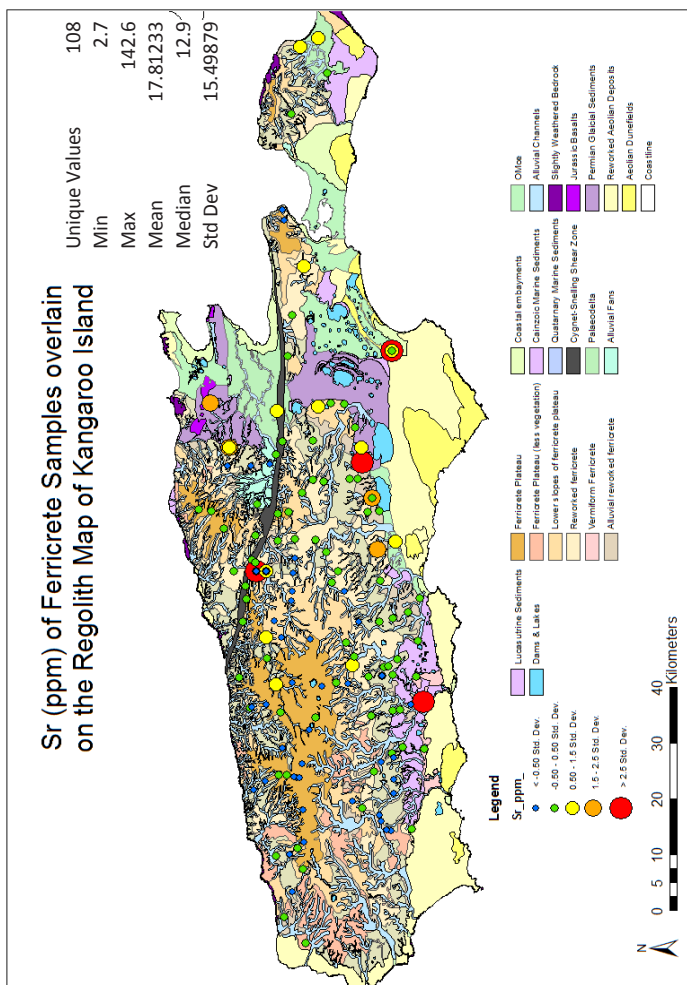
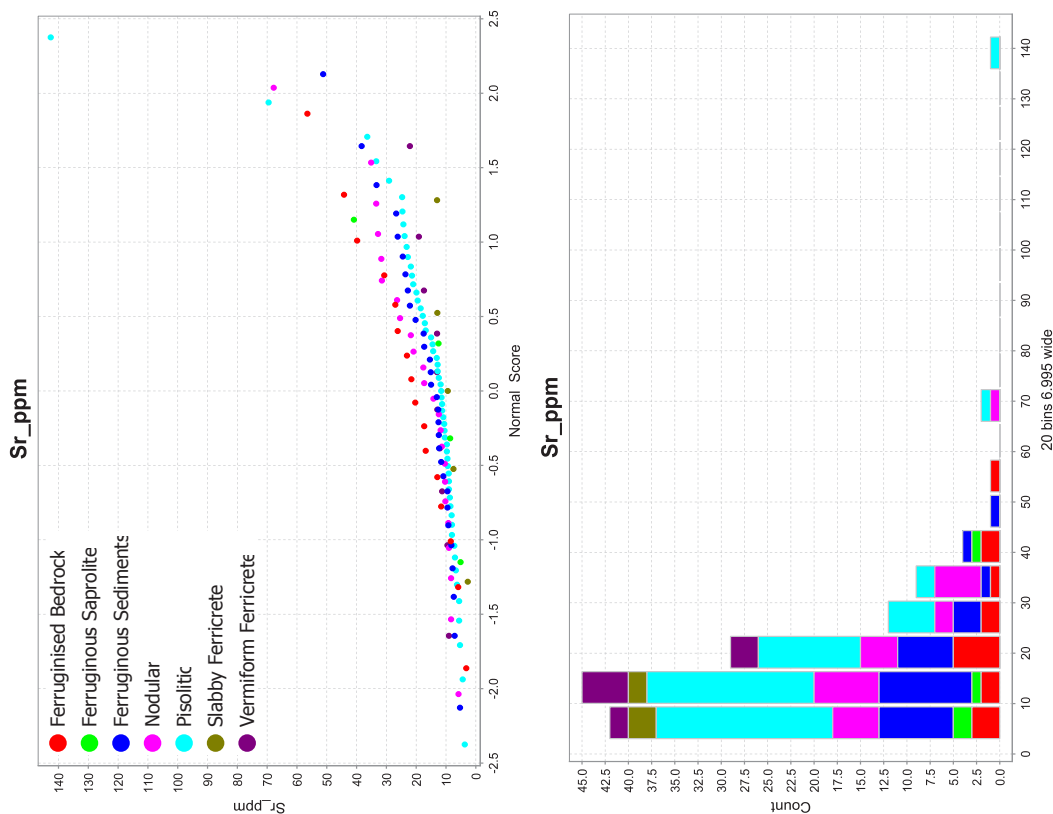


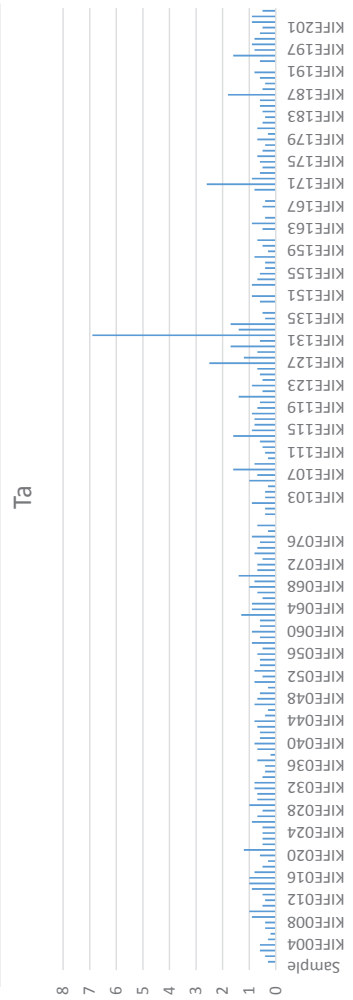
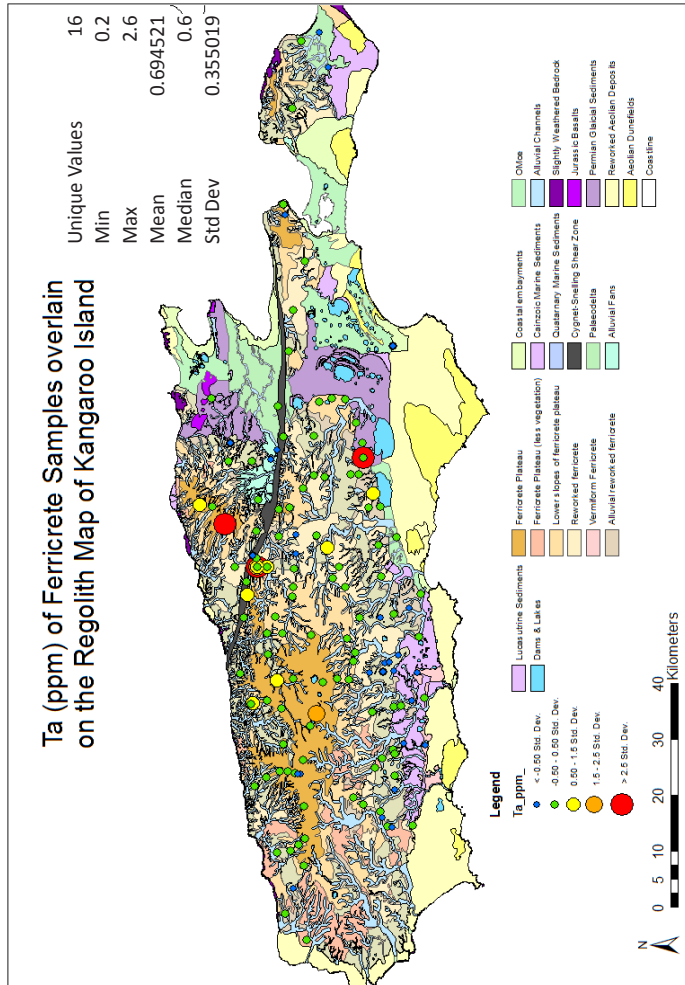
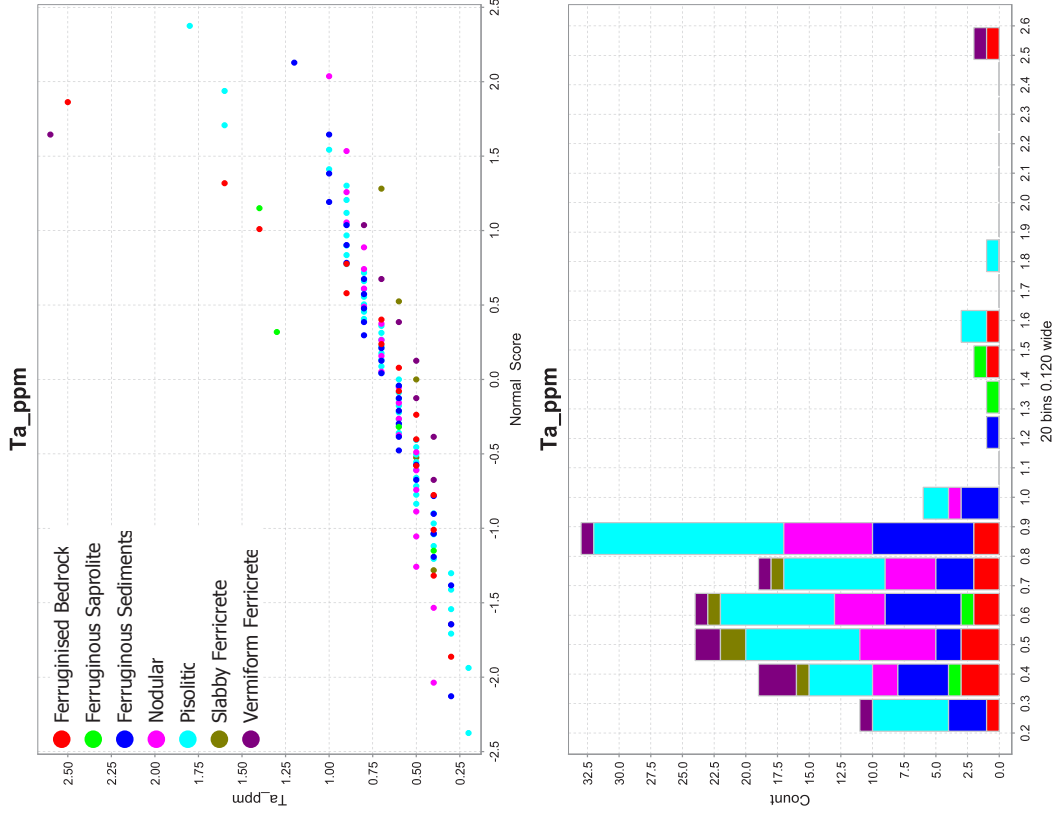


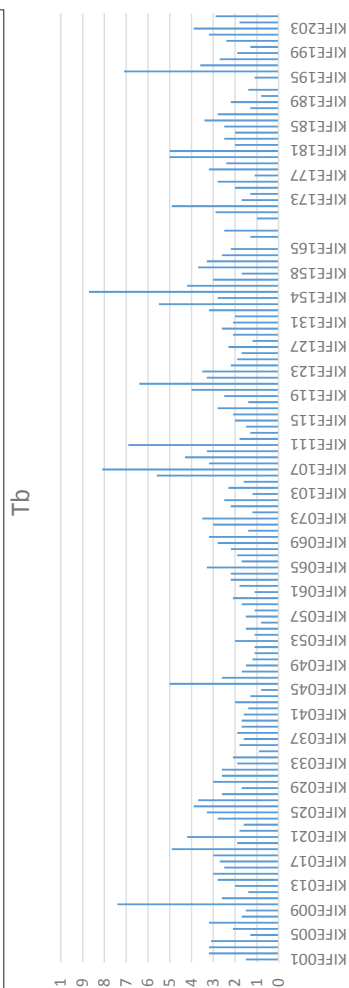
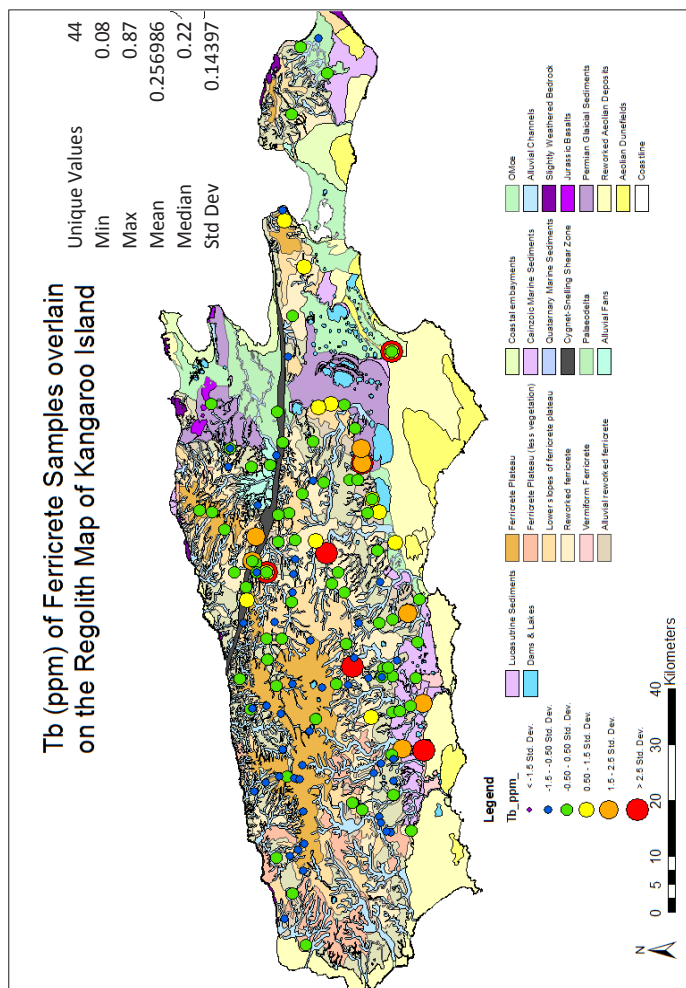
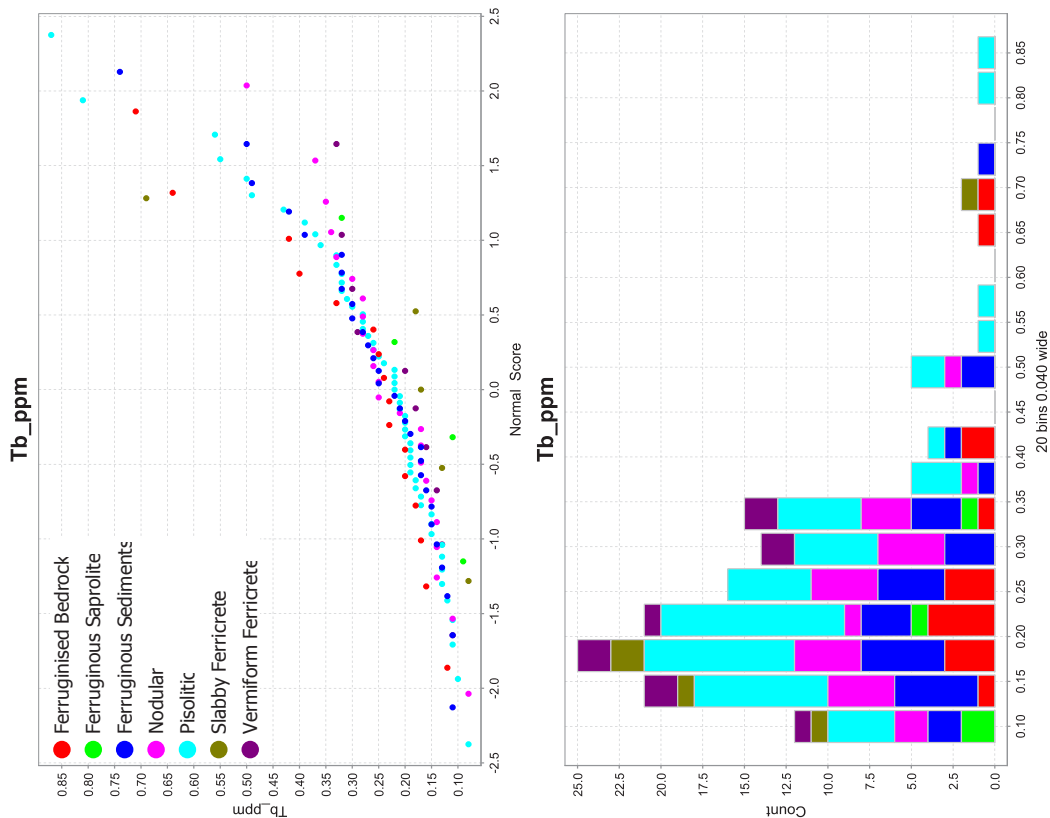


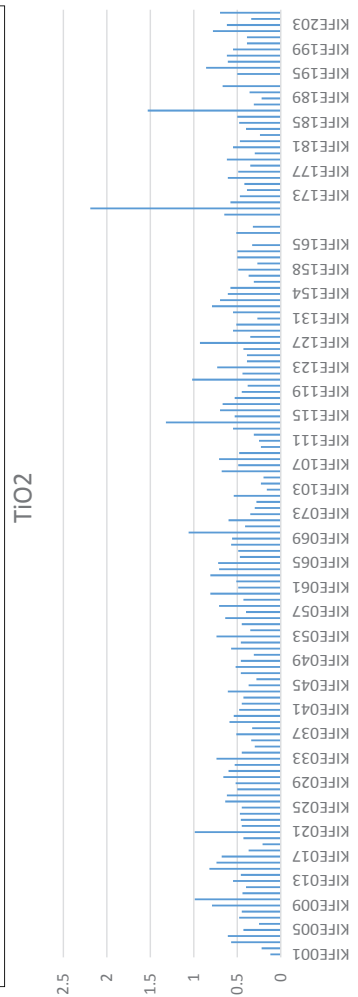
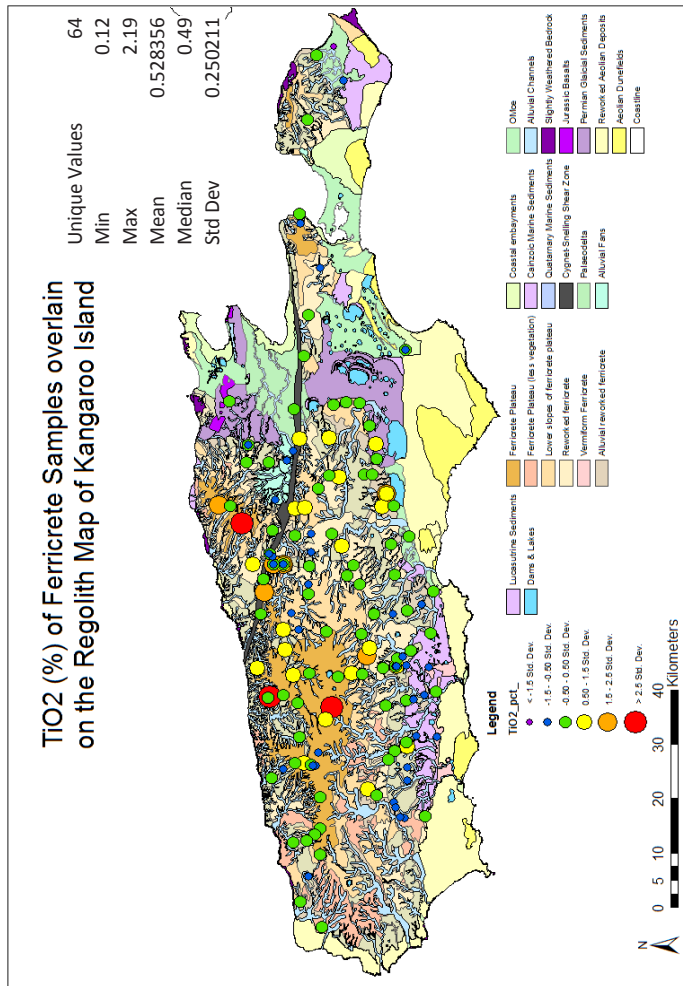
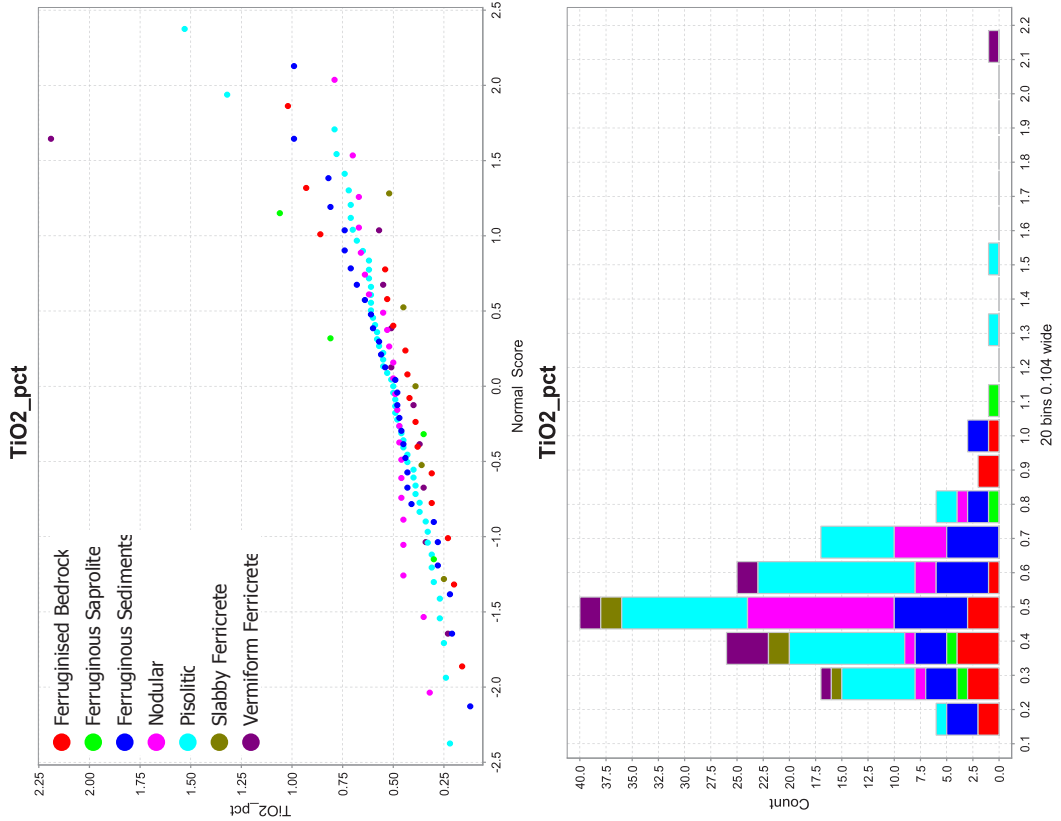


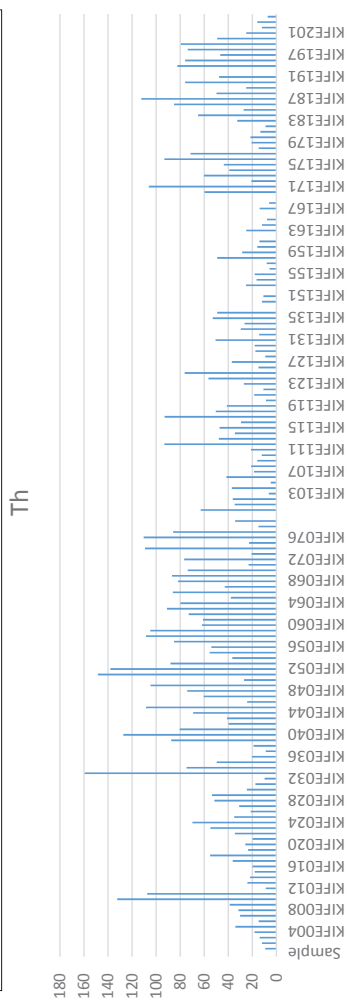
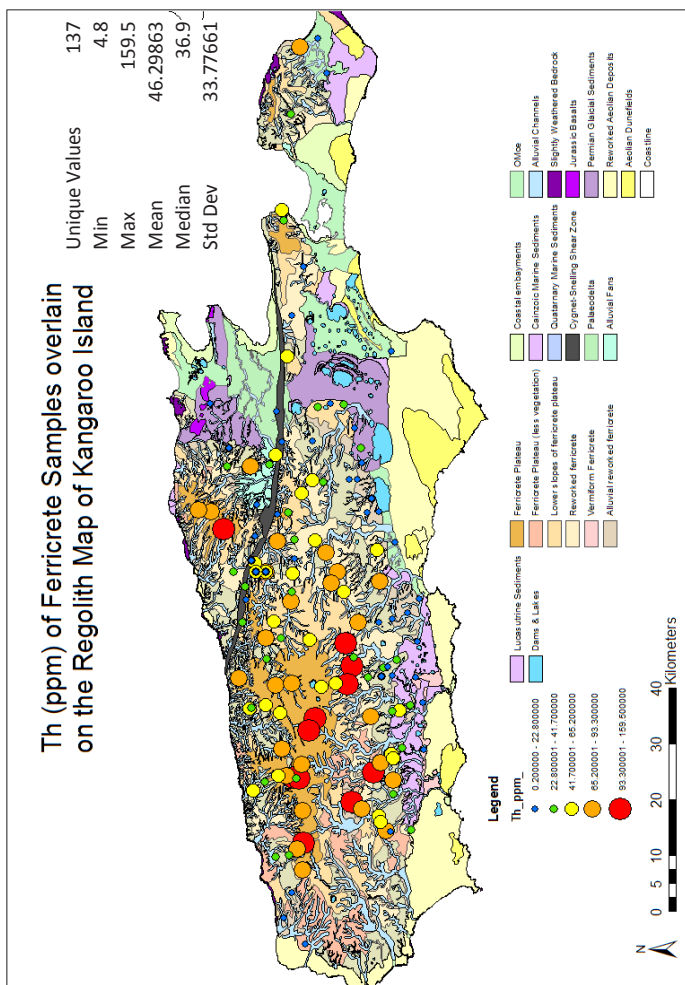
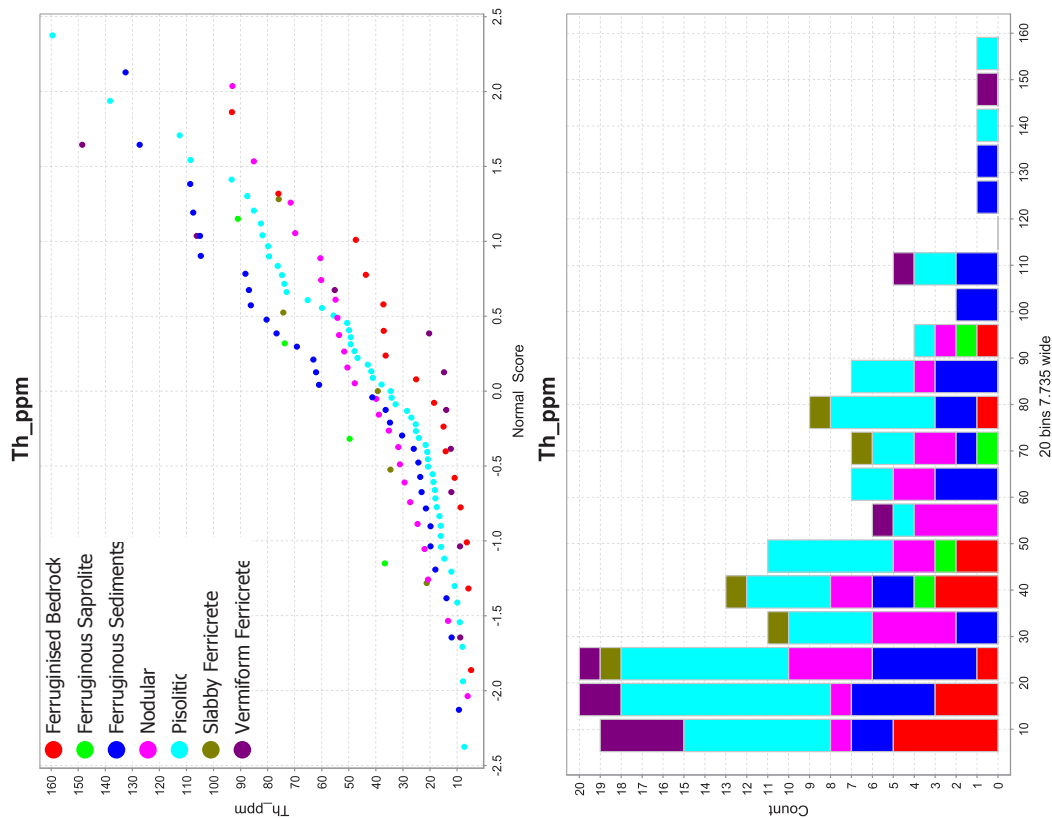


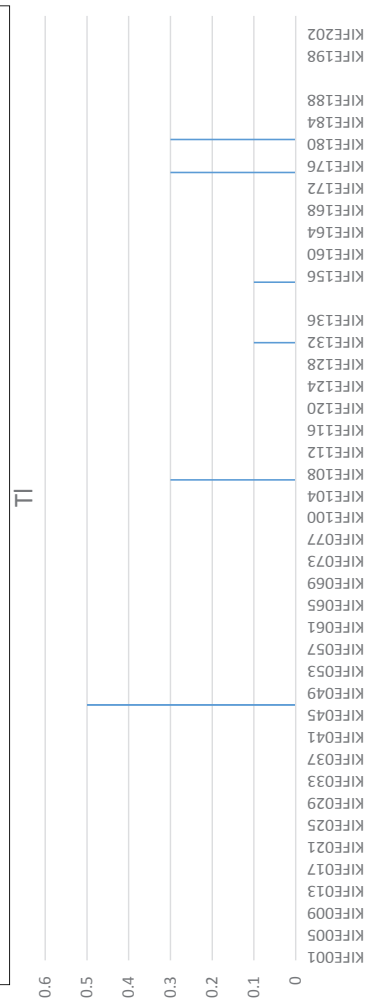
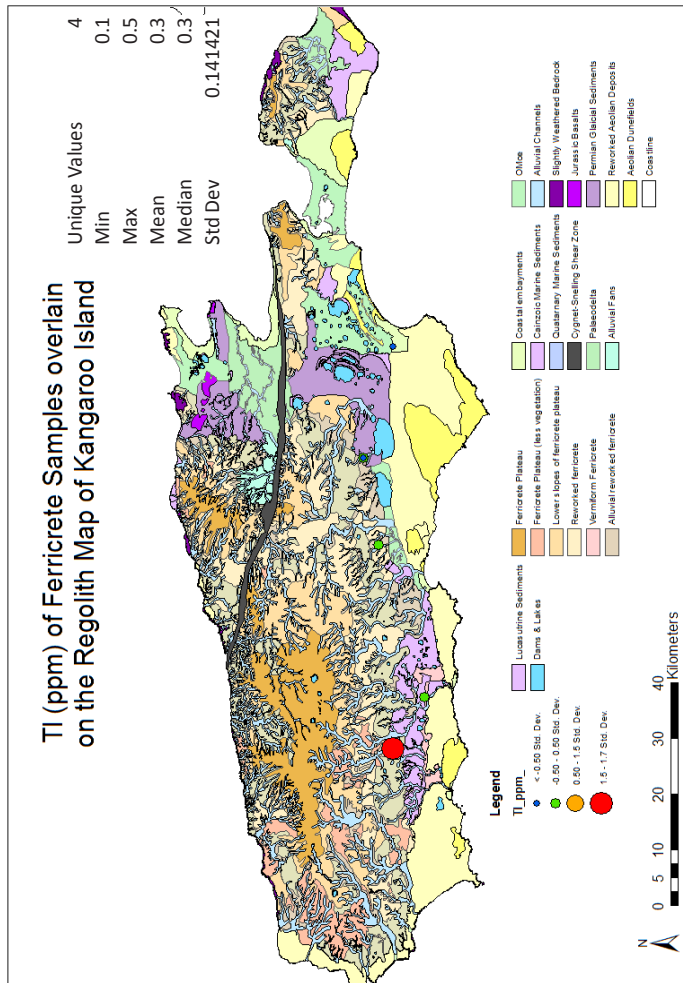
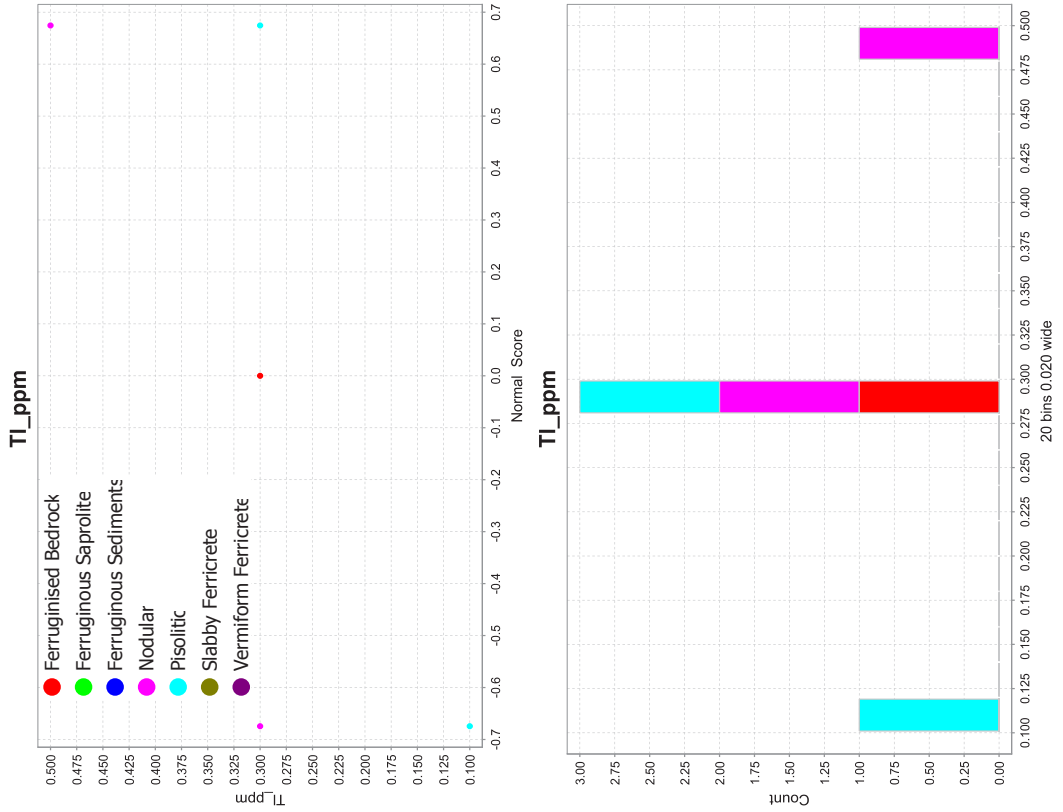


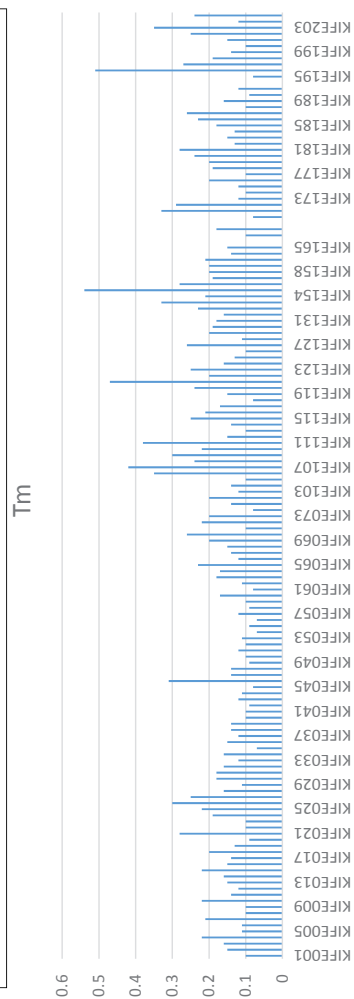
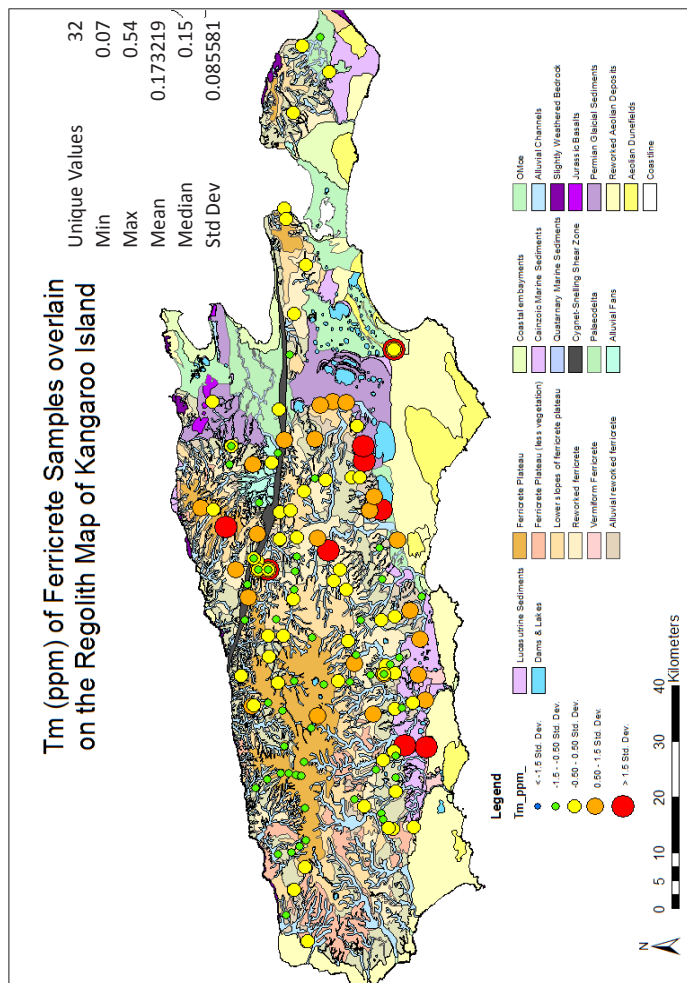
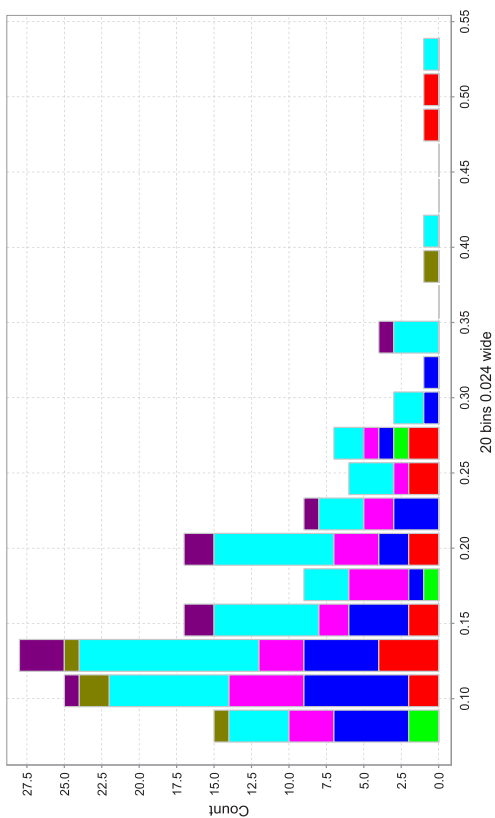
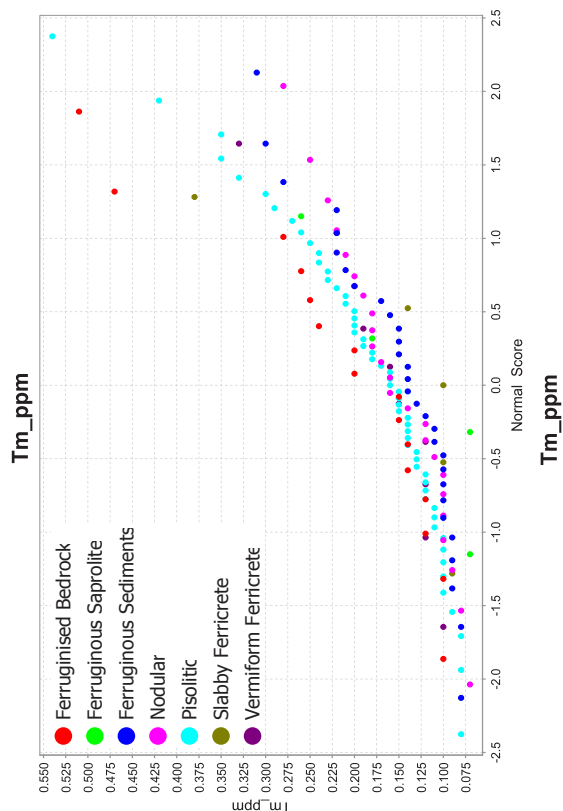


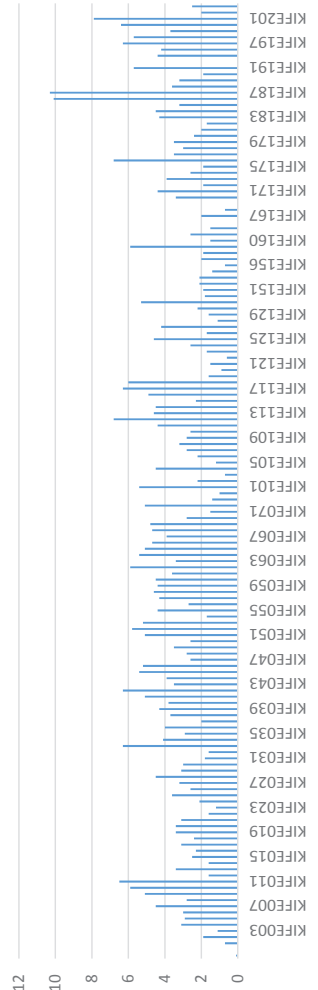
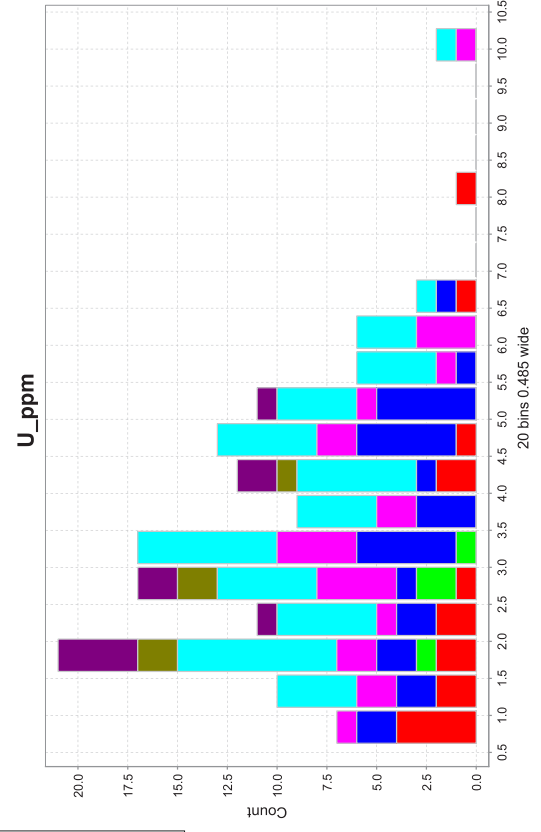
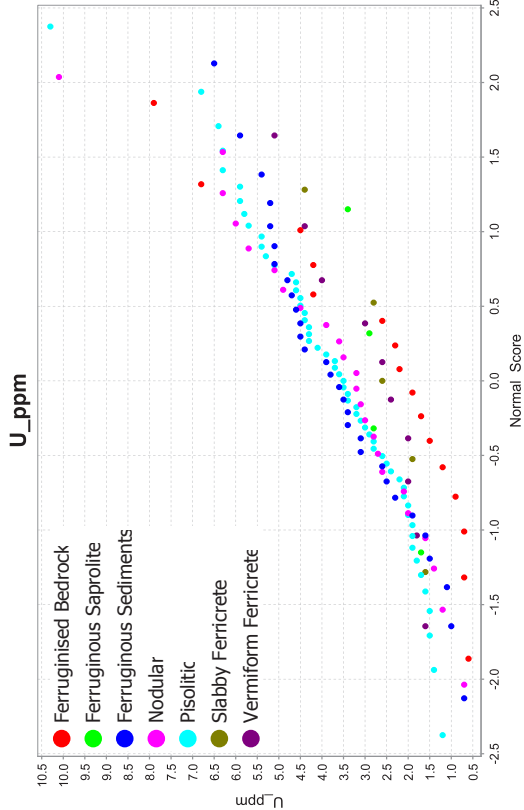
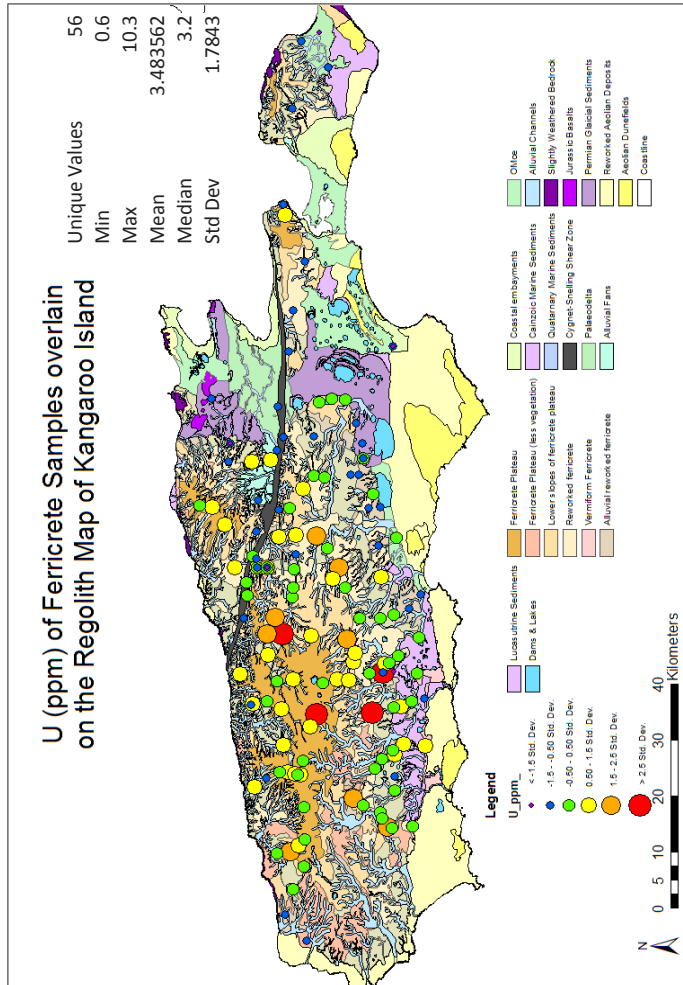


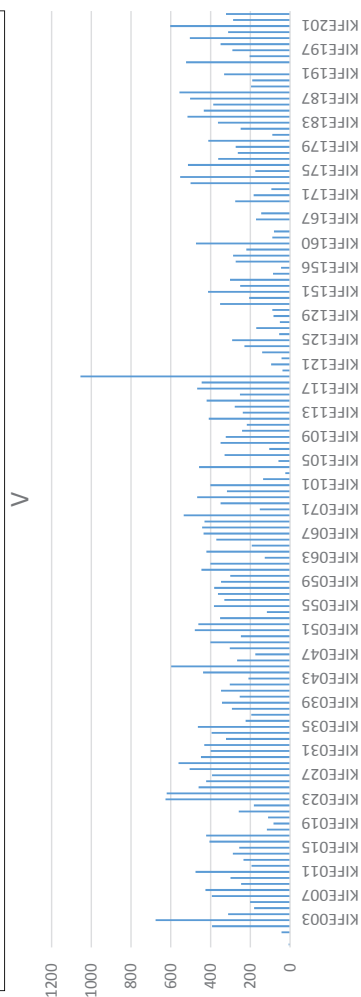
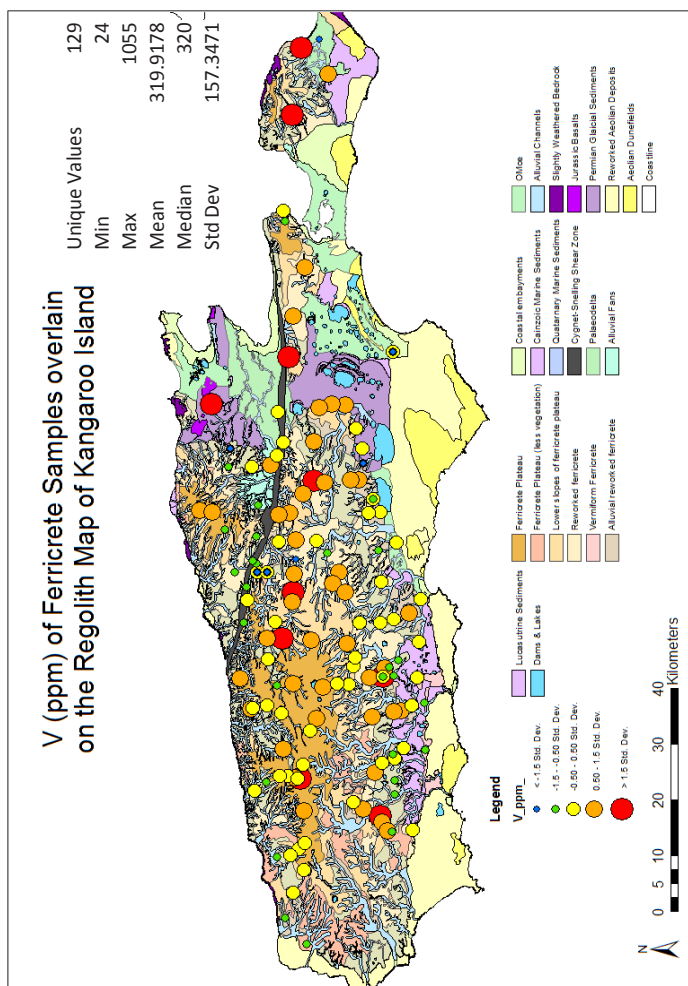
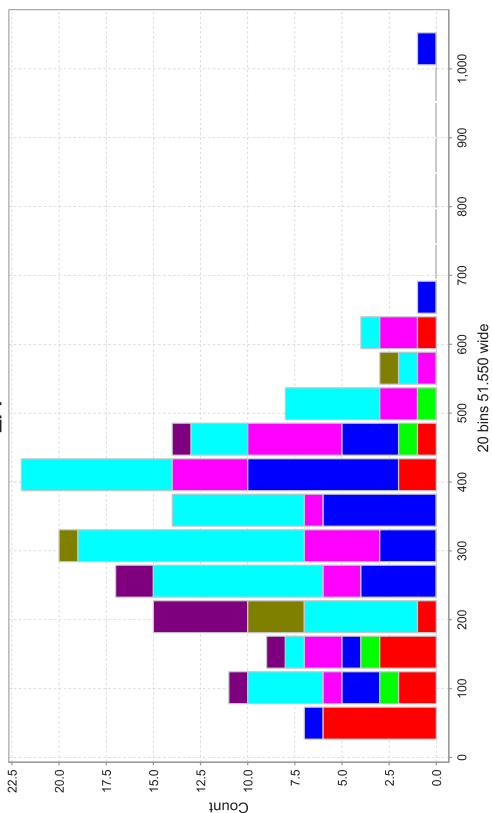
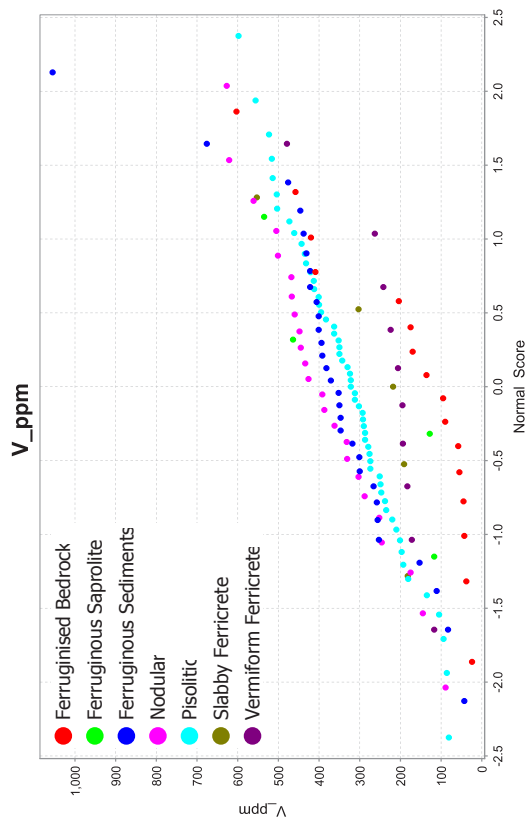


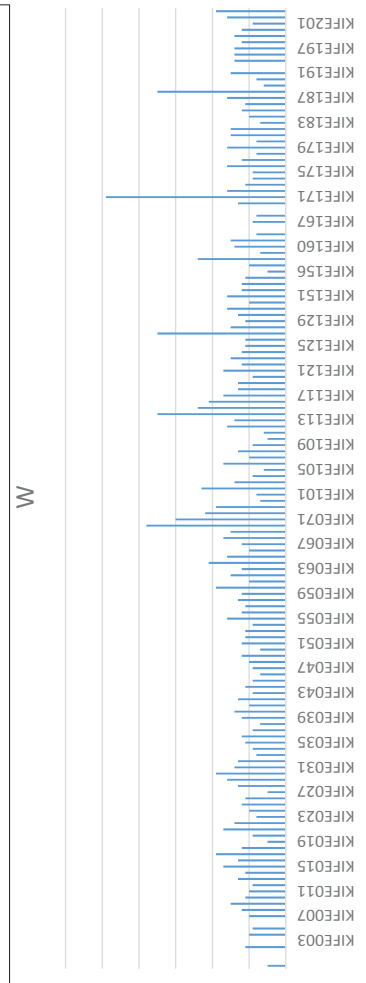
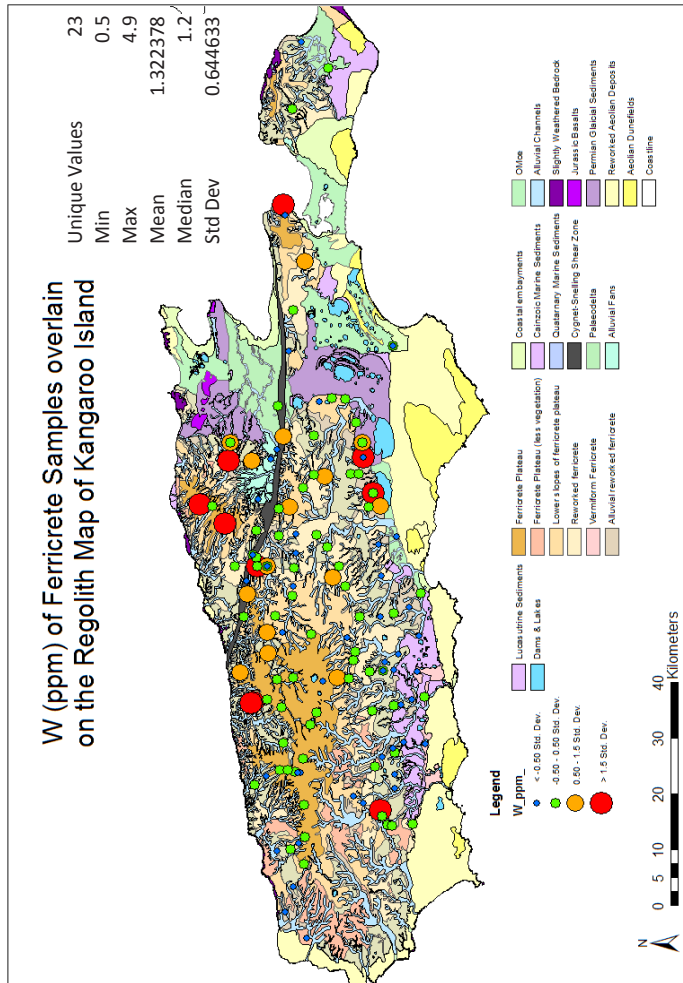
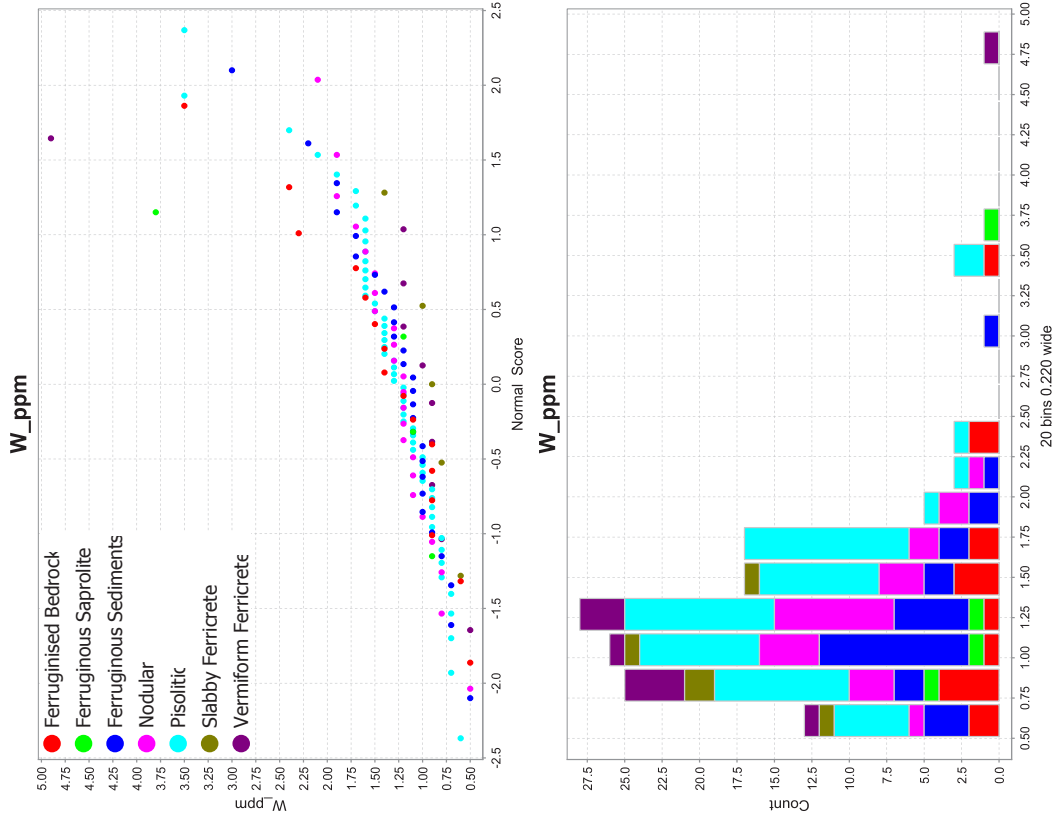


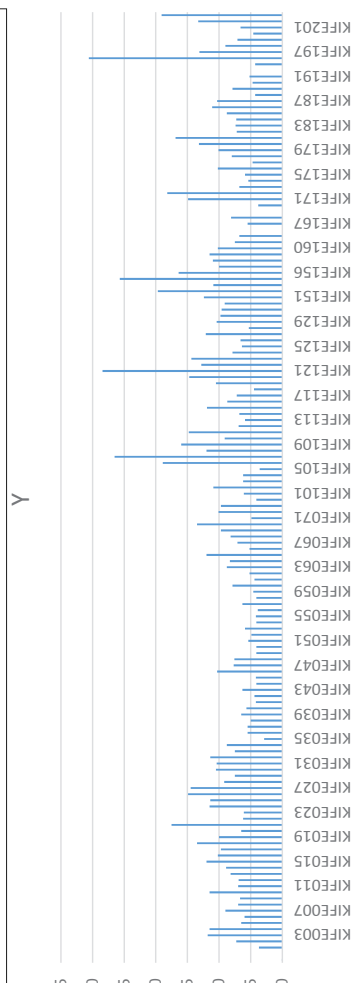
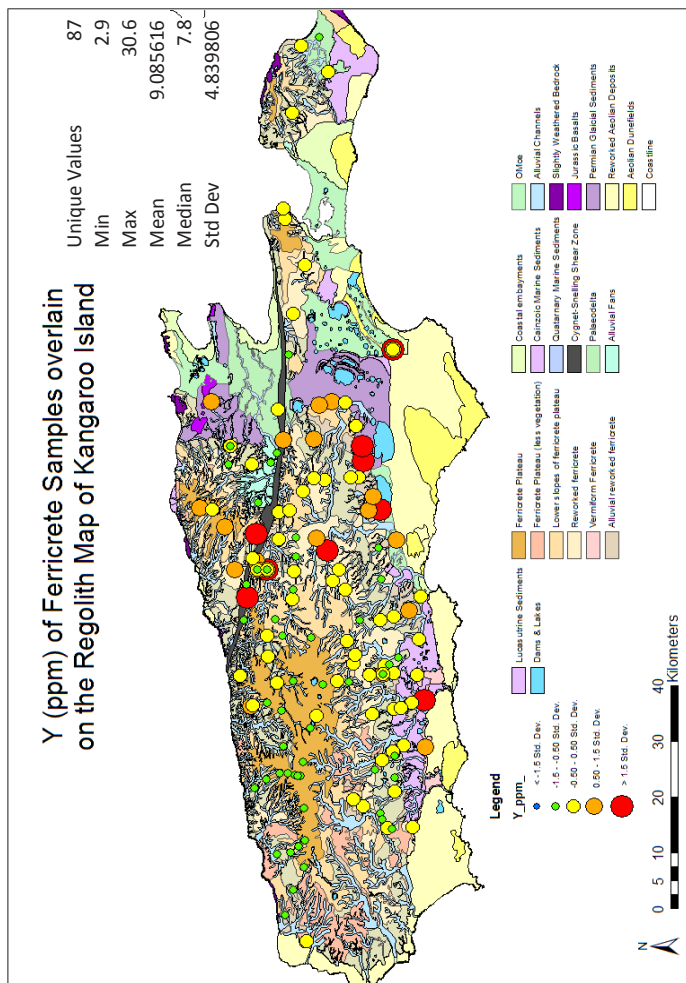
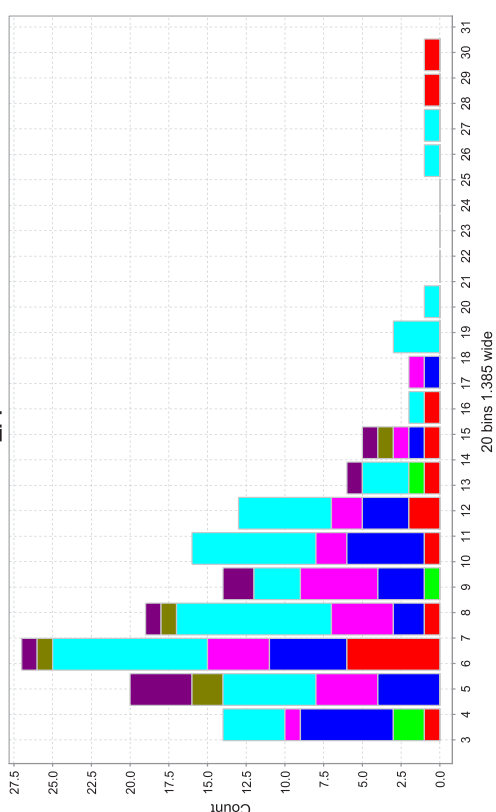
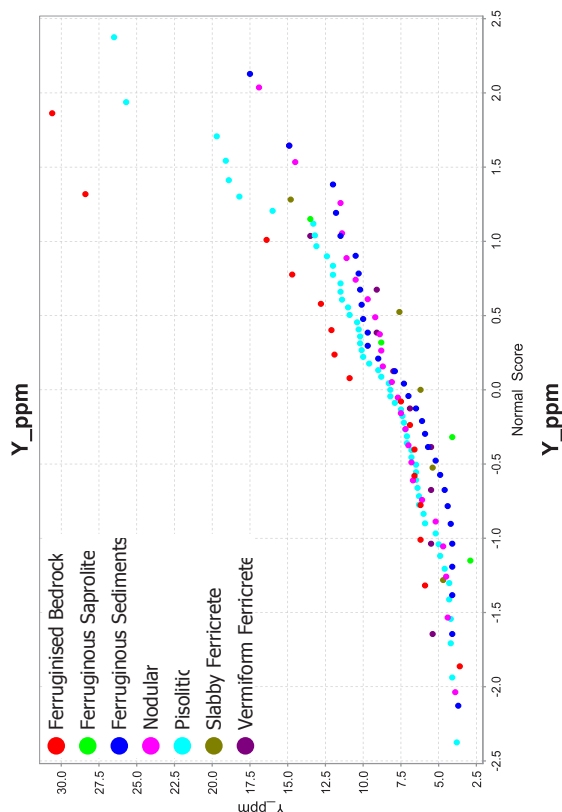


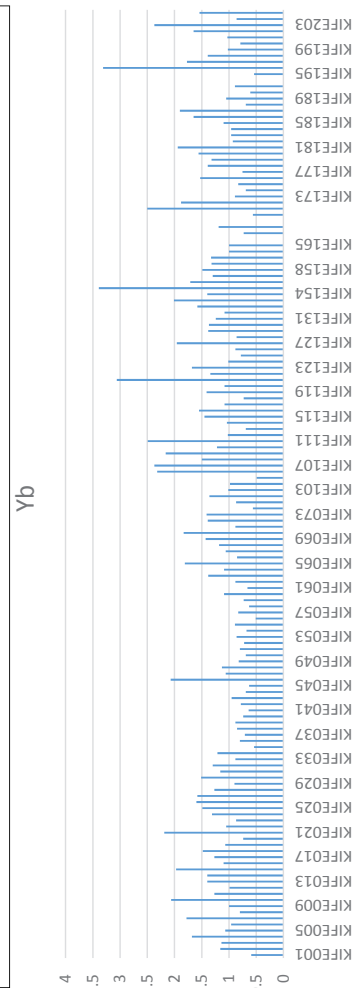
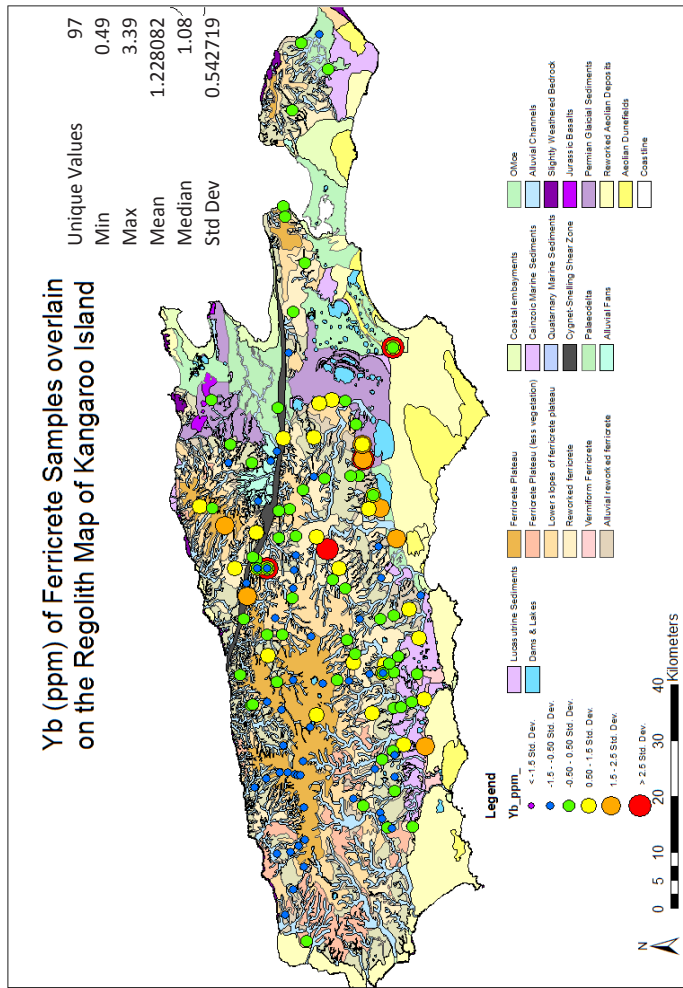
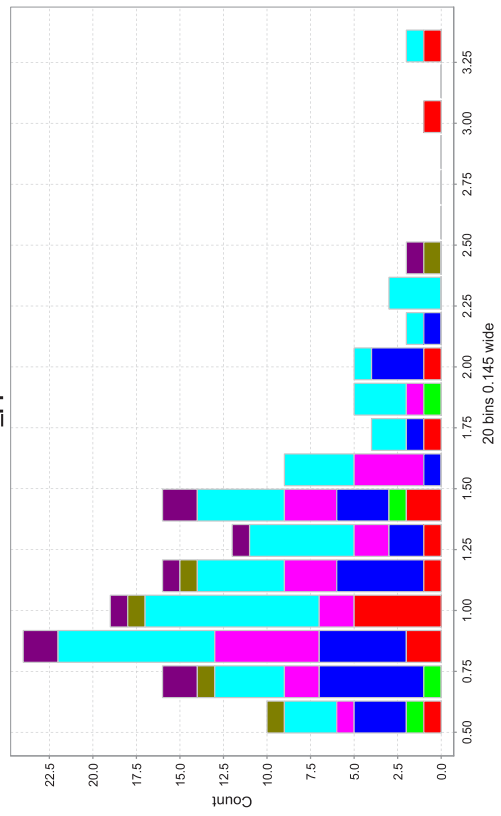
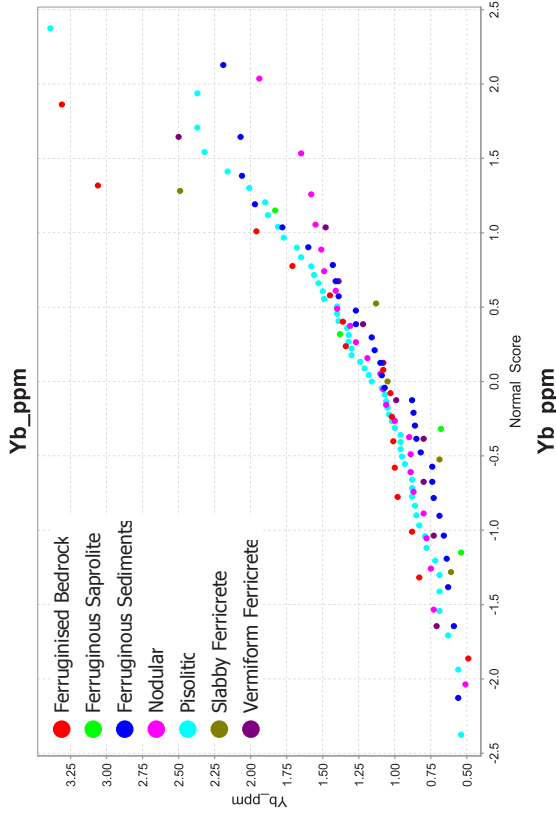


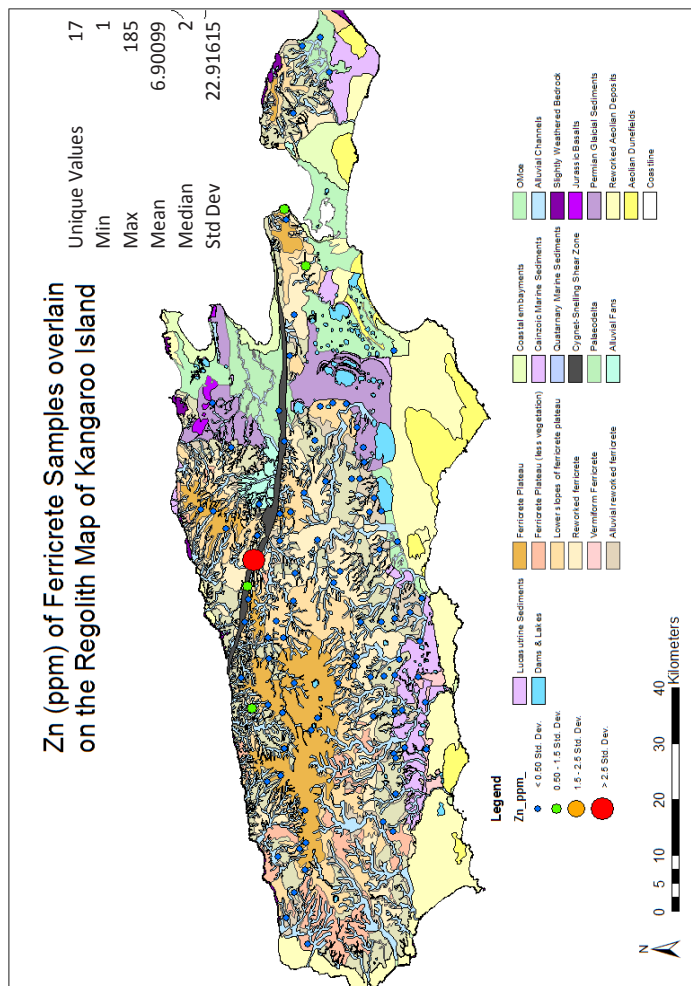
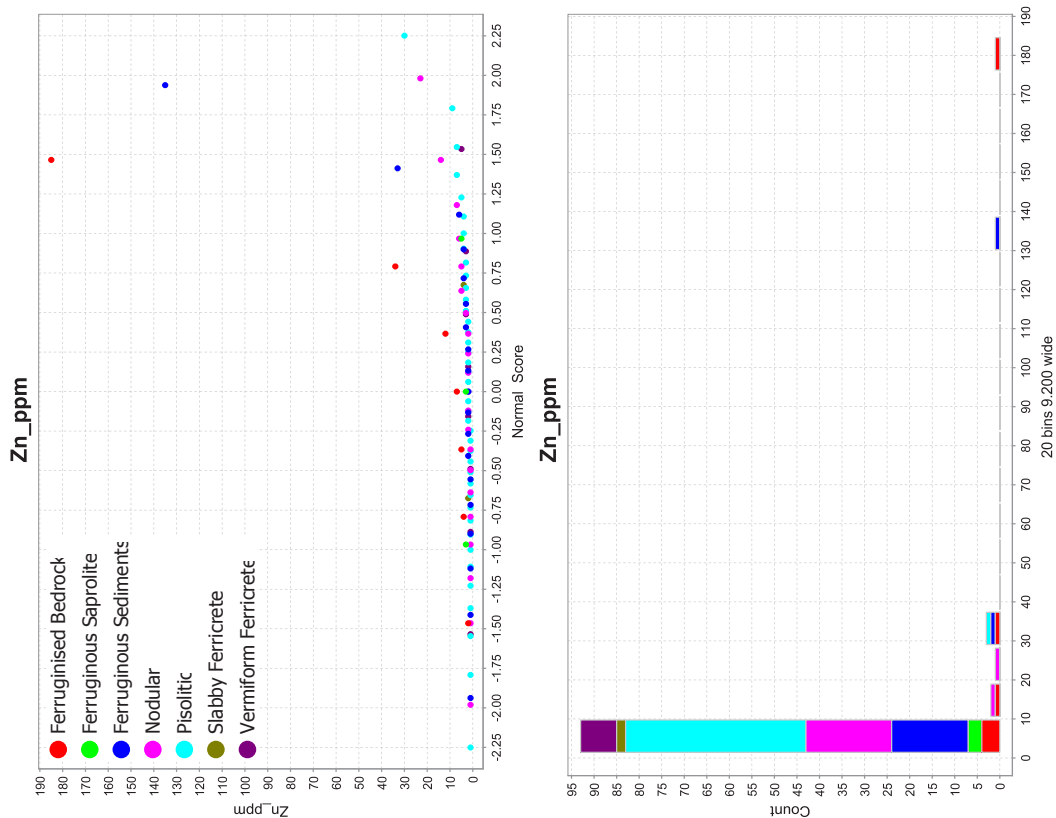


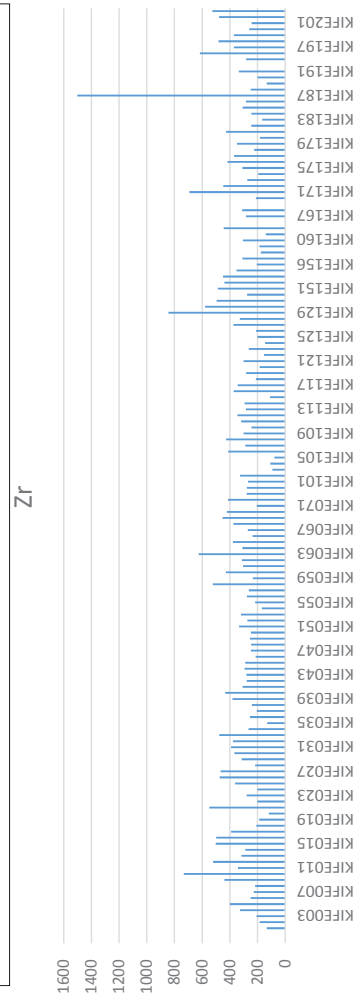
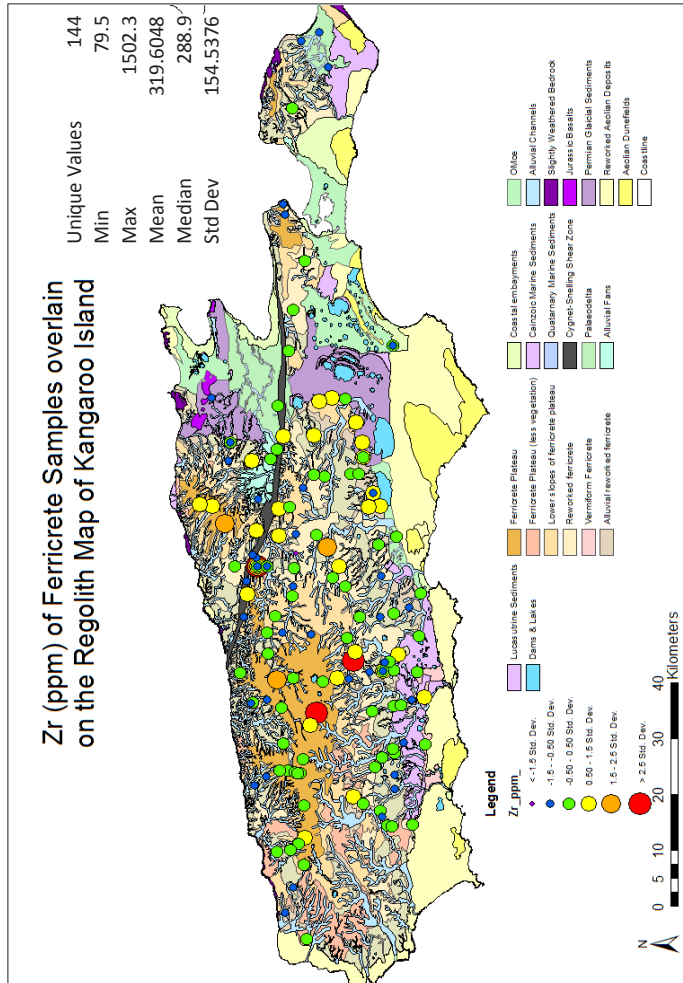
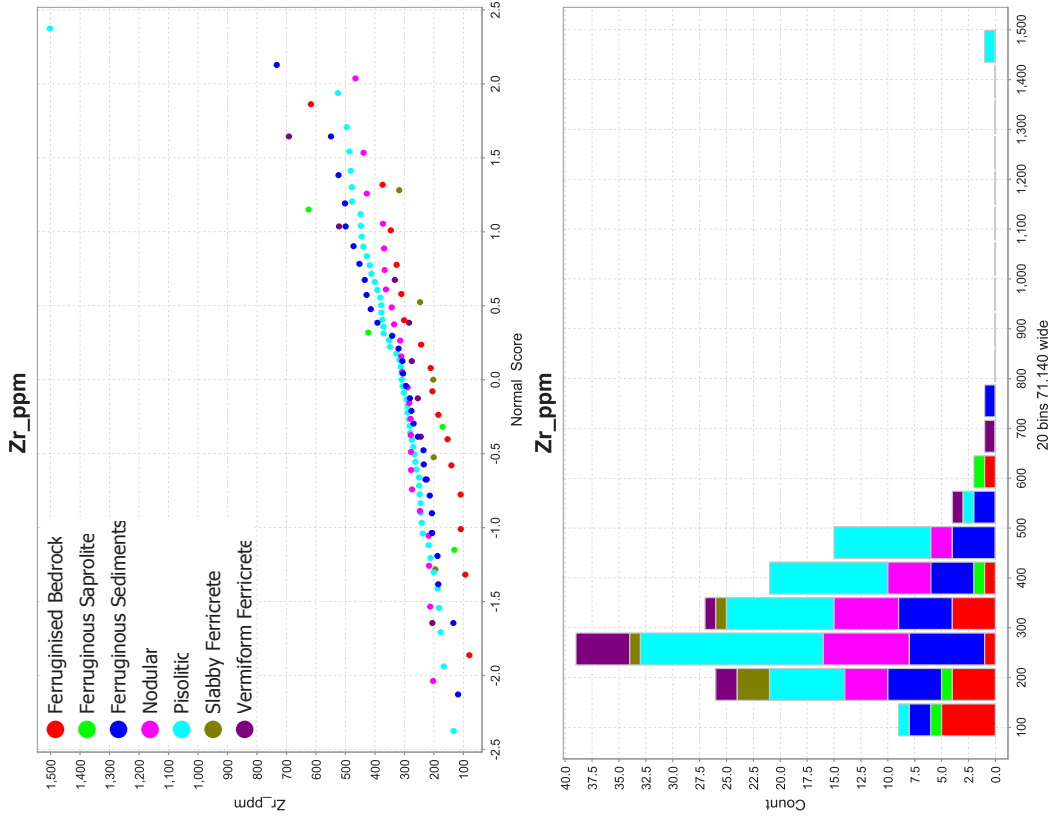




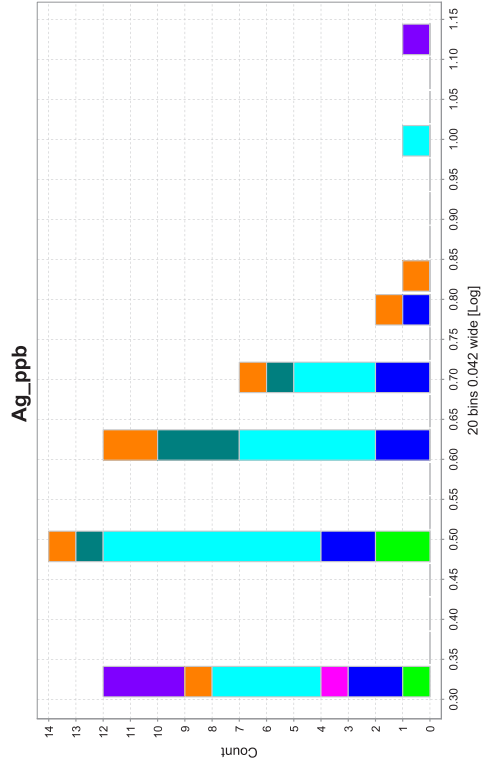
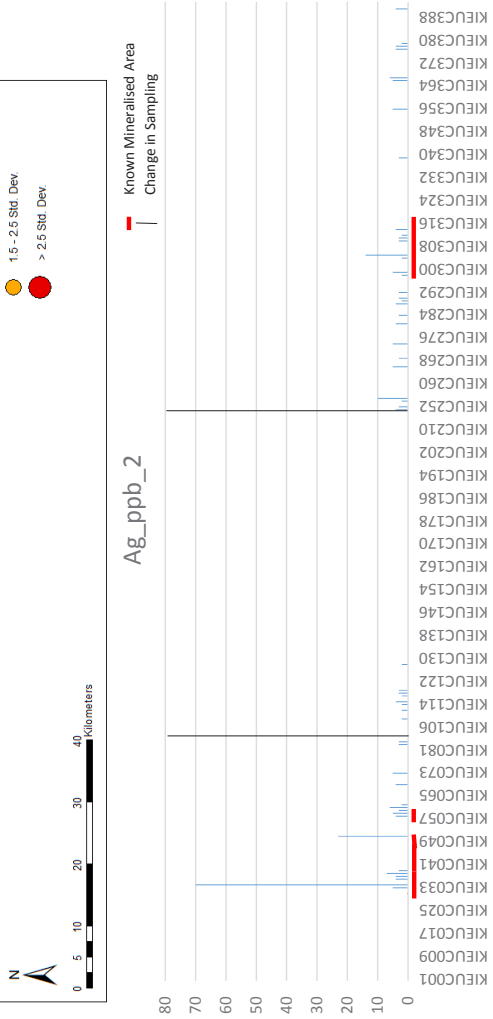
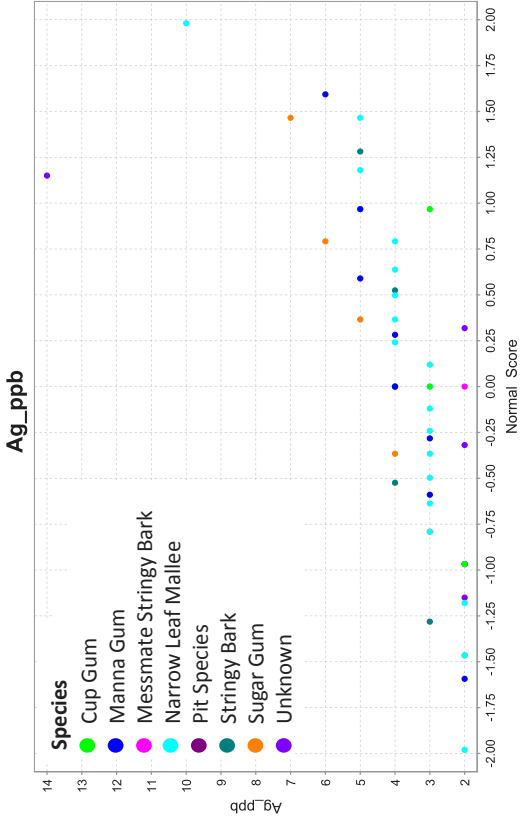
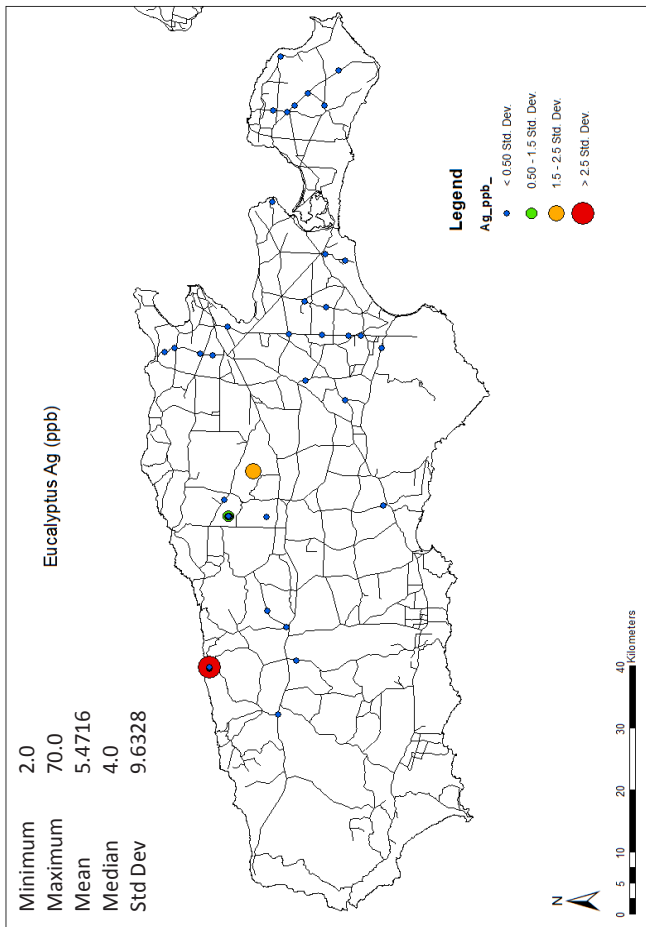


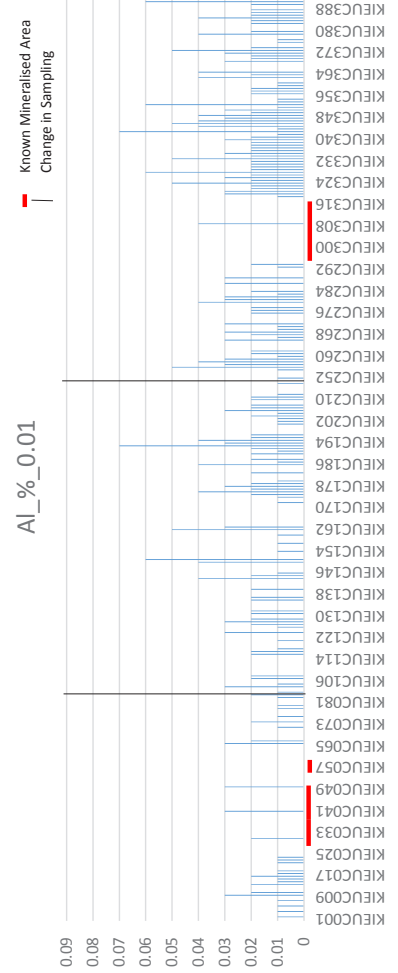
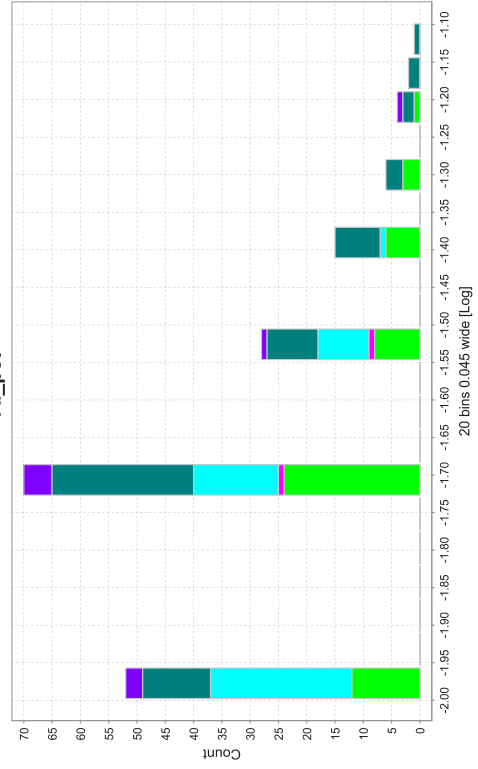
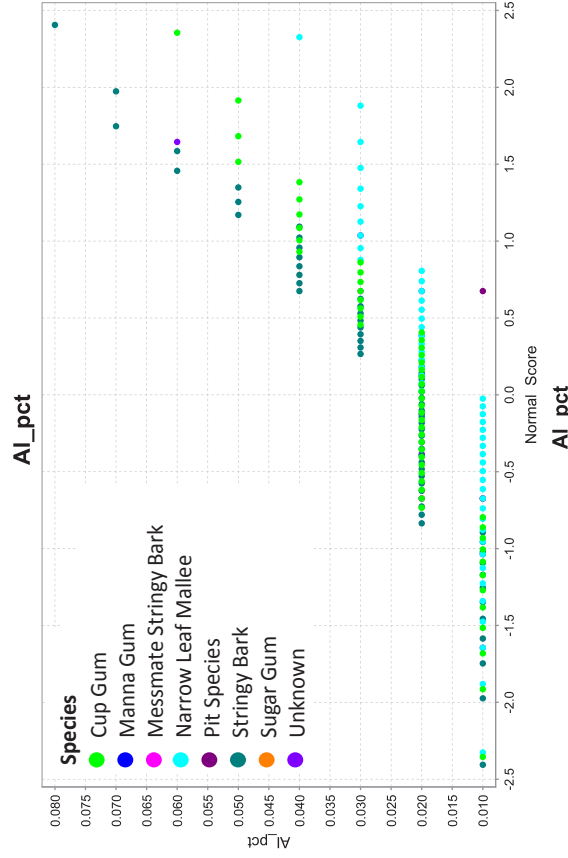
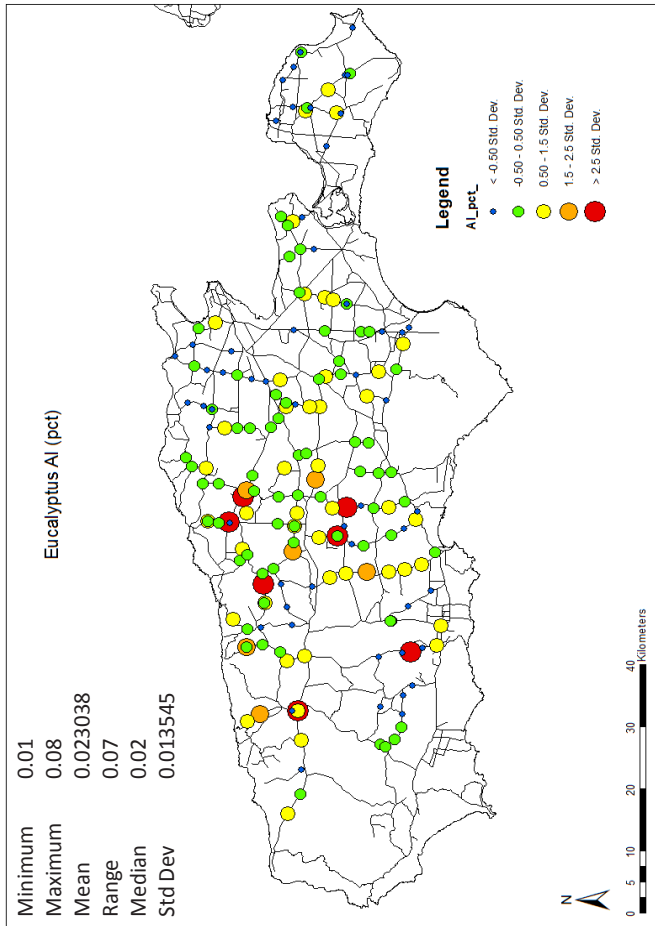


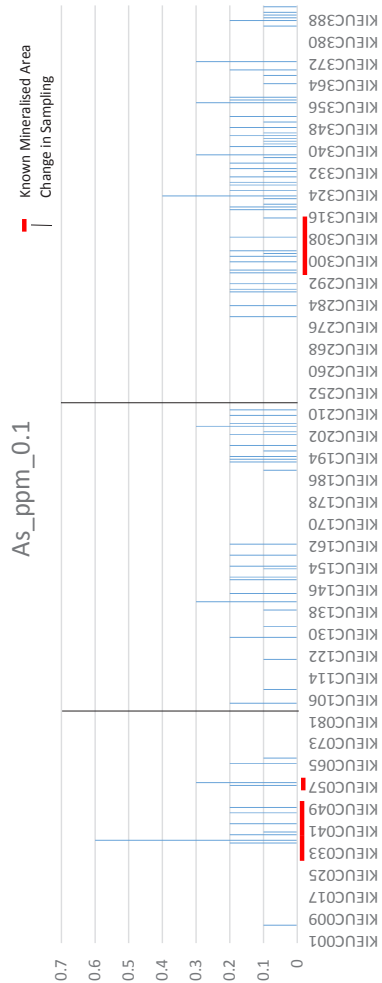
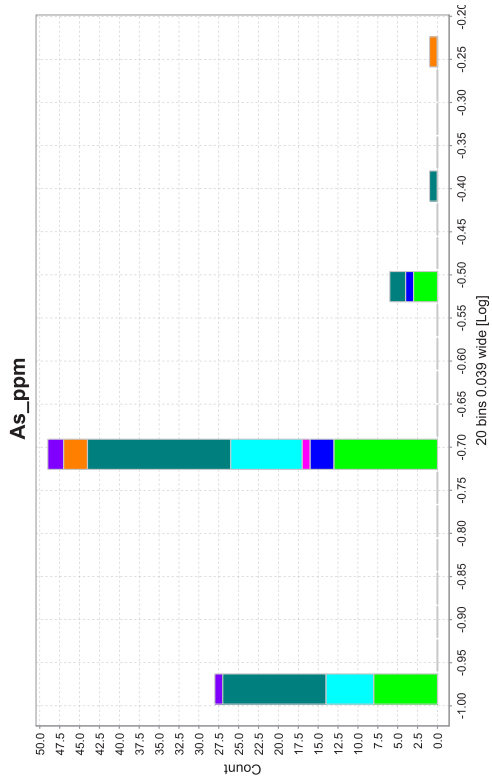
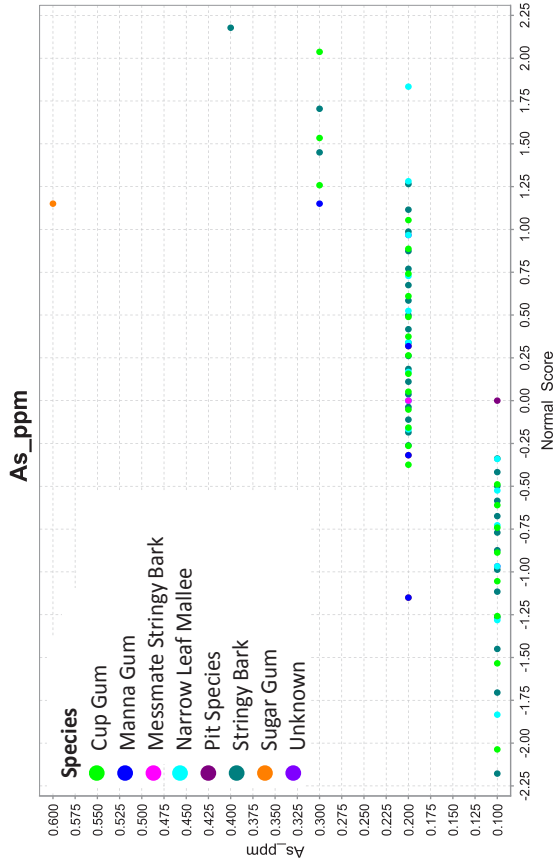
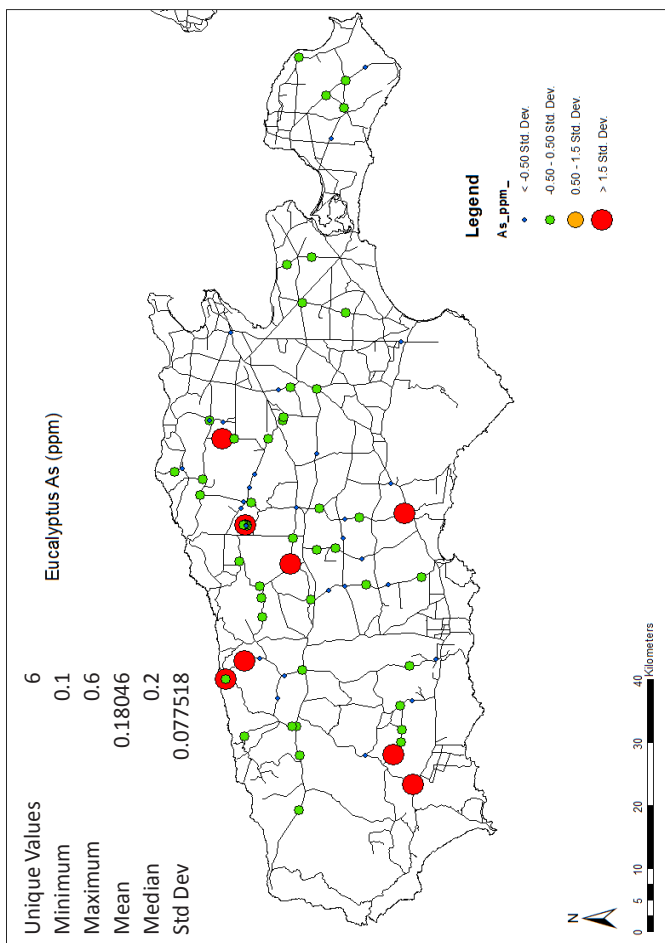


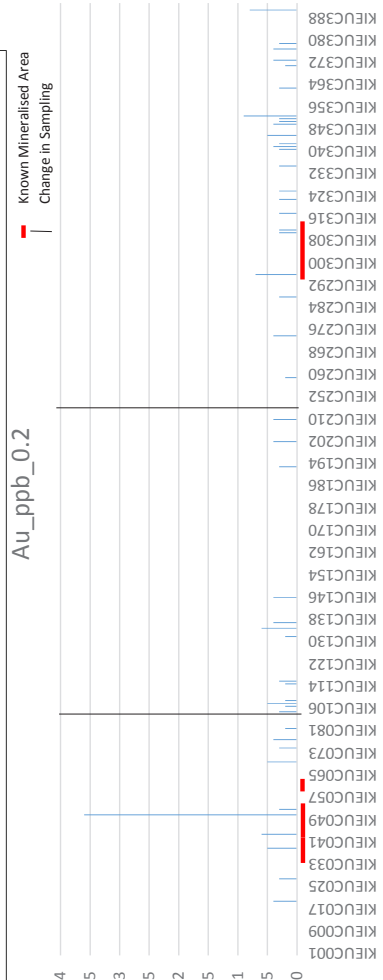
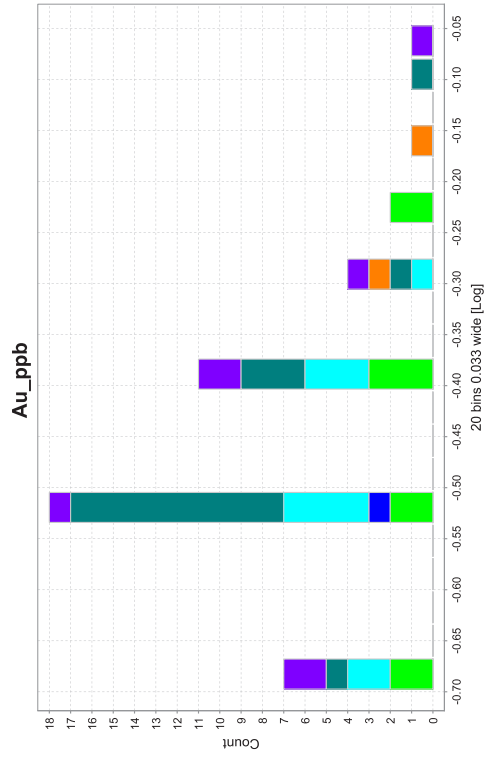
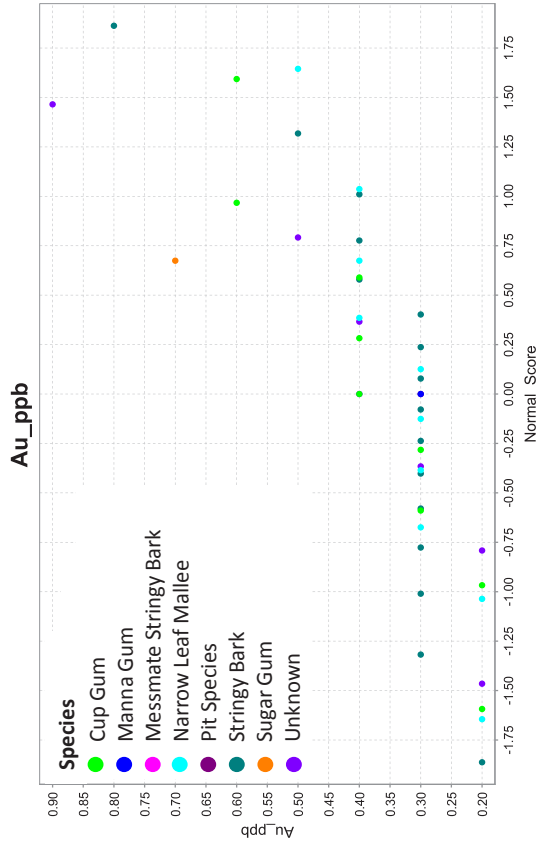
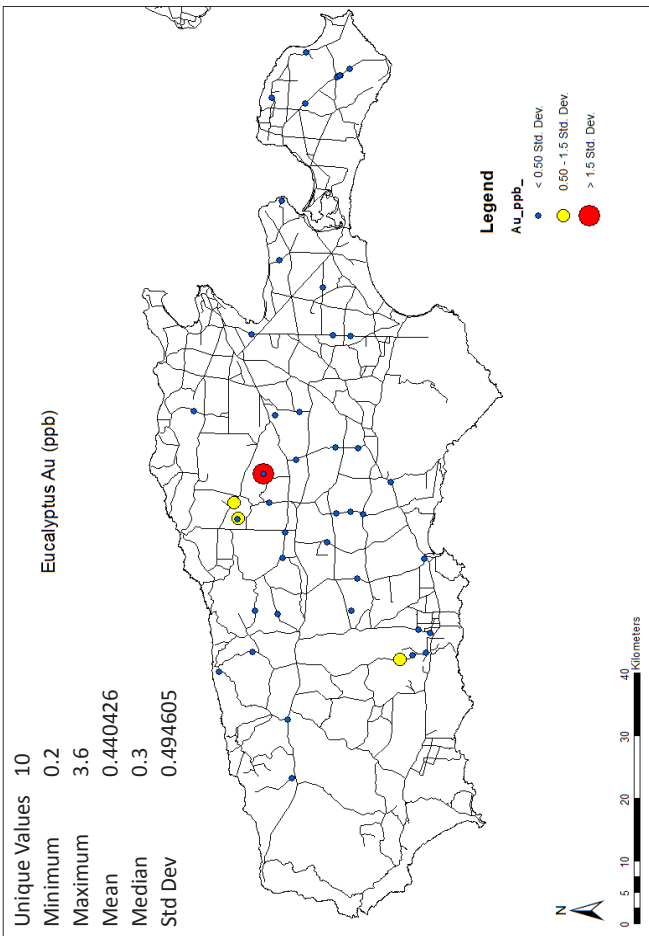


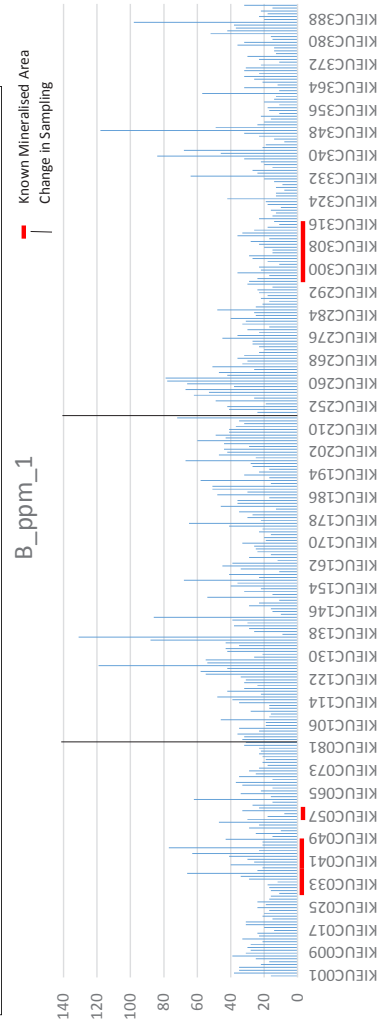
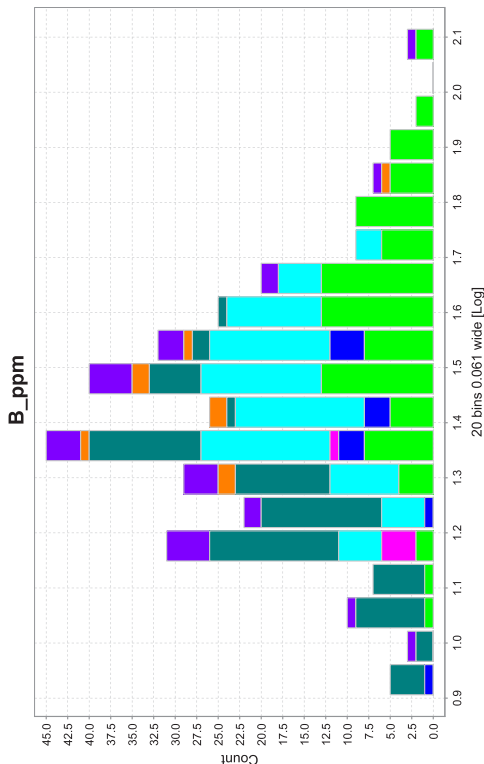
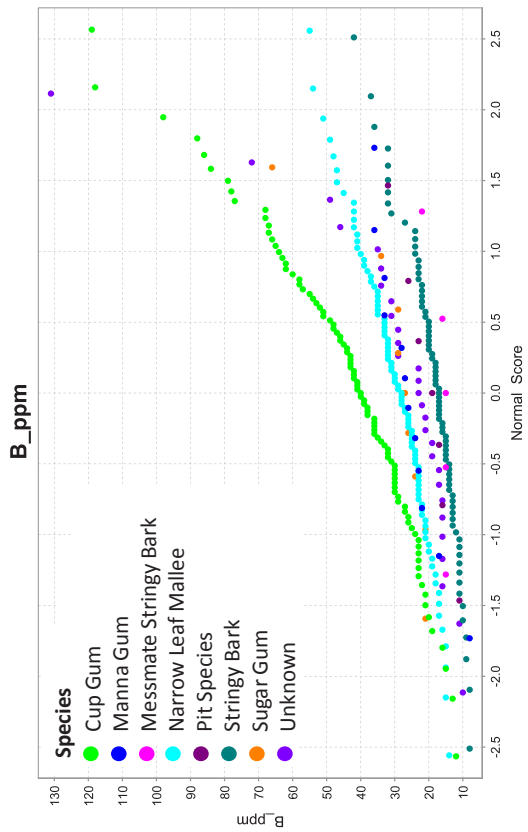
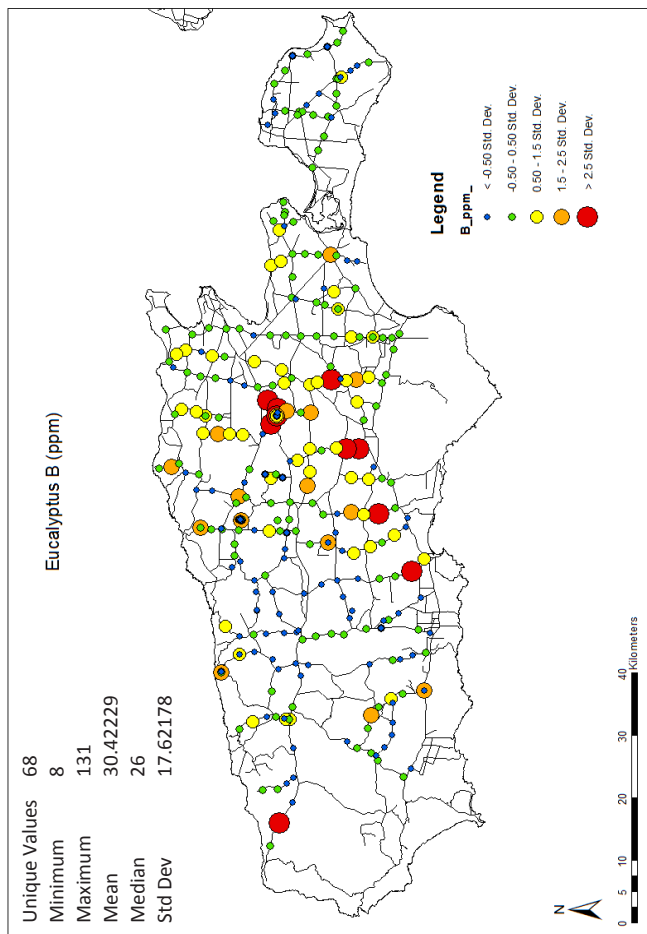
Appendix C: Eucalypt Maps and Graphs

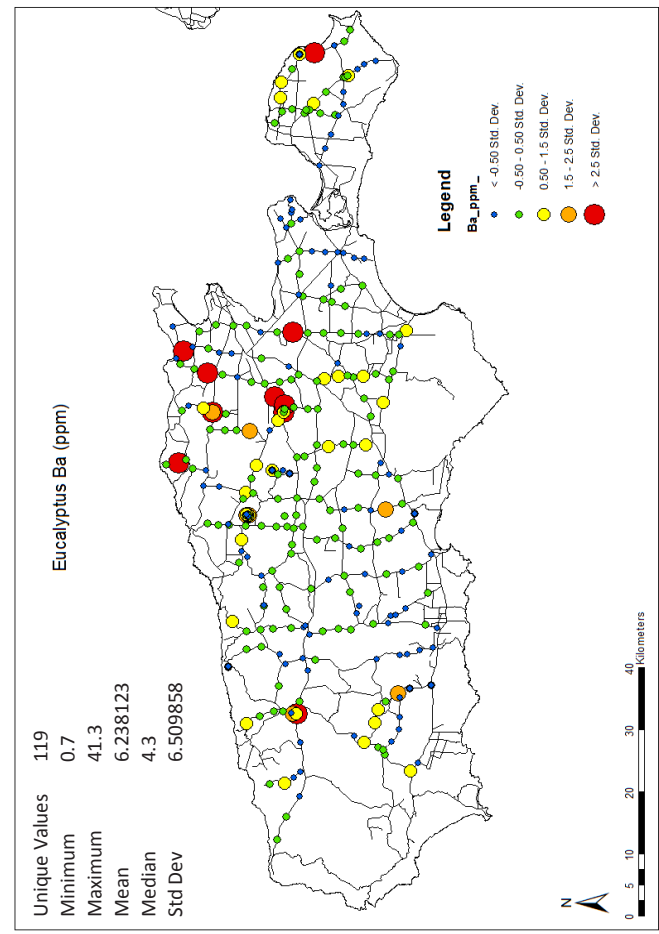
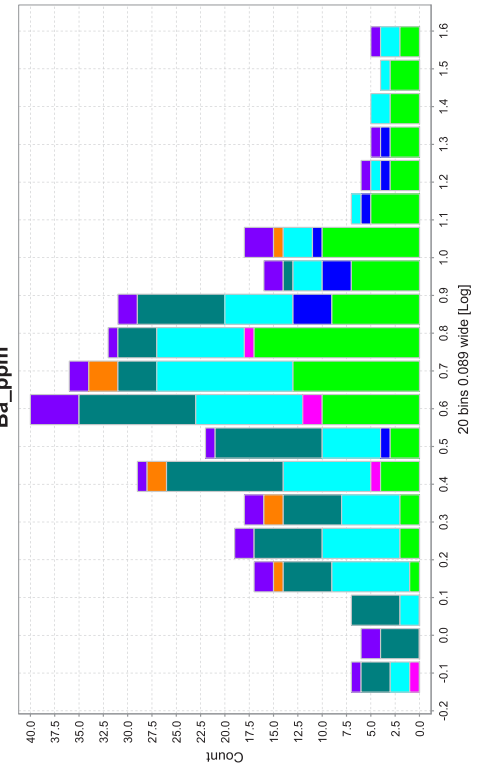
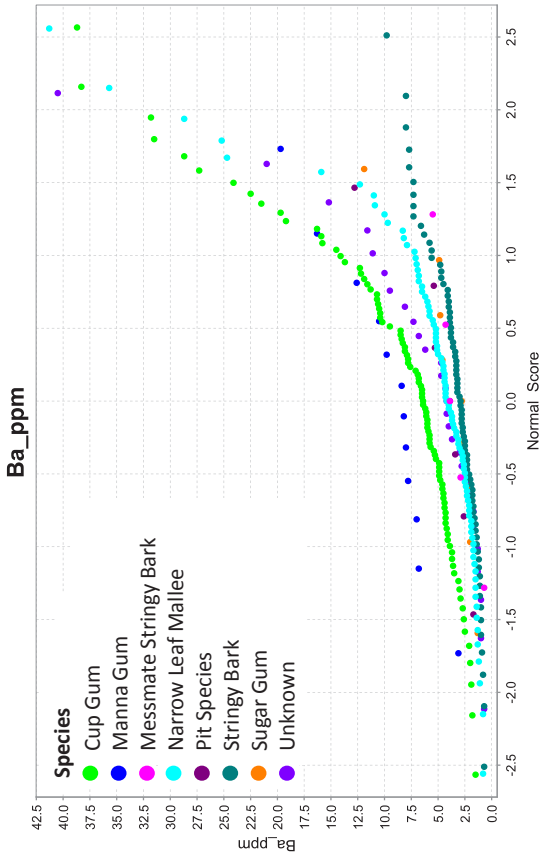


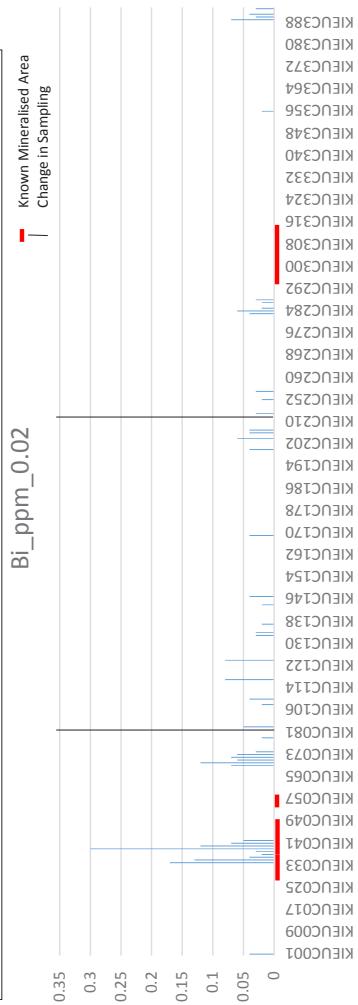
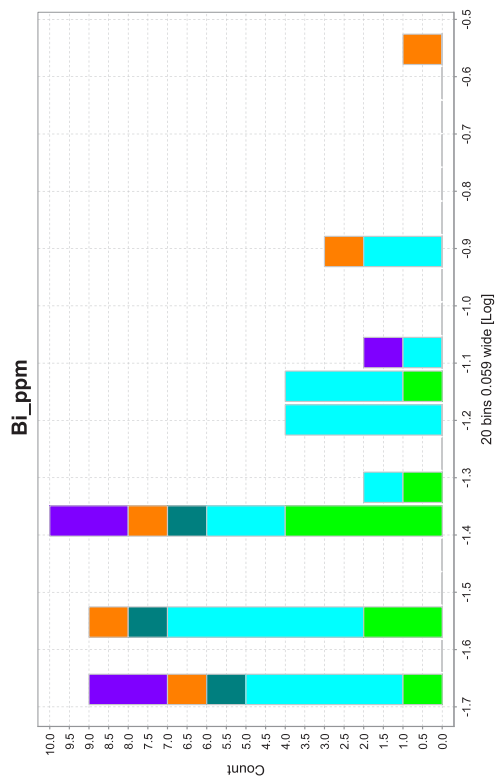
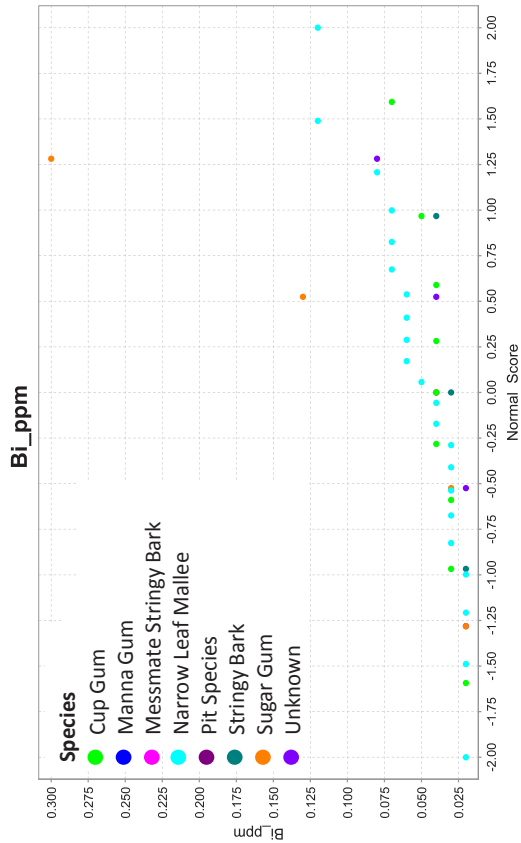
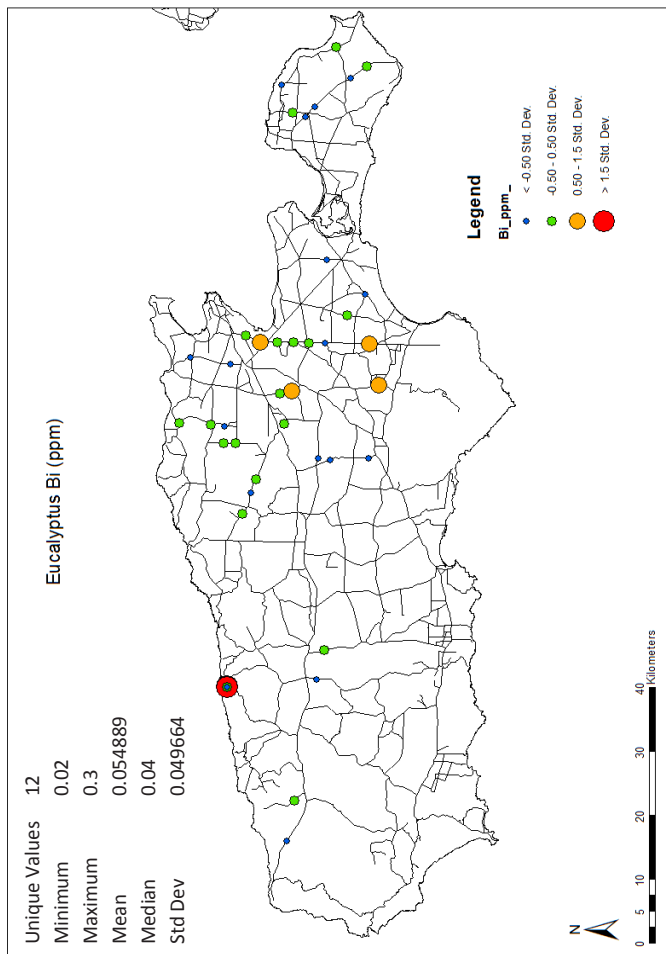


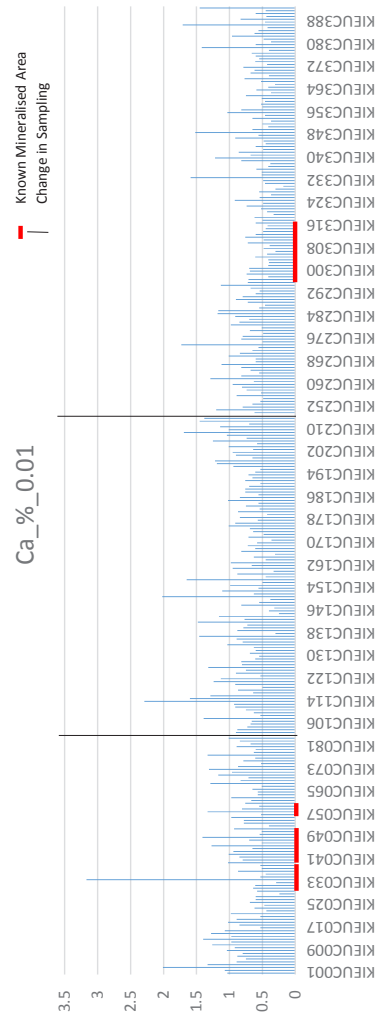
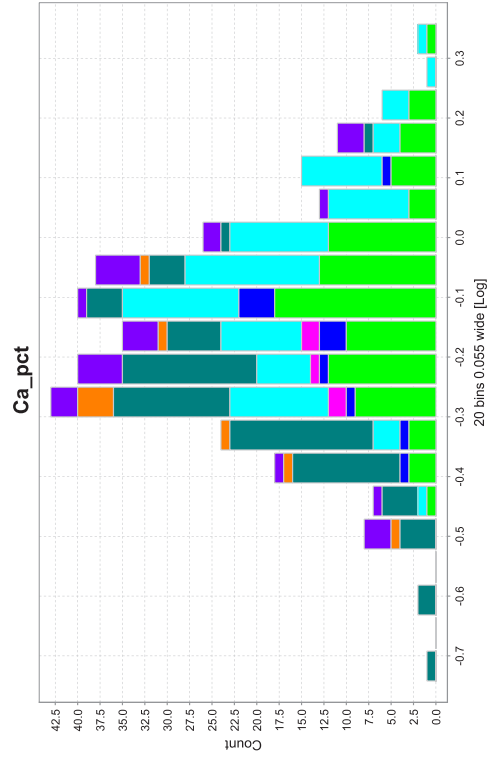
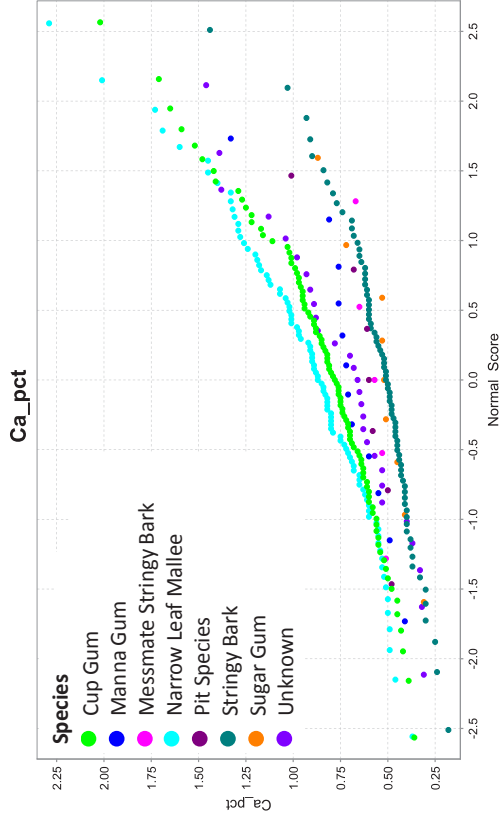
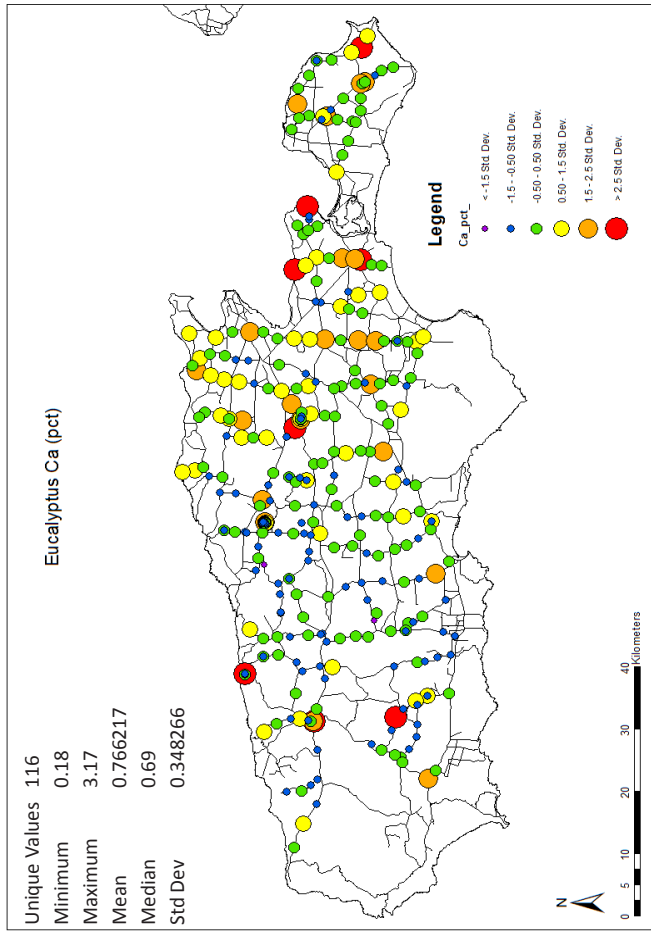


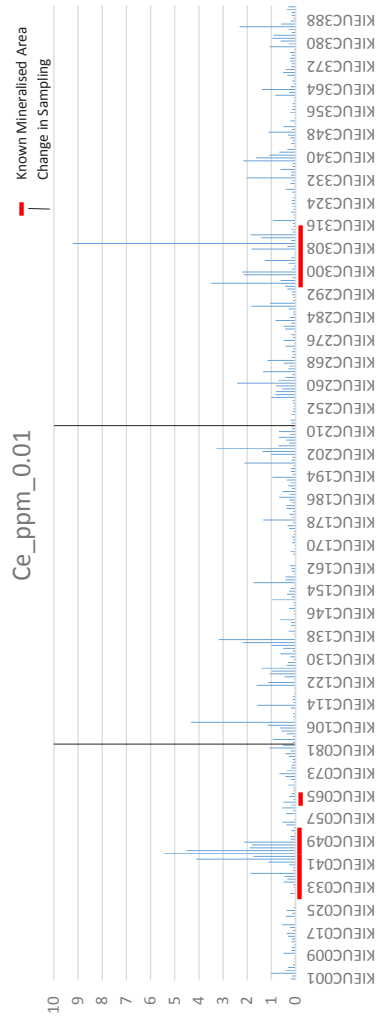
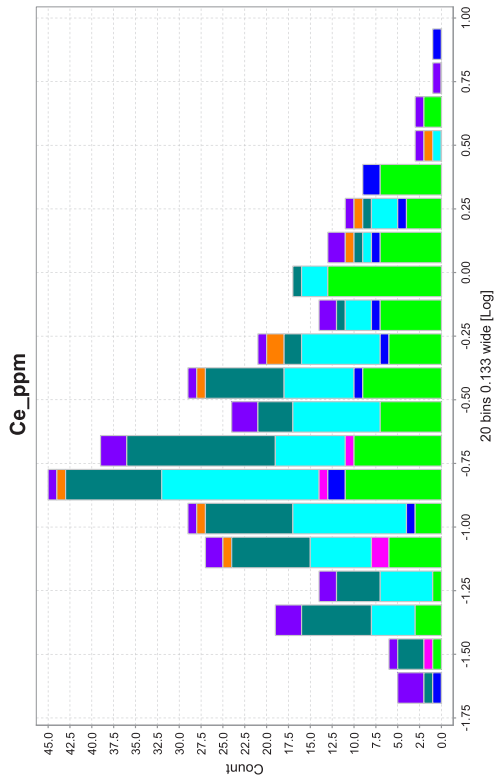
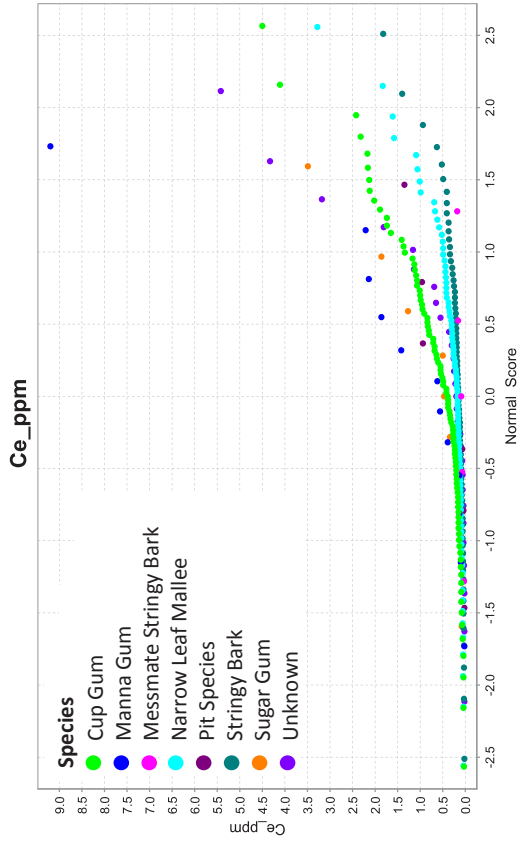
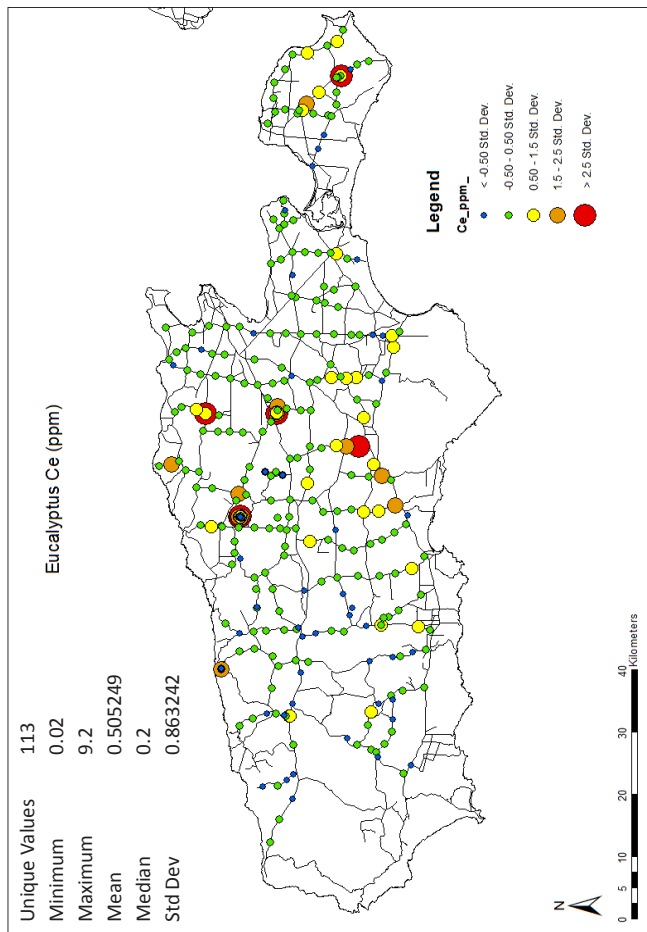


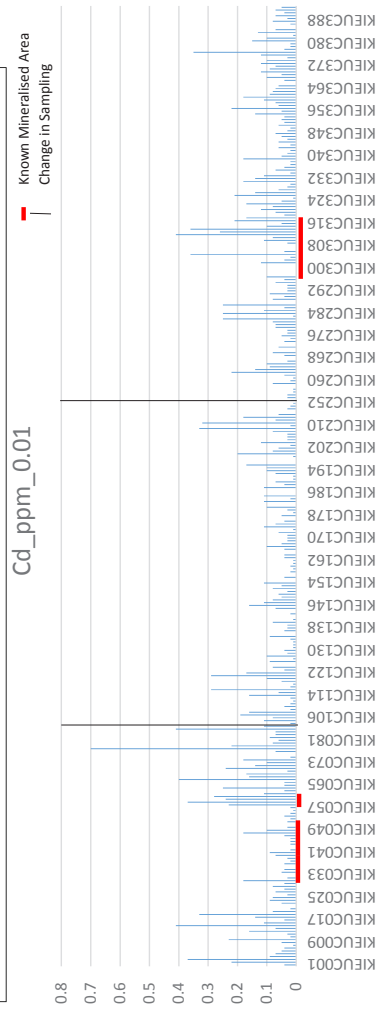
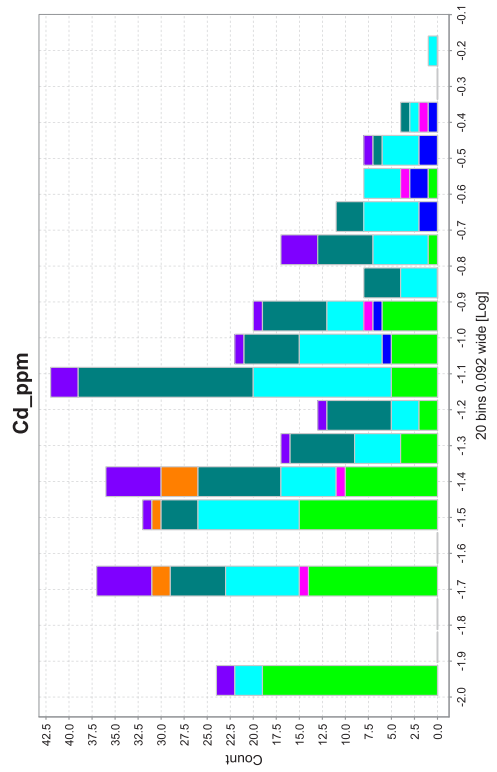
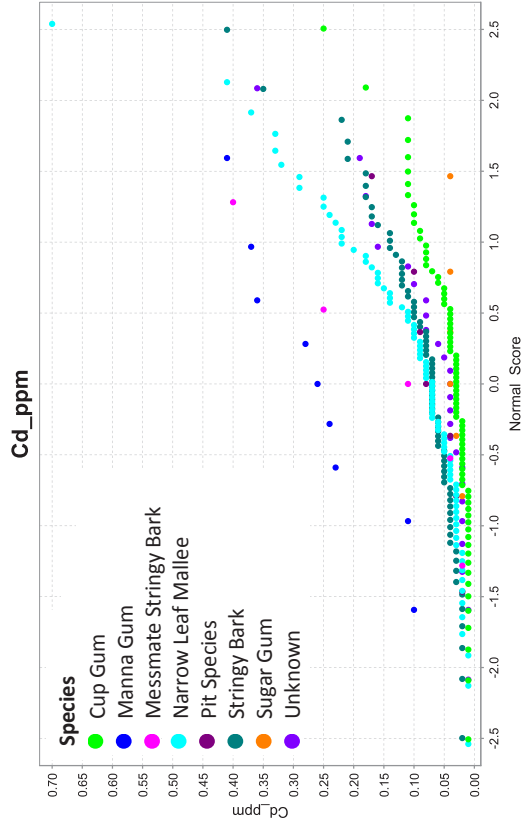
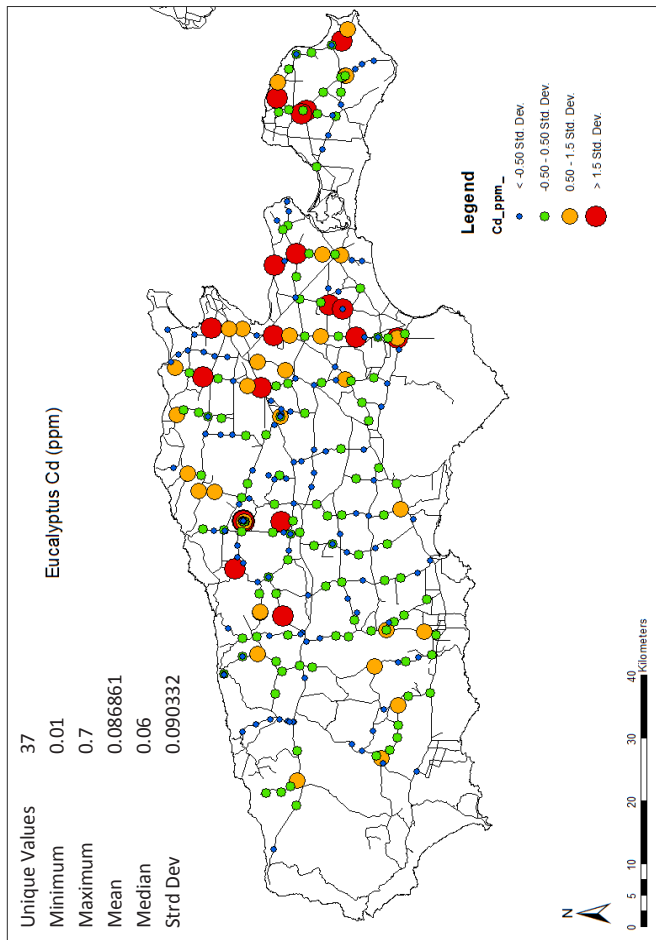


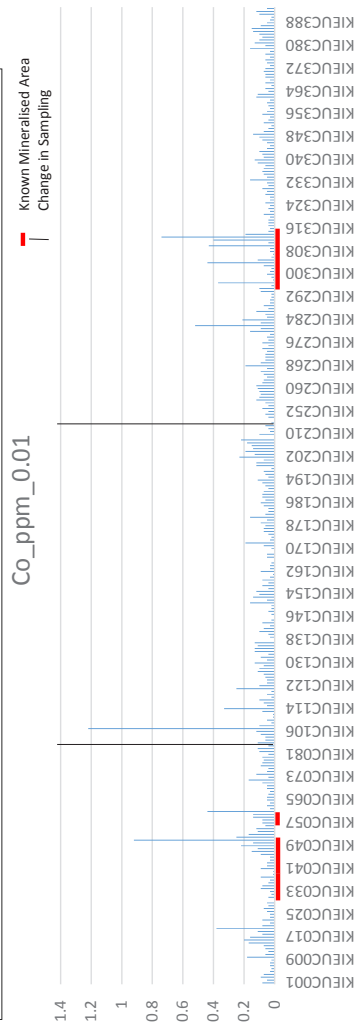
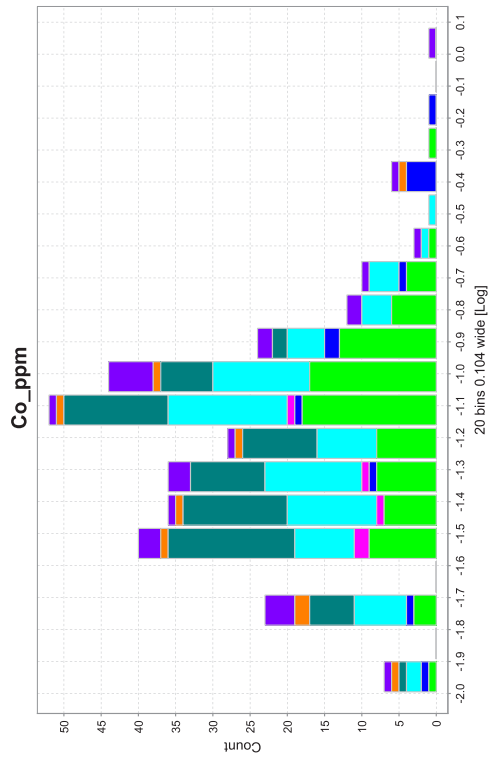
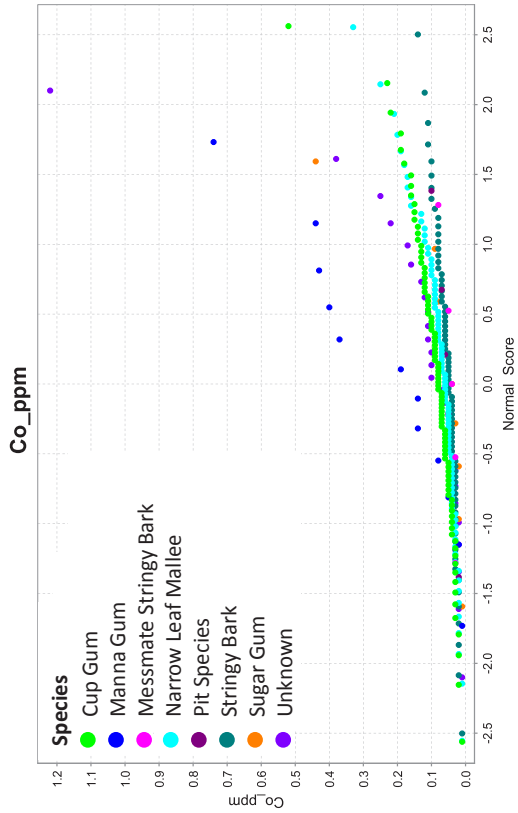
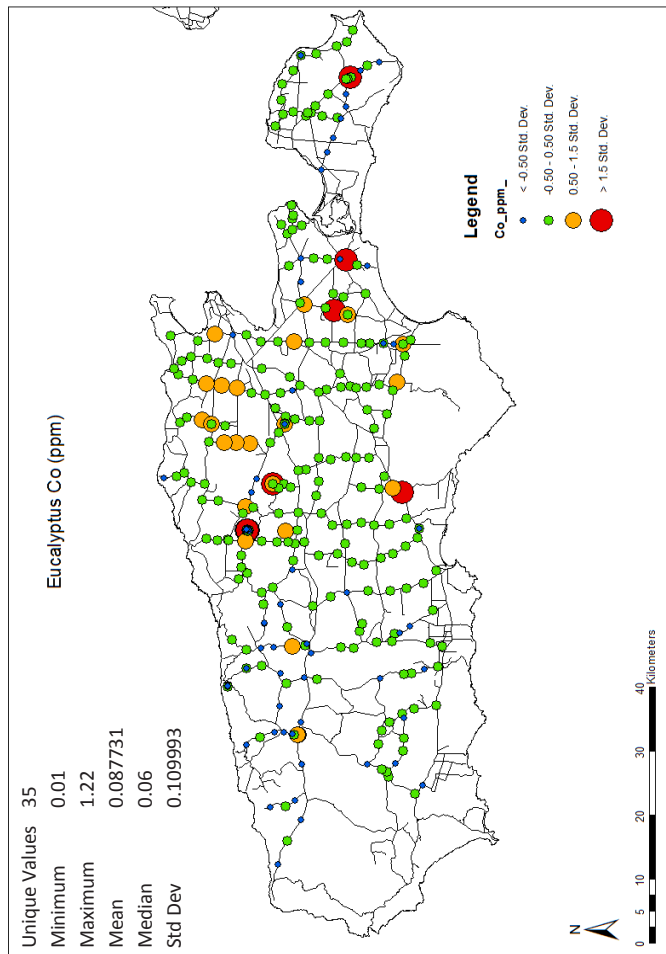


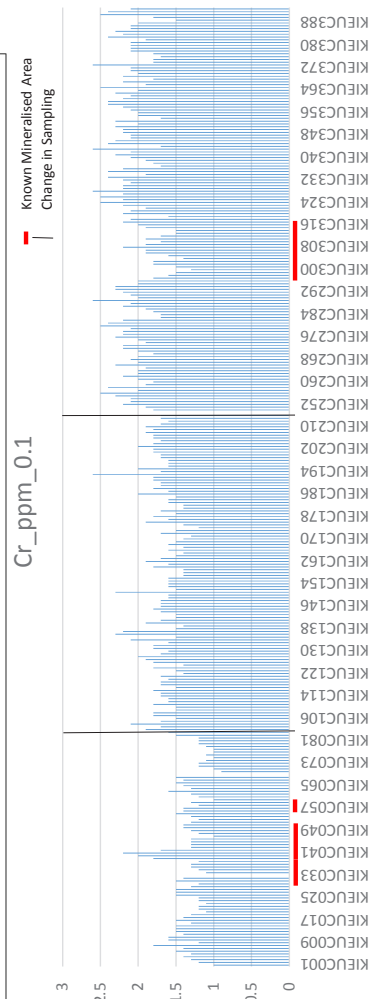
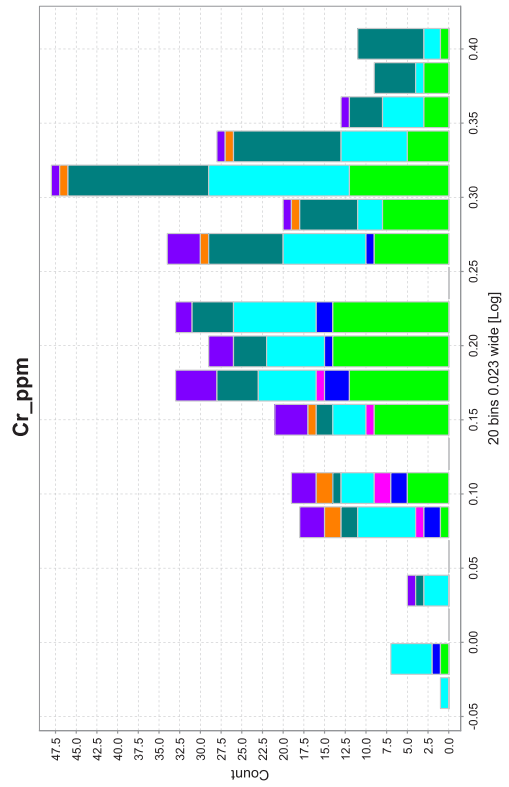
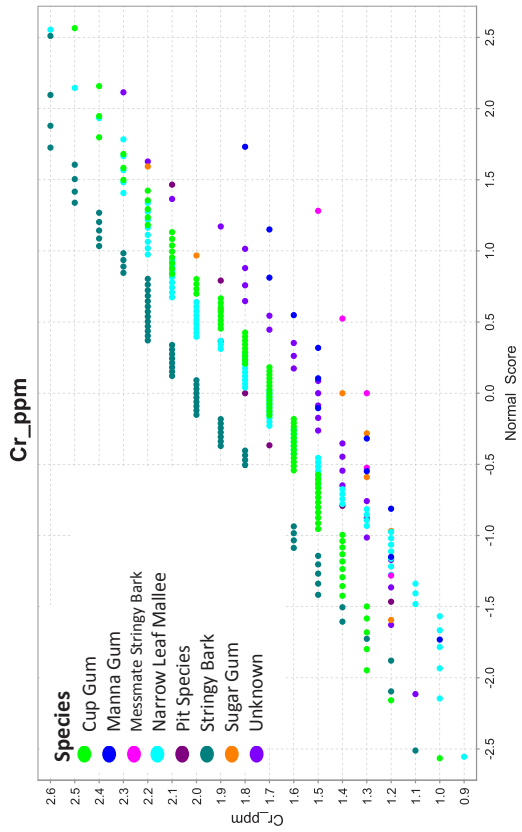
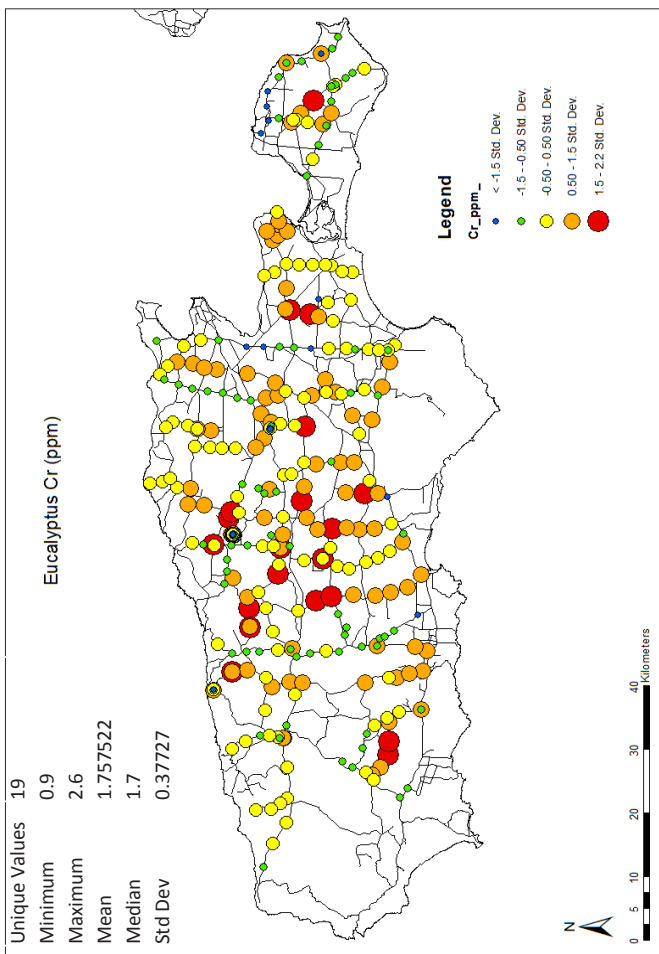


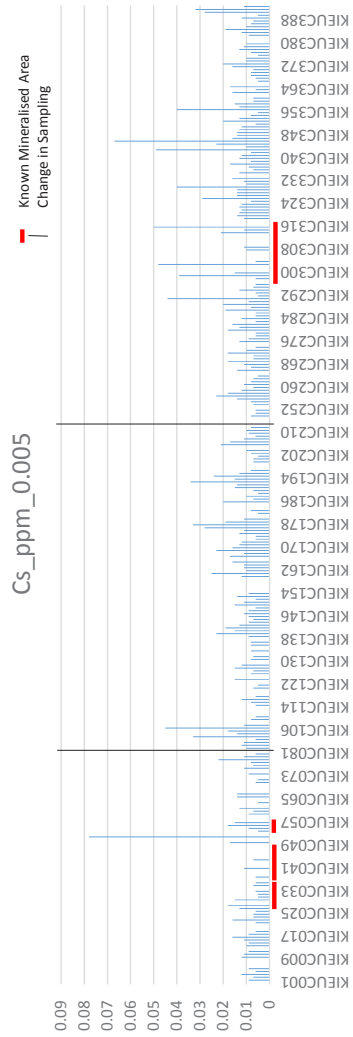
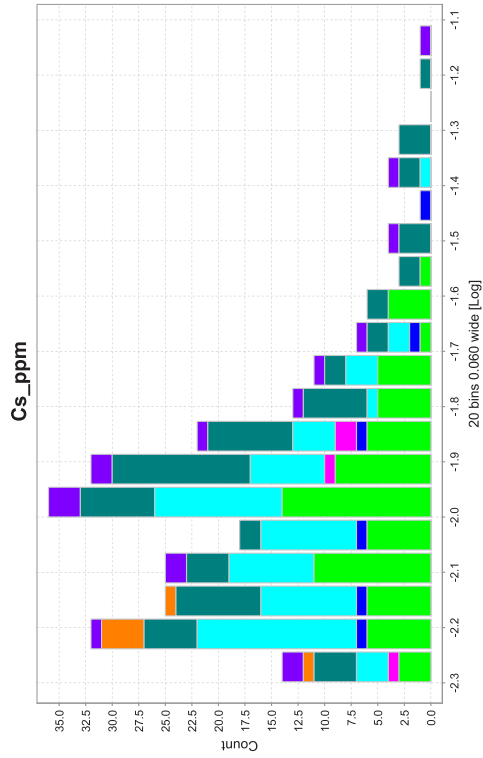
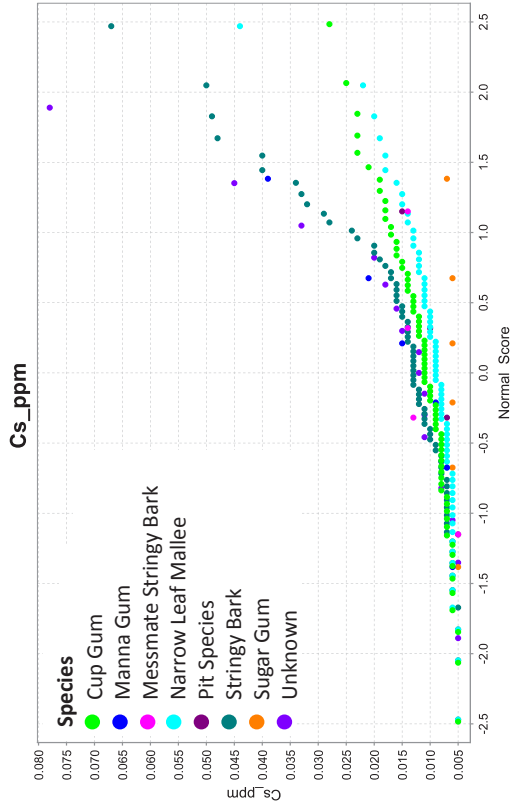
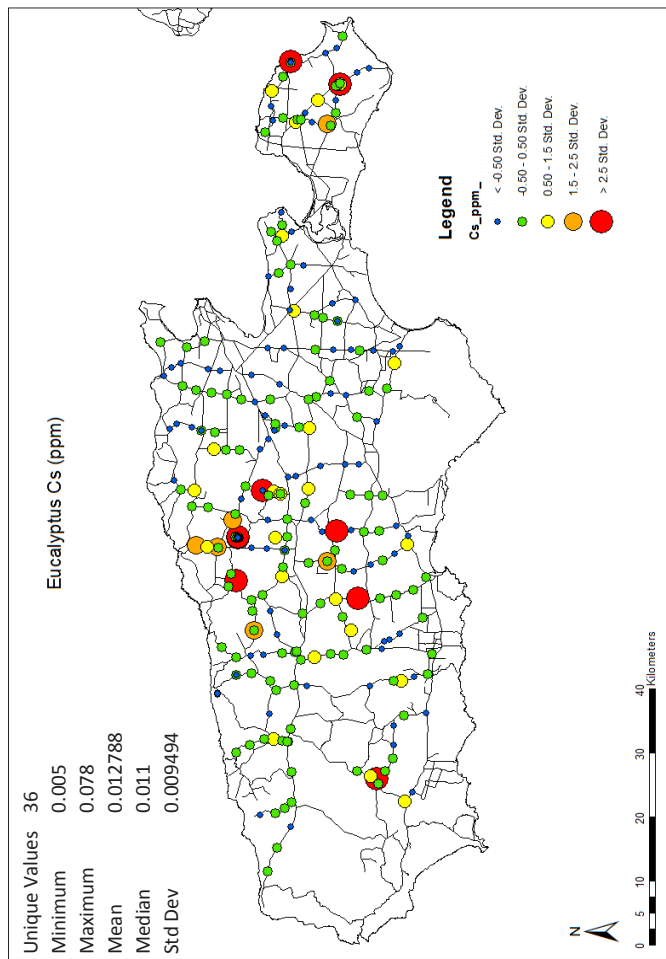


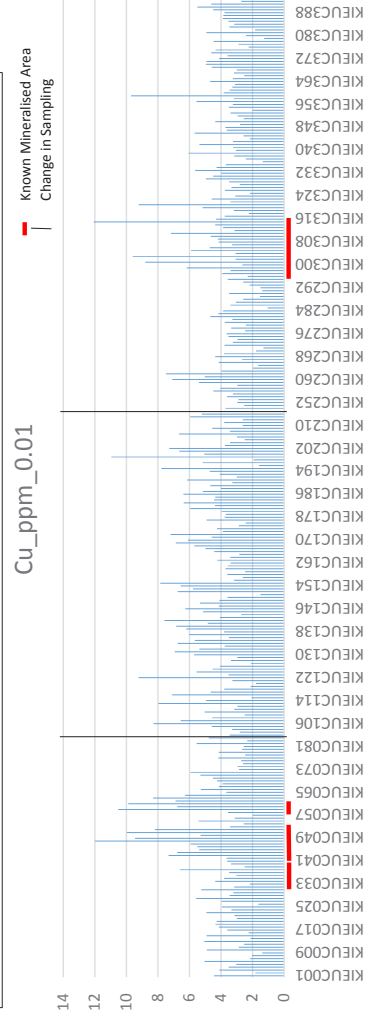
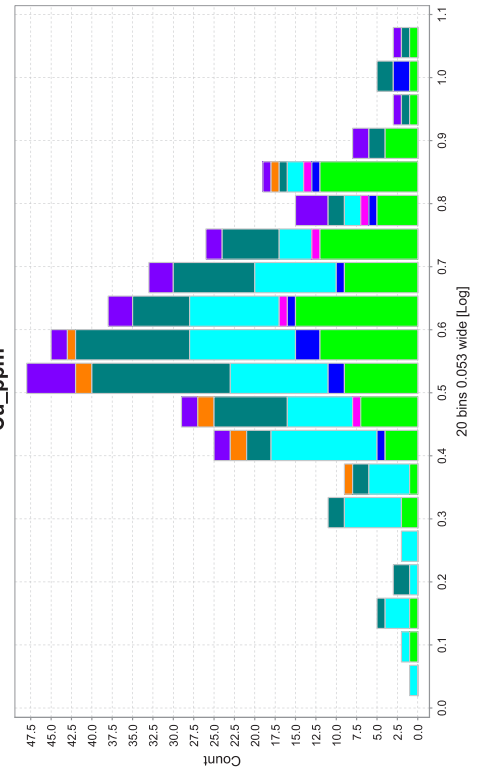
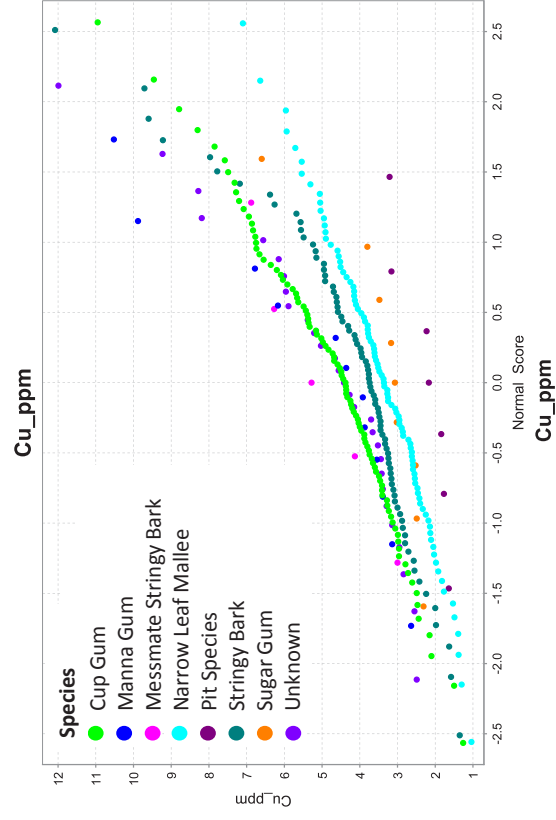
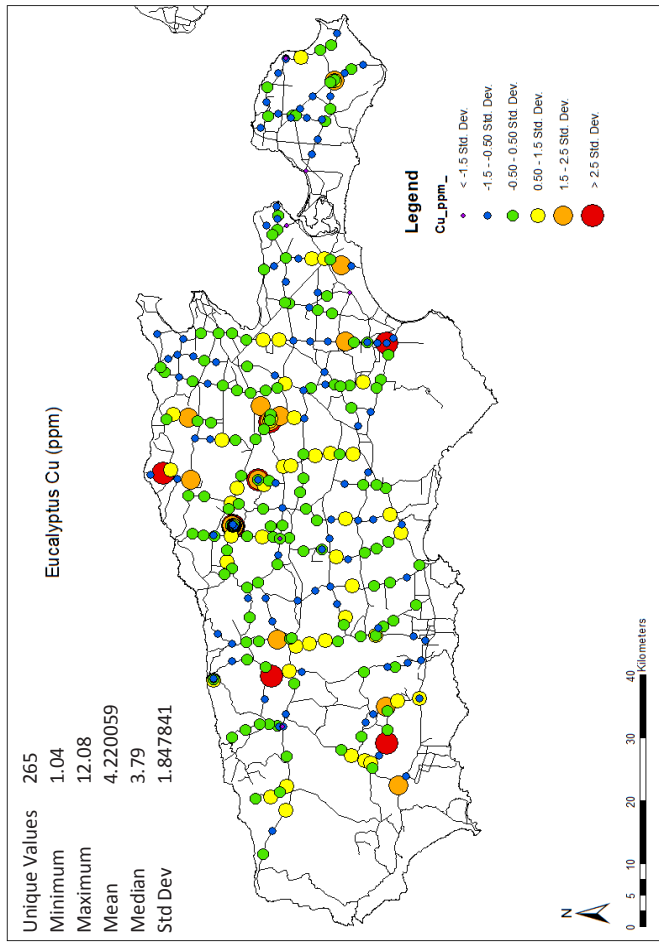


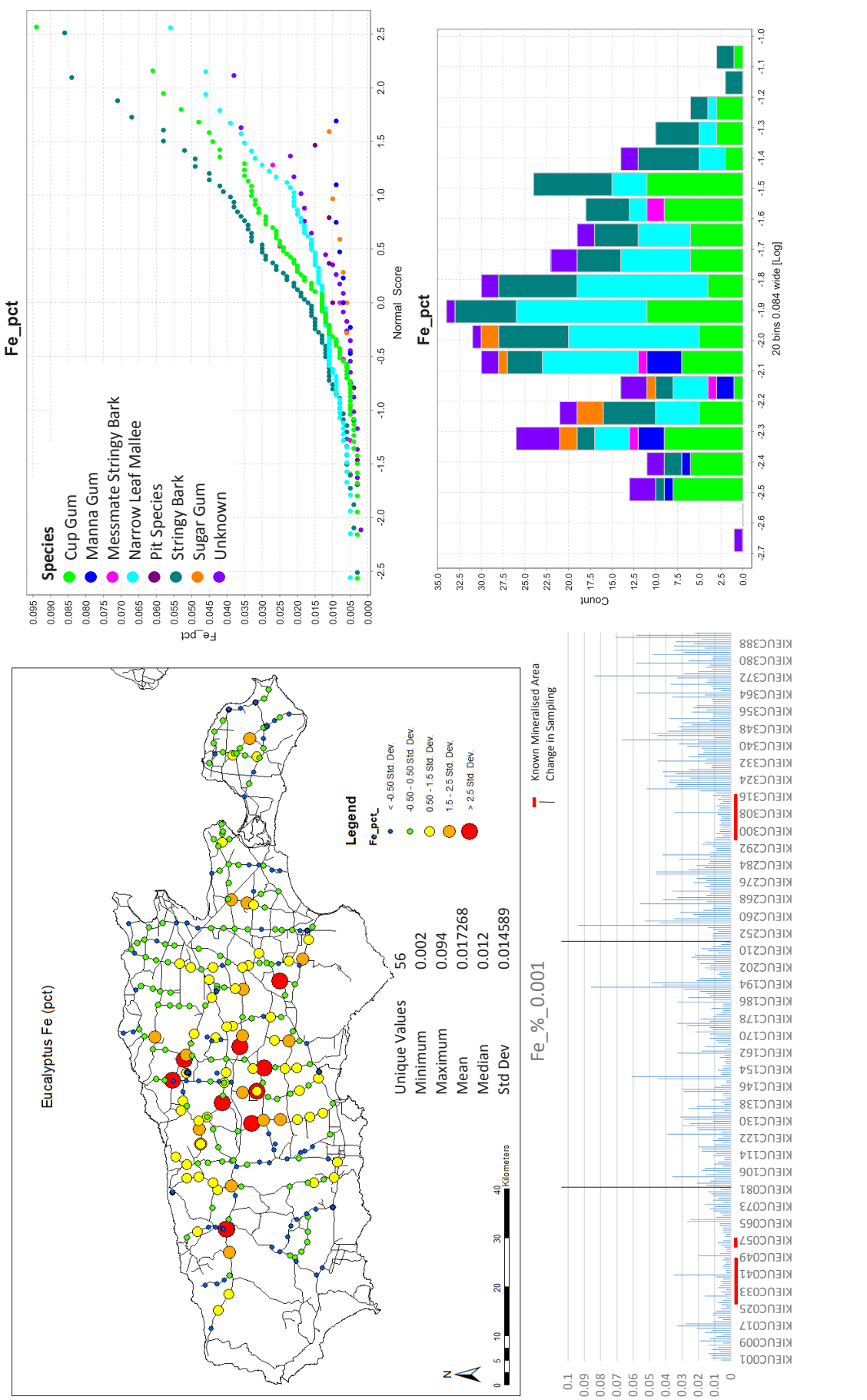


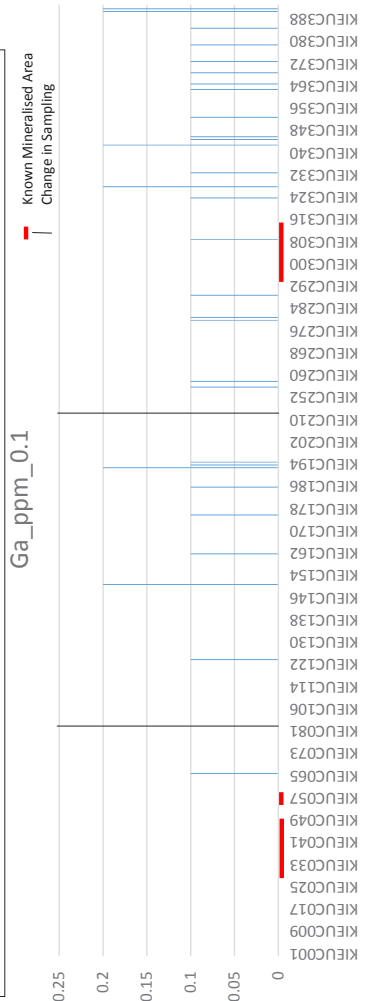
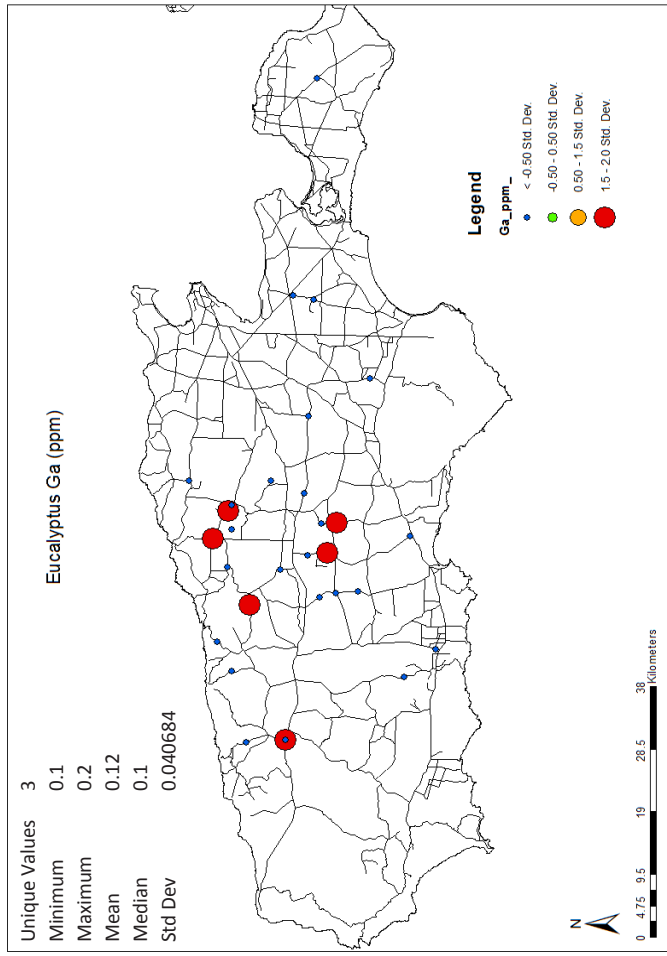
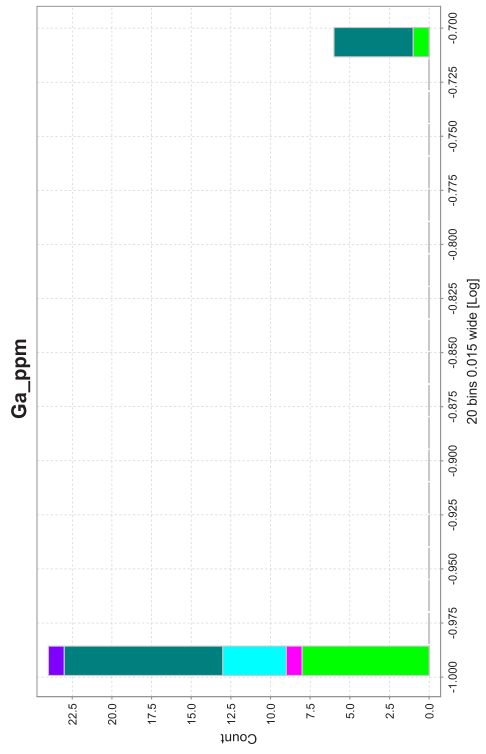
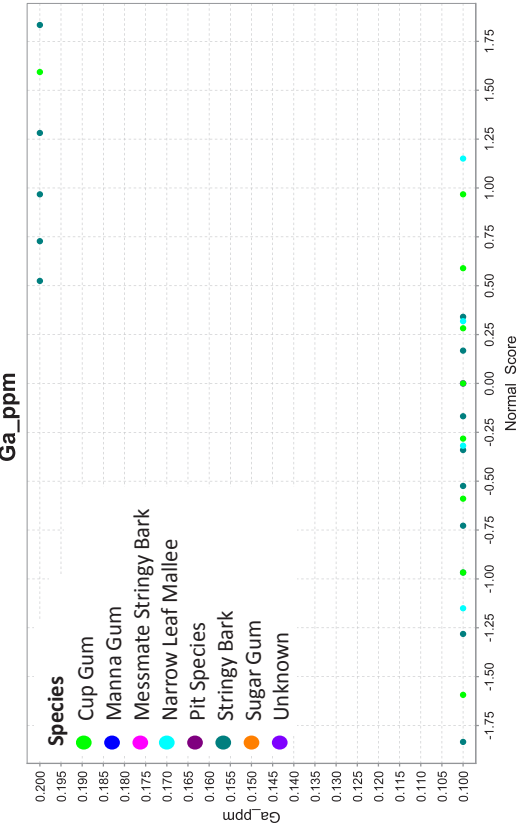


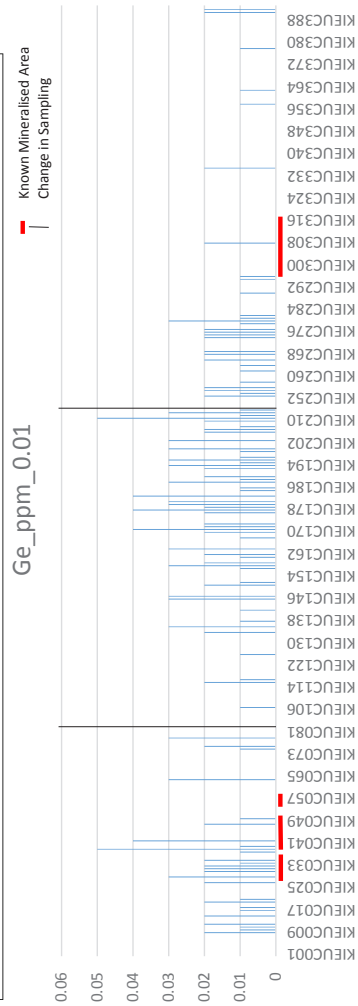
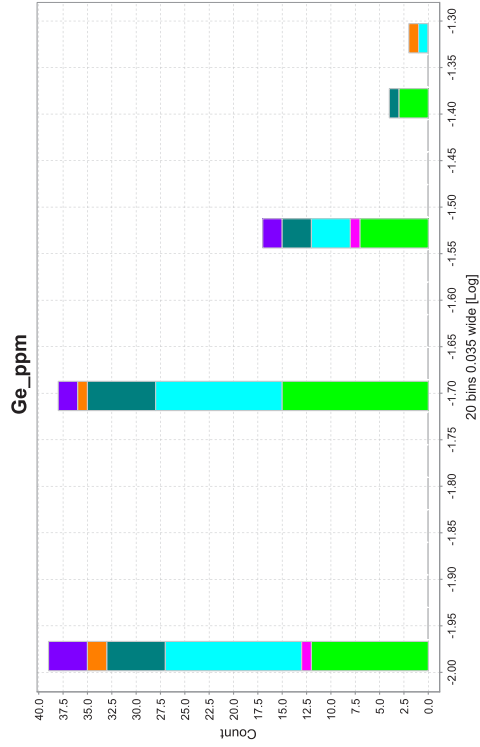
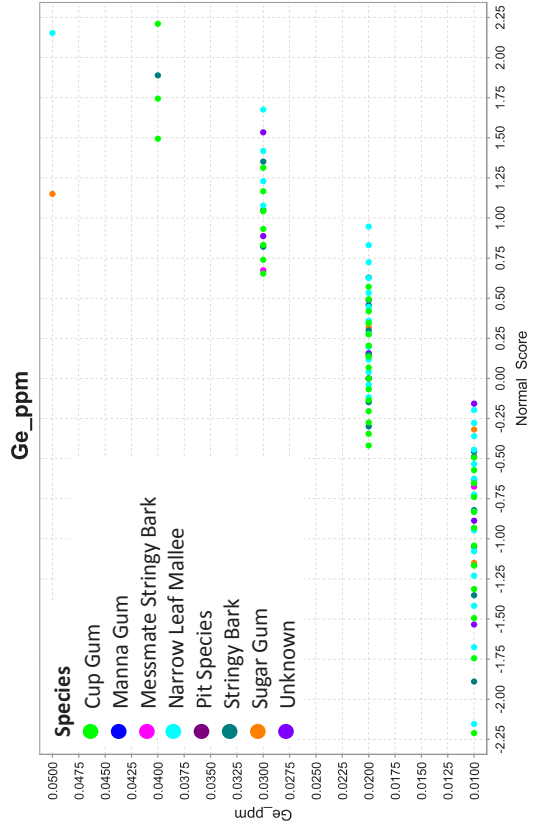
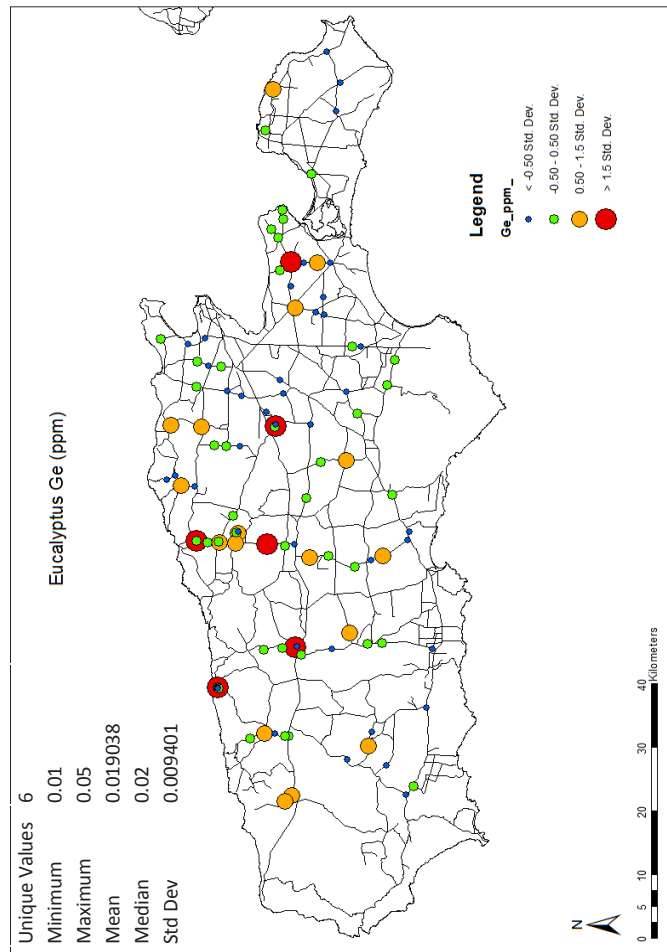


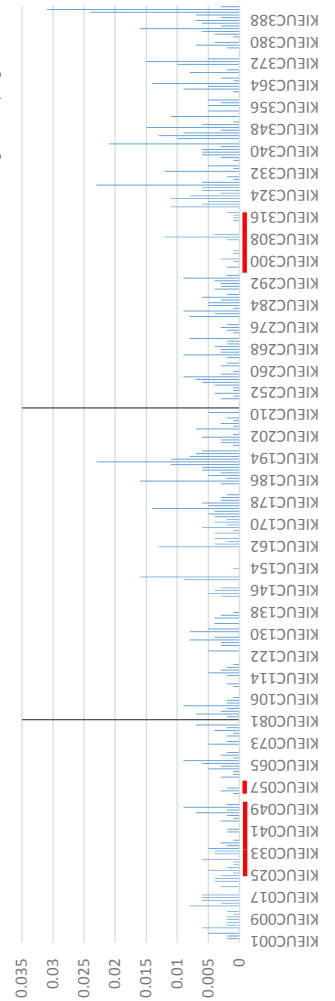
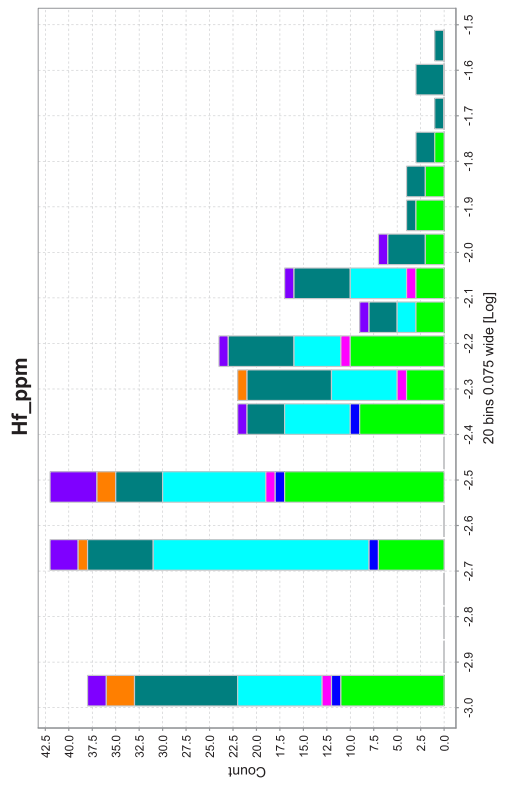
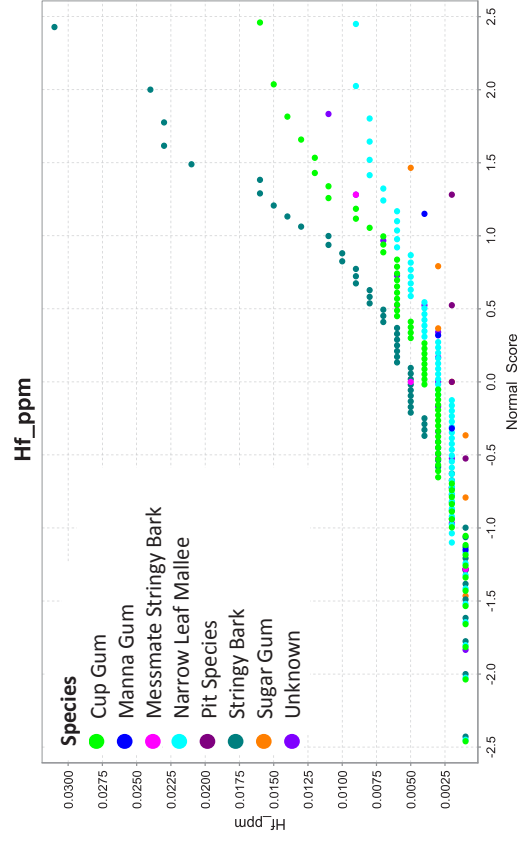
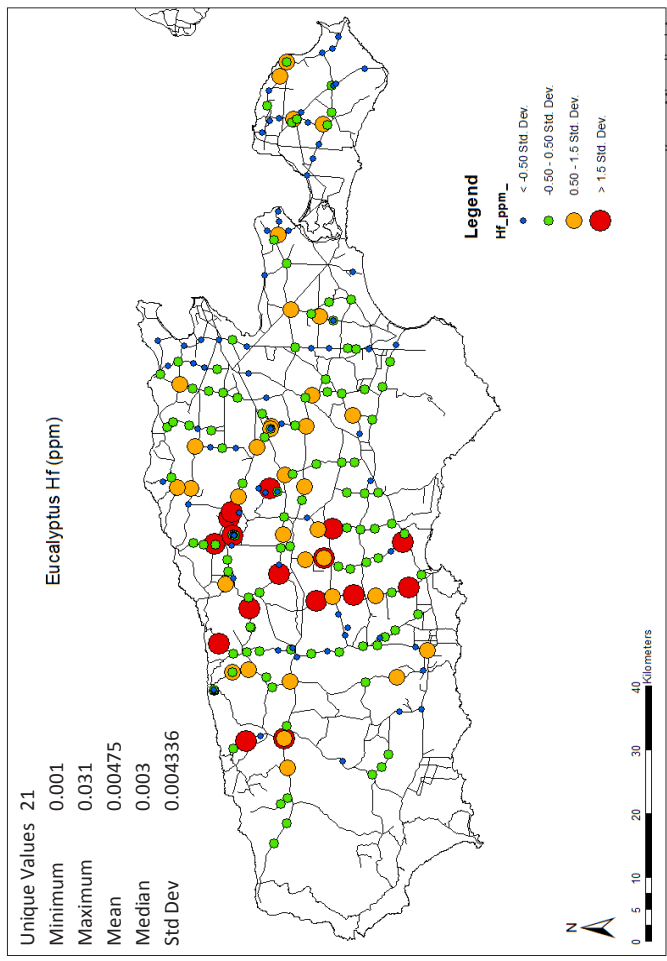


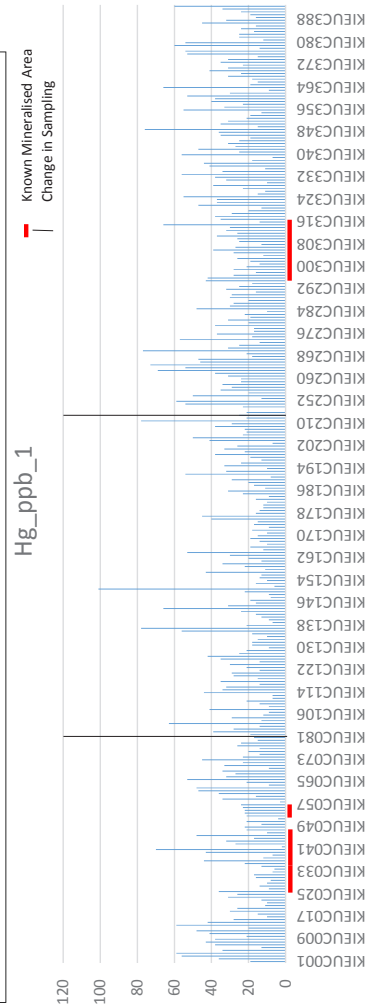
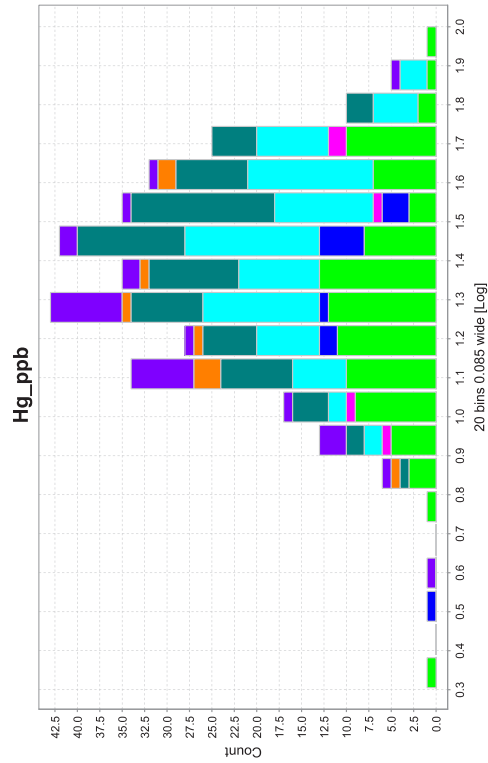
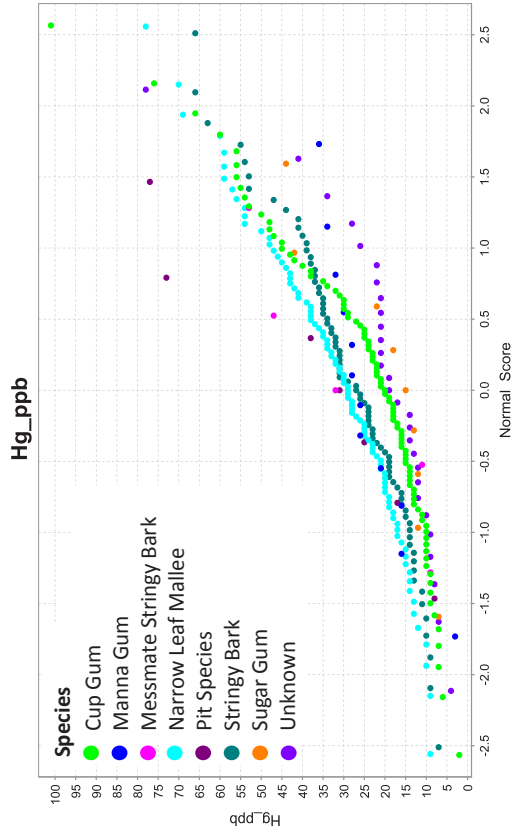
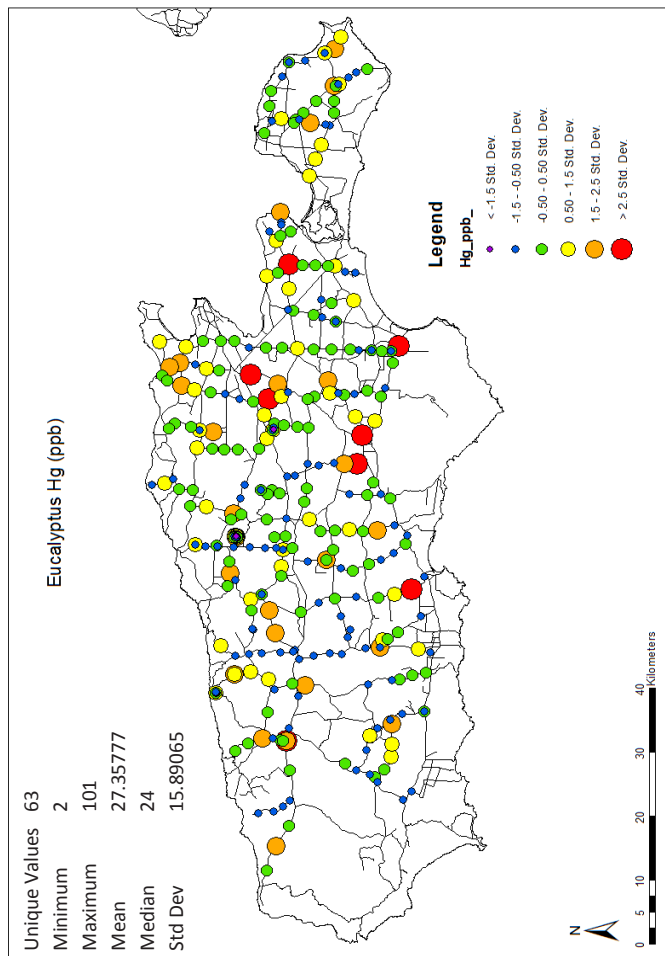


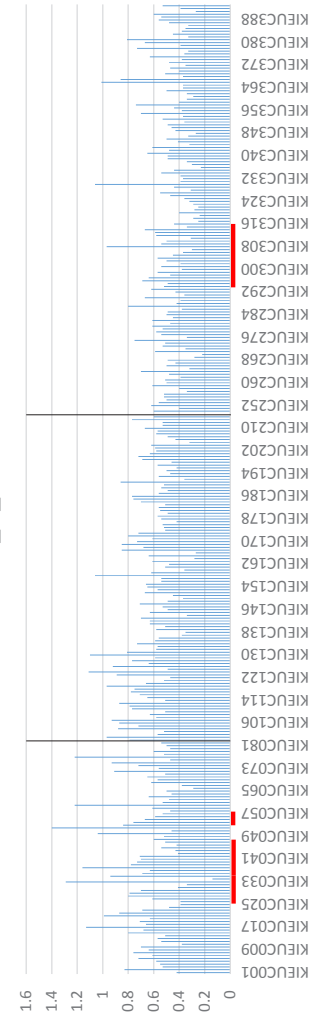
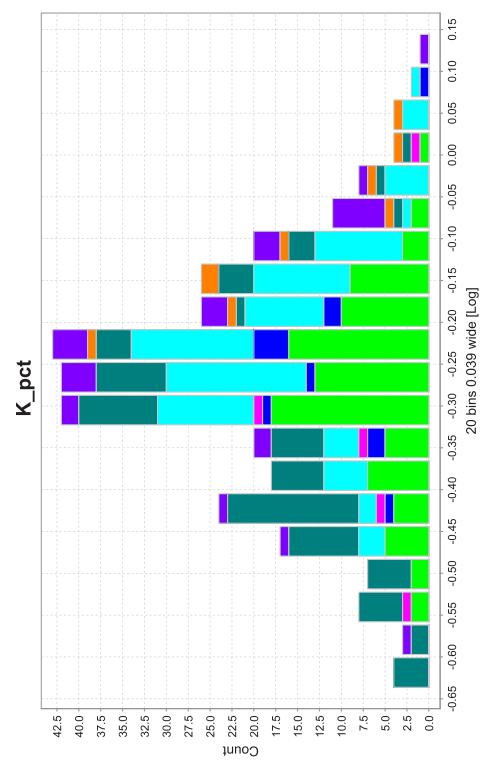
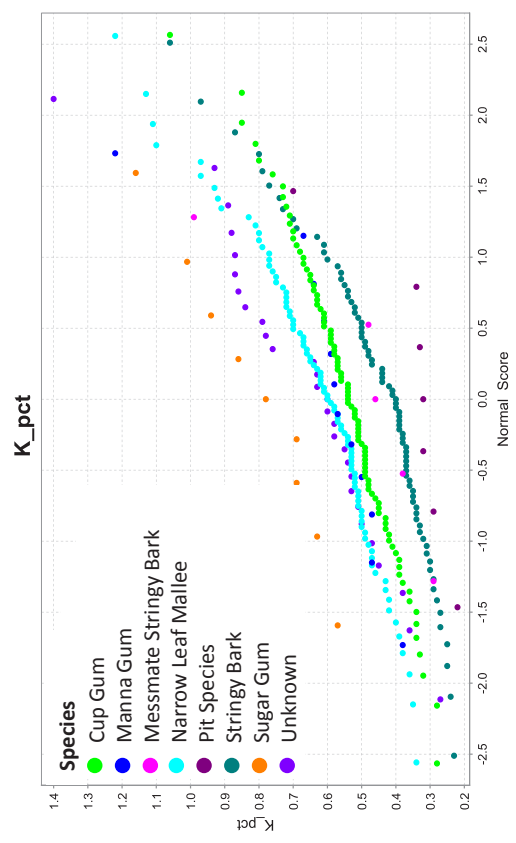
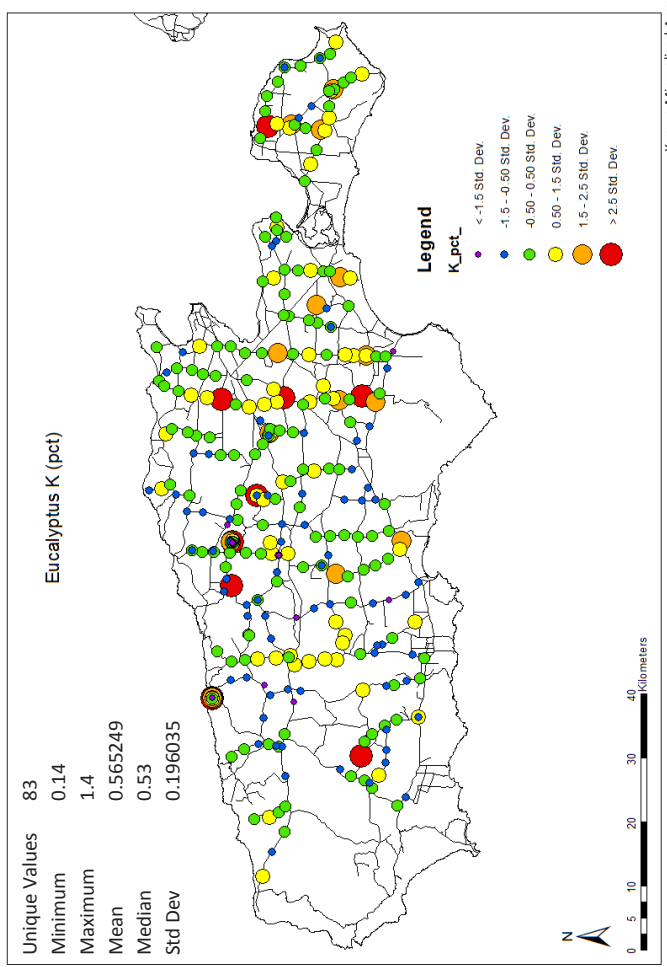


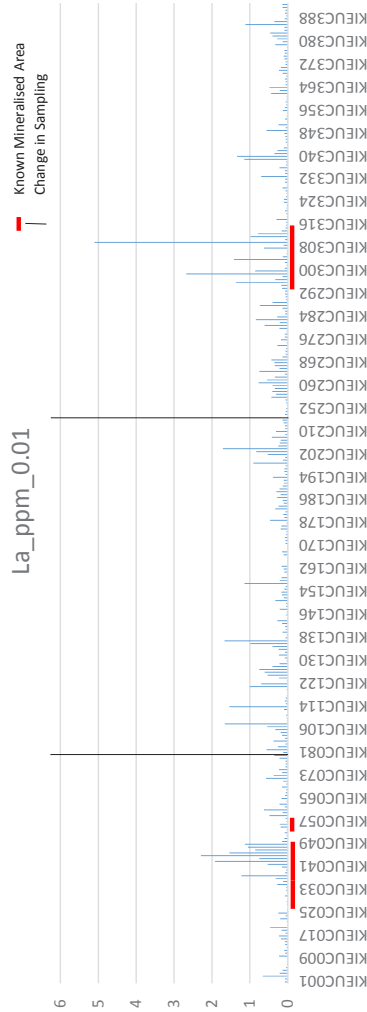
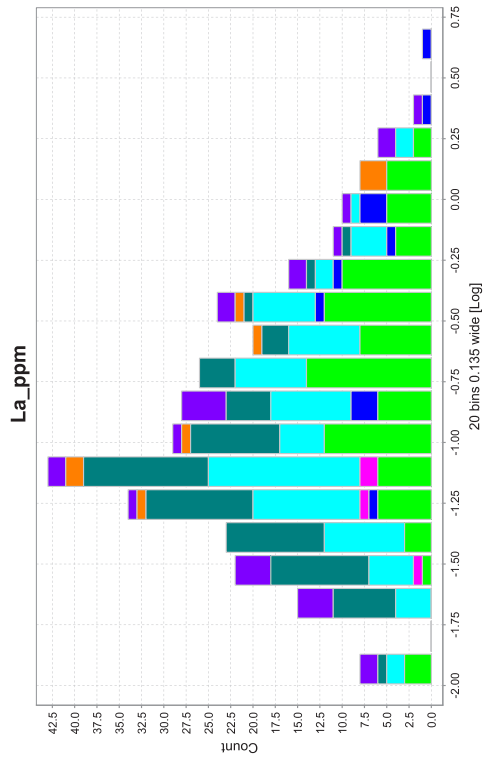
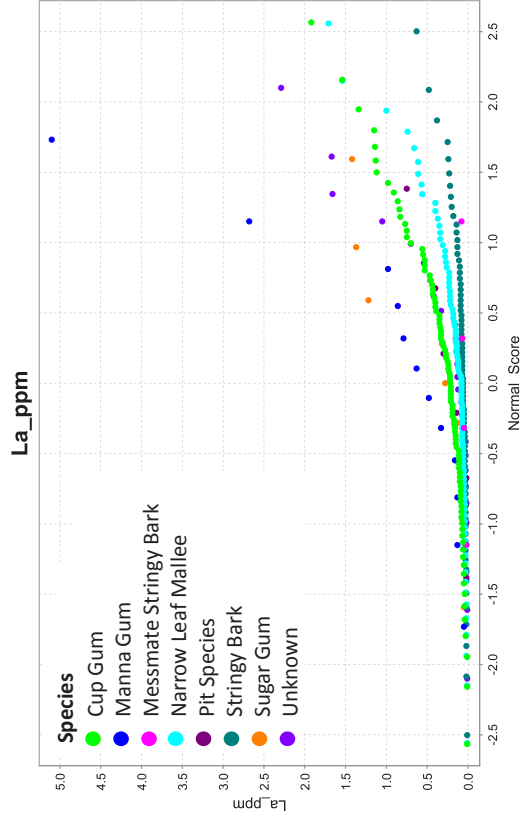
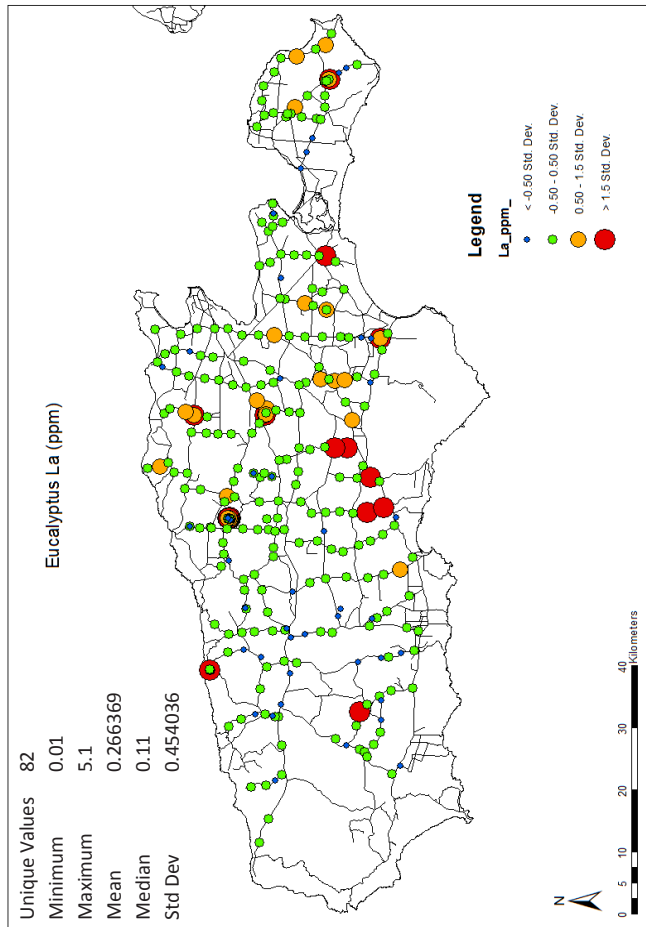


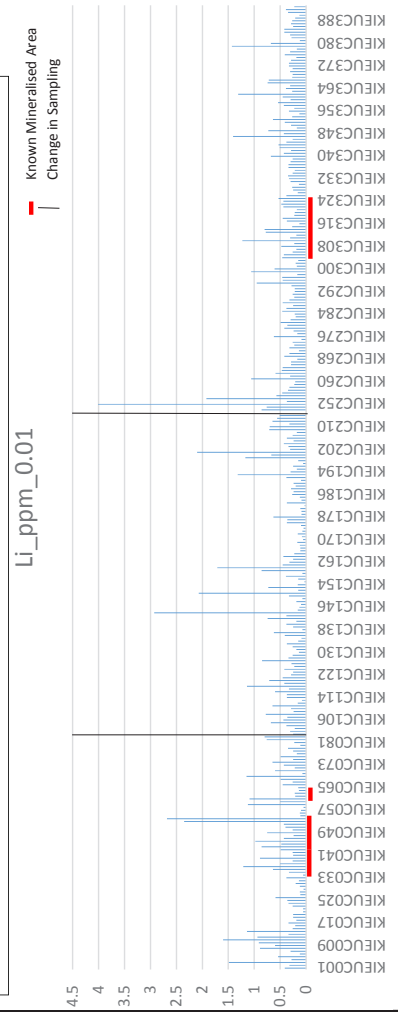
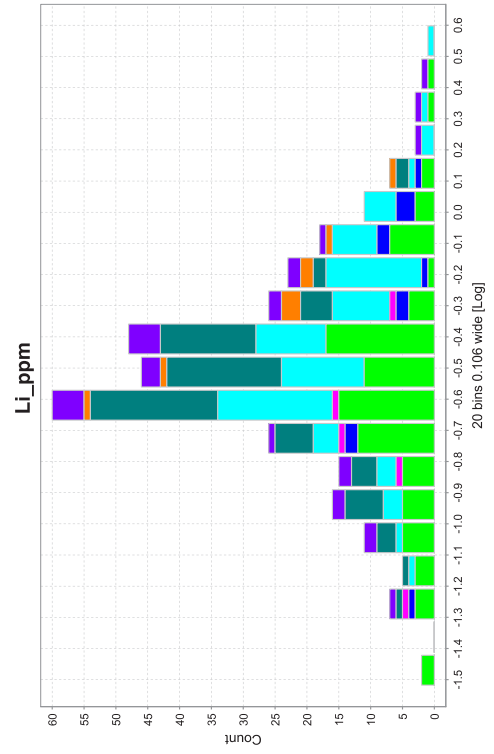
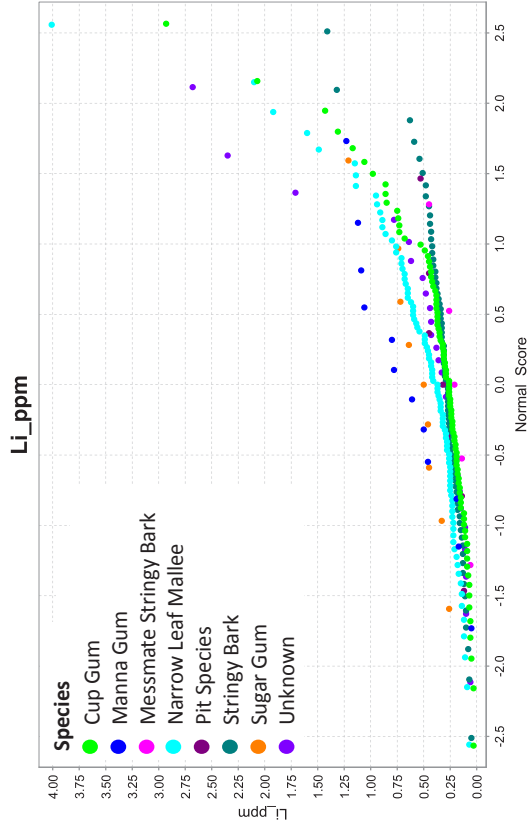
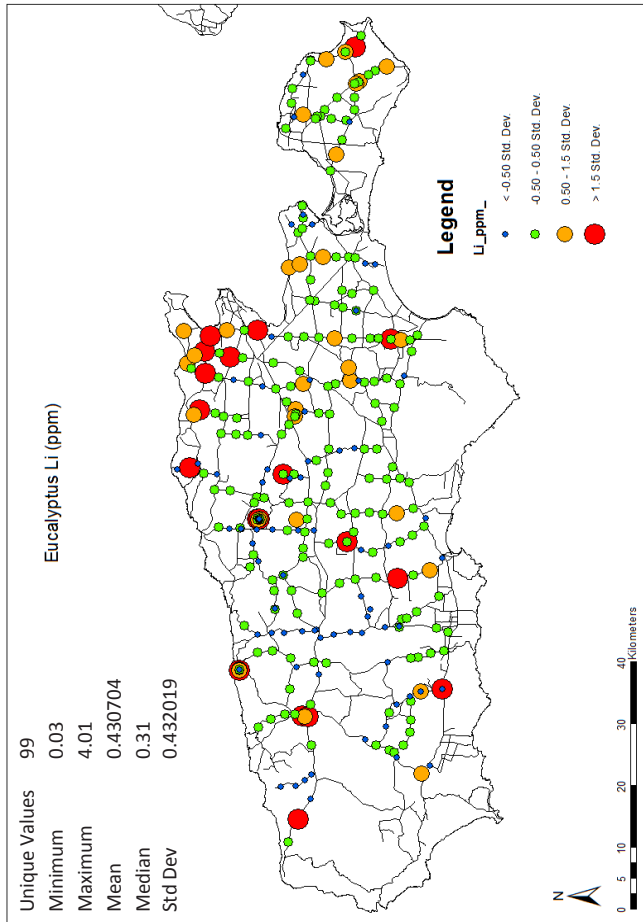


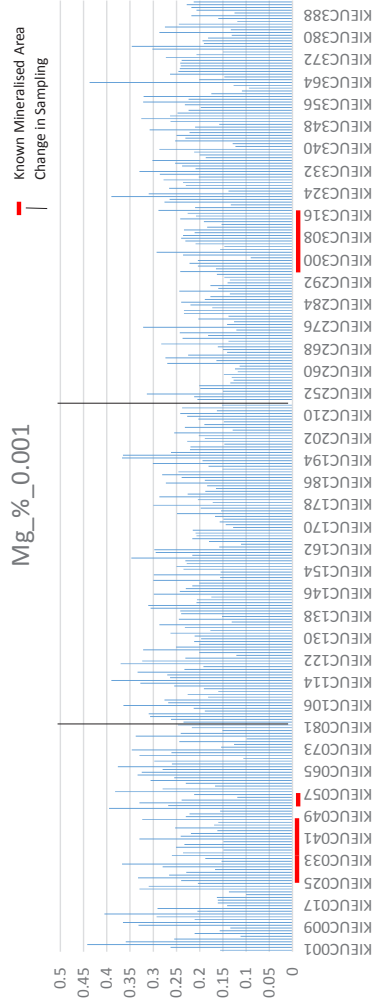
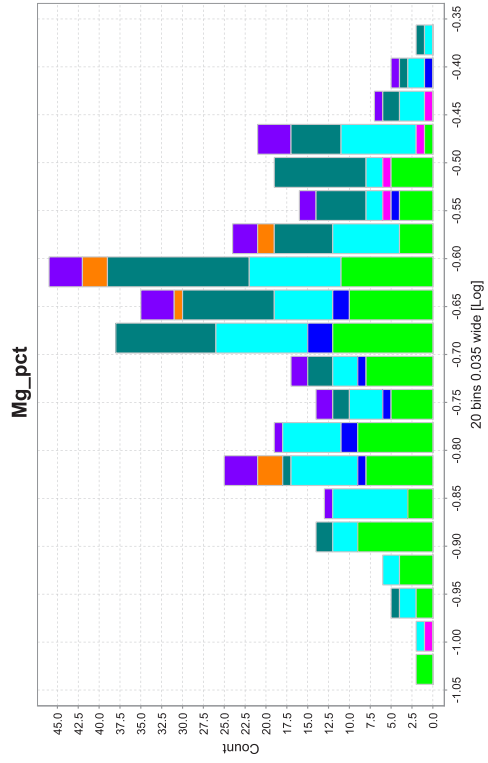
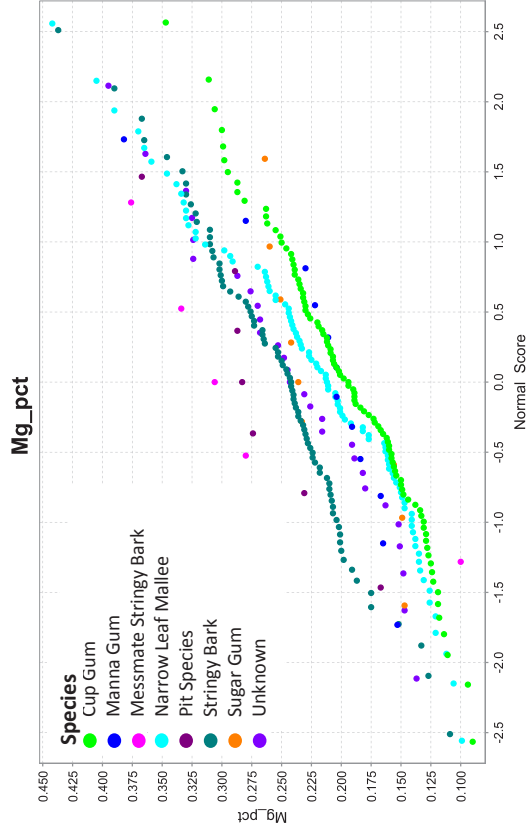
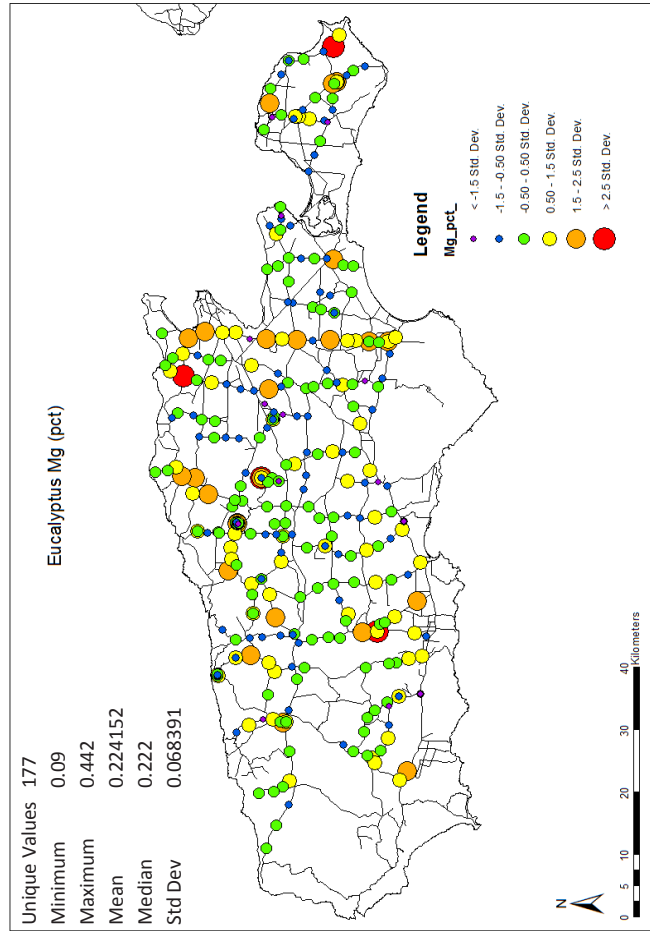


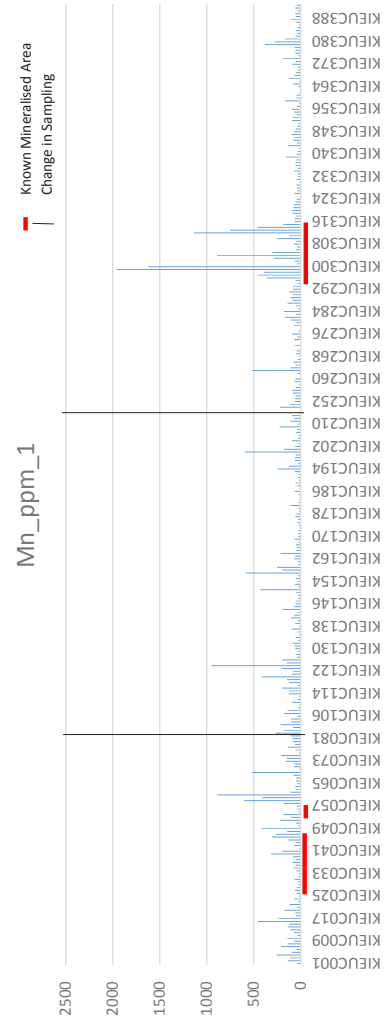
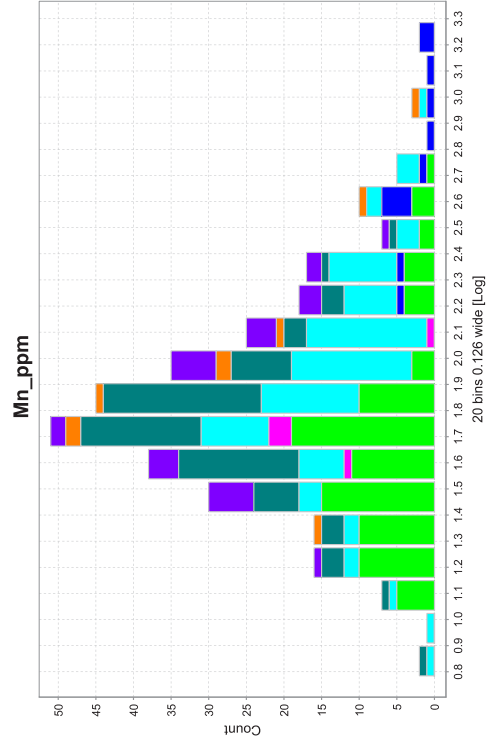
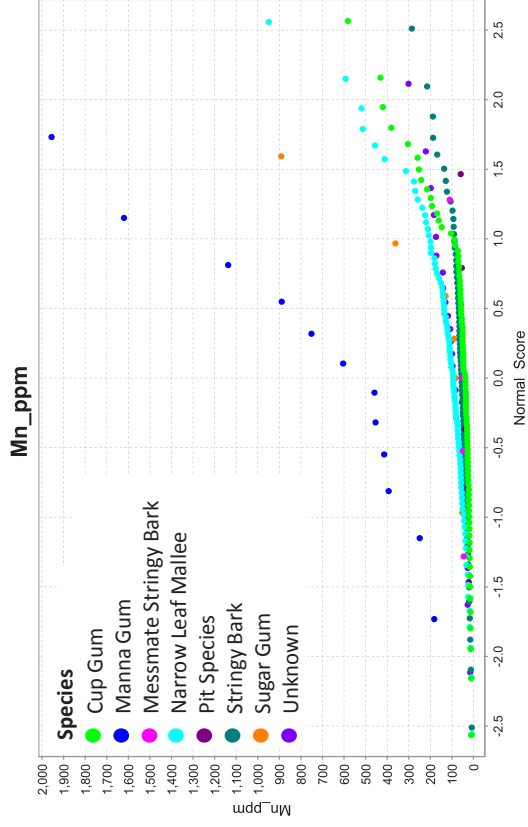
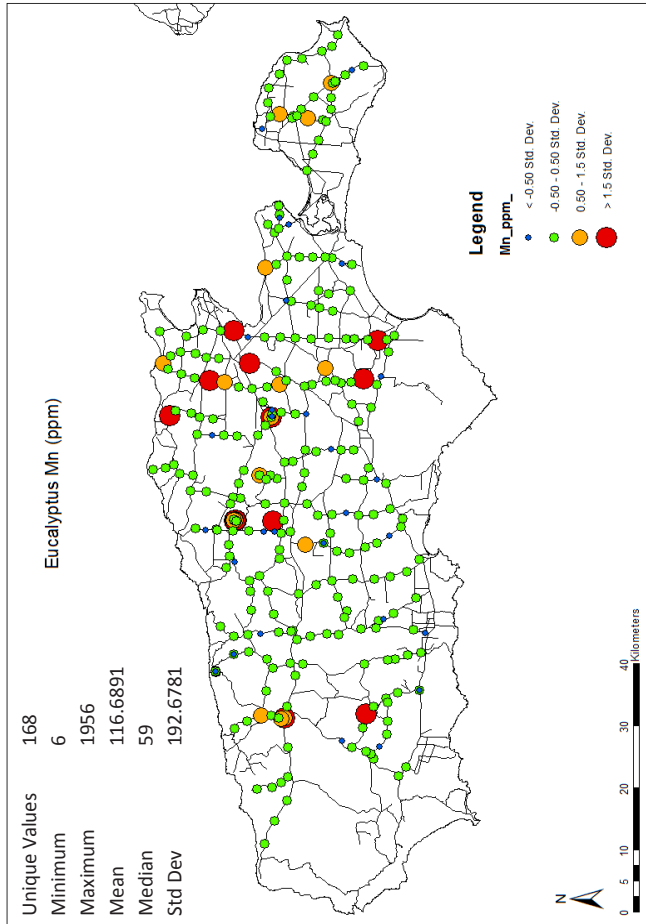


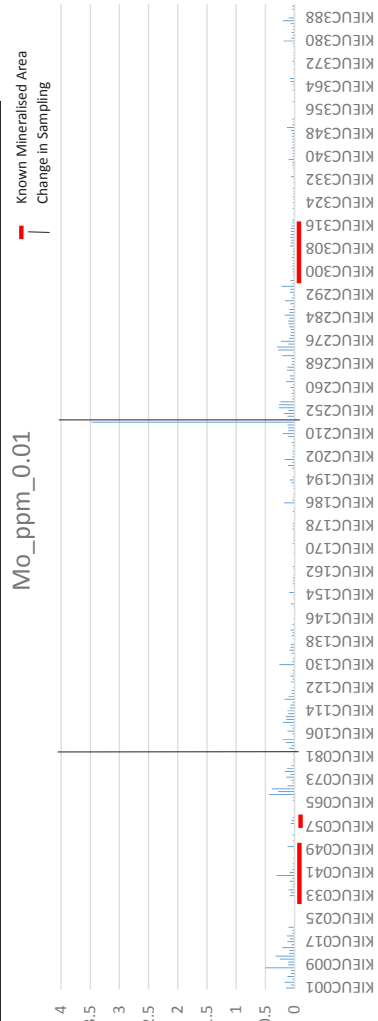
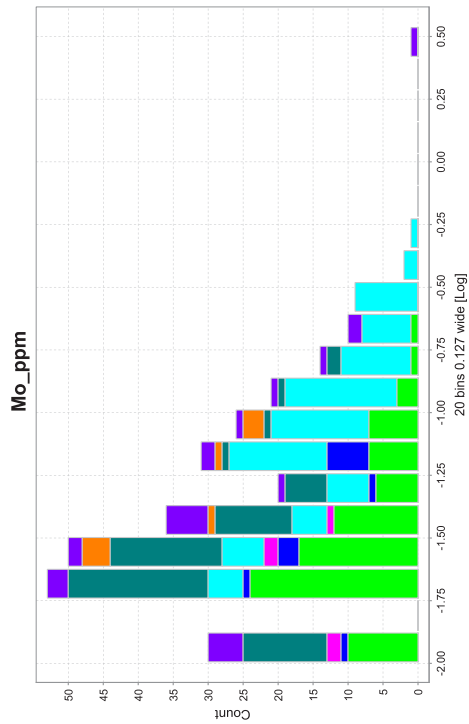
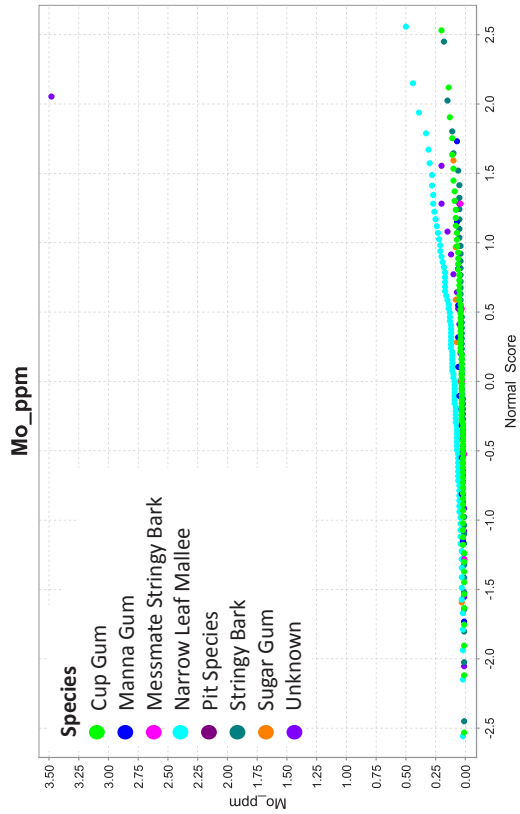
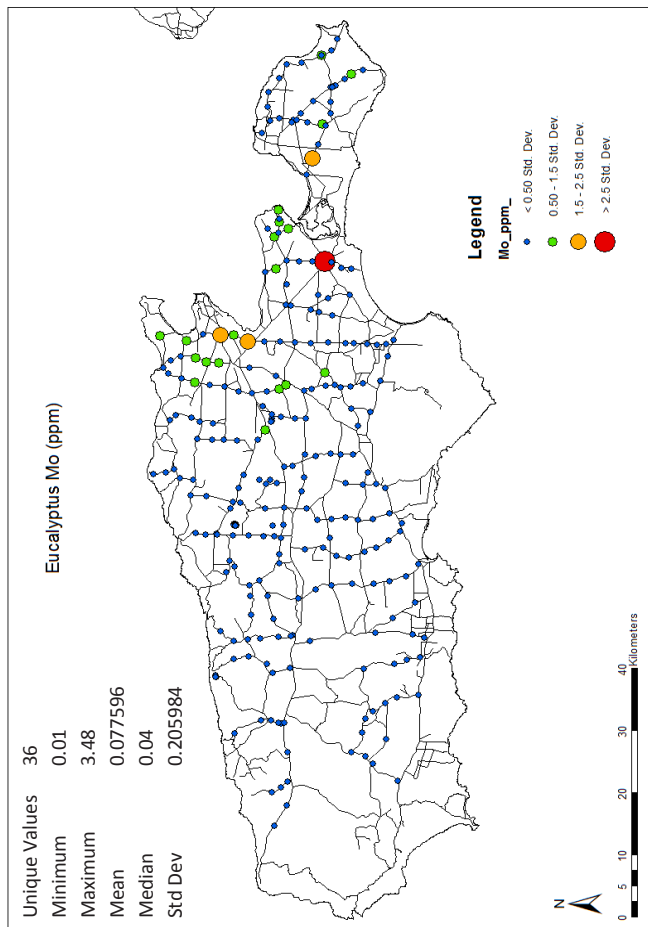


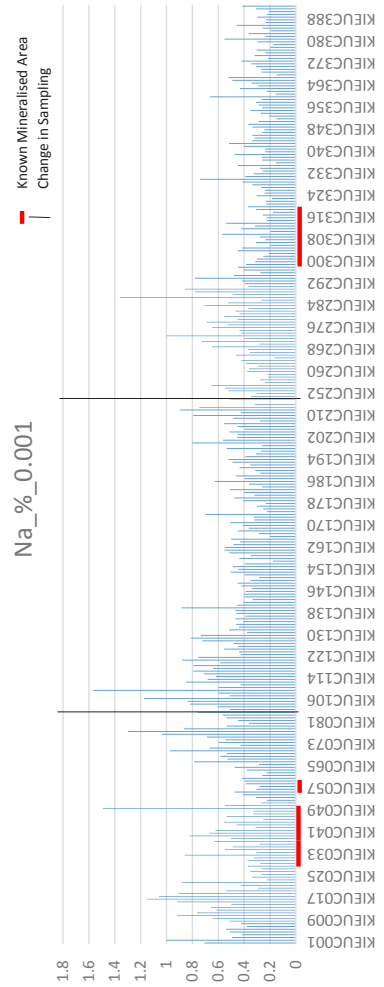
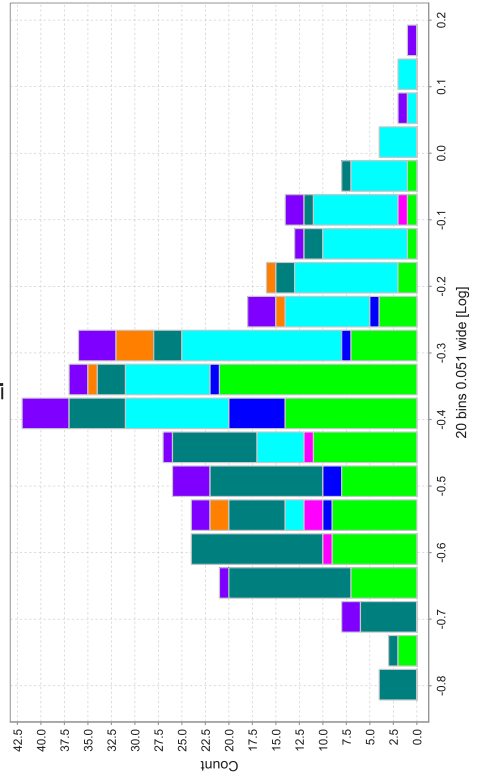
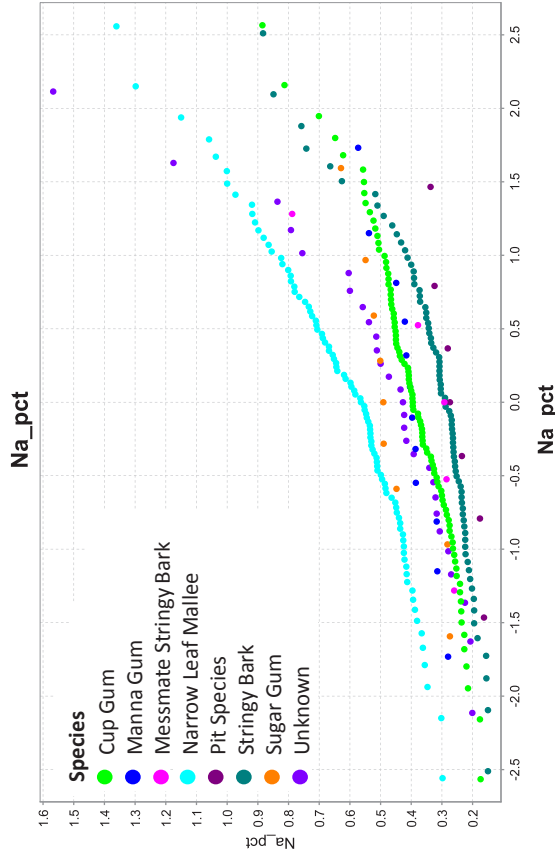
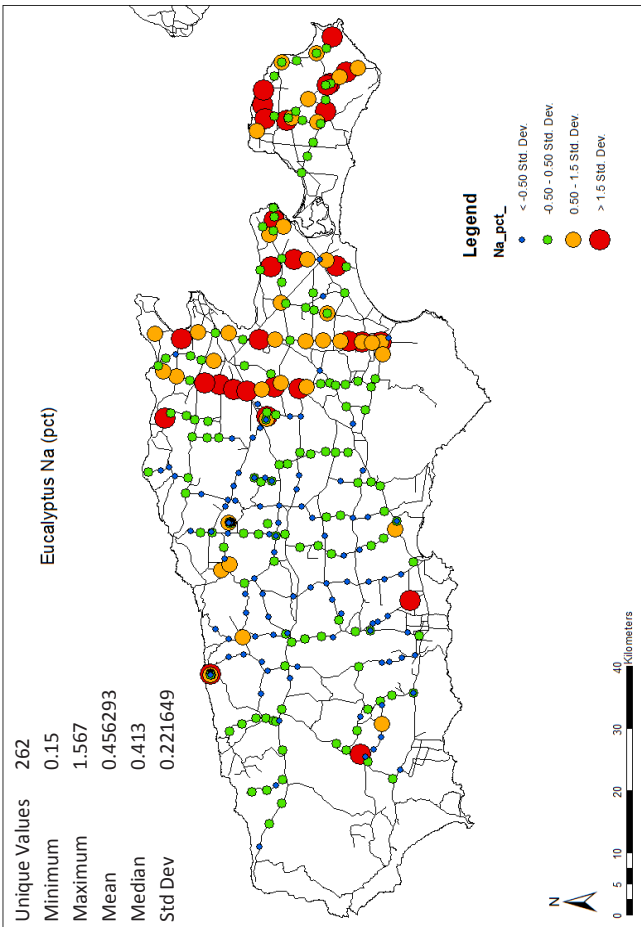


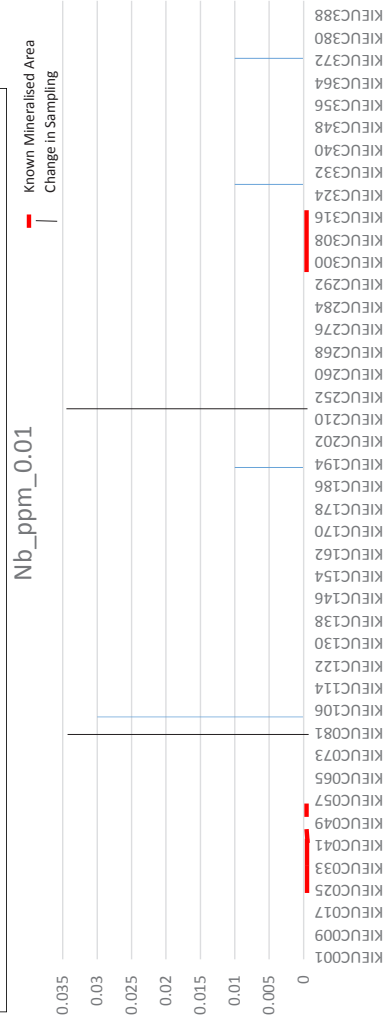
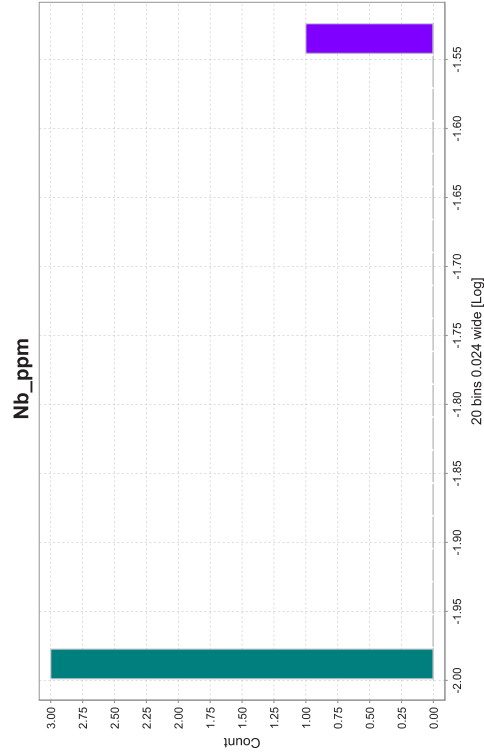
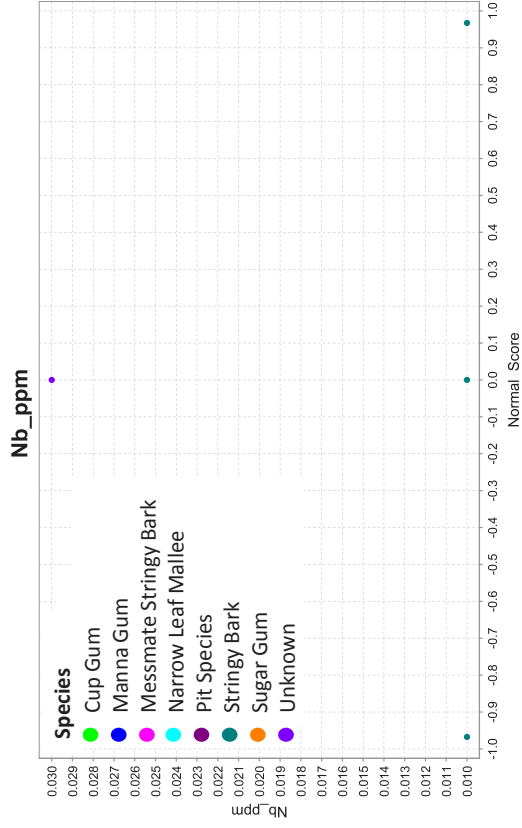
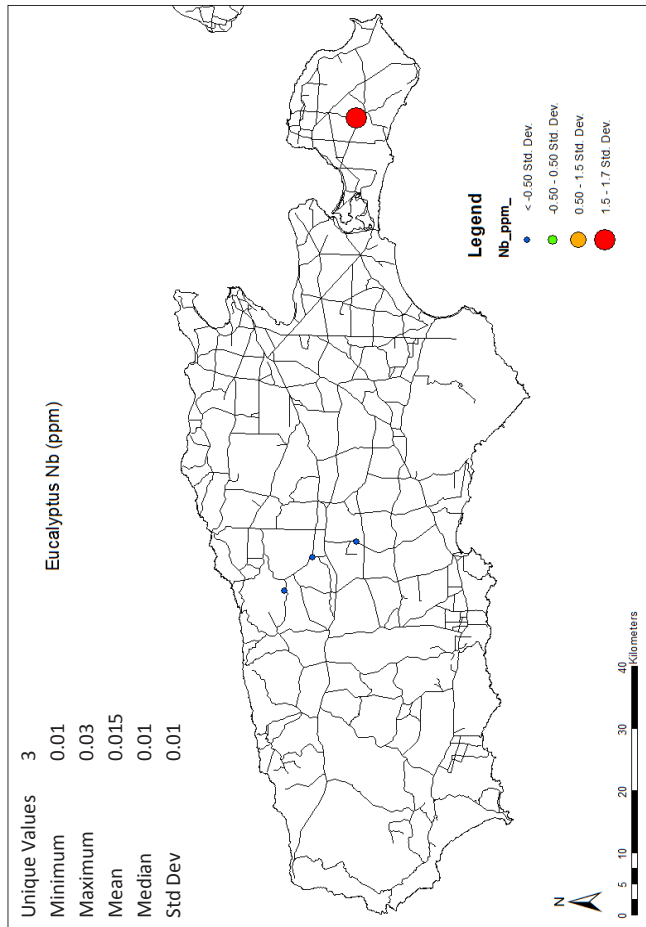


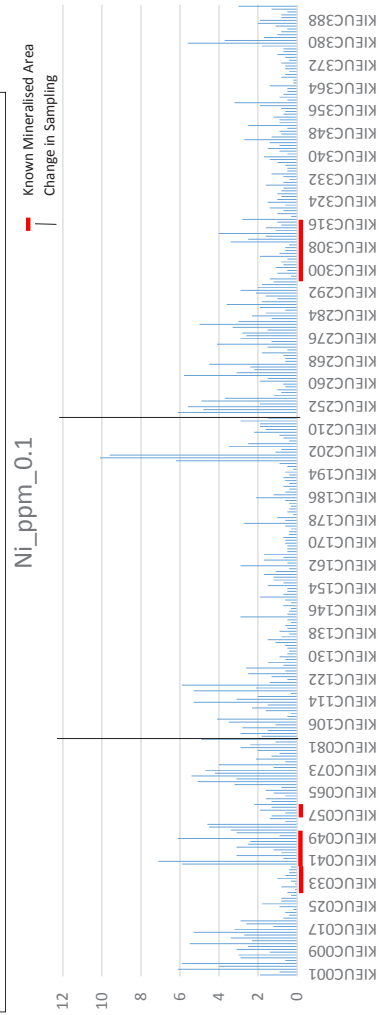
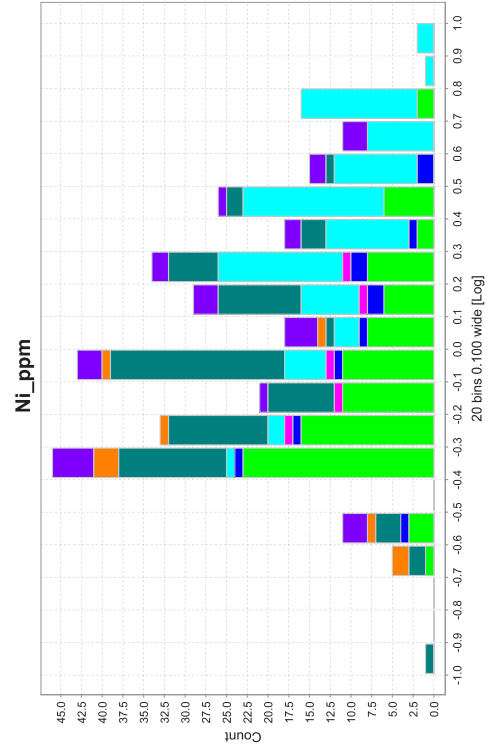
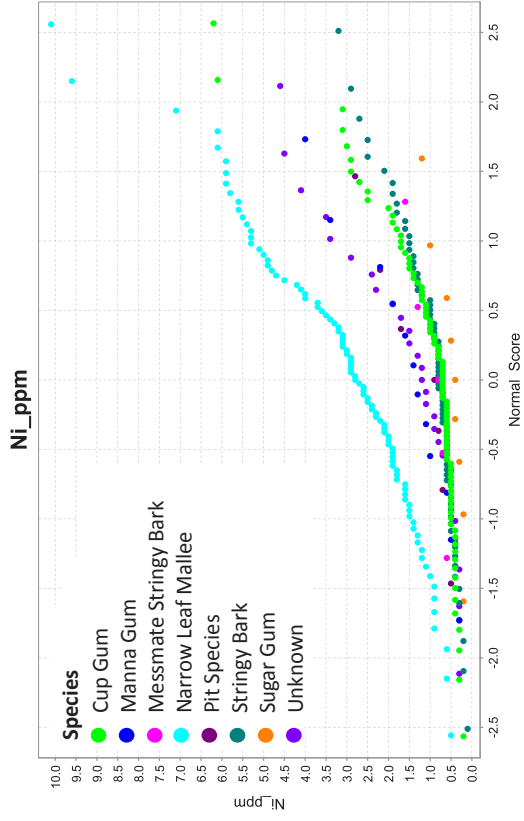
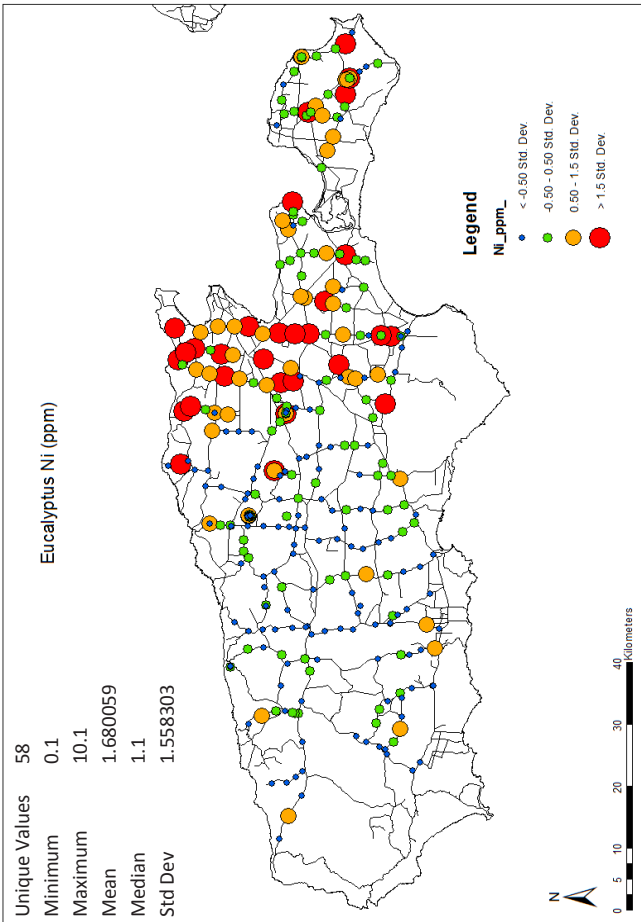


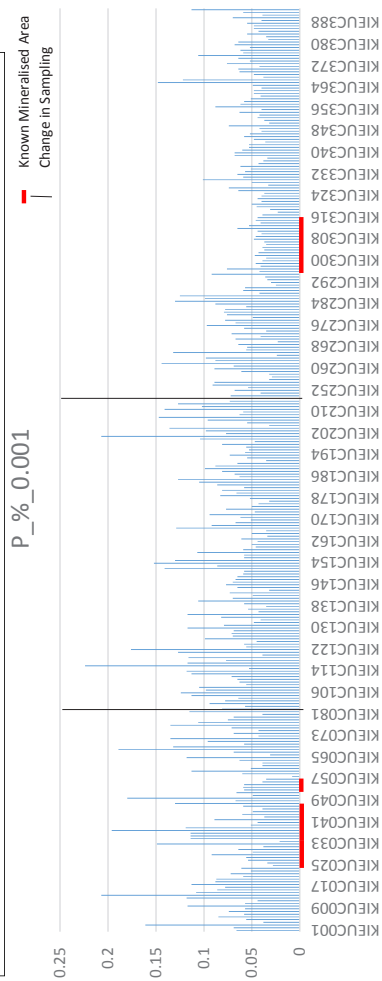
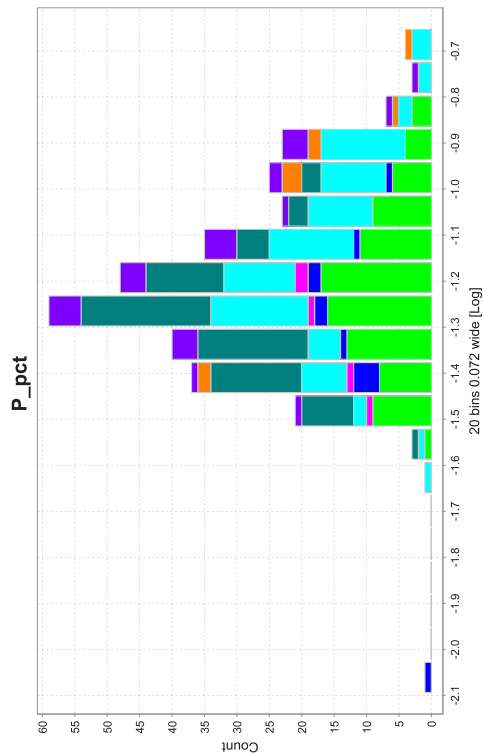
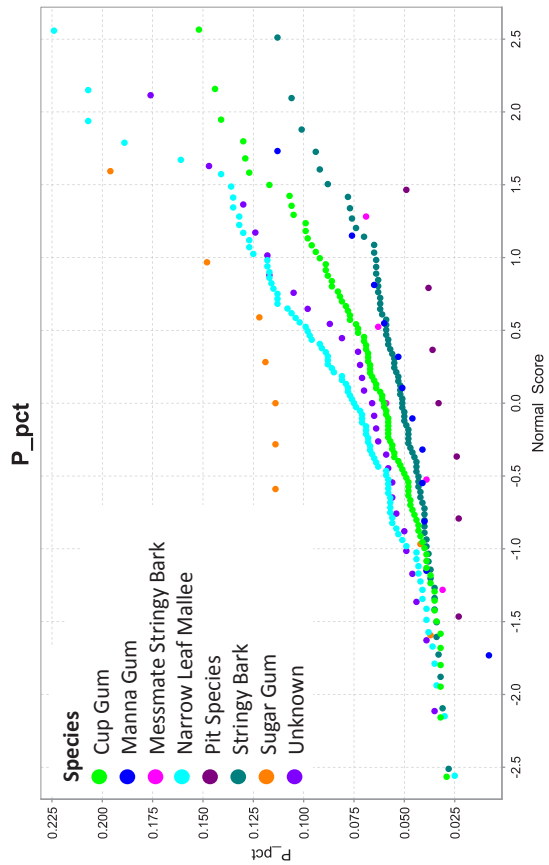
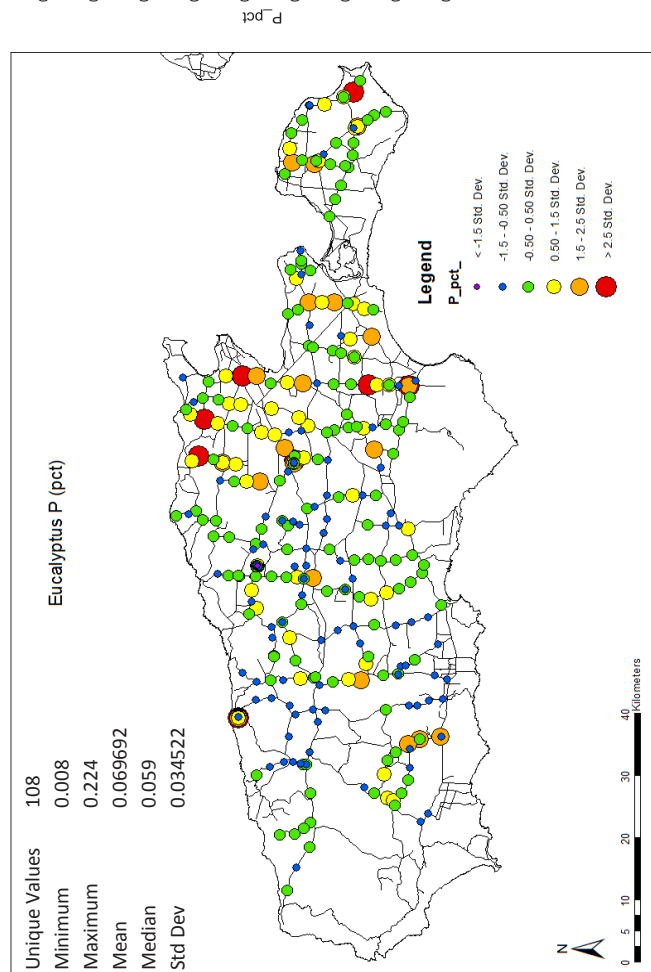


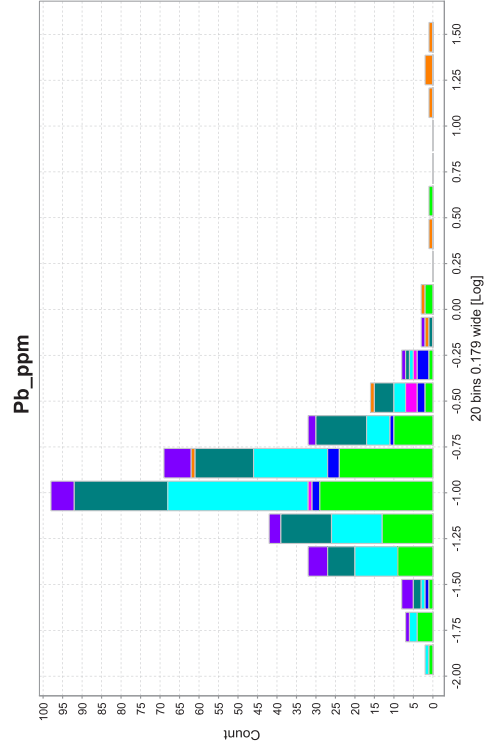
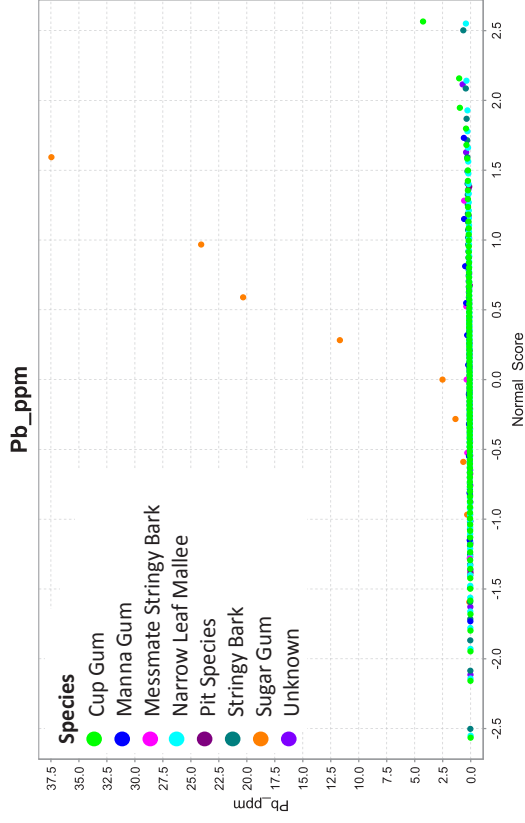
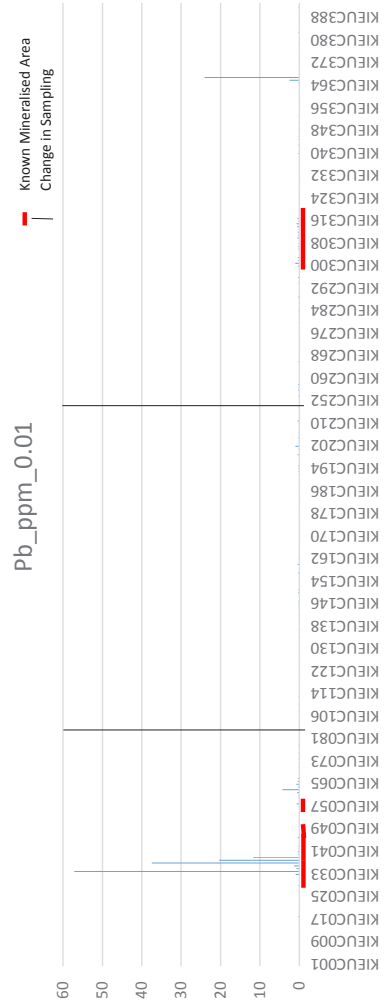
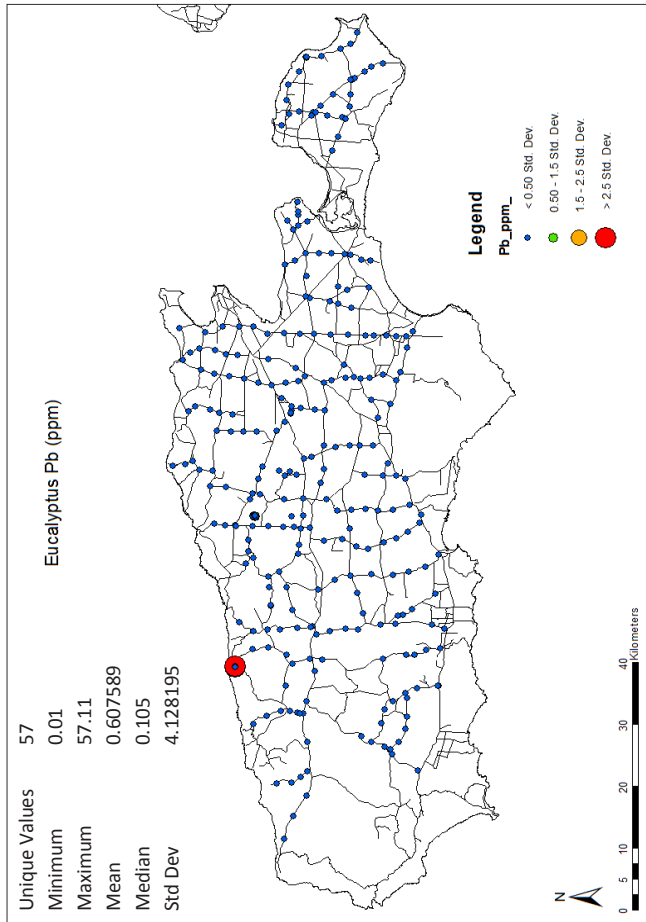


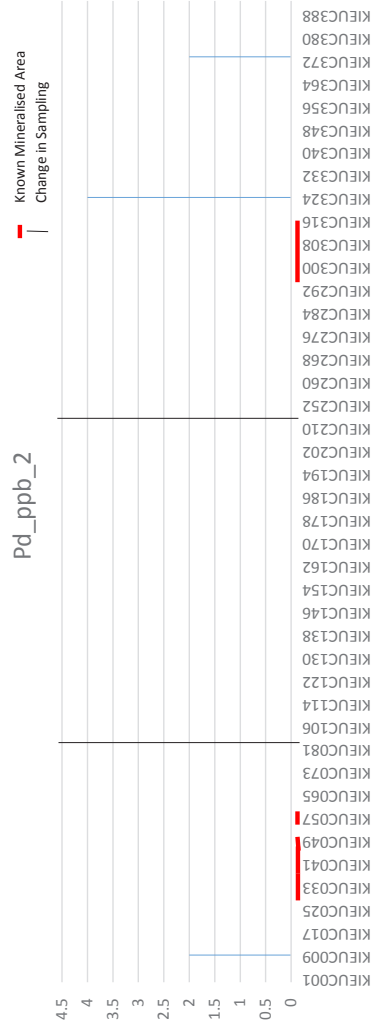
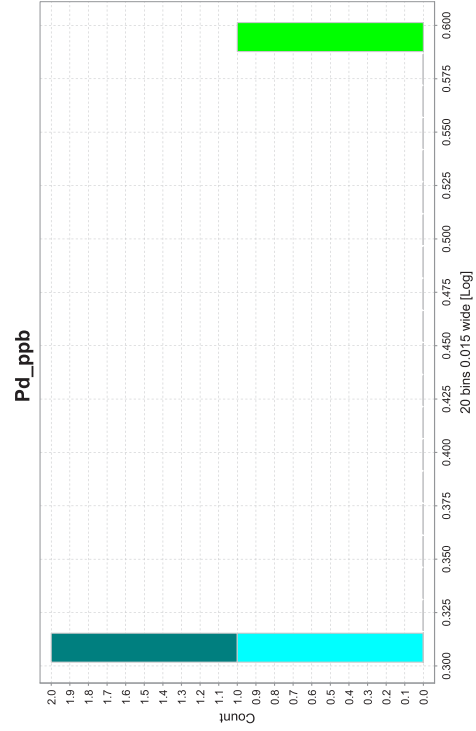
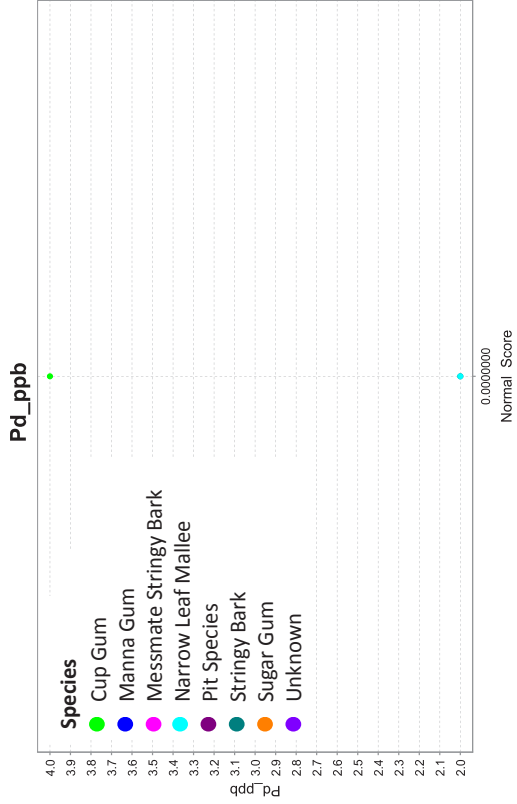
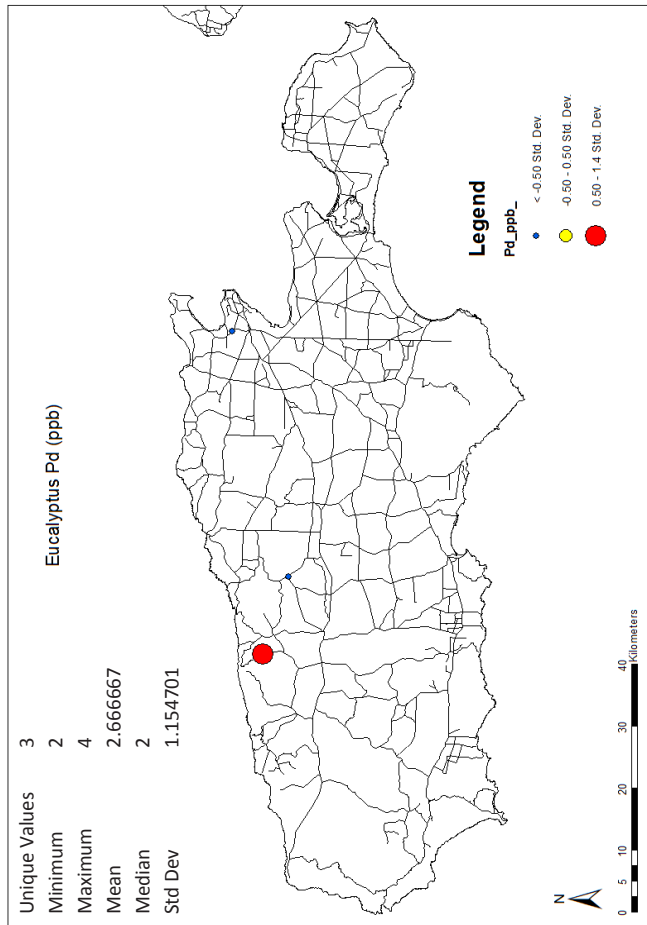


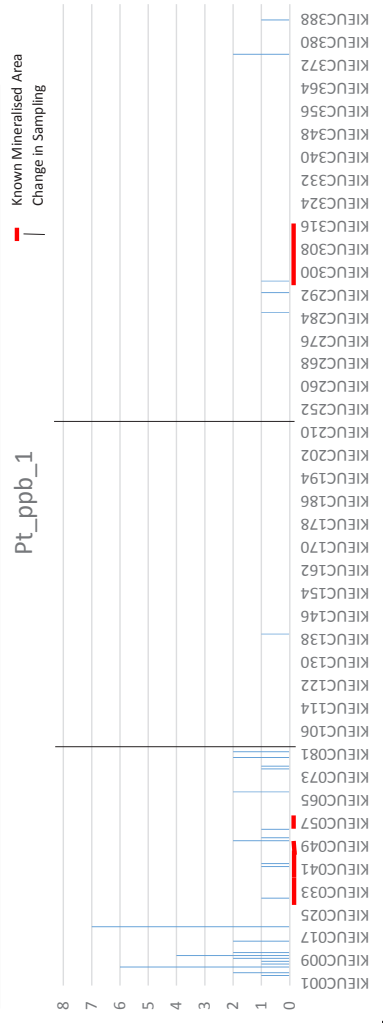
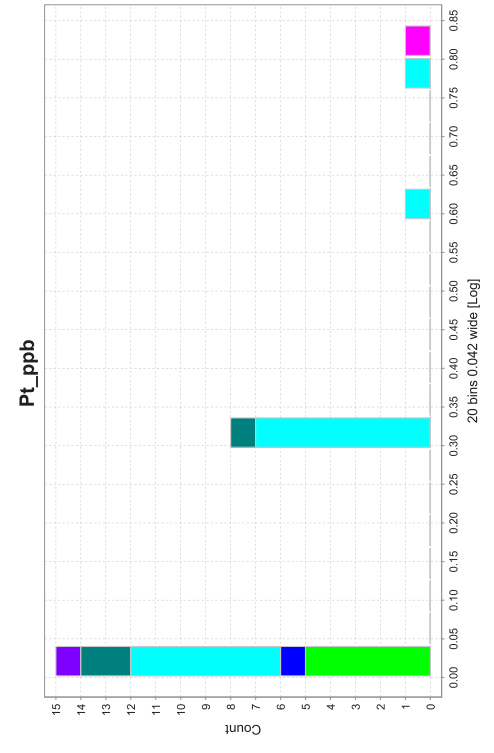
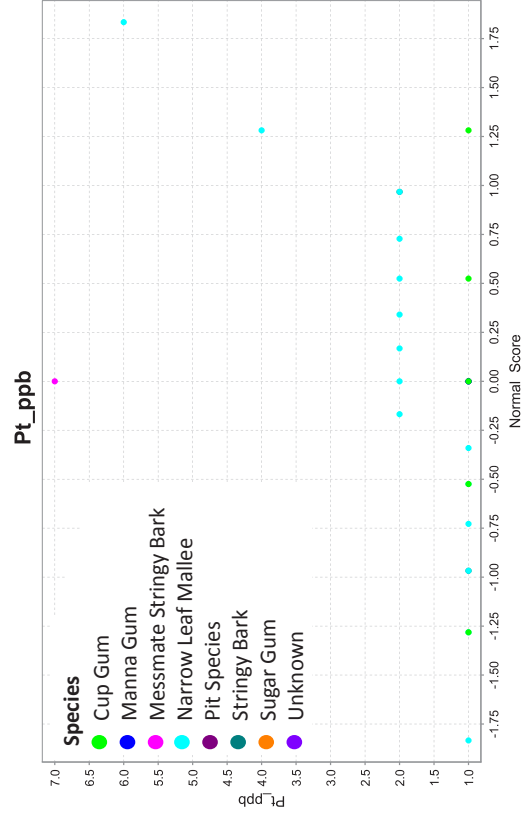
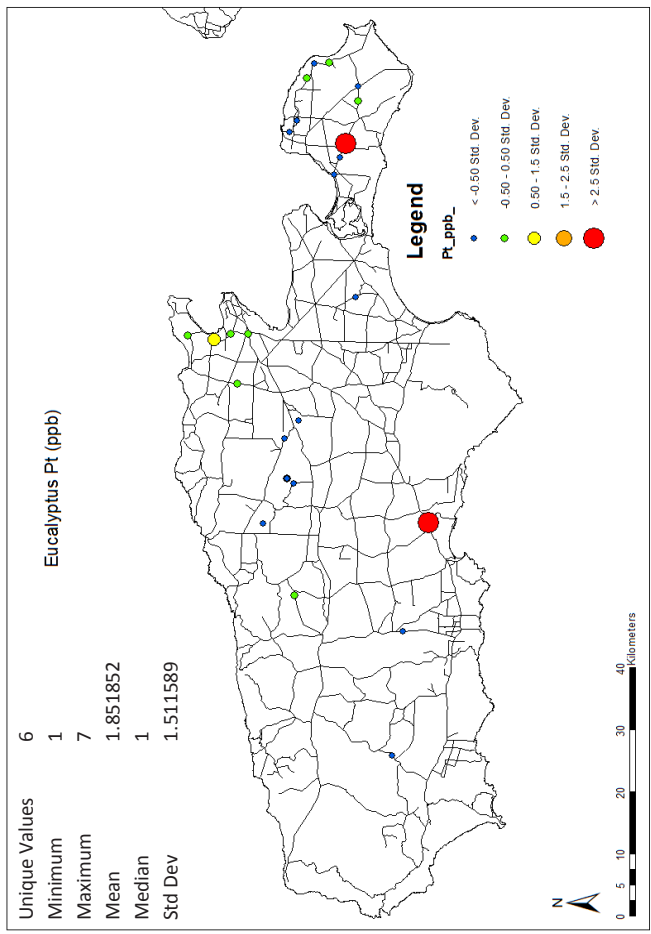


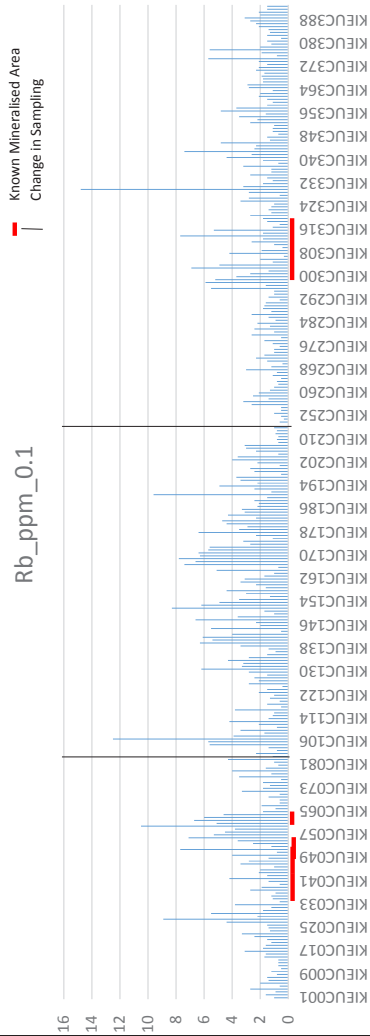
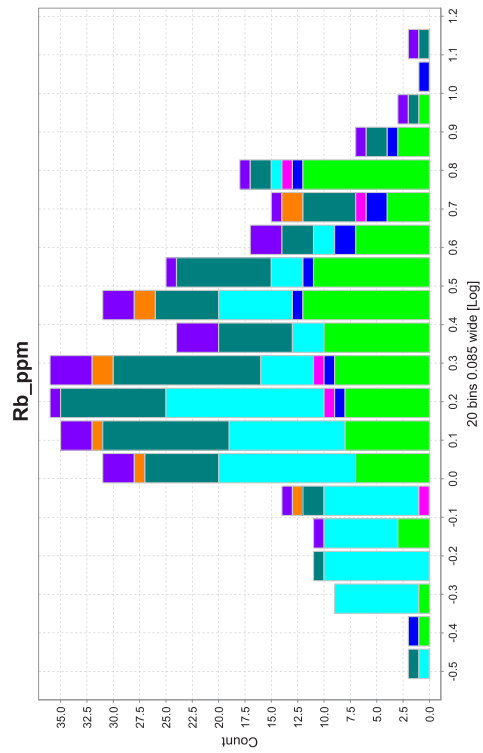
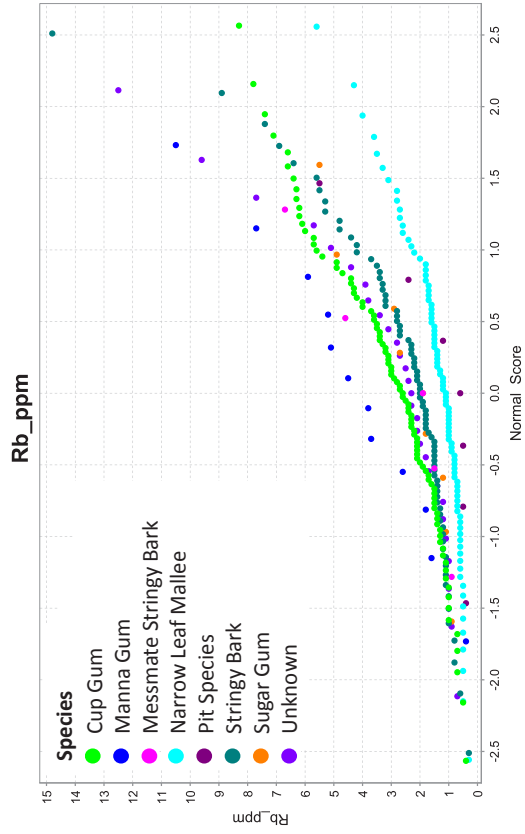
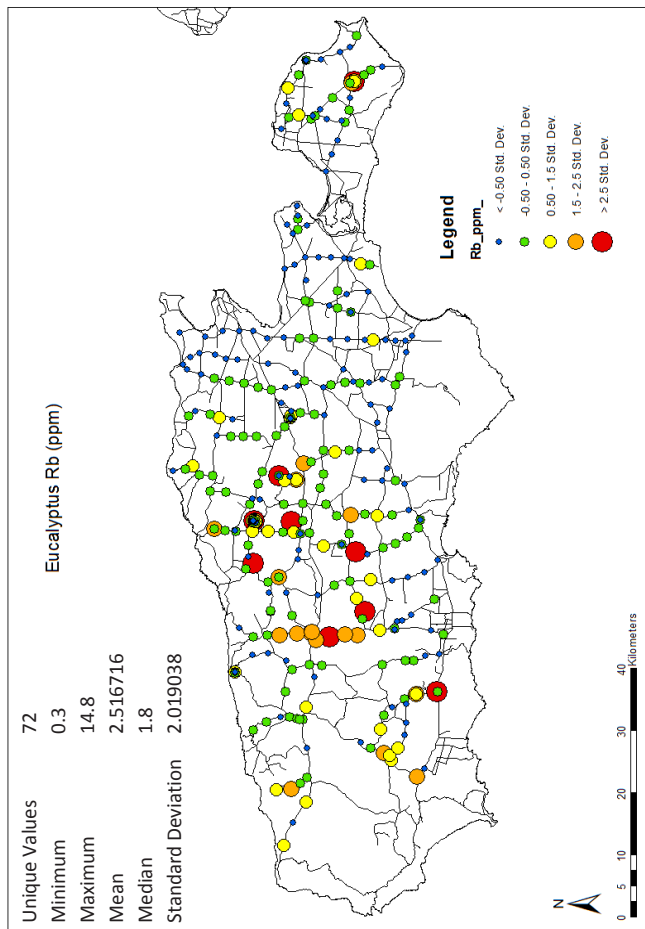


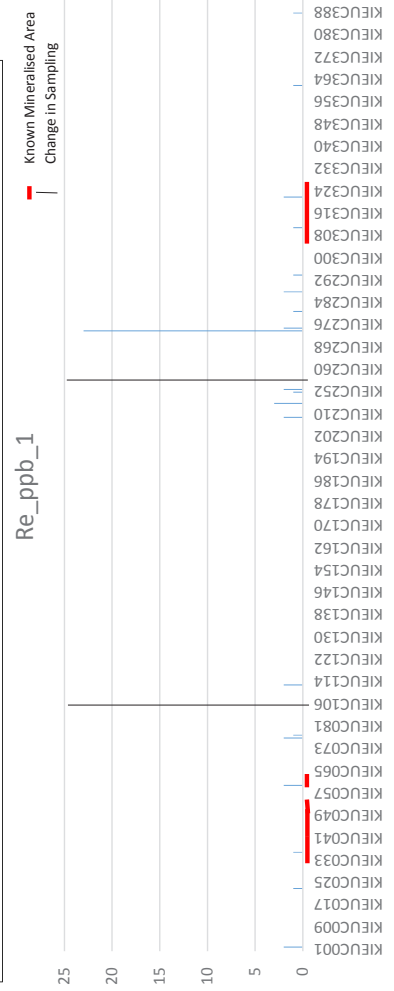
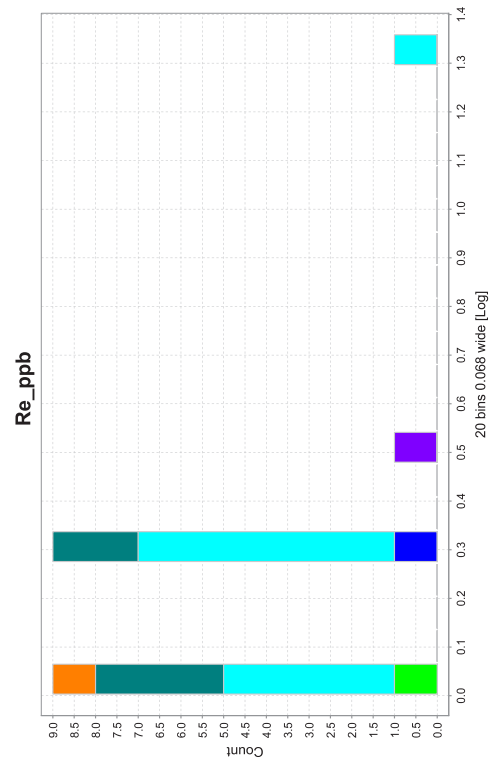
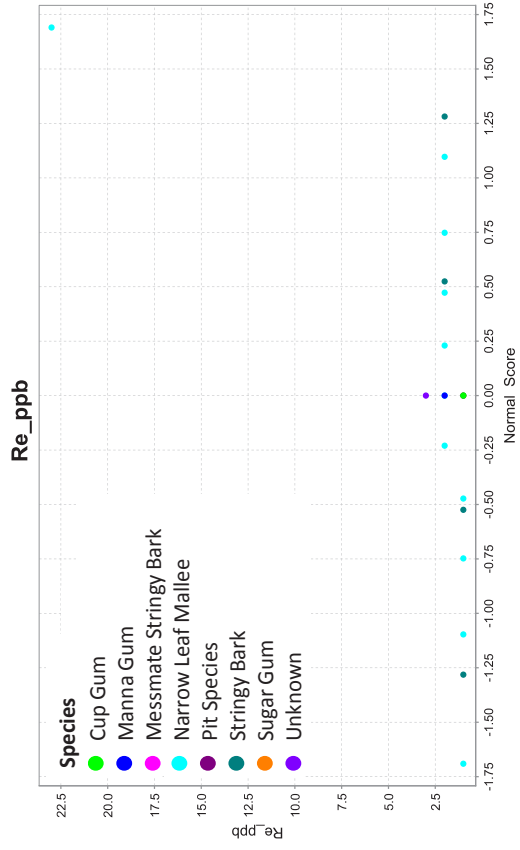
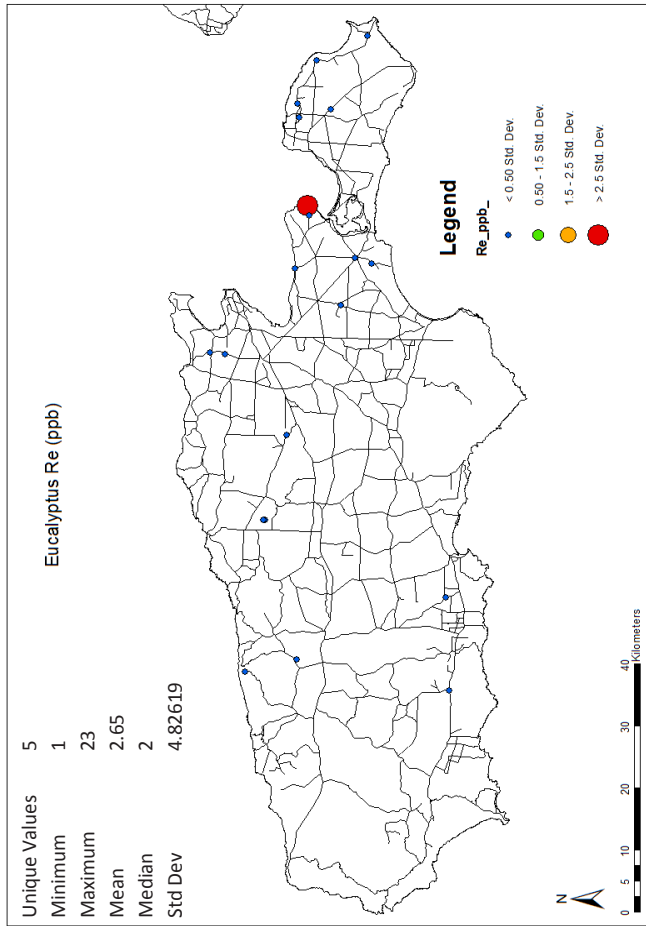


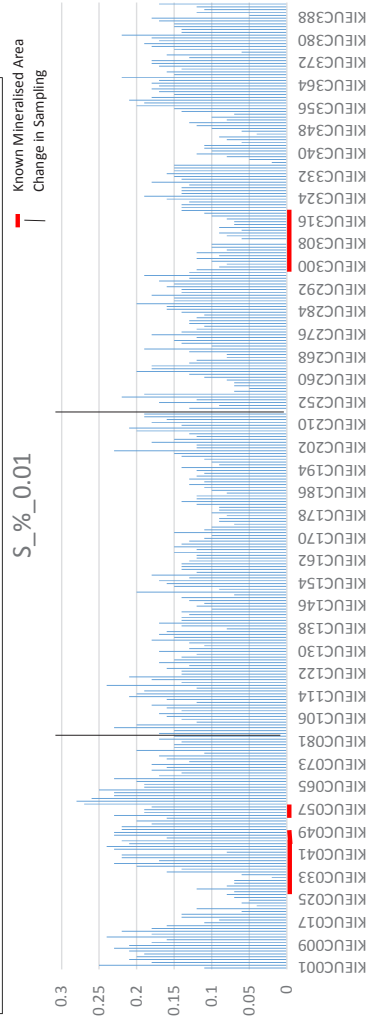
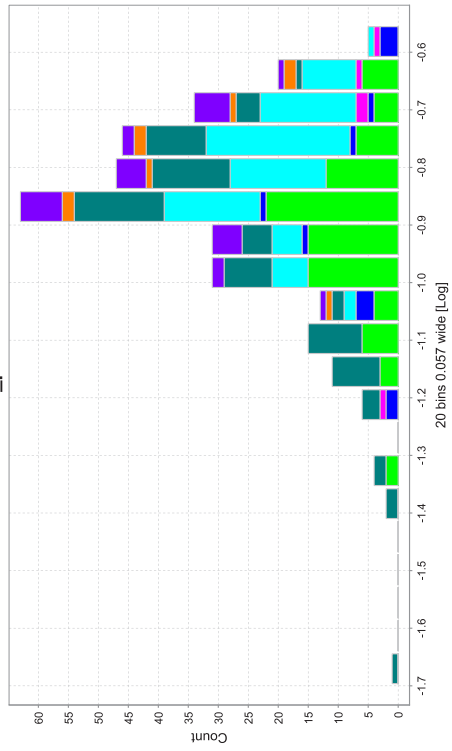
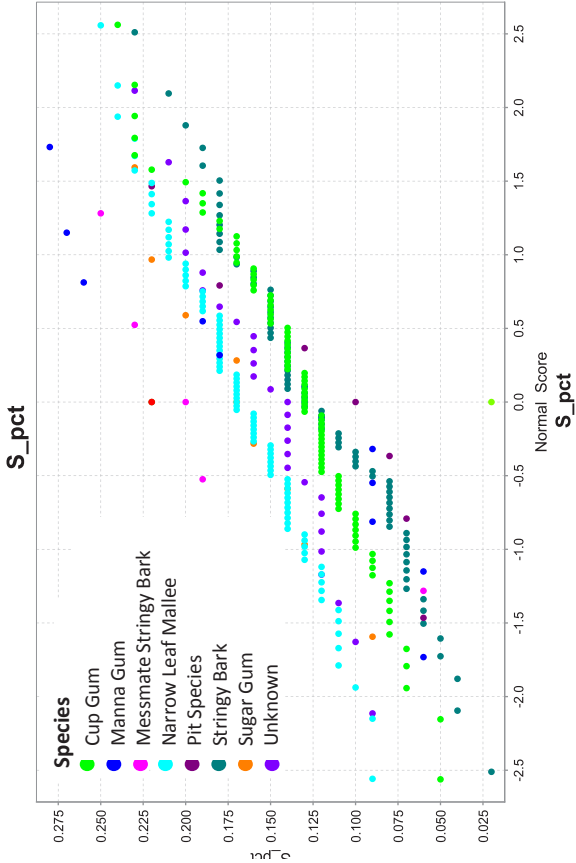
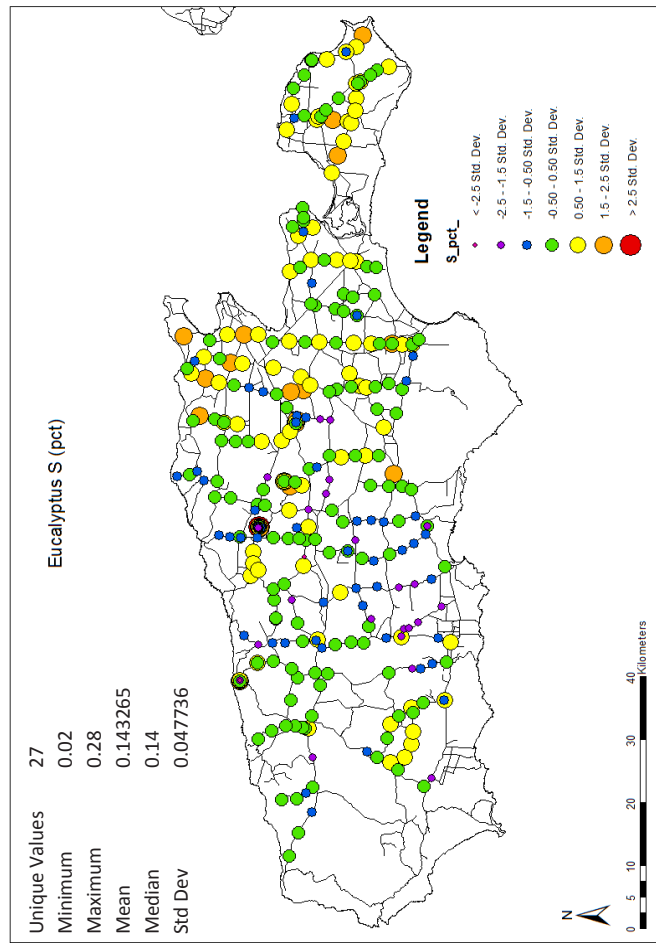


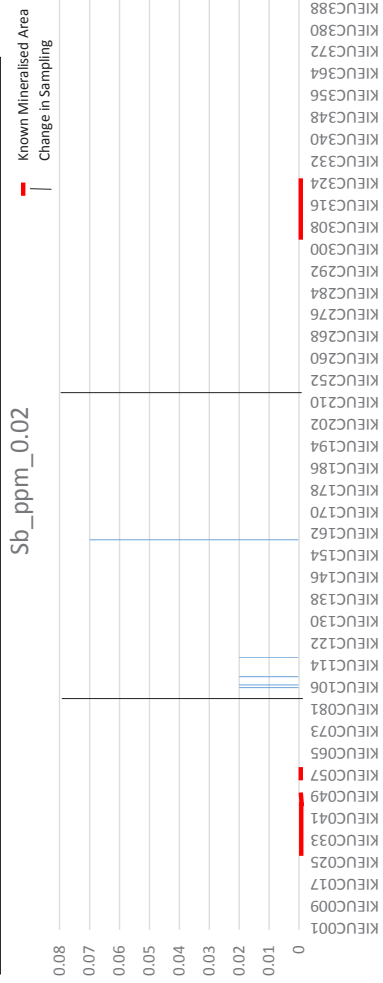
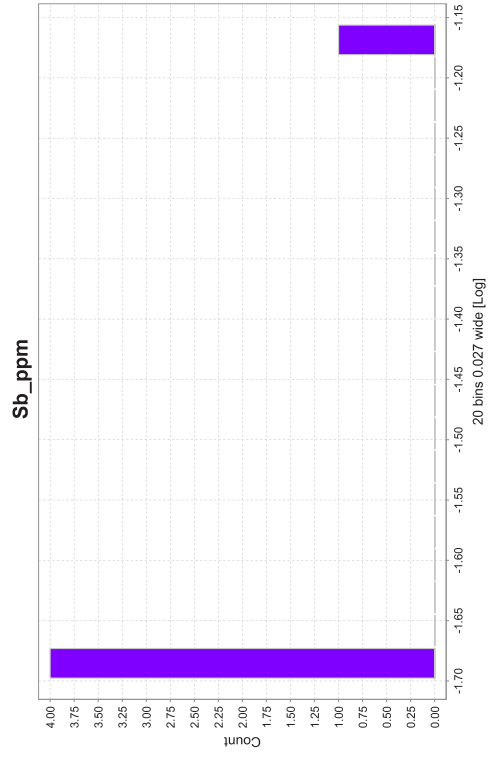
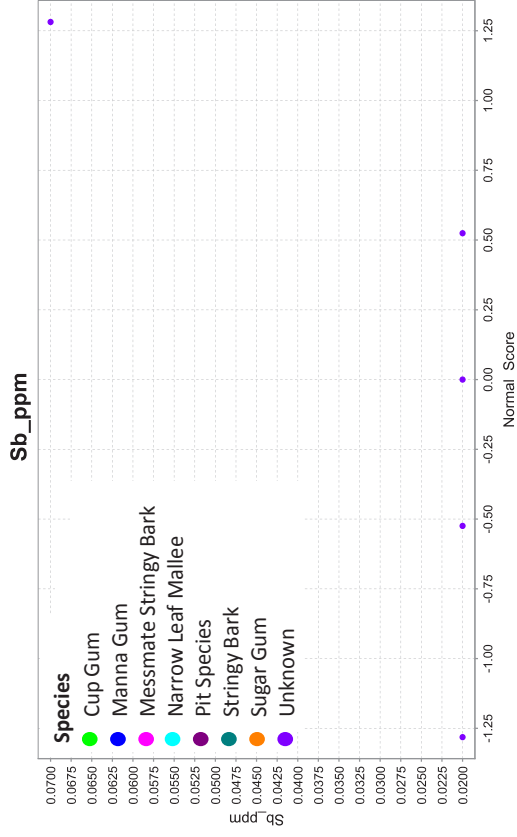
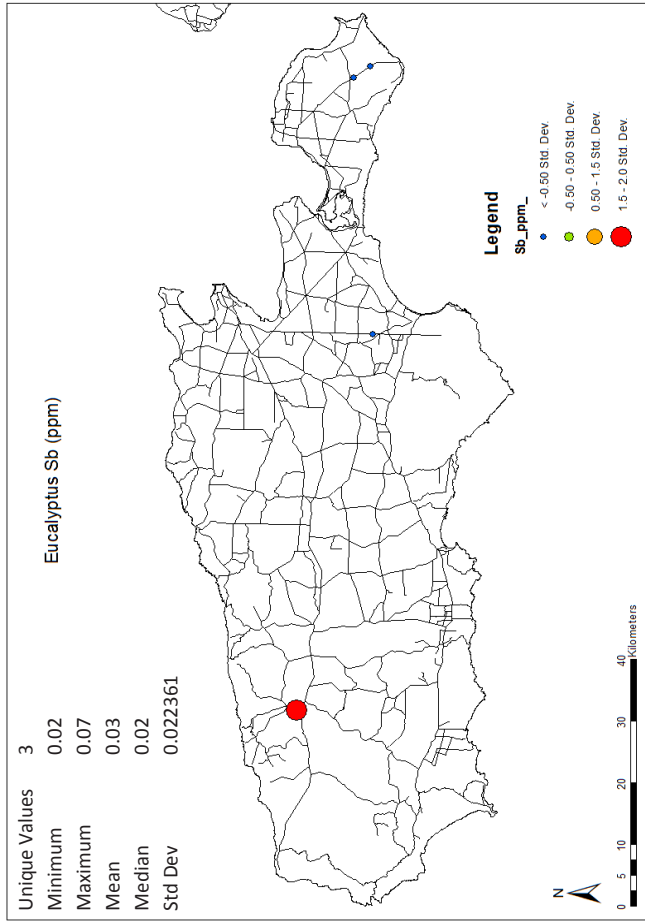


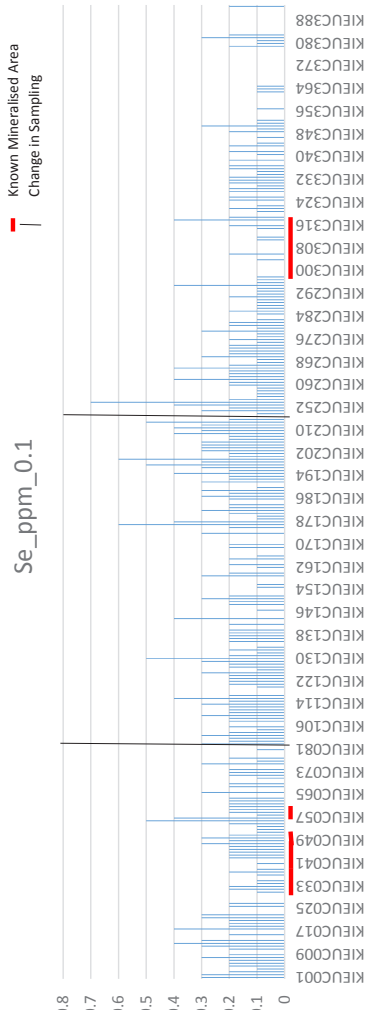
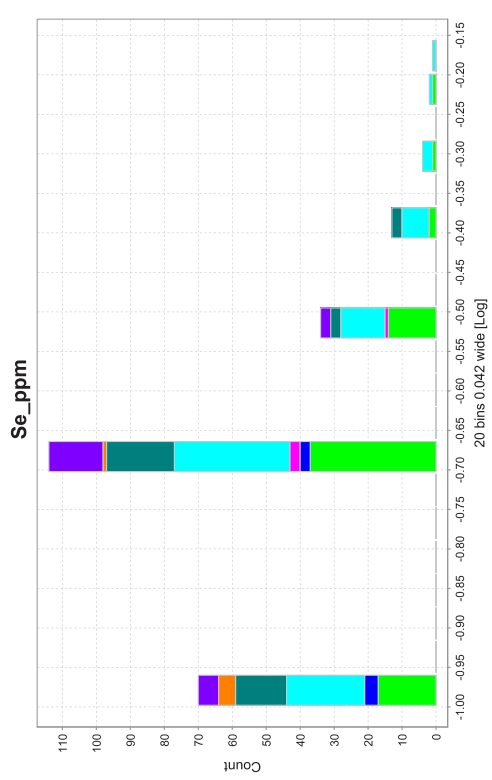
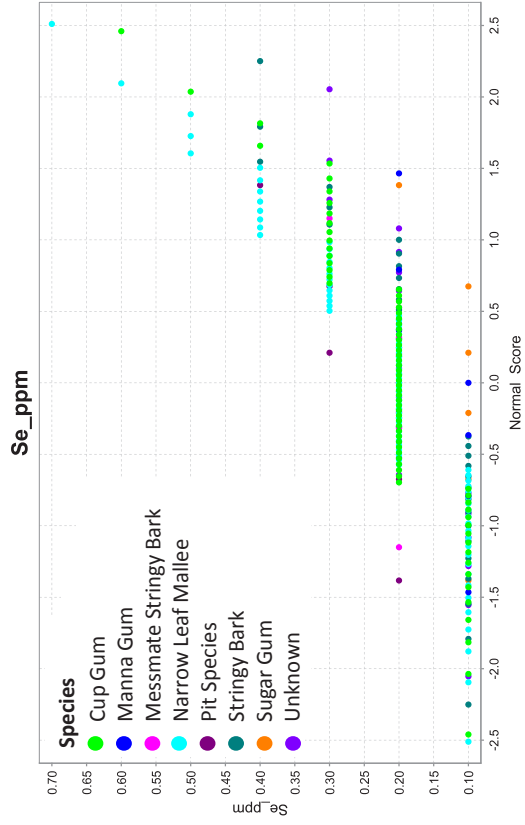
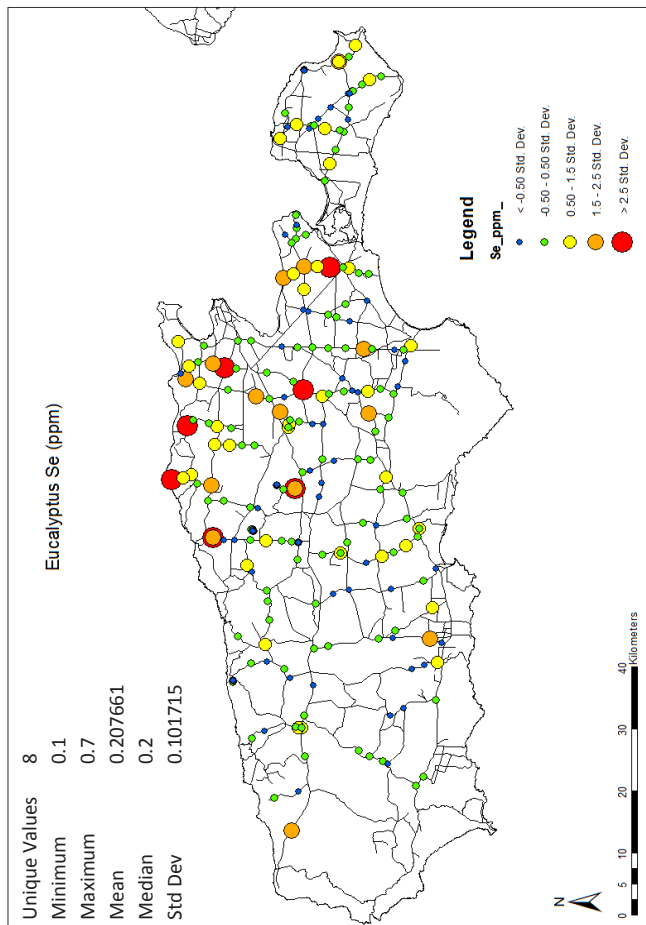


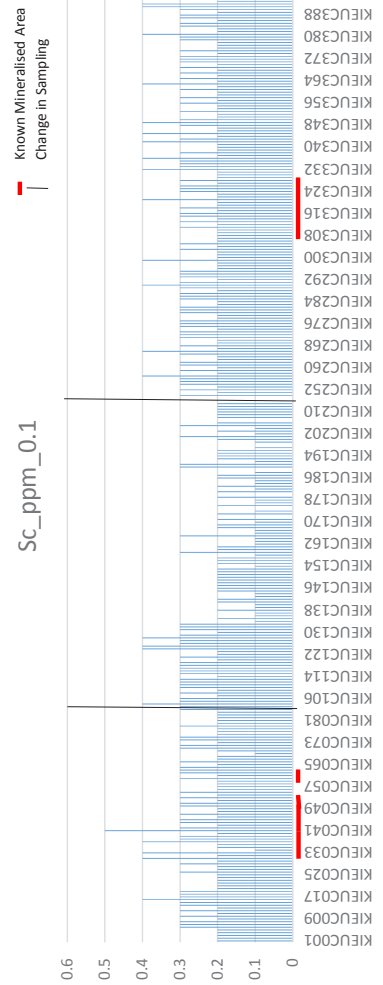
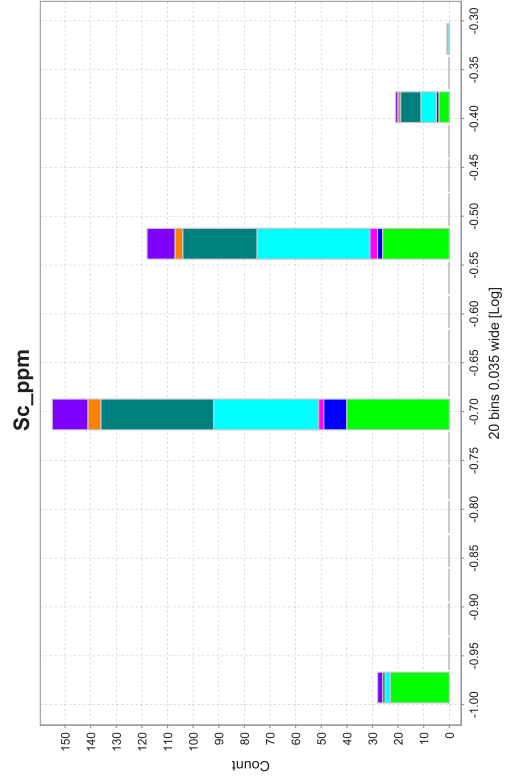
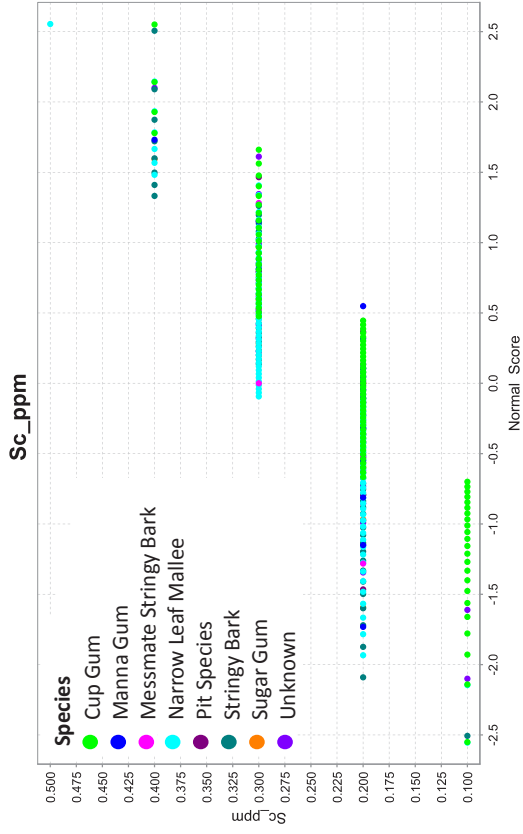
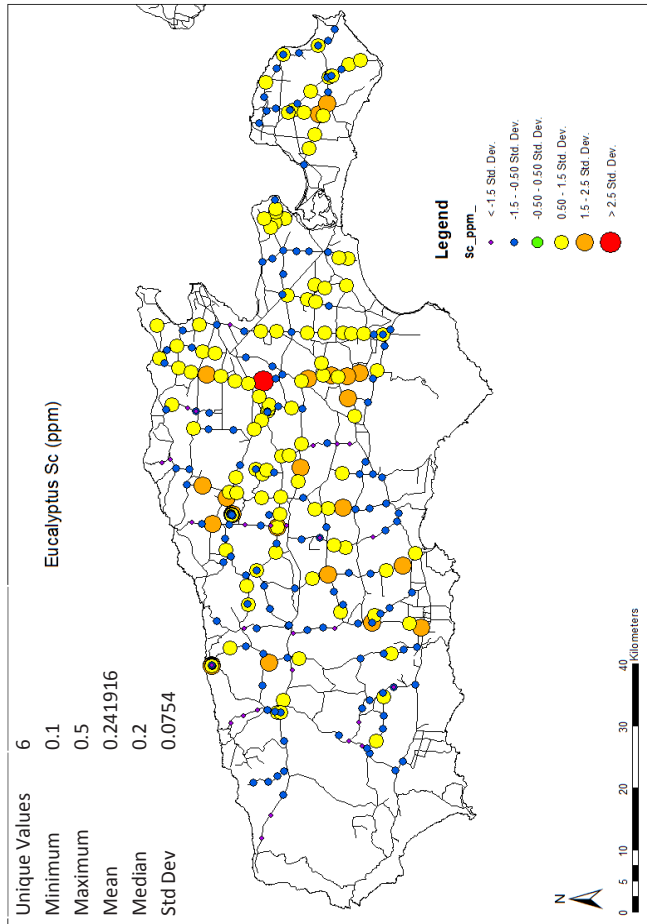


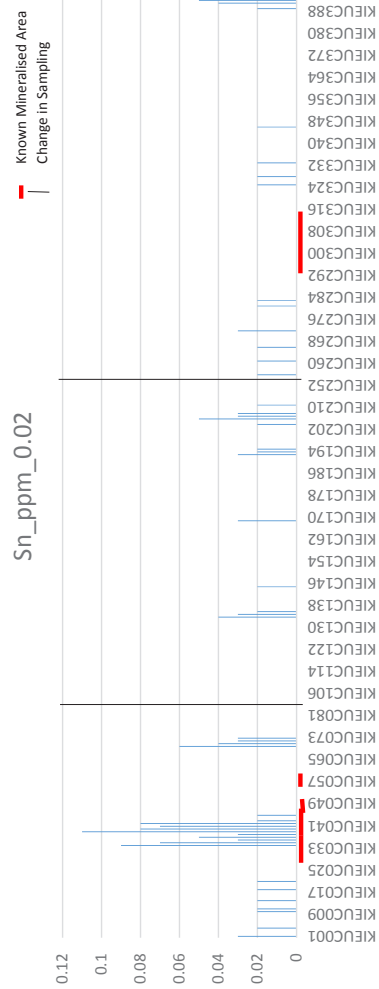
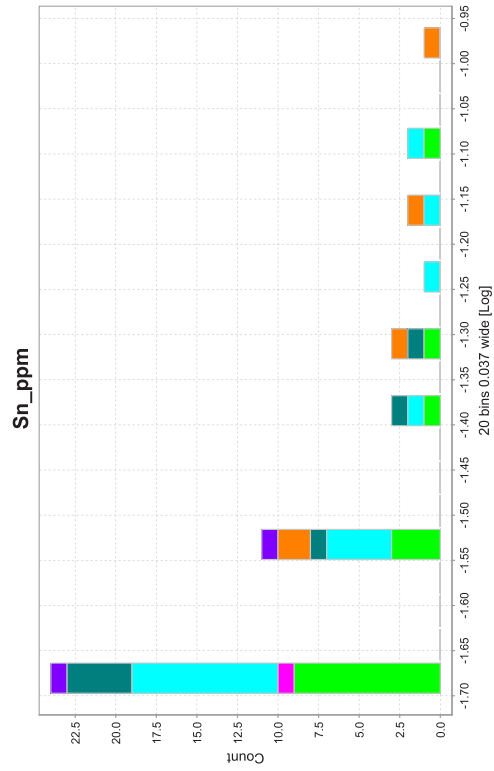
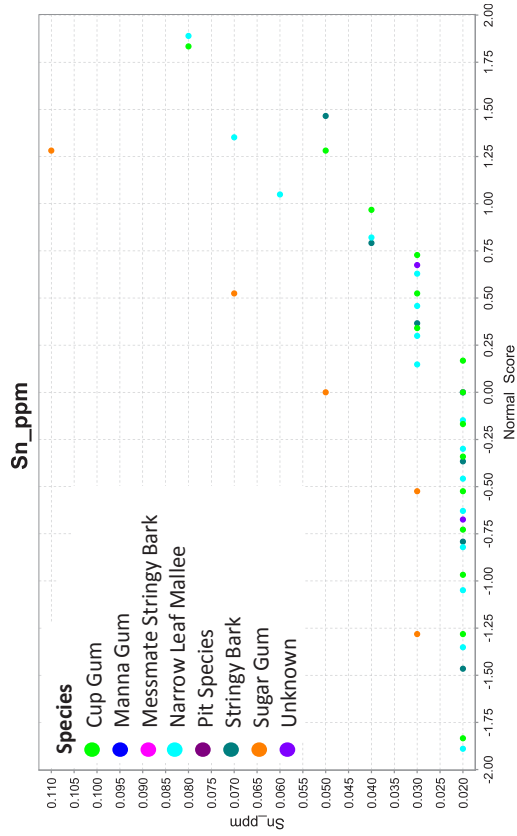
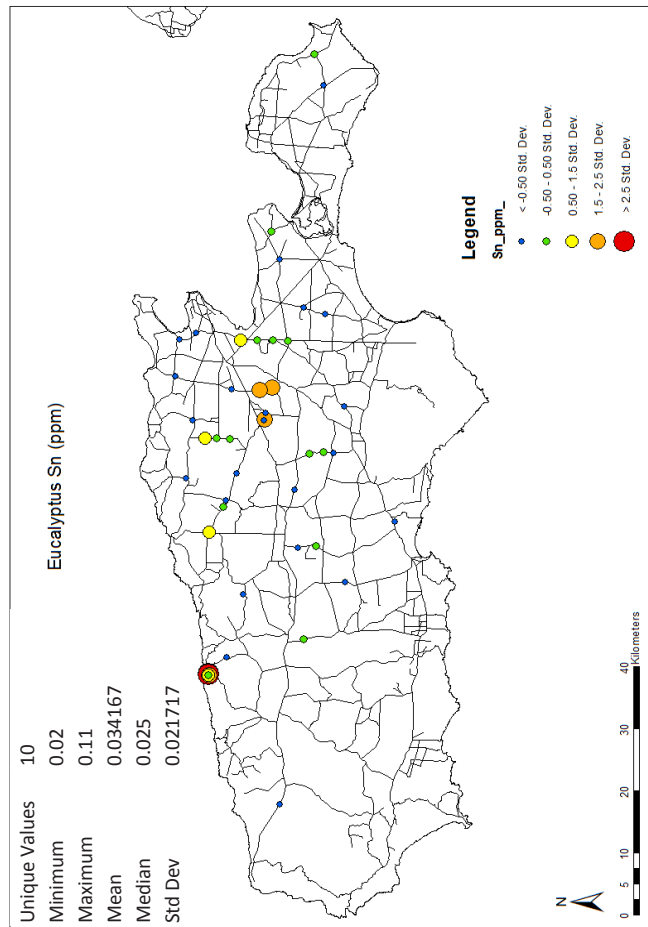


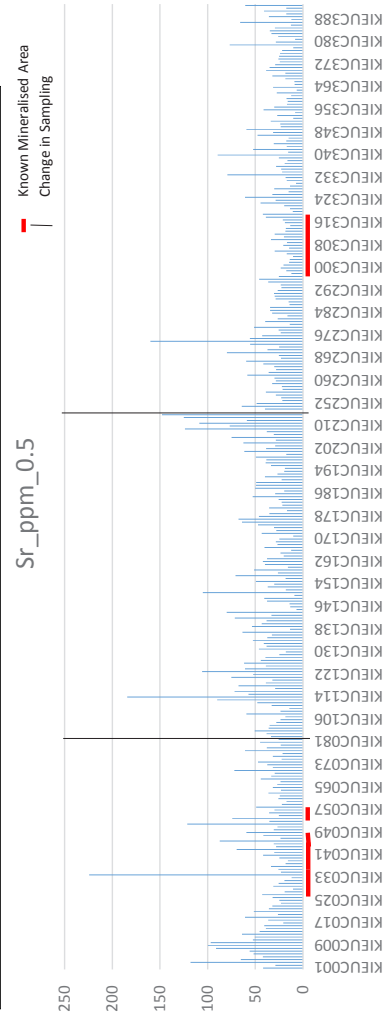
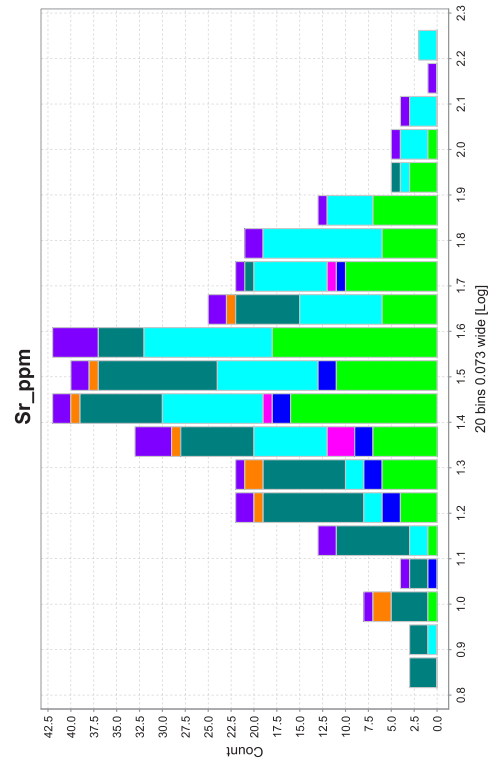
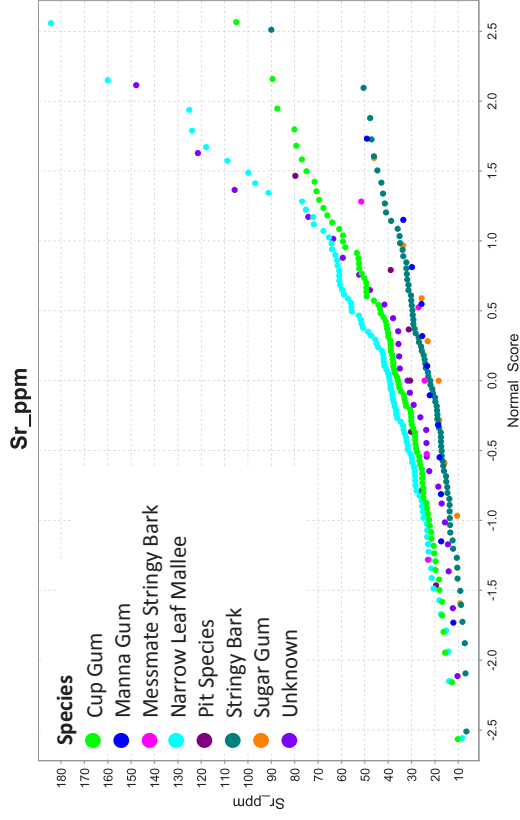
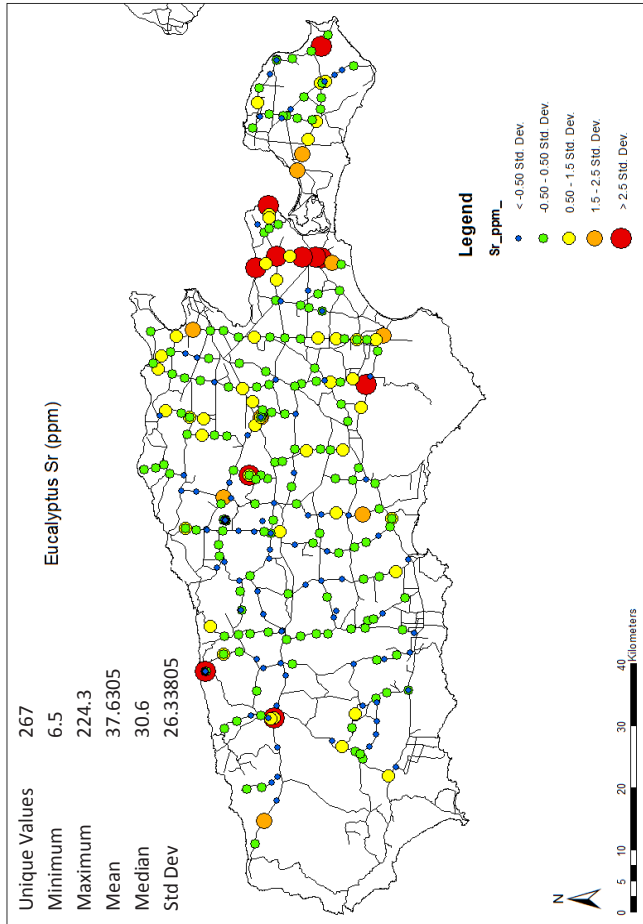


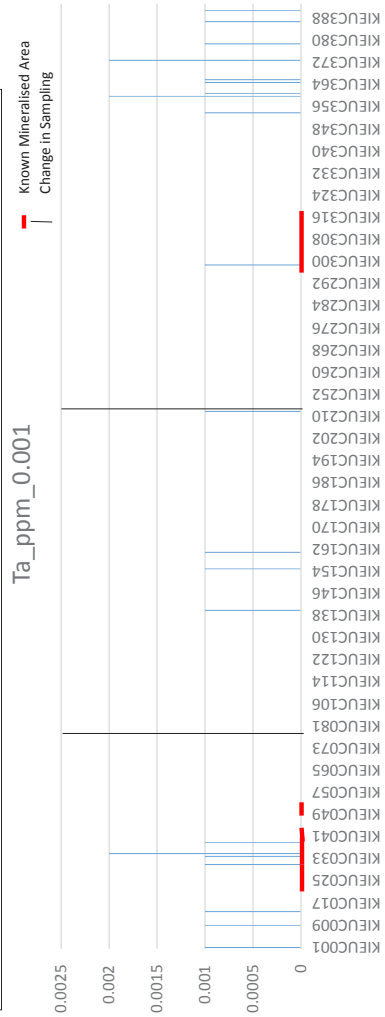
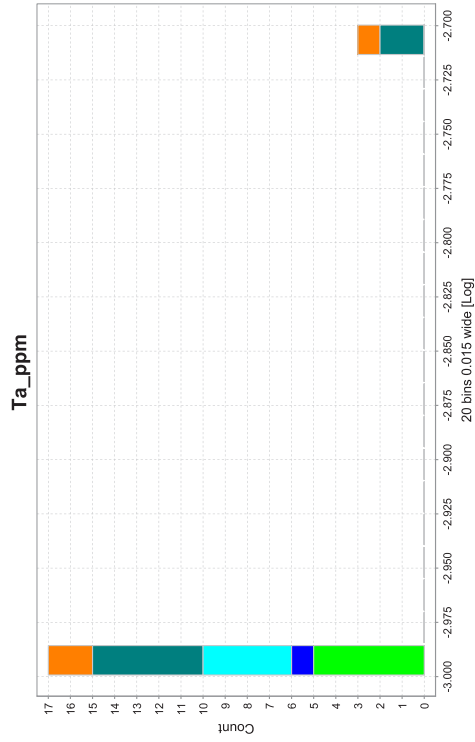
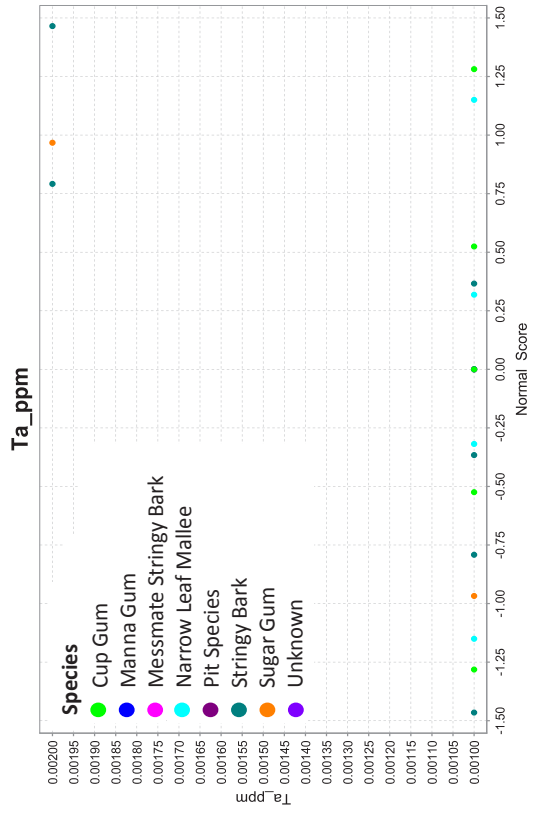
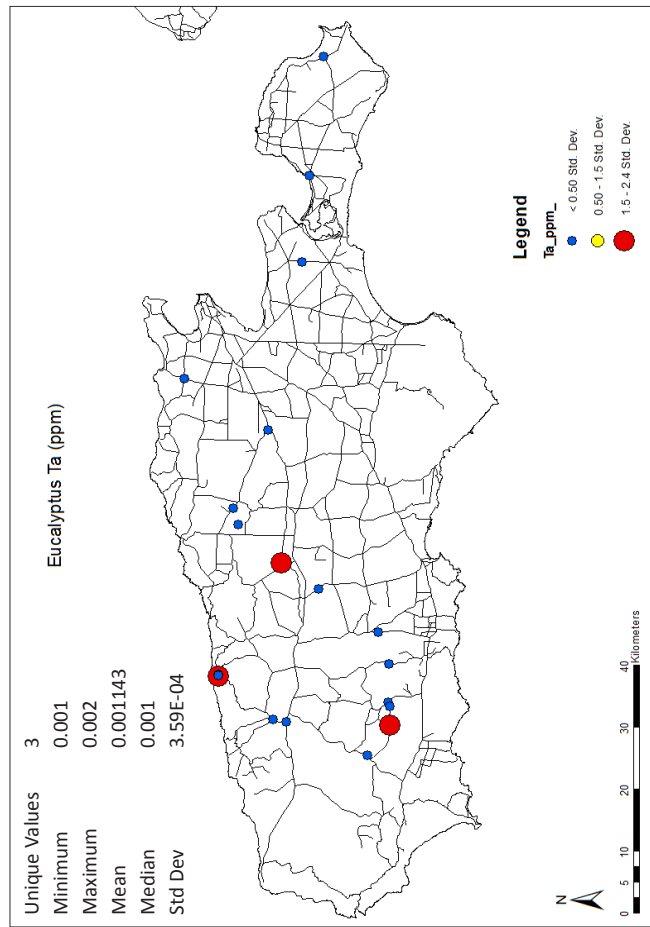


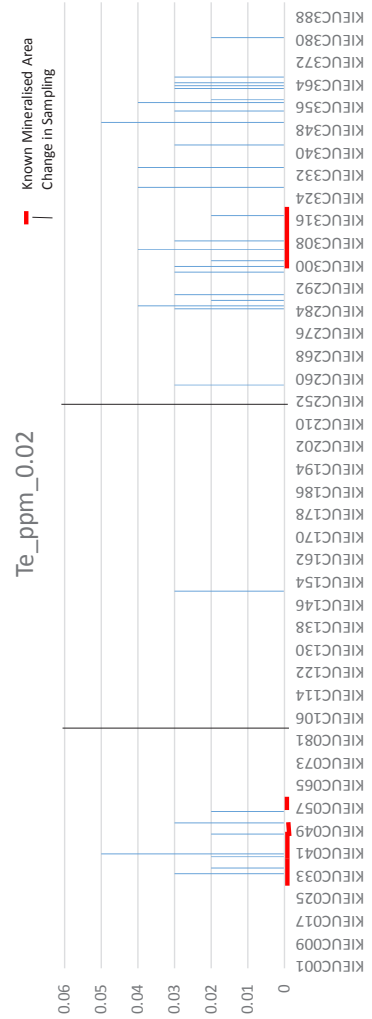
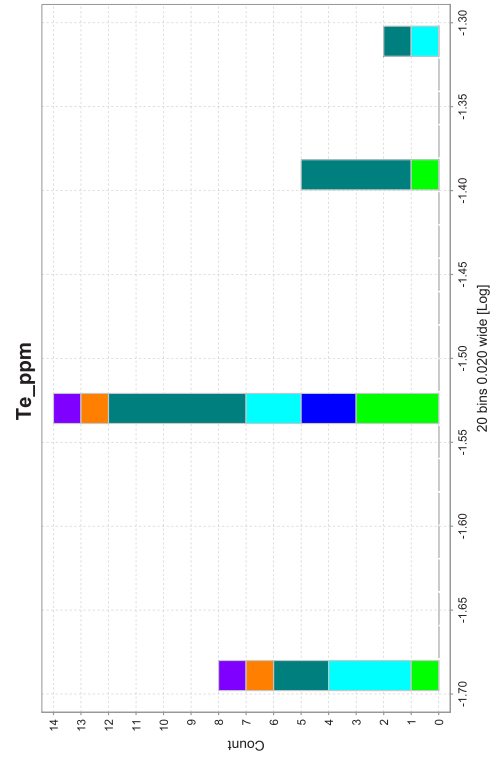
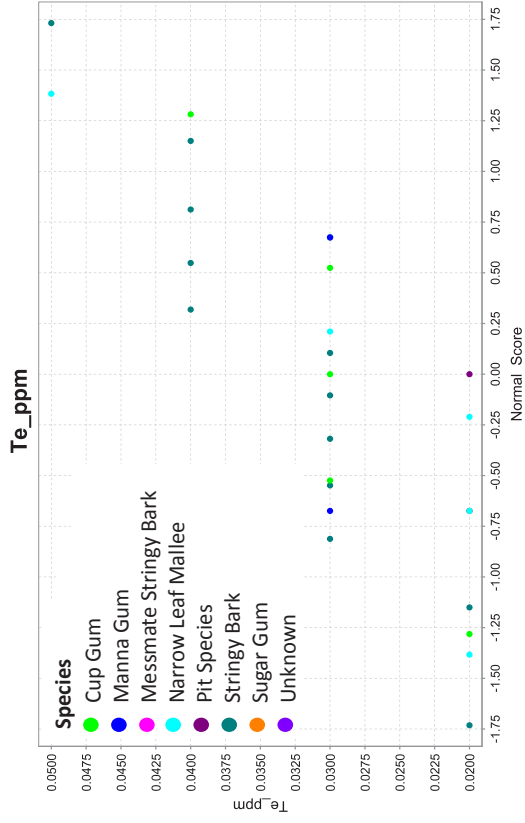
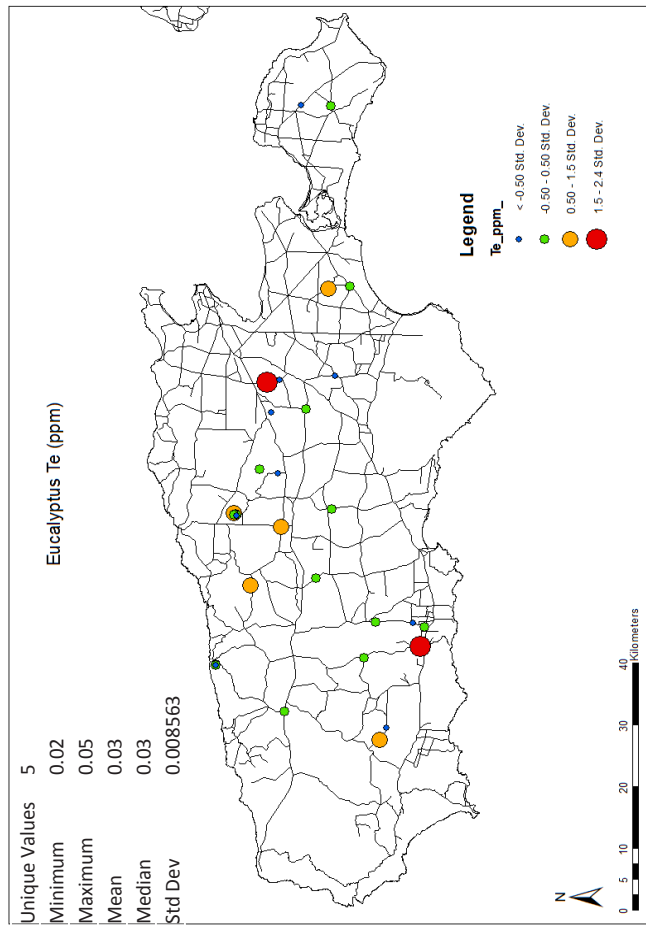


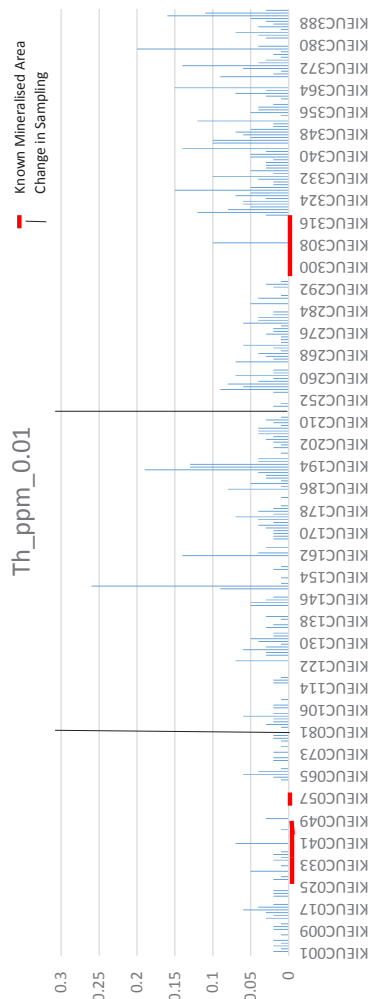
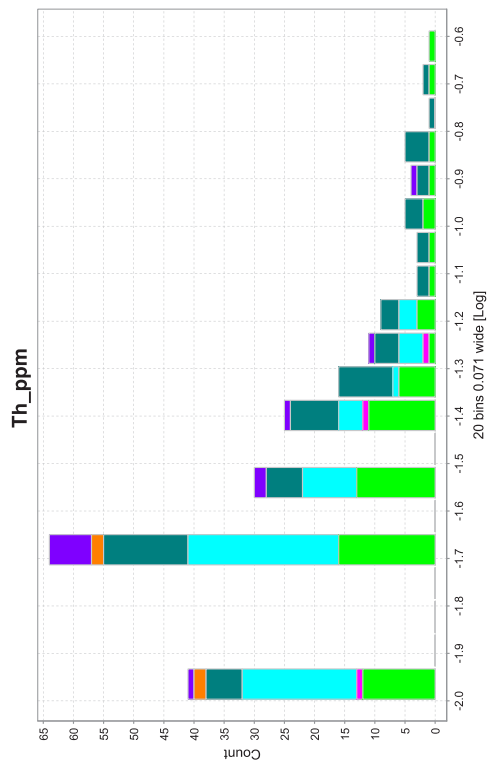
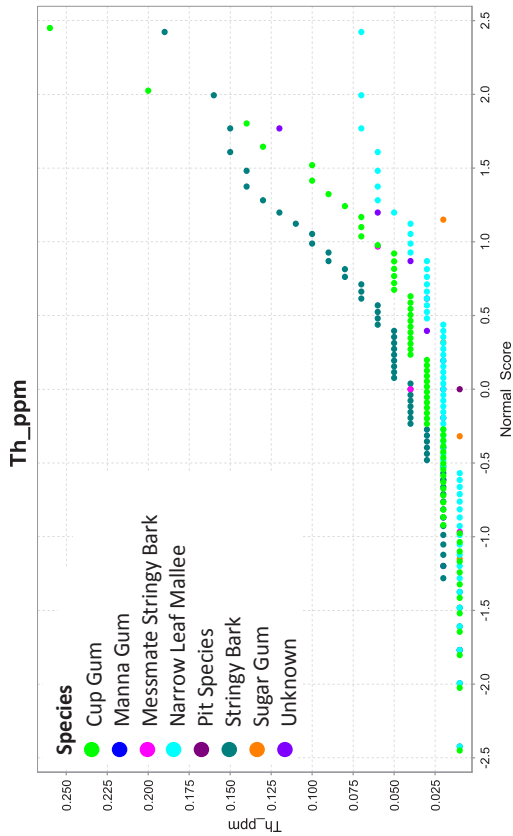
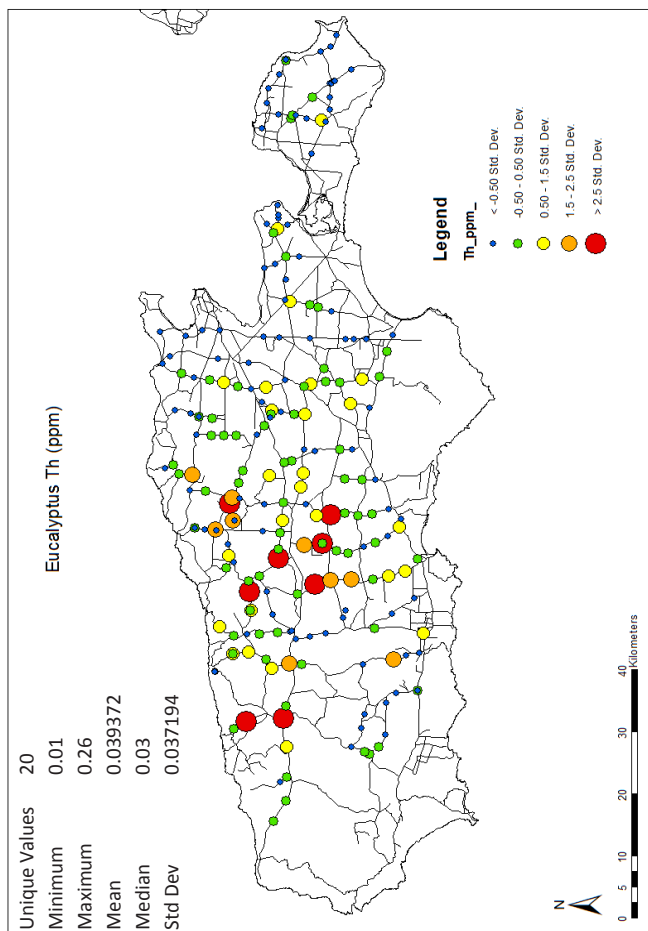


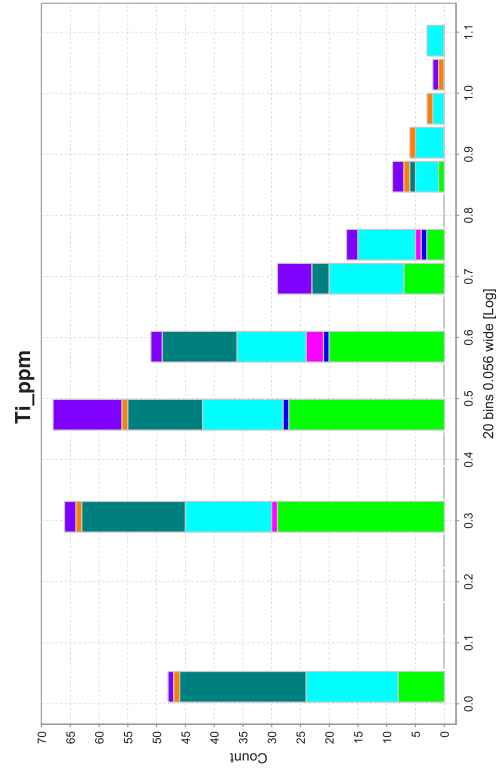
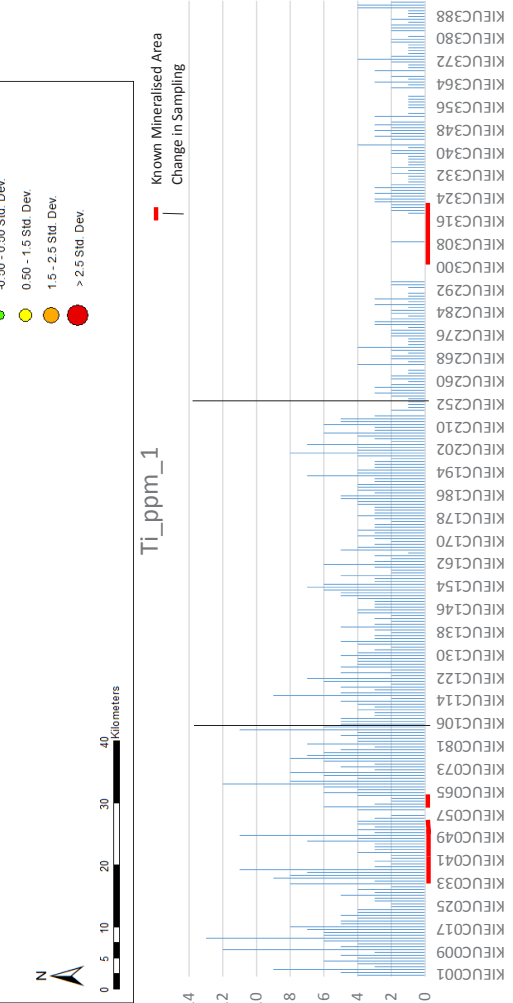
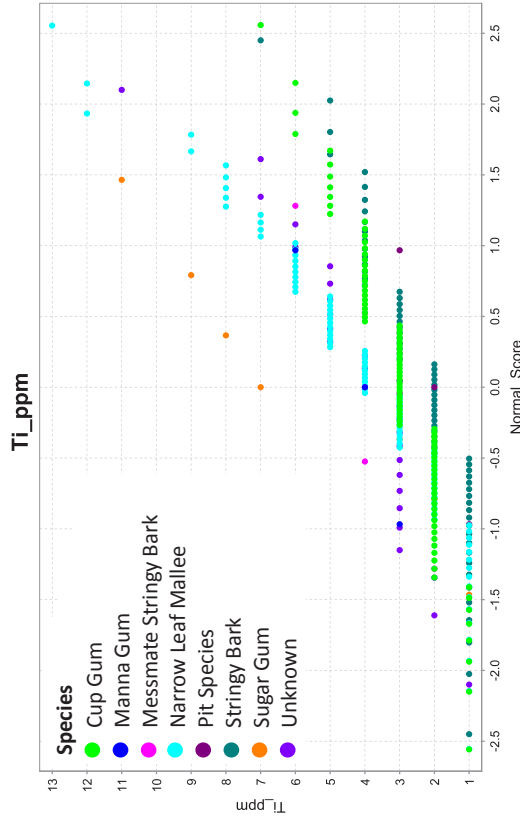
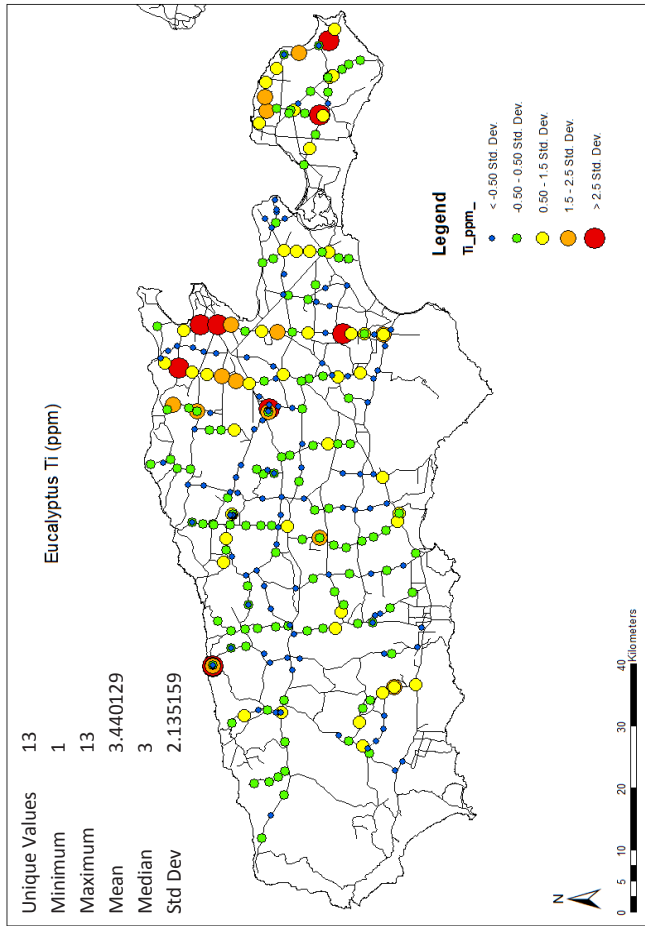


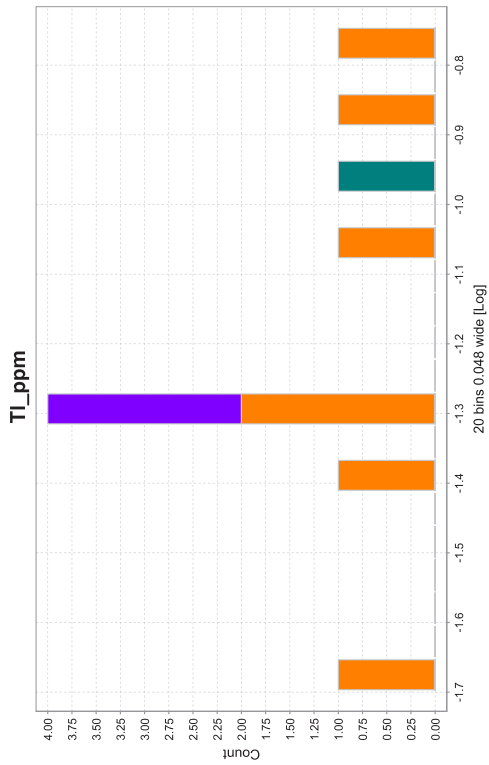
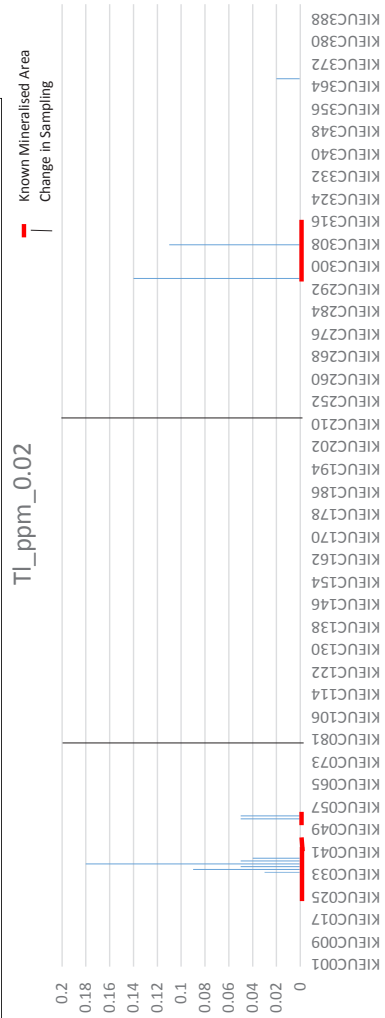
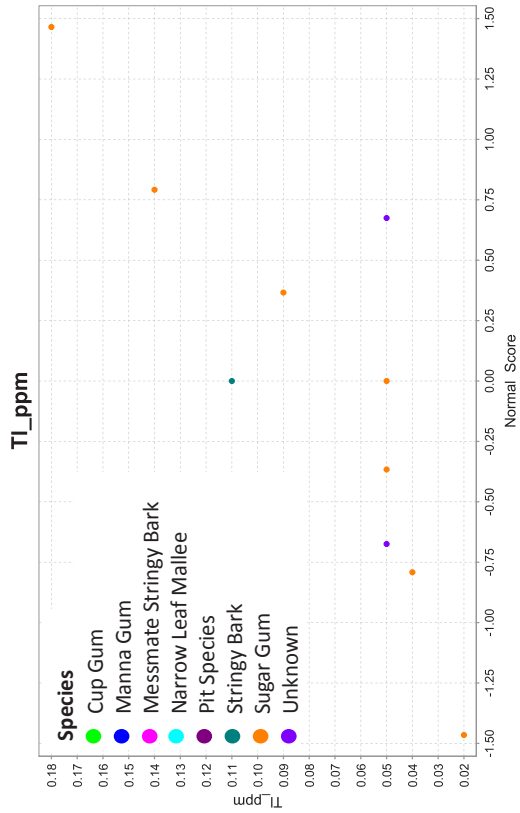
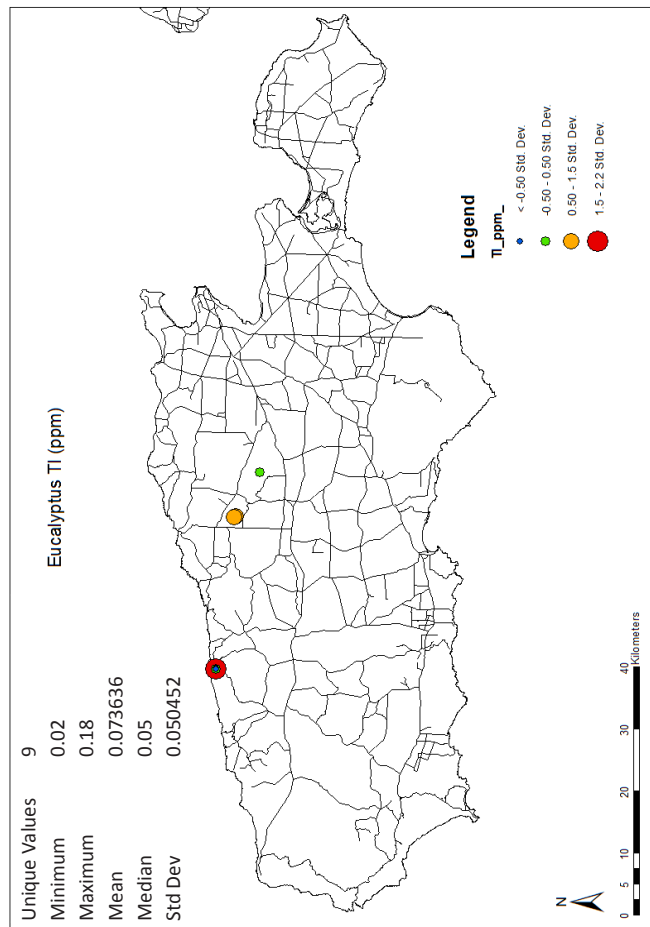


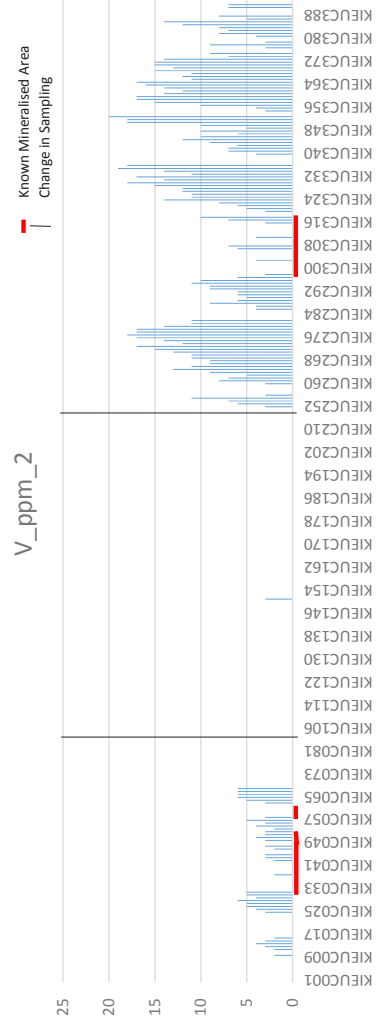
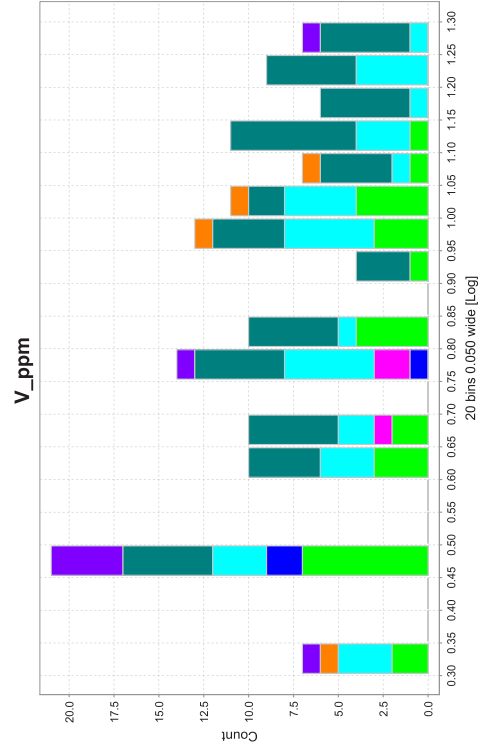
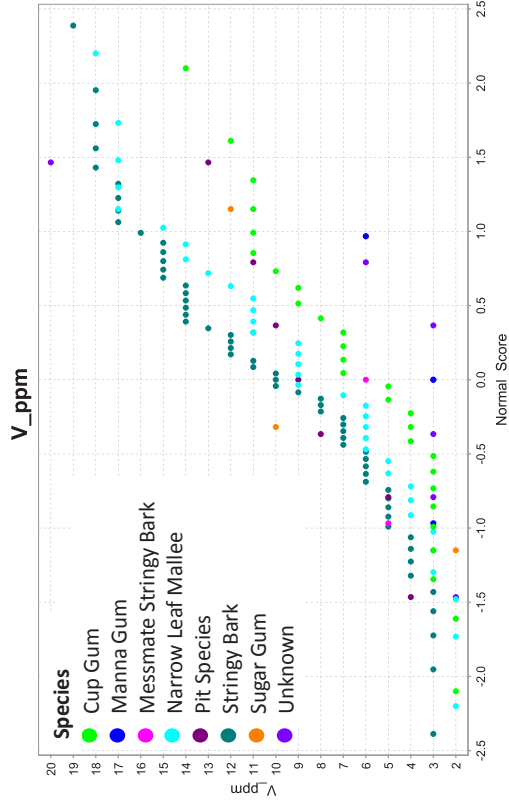
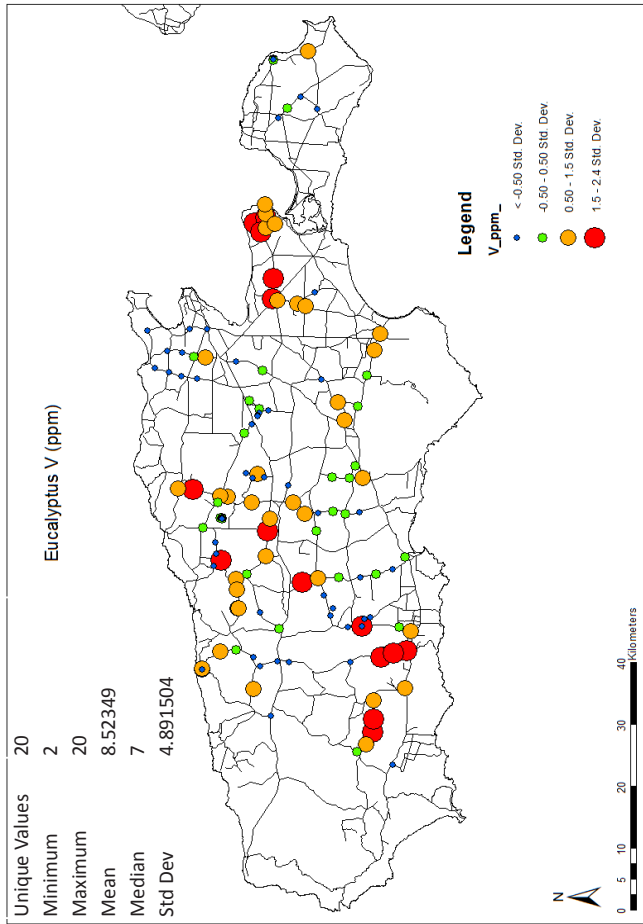


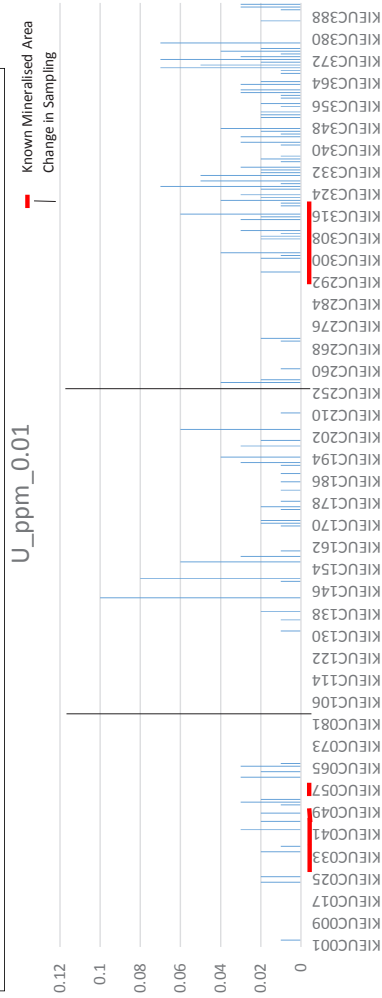
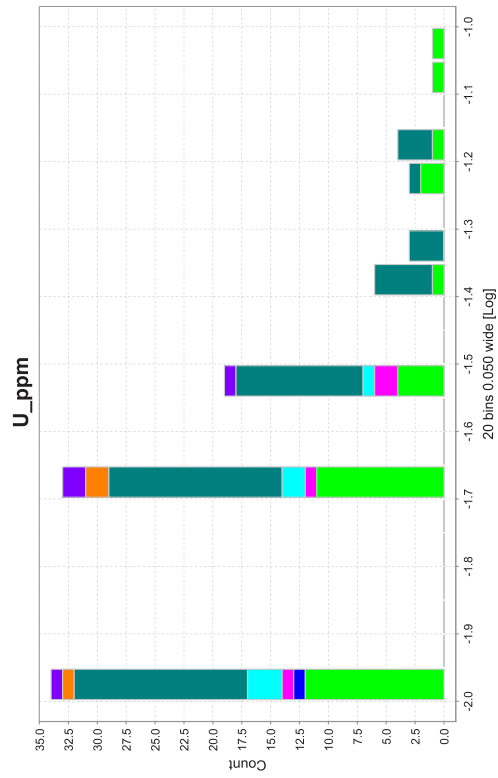
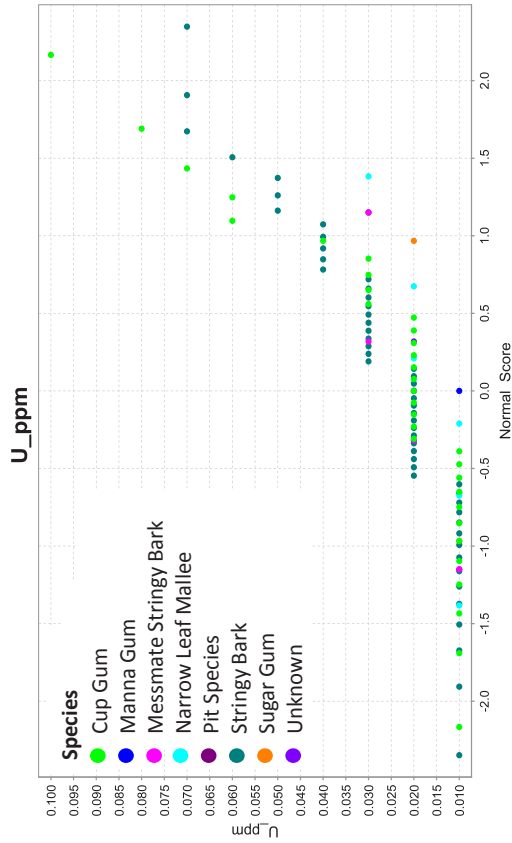
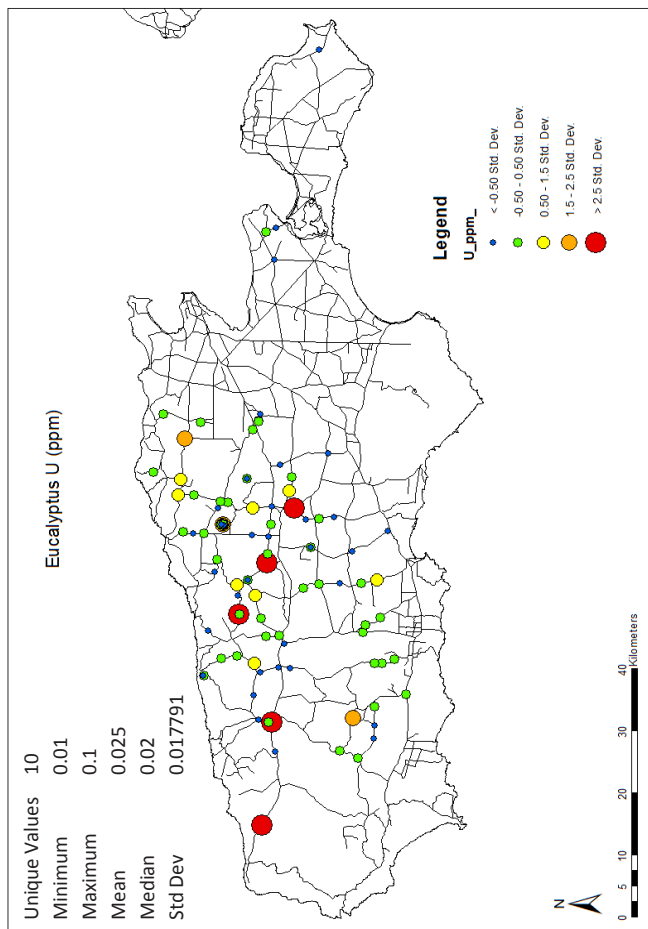


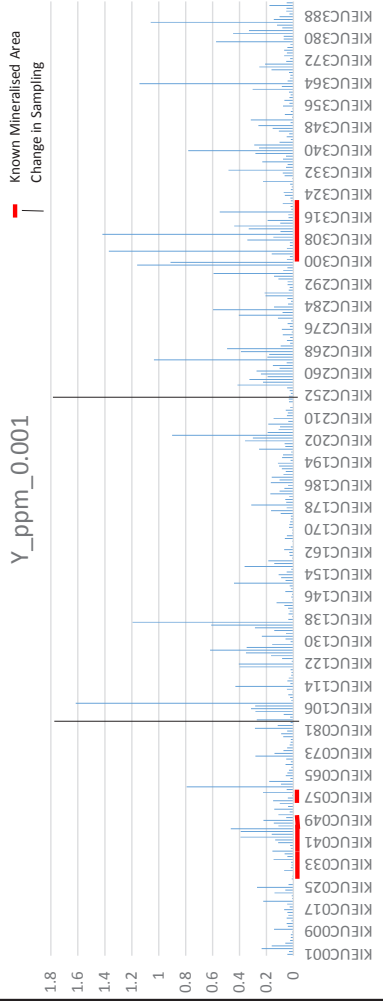
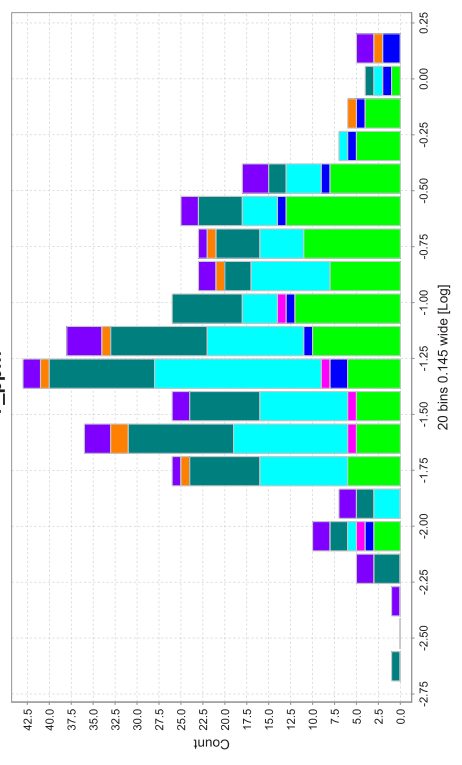
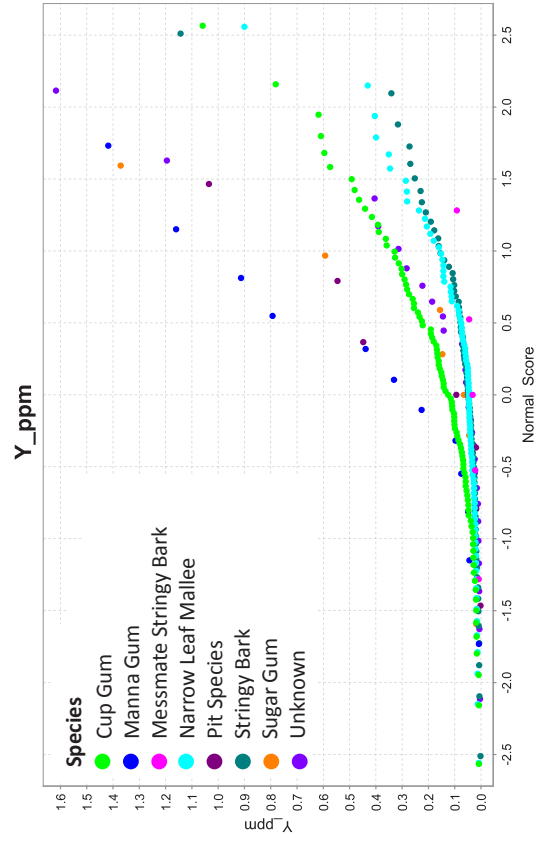
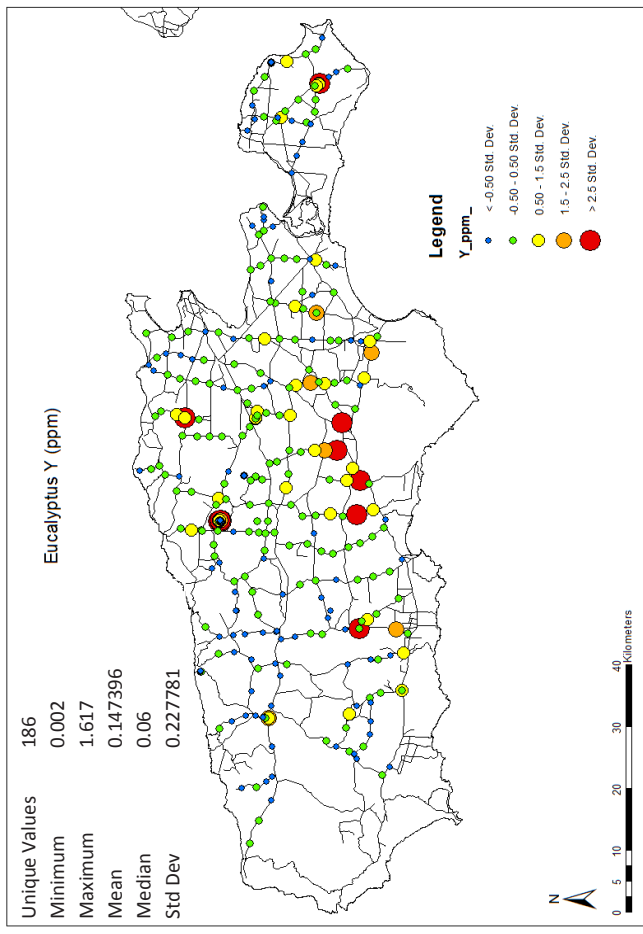


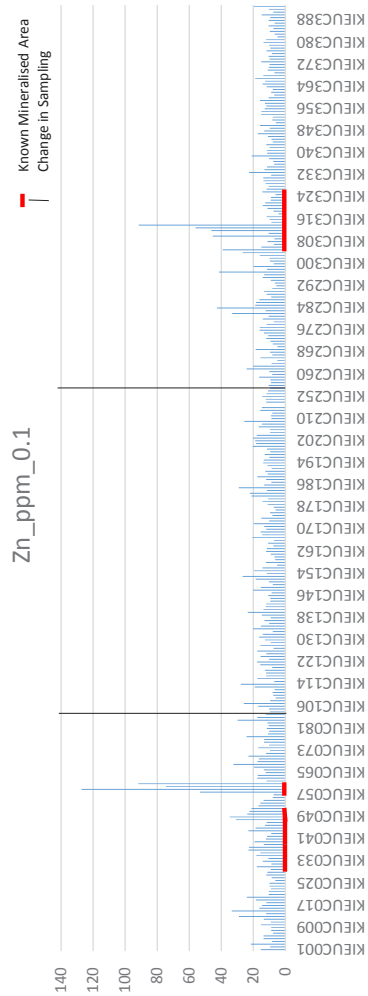
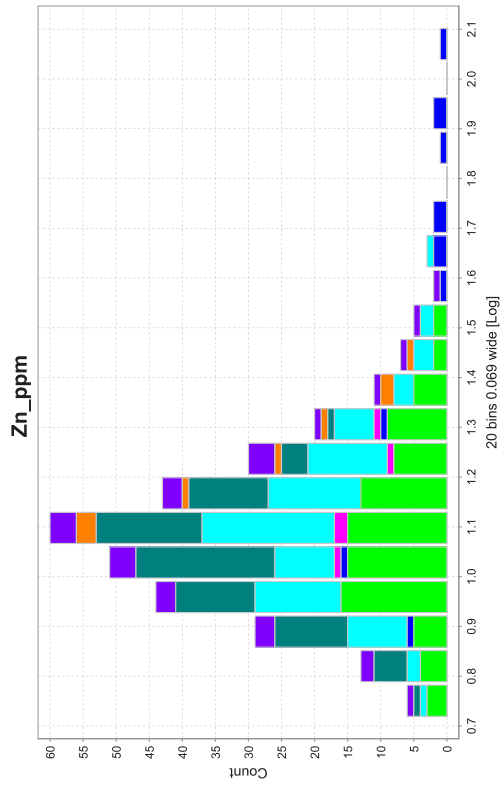
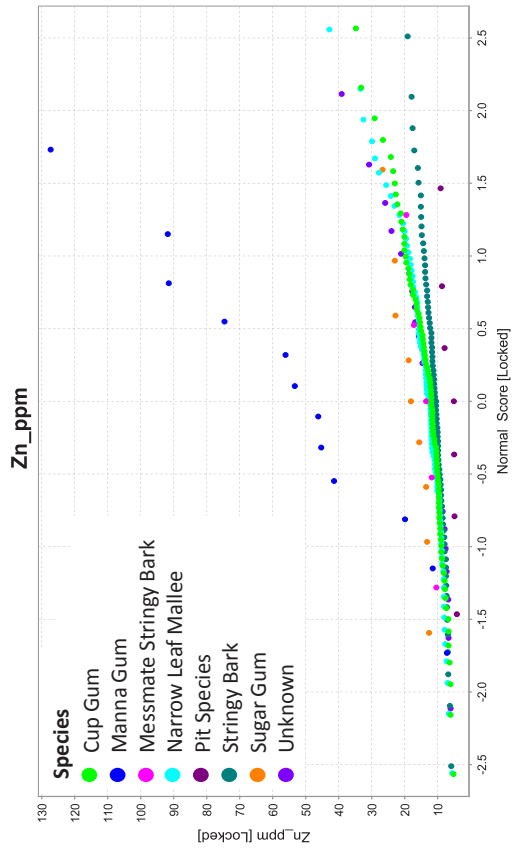
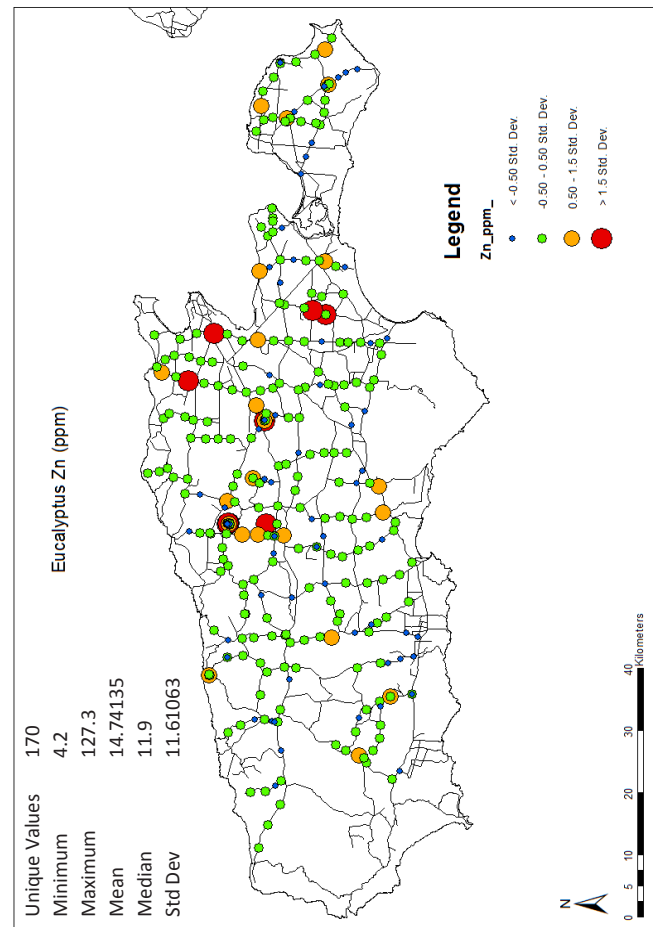


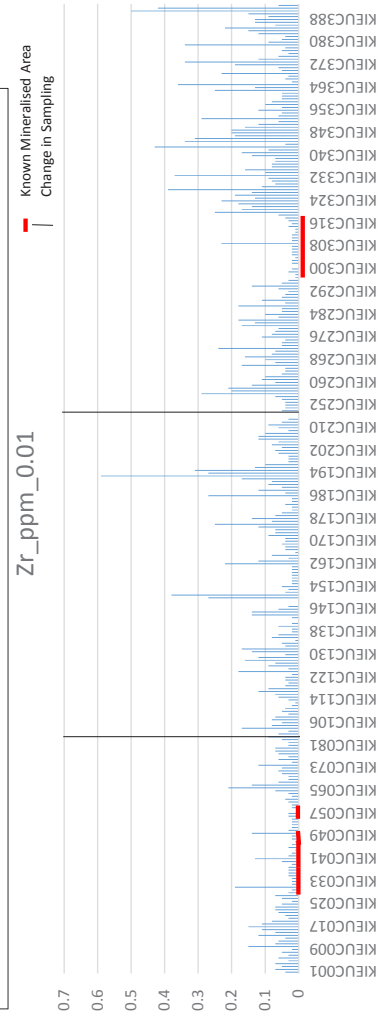
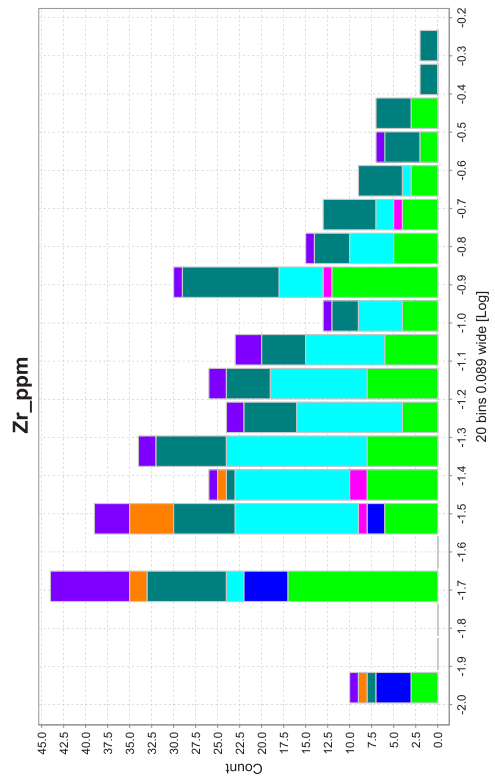
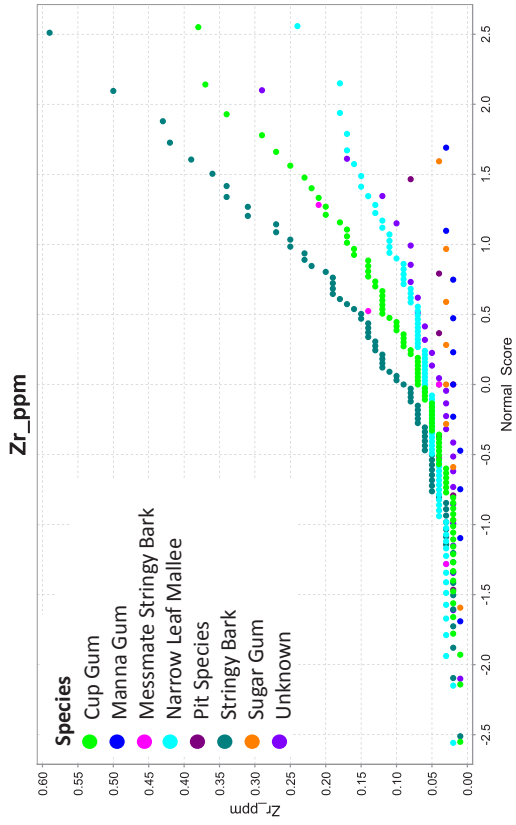
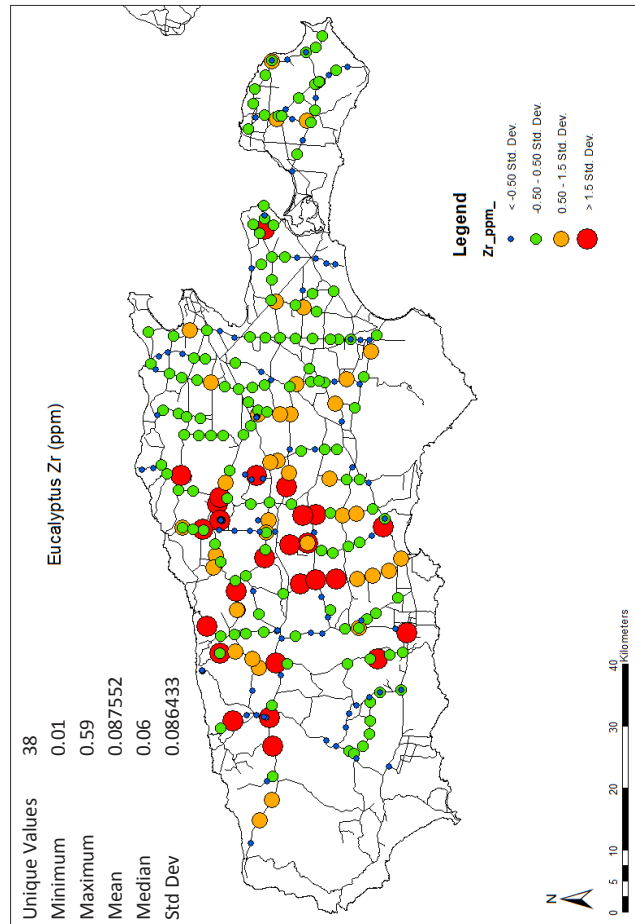




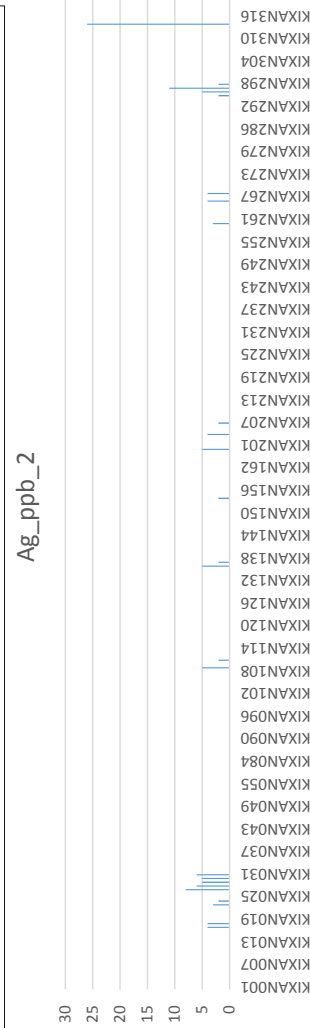
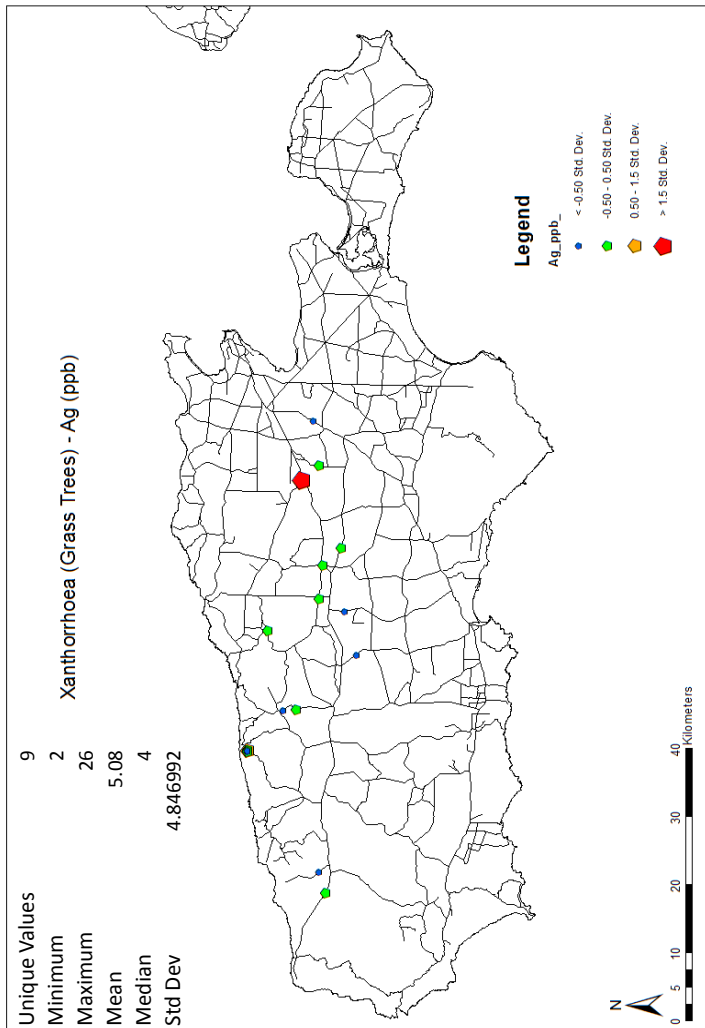
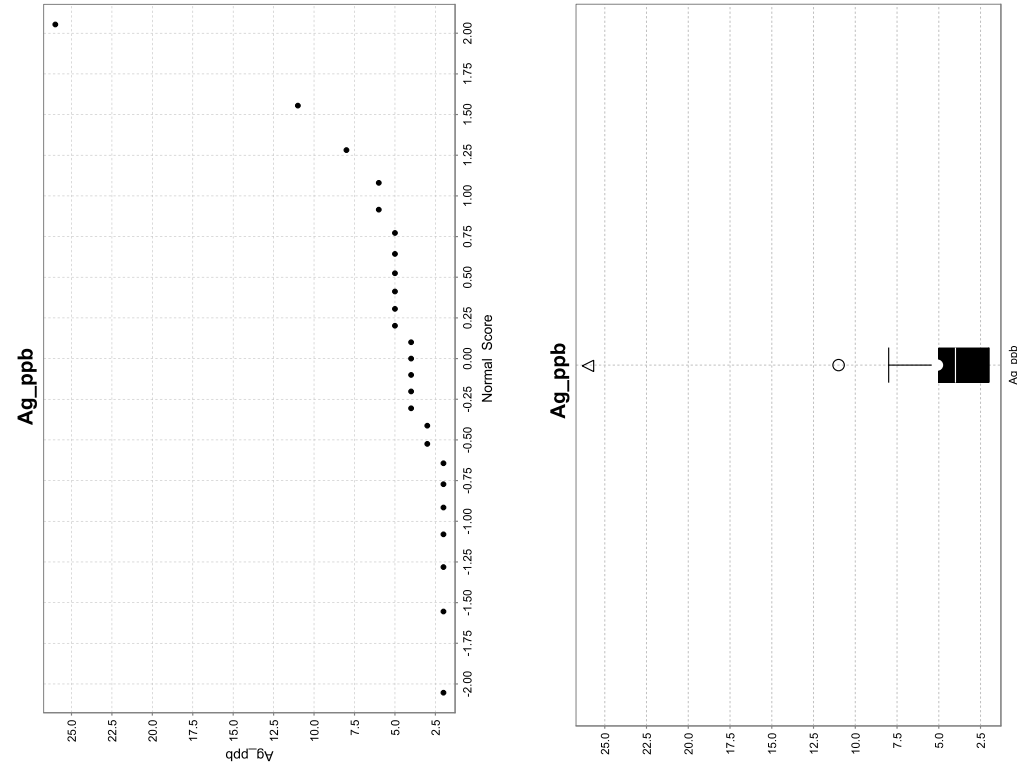


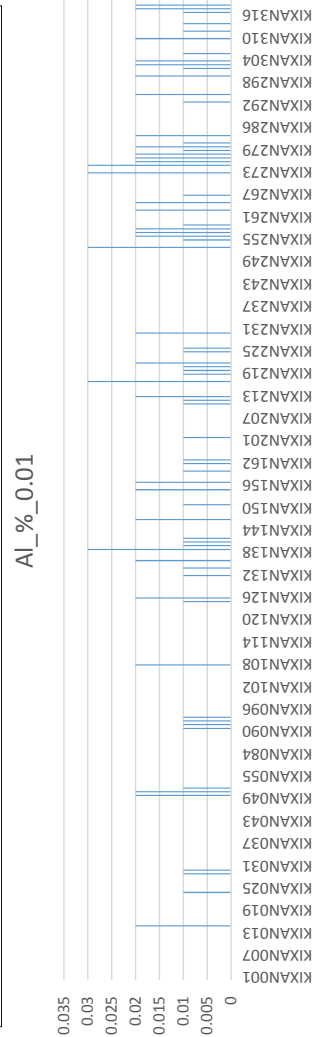
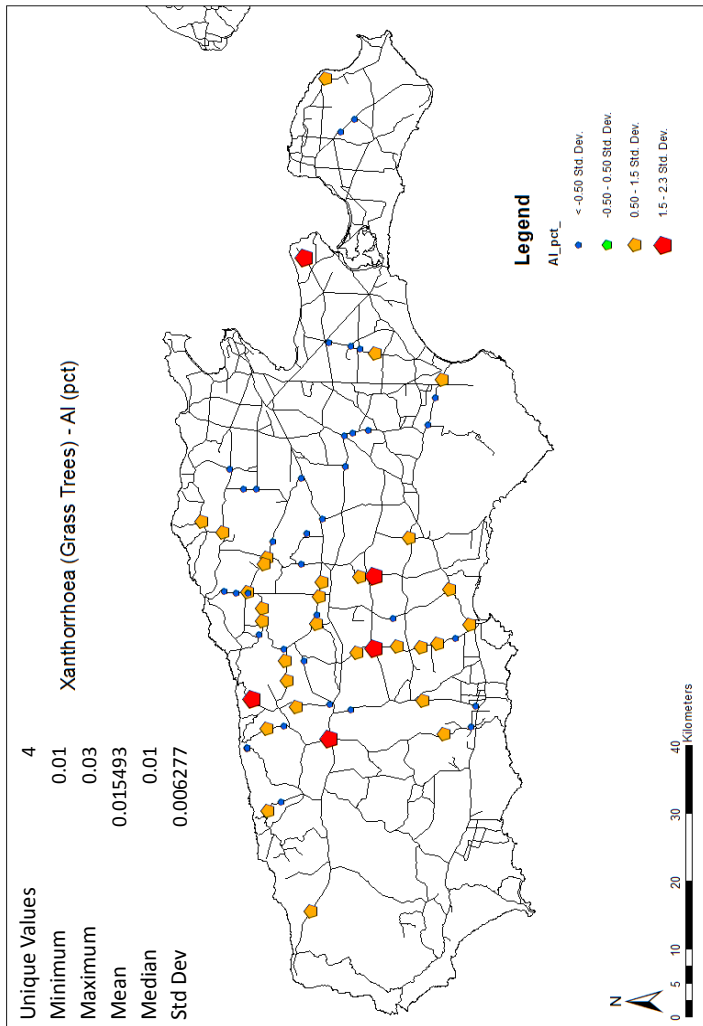
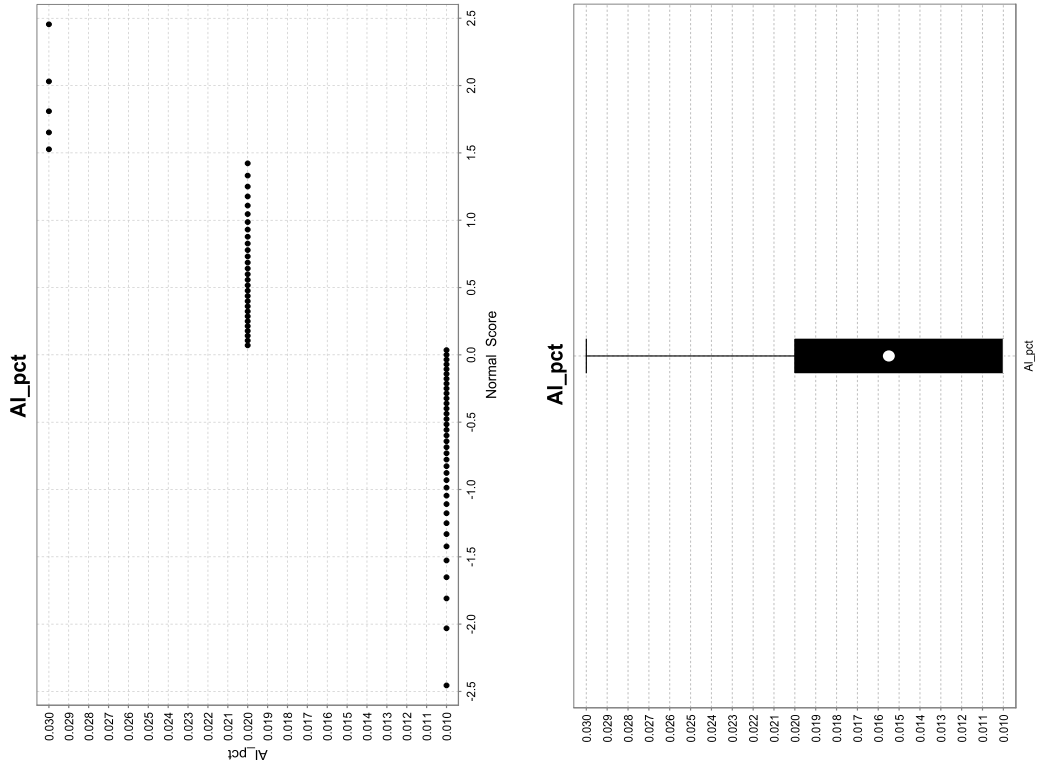


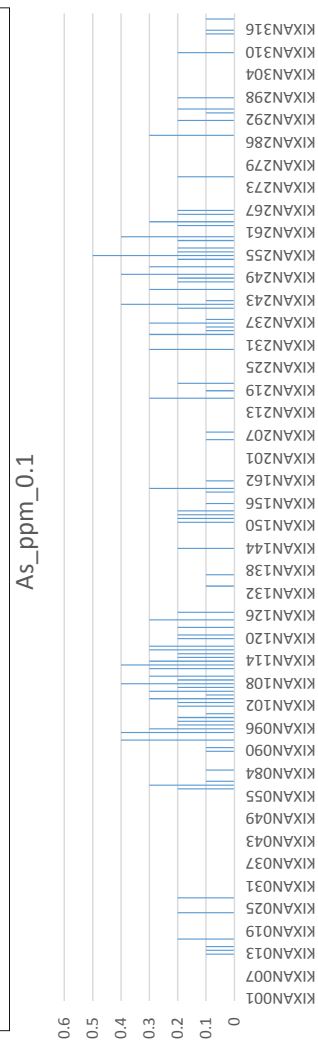
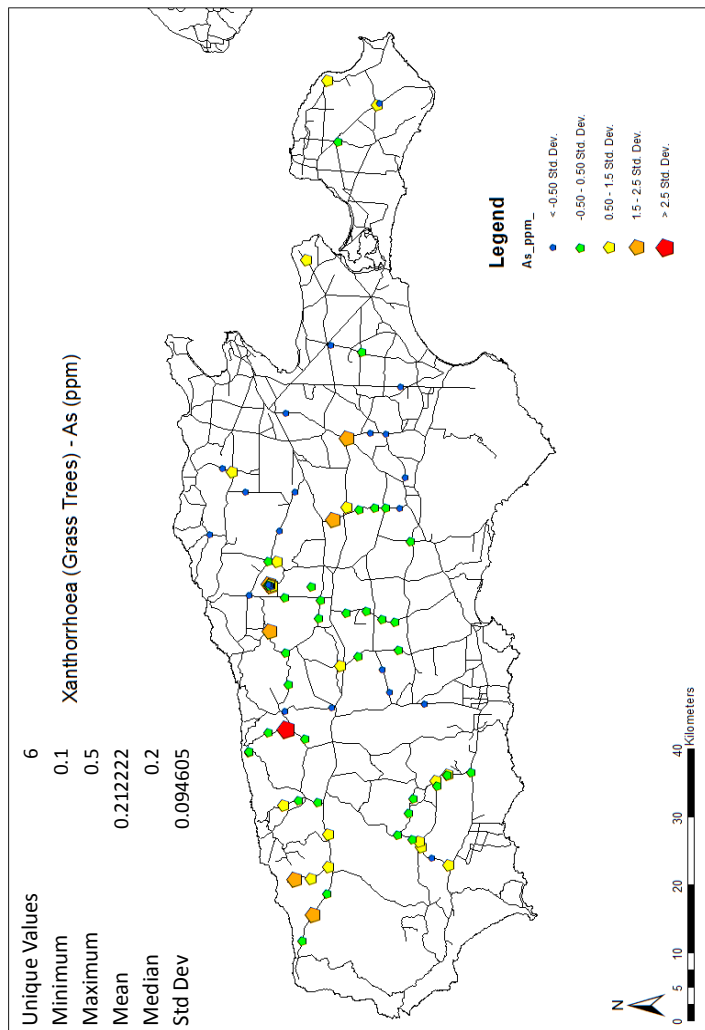
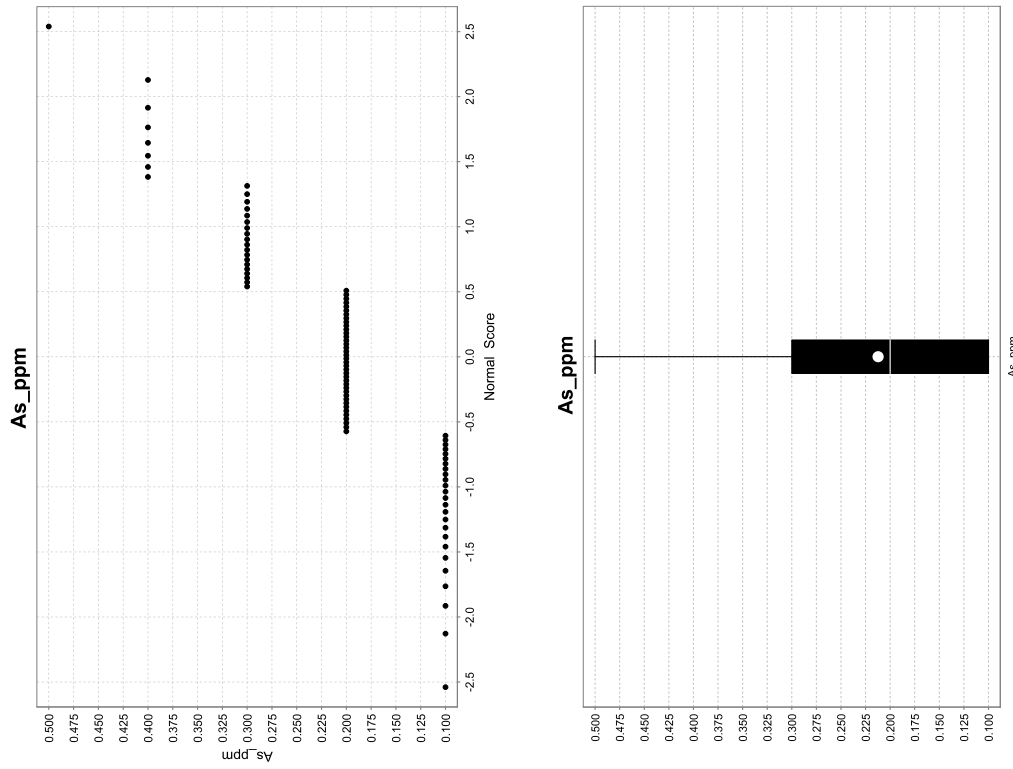


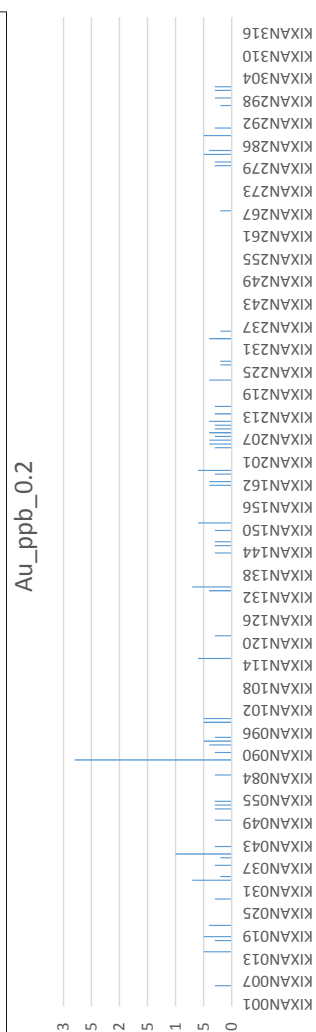
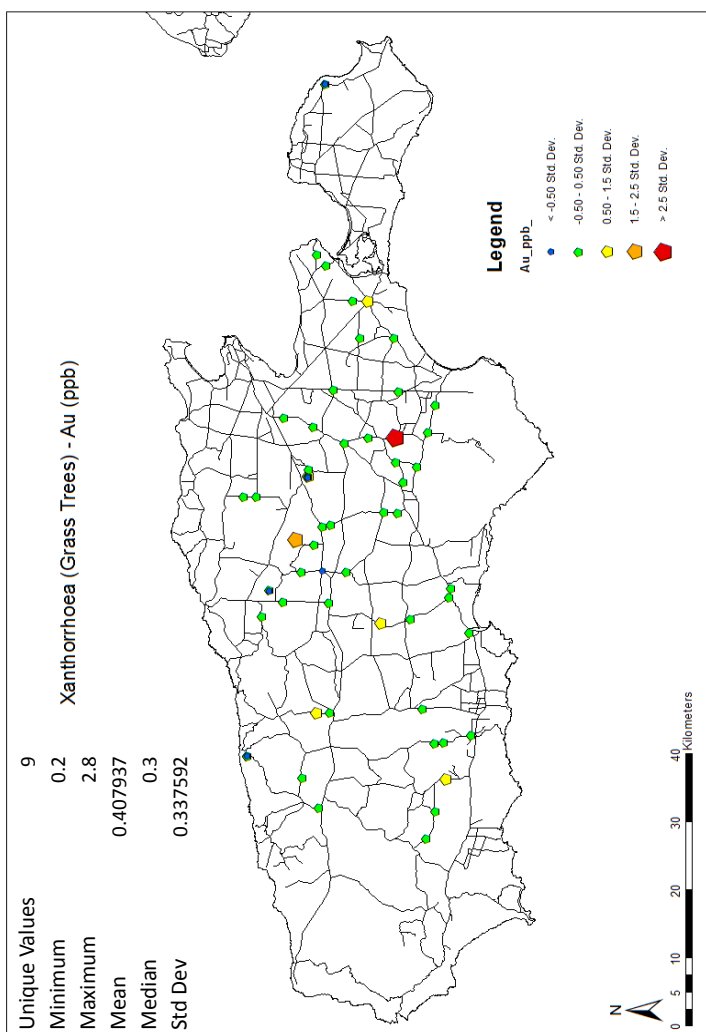
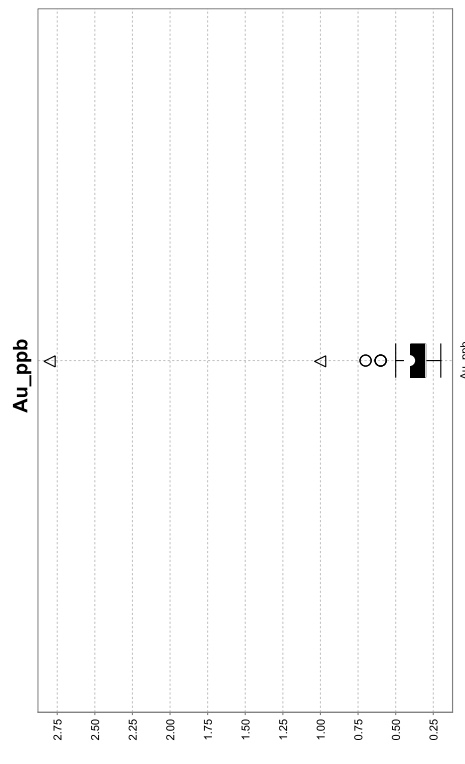
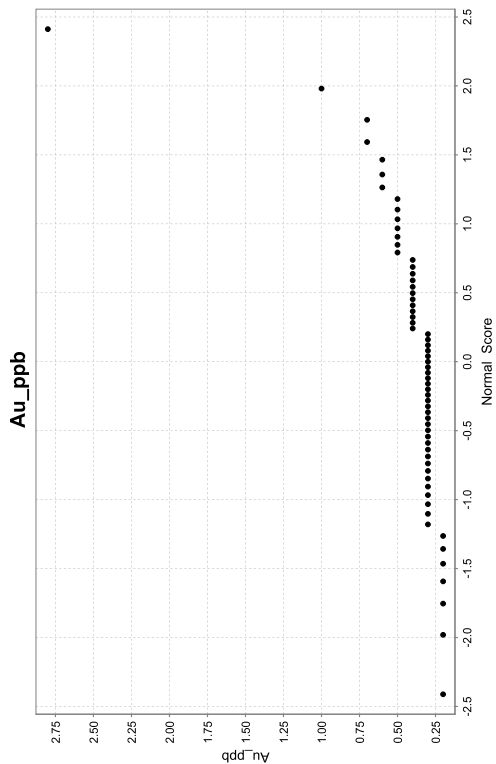


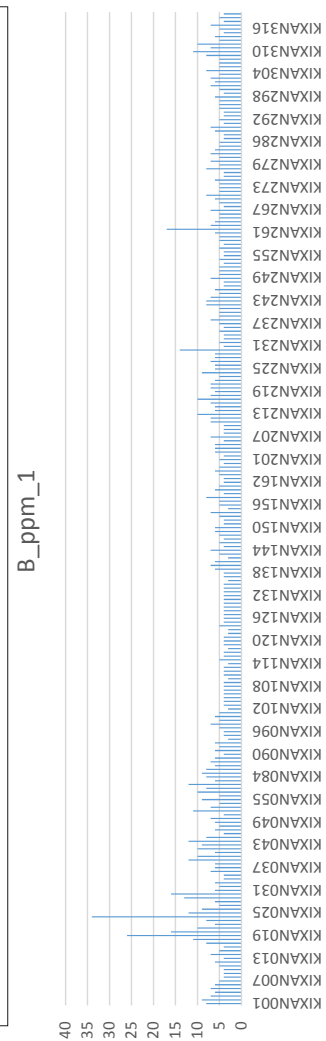
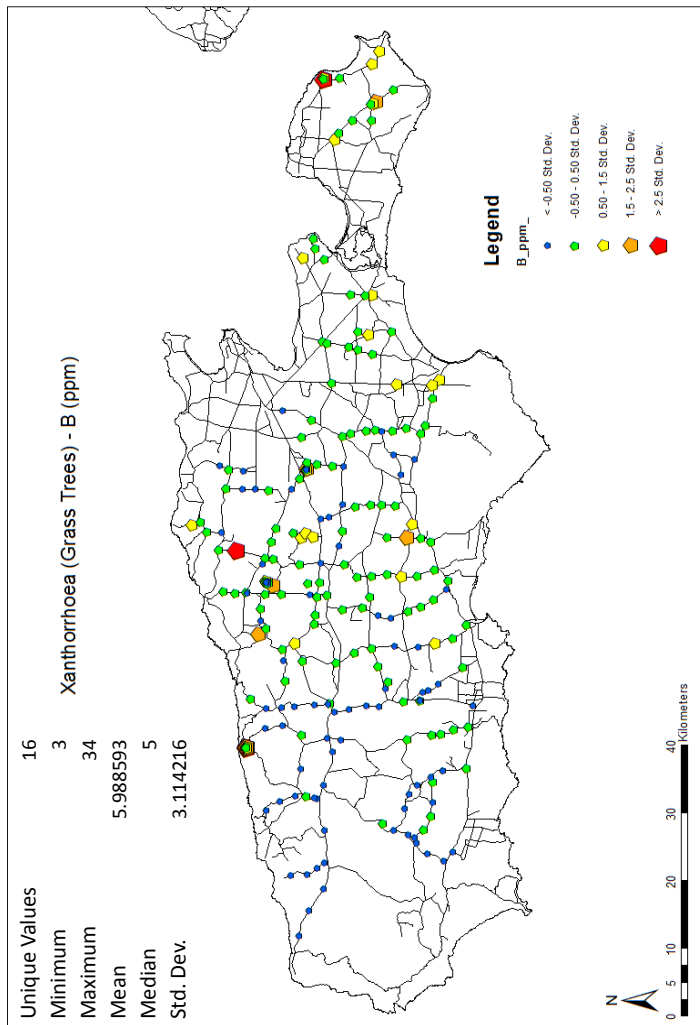
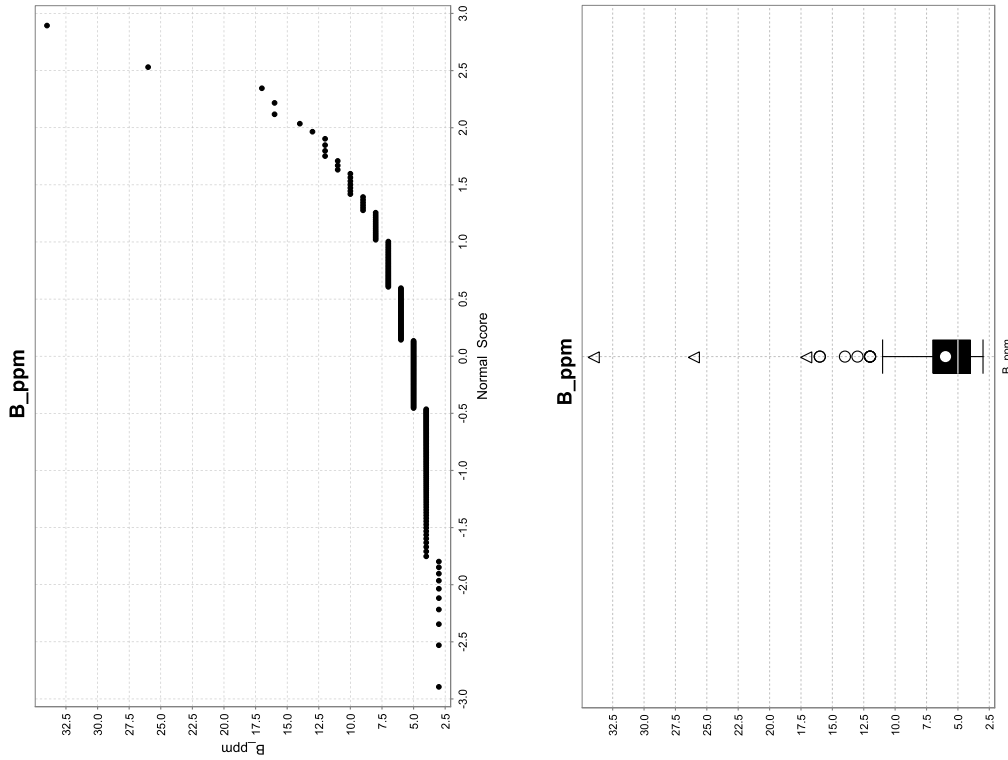
Appendix D: Xanthorrhoea Maps and Graphs

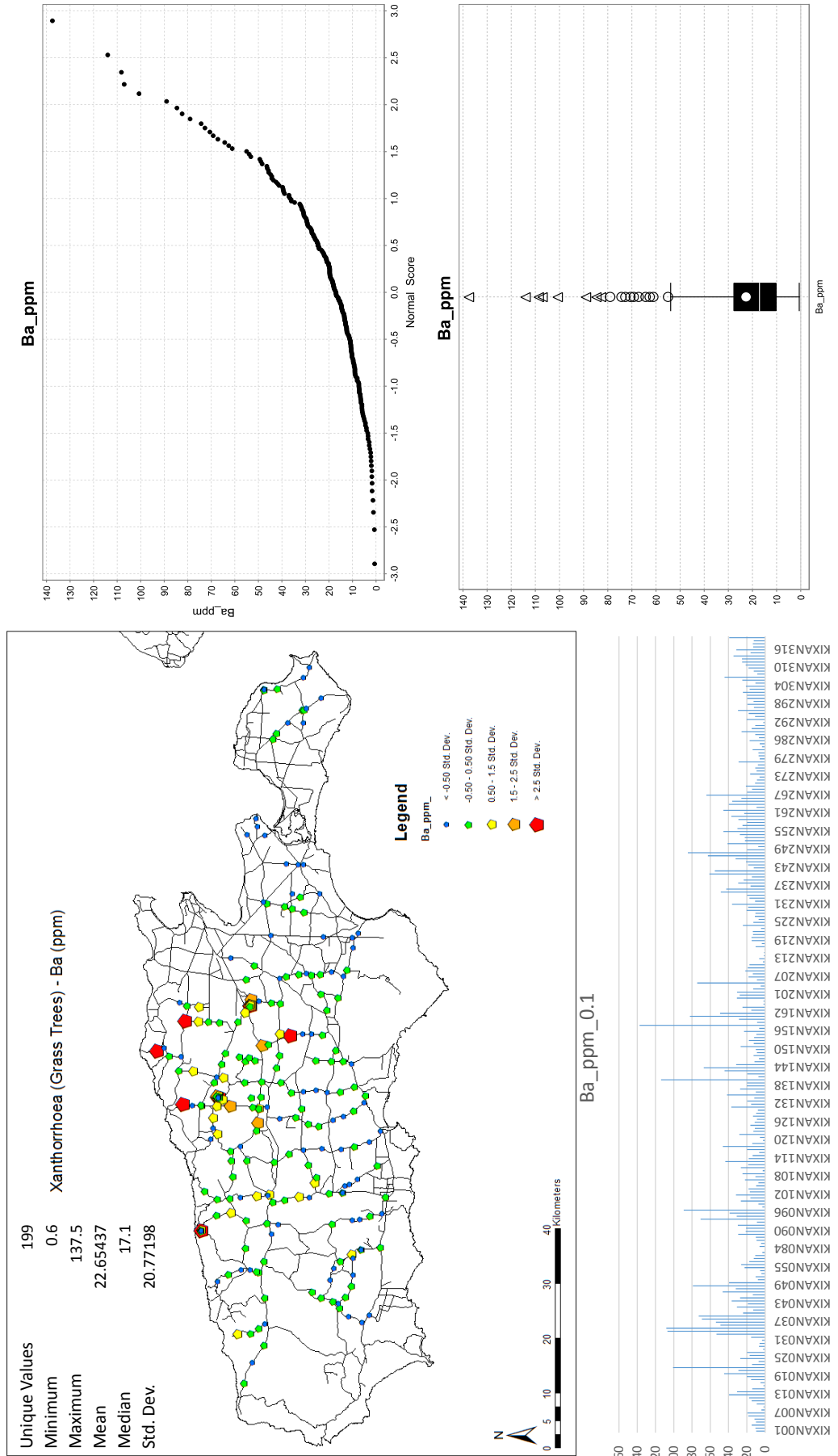


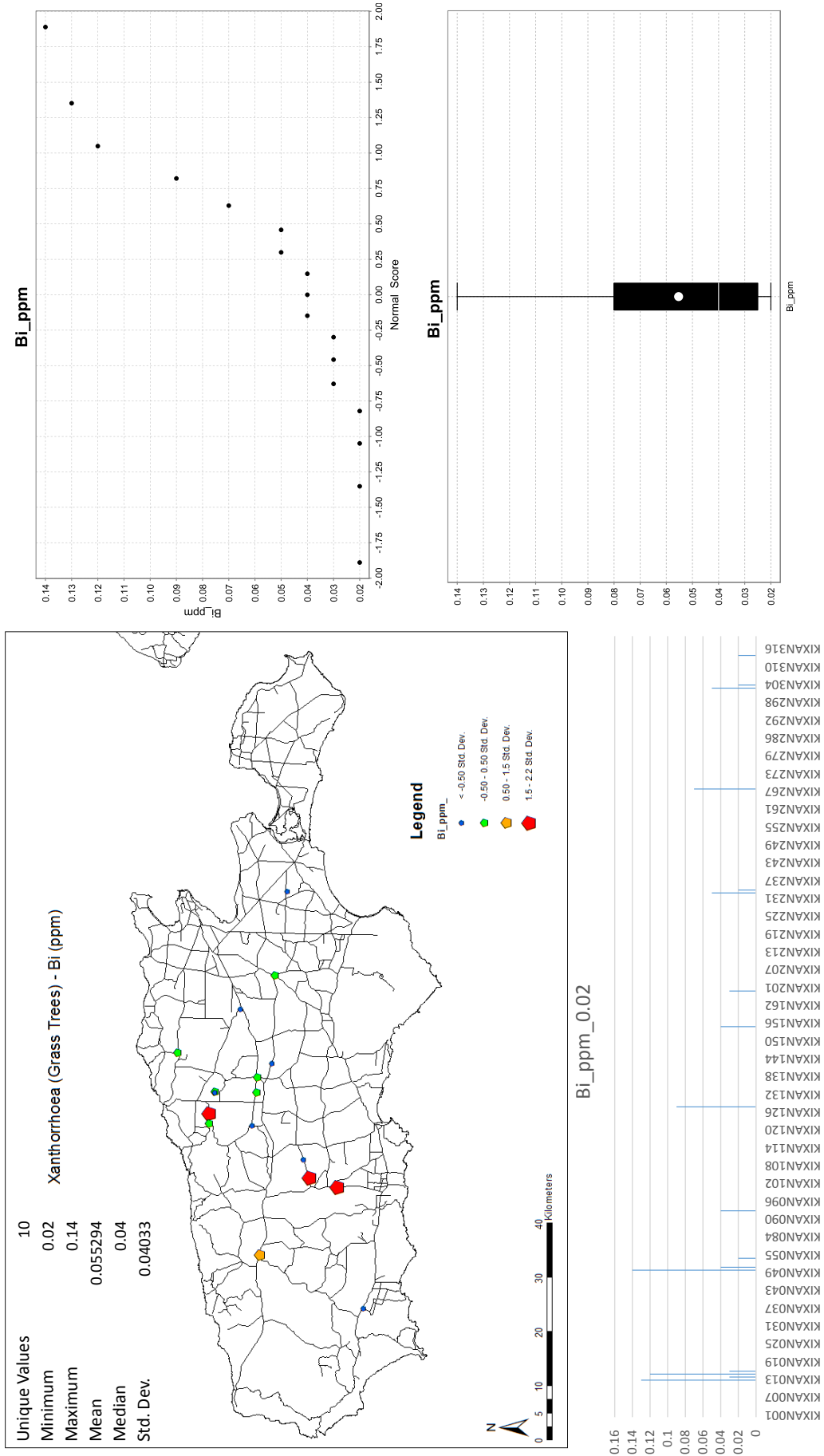


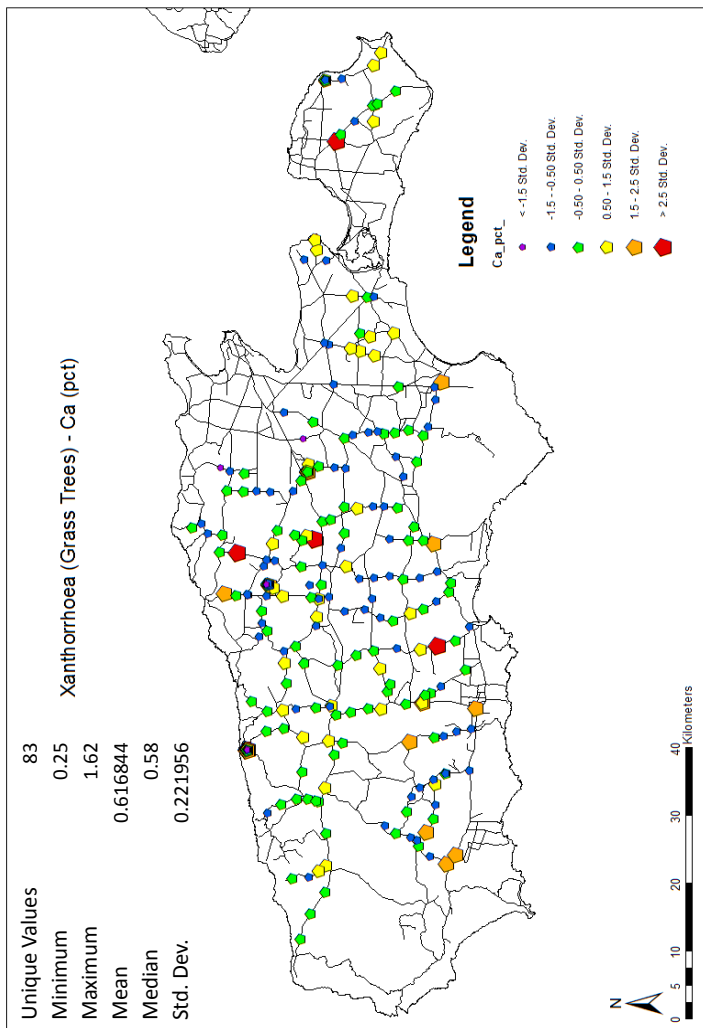
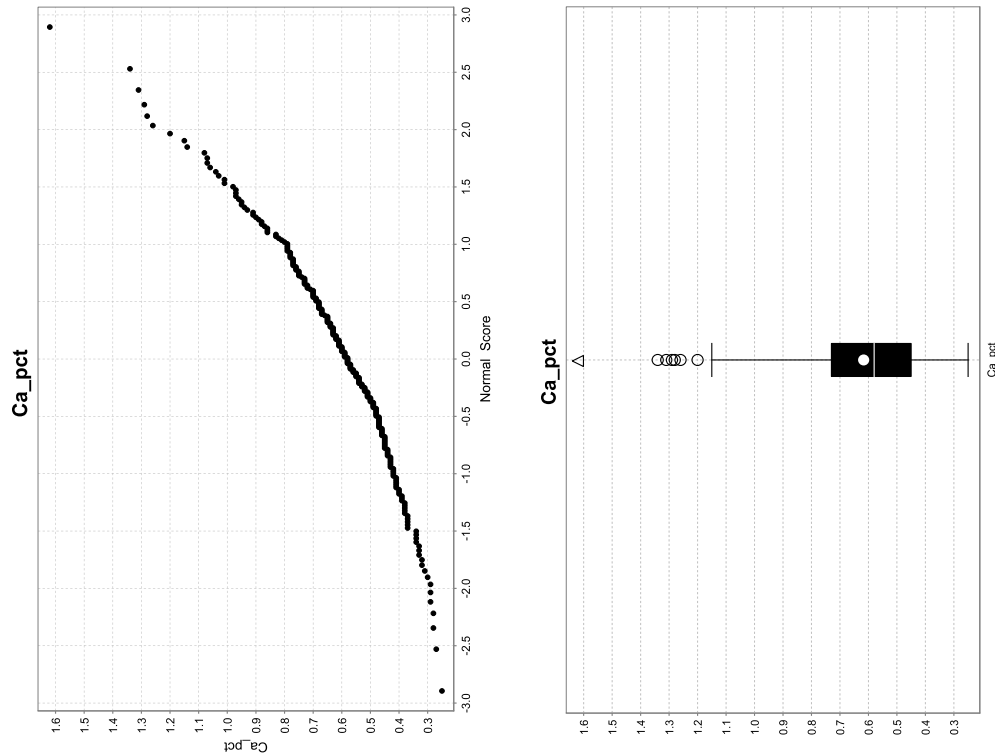






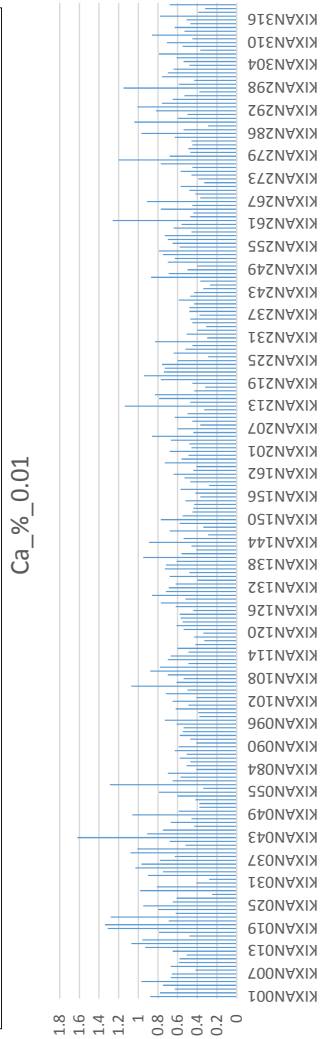


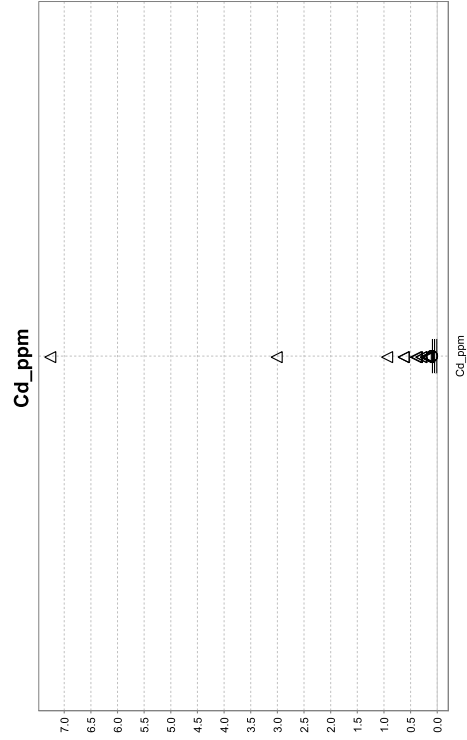
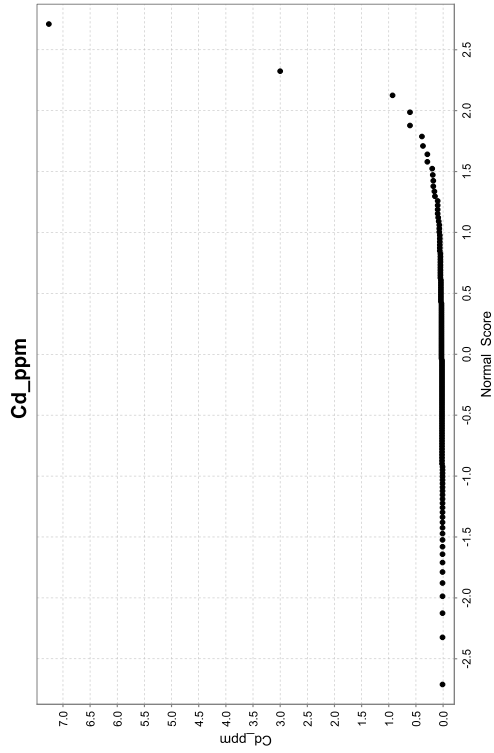
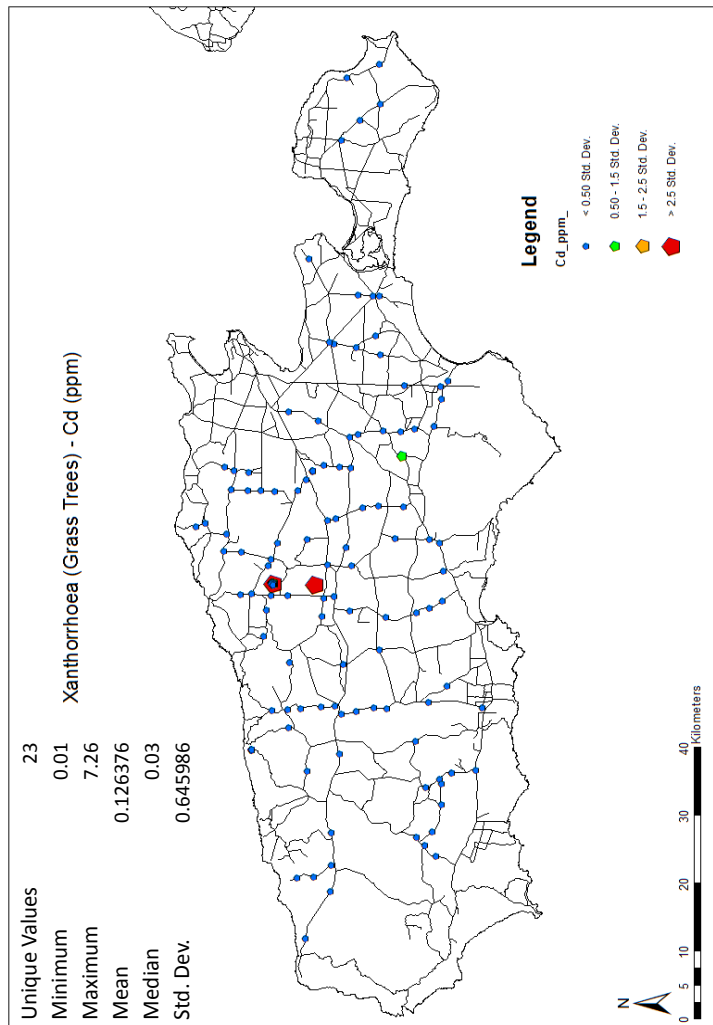


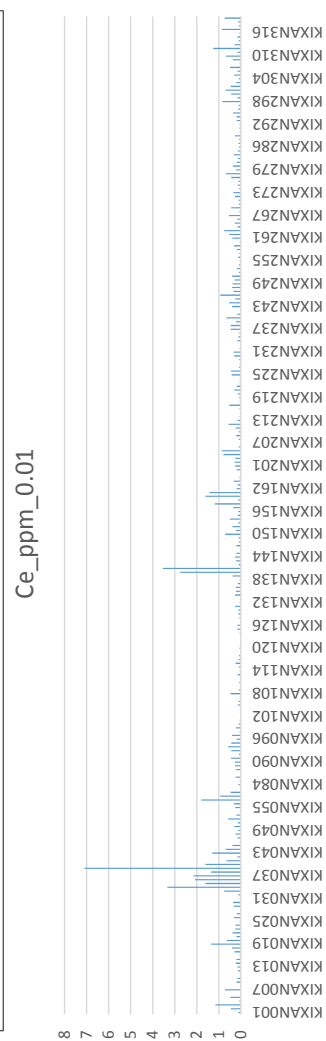
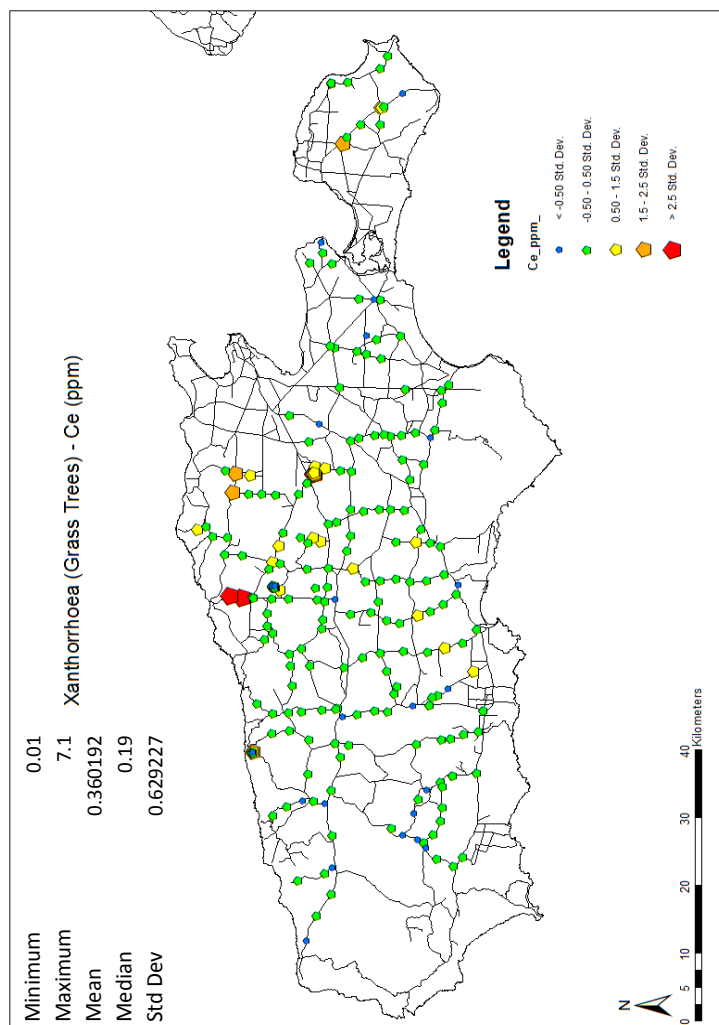
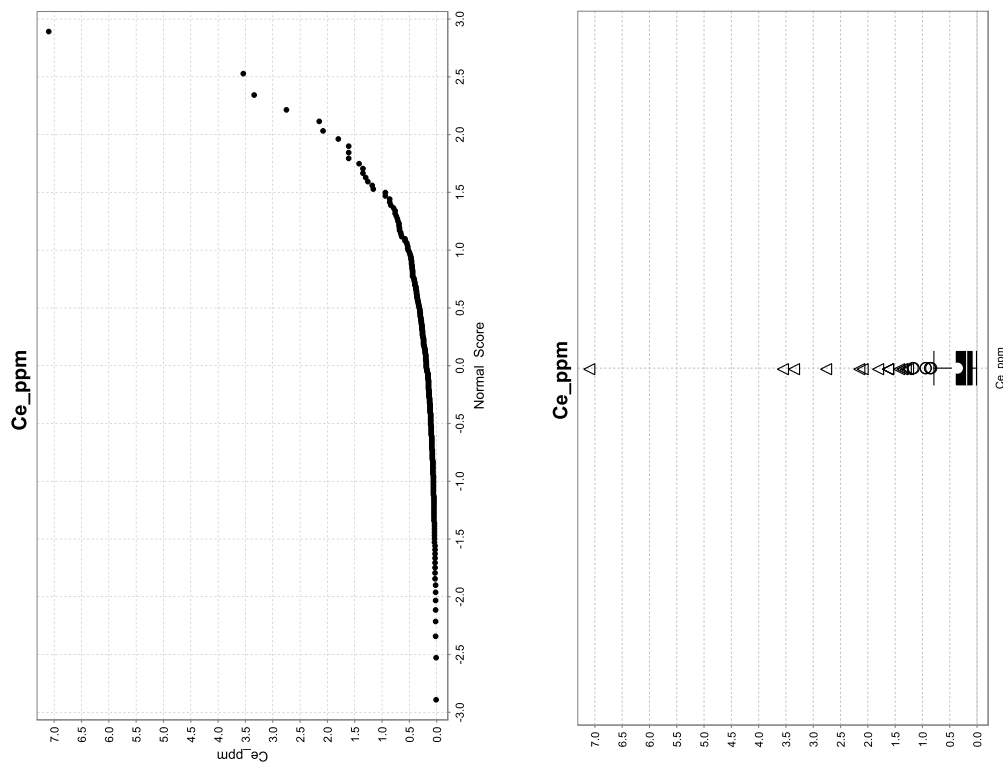


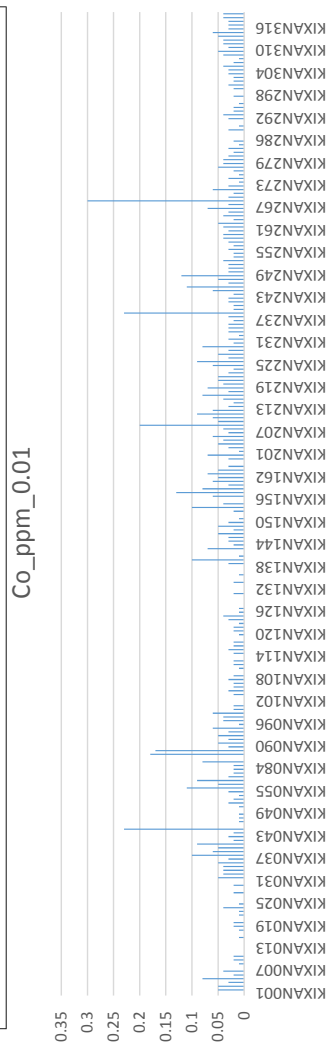
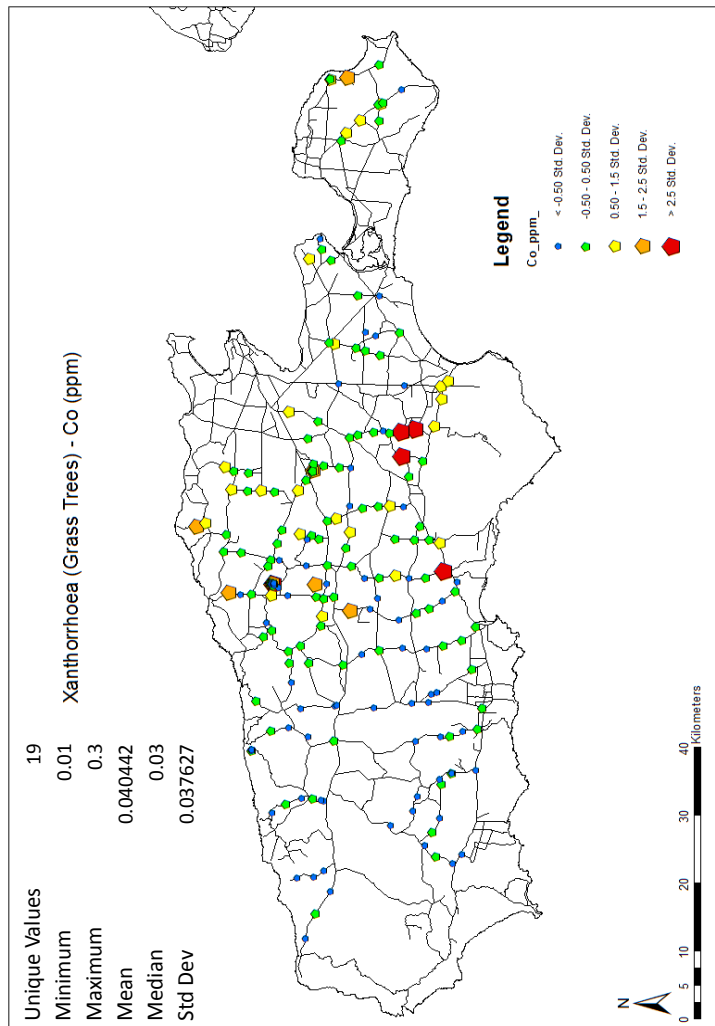
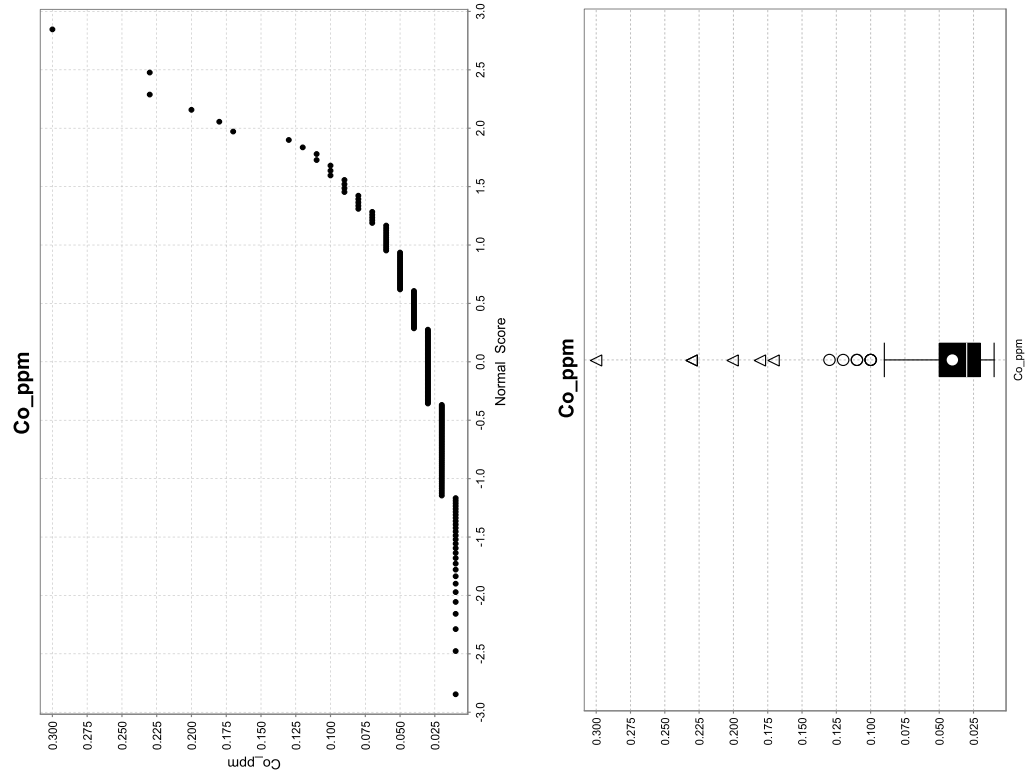
Unique Values 83
Minimum 0.25
Maximum 1.62
Mean 0.616844
Median 0.58
Std. Dev. 0.221956

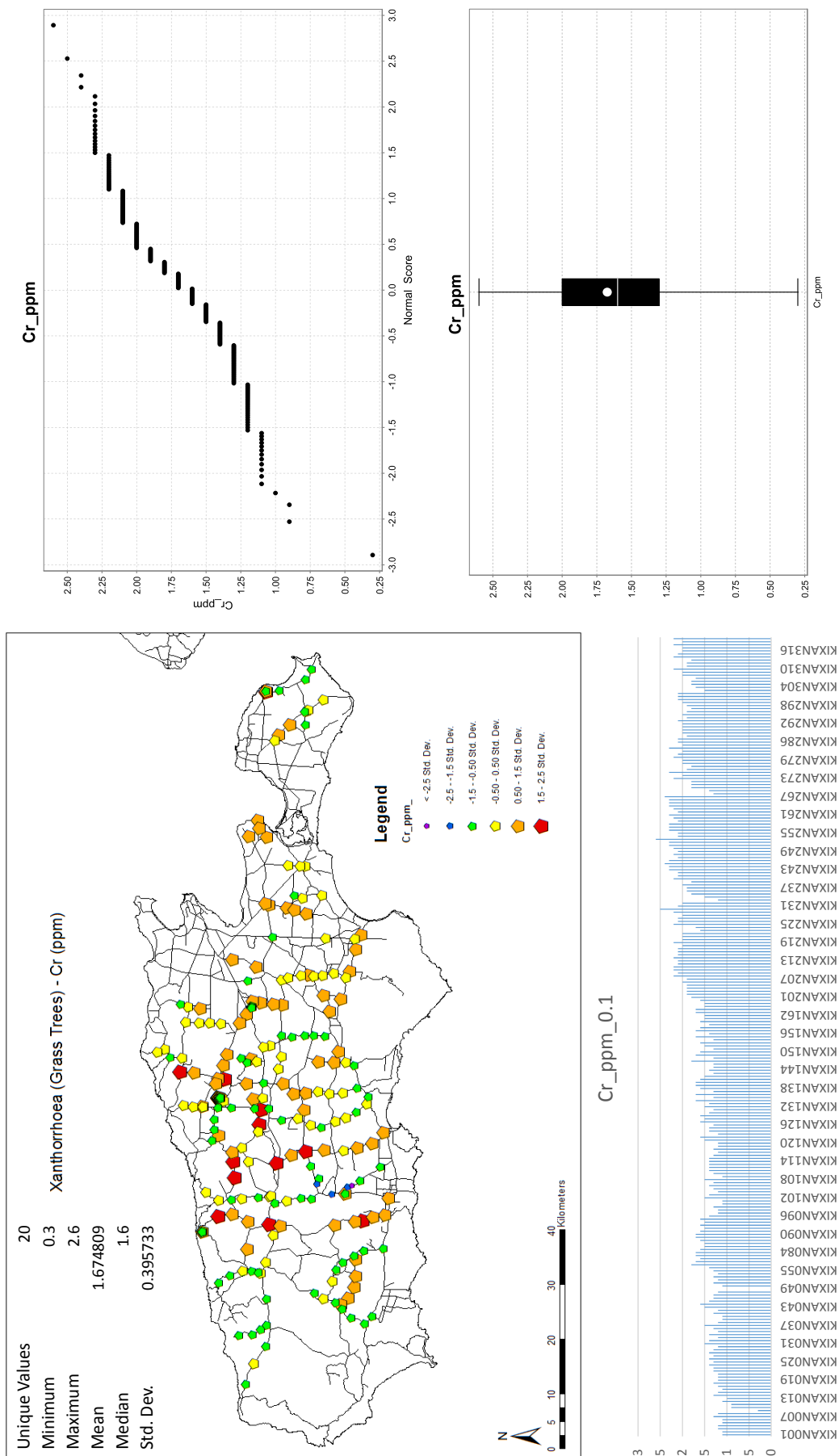
Xanthorrhoea (Grass Trees) - Ca (pct)

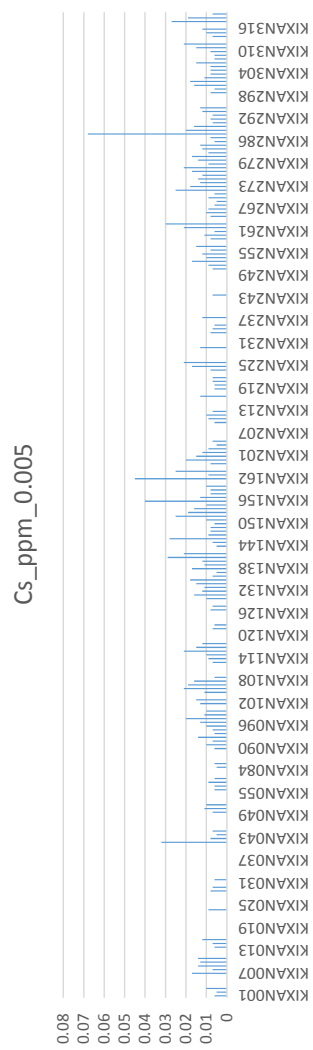
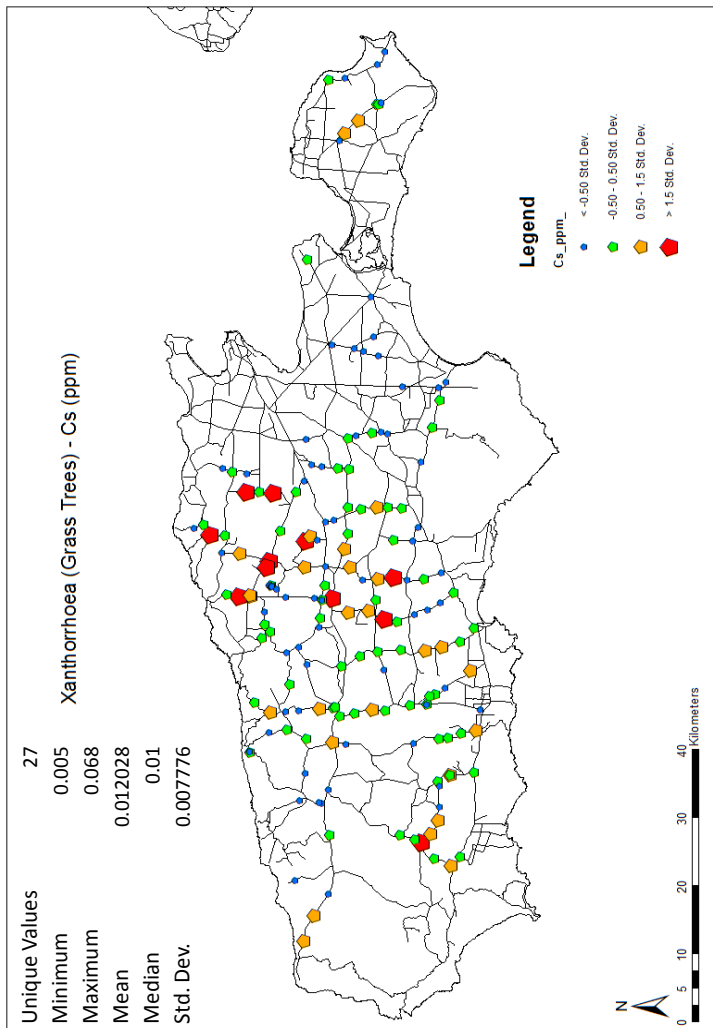
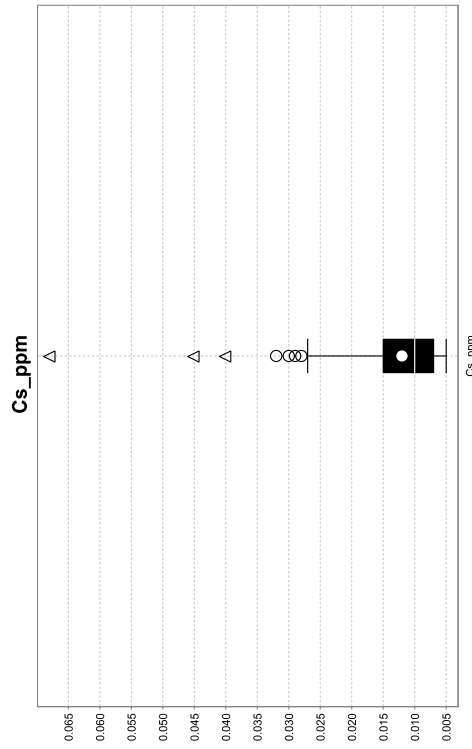
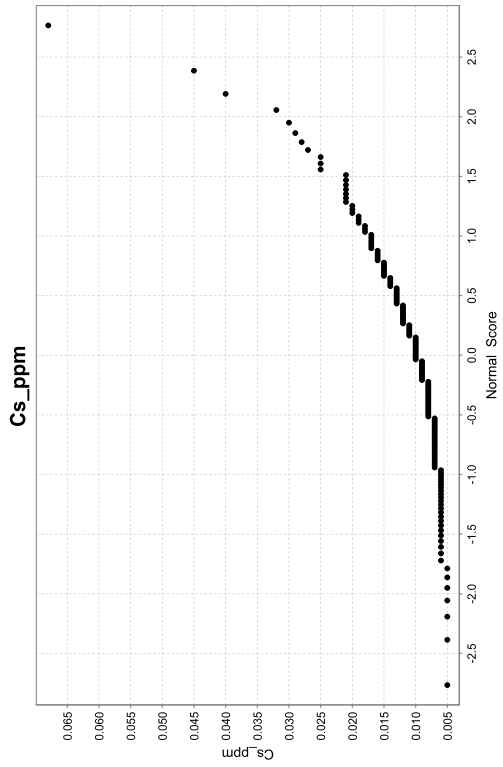


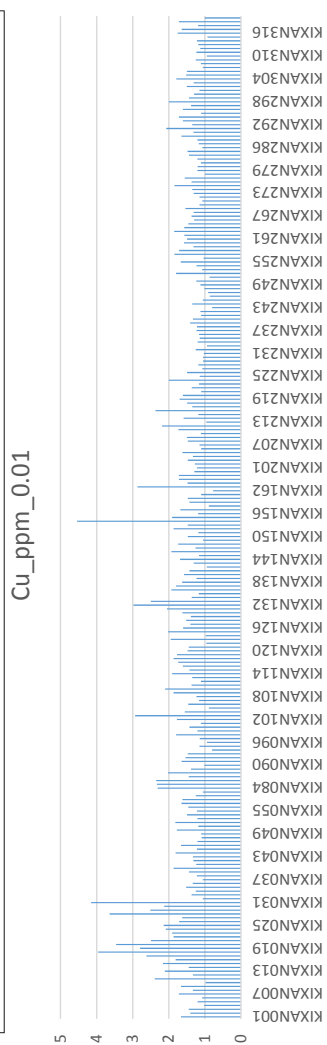
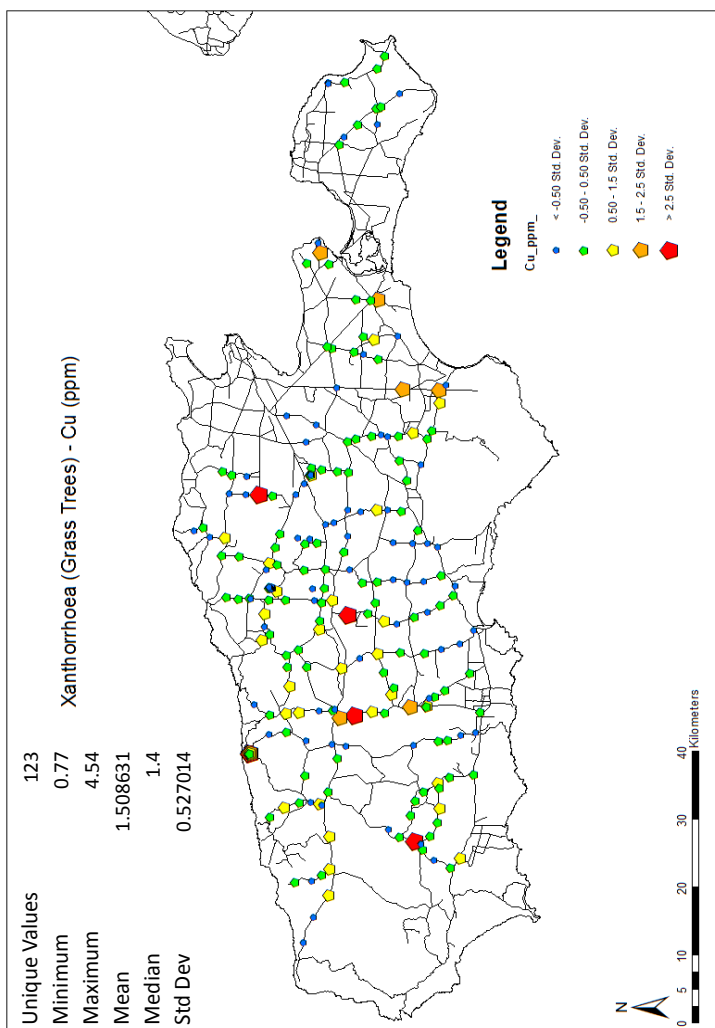
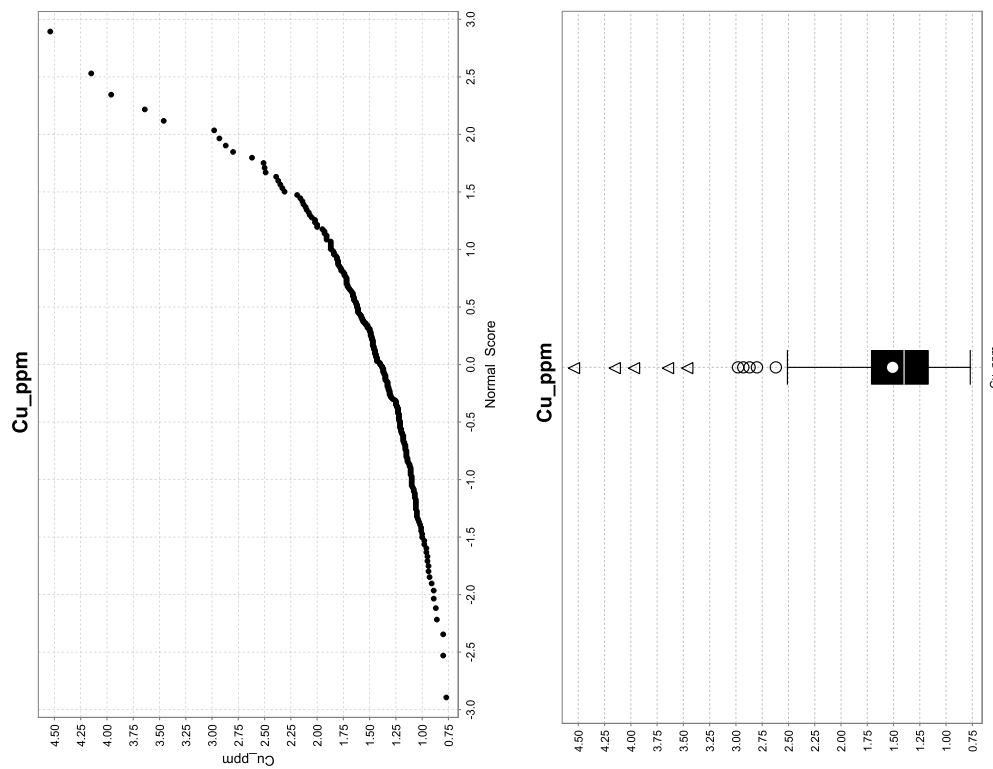


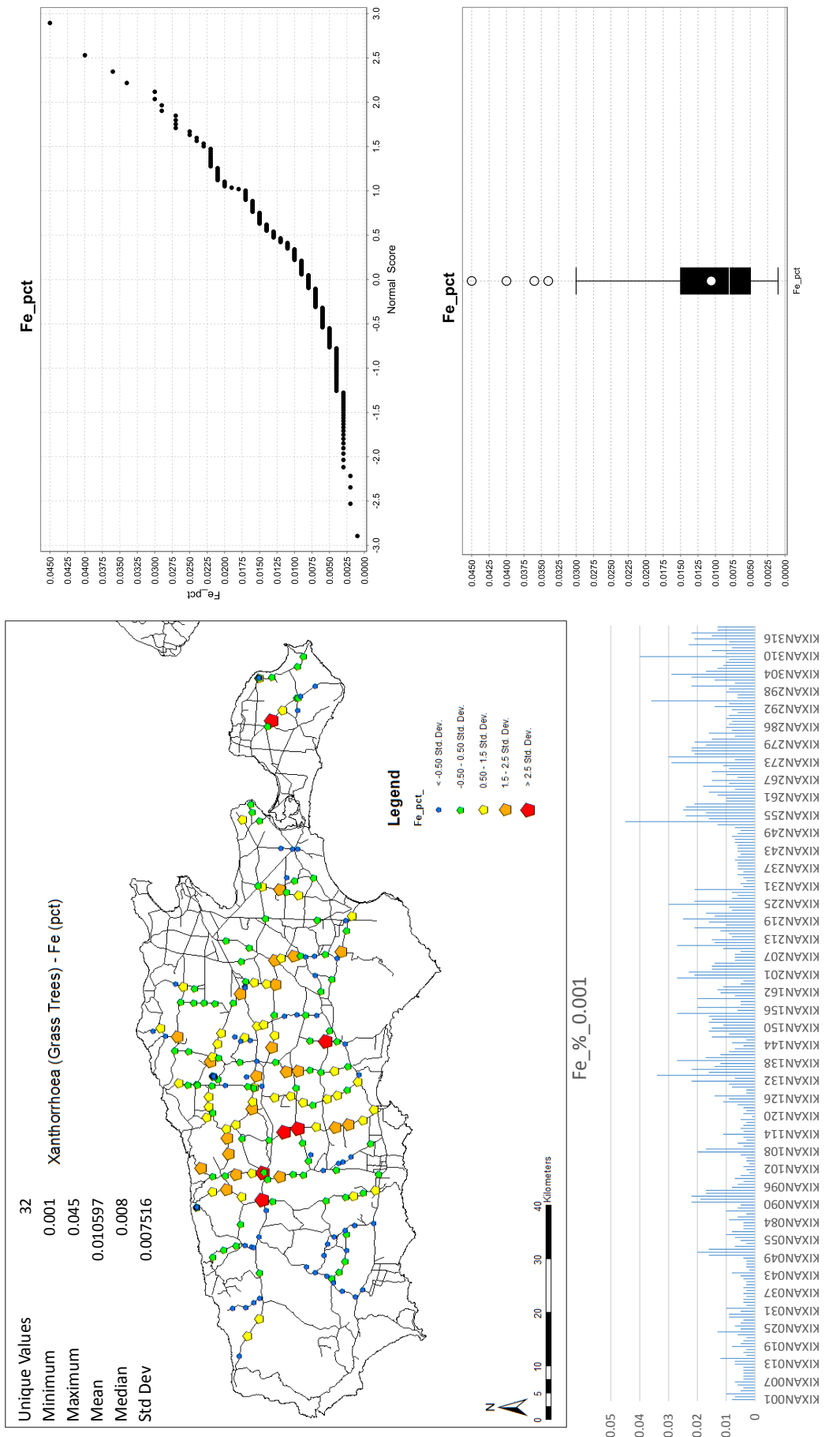


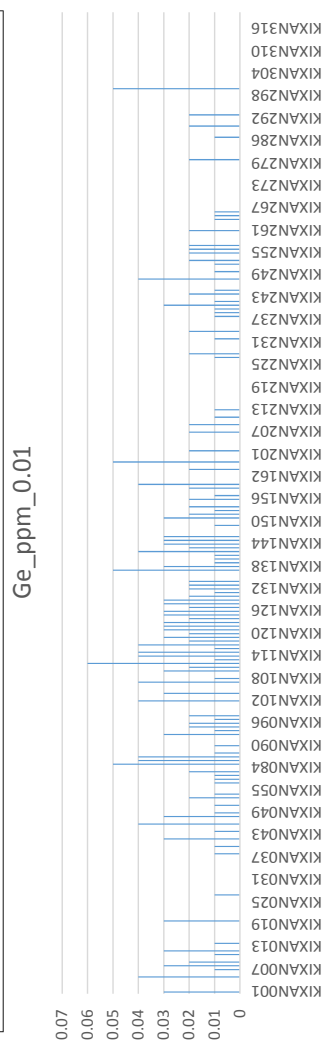
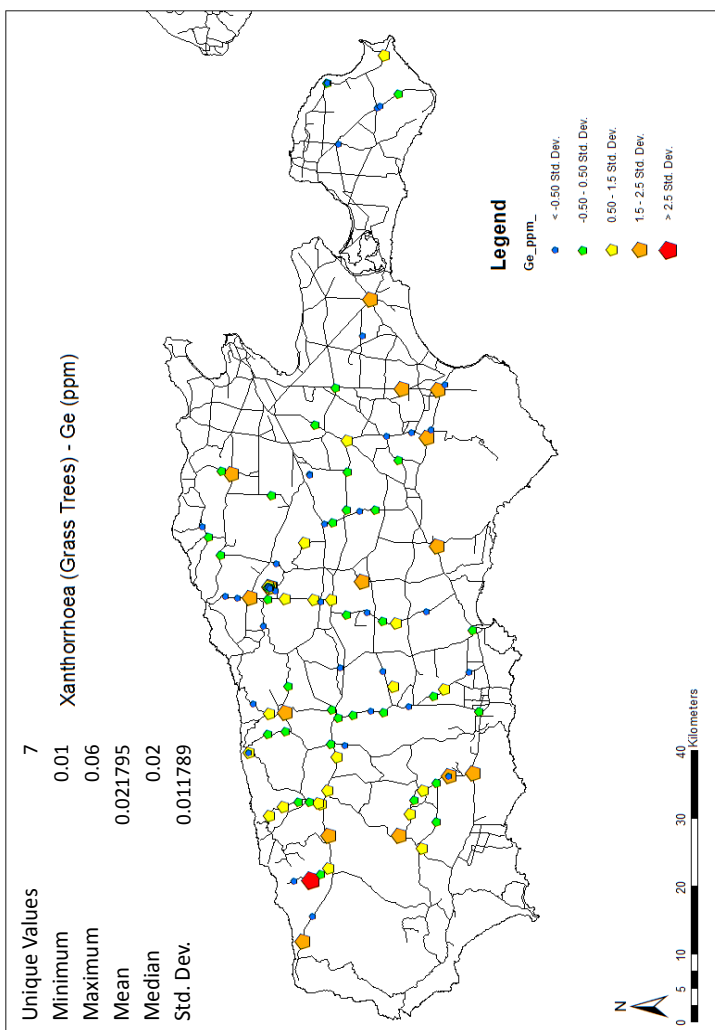
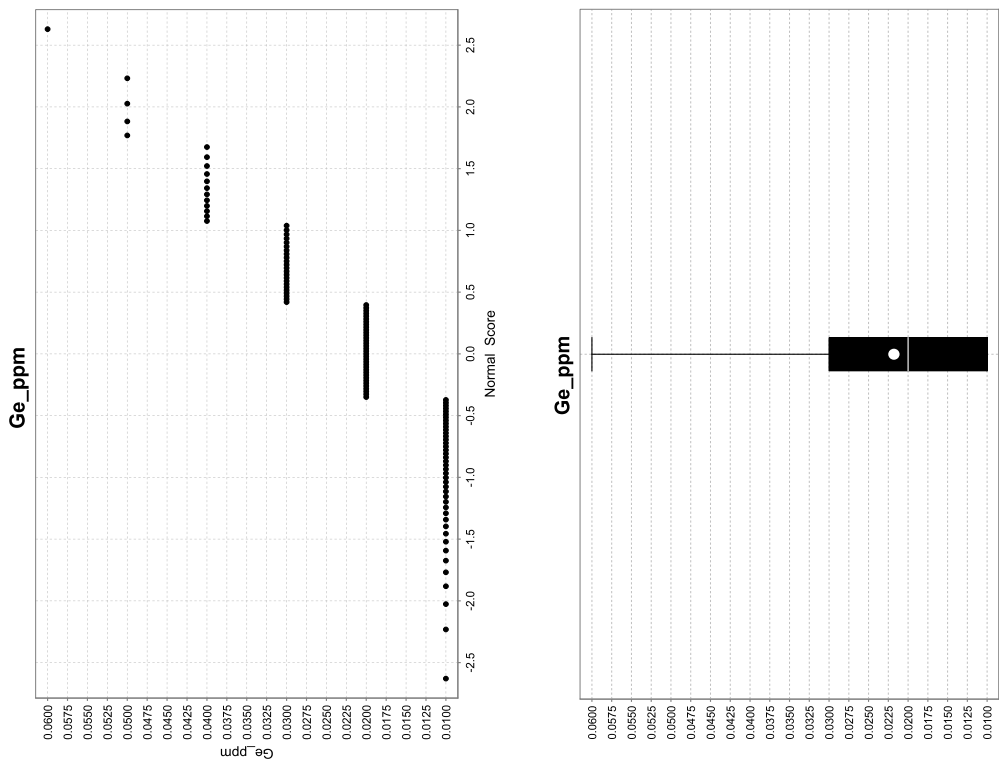


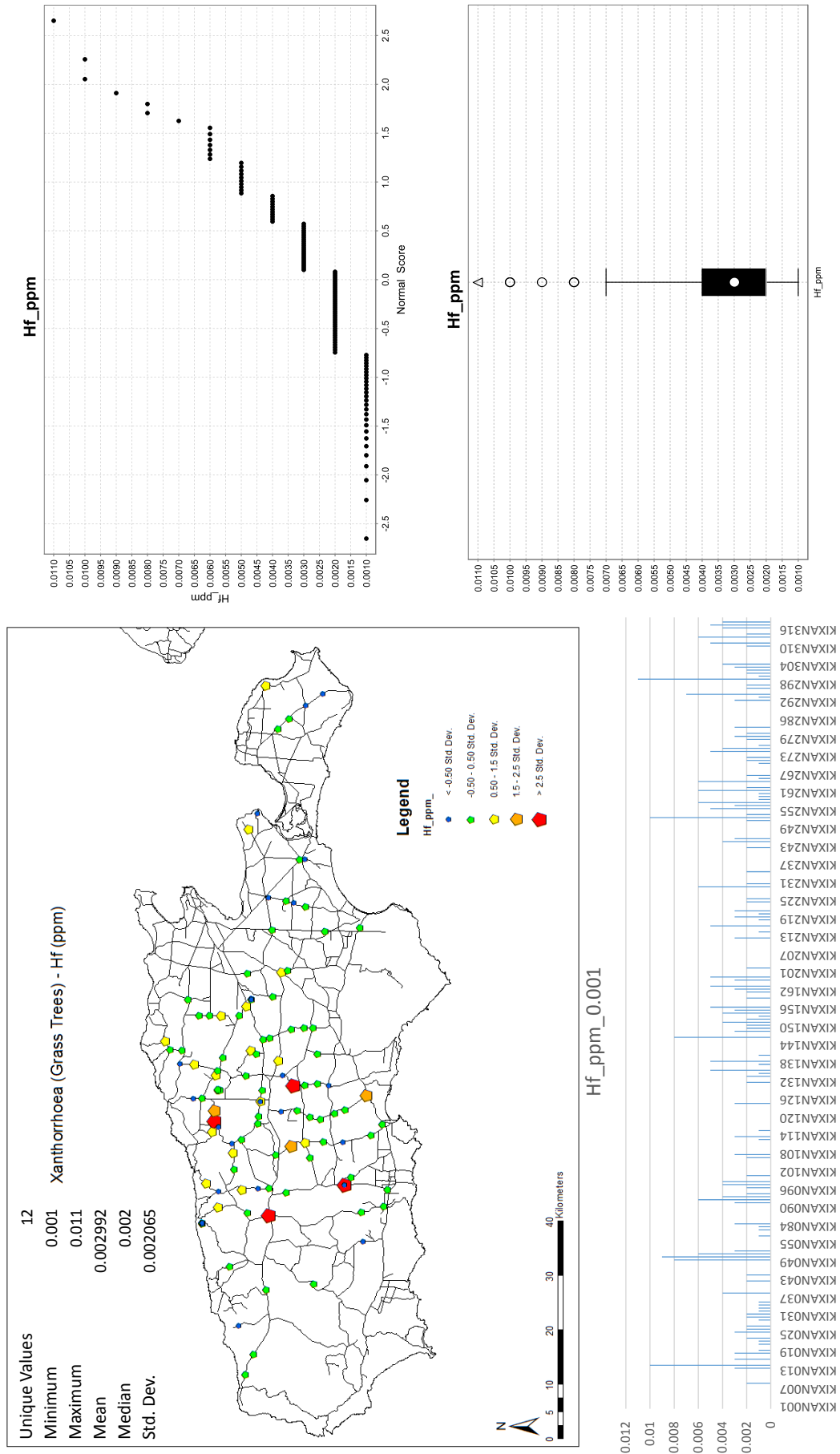


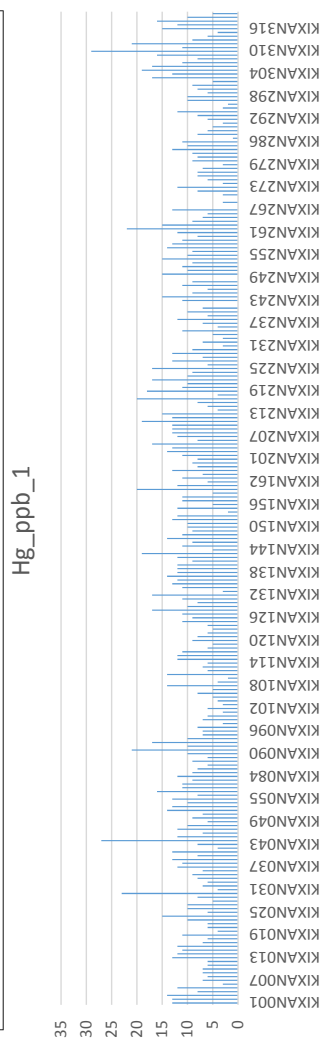
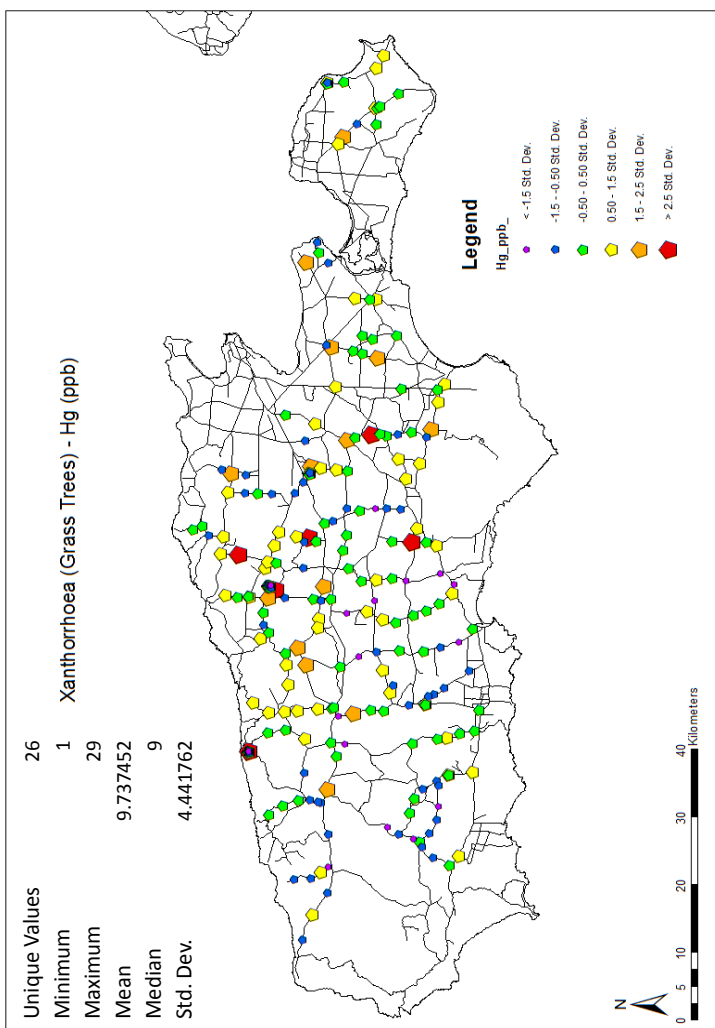
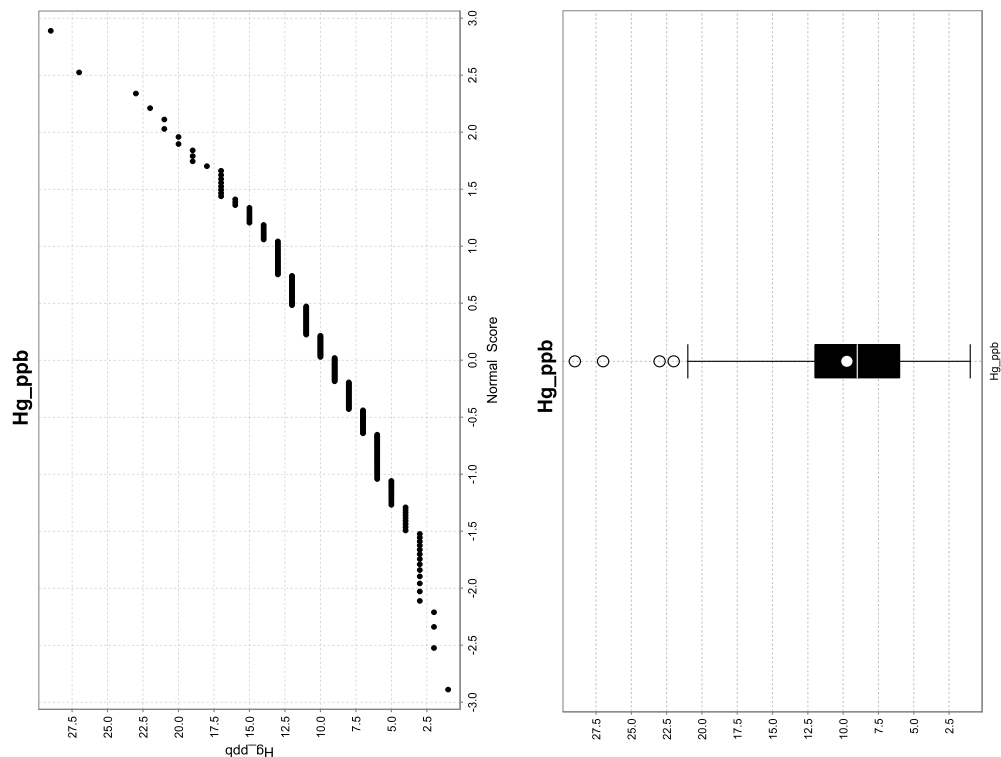


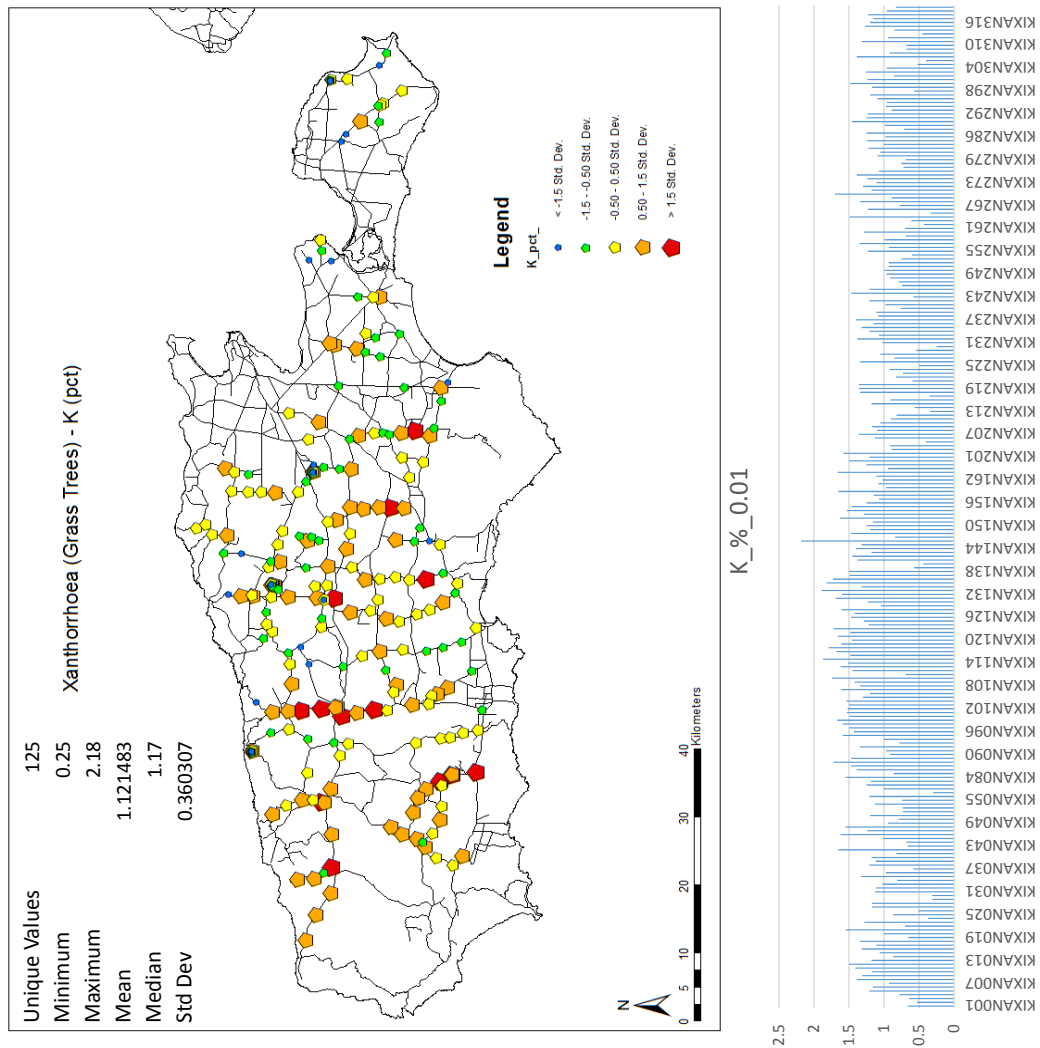
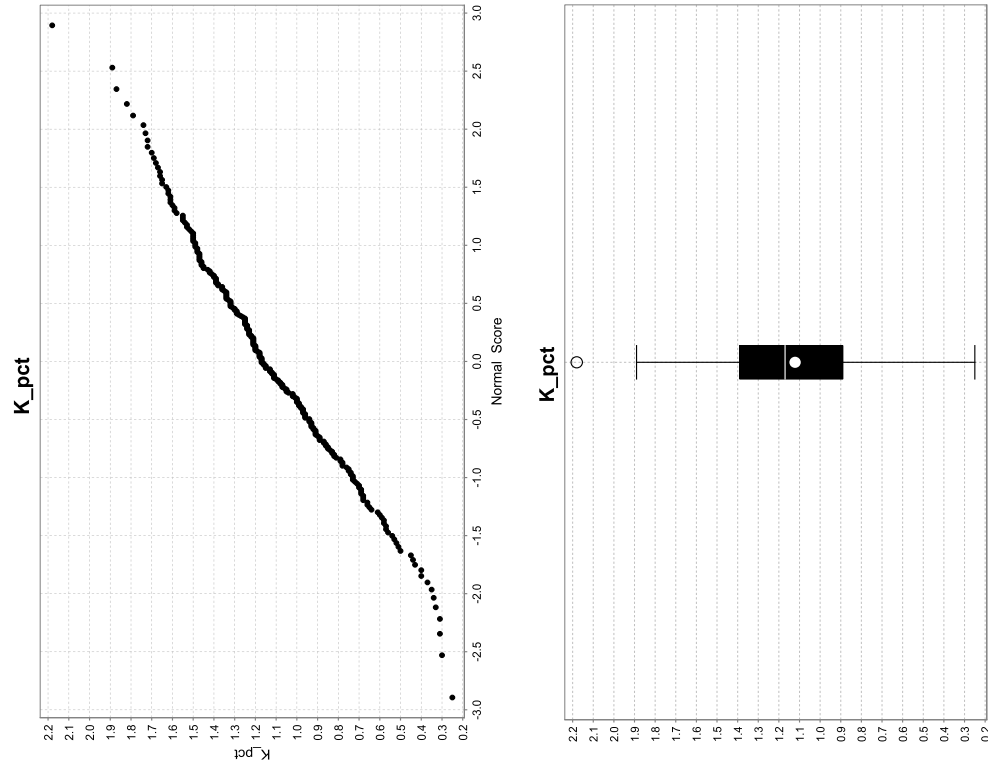


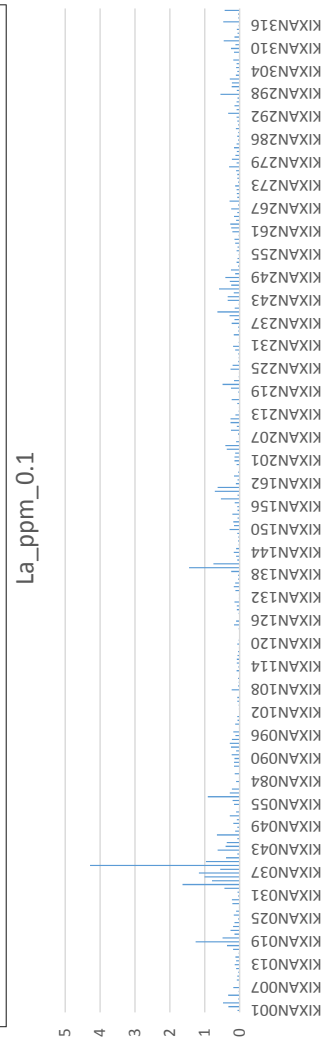
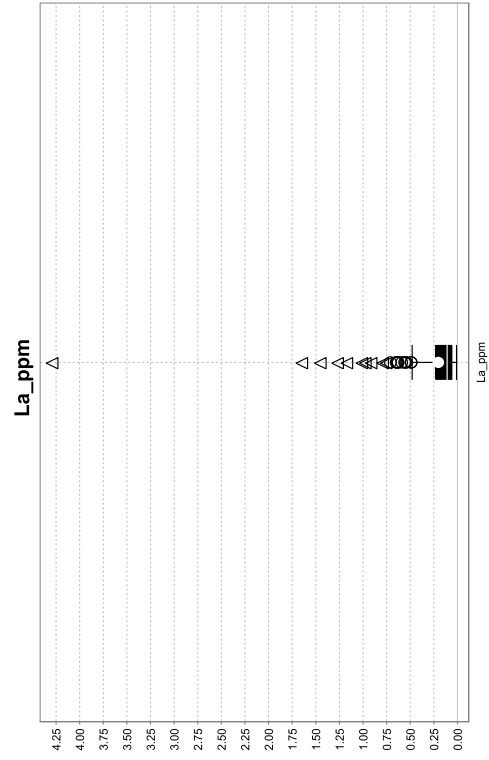
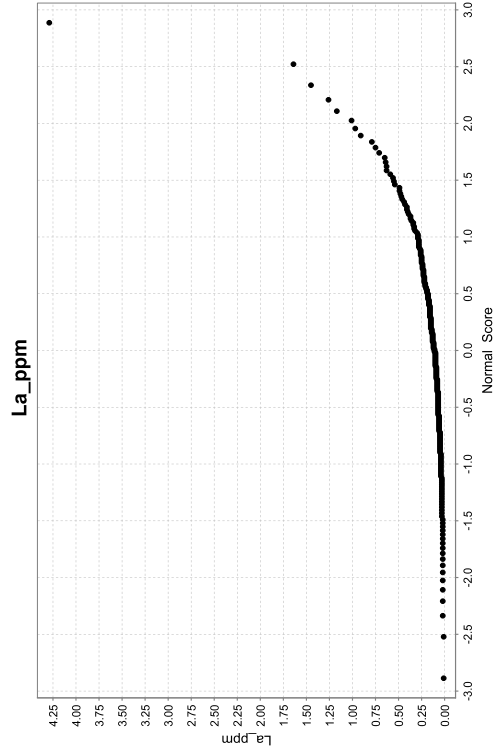
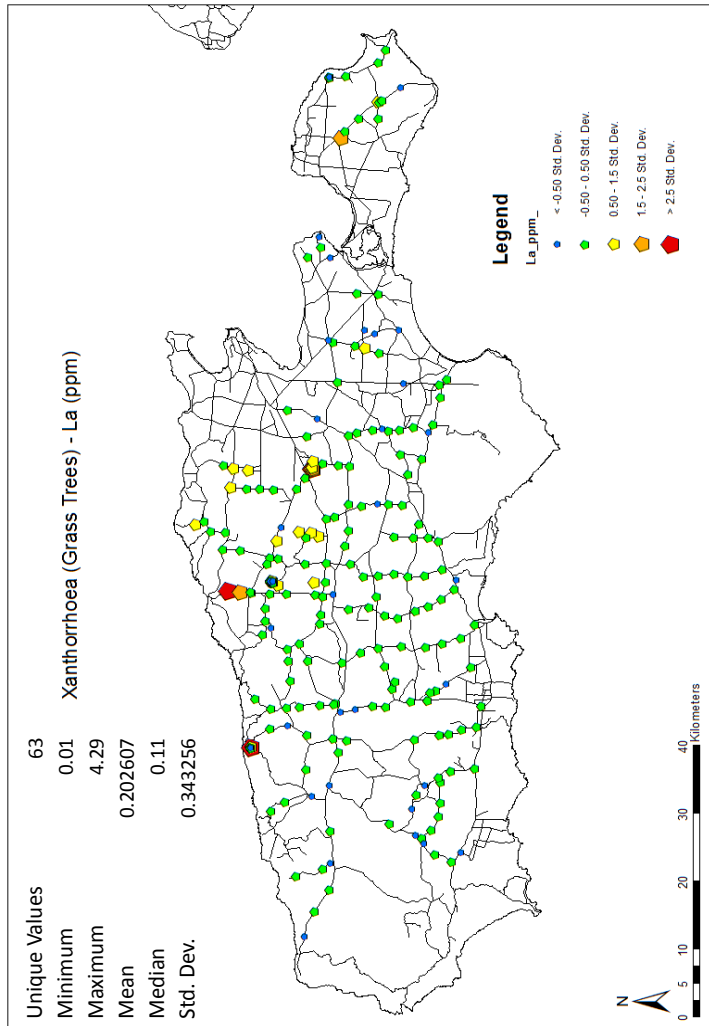


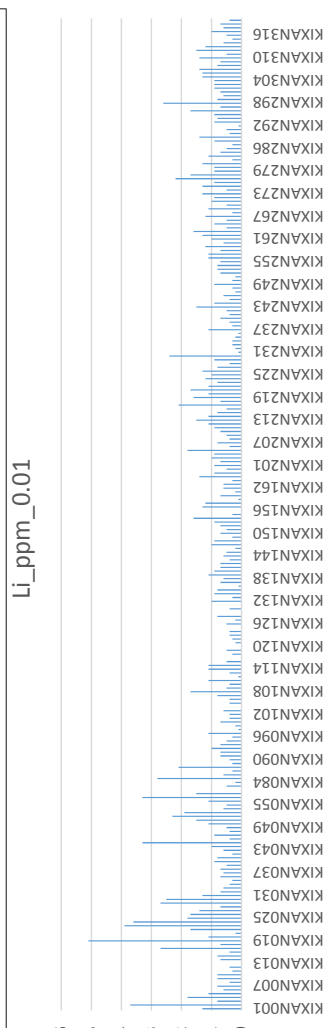
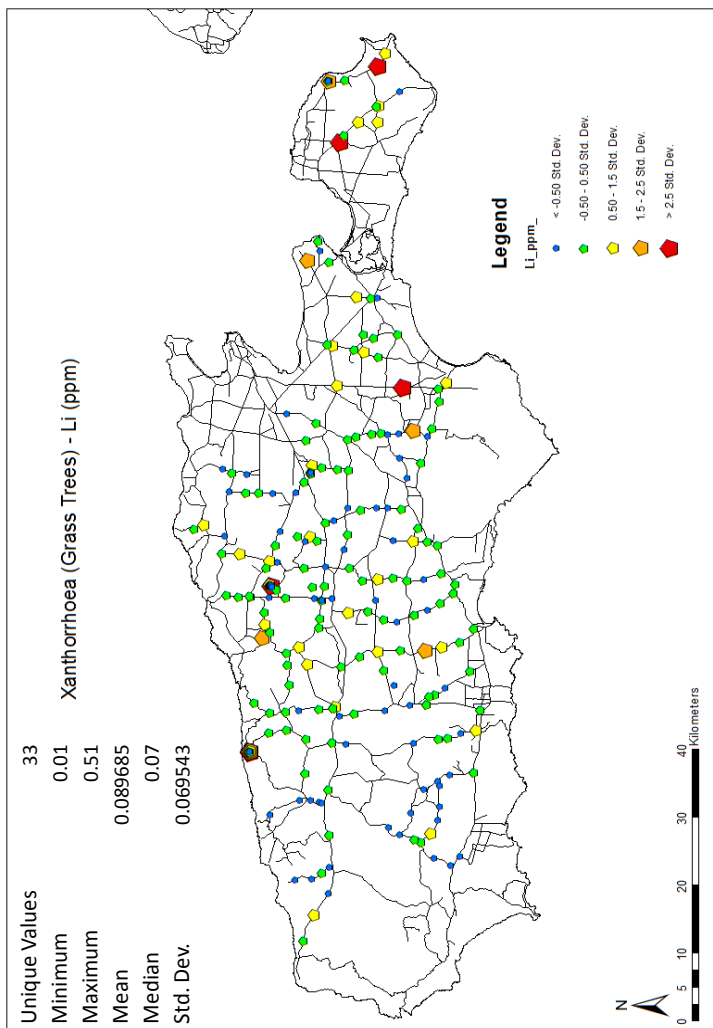
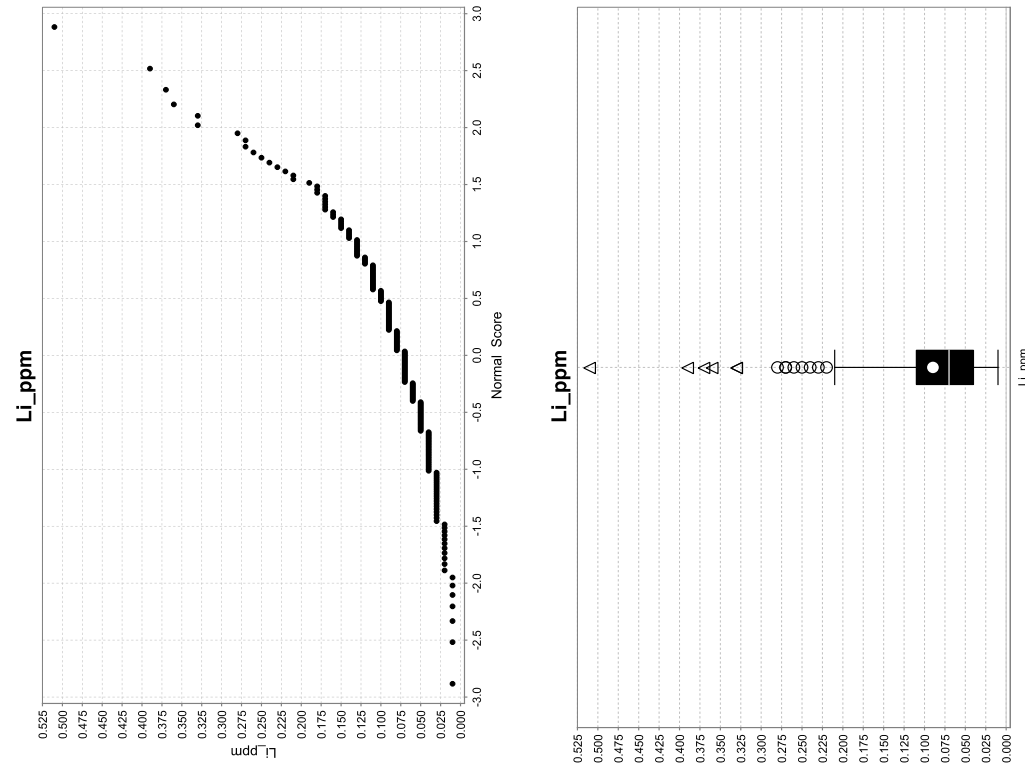


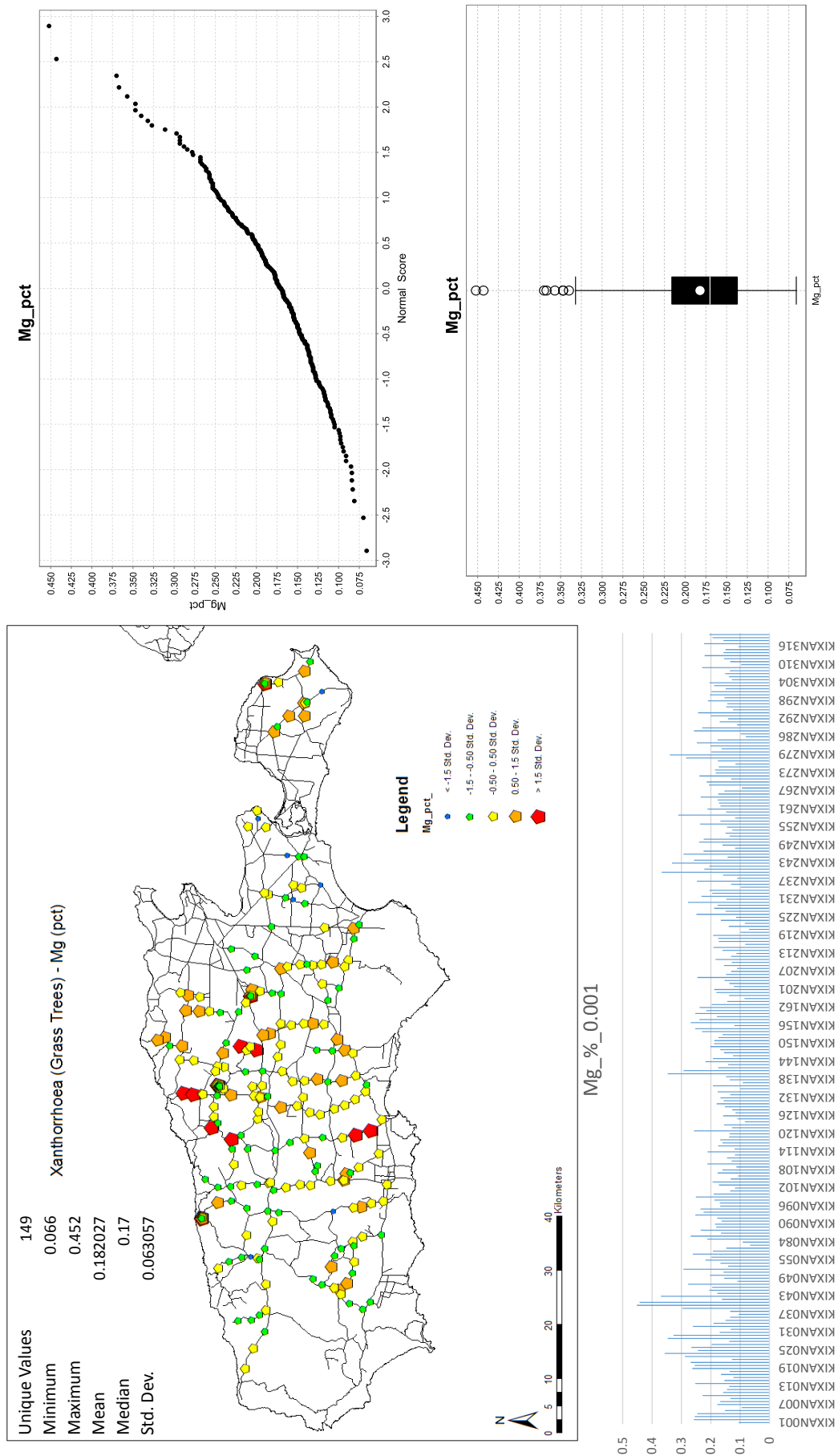


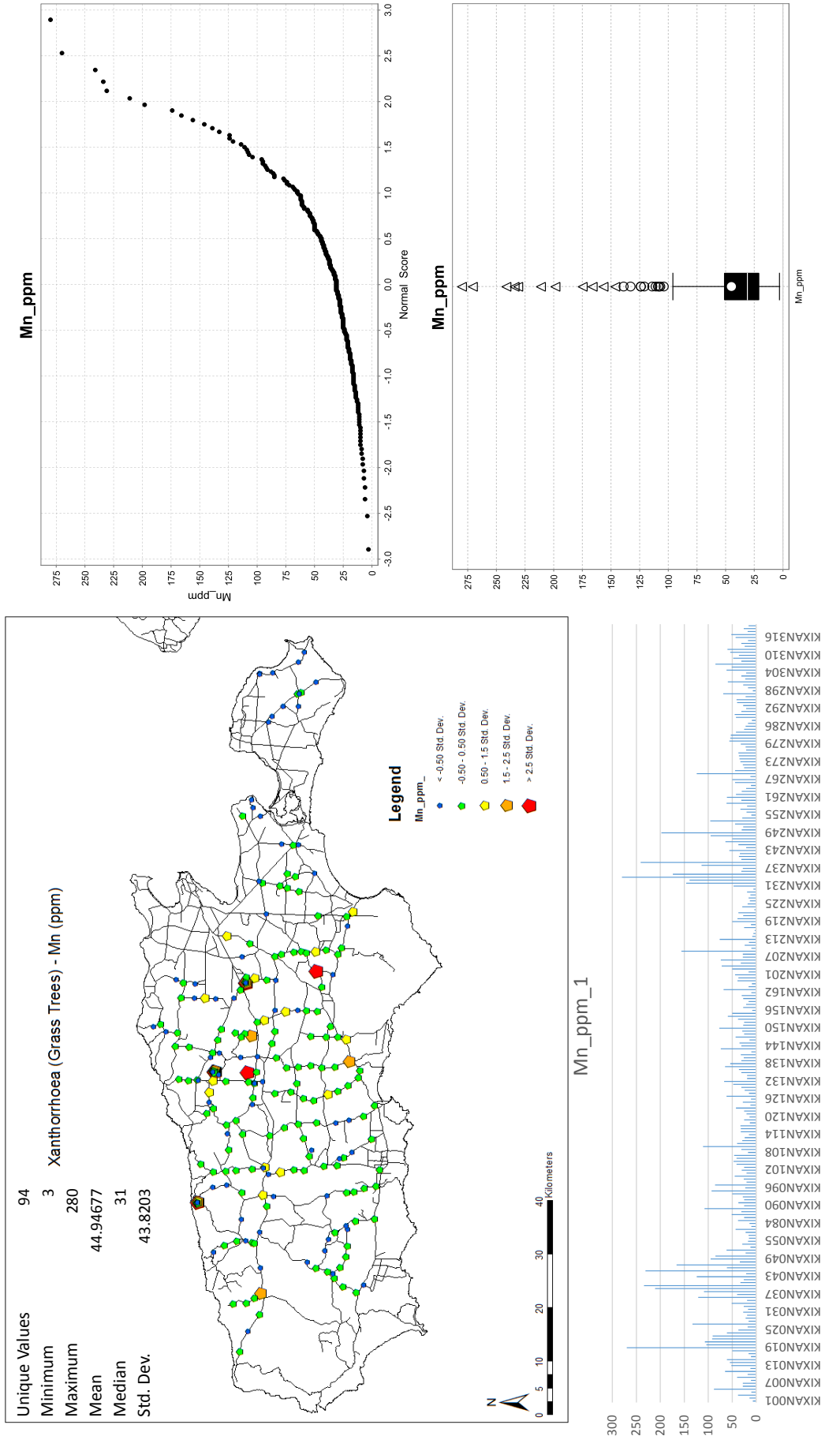


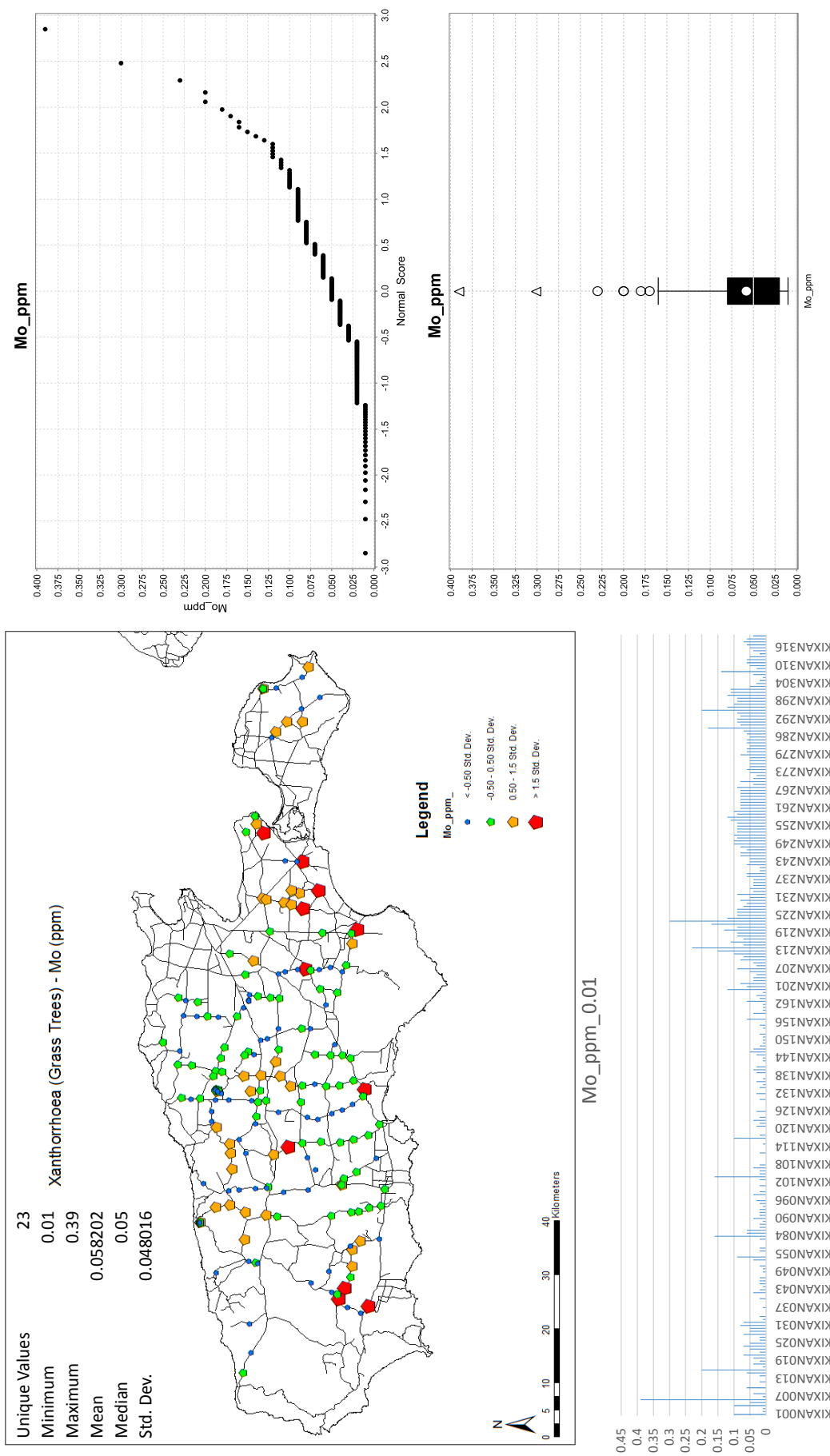


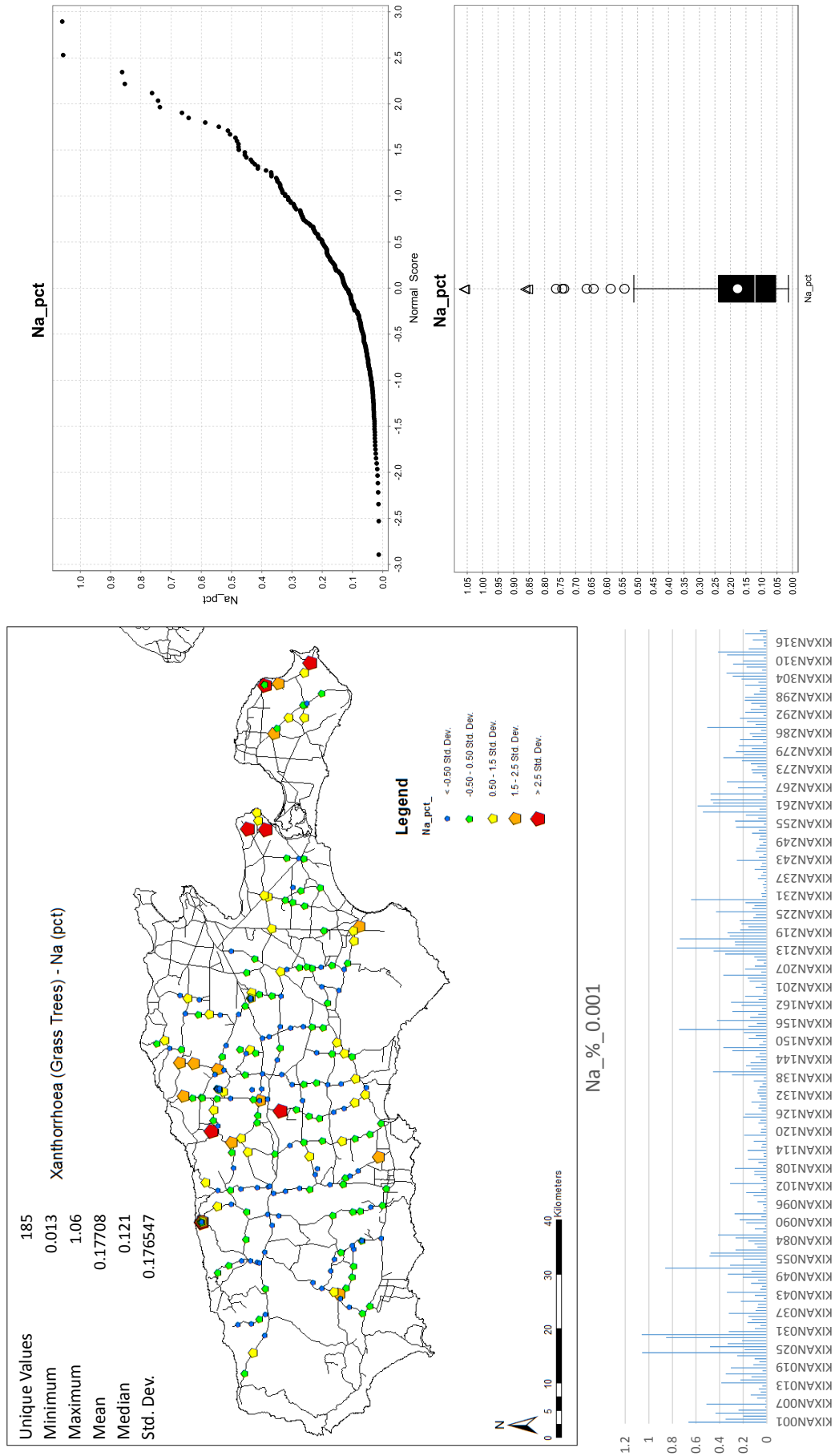


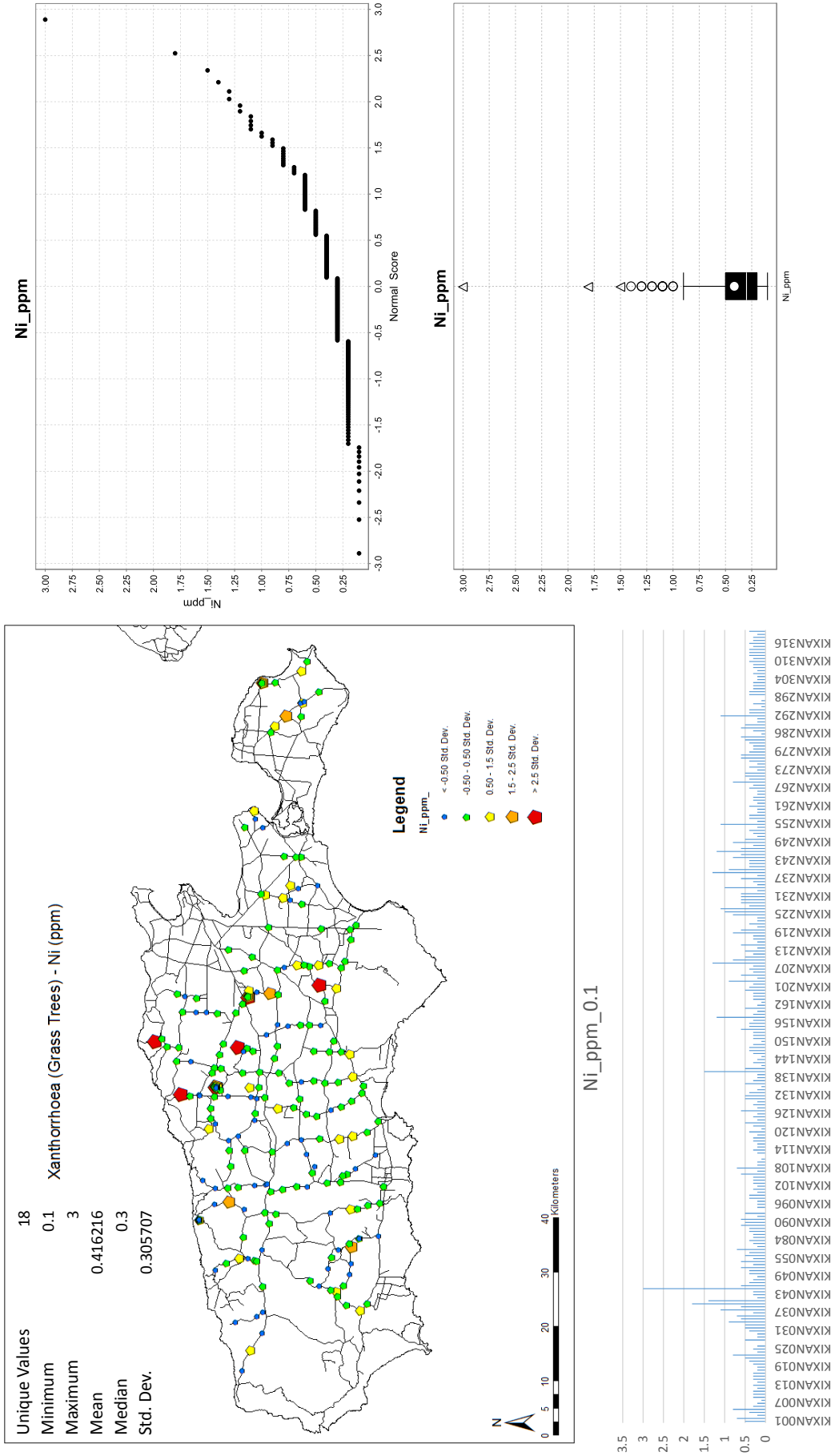


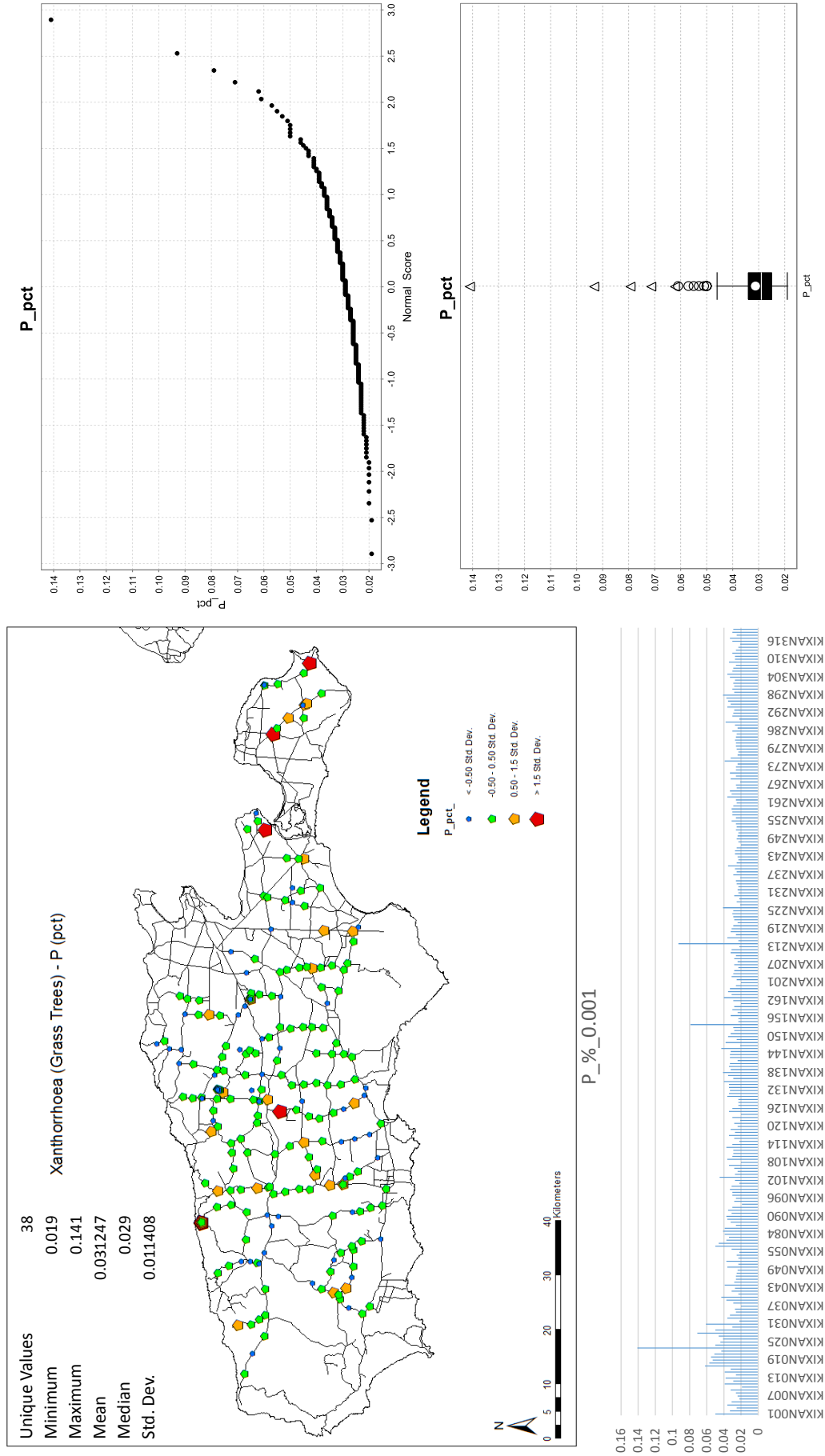


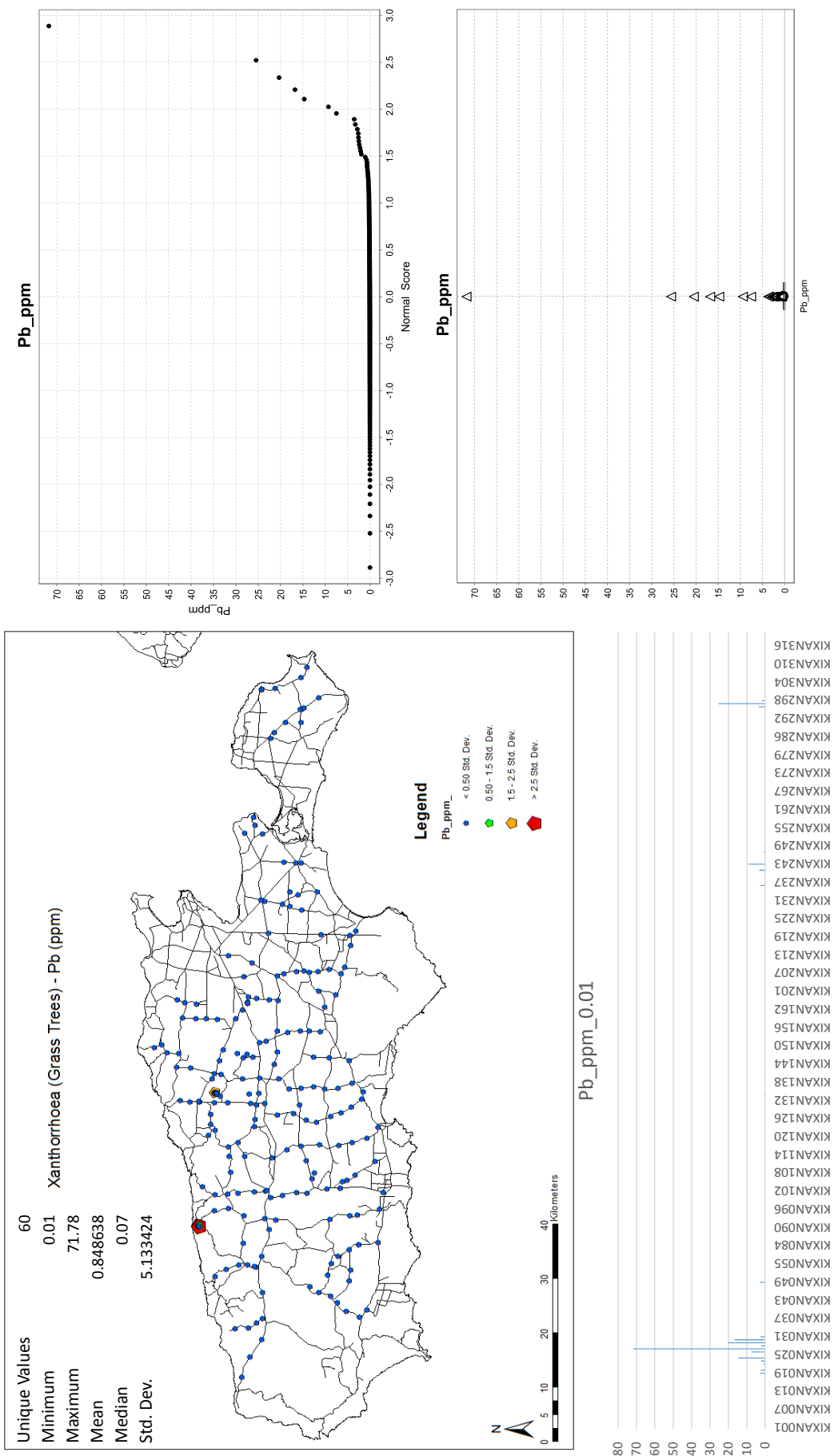


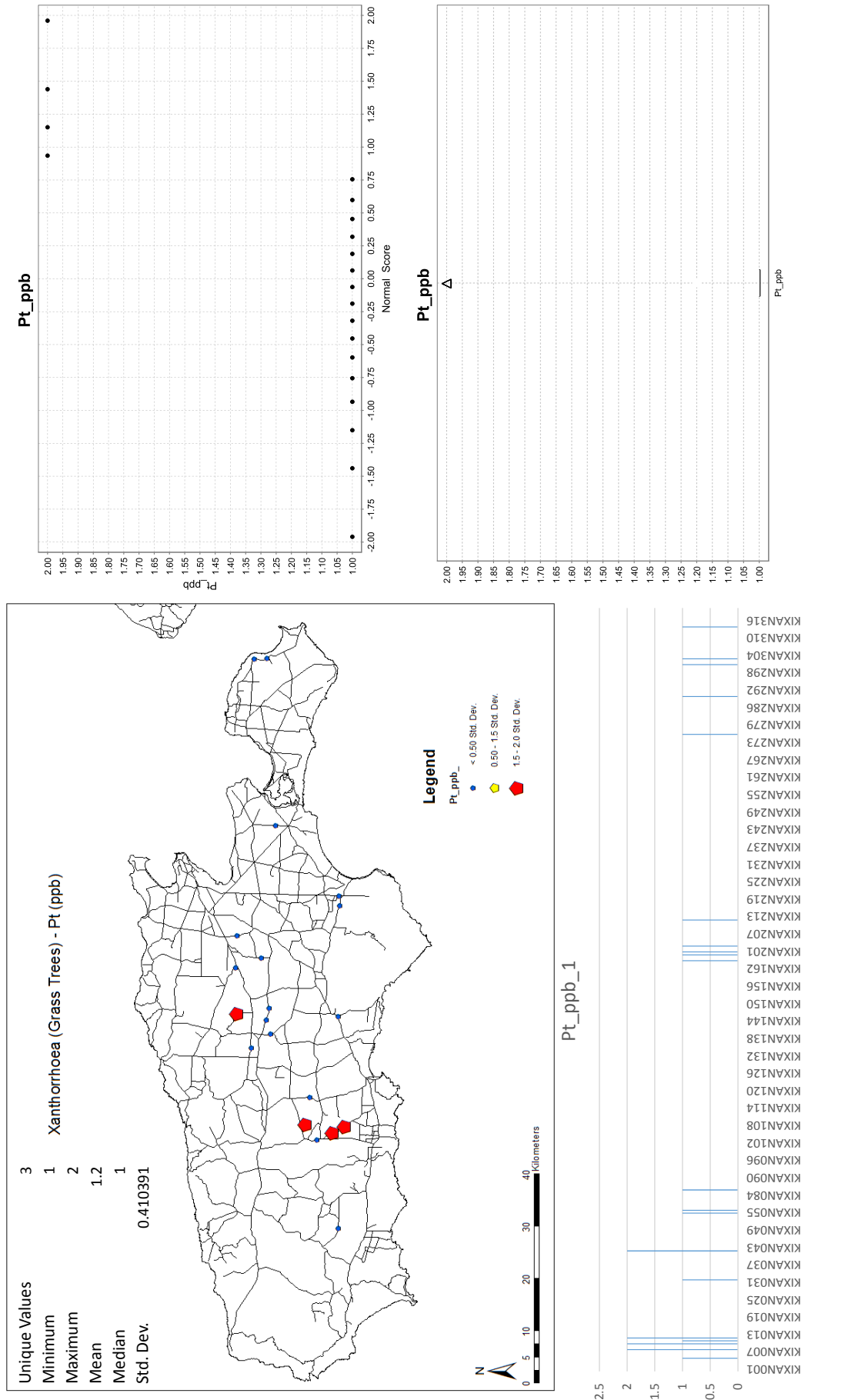


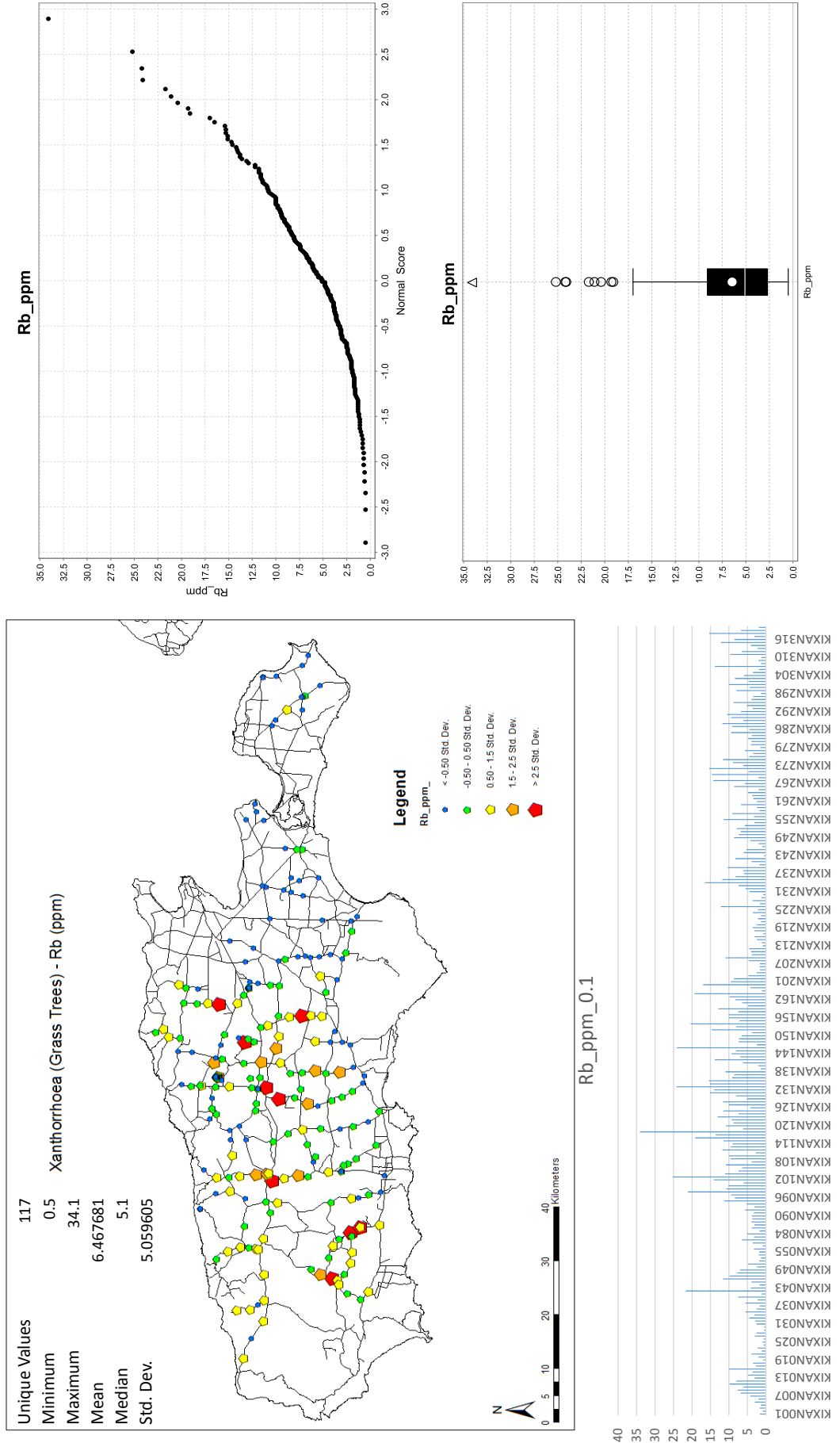


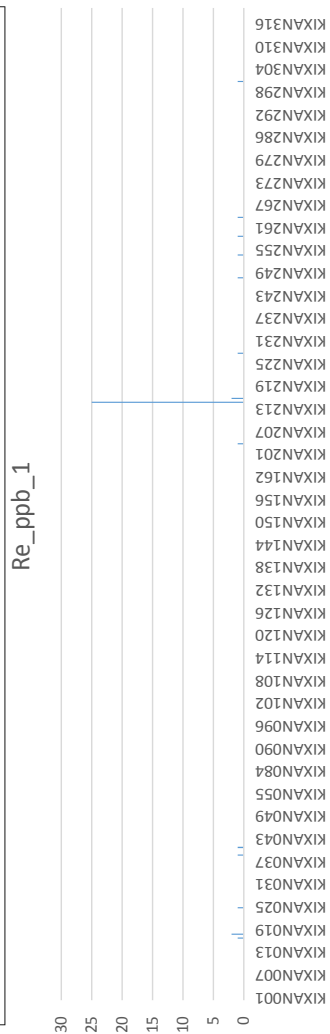
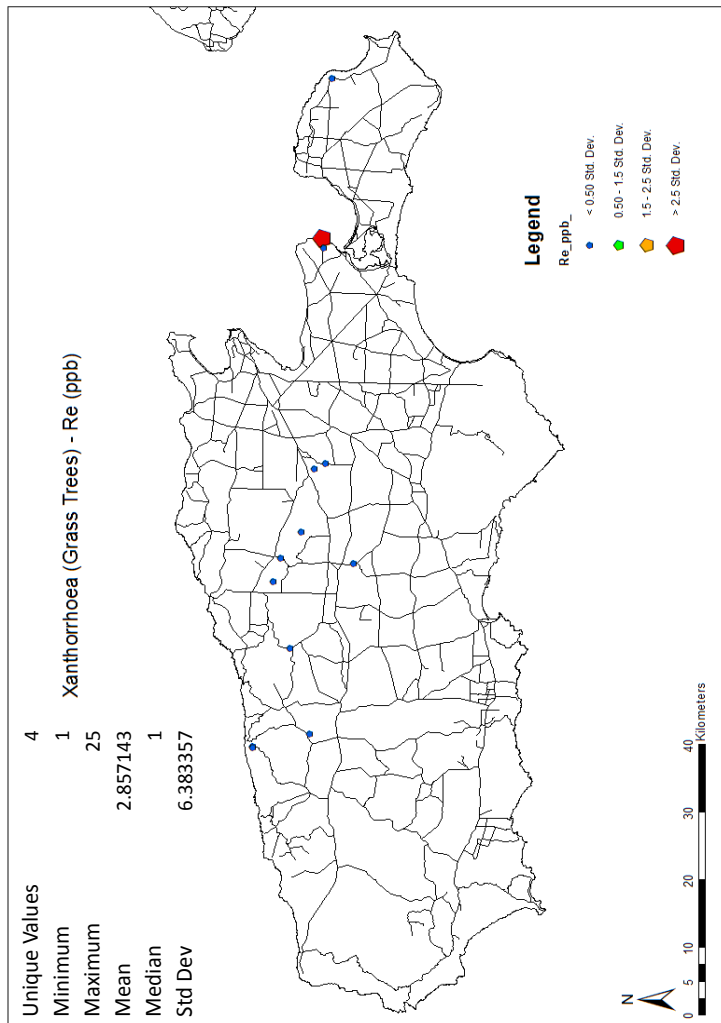
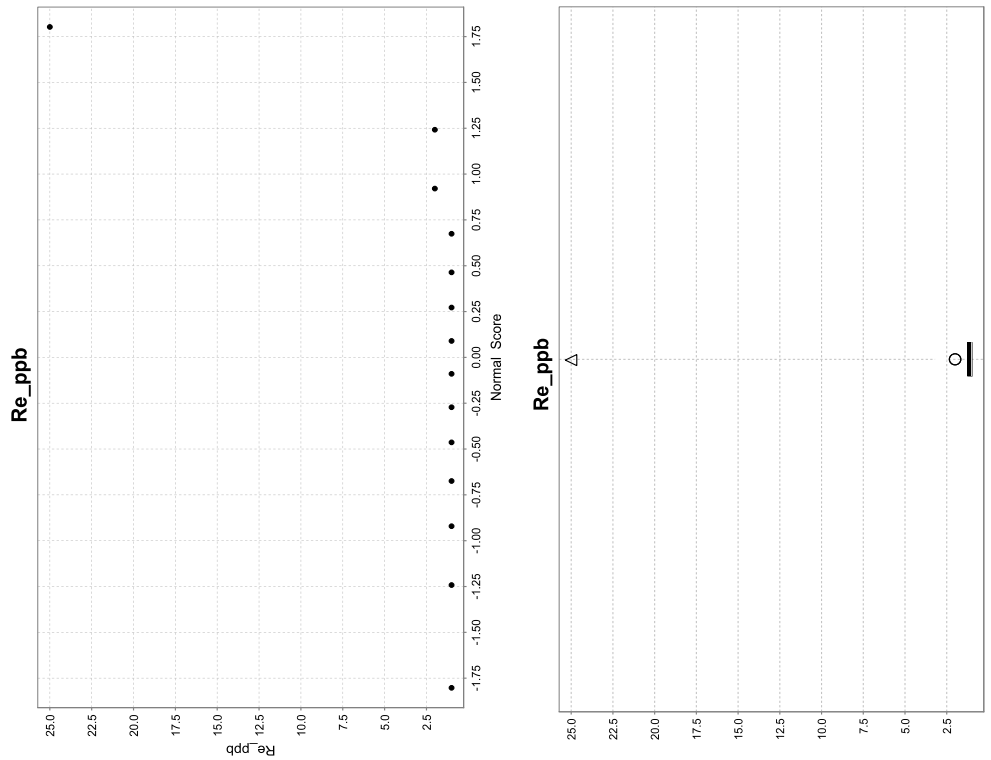












Unique Values 4
 Minimum 1
 Maximum 25
 Mean 2.857143
 Median 1
 Std Dev 6.383357

Xanthorrhoea (Grass Trees) - Re (ppb)

